Abiotic Transformations of Pesticides in Prairie Potholes

A DISSERTATION
SUBMITTED TO THE FACULTY OF THE GRADUATE SCHOOL
OF THE UNIVERSITY OF MINNESOTA
BY

Teng Zeng

IN PARTIAL FULFILLMENT OF THE REQUIREMENTS
FOR THE DEGREE OF
DOCTOR OF PHILOSOPHY

Adviser: Dr. William A. Arnold

August 2012

© Teng Zeng 2012

Acknowledgements

I owe my gratitude to many people who have helped me get to this destination.

My deepest gratitude goes to my advisor, Dr. William A. Arnold. I have been fortunate to have Bill as an advisor who gave me the freedom to explore on my own, and at the same time the guidance and encouragement to overcome unexpected challenges and crisis situations. In particular, I am thankful to Bill for holding me to a high research standard, for helping me sort out the technical details of my work, and for carefully reading and commenting every piece of my writing. More importantly, Bill taught me to be a versatile environmental chemist.

I must thank my dissertation committee members, Dr. Paige J. Novak, Dr. R. Lee Penn, and Dr. Paul D. Capel, for reading previous drafts of this dissertation and providing many valuable comments that improved the presentation and contents of this dissertation. I am especially grateful to Paige for her willingness to serve as my committee chair with relatively short notice. I am also thankful to Dr. Raymond M. Hozalski, who served on my written and oral exam committee and generously allowed me to use large portions of his laboratory space.

I am also indebted to our research collaborators Dr. Yu-Ping Chin and Kate L. Ziegelgruber at the Ohio State University as well as Dr. David N. Mushet at the U.S. Geological Survey Northern Prairie Wildlife Research Center. Special thanks are due to Yo for teaching me the art of sediment coring and porewater extraction and for providing thorough review and constructive comments on my manuscripts. I would like to thank Kate for helping me with sediment sample processing and DOC analysis. I also would

like to express my gratitude to Dave for guiding us through sampling sites and for sharing his first-hand experience with prairie potholes.

I would like to offer special thanks to Dr. Brandy M. Toner for introducing me to the remarkable XANES technique and for sharing her valuable beamtime and beamline wisdom. Without Brandy's input, there would not have been Chapter 5 of this dissertation. I also would like to thank Dr. Matthew A. Marcus and Dr. Sirine C. Fakra at the ALS Beamline 10.3.2 for their expert guidance and consistent support during my beamtime. I further wish to thank members of the Toner research group, especially Brandi Cron, Jeffry Sorensen, Jill Coleman Wasik, and Sarah Nicholas, for assisting me with XANES data collection and analysis.

I would like to express my appreciation to Dr. Edward L. Cussler for providing focused and constructive commentary on my dissertation practice talk. Ed also guided me through a paint research project and has taught me innumerable lessons and insights on the workings of academic research in general.

I am grateful to my fellow graduate students within the Environmental Engineering and Chemistry group, past and present. I would like to thank Amanda Stemig, Andy McCabe, Cale Anger, David Tan, Erin Surdo, Hao Pang, Megan Kelly, Noah Hensley, Jay Roth, Fabrizio Sabba, Greg LeFevre, Mark Krzmarzick, Nate Fleishhacker, Pat McNamara, Andrew Rescorla, Kathryn Wilkinson, Srijan Aggarwal, Alina Grigorescu, and Tucker Burch for their help, talents, and friendship along the way. On the more personal side, I wish to thank Andrew, Fab, Pat, and Srijan for their steadfast encouragement and Megan for always brightening up the office.

Most importantly, none of this would have been possible without the love and support of my parents and my girlfriend Lydia.

Finally, I appreciate the financial support from the Department of Civil Engineering and the National Science Foundation.

Dedication

This dissertation is dedicated to my parents.

Abstract

The prairie pothole region (PPR) is among the most extensively altered ecosystems on Earth. This region covers approximately 780,000 km^2 of central North America, and contains numerous glacially formed wetlands embedded in an agricultural landscape. These wetlands, commonly known as prairie pothole lakes (PPLs), provide essential ecosystem services. Over the last 150 years, agricultural drainage has resulted in severe loss of native prairie wetlands. The remaining PPLs continue to be threatened by nonpoint source pesticide pollution from agriculture. Currently, little is known about the fate and persistence of pesticides in PPLs. In this work, the abiotic transformations of commonly used pesticides in PPL sediment porewaters and surface water were explored. Chloroacetanilide and dinitroaniline pesticides were found to react rapidly with naturally abundant reduced sulfur species (i.e., hydrogen sulfide and polysulfides) in sediment porewaters via nucleophilic substitution and reduction reactions, respectively. Dissolved organic matter (DOM) was also found to play a vital role in the reductive transformation. Next, the photodegradation of a suite of pesticides was investigated in PPL surface water under both simulated and natural sunlight. Enhanced pesticide removal rates pointed to the importance of indirect photolysis pathways involving photochemically produced reactive intermediates such as singlet oxygen and triplet excited-state DOM. Finally, the sedimentary sulfur speciation was examined by sulfur *K*-edge X-ray absorption near-edge structure (XANES) spectroscopy. Sulfur species in PPL sediments were found to consist of organic (di)sulfides, sulfonate, sulfate, and the mineral pyrite. Notably, the fractional abundances of reduced and oxidized sulfur species fluctuate on a seasonal basis.

Table of Contents

List of Tables

List of Figures

Chapter 1: Introduction

1.1 Pesticides in the Aquatic Environments

Each year, three to seven million tons (i.e., 6 to 14 billion pounds) of pesticides are manufactured globally to maintain and increase crop production to meet the increasing food demand driven by population growth.[1] It has been projected that global pesticide use will increase by 2.7-fold from 2000 to 2050, accompanied by a loss of 10^9 hectares of natural ecosystems to agricultural expansion during this 50-year period.[1] Owing to the ecotoxicity of pesticides and their metabolites, concerns have been raised regarding the exposure risks of biota and humans to these chemicals.[2] The mitigation of pesticide pollution is therefore considered as a key element in agricultural management strategies for maintaining the ecological integrity of the environment.[1,2] In the United States, more than 900 pesticides have been registered for use since 1967, and approximately 1 billion pounds of conventional pesticides (i.e., herbicides, insecticides, fungicides, and a mixed group of fumigants, nematicides, and other pesticides) are consumed annually to control weeds, insects, fungi, and other pests (Figure 1.1).[3] A 10-year study conducted by the U.S. Geological Survey's (USGS) National Water-Quality Assessment program has reported the widespread occurrence and elevated concentrations of pesticides in surface streams and groundwater impacted by agriculture.[3] Pesticides or their degradates were detected more than 97% and 61% of the time during the year in water samples collected from streams and shallow groundwater in investigated agricultural areas, respectively, with triazines and chloroacetanilides being the most frequently detected.[3] Of these, annual mean concentrations of pesticides exceeded one or more human-health benchmarks and water-quality benchmarks for aquatic life and

wildlife in 10% and 57% of streams with agricultural watersheds, respectively.[3] Over the past decade, many other studies have also documented the occurrence of a wide array of pesticides in various aquatic environments throughout the world.[4-11]

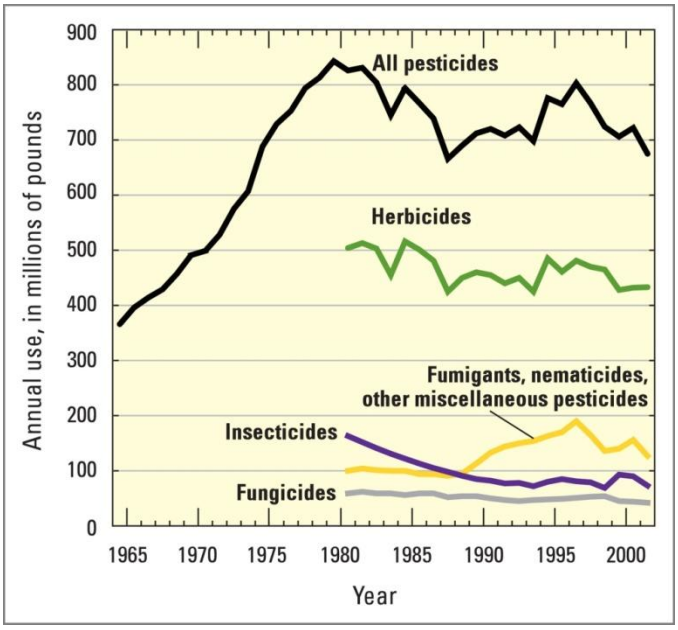

Figure 1.1 Trend of total agricultural use of pesticides in the United States from 1964 to 2001. Figure adapted from Gilliom et al. (2006).

Pesticides can enter natural waters from agricultural fields through multiple routes. Nonpoint source surface runoff is one of the predominant pathways and is typically governed by weather (e.g., rainfall intensity/duration, wind speed), soil (e.g., organic matter content, permeability), management practices (e.g., irrigation, sediment erosion control, vegetative buffer strips), as well as properties of the pesticides themselves (e.g., volatility, water solubility, sorption affinity).[12-14] The biological (e.g., algae, microbial community), chemical (e.g., pH, dissolved oxygen, dissolved organic matter, suspended particles, alkalinity), and physical (e.g., depth, temperature) conditions of downstream water bodies can all affect the partitioning and persistence of pesticides.[12-

[14] Pesticides may sorb to particles and deposit in sediments, volatilize into the atmosphere, accumulate in aquatic biota, be biodegraded by microorganisms, or undergo abiotic transformations (e.g., hydrolysis, redox reactions, and photolysis).[15,16] As with other anthropogenic contaminants, predictions of the transport and fate of pesticides in natural waters require assessment of the transformation rates and mechanisms.

1.2 Prairie Pothole Region of North America

Climate, hydrologic forces, geologic modifications, human activities, and many other processes have shaped the Earth's landscape and led to the formation of a diverse collection of wetlands from mountaintops to seacoasts.[17] The prairie pothole region (PPR), which encompasses approximately 780,000 km^2 of the north-central United States and south-central Canada, contains a high density of small, shallow, depressional wetlands embedded in a complex landscape of moraines, glacial meltwater channels, outwash plains, and lacustrine plains (Figure 1.2).[18-20] These wetlands, commonly known as prairie pothole lakes (PPLs) or sloughs, formed about 16,000 years ago upon the retreat of late Pleistocene glaciers.[21] PPLs are often defined as isolated wetlands[21] because most of them lack surface inflows or outflows due to their origin and relative youth.[22] PPLs mainly receive water from direct precipitation, upland runoff, and groundwater discharge, with evapotranspiration contributing to the largest fraction of water loss.[18] Their size, shape, and water levels constantly fluctuate in respond to significant changes in seasonal and interannual climate conditions.[20] Many shallow PPLs are only temporarily or seasonally ponded while deeper ones may have standing water most of (semipermanent) or all (permanent) the time.[23] Owing to their dynamic nature,

the ecological functions of PPLs are also highly variable.[24] Collectively, the PPLs and their associated watersheds constitute one of the largest inland wetland systems on Earth,[19] and are of unparalleled importance to a diverse community of waterfowl, invertebrates, and plants.[25] The PPR represents one of the major waterfowl breeding habitats and migration corridors in North America.[26] It is a critical breeding habitat for about 21.6 million ducks of 12 species and produces from 50% to 75% of the continent's duck population.[20,27] In terms of primary productivity (vegetation), the PPR ranks with the tropical rain forests.[28] Moreover, PPLs provide additional ecological functions such as groundwater recharge, floodwater storage, sediment and pollutant reduction and carbon sequestration.[29-31]

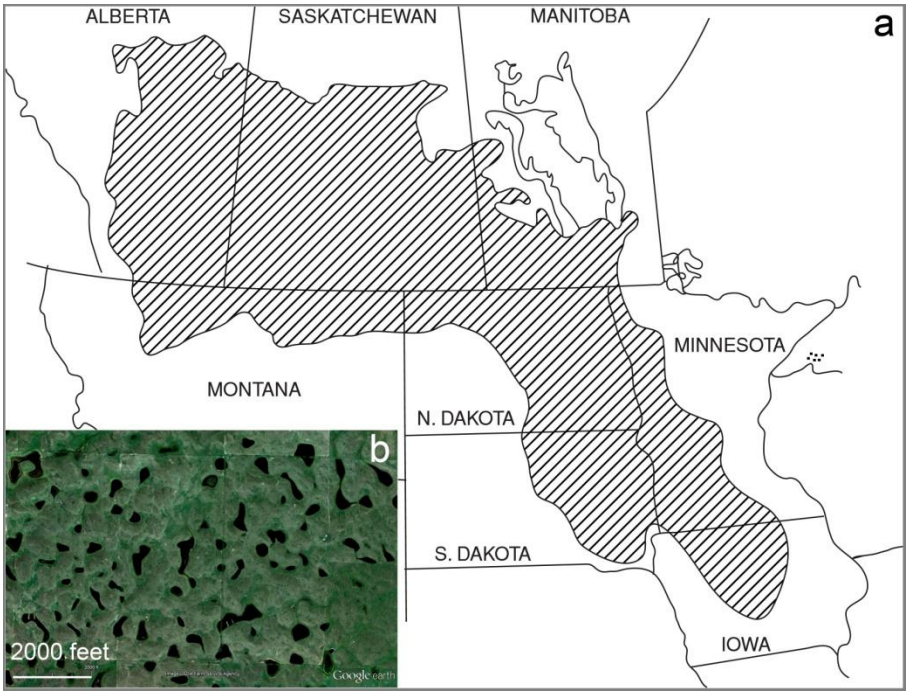

Figure 1.2 The prairie pothole region of North America: (a) The PPR runs from central Iowa through eastern South and North Dakota and western Minnesota in the US and across southern Manitoba, Saskatchewan, and Alberta in Canada. Map adapted from van der Valk (2005). (b) Satellite image of typical PPR landscape in North Dakota *[47°23'33.91"N and 100°37'57.71"W. Google Earth®. (Accessed July 2012)]*.

PPLs were once the most common wetland ecosystem in North America. Historically, 23% of the PPR landscape was covered by wetlands with a density of 5-90 potholes/km^2. [19,32] There may have been over 20 million PPLs prior to European settlement.[30] Temporary and seasonal PPLs were estimated to comprise approximately 60% and 35%, respectively, of all potholes with semipermanent and permanent ones making up less than 5% of the total.[23,32] Since European settlement (i.e., the last quarter of the 19th century), agriculture has become a primary socioeconomic driving force throughout the PPR.[33] Drainage to create more farmland has been the major factor leading to the loss of PPLs. For instance, a significant portions of the PPR in Iowa, western Minnesota, and eastern North and South Dakota have experienced comprehensive drainage through drainage tile, ditch networks, and streams.[34] In the U.S., the loss of native PPLs reached 35% in South Dakota, 50% in North Dakota, 90% in Iowa, and over 85% in Minnesota by the 1980s.[32,35] Since the 1980s, 4.3% of the Minnesota PPR wetland has been drained with losses varying from 0 to 15% among ecological subsections (Figure 1.3).[36] In Canada, the magnitude of loss is estimated to be around 40-70% since settlement.[37] The large-scale drainage of PPLs and removal of vegetation buffers have exerted a profound and negative impact on native prairie wildlife, thereby compromising the overall biodiversity and productivity of these landscapes.[38] For instance, a five-county area in central western Minnesota historically estimated to support up to 0.3 million breeding duck pairs is only able to support less than 60,000 breeding pairs today.[32] The number of plant species in the PPR has declined to roughly half of that found at the time of European settlement.[39] In the past two decades, there has been a

growing awareness of the ecological importance of PPLs and of the need to ameliorate their loss. Significant advances (e.g., the Wetland Reserve Program and the Conservation Reserve Program) have been made in conserving and restoring PPLs.[40,41] In recent years, however, there have been renewed incentives to expand agriculture in the PPR for production of organic crops and corn-based biofuels.[32,41]

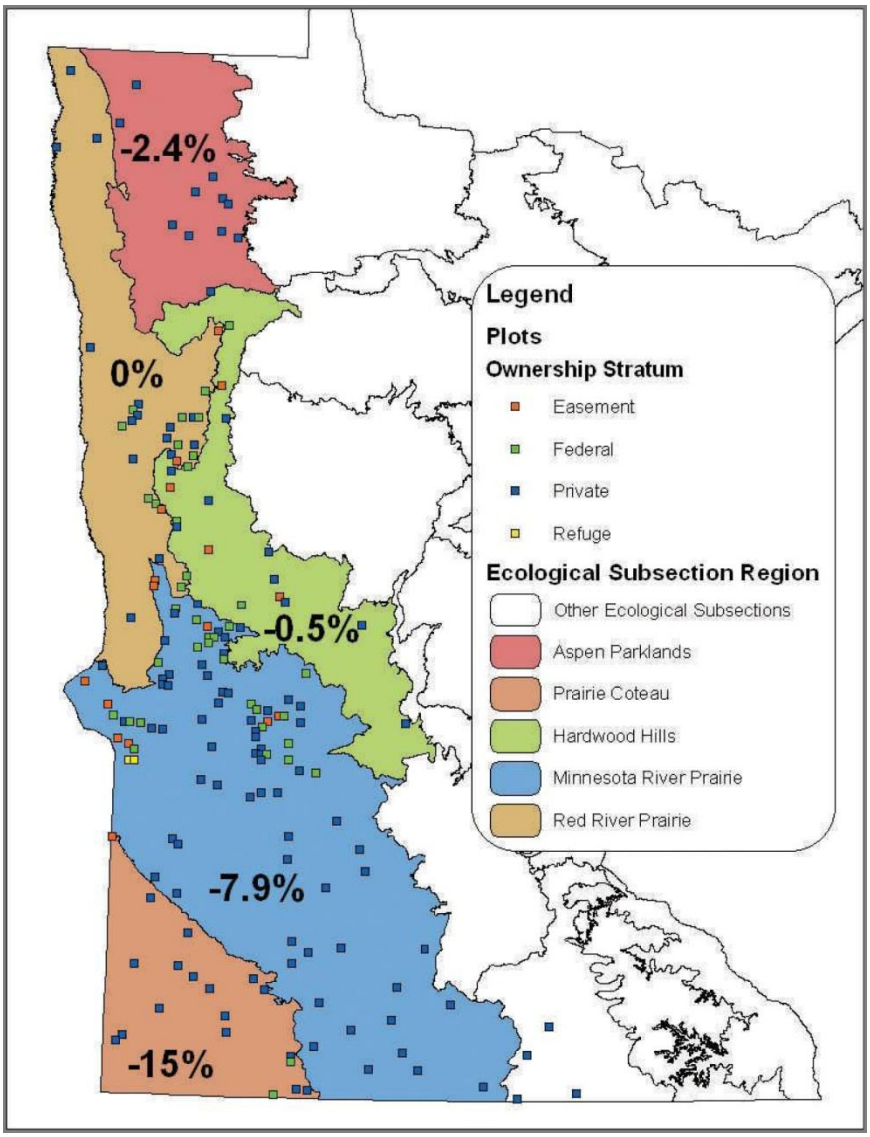

Figure 1.3 The prairie pothole region of western Minnesota showing locations percentage change of wetland area by ecological subsections (1980-2007). Figure adapted from Oslund et al. (2010).

The remaining PPLs have become interspersed within a matrix of agricultural lands and are thus directly and indirectly impacted by adjacent land use and management practices. In particular, many PPLs are located on or closely surrounded by farmland.[42] As a result, PPLs are at a high risk of trapping nonpoint source agricultural pollutants, such as pesticides and nitrogen and phosphorus fertilizers.[43-45] Furthermore, the establishment of drainage networks, either using surface channels or drainage tiles artificially joined PPLs to the existing natural streams, rivers, and lakes.[32] The increasing connectivity of PPLs may potentially increase contaminant fluxes into downstream aquatic systems. For instance, nitrate concentrations in two Mississippi River tributaries originating in the PPR, the Minnesota and Des Moines River, have increased ~13 times and ~6 times, respectively, between 1906 and 1996, making them two of the greatest contributors to hypoxia in the Gulf of Mexico.[46]

Since 1960s, both the quantity and spectrum of pesticides applied in the PPR have significantly increased.[42] Most of the agricultural area is treated annually with at least two to three different pesticides along with fertilizers.[44] Pesticides may enter PPLs by application drift,[47] deposition of wind-eroded soil,[48] surface runoff,[49,50] and wet and dry atmospheric deposition.[51] A number of pesticides, such as 2,4-D, atrazine, bentazon, bromoxynil, clopyralid, dicamba, dichlorprop, diuron, MCPA, mecoprop, metolachlor, and trifluralin, have been detected in prairie aquatic ecosystems.[52-55] Pesticides entering prairie wetlands were shown to greatly lower the population sizes of aquatic invertebrates as well as the reproductive success and survival rates of waterfowl.[47,56-58] Thus, concerns have been raised about the negative impact of pesticides on the water quality of prairie

wetlands and their disruptive effects on the ecological integrity of the region.[42,57] Knowledge about the transformation of pesticides in the PPL water column and sediment, however, is still rather limited.

1.3 Aqueous Inorganic Sulfur Chemistry: Bisufide and Polysulfides

Sulfur (S) is not only an essential element for all living organisms (i.e., the 6th most abundant element in biomass; ~1% of dry weight)[59] being a constituent of amino acids, coenzymes, and vitamins, but also fulfills many diverse roles in complex economic, ecological, and geochemical aspects of life on Earth.[60] Sulfur occurs in a range of oxidation states, ranging from –2 (as in sulfide) to +6 (as in sulfate), and readily forms a variety of organic and inorganic species. Sulfate (SO_4^{2-}) is the most thermodynamically stable form of S. In anoxic *aqueous* environments, hydrogen sulfide (H_2S) is the major dissolved reduced S species, and is formed as a result of dissimilatory sulfate reduction associated with organic carbon mineralization (Equation (1.1)):

$$SO_4^{2-} + 8e^- + 9H^+ \rightarrow HS^- + 4H_2O \qquad (1.1)$$

Re-oxidation of bisulfide (HS^-) at the oxic-anoxic interface regenerates sulfate but also leads to the formation of a range of partially oxidized S species, such as polysulfides (S_n^{2-}; n = 2-8), thiosulfate ($S_2O_3^{2-}$), elemental sulfur (S_8), polythionate ($S_xO_6^{2-}$; x = 3-5), and sulfite (SO_3^{2-}) (Figure 1.4).[61-64]

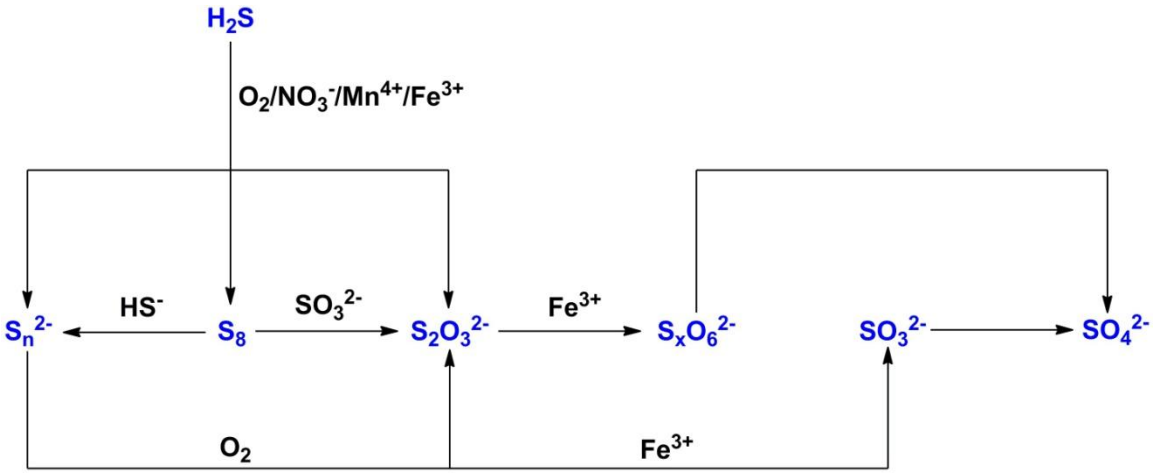

Figure 1.4 Schematic diagram of formation pathways of major inorganic S species in anoxic aqueous environments.

Polysulfides form by the reaction of bisulfide with *excess* elemental sulfur (Equation (1.2)):[65]

$$HS^- + (n-1)/8\ S_{8(s)} \leftrightharpoons S_n^{2-} + H^+ \qquad (1.2)$$

Equilibrium constants and acid dissociation constants for these reactions have been well documented.[66,67] The relative abundance of different polysulfide species strongly depends on the pH of the system (Figure 1.5). At higher pH, the formation of polysulfide dianions is favored, while at neutral pH, the hydropolysulfide anions (HS_n^-) and bisulfide are favored. It should be noted that the speciation of polysulfides in a system undersaturated with respect to S_8 is expected to be dominated by polysulfides with shorter S chain length (e.g., disulfide (S_2^{2-}) and trisulfide(S_3^{2-})), whereas a system saturated with S_8 will be dominated by polysulfides with longer S chain length (e.g., tetrasulfide (S_4^{2-}) and pentasulfide (S_5^{2-})) .[68] Polysulfides are an important component of dissolved S in marine, estuarine, and lacustrine sediment porewaters,[69-72] and they potentially play a role in the cycling of metals (e.g, iron).[66,73,74] The concentrations of hydrogen sulfide and

polysulfides in anoxic sedimentary environments have been reported to reach as high as 6.4 mM and 0.43 mM, respectively.[73,75]

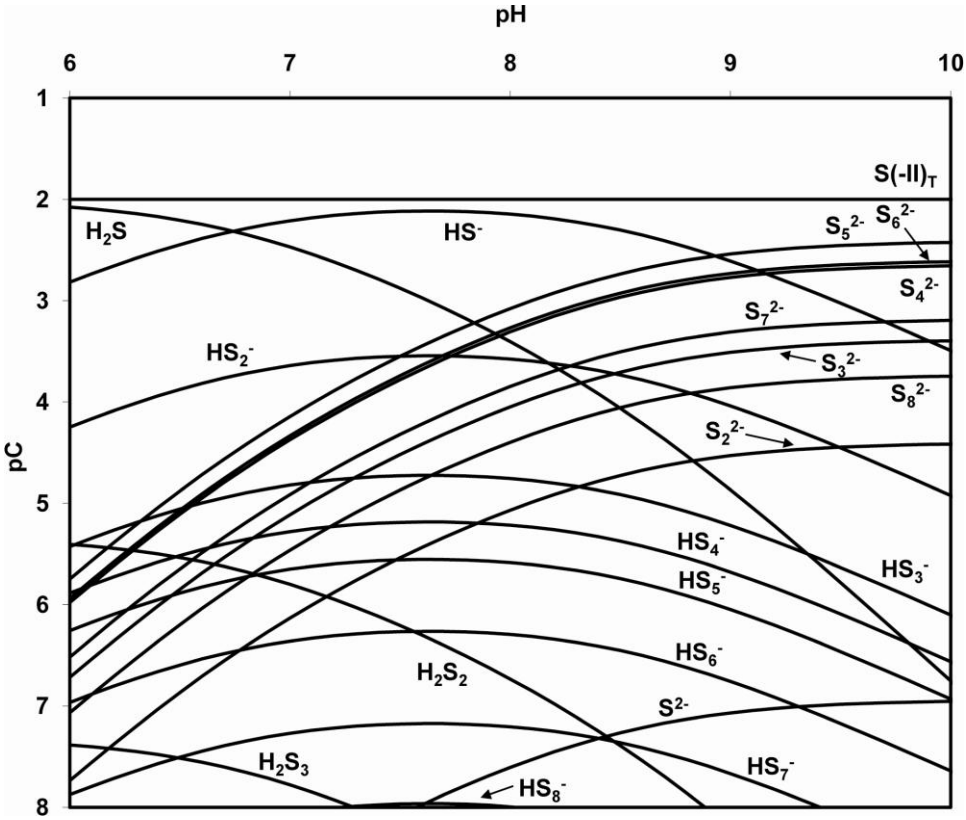

Figure 1.5 Polysulfide speciation in a HS^- solution in equilibrium with excess S_8. Total reduced sulfur ($[S(-II)]_T$) = 10 mM; Ionic strength = 0.2; Equilibrium constants and acid dissociation constants (corrected for ionic strength) from Kamyshny et al. (2004) were used.

Both hydrogen sulfide and polysulfides exhibit high nucleophilicity and redox reactivity. Extensive research over the past two decades has demonstrated that HS^- and S_n^{2-} can act as nucleophiles and/or reductants to promote the rapid transformation of a wide array of pesticides in both well-defined aqueous systems[76-92] and natural sulfidic waters.[93,94] For instance, chloroacetanilide pesticides (e.g., metolachlor) undergo nucleophilic aliphatic (S_N2) substitution reactions with HS^- and S_n^{2-} by displacement of a chlorine atom (Figure 1.6a).[95] Moreover, S_n^{2-} was found to exhibit a considerably greater

reactivity towards chloroacetanilides than HS^-,[95] presumably due to its higher polarizability and lower solvation energies.[89] Dinitroaniline pesticides (e.g., trifluralin), on the other hand, were found to undergo nitro-reduction reaction in the presence of HS^- alone, but the *direct* reduction rates were relatively slow under environmentally relevant conditions (Figure 1.6b).[78] In the presence of dissolved organic matter (DOM), however, the reduction rates were accelerated by orders of magnitude, which was attributed to the electron transfer capacity of redox-labile functional groups (e.g., hydroquinone moieties) in DOM that shuttle electrons between HS^- (i.e., bulk electron donors) and dinitroanilines.[78] Although S_n^{2-} has been shown to be a kinetically more reactive reductant than HS^-,[93] its reactivity towards dinitroanilines is unknown.

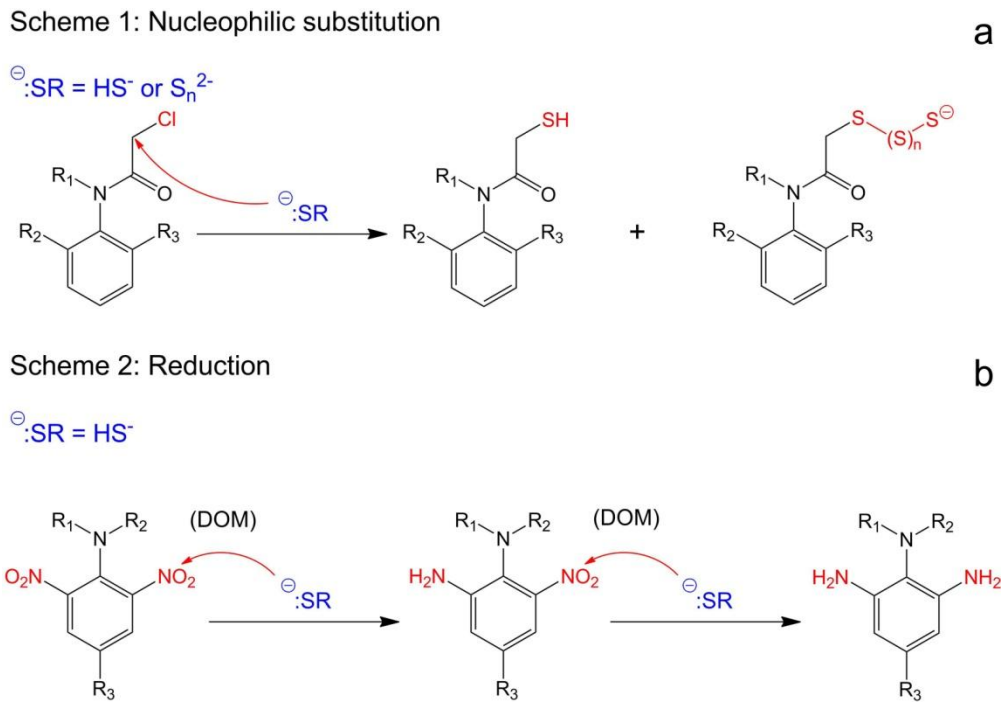

Figure 1.6 Diagrams of nucleophilic substitution and reduction reactions: (a) Nucleophilic aliphatic substitution of chloroacetanilides with HS^- and S_n^{2-} based on Loch et al. (2002)[95]; (b) Sequential reduction of dinitroanilines with HS- based on Wang and Arnold (2003). "DOM" denotes dissolved organic matter added as the electron transfer mediator.

One unique aspect of PPLs is that many of them have evolved high concentrations of sulfate in the surface water (typically on the order of 10-100 mM[33]) due to seasonal evaporation and groundwater recharge, suggesting that microbially-driven sulfate reduction may represent a predominant process in PPL anoxic sediments. Thus, reduced inorganic S species formed upon sulfate reduction, in particular HS^- and S_n^{2-}, are likely to be enriched in interstitial porewaters. To date, no information exists pertaining to the abundance of these reduced S species in PPL sediment porewaters, and they would presumably act as both nucleophiles and reductants to promote the abiotic degradation of pesticides. In addition, dissolved organic matter, if present in appreciable amounts in PPL porewaters, may serve as the electron transfer mediator to facilitate the in reduction reactions of pesticides. Although previous research has suggested that partitioning to sediments can be a major dissipation pathway for pesticides entering PPLs,[96-98] the fate of pesticides in the sedimentary environment remains unclear.

1.4 Aquatic Photochemistry: Direct and Indirect Photolysis

When light interacts with a compound, a number of processes can potentially occur. Most are photophysical processes (i.e., the chemical structure of the compound is unaltered in the end); others, however, are photochemical processes (i.e., the compound undergoes chemical structural changes).[99,100] As the major radiation source in nature, sunlight has a spectral range of approximately 290-800 nm, corresponding to an energy range of 414-150 kJ/mol (or 98.6-35.8 kcal/mol).[101] These energies are sufficiently high to induce a wide range of chemical reactions, because a large portion of bond dissociation energies fall within this energy range.[99] Thus, photochemical processes play a vital role

in the environmental fate of natural and anthropogenic compounds.[102] Photolysis in natural waters occurs in the upper most portion of the water column known as the photic zone and is affected by the water depth and light attenuation.[103] Within the photic zone, photoreactions fall into two main categories: *direct* photolysis and *indirect* photolysis. Compounds may react solely via direct or indirect photolysis, or by a combination of the two.[104]

Direct photolysis occurs when a compound directly absorbs light energy and undergoes chemical transformations after becoming electronically excited (Figure 1.7). For a compound to undergo direct photolysis, it must absorb light with wavelength greater than 290 nm.[105] The light-absorbing functional groups in a compound are often called chromophores, which undergo chemical changes as a direct consequence of absorbing photons.[100] Conjugated π-electron structures, including double bonds, carbonyl, carboxylate, nitro and phenolate groups, are the major chromophores in natural organic matter and anthropogenic organic compounds.[100] Direct photolysis is an important pathway for the photodegradation of organic contaminants commonly detected in natural waters. Previous research has shown that pesticides (e.g., trifluralin and bentazon),[106,107] polycyclic aromatic hydrocarbons (e.g., pyrene, phenanthrene, and naphthalene),[108-111] alkyl nitrosamines (e.g., *N*-nitrosodimethylamine),[112] phytoestrogens (genistein and daidzein)[113,114] and several categories of pharmaceutical and personal care products, including anti-anxiety drugs (e.g., diazepam),[115] anti-bacterial/viral drugs (e.g., sulfamethoxazole, nitrofurantoin, ciprofloxacin, and oseltamivir),[116-120] anti-inflammatory drugs (e.g., diclofenac, ibuprofen, naproxen, and mefenamic acid),[121-125] hormones (e.g.,

estriol and 17β-estradiol),[124] anti-bacterial agents (e.g., triclosan and its chlorinated derivatives),[126-128] and sunscreen agents (e.g., ensulizole and octyl methoxycinnamate),[129,130] can all undergo direct photolysis under environmental relevant conditions.

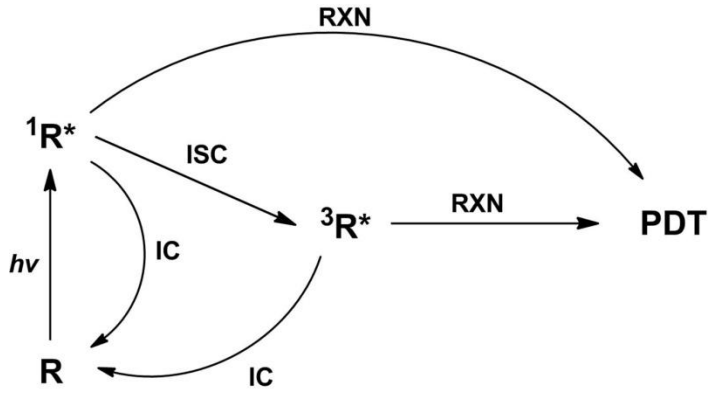

Figure 1.7 Schematic pathways of direct photolysis. R – ground-state reactant, $^1R^*$ – singlet-state reactant, $^3R^*$ – triplet-state reactant, PDT – product, IC – internal conversion, ISC – intersystem crossing, RXN – chemical reaction.

Indirect photolysis occurs when another chemical species, termed a photosensitizer, becomes electronically excited due to light absorption and then either reacts directly with the compound of interest or produces reactive intermediates which further transform the compound (Figure 1.8). Indirect photolysis is more important in the case of compounds that absorb little sunlight or that are stable with respect to direct photolysis. Natural waters contain a variety of constituents (e.g., dissolved organic matters (DOM), nitrate and nitrite, and iron) that are capable of producing reactive intermediates and the photoreactivity of the water depends on its overall composition.

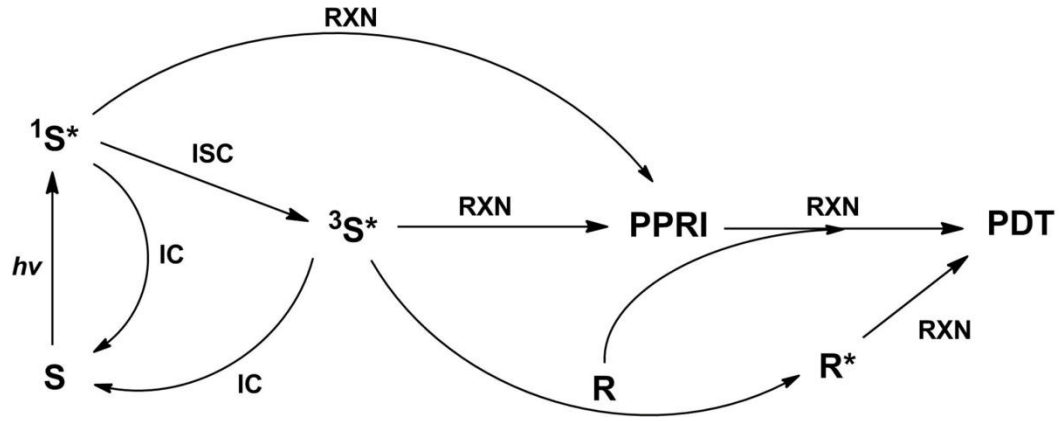

Figure 1.8 Schematic pathways of indirect photolysis. S – ground-state sensitizer, $^{1}S^{*}$– singlet-state sensitizer, $^{3}S^{*}$ – triplet-state sensitizer, R – ground-state reactant, R^{*} – excited-state reactant, PPRI – photochemically produced reactive intermediate, PDT – product, IC – internal conversion, ISC – intersystem crossing, RXN – chemical reaction.

Dissolved organic matter is a complex, heterogeneous mixture of organic compounds that are ubiquitous to natural waters and can influence a number of biogeochemical processes in aquatic systems.[131] It is well known that DOM can sensitize several indirect photolytic pathways by generating photochemically produced reactive intermediates (PPRIs; Figure 1.9), and the reaction mechanisms often vary both with the compound of interest and origin of the DOM.[132] Specifically, short-lived singlet-state DOM ($^{1}DOM^{*}$) can undergo intersystem crossing to a more stable, lower-energy triplet state ($^{3}DOM^{*}$), which can 1) react directly with compounds, 2) generate a suite of reactive intermediates, including hydroxyl radical ($^{\bullet}OH$), singlet oxygen ($^{1}O_2$), superoxide ($O_2^{-\bullet}$), peroxyl radicals ($ROO^{\bullet}$), and hydrogen peroxide (H_2O_2).[131-143] Superoxide can further react with itself or hydroperoxyl radical ($HO_2^{\bullet}$) to produce H_2O_2 through a dismutation process,[131] whereas hydroxyl radical can react with some inorganic water constituents and yield long-lived radicals such as bicarbonate radical ($CO_3^{-\bullet}$).[132] Singlet-state DOM ($^{1}DOM^{*}$) can also release energy by ejecting electrons, producing

solvated electron (e^-_{aq}) [144-147]. Conversely, DOM also retards phototransformation by screening reactive wavelengths of light or acting as a scavenger of PPRIs.[131] Therefore, DOM acts as both a source and sink (or quencher) of PPRIs in natural waters, which further complicates its role in indirect photolysis.[131]

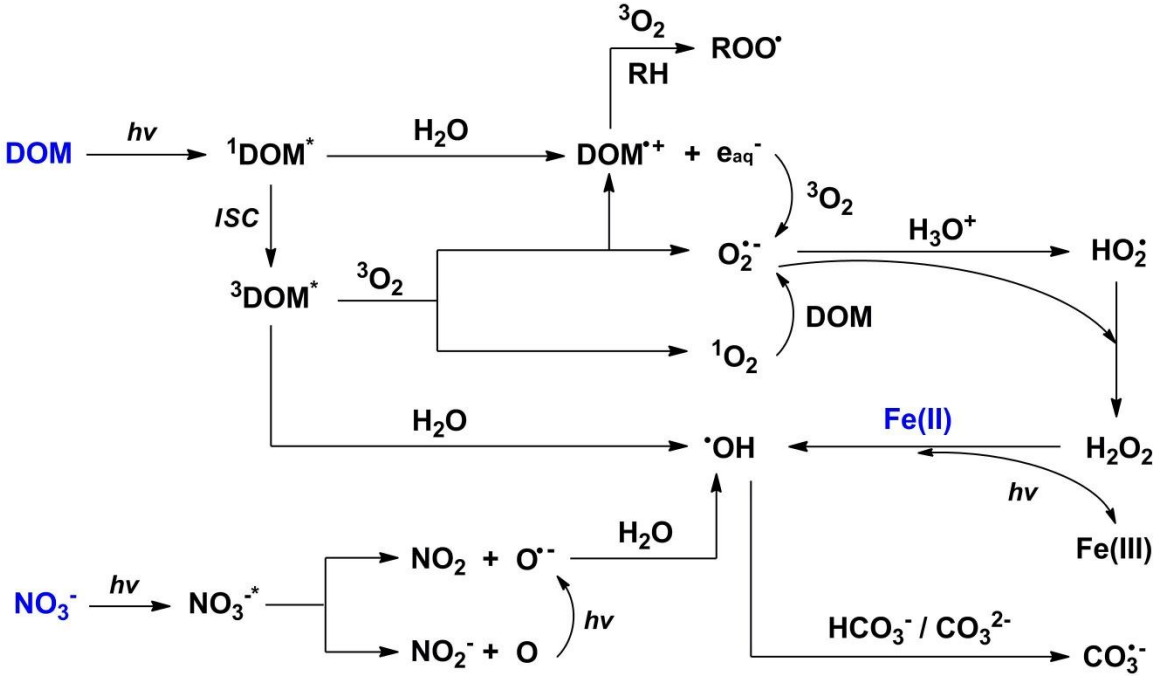

Figure 1.9 Indirect photochemical productions of PPRIs from the photolysis of different sensitizers (DOM, nitrate, and iron(II)) in natural waters.

Although the concentrations of PPRIs vary widely (10^{-18} - 10^{-9} M), they are substantially lower than other major chemical species in natural waters. These concentrations, however, are often sufficient to be important in the processing of dissolved chemical species.[143] Many studies have demonstrated that photochemical processes mediate the transformation of pesticides in natural waters through direct and indirect pathways. The relative importance of direct and indirect processes depends on the properties of pesticides as well as other chemical constituents in water.[148] For instance, trifluralin can absorb sunlight and mainly undergoes direct photolysis,[107]

whereas atrazine and metolachlor mainly react via indirect photolysis mediated by nitrate and DOM.[149,150]

Most PPLs have large surface areas with relatively shallow depths (typically < 1.5 m deep[42]), which greatly increases the potential for sunlight to penetrate the water column. In addition, the surface water of PPLs often contains high levels of DOM (up to 100 mg C/L), which is capable of acting as photosensitizer for the production of PPRIs that promote the degradation of pesticides through indirect photolysis. Taken together, PPLs may possess high near-surface photoreactivity. For many pesticides, direct photolysis is often a less important pathway because they do not readily absorb sunlight. Thus, indirect photolysis of pesticides may play a vital role in PPLs. Although a handful of studies have suggested that photolysis could be an important pathway for pesticide removal in natural and engineered wetlands,[151-153] little is known about to what extent such process occurs in the surface water of PPLs.

1.5 X-ray Absorption Near-Edge Structure (XANES) spectroscopy

Sediments are arguably one of the most complex biogeochemical systems on Earth. They comprise a highly heterogeneous assemblage of water, mineral particles, and organic materials, and their chemical, physical, and biological properties evolve over time at varying rates.[154] Sedimentary environments constitute a critical component of the global S cycle.[155] For instance, sulfur is typically enriched in lacustrine sediments (0.03-6.4% by weight) relative to crustal materials (0.003-0.27% by weight) and surface soils (0.005-0.20% by weight).[156] Studying the geochemical transformations of S in sediments, however, is complicated by the co-existence of a wide range of aqueous and solid-phase

inorganic and organic S species, as well as the methodological challenges posed by the heterogeneity of sediments.[63] The chemistry of S in aqueous environmental systems has been well constrained (as discussed in Section 1.3). In contrast, advances in knowledge of solid-phase S remains have relied heavily on destructive wet-chemical methods to extract operationally-defined fractions.[157-161] For instance, acid-volatile sulfide (AVS) has been frequently taken as a measurement for iron monosulfide in sediment samples.[162,163] Although these conventional techniques offer insightful information, they are indirect in their characterization and thus lack accuracy and details of S speciation.[163,164] Over the past two decades, synchrotron-radiation-based sulfur *K*-edge X-ray absorption near-edge structure (XANES) spectroscopy has emerged as a powerful tool for determining the S speciation in compositionally complex environmental samples, such as sediments,[75,165-169] soils,[164,170-176] biological tissues,[177,178] as well as deep-sea hydrothermal plume particles.[179] The key advantage of using a synchrotron radiation source to perform X-ray absorption spectroscopy lies in that the radiation is tunable over a broad energy range and is highly intense and polarized, leading to more flexibility and higher sensitivity.[180]

XANES is an *in situ*, non-destructive method that has the potential for directly identifying and quantifying different chemical species (functional groups) of S. The general principle of sulfur XANES is given in Figure 1.10a. Upon the absorption of a synchrotron generated X-ray photon by an S atom, a core-level electron is transmitted to unoccupied or partially occupied higher energy levels (e.g., $1s \rightarrow 3p$; *K*-edge) and subsequently ejected into the continuum as a photoelectron. The vacancy left by each expelled electron is then filled by an electron from a higher energy level, and

fluorescence (or alternatively an Auger electron, especially for lighter elements) is emitted to compensate for the energy difference between the two electron levels.[181] An X-ray absorption spectrum is produced by the photo-electric effect (Figure 1.10b). An intense jump in the spectrum (i.e., absorption edge) occurs when the X-ray photon has sufficient energy to excite the core-level electron and the fine structure usually appears as a peak (i.e., white-line peak).[64] Spectral oscillations in the 0-50 eV range directly above the absorption edge, which correspond to the continuum transition (i.e., the ejection of photoelectron), are commonly defined as the X-ray absorption near-edge structure (XANES), while oscillations that persist beyond the XANES region (e.g. up to several hundred eV) are defined as the extended X-ray absorption fine structure (EXAFS).[64,181] The energy position and intensity of absorption edge is sensitive to the electronic configuration (i.e., oxidation state) of the S atom and its local bonding environment.[64] The XANES spectrum, therefore, allows differentiation of various S oxidation states and functional groups present in a sample.

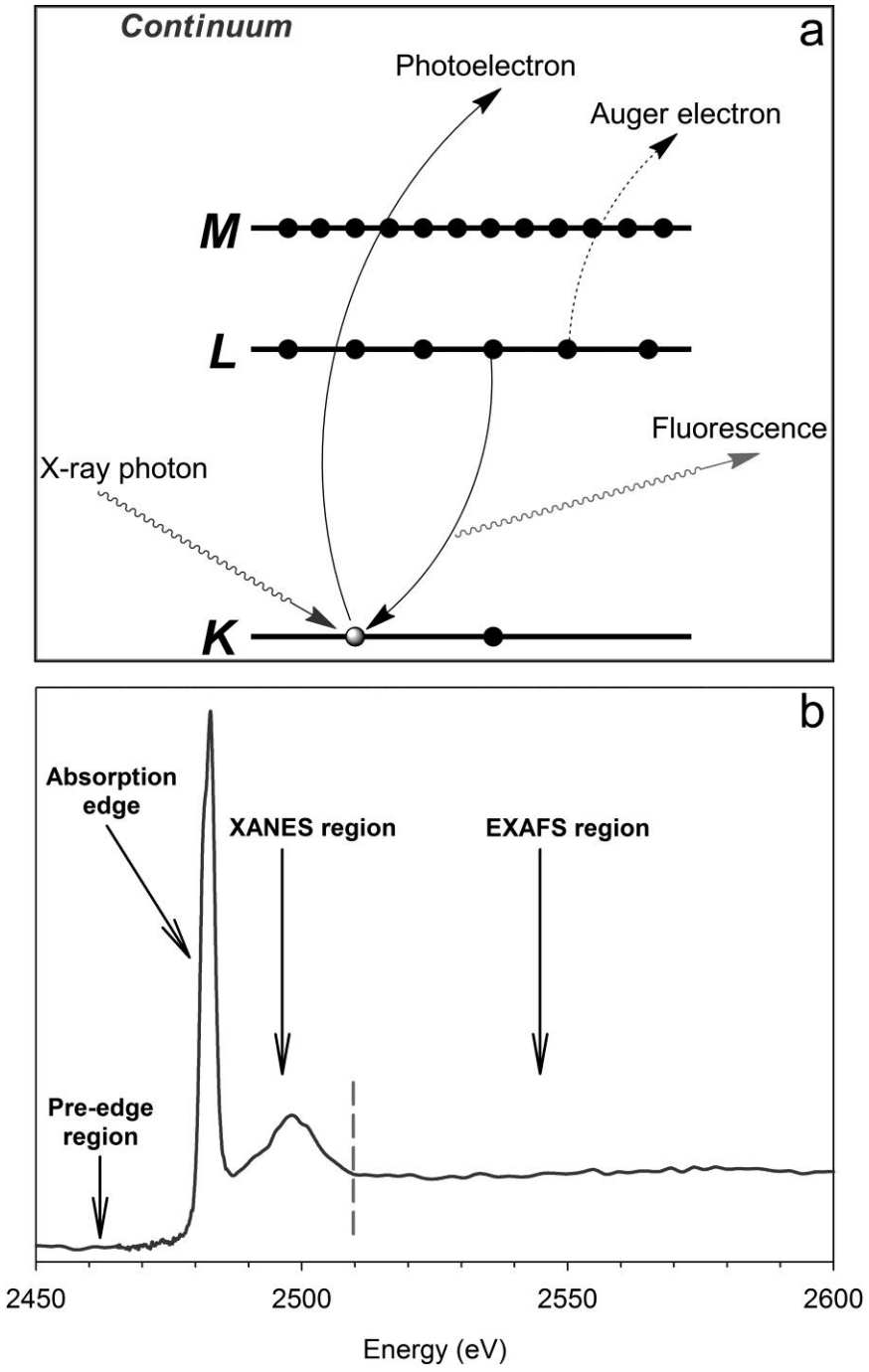

Figure 1.10 Principle of sulfur *K*-edge XANES spectroscopy: (a) Schematic diagram of the excitation of an atom by an X-ray photon and decay of the excited state by either X-ray fluorescence or by the Auger effect. *K*, *L*, and *M* denote the core electron levels; (b) X-ray absorption spectrum of sodium dodecyl sulfate showing the absorption edge, XANES and EXAFS energy regions.

The qualitative and quantitative analyses of S speciation are achieved through deconvolution of the XANES spectra. The fractional contribution of different S species to the total S in a sample can be estimated using two approaches: (1) Linear combination fitting (LCF) by a least-squares linear combination of experimental XANES spectra of model S compounds, and (2) Gaussian curve fitting (GCF) with a number of theoretical Gaussian peaks (theoretically corresponding to the $1s \rightarrow 3p$ transition) along with arctangent step functions (theoretically corresponding to the ejection of photoelectron).[182] LCF requires the availability of a large set of model S compounds but allows a more detailed picture of S speciation to be obtained, especially for the identification and quantification of organic S.[173] GCF is inherently limited by the use of non-realistic spectral profiles that do not strictly discern the subtle variations of the absorption edge of different S species.[182,183] LCF thus is more reliable than GCF, especially when combined with principal component analysis to identify S species that are likely to be present or absent in the samples of interest.[184] In light of its non-destructive, direct nature, sulfur *K*-edge XANES spectroscopy has gained its popularity in sediment S research and has successfully been applied to determine S speciation in whole marine,[165,166] estuarine,[75,168,169] and lacustrine[167] sediment samples as well as sedimentary organic matter extracts.[185]

Given the high sulfate levels in PPL surface water, it is expected that PPL sediments serve as a major sink of S and may exert a strong influence on the regional S cycling. To date, there has been only one study that applied XANES spectroscopy to investigate the S speciation in low-S prairie wetland soils collected from Saskatchewan,

Canada.[170] The relative contribution of reduced inorganic and organic S species in the PPL sediments, however, has not been adequately characterized. Moreover, the spatial and temporal variability in the sedimentary S speciation remains unexplored. A more complete picture of S biogeochemistry in PPLs, therefore, would be a key component in understanding the ecosystem functions and evolution of these wetland systems and their future development.

1.6 Scope of Dissertation

The central hypothesis of this work was that the unique hydrogeochemistry of PPLs would promote the natural attenuation of pesticides. The main objective of this work was to identify and assess the significance of abiotic natural transformations pathways influencing the fate of commonly used pesticides in prairie wetlands. This work combined the investigation of pesticide reaction kinetics with characterization of relevant reactive chemical species. To this end, a series of laboratory batch experiments were performed using surface water and sediment samples collected from two PPLs in the USGS Cottonwood Lake study area, Stutsman County, North Dakota.[186] This dissertation is organized as follows:

Chapter 2 characterizes the bulk chemistry of PPL surface water and sediment porewaters sampled seasonally through 2010, and presents the evaluation of the reactivity of four chloroacetanilide pesticides with reduced S species (i.e., HS^- and S_n^{2-}) in PPL sediment porewaters. The reaction products are identified to verify the involvement of HS^- and S_n^{2-} in nucleophilic substitution reactions.

Chapter 3 presents the evaluation of the reactivity of seven dinitroaniline pesticides with reduced S species (i.e., HS^- and S_n^{2-}) in PPL sediment porewaters. The role of DOM as an electron transfer mediator is also assessed. The reaction products are identified to verify that the transformation process is a reduction reaction.

Chapter 4 examines the photodegradation of sixteen pesticides in PPL surface water under both simulated and natural sunlight with a focus on quantifying indirect photolysis pathways. The steady-state concentrations of four PPRIs (i.e., $CO_3^{\bullet-}$, $^{\bullet}OH$, $^1O_2$ and $^3DOM^*$) are measured to gain insight into the relative importance of each to the overall pesticide photolysis.

Chapter 5 illustrates the applicability of sulfur XANES spectroscopy to identify and quantify the solid-phase S species in PPL sediments. The seasonal dynamics of sedimentary S speciation is assessed to probe the environmental factors governing S cycling.

Chapter 6 provides an overall summary of findings from Chapter 2 to 5 and discusses implications for future research.

1.7 References

1. Tilman, D.; Fargione, J.; Wolff, B.; D'Antonio, C.; Dobson, A.; Howarth, R.; Schindler, D.; Schlesinger, W. H.; Simberloff, D.; Swackhamer, D., Forecasting agriculturally driven global environmental change. *Science* **2001,** *292*, 281-284.
2. Schwarzenbach, R. P.; Egli, T.; Hofstetter, T. B.; von Gunten, U.; Wehrli, B., Global water pollution and human health. *Annu. Rev. Environ. Resour.* **2010,** *35*, 109-136.
3. Gilliom, R. J.; Barbash, J. E.; Crawford, C. G.; Hamilton, P. A.; Martin, J. D.; Nakagaki, N.; Nowell, L. H.; Scott, J. C.; Stackelberg, P. E.; Thelin, G. P.; Wolock, D. M. *The quality of our Nation's waters - Pesticides in the Nation's stream and ground water, 1992-2001*; National Water-Quality Assessment Program, U.S. Geological Survey Circular 1291; Reston, VA, 2006; pp 1-172.
4. Li, Y.; Zhang, J. B., Agricultural diffuse pollution from fertilisers and pesticides in China. *Water Sci. Technol.* **1999,** *39*, 25-32.
5. Huber, A.; Bach, M.; Frede, H. G., Pollution of surface waters with pesticides in Germany: modeling non-point source inputs. *Agric., Ecosyst. Environ.* **2000,** *80*, 191-204.
6. Kishimba, M. A.; Henry, L.; Mwevura, H.; Mmochi, A. J.; Mihale, M.; Hellar, H., The status of pesticide pollution in Tanzania. *Talanta* **2004,** *64*, 48-53.
7. Konstantinou, I. K.; Hela, D. G.; Albanis, T. A., The status of pesticide pollution in surface waters (rivers and lakes) of Greece. Part I. Review on occurrence and levels. *Environ. Pollut.* **2006,** *141*, 555-570.
8. Sarkar, S. K.; Bhattacharya, B. D.; Bhattacharya, A.; Chatterjee, M.; Alam, A.; Satpathy, K. K.; Jonathan, M. P., Occurrence, distribution and possible sources of organochlorine pesticide residues in tropical coastal environment of India: An overview. *Environ. Int.* **2008,** *34*, 1062-1071.
9. Menezes, C. T.; Heller, L., A method for prioritization of areas for pesticides surveillance on surface waters: A study in Minas Gerais, Brazil. *Water Sci. Technol.* **2008,** *57*, 1693-1698.
10. Williamson, S.; Ball, A.; Pretty, J., Trends in pesticide use and drivers for safer pest management in four African countries. *Crop Protect.* **2008,** *27*, 1327-1334.
11. Atapattu, S. S.; Kodituwakku, D. C., Agriculture in South Asia and its implications on downstream health and sustainability: A review. *Agric. Water Manage.* **2009,** *96*, 361-373.
12. Capel, P. D.; Larson, S. J., Effect of scale on the behavior of atrazine in surface waters. *Environ. Sci. Technol.* **2001,** *35*, 648-657.
13. Capel, P. D.; Larson, S. J.; Winterstein, T. A., The behaviour of 39 pesticides in surface waters as a function of scale. *Hydrol. Processes* **2001,** *15*, 1251-1269.
14. Capel, P. D.; McCarthy, K. A.; Barbash, J. E., National, holistic, watershed-scale approach to understand the sources, transport, and fate of agricultural chemicals. *J. Environ. Qual.* **2008,** *37*, 983-993.
15. Katagi, T., Behavior of pesticides in water-sediment systems. In *Reviews of Environmental Contamination and Toxicology*, Ware, G. W.; Albert, L. A.; Voogt, P.;

Gerba, C. P.; Hutzinger, O.; Knaak, J. B.; Mayer, F. L.; Morgan, D. P.; Park, D. L.; Tjeerdema, R. S.; Whitacre, D. M.; Yang, R. S. H.; Gunther, F. A., Eds. Springer-Verlag New York, LLC.: Secaucus, NJ 2006; Vol. 187, pp 133-251.
16. Barbash, J. E., The geochemistry of pesticides. In *Treatise on Geochemistry - Environmental Geochemistry*, Holland, H. D.; Turekian, K. K., Eds. Elsevier Ltd.: Oxford, UK, 2007; Vol. 9, pp 1-43.
17. Zedler, J. B.; Kercher, S., Wetland resources: Status, trends, ecosystem services, and restorability. *Annu. Rev. Environ. Resour.* **2005,** *30*, 39-74.
18. Winter, T. C., Hydrologic studies of wetlands in the Northern Prairie. In *Northern Prairie Wetlands*, Van der Valk, A. G., Ed. Iowa State University Press: Ames, IA, 1989; pp 16-54.
19. van der Valk, A. G., The prairie potholes of North America. In *The World's Largest Wetlands*, Fraser, L. H.; Keddy, P. A., Eds. Cambridge University Press: Cambridge, UK, 2005; pp 393-423.
20. Mitsch, W.; Hernandez, M., Landscape and climate change threats to wetlands of North and Central America. *Aquat. Sci.* **2012**, 1-17.
21. Tiner, R. W., Geographically isolated wetlands of the United States. *Wetlands* **2003,** *23*, 494-516.
22. LaBaugh, J. W.; Winter, T. C.; Rosenberry, D. O., Hydrological functions of prairie wetlands. *Great Plains Res.* **1998,** *8*, 17-37.
23. Stewart, R. E.; Kantrud, H. A. *Classification of natural ponds and lakes in the glaciated prairie region*; Bureau of Sport Fisheries and Wildlife, U.S. Fish and Wildlife Service, Resource Publication 92; Washington, DC, 1971; pp 1-57.
24. Euliss, N. H.; LaBaugh, J. W.; Fredrickson, L. H.; Mushet, D. M.; Laubhan, M. K.; Swanson, G. A.; Winter, T. C.; Rosenberry, D. O.; Nelson, R. D., The wetland continuum: A conceptual framework for interpreting biological studies. *Wetlands* **2004,** *24*, 448-458.
25. Kantrud, H. A.; Krapu, G. L.; Swanson, G. A. *Prairie basin wetlands of the Dakotas: A community profile*; U.S. Fish and Wildlife Service, Biological Report 85: Washington, DC, 1989; pp 1-111.
26. Batt, B. D. J.; Anderson, M. G.; Anderson, C. D.; Caswell, F. D., The use of prairie potholes by North American ducks. In *Northern Prairie Wetlands*, Van der Valk, A. G., Ed. Iowa State University Press: Ames, IA, 1989; pp 204-227.
27. Smith, G. W. *A critical review of the aerial and ground surveys of breeding waterfowl in North America*; U.S. Fish and Wildlife Service, National Biological Service, Biological Science Report 5; Washington, DC, 1995; pp 1-252.
28. Tiner, R. W., *Wetlands of the United States: Current status and recent trends*. National Wetlands Inventory, U.S. Fish and Wildlife Service: Washington, DC, 1984.
29. Adamus, P. R. *Condition, values, and loss of natural functions of prairie wetlands of the north-central United States*; EPA 600-R-92-249; U.S. Environmental Protection Agency: Washington, DC, 1998. http://water.epa.gov/type/wetlands/assessment/appendixb.cfm (Accessed July, 2012).
30. Euliss, J. N. H.; Gleason, R. A.; Olness, A.; McDougal, R. L.; Murkin, H. R.; Robarts, R. D.; Bourbonniere, R. A.; Warner, B. G., North American prairie wetlands are

important nonforested land-based carbon storage sites. *Sci. Total Environ.* **2006,** *361*, 179-188.
31. Gleason, R. A.; Laubhan, M. K.; Euliss, N. H. *Ecosystem services derived from wetland conservation practices in the United States prairie pothole region with an emphasis on the U.S. Department of Agriculture Conservation Reserve and Wetlands Reserve Programs*; U. S. Geological Survey Professional Paper 1745: Reston, VA, 2008; pp 1-58.
32. Johnson, R. R.; Oslund, F. T.; Hertel, D. R., The past, present, and future of prairie potholes in the United States. *J. Soil Water Conserv.* **2008,** *63*, 84A-87A.
33. LaBaugh, J. W., Chemical characterisitcs of water in Northern Prairie Wetlands. *Northern Prairie Wetlands* **1988**, 56-90.
34. Anteau, M., Do interactions of land use and climate affect productivity of waterbirds and prairie-pothole wetlands? *Wetlands* **2012,** *32*, 1-9.
35. Dahl, T. E. *Wetland losses in the United States 1780's to 1980's*; U.S. Fish and Wildlife Service: Washington, DC, 1990; pp 1-13.
36. Oslund, F. T.; Johnson, R. R.; Hertel, D. R., Assessing wetland changes in the prairie pothole region of Minnesota from 1980 to 2007. *J. Fish Wildl. Manag.* **2010,** *1*, 131-135.
37. Dahl, T. E.; Watmough, M. D., Current approaches to wetland status and trends monitoring in prairie Canada and the continental United States of America. *Can. J. Remote Sens.* **2007,** *33*, S17-S27.
38. Samson, F.; Knopf, F., Prairie conservation in North America. *Bioscience* **1994,** *44*, 418-421.
39. Galatowitsch, S. M.; van der Valk, A. G., Natural revegetation during restoration of wetlands in the southern prairie-pothole region of North America. In *Restoration of Temperate Wetlands*, Wheeler, B. D.; Shaw, S. S.; Fojt, W. J.; Robertson, R. A., Eds. John Wiley & Sons, Inc.: Chichester, UK, 1995; pp 129-142.
40. Dahl, T. E. *Status and trends of wetlands in the conterminous United States, 1998-2004*; U.S. Fish and Wildlife Service; U.S. Fish and Wildlife Service: Washington, DC, 2006; pp 1-112.
41. Watmough, M. D.; Schmoll, M. J. *Environment Canada's prairie and northern region habitat monitoring program phase II: Recent habitat trends in the Prairie Habitat Joint Venture*; Environment Canada, Canadian Wildlife Service, Technical Report Series No. 493; Environment Canada, Canadian Wildlife Service, Technical Report Series No. 493: Edmonton, Canada, 2007; pp 1-135.
42. Goldsborough, L. G.; Crumpton, W. G., Distribution and environmental fate of pesticides in prairie wetlands. *Great Plains Res.* **1998,** *8*, 73-95.
43. Neely, R. K.; Baker, J. L., Nitrogen and phosphorous dynamics and the fate of agricultural runoff. In *Northern Prairie Wetlands*, Van der Valk, A. G., Ed. Iowa State University Press: Ames, IA, 1989; pp 92-131.
44. Olness, A.; Staricka, J. A.; Daniel, J. A., Oxidation-reduction and groundwater contamination in the Prairie Pothole region of the Northern Great Plains. In *Water for Agriculture and Wildlife and the Environment -- Win-Win Opportunities: Proceedings of*

the 1996 USCID Wetlands Seminar, Schaack, J.; Anderson, S. S., Eds. U.S. Committee on Irrigation and Drainage: Denver, CO, 1996; pp 115-131.
45. Detenbeck, N. E.; Elonen, C. M.; Taylor, D. L.; Cotter, A. M.; Puglisi, F. A.; Sanville, W. D., Effects of agricultural activities and best management practices on water quality of seasonal prairie pothole wetlands. *Wetlands Ecol. Manage.* **2002,** *10*, 335-354.
46. Goolsby, D. A.; Battaglin, W. A.; Lawrence, G. B.; Artz, R. S.; Aulenbach, B. T.; Hooper, R. P.; Keeny, D. R.; Stensland, G. J. *Flux and sources of nutrients in the Mississippi-Atchafalaya River basin*; Costal Ocean Program, National Oceanic and Atmospheric Administration, Decision Analysis Series No. 17; Silver Spring, MD, 1999; pp 1-151.
47. Wolf, T. M.; Cessna, A. J., Protecting aquatic and riparian areas from pesticide drift. In *International Conference on Pesticide Application for Drift Management*, Washington State University Press: Pullman, WA 2004; pp 59-71.
48. Larney, F. J.; Cessna, A. J.; Bullock, M. S., Herbicide transport on wind-eroded sediment. *J. Environ. Qual.* **1999,** *28*, 1412-1421.
49. Waite, D. T.; Sommerstad, H.; Grover, R.; Kerr, L.; Westcott, N. D., Pesticides in ground water, surface water and spring runoff in a small saskatchewan watershed. *Environ. Toxicol. Chem.* **1992,** *11*, 741-748.
50. Cessna, A. J.; Elliott, J. A.; Best, K. B.; Grover, R.; Nicholaichuk, W., Transport of nutrients and postemergence-applied herbicides in runoff from corrugation irrigation of wheat. In *Herbicide Metabolites in Surface Water and Groundwater*, American Chemical Society: Washington, DC, 1996; Vol. 630, pp 151-164.
51. Yao, Y.; Tuduri, L.; Harner, T.; Blanchard, P.; Waite, D.; Poissant, L.; Murphy, C.; Belzer, W.; Aulagnier, F.; Li, Y.-F.; Sverko, E., Spatial and temporal distribution of pesticide air concentrations in Canadian agricultural regions. *Atmos. Environ.* **2006,** *40*, 4339-4351.
52. Donald, D. B.; Narine, P. G.; Lynne, Q.-A.; Kevin, C., Diffuse geographic distribution of herbicides in northern prairie wetlands. *Environ. Toxicol. Chem.* **2001,** *20*, 273-279.
53. Donald, D. B.; Cessna, A. J.; Sverko, E.; Glozier, N. E., Pesticides in surface drinking-water supplies of the northern Great Plains. *Environ. Health Perspect.* **2007,** *115*, 1183-1191.
54. Degenhardt, D.; Cessna, A. J.; Raina, R.; Farenhorst, A.; Pennock, D. J., Dissipation of six acid herbicides in water and sediment of two Canadian prairie wetlands. *Environ. Toxicol. Chem.* **2011,** *30*, 1982-1989.
55. Johnson, J.; Gray, J. *Surface Water Pesticide Monitoring and Assessment Project, 2010*; Pesticide Water Quality Program, North Dakota Department of Agriculture; Bismarck, ND, 2011.
56. Grue, C. E.; Tome, M. W.; Swanson, G. A.; Borthwick, S. M.; DeWeese, L. R., Agricultural chemicals and the quality of prairie-pothole wetlands for adult and juvenile waterfowl - What are the concerns? In *Proceedings of the National Symposium on Protection of Wetlands from Agricultural Impacts*, Stuber, P. J., Ed. U.S. Fish and Wildlife Service Biological Report 88(16): Washington, DC, 1988; pp 55-64.

57. Donald, D. B.; Syrgiannis, J.; Hunter, F.; Weiss, G., Agricultural pesticides threaten the ecological integrity of northern prairie wetlands. *Sci. Total Environ.* **1999,** *231*, 173-181.
58. Sura, S.; Waiser, M.; Tumber, V.; Lawrence, J. R.; Cessna, A. J.; Glozier, N., Effects of glyphosate and two herbicide mixtures on microbial communities in prairie wetland ecosystems: A mesocosm approach. *J. Environ. Qual.* **2012,** *41*, 732-743.
59. Sievert, S. M.; Kiene, R. P.; Schulz-Vogt, H. N., The sulfur cycle. *Oceanography* **2007,** *20*, 117-123.
60. Vairavamurthy, M. A.; Orr, W. L.; Manowitz, B., Geochemical transformations of sedimentary sulfur: An introduction. In *Geochemical Transformations of Sedimentary Sulfur*, Vairavamurthy, M. A.; Schoonen, M. A. A.; Eglinton, T. I.; Luther III, G. W.; Manowitz, B., Eds. American Chemical Society: Washington, DC, 1995; Vol. 612, pp 1-14.
61. Chen, K. Y.; Morris, J. C., Kinetics of oxidation of aqueous sulfide by oxygen. *Environ. Sci. Technol.* **1972,** *6*, 529-537.
62. Hoffmann, M. R., Kinetics and mechanism of oxidation of hydrogen sulfide by hydrogen peroxide in acidic solution. *Environ. Sci. Technol.* **1977,** *11*, 61-66.
63. Luther III, G. W.; Church, T. M., An overview of the environmental chemistry of sulphur in wetland systems. In *Sulphur Cycling on the Continents: Wetlands, Terrestrial Ecosystems, and Associated Water Bodies*, Howarth, R. W.; Stewart, J. W. B.; Ivanov, M. V., Eds. SCOPE, John Wiley & Sons, Inc.: Somerset, NJ, 1992; pp 125-142.
64. Vairavamurthy, M. A.; Manowitz, B.; Zhou, W.; Jeon, Y., Determination of hydrogen sulfide oxidation products by Sulfur *K*-edge X-ray absorption near-edge structure spectroscopy. In *Environmental Geochemistry of Sulfide Oxidation*, Alpers, C. N.; Blowes, D. W., Eds. American Chemical Society: Washington DC, 1994; Vol. 550, pp 412-430.
65. Giggenbach, W., Optical spectra and equilibrium distribution of polysulfide ions in aqueous solution at 20.deg. *Inorg. Chem.* **1972,** *11*, 1201-1207.
66. Shea, D.; Helz, G. R., The solubility of copper in sulfidic waters - sulfide and polysulfide complexes in equilibrium with covellite. *Geochim. Cosmochim. Acta* **1988,** *52*, 1815-1825.
67. Kamyshny, A.; Goifman, A.; Gun, J.; Rizkov, D.; Lev, O., Equilibrium distribution of polysulfide ions in aqueous solutions at 25 degrees C: A new approach for the study of polysulfides equilibria. *Environ. Sci. Technol.* **2004,** *38*, 6633-6644.
68. Gun, J.; Goifman, A.; Shkrob, I.; Kamyshny, A.; Ginzburg, B.; Hadas, O.; Dor, I.; Modestov, A. D.; Lev, O., Formation of polysulfides in an oxygen rich freshwater lake and their role in the production of volatile sulfur compounds in aquatic systems. *Environ. Sci. Technol.* **2000,** *34*, 4741-4746.
69. MacCrehan, W.; Shea, D., Temporal relationship of thiols to inorganic sulfur compounds in anoxic Chesapeake Bay sediment porewater. In *Geochemical Transformations of Sedimentary Sulfur*, Vairavamurthy, M. A.; Schoonen, M. A. A.; Eglinton, T. I.; Luther III, G. W.; Manowitz, B., Eds. American Chemical Society: Washington, DC, 1995; Vol. 612, pp 294-310.

70. Overmann, J.; Beatty, J. T.; Krouse, H. R.; Hall, K. J., The sulfur cycle in the chemocline of a meromictic salt lake. *Limnol. Oceanogr.* **1996,** *41*, 147-156.
71. Ciglenecki, I.; Kodba, Z.; Cosovic, B., Sulfur species in Rogoznica Lake. *Mar. Chem.* **1996,** *53*, 101-110.
72. Bura-Nakic, E.; Helz, G. R.; Ciglenecki, I.; Cosovic, B., Reduced sulfur species in a stratified seawater lake (Rogoznica Lake, Croatia); seasonal variations and argument for organic carriers of reactive sulfur. *Geochim. Cosmochim. Acta* **2009,** *73*, 3738-3751.
73. Boulegue, J.; Lord III, C. J.; Church, T. M., Sulfur speciation and associated trace metals (Fe, Cu) in the pore waters of Great Marsh, Delaware. *Geochim. Cosmochim. Acta* **1982,** *46*, 453-464.
74. Luther, G. W., III; Meyerson, A. L.; Rogers, K.; Hall, F., Tidal and seasonal variations of sulfate ion in a New Jersey marsh system. *Estuaries* **1982,** *5*, 189-196.
75. Morgan, B.; Burton, E. D.; Rate, A. W., Iron monosulfide enrichment and the presence of organosulfur in eutrophic estuarine sediments. *Chem. Geol.* **2012,** *296–297*, 119-130.
76. Stamper, D. M.; Traina, S. J.; Tuovinen, O. H., Anaerobic transformation of alachlor, propachlor, and metolachlor with sulfide. *J. Environ. Qual.* **1997,** *26*, 488-494.
77. Lippa, K. A.; Roberts, A. L., Nucleophilic aromatic substitution reactions of chloroazines with bisulfide (HS^-) and polysulfides (S_n^{2-}). *Environ. Sci. Technol.* **2002,** *36*, 2008-2018.
78. Wang, S.; Arnold, W. A., Abiotic reduction of dinitroaniline herbicides. *Water Res.* **2003,** *37*, 4191-4201.
79. Jans, U.; Miah, M. H., Reaction of chlorpyrifos-methyl in aqueous hydrogen sulfide/bisulfide solutions. *J. Agric. Food. Chem.* **2003,** *51*, 1956-1960.
80. Lippa, K. A.; Demel, S.; Lau, I. H.; Roberts, A. L., Kinetics and mechanism of the nucleophilic displacement reactions of chloroacetanilide herbicides: Investigation of α-substituent effects. *J. Agric. Food. Chem.* **2004,** *52*, 3010-3021.
81. Yang, W.; Gan, J. J.; Bondarenko, S.; Liu, W., Nucleophilic radical substitution reaction of triazine herbicides with polysulfides. *J. Agric. Food. Chem.* **2004,** *52*, 7051-7055.
82. Lippa, K. A.; Roberts, A. L., Correlation analyses for bimolecular nucleophilic substitution reactions of chloroacetanilide herbicides and their structural analogs with environmentally relevant nucleophiles. *Environ. Toxicol. Chem.* **2005,** *24*, 2401-2409.
83. Bondarenko, S.; Zheng, W.; Yates, S. R.; Gan, J., Dehalogenation of halogenated fumigants by polysulfide salts. *J. Agric. Food. Chem.* **2006,** *54*, 5503-5508.
84. Gan, J. Y., Enhanced degradation of chloroacetanilide herbicides by polysulfide salts. In *Proceedings of the 2006 USDA-CSREES National Water Quality Conference*, USDA-NIFA National Integrated Water Quality Program: Washington, DC, 2006.
85. Gan, Q.; Jans, U., Reaction of thiometon and disulfoton with reduced sulfur species in simulated natural environment. *J. Agric. Food. Chem.* **2006,** *54*, 7753-7760.
86. Gan, Q.; Singh, R. M.; Jans, U., Degradation of naled and dichlorvos promoted by reduced sulfur species in well-defined anoxic aqueous solutions. *Environ. Sci. Technol.* **2006,** *40*, 778-783.

87. Gan, Q.; Singh, R. M.; Wu, T.; Jans, U., Kinetics and mechanism of degradation of dichlorvos in aqueous solutions containing reduced sulfur species. *Environ. Sci. Technol.* **2006,** *40*, 5717-5723.
88. Guo, X.; Jans, U., Kinetics and mechanism of the degradation of methyl parathion in aqueous hydrogen sulfide solution: Investigation of natural organic matter effects. *Environ. Sci. Technol.* **2006,** *40*, 900-906.
89. Wu, T.; Gan, Q.; Jans, U., Nucleophilic substitution of phosphorothionate ester pesticides with bisulfide (HS^-) and polysulfides (S_n^{2-}). *Environ. Sci. Technol.* **2006,** *40*, 5428-5434.
90. Wu, T.; Jans, U., Nucleophilic substitution reactions of chlorpyrifos-methyl with sulfur species. *Environ. Sci. Technol.* **2006,** *40*, 784-790.
91. Zheng, W.; Yates, S. R.; Papiernik, S. K.; Guo, M.; Gan, J., Dechlorination of chloropicrin and 1,3-dichloropropene by hydrogen sulfide species: Redox and nucleophilic substitution reactions. *J. Agric. Food. Chem.* **2006,** *54*, 2280-2287.
92. Gan, Q.; Jans, U., Nucleophilic reactions of phorate and terbufos with reduced sulfur species under anoxic conditions. *J. Agric. Food. Chem.* **2007,** *55*, 3546-3554.
93. Miller, P. L.; Vasudevan, D.; Gschwend, P. M.; Roberts, A. L., Transformation of hexachloroethane in a sulfidic natural water. *Environ. Sci. Technol.* **1998,** *32*, 1269-1275.
94. Lippa, K. A. Reactions of chloro-*s*-triazine and chloroacetanilide agrochemicals with reduced sulfur nucleophiles. Ph.D. Dissertation, The Johns Hopkins University, Baltimore, MD, 2002.
95. Loch, A. R.; Lippa, K. A.; Carlson, D. L.; Chin, Y.-P.; Traina, S. J.; Roberts, A. L., Nucleophilic aliphatic substitution reactions of propachlor, alachlor, and metolachlor with bisulfide (HS^-) and polysulfides (S_n^{2-}). *Environ. Sci. Technol.* **2002,** *36*, 4065-4073.
96. Huckins, J. N.; Petty, J. D.; England, D. C., Distribution and impact of trifluralin, atrazine, and fonofos residues in microcosms simulating a northern prairie wetland. *Chemosphere* **1986,** *15*, 563-588.
97. Cessna, A. J.; Donald, D. B.; Bailey, J.; Waiser, M.; Headley, J. V., Persistence of the sulfonylurea herbicides thifensulfuron-methyl, ethametsulfuron-methyl, and metsulfuron-methyl in farm dugouts (ponds). *J. Environ. Qual.* **2006,** *35*, 2395-2401.
98. Degenhardt, D.; Humphries, D.; Cessna, A. J.; Messing, P.; Badiou, P. H.; Raina, R.; Farenhorst, A.; Pennock, D. J., Dissipation of glyphosate and aminomethylphosphonic acid in water and sediment of two Canadian prairie wetlands. *J. Environ. Sci. Health, Part B* **2012,** *47*, 631-639.
99. Anslyn, E. V.; Dougherty, D. A., *Modern Physical Organic Chemistry*. University Science Books: Sausalito, CA, 2006.
100. Schwarzenbach, R. P.; Gschwend, P. M.; Imboden, D. M., *Environmental Organic Chemistry*. John Wiley & Sons, Inc.: Hoboken, NJ, 2003.
101. Leifer, A., *The Kinetics of Environmental Aquatic Photochemistry: Theory and Practice*. American Chemical Society: Washington, DC, 1988.
102. Larson, R. A.; Weber, E. J., *Reaction Mechanisms in Environmental Organic Chemistry*. CRC Press, Inc.: Boca Raton, FL, 1994.
103. Zepp, R. G.; Cline, D. M., Rates of direct photolysis in aquatic environment. *Environ. Sci. Technol.* **1977,** *11*, 359-366.

104. Arnold, W. A.; McNeill, K.; Petrovic, M.; Barcel, D., Transformation of pharmaceuticals in the environment: Photolysis and other abiotic processes. In *Comprehensive Analytical Chemistry*, Elsevier: 2007; Vol. Volume 50, pp 361-385.
105. Vione, D.; Maurino, V.; Minero, C.; Pelizzetti, E., Reactions induced in natural waters by irradiation of nitrate and nitrite ions. In *The Handbook of Environmental Chemistry Vol. 2-M (Environmental Photochemistry Part II)*, Boule, P.; Bahnemann, D. W.; Robertson, P. K. J., Eds. Springer: Berlin, Germany, 2005; pp 221-253.
106. Chiron, S.; Barcel ó, D.; Abian, J.; Ferrer, M.; Sanchez-Baeza, F.; Messeguer, A., Comparative photodegradation rates of alachlor and bentazone in natural water and determination of breakdown products. *Environ. Toxicol. Chem.* **1995,** *14*, 1287-1298.
107. Dimou, A. D.; Sakkas, V. A.; Albanis, T. A., Trifluralin photolysis in natural waters and under the presence of isolated organic matter and nitrate ions: Kinetics and photoproduct analysis. *J. Photochem. Photobiol. A: Chem.* **2004,** *163*, 473-480.
108. Fasnacht, M. P.; Blough, N. V., Aqueous photodegradation of polycyclic aromatic hydrocarbons. *Environ. Sci. Technol.* **2002,** *36*, 4364-4369.
109. Fasnacht, M. P.; Blough, N. V., Mechanisms of the aqueous photodegradation of polycyclic aromatic hydrocarbons. *Environ. Sci. Technol.* **2003,** *37*, 5767-5772.
110. Fasnacht, M. P.; Blough, N. V., Kinetic analysis of the photodegradation of polycyclic aromatic hydrocarbons in aqueous solution. *Aquat. Sci.* **2003,** *65*, 352-358.
111. Jacobs, L. E.; Weavers, L. K.; Chin, Y. P., Direct and indirect photolysis of polycyclic aromatic hydrocarbons in nitrate-rich surface waters. *Environ. Toxicol. Chem.* **2008,** *27*, 1643-1648.
112. Plumlee, M. H.; Reinhard, M., Photochemical attenuation of *N*-nitrosodimethylamine (NDMA) and other nitrosamines in surface water. *Environ. Sci. Technol.* **2007,** *41*, 6170-6176.
113. Kelly, M. M.; Arnold, W. A., Direct and indirect photolysis of the phytoestrogens genistein and daidzein. *Environ. Sci. Technol.* **2012,** *46*, 5396-5403.
114. Felcyn, J. R.; Davis, J. C. C.; Tran, L. H.; Berude, J. C.; Latch, D. E., Aquatic photochemistry of isoflavone phytoestrogens: Degradation kinetics and pathways. *Environ. Sci. Technol.* **2012,** *46*, 6698-6704.
115. West, C. E.; Rowland, S. J., Aqueous phototransformation of diazepam and related human metabolites under simulated sunlight. *Environ. Sci. Technol.* **2012,** *46*, 4749-4756.
116. Boreen, A. L.; Arnold, W. A.; McNeill, K., Photochemical fate of sulfa drugs in the aquatic environment: Sulfa drugs containing five-membered heterocyclic groups. *Environ. Sci. Technol.* **2004,** *38*, 3933-3940.
117. Edhlund, B. L.; Arnold, W. A.; McNeill, K., Aquatic photochemistry of nitrofuran antibiotics. *Environ. Sci. Technol.* **2006,** *40*, 5422-5427.
118. Ge, L.; Chen, J.; Wei, X.; Zhang, S.; Qiao, X.; Cai, X.; Xie, Q., Aquatic photochemistry of fluoroquinolone antibiotics: Kinetics, pathways, and multivariate effects of main water constituents. *Environ. Sci. Technol.* **2010,** *44*, 2400-2405.
119. Ryan, C. C.; Tan, D. T.; Arnold, W. A., Direct and indirect photolysis of sulfamethoxazole and trimethoprim in wastewater treatment plant effluent. *Water Res.* **2011,** *45*, 1280-1286.

120. Gonçalves, C.; Pérez, S.; Osorio, V.; Petrovic, M.; Alpendurada, M. F.; Barceló, D., Photofate of oseltamivir (Tamiflu) and oseltamivir carboxylate under natural and simulated solar irradiation: Kinetics, identification of the transformation products, and environmental occurrence. *Environ. Sci. Technol.* **2011,** *45*, 4307-4314.
121. Latch, D. E.; Stender, B. L.; Packer, J. L.; Arnold, W. A.; McNeill, K., Photochemical fate of pharmaceuticals in the environment: Cimetidine and ranitidine. *Environ. Sci. Technol.* **2003,** *37*, 3342-3350.
122. Packer, J. L.; Werner, J. J.; Latch, D. E.; McNeill, K.; Arnold, W. A., Photochemical fate of pharmaceuticals in the environment: Naproxen, diclofenac, clofibric acid, and ibuprofen. *Aquatic Sciences - Research Across Boundaries* **2003,** *65*, 342-351.
123. Werner, J. J.; McNeill, K.; Arnold, W. A., Environmental photodegradation of mefenamic acid. *Chemosphere* **2005,** *58*, 1339-1346.
124. Lin, A. Y. C.; Reinhard, M., Photodegradation of common environmental pharmaceuticals and estrogens in river water. *Environ. Toxicol. Chem.* **2005,** *24*, 1303-1309.
125. Liu, Q.-T.; Williams, H. E., Kinetics and degradation products for direct photolysis of β-blockers in water. *Environ. Sci. Technol.* **2007,** *41*, 803-810.
126. Tixier, C.; Singer, H. P.; Canonica, S.; Müller, S. R., Phototransformation of triclosan in surface waters: A relevant elimination process for this widely used biocide - Laboratory studies, field measurements, and modeling. *Environ. Sci. Technol.* **2002,** *36*, 3482-3489.
127. Latch, D. E.; Packer, J. L.; Arnold, W. A.; McNeill, K., Photochemical conversion of triclosan to 2,8-dichlorodibenzo-p-dioxin in aqueous solution. *J. Photochem. Photobiol. A: Chem.* **2003,** *158*, 63-66.
128. Buth, J. M.; Grandbois, M.; Vikesland, P. J.; McNeill, K.; Arnold, W. A., Aquatic photochemistry of chlorinated triclosan derivatives: Potential source of polychlorodibenzo-P-dioxins. *Environ. Toxicol. Chem.* **2009,** *28*, 2555-2563.
129. Zhang, S.; Chen, J.; Qiao, X.; Ge, L.; Cai, X.; Na, G., Quantum chemical investigation and experimental verification on the aquatic photochemistry of the sunscreen 2-phenylbenzimidazole-5-sulfonic acid. *Environ. Sci. Technol.* **2010,** *44*, 7484-7490.
130. MacManus-Spencer, L. A.; Tse, M. L.; Klein, J. L.; Kracunas, A. E., Aqueous photolysis of the organic ultraviolet filter chemical octyl methoxycinnamate. *Environ. Sci. Technol.* **2011,** *45*, 3931-3937.
131. Hoigné, J.; Faust, B. C.; Haag, W. R.; Scully, F. E.; Zepp, R. G., Aquatic humic substances as sources and sinks of photochemically produced transient reactants. In *Aquatic Humic Substances*, Suffet, I. H.; MacCarthy, P., Eds. American Chemical Society: Washington DC, 1989; Vol. 219, pp 363-381.
132. Cooper, W. J.; Zika, R. G.; Petasne, R. G.; Fischer, A. M., Sunlight-induced photochemistry of humic substances in natural waters: Major reactive species. In *Aquatic Humic Substances*, Suffet, I. H.; MacCarthy, P., Eds. American Chemical Society: Washington DC, 1989; Vol. 219, pp 333-362.

133. Zepp, R. G.; Wolfe, N. L.; Baughman, G. L.; Hollis, R. C., Singlet oxygen in natural waters. *Nature* **1977,** *267*, 421-423.
134. Mill, T.; Hendry, D. G.; Richardson, H., Free-radical oxidants in natural waters. *Science* **1980,** *207*, 886-887.
135. Zepp, R. G.; Baughman, G. L.; Schlotzhauer, P. F., Comparison of photochemical behavior of various humic substances in water: II. Photosensitized oxygenations. *Chemosphere* **1981,** *10*, 119-126.
136. Cooper, W. J.; Zika, R. G., Photochemical formation of hydrogen peroxide in surface and ground waters exposed to sunlight. *Science* **1983,** *220*, 711-712.
137. Draper, W. M.; Crosby, D. G., The photochemical generation of hydrogen peroxide in natural waters. *Arch. Environ. Contam. Toxicol.* **1983,** *12*, 121-126.
138. Baxter, R. M.; Carey, J. H., Evidence for photochemical generation of superoxide ion in humic waters. *Nature* **1983,** *306*, 575-576.
139. Zepp, R. G.; Schlotzhauer, P. F.; Sink, R. M., Photosensitized transformations involving electronic energy transfer in natural waters: role of humic substances. *Environ. Sci. Technol.* **1985,** *19*, 74-81.
140. Haag, W. R.; Hoigné, J., Photo-sensitized oxidation in natural water via $^{\bullet}OH$ radicals. *Chemosphere* **1985,** *14*, 1659-1671.
141. Haag, W. R.; Hoigné, J., Singlet oxygen in surface waters. 3. Photochemical formation and steady-state concentrations in various types of waters. *Environ. Sci. Technol.* **1986,** *20*, 341-348.
142. Mopper, K.; Zhou, X., Hydroxyl radical photoproduction in the sea and its potential impact on marine processes. *Science* **1990,** *250*, 661-664.
143. Mill, T., Predicting photoreaction rates in surface waters. *Chemosphere* **1999,** *38*, 1379-1390.
144. Fischer, A. M.; Kliger, D. S.; Winterle, J. S.; Mill, T., Direct observation of phototransients in natural waters. *Chemosphere* **1985,** *14*, 1299-1306.
145. Zepp, R. G.; Braun, A. M.; Hoigne, J.; Leenheer, J. A., Photoproduction of hydrated electrons from natural organic solutes in aquatic environments. *Environ. Sci. Technol.* **1987,** *21*, 485-490.
146. Thomas-Smith, T. E.; Blough, N. V., Photoproduction of hydrated electron from constituents of natural waters. *Environ. Sci. Technol.* **2001,** *35*, 2721-2726.
147. Wang, W.; Zafiriou, O. C.; Chan, I.-Y.; Zepp, R. G.; Blough, N. V., Production of hydrated electrons from photoionization of dissolved organic matter in natural waters. *Environ. Sci. Technol.* **2007,** *41*, 1601-1607.
148. Lam, M. W.; Tantuco, K.; Mabury, S. A., PhotoFate: A new approach in accounting for the contribution of indirect photolysis of pesticides and pharmaceuticals in surface waters. *Environ. Sci. Technol.* **2003,** *37*, 899-907.
149. Kochany, J.; Maguire, R. J., Sunlight photodegradation of metolachlor in water. *J. Agric. Food. Chem.* **1994,** *42*, 406-412.
150. Torrents, A.; Anderson, B. G.; Bilboulian, S.; Johnson, W. E.; Hapeman, C. J., Atrazine photolysis: Mechanistic investigations of direct and nitrate-mediated hydroxy radical processes and the influence of dissolved organic carbon from the Chesapeake Bay. *Environ. Sci. Technol.* **1997,** *31*, 1476-1482.

151. Miller, P. L.; Chin, Y.-P., Photoinduced degradation of carbaryl in a wetland surface water. *J. Agric. Food. Chem.* **2002,** *50*, 6758-6765.
152. Schulz, R.; Hahn, C.; Bennett, E. R.; Dabrowski, J. M.; Thiere, G.; Peall, S. K. C., Fate and effects of azinphos-methyl in a flow-through wetland in South Africa. *Environ. Sci. Technol.* **2003,** *37*, 2139-2144.
153. Miller, P. L.; Chin, Y.-P., Indirect photolysis promoted by natural and engineered wetland water constituents: Processes leading to alachlor degradation. *Environ. Sci. Technol.* **2005,** *39*, 4454-4462.
154. Hedges, J. I.; Oades, J. M., Comparative organic geochemistries of soils and marine sediments. *Org. Geochem.* **1997,** *27*, 319-361.
155. Goldhaber, M. B., Sulfur-rich sediments. In *Treatise on Geochemistry - Sediments, Diagenesis, and Sedimentary Rocks*, Mackenzie, F. T., Ed. Elsevier Ltd.: Oxford, UK, 2003; Vol. 7, pp 257-288.
156. Urban, N. R., Retention of sulfur in lake sediments. In *Environmental Chemistry of Lakes and Reservoirs*, Baker, L. A., Ed. American Chemical Society: Washington, DC, 1994; Vol. 237, pp 323-369.
157. Freney, J., Some observations on the nature of organic sulphur compounds in soil. *Aust. J. Agric. Res.* **1961,** *12*, 424-432.
158. Pruden, G.; Bloomfield, C., The determination of iron(II) sulphide in soil in the presence of iron(III) oxide. *Analyst* **1968,** *93*, 532-534.
159. Freney, J. R.; Melville, G. E.; Williams, C. H., The determination of carbon bonded sulfur in soil. *Soil Sci.* **1970,** *109*, 310-318.
160. Dick, W. A.; Tabatabai, M. A., Ion chromatographic determination of sulfate and nitrate in soils. *Soil Sci. Soc. Am. J.* **1979,** *43*, 899-904.
161. Canfield, D. E.; Raiswell, R.; Westrich, J. T.; Reaves, C. M.; Berner, R. A., The use of chromium reduction in the analysis of reduced inorganic sulfur in sediments and shales. *Chem. Geol.* **1986,** *54*, 149-155.
162. Berner, R. A., Iron sulfides formed from aqueous solution at low temperatures and atmospheric pressure. *J. Geol. (Chicago, IL, U. S.)* **1964,** *72*, 293-306.
163. Rickard, D.; Morse, J. W., Acid volatile sulfide (AVS). *Mar. Chem.* **2005,** *97*, 141-197.
164. Prietzel, J.; Thieme, J.; Neuhäusler, U.; Susini, J.; Kögel-Knabner, I., Speciation of sulphur in soils and soil particles by X-ray spectromicroscopy. *Eur. J. Soil Sci.* **2003,** *54*, 423-433.
165. Vairavamurthy, M. A.; Zhou, W.; Eglinton, T.; Manowitz, B., Sulfonates: A novel class of organic sulfur compounds in marine sediments. *Geochim. Cosmochim. Acta* **1994,** *58*, 4681-4687.
166. Vairavamurthy, M. A.; Wang, S.; Khandelwal, B.; Manowitz, B.; Ferdelman, T.; Fossing, H., Sulfur transformations in early diagenetic sediments from the Bay of Conception, off Chile. In *Geochemical Transformations of Sedimentary Sulfur*, Vairavamurthy, M. A.; Schoonen, M. A. A.; Eglinton, T. I.; Luther III, G. W.; Manowitz, B., Eds. American Chemical Society: Washington, DC, 1995; Vol. 612, pp 38-58.

167. Bostick, B. C.; Theissen, K. M.; Dunbar, R. B.; Vairavamurthy, M. A., Record of redox status in laminated sediments from Lake Titicaca: A sulfur *K*-edge X-ray absorption near edge structure (XANES) study. *Chem. Geol.* **2005,** *219*, 163-174.
168. Burton, E. D.; Bush, R. T.; Sullivan, L. A.; Hocking, R. K.; Mitchell, D. R. G.; Johnston, S. G.; Fitzpatrick, R. W.; Raven, M.; McClure, S.; Jang, L. Y., Iron-monosulfide oxidation in natural sediments: Resolving microbially mediated S transformations using XANES, electron microscopy, and selective extractions. *Environ. Sci. Technol.* **2009,** *43*, 3128-3134.
169. Burton, E. D.; Bush, R. T.; Johnston, S. G.; Sullivan, L. A.; Keene, A. F., Sulfur biogeochemical cycling and novel Fe–S mineralization pathways in a tidally re-flooded wetland. *Geochim. Cosmochim. Acta* **2011,** *75*, 3434-3451.
170. Jokic, A.; Cutler, J. N.; Ponomarenko, E.; van der Kamp, G.; Anderson, D. W., Organic carbon and sulphur compounds in wetland soils: Insights on structure and transformation processes using *K*-edge XANES and NMR spectroscopy. *Geochim. Cosmochim. Acta* **2003,** *67*, 2585-2597.
171. Solomon, D.; Lehmann, J.; Lobe, I.; Martinez, C. E.; Tveitnes, S.; Du Preez, C. C.; Amelung, W., Sulphur speciation and biogeochemical cycling in long-term arable cropping of subtropical soils: evidence from wet-chemical reduction and S *K*-edge XANES spectroscopy. *Eur. J. Soil Sci.* **2005,** *56*, 621-634.
172. Prietzel, J.; Thieme, J.; Tyufekchieva, N.; Paterson, D.; McNulty, I.; Kögel-Knabner, I., Sulfur speciation in well-aerated and wetland soils in a forested catchment assessed by sulfur *K*-edge X-ray absorption near-edge spectroscopy (XANES). *J. Plant Nutr. Soil Sci.* **2009,** *172*, 393-403.
173. Prietzel, J.; Botzaki, A.; Tyufekchieva, N.; Brettholle, M.; Thieme, J. r.; Klysubun, W., Sulfur speciation in soil by S *K*-edge XANES spectroscopy: Comparison of spectral deconvolution and linear combination fitting. *Environ. Sci. Technol.* **2011,** *45*, 2878-2886.
174. Prietzel, J.; Kögel-Knabner, I.; Thieme, J.; Paterson, D.; McNulty, I., Microheterogeneity of element distribution and sulfur speciation in an organic surface horizon of a forested Histosol as revealed by synchrotron-based X-ray spectromicroscopy. *Org. Geochem.* **2011,** *42*, 1308-1314.
175. Solomon, D.; Lehmann, J.; de Zarruk, K. K.; Dathe, J.; Kinyangi, J.; Liang, B.; Machado, S., Speciation and long- and short-term molecular-level dynamics of soil organic sulfur studied by X-ray absorption near-edge structure spectroscopy. *J. Environ. Qual.* **2011,** *40*, 704-718.
176. Boye, K.; Almkvist, G.; Nilsson, S. I.; Eriksen, J.; Persson, I., Quantification of chemical sulphur species in bulk soil and organic sulphur fractions by S K-edge XANES spectroscopy. *Eur. J. Soil Sci.* **2011,** *62*, 874-881.
177. Pickering, I. J.; Prince, R. C.; Divers, T.; George, G. N., Sulfur K-edge X-ray absorption spectroscopy for determining the chemical speciation of sulfur in biological systems. *FEBS Lett.* **1998,** *441*, 11-14.
178. Rompel, A.; Cinco, R. M.; Latimer, M. J.; McDermott, A. E.; Guiles, R. D.; Quintanilha, A.; Krauss, R. M.; Sauer, K.; Yachandra, V. K.; Klein, M. P., Sulfur K-edge

x-ray absorption spectroscopy: A spectroscopic tool to examine the redox state of S-containing metabolites in vivo. *Proc. Natl. Acad. Sci. U. S. A.* **1998,** *95*, 6122-6127.
179. Breier, J. A.; Toner, B. M.; Fakra, S. C.; Marcus, M. A.; White, S. N.; Thurnherr, A. M.; German, C. R., Sulfur, sulfides, oxides and organic matter aggregated in submarine hydrothermal plumes at 9° 50′ N East Pacific Rise. *Geochim. Cosmochim. Acta* **2012,** *88*, 216-236.
180. Lombi, E.; Hettiarachchi, G. M.; Scheckel, K. G., Advanced in situ spectroscopic techniques and their applications in Environmental Biogeochemistry: Introduction to the special section. *J. Environ. Qual.* **2011,** *40*, 659-666.
181. Lombi, E.; Susini, J., Synchrotron-based techniques for plant and soil science: Opportunities, challenges and future perspectives. *Plant Soil* **2009,** *320*, 1-35.
182. Orthous-Daunay, F. R.; Quirico, E.; Lemelle, L.; Beck, P.; deAndrade, V.; Simionovici, A.; Derenne, S., Speciation of sulfur in the insoluble organic matter from carbonaceous chondrites by XANES spectroscopy. *Earth. Planet. Sci. Lett.* **2010,** *300*, 321-328.
183. Almkvist, G.; Boye, K.; Persson, I., *K*-edge XANES analysis of sulfur compounds: An investigation of the relative intensities using internal calibration. *J. Synchrotron Radiat.* **2010,** *17*, 683-688.
184. Beauchemin, S.; Hesterberg, D.; Beauchemin, M., Principal component analysis approach for modeling sulfur *K*-XANES spectra of humic acids. *Soil Sci. Soc. Am. J.* **2002,** *66*, 83-91.
185. Vairavamurthy, M. A.; Maletic, D.; Wang, S.; Manowitz, B.; Eglinton, T.; Lyons, T., Characterization of sulfur-containing functional groups in sedimentary humic substances by X-ray absorption near-edge structure spectroscopy. *Energy Fuels* **1997,** *11*, 546-553.
186. Mushet, D. M.; Euliss, N. H. *The Cottonwood Lake study area, a long-term wetland ecosystem monitoring site*; U.S. Geological Survey Fact Sheet 2012-3040: Reston, VA 2012; pp 1-2.

Chapter 2: Abiotic Transformation of Pesticides in Prairie Pothole Porewaters: Nucleophilic Reactions[1]

1 A version of this chapter has been published as: Zeng, T.; Ziegelgruber, K. L.; Chin, Y.-P.; Arnold, W. A., Pesticide processing potential in prairie pothole porewaters. *Environ. Sci. Technol.* **2011,** *45*, 6814-6822.

Prairie pothole lakes (PPLs) are located within the extensively farmed Great Plains region of North America, and many are negatively impacted by nonpoint source pesticide pollution. To date, the environmental fate of pesticides in these lakes remains largely unknown. In this study, two PPLs in the Cottonwood Lake study area of North Dakota, USA were sampled, and transformations of four chloroacetanilide pesticides in sediment porewaters were examined. The reduced sulfur species in the porewaters, such as bisulfide (HS^-) and polysulfides (S_n^{2-}), readily transformed the target pesticides into sulfur-substituted products. While HS^- and S_n^{2-} played a dominant role, other reactive constituents in PPL porewaters also contributed to the transformation. Results from this study revealed that abiotic reactions with reduced sulfur species could represent an important removal pathway for pesticides entering PPLs.

2.1 Introduction

The prairie pothole region (PPR), which covers approximately 700,000 km^2 of the north-central United States and south-central Canada, hosts a high density of water-filled basins formed glacially during the late Pleistocene Epoch.[1,2] These small, shallow water bodies, often known as prairie pothole lakes (PPLs), are important hydrological and ecological features.[3] In particular, PPLs support a diverse community of waterfowl, invertebrates, and aquatic plants.[2] The PPR is dominated by agricultural land uses[4], and crops grown within this region mainly consist of corn, wheat, sunflower, and soybeans to which pesticides are regularly applied.[5,6] Both the types and quantity of pesticides used in the PPR have increased dramatically over the past decades.[7,8] Numerous PPLs are located on or immediately bordered by farmland.[7] Thus, they are highly susceptible to nonpoint

source pesticide contamination.[9,10] Concerns have been raised about the disruptive effects of pesticides on the reproduction and survival of nontarget prairie wetland wildlife.[11-14] Upon application, the persistence of pesticides in prairie wetlands is controlled by various abiotic and biotic processes.[8] Previous studies have suggested that infiltration through sediment with concomitant sorption to the sediment is a major pathway for the dissipation of pesticides from the water column of PPLs.[15-18] Moreover, pesticides sorbed on redox-sensitive surfaces of sediment particles may solubilize under anoxic conditions and leach into groundwater if the pothole serves as a groundwater recharge site.[9] The ultimate fate of these pesticides in the PPL water column and sediment, however, remains an open question.

One unique aspect of PPLs is that many of them have evolved high concentrations of sulfate (mM levels).[19-22] The source of sulfate in these lakes is generally attributed to the recharge by highly brinish groundwater circulating through the deeply-buried evaporites[23] or shallower bedrock[24]. Recent sulfur isotope data have further traced the source of dissolved sulfate in groundwater to the oxidation of Pierre Shale-derived pyrite.[25,26] Evaporative concentration during the dry season then causes the accumulation of sulfate over time.[27] The sulfur biogeochemistry in PPLs may be similar to that in marine environments, and reduced sulfur species, such as bisulfide (HS^-) and polysulfides (S_n^{2-}), are likely present in sediment porewaters. In anoxic sediments, the microbially driven reduction of sulfate leads to the formation of bisulfide, which can further react with elemental sulfur to form polysulfide species. The concentrations of hydrogen sulfide and polysulfides in estuarine and salt marsh sediment porewaters have been reported as

high as 6.3 mM and 0.43 mM, respectively[28-30], and comparable levels may exist in PPLs. Reduced sulfur species not only participate in the biogeochemical cycling of inorganic and organic sulfur[31], but also play vital roles in environmentally relevant processes because of their high reductive reactivity and nucleophilicity.[32,33] Laboratory studies have demonstrated that HS^- and S_n^{2-} are capable of promoting the transformations of a wide array of anthropogenic pollutants including pesticides.[34-41] No information exists pertaining to the abundance of reduced sulfur species in PPL porewaters, and these highly reactive species would presumably affect the fate of pesticides that enter these systems.

The primary goal of this study was to quantify the role of reduced sulfur species in the abiotic transformation of pesticides in PPL sediment porewaters. Chloroacetanilide pesticides were selected as probe compounds due to their extensive use in the PPR[42], and prior research has emphasized nucleophilic substitution (S_N2) reactions of these pesticides in the presence of HS^- and S_n^{2-}.[38,43] We hypothesized that reduced sulfur species, if present in appreciable amounts in PPL porewaters, could represent potent environmental "reagents" to promote the removal of pesticides. This hypothesis was tested by monitoring the reaction kinetics and identifying transformation products of four chloroacetanilides (propachlor, alachlor, acetochlor, and metolachlor) in native and filter-sterilized porewaters under anoxic conditions.

2.2 Experimental Section

2.2.1 Chemicals, Reagents, and Glassware

Propachlor (2-chloro-*N*-isopropyl-*N*-phenylacetamide; 99.9%), alachlor (2-chloro-*N*-(2,6-diethylphenyl)-*N*-(methoxymethyl)acetamide; 99.2%), acetochlor (2-

chloro-*N*-(ethoxymethyl)-*N*-(2-ethyl-6-methylphenyl)acetamide; 97.3%), metolachlor (2-chloro-*N*-(2-ethyl-6-methylphenyl)-*N*-(1-methoxypropan-2-yl)acetamide; 97.6%), and terbuthylazine (N^2-(*tert*-butyl)-6-chloro-N^4-ethyl-1,3,5-triazine-2,4-diamine; 98.8%) were obtained from Fluka. Methanol (Chromasolv for HPLC, ≥99.9%), toluene (Chromasolv for HPLC, ≥99.9%), 3-[*N*-morpholino]propanesulfonic acid (MOPS; 99.5%), silver nitrate ($AgNO_3$; ≥99.0%), sodium sulfate (≥99.0%), sodium nitrate (≥99.0%), and methyl iodide (99.5%) were obtained from Sigma-Aldrich. Ferric chloride hexahydrate (≥98.0%) was obtained from Sigma. Sodium sulfide nonahydrate ($Na_2S{\cdot}9H_2O$; ≥99.99%) and *N*,*N*-dimethyl-*p*-phenylenediamine sulfate salt (DMPD; 98%) were obtained from Aldrich. Dimethyldisulfide (Me_2S_2; 99%), dimethyltrisulfide (Me_2S_3; 98%), sodium tetrasulfide (Na_2S_4; technical grade, 90+%), and 2-nitro-*m*-xylene (99%) were obtained from Alfa Aesar. *n*-Hexane (UltimAR grade, ≥95% *n*-hexane), sodium hydroxide (> 99%), sodium carbonate (≥ 99.5%), sodium bicarbonate (99.7-100.3%), sodium chloride (100%), sodium borate decahydrate (>99%), sodium thiosulfate pentahydrate (100.1%), potassium iodide (100.2%), hydrochloric acid (≥36.5-38.0%), nitric acid (≥68.0-70.0%), iodine (100%) and starch powder were obtained from Mallinckrodt. All chemicals were used as received without further purification. All deoxygenated aqueous solutions were prepared using ultrapure water (resistivity 18.2 MΩ·cm, Millipore Corp.). Standard solutions of pesticides were prepared in *n*-hexane. Pesticide stock solutions for spiking aqueous samples were prepared in deoxygenated methanol.

All glassware was soaked in 1N HNO_3 solution overnight and rinsed 3 times with ultrapure water, followed by 3 times with methanol. Non-volumetric glassware was then

baked at 550 ℃ in a Thermolyne Type 6000 furnace for a minimum of 4 h. Volumetric glassware was air-dried overnight in a fume hood. All glass syringes, stainless steel luer ends, and stainless steel needles were rinsed 3 times with ultrapure water, followed by 3 times with methanol, and autoclaved in a Consolidated SSR-3A-PB sterilizer at 121 ℃ for 30 min.

2.2.2 Field Sampling and Sample Analysis

Four batches of lake sediment cores and surface water were sampled throughout 2010 from selected PPLs (i.e., Lake P1 and P8) in the U.S. Geological Survey (USGS) Cottonwood Lake study area, Jamestown, North Dakota (Figure 2.1). Surface water samples were collected using acid-washed glass jars and were stored in the dark at 4 ℃. The pH, dissolved oxygen (DO), and conductivity of these water samples were measured within 24 h of sampling. The concentrations of sulfate, chloride, and nitrate were measured by a Metrohm 761 compact ion chromatograph with a Metrosep A Supp 5 anion column (150 mm × 4.0 mm i.d.; eluent: 3.2 mM sodium carbonate/1.0 mM sodium bicarbonate; flow rate: 0.7 mL/min). Dissolved organic carbon (DOC) was measured on a Shimadzu TOC-V_{CPN} total organic carbon analyzer. Samples were acidified and purged with carbon-free air to remove any inorganic carbon prior to analysis. Duplicate water samples were also extracted and analyzed to screen for the presence of pesticides following a USGS protocol.[44]

Figure 2.1 Satellite image of the USGS Cottonwood Lake study area and specific sampling lakes (P1 and P8). P1 is an intermediate elevation flow-through lake, while P8 is a topographically low discharge lake.[27,45] *[47º05'57.30"N and 99º06'04.78"W. Google Earth®. June 23, 2009. (Accessed February 2011)].*

Sediment cores were collected using a punch-core technique[46] and transported to the University of Minnesota within 24 h. Bulk porewaters were collected by sediment centrifugation in a Beckman JA-10 rotor (3 times at 5000 rpm for 30 min). For each lake, extracted porewaters were combined and thoroughly mixed to create one homogenous sample for pesticide transformation studies. Both sediment and porewaters were transferred into an anaerobic glove box (95% N_2/5% H_2, Pd catalyst, Coy Laboratory Products Inc.), and further manipulations of these air-sensitive samples were conducted in the glove box.

Prior to pesticide transformation experiments, sub-samples of porewaters were analyzed for the abundance of reduced sulfur species (i.e., HS^- and S_n^{2-}). DOC was measured as described above after dilution of the samples with deoxygenated ultrapure

water by ~20 fold. Anion and cation concentrations were analyzed by ion chromatography (IC) and inductively coupled plasma-mass spectrometry (ICP-MS), respectively (see Appendix A.1).

2.2.3 Analysis of Porewater Total Hydrogen Sulfide

The total hydrogen sulfide concentration ($[H_2S]_T$), representing the sum of all hydrogen sulfide species ($[H_2S]+[HS^-]+[S^{2-}]$), was determined by the methylene blue method.[47] The diamine reagent was prepared by dissolving 4.0 g of DMPD and 6.0 g of ferric chloride in 100 mL of deoxygenated 50% (v/v) HCl. A 1-mL aliquot of porewater sample (diluted if necessary) or H_2S standard solution was mixed with 80 μL of diamine reagent, and the mixture was then allowed to react for 20 min for color development. The resultant methylene blue solution was diluted with ultrapure water in a ratio of 1:50 (v/v), and the absorbance of diluted solution was measured at 670 nm by a Shimadzu UV-1601 PC spectrophotometer using 1-cm path length quartz cuvettes. All operations prior to UV/vis analysis were conducted in the anaerobic glove box.

Triplicate porewater samples were analyzed along with a set of freshly-prepared H_2S standard solutions (prepared with $Na_2S{\cdot}9H_2O$ crystals). The concentrations of hydrogen sulfide species in the porewaters were computed using the measured $[H_2S]_T$, pH, and the acid dissociation constants from Shea and Helz.[48] The pH of porewaters was measured by a Fisher Accumet AP62 portable pH/mV/ion meter with an Orion Ross combination pH electrode. The ionic strength (I) was computed based on the conductivity measured with an Orbeco Model 72 conductance/TDS meter using the Russell approximation ($I = 1.6 \times 10^{-5} \times$ conductivity in μS/cm).[49] Although the methylene blue

method was initially developed for measuring free hydrogen sulfide, it is not necessarily specific[50,51] and can be biased by the presence of polysulfides.[52,53] Nevertheless, the interference from polysulfides should be minimal if present at low concentrations relative to $[H_2S]_T$.[54,55]

2.2.4 Analysis of Porewater Total Polysulfides

The total polysulfide concentration ($[H_2S_n]_T$), representing the sum of polysulfide species ($[H_2S_n]+[HS_n^-]+[S_n^{2-}]$; n = 2-5), was determined by a modified methylation method.[56,57] This method uses methyl iodide to derivatize polysulfides to corresponding dimethylpolysulfides (DMPS), which can be directly analyzed by gas chromatography-mass spectrometry (GC-MS).

A 1-mL aliquot of porewater sample (diluted if necessary) was mixed with 200 μL of neat methyl iodide in the anaerobic glove box and heated at 60 ℃ in a water bath for 1 h. After cooling to room temperature, the mixture was extracted with 0.5 mL *n*-hexane (containing 36 μM 2-nitro-*m*-xylene as an internal standard) by vortexing for 1 min. Triplicate porewater samples were extracted and analyzed by GC-MS along with DMPS external standard solutions.

The concentrations of DMPS were quantified by a Hewlett-Packard G1800A GCD Series gas chromatograph equipped with a Hewlett-Packard 5972 Series mass selective detector (MSD). The instrument was operated with ultrapure helium as the carrier gas (at flow rate 0.9 mL/min) in splitless mode with a HP-5MS fused silica capillary column ((5%-phenyl)-methylpolysiloxane bonded phase; 30 m × 0.25mm i.d. × 0.25 μm film thickness; J & W Scientific Inc.). The following conditions were used: 1 μL

sample injection, inlet temperature 250 ℃, MSD transfer line temperature 250 ℃, MSD source temperature 150 ℃, initial column temperature 40 ℃ (hold for 8 min), then 10 ℃/min to 290 ℃ (hold for 2 min). The MSD was operated in electron impact (EI) mode at 70 eV to generate mass spectra and was programmed to monitor for selected ion mass/charge (*m/z*) ratios in selective ion monitoring (SIM) mode.

Qualitative identification of polysulfides on the GC-MS was accomplished by methylation of a relatively concentrated Na_2S_4 solution. The total ion chromatogram (TIC) of methylated Na_2S_4 solution was obtained under the same chromatographic conditions as described above but using full-scan mode with the *m/z* ratio ranging from 50-400. The TIC revealed the presence of a series of DMPS with sulfur chain lengths ranging from 2-5, and was used to compare with TICs of methylated porewaters for identification of potential DMPS formation (see Figure 2.1). Only Me_2S_2 and Me_2S_3 were identified in methylated porewater samples, suggesting that either polysulfides with higher chain lengths were not present or partial rearrangement of sulfur chain occurred during methylation.[58,59] Although methods based on methylation are not suitable for quantifying individual polysulfide species[60], it can provide a reasonable quantitative assessment of total polysulfides except for low polysulfide concentrations (< 0.5 μM).[56,57,61] Thus, the total polysulfide concentration in the porewaters was approximated as the concentration of polysulfides recovered as Me_2S_2 and Me_2S_3 (see Appendix A.2).[56,57]

2.2.5 Batch Kinetic Studies and Product Derivatization

All pesticide transformation studies were performed at 23±2 ℃ in the glove box. Batch kinetic experiments used porewaters from Lake P1 in 10 mL glass syringes. Experiments were run in triplicate with native porewaters (pH 8.62) and in duplicate with pH-adjusted porewaters (pH 7.43 and 9.53). Porewaters were adjusted with deoxygenated HCl and NaOH solutions to desired pH values and were equilibrated for 2 weeks before use. Selected porewaters were filter-sterilized through 0.2 μm syringe filters (PTFE Acrodisc CR13, Pall Corp.) as they were transferred into syringes. Reactions were initiated by spiking a 50-μL aliquot of pesticide stock solution into the syringes to yield an initial concentration of 8-12 μM. The syringes were then vigorously mixed on a touch vortexer and purged of any headspace to minimize the volatilization of pesticides. The syringes were also wrapped with aluminum foil to prevent photolysis. A 0.5-mL aliquot was withdrawn at specific time intervals (over 2 to 6 half lives) and extracted with 0.5 mL of *n*-hexane (containing 8.7 μM terbuthylazine as an internal standard) by vortexing for 1 min. Extraction efficiencies for pesticides were 90-95%. The exact volumes of aqueous sample and hexane were determined gravimetrically. Control syringes containing 5 mM deoxygenated MOPS buffer were prepared, sampled, and extracted in the same manner to account for the loss of pesticides due to other processes such as sorption or hydrolysis. At the end of kinetic experiments, the pesticide transformation products were derivatized with methyl iodide[38] and extracted by *n*-hexane. All hexane extracts were analyzed by GC-MS.

2.2.6 Chloroacetanilide and Product Analysis

Concentrations of chloroacetanilide pesticides in *n*-hexane extracts were analyzed using the same GC-MS system described above. The instrument was operated with ultrapure helium as the carrier gas (at flow rate 0.9 mL/min) in splitless mode with a Rtx-5 fused silica capillary column (5% diphenyl/95% dimethyl polysiloxane bonded phase; 30 m × 0.25mm i.d. × 0.25 μm film thickness; Restek Crop.). The following conditions were used for pesticide analysis: 1 μL sample injection, inlet temperature 250 ℃, MSD transfer line temperature 260 ℃, MSD source temperature 150 ℃, initial column temperature 40 ℃ (hold for 2 min), initial rate 25 ℃/min to 140 ℃, then 7 ℃/min to 210 ℃, and then 25 ℃/min to 280 ℃ (hold for 5 min). The MSD was operated in EI mode at 70 eV to generate mass spectra and was programmed to monitor for selected ion *m/z* ratios in SIM mode. The transformation products of pesticides were identified under the same chromatographic conditions but using full-scan mode with the *m/z* ratio ranging from 50-400.

2.2.7 Data Analysis

Reactions were modeled assuming pseudo-first-order kinetics. Data fitting and analysis were performed using *SigmaPlot 10* (Systat Software Inc.).

2.3 Results and Discussion

2.3.1 Water Chemistry of PPLs

Characteristics of surface water and porewaters from Lake P1 and P8 are presented in Table 2.1 and Table 2.2, respectively. Although these two lakes are adjacent to each other, the sulfate level is significantly higher in P1, which can be explained by

their relative altitudes and the influence of water table gradient on groundwater flow.[27,45] The nitrate levels in both lakes are low (less than 1 mg/L). DOC levels in these lakes are higher than those reported for most surface waters[62], but are similar to values reported for Cottonwood Lake area[63] and Canadian PPLs.[21,22,64] Additionally, no target pesticides were detected in water samples collected over the 1-year period.

Table 2.1 Characteristics of PPL surface water.

Sampling date	Lake	pH	DO (mg/L)	Conductivity (μS/cm)	Sulfate (mg/L)[a]	DOC (mg/L)[a]
Jan 2010	P1	8.14	9.0	4.68×10^4	2912 ± 73	38.94 ± 0.46
Apr 2010	P1	8.38	6.5	2.99×10^4	1828 ± 3	35.87 ± 0.86
	P8	7.87	7.5	1.51×10^4	496 ± 2	22.05 ± 0.25
Jun 2010	P1	8.35	6.9	3.08×10^4	1849 ± 30	30.10 ± 0.14
	P8	8.12	7.3	1.50×10^4	578 ± 2	22.14 ± 0.18
Sep 2010	P8	8.05	5.5	1.77×10^4	667 ± 7	28.70 ± 0.02

[a] Triplicate measurements and errors represent one standard deviation. [b] N.D. = not detected.

Table 2.2 Characteristics of PPL sediment porewaters.

Sampling date	Lake	pH	$[H_2S]_T$ (μM)	$[H_2S_n]_{T, calc}$ (μM)	$[Me_2S_2]$ (μM)	$[Me_2S_3]$ (μM)	DOC (mg/L)
Apr 2010	P1	8.62	2370 ± 27[a]	79.1 ± 5.9[b]	77.8 ± 5.9[c]	1.3 ± 0.4[c]	72.1 ± 0.4
	P8	8.53	2056 ± 47[a]	43.5 ± 1.5[b]	42.9 ± 1.5[c]	0.6 ± 0.1[c]	124.4 ± 0.4

Jun 2010	P1	7.84	892 ± 84[a,d]	N.A.[e]	N.A.[e]	N.A.[e]	105.7 ± 0.2[d]
	P8	7.48	896 ± 126[a,d]	N.A.[e]	N.A.[e]	N.A.[e]	65.3 ± 0.2[d]
Sep 2010	P1	7.36	1953 ± 53[a]	78.6 ± 6.9[b]	76.3 ± 6.9[c]	2.3 ± 0.3[c]	108.7 ± 0.2
	P8	7.45	1602 ± 64[a]	46.0 ± 3.0[b]	45.0 ± 3.0[c]	1.0 ± 0.1[c]	121.1 ± 0.5

[a] Triplicate measurements by the methylene blue method and errors represent one standard deviation. [b] Sum of measured Me_2S_2 and Me_2S_3 concentrations in methylated native porewater samples after correcting for methylation and extraction efficiencies (i.e., $[H_2S_n]_{T,\ calc}$ = ($[Me_2S_2]$ + $[Me_2S_3]$) / (Methylation efficiency × Extraction efficiency)). Methylation efficiencies for Me_2S_2 and Me_2S_3 are assumed to be 100%. Measured extraction efficiencies for Me_2S_2 and Me_2S_3 are 95.6% and 96.2%, respectively. Errors were calculated through propagation of errors associated with $[Me_2S_2]$ and $[Me_2S_3]$. [c] Triplicate measurements by the methylation method and errors represent one standard deviation. [d] Average values from porewater samples collected at 2-21 cm depths below the sediment-water interface and errors represent one standard deviation. [e] N.A. = not available.

Observed total hydrogen sulfide concentrations in PPL porewaters were 1-2 mM, which are comparable to the sulfide levels measured in other marine porewaters[28-30,52,65] and sulfidic lake waters.[66-69] Observed total polysulfide concentrations were 40-80 μM, which fall at the low end of polysulfide concentration range reported for other porewaters[29,52] and lake waters.[33,48,53,66] Additionally, the measured polysulfide concentrations are much less than the predicted polysulfide concentrations from the equilibrium speciation calculations (see Figure A.2), suggesting that these porewaters are undersaturated with respect to elemental sulfur. DOC levels in these PPL porewaters are among the highest ever recorded for a freshwater limnological system.[46,58,70,71] Indeed PPL porewater DOC concentrations are up to an order of magnitude higher than typically reported for wetlands and lakes.

2.3.2 Transformations of Pesticides in PPL Porewaters

As shown by the example time courses in Figure 2.2, all pesticides readily underwent degradation in native and filter-sterilized porewaters.

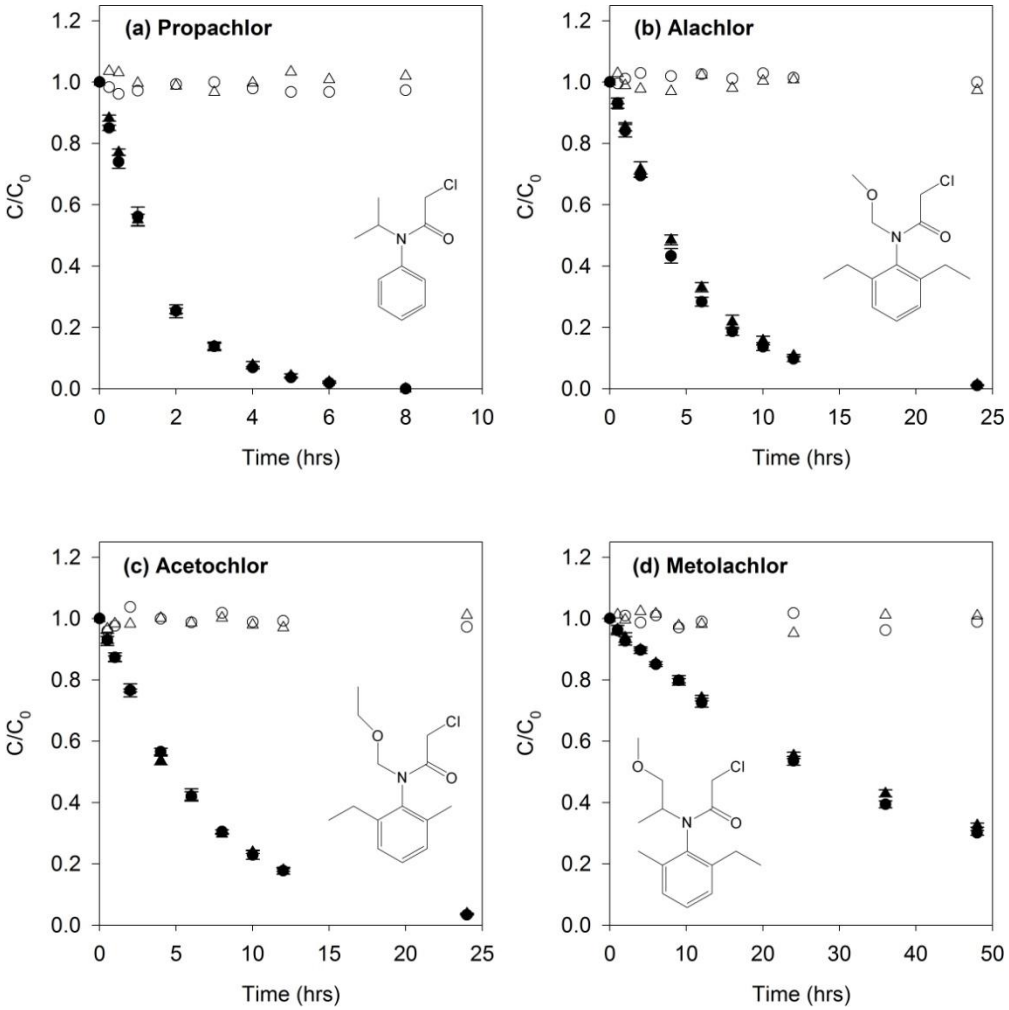

Figure 2.2 Transformations of chloroacetanilides in native (▲) and filter-sterilized (●) P1 porewaters (Apr 2010): (a) propachlor; (b) alachlor; (c) acetochlor; (d) metolachlor. Open symbols are buffer controls. Error bars represent one standard deviation of triplicate samples; where absent, bars fall within symbols. Note differences in time scales. $[H_2S]_T$ and $[H_2S_n]_{T,\,calc}$ in native and filter-sterilized porewaters are provided in Table A.4.

The reactivity of pesticides decreased in the following order: propachlor > alachlor > acetochlor > metolachlor, which parallels the reactivity trend reported in HS^- and S_n^{2-} fortified solutions.[38,72,73] The reaction rate constants of pesticides are similar in native and filter-sterilized porewaters ($k_{obs,\ filtered}/k_{obs,\ unfiltered} \approx 1.00$, see Table 2.3), indicating that biodegradation or reaction with mineral particles was insignificant. All

pesticides were unreactive in buffer controls, which is consistent with previous findings of minimal hydrolysis of these pesticides under environmentally relevant conditions.[74]

Table 2.3 Pseudo-first-order rate constants for reactions of pesticides in PPL porewaters

Chloroacetanilide	pH	$k_{obs,\ filtered}$ (hr^{-1})[a]	$k_{obs,\ unfiltered}$ (hr^{-1})[a]	$k_{obs,\ filtered}$ / $k_{obs,\ unfiltered}$[b]
Propachlor	7.43	0.7624 (±0.0075)	0.7154 (±0.0064)	1.07
	8.62	0.6671 (±0.0042)	0.6476 (±0.0095)	1.03
	9.53	1.0465 (±0.0087)	1.0155 (±0.0106)	1.03
Alachlor	7.43	0.1462 (±0.0028)	0.1331 (±0.0009)	1.10
	8.62	0.1919 (±0.0019)	0.1831 (±0.0011)	1.05
	9.53	0.3071 (±0.0029)	0.2661 (±0.0025)	1.15
Acetochlor	7.43	0.1530 (±0.0017)	0.1507 (±0.0021)	1.02
	8.62	0.1430 (±0.0010)	0.1375 (±0.0015)	1.04
	9.53	0.2169 (±0.0027)	0.2058 (±0.0028)	1.05
Metolachlor	7.43	0.0188 (±0.0002)	0.0160 (±0.0002)	1.18
	8.62	0.0251 (±0.0003)	0.0232 (±0.0003)	1.08
	9.53	0.1614 (±0.0013)	0.1611 (±0.0015)	1.00

[a] Rate constant measured in filter-sterilized or unfiltered P1 porewaters (Apr 2010). Errors represent one standard deviation from duplicate (pH 7.43 and 9.53) or triplicate (pH 8.62) experiments. [b] Calculated as $k_{obs,filtered}$ / $k_{obs,\ unfiltered}$.

2.3.3 Roles of Bisulfide and Polysulfides

Transformations of chloroacetanilide pesticides were studied in pH-adjusted porewaters to evaluate the relative importance of HS^- and S_n^{2-}. As shown by Figure 2.3, semilogarithmic plots for disappearance of the parent compounds indicate that reactions followed pseudo-first-order kinetics at all pH values.

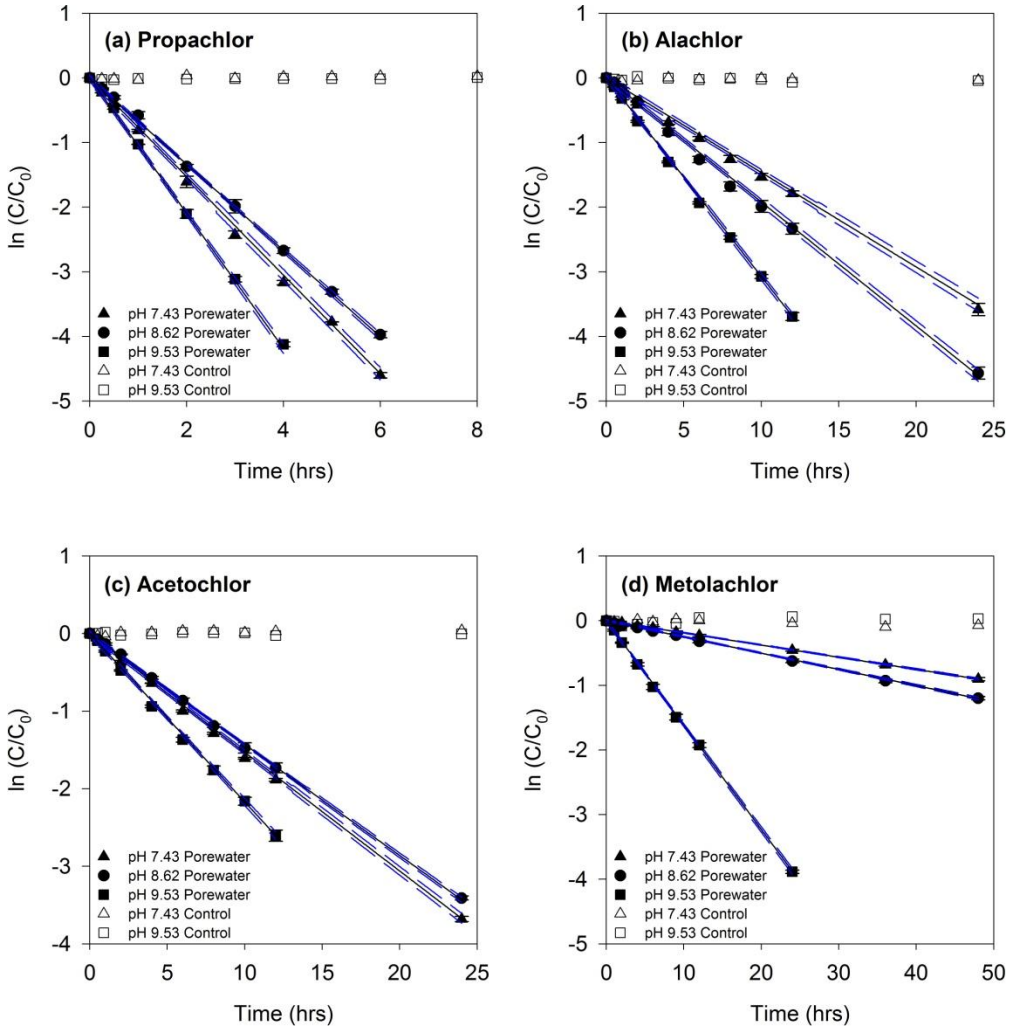

Figure 2.3 Comparison of chloroacetanilide reactivity in pH-adjusted, filter-sterilized P1 porewaters (Apr 2010): (a) propachlor; (b) alachlor; (c) acetochlor; (d) metolachlor. Error bars represent one standard deviation of duplicate (pH 7.43 and 9.53) or triplicate (native, pH 8.62) samples; where absent, bars fall within symbols. Solid lines represent linear regressions and dashed lines represent 95% confidence intervals. $R^2 > 0.99$ in all cases. $[H_2S]_T$ and $[H_2S_n]_{T,\,calc}$ in filter-sterilized porewaters are provided in Table A.4.

It was anticipated that adjustment to higher pH would result in an increase in the abundance of S_n^{2-} (Equation (2.1)), thereby accelerating the reaction of the pesticides due to the greater reactivity of S_n^{2-}.

$$HS^- + (n-1)/8\ S_{8(s)} \leftrightharpoons S_n^{2-} + H^+ \qquad (2.1)$$

For both alachlor and metolachlor, enhanced reactivity was observed with increasing pH. For propachlor and acetochlor, however, the reaction rates increased for both pH 7.43 and 9.53 relative to pH 8.62 (Figure 2.3). Similar results were seen in unfiltered porewaters (see Table 2.3; Figure A.3**).**

The overall reaction rate is quantified by summing the rate constants for all concurrent processes assuming pseudo-first-order kinetics (Equation (2.2)):

$$-\frac{dC}{dt} = k_{obs} \cdot C = \left(k_{HS^-} \cdot [HS^-] + k_{S_n^{2-}} \cdot \Sigma [S_n^{2-}] + k_{other} \right) \cdot C \qquad (2.2)$$

where C is the concentration of the chloroacetanilide, k_{HS^-} and $k_{S_n^{2-}}$ are the second-order rate constants for reactions with HS^- and S_n^{2-} (summarized in Table A.5), and k_{other} is the rate constant for other parallel reactions. The contributions of HS^- and S_n^{2-} to k_{obs} can be estimated by multiplying their calculated concentrations in the porewaters (see Table A.4) and the second-order rate constants. With this approximation, the percent contributions of HS^- and S_n^{2-} to the overall pesticide transformation are illustrated in Figure 2.4 for filter-sterilized porewaters. Figure A.4 is a similar plot for unfiltered porewaters, and Table A.6 contains the calculated pseudo-first order rate constants.

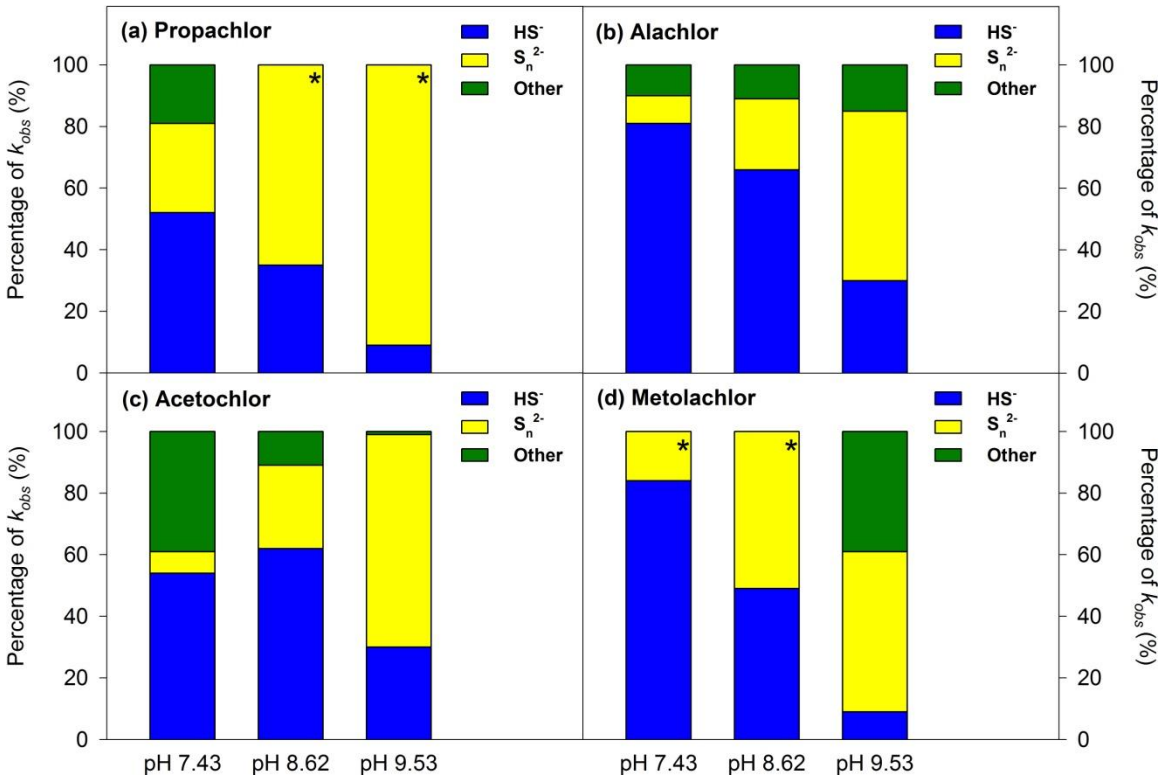

Figure 2.4 Percent contributions of HS^-, S_n^{2-}, and other processes to transformations of chloroacetanilides in pH-adjusted, filter-sterilized P1 porewaters (Apr 2010): (a) propachlor; (b) alachlor; (c) acetochlor; (d) metolachlor. Stacked bars plotted based on values calculated from Table A.4 and Table A.5. Bars with an asterisk mark designate the joint contribution of HS^- and S_n^{2-} up to 100% of k_{obs} even though the predicted contributions of HS^- and S_n^{2-} to k_{obs} are greater than the experimental value of k_{obs} in these cases. See text and Appendix A.8 for additional details.

Overall, the contribution of HS^- decreases with increasing pH, whereas the contribution of S_n^{2-} increases with increasing pH. At pH 7.43, the reaction with HS^- accounts for the major fraction (50-85%) of k_{obs}. Polysulfides are inherently more reactive nucleophiles, but because their concentrations are two orders of magnitude lower than that of HS^-, the overall influence of S_n^{2-} is secondary (10-30%). Meanwhile, the contribution from other concurrent processes seems to represent a non-negligible portion (0-40%) of k_{obs}, indicating that some porewater constituent(s) other than HS^- and S_n^{2-} mediate the transformations of these pesticides. The joint contribution from HS^- and S_n^{2-}

somewhat overestimates the observed disappearance of metolachlor, suggesting that depletion of reduced sulfur species might occur during the reaction. At pH 8.62, a major fraction (35-65%) of k_{obs} is still attributable to HS^-, while a comparable contribution (25-65%) to k_{obs} stems from S_n^{2-} owing to its increasing abundance at this pH. Inclusion of reaction with S_n^{2-} actually overpredicts k_{obs} for the reactions of propachlor and metolachlor. At pH 9.53, with a further increase in S_n^{2-} relative to HS^-, S_n^{2-} contributes substantially (50-90%) to k_{obs}. But again, the possible contribution from other reagents cannot be ruled out. It should be noted that the contribution of S_n^{2-} can be biased (i.e., overprediction of k_{obs}) by the uncertainties associated with the approximation that total polysulfides are equal to the recovered DMPS. It should be noted that observed sulfite (SO_3^{2-}) and thiosulfate ($S_2O_3^{2-}$) concentrations in native porewaters reached approximately 40 μM and 80 μM, respectively (see Table A.1), which are comparable to the levels reported for marine sediment porewaters.[28,75] At pH 8.62, the joint contribution of sulfite and thiosulfate, however, can only account for less than 0.3% of k_{obs} due to their relatively low reactivity (see Table A.5 and Table A.7). Thus, the roles of sulfite and thiosulfate are considered unimportant in the transformation of chloroacetanilides.

Previous research has demonstrated that redox-active moieties in dissolved organic matter (DOM) can function as effective electron-transfer mediators[36,76] or direct reductants[77] in the reductive dehalogenation of halogenated organic contaminants, but the reactivity of DOM moieties is strongly pH-dependent and may drop significantly with increasing pH.[78,79] Given the high DOC levels in these porewaters (see Table 2.2), this appears to be a plausible explanation for the remaining degradation that cannot be

attributed to reduced sulfur species, provided that the DOM-mediated processes do not inhibit the competing nucleophilic substitution reaction. Due to the high reduced sulfur concentrations, it is possible that the organic sulfur compounds in the porewaters is high and formed via pathways such as the Michael addition.[80] In marine sediment porewaters, several organosulfur compounds, such as glutathione and cysteine, have been reported to reach concentrations as high as 2.4 mM and 12.4 μM, respectively.[32] Organocsulfur compounds containing thiol group (i.e., R-SH) have been shown to promote nucleophilic substitution reactions at halogen atoms with halogenated organic pollutants as well as chloroacetanilide pesticides.[36,76,81-85] For instance, glutathione can conjugate with chloroacetanilides via the nucleophilic displacement of chlorine.[83,84] The potential therefore exists for these organosulfur species to react with pesticides. The role of DOM and organosulfur compounds in pesticide transformation processes, however, is beyond the scope of this paper.

To further test the importance of reduced sulfur species with respect to the fate of chloroacetanilides, the transformation of propachlor was investigated in $AgNO_3$-amended porewaters. Varying amounts of $AgNO_3$ crystals were added to native porewaters to lower the reduced sulfur concentrations. It was found that the reaction rate of propachlor decreased with increasing doses of $AgNO_3$ (see Table A.8 and Figure A.5**)**. This supports a critical role for reduced sulfur species in the transformation of pesticides in PPL porewaters.

2.3.4 Transformation Products of Chloroacetanilides

All chloroacetanilides appeared to react with HS^- and S_n^{2-} via the S_N2 mechanism (i.e., displacement of chlorine) to form the corresponding mercaptoacetanilides. Products of chloroacetanilides exhibited mass spectra consistent with the presence of sulfur atoms as reported by Loch et al.[38] As shown in Figure 2.5 for propachlor, the major products were the monosulfur (1S)- and disulfur (2S)-substituted methyl derivatives (i.e., RS_nCH_3, n = 1 or 2). Corresponding products were found for the other three pesticides (see Figure A.6, Figure A.7, and Figure A.8). The 1S-substituted product may result from reaction with either HS^- or S_n^{2-}, while the 2S-substituted product arises from reaction with S_n^{2-}. Although none of the identified reaction products contained higher polysulfide linkages, the number of sulfur atoms in the final methylated products may not necessarily reflect their parent structures as disproportion of sulfur chains can occur.[38] Finally, no reductive dechlorination products were observed, suggesting that reduction was not a major pathway for transformations of chloroacetanilides in these porewaters.

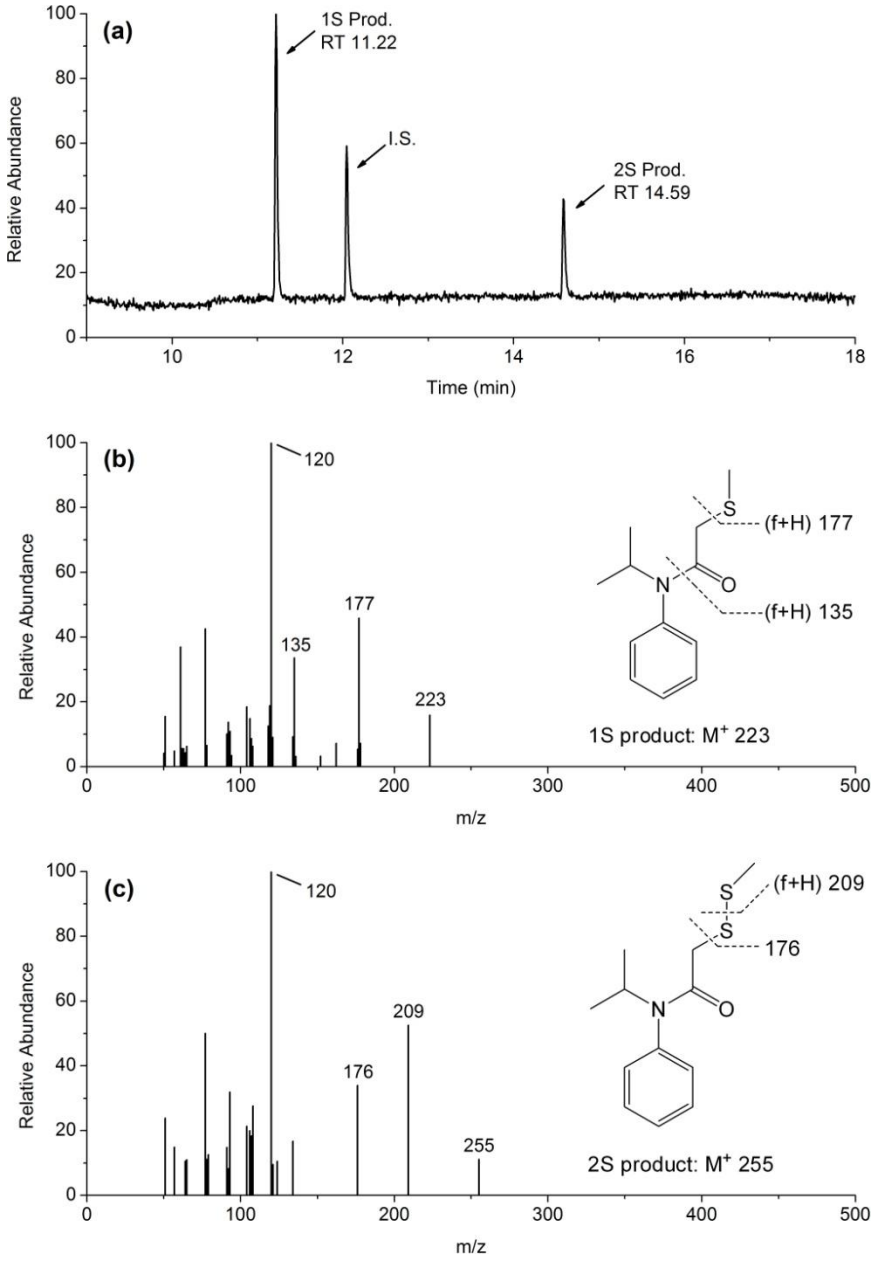

Figure 2.5 Total ion chromatogram (TIC) and mass spectra of methylated products obtained in the reaction of propachlor with porewaters: (a) TIC of propachlor products; (b) Mass spectrum of 1S-substituted product; (c) Mass spectrum of 2S-substituted product. . "I.S." denotes the internal standard (i.e., terbuthylazine). "RT" denotes the retention time (min). "1S" and "2S" denote the number of sulfur atoms in the products.

2.4 Summary

Bisulfide and polysulfides seem to dominate the reaction of chloroacetanilides in these PPL porewaters. Because the sulfur biogeochemistry in PPLs is strongly linked to the local climate and hydrology, the distribution and abundance of reduced sulfur species may shift spatially and temporally, which can in turn affect the ultimate fate of pesticides in PPLs. Although the current study focuses on the behavior of chloroacetanilides, other commonly used *s*-triazine[37,86] and organophosphorus pesticides[40,41,79,87-91] may be transformed in PPL porewaters via similar pathways as seen from previous laboratory studies. This research not only demonstrates that PPLs can act as "natural reactors" for the attenuation of pesticides, but also offers practical insights into the modeling of pesticide fate in PPLs and provides compelling reasons for the proper conservation and restoration of PPLs

2.5 References

1. van der Valk, A. G., The prairie potholes of North America. In *The World's Largest Wetlands*, Fraser, L. H.; Keddy, P. A., Eds. Cambridge University Press: Cambridge, UK, 2005; pp 393-423.
2. Kantrud, H. A.; Krapu, G. L.; Swanson, G. A. *Prairie basin wetlands of the Dakotas: A community profile*; U.S. Fish and Wildlife Service, Biological Report 85: Washington, DC, 1989; pp 1-111.
3. Gleason, R. A.; Euliss, N. H.; Tangen, B. A.; Laubhan, M. K.; Browne, B. A., USDA conservation program and practice effects on wetland ecosystem services in the Prairie Pothole Region. *Ecol. Appl.* **2011,** *21*, S65-S81.
4. Johnson, R. R.; Oslund, F. T.; Hertel, D. R., The past, present, and future of prairie potholes in the United States. *J. Soil Water Conserv.* **2008,** *63*, 84A-87A.
5. U.S. Department of Agriculture, National Agricultural Statistical Services. *2009 State Agriculture Overview - North Dakota*; http://www.nass.usda.gov/Statistics_by_State/Ag_Overview/AgOverview_ND.pdf (Accessed February, 2011).
6. U.S. Department of Agriculture, National Agricultural Statistical Services. *Agricultural Chemical Usage - Field Crops*;

http://usda.mannlib.cornell.edu/MannUsda/viewDocumentInfo.do?documentID=1560 (Accessed February, 2011).
7. Grue, C. E.; DeWeese, L. R.; Mineau, P.; Swanson, G. A.; Foster, J. R.; Arnold, P. M.; Huckins, J. N.; Sheehan, P. L.; Marshall, W. K.; Ludden, A. P., Potential impacts of agricultural chemicals on waterfowl and other wildlife inhabiting prairie wetlands: An evaluation of research needs and approaches. In *Transactions North American Wildlife and Natural Resources Conference*, McCabe, R. E., Ed. Wildlife Management Institute: Washington, DC, 1986; Vol. 51, pp 357-383.
8. Goldsborough, L. G.; Crumpton, W. G., Distribution and environmental fate of pesticides in prairie wetlands. *Great Plains Res.* **1998,** *8*, 73-95.
9. Olness, A.; Staricka, J. A.; Daniel, J. A., Oxidation-reduction and groundwater contamination in the Prairie Pothole region of the Northern Great Plains. In *Water for Agriculture and Wildlife and the Environment -- Win-Win Opportunities: Proceedings of the 1996 USCID Wetlands Seminar*, Schaack, J.; Anderson, S. S., Eds. U.S. Committee on Irrigation and Drainage: Denver, CO, 1996; pp 115-131.
10. Detenbeck, N. E.; Elonen, C. M.; Taylor, D. L.; Cotter, A. M.; Puglisi, F. A.; Sanville, W. D., Effects of agricultural activities and best management practices on water quality of seasonal prairie pothole wetlands. *Wetlands Ecol. Manage.* **2002,** *10*, 335-354.
11. Grue, C. E.; Tome, M. W.; Swanson, G. A.; Borthwick, S. M.; DeWeese, L. R., Agricultural chemicals and the quality of prairie-pothole wetlands for adult and juvenile waterfowl - What are the concerns? In *Proceedings of the National Symposium on Protection of Wetlands from Agricultural Impacts*, Stuber, P. J., Ed. U.S. Fish and Wildlife Service Biological Report 88(16): Washington, DC, 1988; pp 55-64.
12. Donald, D. B.; Syrgiannis, J.; Hunter, F.; Weiss, G., Agricultural pesticides threaten the ecological integrity of northern prairie wetlands. *Sci. Total Environ.* **1999,** *231*, 173-181.
13. Wolf, T. M.; Cessna, A. J., Protecting aquatic and riparian areas from pesticide drift. In *International Conference on Pesticide Application for Drift Management*, Washington State University Press: Pullman, WA 2004; pp 59-71.
14. Sura, S.; Waiser, M.; Tumber, V.; Lawrence, J. R.; Cessna, A. J.; Glozier, N., Effects of glyphosate and two herbicide mixtures on microbial communities in prairie wetland ecosystems: A mesocosm approach. *J. Environ. Qual.* **2012,** *41*, 732-743.
15. Huckins, J. N.; Petty, J. D.; England, D. C., Distribution and impact of trifluralin, atrazine, and fonofos residues in microcosms simulating a northern prairie wetland. *Chemosphere* **1986,** *15*, 563-588.
16. Cessna, A. J.; Donald, D. B.; Bailey, J.; Waiser, M.; Headley, J. V., Persistence of the sulfonylurea herbicides thifensulfuron-methyl, ethametsulfuron-methyl, and metsulfuron-methyl in farm dugouts (ponds). *J. Environ. Qual.* **2006,** *35*, 2395-2401.
17. Degenhardt, D.; Cessna, A. J.; Raina, R.; Farenhorst, A.; Pennock, D. J., Dissipation of six acid herbicides in water and sediment of two Canadian prairie wetlands. *Environ. Toxicol. Chem.* **2011,** *30*, 1982-1989.
18. Degenhardt, D.; Humphries, D.; Cessna, A. J.; Messing, P.; Badiou, P. H.; Raina, R.; Farenhorst, A.; Pennock, D. J., Dissipation of glyphosate and

aminomethylphosphonic acid in water and sediment of two Canadian prairie wetlands. *J. Environ. Sci. Health, Part B* **2012,** *47*, 631-639.
19. Driver, E. A.; Peden, D. G., The chemistry of surface water in prairie ponds. *Hydrobiologia* **1977,** *53*, 33-48.
20. LaBaugh, J. W., Chemical characteristics of water in northern prairie wetlands. In *Northern Prairie Wetlands*, Van der Valk, A. G., Ed. Iowa State University Press: Ames, IA, 1989; pp 56-90.
21. Hall, B. D.; Baron, L. A.; Somers, C. M., Mercury concentrations in surface water and harvested waterfowl from the prairie pothole region of Saskatchewan. *Environ. Sci. Technol.* **2009,** *43*, 8759-8766.
22. Bates, L. M.; Hall, B. D., Concentrations of methylmercury in invertebrates from wetlands of the Prairie Pothole Region of North America. *Environ. Pollut.* **2012,** *160*, 153-160.
23. Grossman, I. G. Origin of the sodium sulfate deposits of the northern Great Plains of Canada and the United States. U.S. Geological Survey Professional Paper 600-B: Denver, CO, 1968; pp B104-B109.
24. Lemke, R. W. Geology of the Souris River area, North Dakota. U.S. Geological Survey Professional Paper 325: Denver, CO, 1960.
25. Goldhaber, M. B.; Mills, C. T.; Stricker, C. A.; Morrison, J. M., The role of critical zone processes in the evolution of the Prairie Pothole Region wetlands. *Appl. Geochem.* **2011,** *26, Supplement*, S32-S35.
26. Mills, C. T.; Goldhaber, M. B.; Stricker, C. A.; Holloway, J. M.; Morrison, J. M.; Ellefsen, K. J.; Rosenberry, D. O.; Thurston, R. S., Using stable isotopes to understand hydrochemical processes in and around a Prairie Pothole wetland in the Northern Great Plains, USA. *Appl. Geochem.* **2011,** *26, Supplement*, S97-S100.
27. Sloan, C. E. *Ground-water hydrology of prairie potholes in North Dakota. U.S. Geological Survey Professional Paper 585-C*; Department of the Interior: Denver, CO, 1972.
28. MacCrehan, W.; Shea, D., Temporal relationship of thiols to inorganic sulfur compounds in anoxic Chesapeake Bay sediment porewater. In *Geochemical Transformations of Sedimentary Sulfur*, Vairavamurthy, M. A.; Schoonen, M. A. A.; Eglinton, T. I.; Luther III, G. W.; Manowitz, B., Eds. American Chemical Society: Washington, DC, 1995; Vol. 612, pp 294-310.
29. Boulegue, J.; Lord III, C. J.; Church, T. M., Sulfur speciation and associated trace metals (Fe, Cu) in the pore waters of Great Marsh, Delaware. *Geochim. Cosmochim. Acta* **1982,** *46*, 453-464.
30. Morgan, B.; Burton, E. D.; Rate, A. W., Iron monosulfide enrichment and the presence of organosulfur in eutrophic estuarine sediments. *Chem. Geol.* **2012,** *296–297*, 119-130.
31. Vairavamurthy, M. A.; Orr, W. L.; Manowitz, B., Geochemical transformations of sedimentary sulfur: An introduction. In *Geochemical Transformations of Sedimentary Sulfur*, Vairavamurthy, M. A.; Schoonen, M. A. A.; Eglinton, T. I.; Luther III, G. W.; Manowitz, B., Eds. American Chemical Society: Washington, DC, 1995; Vol. 612, pp 1-14.

32. Barbash, J. E.; Reinhard, M., Reactivity of sulfur nucleophiles toward halogenated organic compounds in natural waters. In *Biogenic Sulfur in the Environment*, Saltzman, E. S.; Cooper, W. J., Eds. American Chemical Society: Washington, DC, 1989; Vol. 393, pp 101-138.
33. Miller, P. L.; Vasudevan, D.; Gschwend, P. M.; Roberts, A. L., Transformation of hexachloroethane in a sulfidic natural water. *Environ. Sci. Technol.* **1998,** *32*, 1269-1275.
34. Haag, W. R.; Mill, T., Some reactions of naturally occurring nucleophiles with haloalkanes in water. *Environ. Toxicol. Chem.* **1988,** *7*, 917-924.
35. Roberts, A. L.; Sanborn, P. N.; Gschwend, P. M., Nucleophilic substitution reactions of dihalomethanes with hydrogen sulfide species. *Environ. Sci. Technol.* **1992,** *26*, 2263-2274.
36. Perlinger, J. A.; Angst, W.; Schwarzenbach, R. P., Kinetics of the reduction of hexachloroethane by juglone in solutions containing hydrogen sulfide. *Environ. Sci. Technol.* **1996,** *30*, 3408-3417.
37. Lippa, K. A.; Roberts, A. L., Nucleophilic aromatic substitution reactions of chloroazines with bisulfide (HS^-) and polysulfides (S_n^{2-}). *Environ. Sci. Technol.* **2002,** *36*, 2008-2018.
38. Loch, A. R.; Lippa, K. A.; Carlson, D. L.; Chin, Y.-P.; Traina, S. J.; Roberts, A. L., Nucleophilic aliphatic substitution reactions of propachlor, alachlor, and metolachlor with bisulfide (HS^-) and polysulfides (S_n^{2-}). *Environ. Sci. Technol.* **2002,** *36*, 4065-4073.
39. Wang, S.; Arnold, W. A., Abiotic reduction of dinitroaniline herbicides. *Water Res.* **2003,** *37*, 4191-4201.
40. Gan, Q.; Singh, R. M.; Jans, U., Degradation of naled and dichlorvos promoted by reduced sulfur species in well-defined anoxic aqueous solutions. *Environ. Sci. Technol.* **2006,** *40*, 778-783.
41. Wu, T.; Gan, Q.; Jans, U., Nucleophilic substitution of phosphorothionate ester pesticides with bisulfide (HS^-) and polysulfides (S_n^{2-}). *Environ. Sci. Technol.* **2006,** *40*, 5428-5434.
42. U.S. Geological Survey, Pesticide National Synthesis Project. *2002 Pesticide Use Maps*; http://water.usgs.gov/nawqa/pnsp/usage/maps/compound_listing.php?year=02 (Accessed August, 2011).
43. Stamper, D. M.; Traina, S. J.; Tuovinen, O. H., Anaerobic transformation of alachlor, propachlor, and metolachlor with sulfide. *J. Environ. Qual.* **1997,** *26*, 488-494.
44. Zaugg, S. D.; Sandstrom, M. W.; Smith, S. G.; Fehlberg, K. M. *Methods of analysis by the U.S. Geological Survey National Water Quality Laboratory - Determination of pesticides in water by C-18 solid-phase extraction and capillary-column gas chromatography/mass spectrometry with selected-ion monitoring*; U.S. Geological Survey Open-File Report 95-181: Denver, CO, 1995.
45. Winter, T. C.; Rosenberry, D. O., Hydrology of prairie pothole wetlands during drought and deluge: A 17-year study of the cottonwood lake wetland complex in North Dakota in the perspective of longer term measured and proxy hydrological records. *Clim. Change* **1998,** *40*, 189-209.
46. Hakala, J. A.; Fimmen, R. L.; Chin, Y.-P.; Agrawal, S. G.; Ward, C. P., Assessment of the geochemical reactivity of Fe-DOM complexes in wetland sediment

pore waters using a nitroaromatic probe compound. *Geochim. Cosmochim. Acta* **2009,** *73*, 1382-1393.
47. Cline, J. D., Spectrophotometric determination of hydrogen sulfide in natural waters. *Limnol. Oceanogr.* **1969,** *14*, 454-458.
48. Shea, D.; Helz, G. R., The solubility of copper in sulfidic waters - sulfide and polysulfide complexes in equilibrium with covellite. *Geochim. Cosmochim. Acta* **1988,** *52*, 1815-1825.
49. Russell, L. L. Chemical aspects of ground water recharge with treated wastewater Ph.D. Dissertation, University of California, Berkeley, Berkeley, CA, 1976.
50. Mylon, S. E.; Benoit, G., Subnanomolar detection of acid-labile sulfides by the classical methylene blue method coupled to HPLC. *Environ. Sci. Technol.* **2001,** *35*, 4544-4548.
51. Bowles, K. C.; Ernste, M. J.; Kramer, J. R., Trace sulfide determination in oxic freshwaters. *Anal. Chim. Acta* **2003,** *477*, 113-124.
52. Luther III, G. W.; Giblin, A. E.; Varsolona, R., Polarographic analysis of sulfur species in marine porewaters. *Limnol. Oceanogr.* **1985,** *30*, 727-736.
53. Overmann, J.; Beatty, J. T.; Krouse, H. R.; Hall, K. J., The sulfur cycle in the chemocline of a meromictic salt lake. *Limnol. Oceanogr.* **1996,** *41*, 147-156.
54. Wang, F.; Tessier, A., Zero-valent sulfur and metal speciation in sediment porewaters of freshwater lakes. *Environ. Sci. Technol.* **2009,** *43*, 7252-7257.
55. Jacobs, L. A. Metal geochemistry in anoxic marine basins. Ph.D. Dissertation, University of Washington, Seattle, WA, 1984.
56. Heitz, A.; Kagi, R. I.; Alexander, R., Polysulfide sulfur in pipewall biofilms: Its role in the formation of swampy odour in distribution systems. *Water Sci. Technol.* **2000,** *41*, 271-278.
57. Kristiana, I.; Heitz, A.; Joll, C.; Sathasivan, A., Analysis of polysulfides in drinking water distribution systems using headspace solid-phase microextraction and gas chromatography-mass spectrometry. *J. Chromatogr. A* **2010,** *1217*, 5995-6001.
58. Kishore, K.; Ganesh, K., Polymers containing disulfide, tetrasulfide, diselenide and ditelluride linkages in the main chain. In *Polymer Synthesis/Polymer Engineering*, Springer Berlin / Heidelberg: 1995; Vol. 121, pp 81-121.
59. Steudel, R., The chemistry of organic polysulfanes R-S_n-R (n > 2). *Chem. Rev.* **2002,** *102*, 3905-3945.
60. Kamyshny, A.; Goifman, A.; Gun, J.; Rizkov, D.; Lev, O., Equilibrium distribution of polysulfide ions in aqueous solutions at 25 degrees C: A new approach for the study of polysulfides equilibria. *Environ. Sci. Technol.* **2004,** *38*, 6633-6644.
61. Goifman, A.; Ryzkov, D.; Gun, J.; Kamyshny, A.; Modestov, A. D.; Lev, O., Inorganic polysulfides' quantitation by methyl iodide derivatization: Dimethylpolysulfide formation potential. *Water Sci. Technol.* **2004,** *49*, 179-184.
62. Sobek, S.; Tranvik, L. J.; Prairie, Y. T.; Kortelainen, P.; Cole, J. J., Patterns and regulation of dissolved organic carbon: An analysis of 7,500 widely distributed lakes. *Limnol. Oceanogr.* **2007,** *52*, 1208-1219.

63. Holloway, J. M.; Goldhaber, M. B.; Mills, C. T., Carbon and nitrogen biogeochemistry of a Prairie Pothole wetland, Stutsman County, North Dakota, USA. *Appl. Geochem.* **2011,** *26*, S44-S47.
64. Arts, M. T.; Robarts, R. D.; Kasai, F.; Waiser, M. J.; Tumber, V. P.; Plante, A. J.; Rai, H.; Lange, H. J. d., The attenuation of ultraviolet radiation in high dissolved organic carbon waters of wetlands and lakes on the northern Great Plains. *Limnol. Oceanogr.* **2000,** *45*, 292-299.
65. Kuwabara, J. S.; van Geen, A.; McCorkle, D. C.; Bernhard, J. M., Dissolved sulfide distributions in the water column and sediment pore waters of the Santa Barbara Basin. *Geochim. Cosmochim. Acta* **1999,** *63*, 2199-2209.
66. Ciglenecki, I.; Kodba, Z.; Cosovic, B., Sulfur species in Rogoznica Lake. *Mar. Chem.* **1996,** *53*, 101-110.
67. Fritz, M.; Bachofen, R., Volatile organic sulfur compounds in a meromictic alpine lake. *Acta Hydroch. Hydrob.* **2000,** *28*, 185-192.
68. Luthy, L.; Fritz, M.; Bachofen, R., In situ determination of sulfide turnover rates in a meromictic alpine lake. *Appl. Environ. Microbiol.* **2000,** *66*, 712-717.
69. Lippa, K. A. Reactions of chloro-*s*-triazine and chloroacetanilide agrochemicals with reduced sulfur nucleophiles. Ph.D. Dissertation, The Johns Hopkins University, Baltimore, MD, 2002.
70. Chin, Y.-P.; Traina, S. J.; Swank, C. R.; Backhus, D., Abundance and properties of dissolved organic matter in pore waters of a freshwater wetland. *Limnol. Oceanogr.* **1998,** *43*, 1287-1296.
71. O'Loughlin, E. J.; Chin, Y.-P., Quantification and characterization of dissolved organic carbon and iron in sedimentary porewater from Green Bay, WI, USA. *Biogeochemistry* **2004,** *71*, 371-386.
72. Qin, Y. Abiotic reactions of acetanilide herbicides with bisulfide. M.S. Thesis, Oklahoma State University, Stillwater, OK, 1995.
73. Gan, J. Y., Enhanced degradation of chloroacetanilide herbicides by polysulfide salts. In *Proceedings of the 2006 USDA-CSREES National Water Quality Conference*, USDA-NIFA National Integrated Water Quality Program: Washington, DC, 2006.
74. Carlson, D. L.; Than, K. D.; Roberts, A. L., Acid- and base-catalyzed hydrolysis of chloroacetamide herbicides. *J. Agric. Food. Chem.* **2006,** *54*, 4740-4750.
75. Zopfi, J.; Ferdelman, T. G.; Fossing, H., Distribution and fate of sulfur intermediates-sulfite, tetrathionate, thiosulfate, and elemental sulfur-in marine sediments. *Geol. Soc. Am. Spec. Pap.* **2004,** *379*, 97-116.
76. Perlinger, J. A.; Buschmann, J.; Angst, W.; Schwarzenbach, R. P., Iron porphyrin and mercaptojuglone mediated reduction of polyhalogenated methanes and ethanes in homogeneous aqueous solution. *Environ. Sci. Technol.* **1998,** *32*, 2431-2437.
77. Kappler, A.; Haderlein, S. B., Natural organic matter as reductant for chlorinated aliphatic pollutants. *Environ. Sci. Technol.* **2003,** *37*, 2714-2719.
78. Tratnyek, P. G.; Macalady, D. L., Abiotic reduction of nitro aromatic pesticides in anaerobic laboratory systems. *J. Agric. Food. Chem.* **1989,** *37*, 248-254.

79. Guo, X.; Jans, U., Kinetics and mechanism of the degradation of methyl parathion in aqueous hydrogen sulfide solution: Investigation of natural organic matter effects. *Environ. Sci. Technol.* **2006,** *40*, 900-906.
80. Perlinger, J. A.; Kalluri, V. M.; Venkatapathy, R.; Angst, W., Addition of hydrogen sulfide to juglone. *Environ. Sci. Technol.* **2002,** *36*, 2663-2669.
81. Lindley, H., A study of the kinetics of the reaction between thiol compounds and chloroacetamide. *Biochem. J* **1960,** *74*, 577-584.
82. Li, X. Y.; Jiang, X. K.; Pan, H. Q.; Hu, J. S.; Fu, W. M., Nucleophilic substitutions of perhalofluoroalkanes initiated by halophilic attacks. *Pure Appl. Chem.* **1987,** *59*, 1015-1020.
83. Scarponi, L.; Perucci, P.; Martientti, L., Conjugation of 2-chloroacetanilide herbicides with glutathione: Role of molecular structures and of glutathione S-transferase enzymes. *J. Agric. Food. Chem.* **1991,** *39*, 2010-2013.
84. Field, J. A.; Thurman, E. M., Glutathione conjugation and contaminant transformation. *Environ. Sci. Technol.* **1996,** *30*, 1413-1418.
85. Buschmann, J.; Angst, W.; Schwarzenbach, R. P., Iron porphyrin and cysteine mediated reduction of ten polyhalogenated methanes in homogeneous aqueous solution: Product analyses and mechanistic considerations. *Environ. Sci. Technol.* **1999,** *33*, 1015-1020.
86. Yang, W.; Gan, J. J.; Bondarenko, S.; Liu, W., Nucleophilic radical substitution reaction of triazine herbicides with polysulfides. *J. Agric. Food. Chem.* **2004,** *52*, 7051-7055.
87. Jans, U.; Miah, M. H., Reaction of chlorpyrifos-methyl in aqueous hydrogen sulfide/bisulfide solutions. *J. Agric. Food. Chem.* **2003,** *51*, 1956-1960.
88. Gan, Q.; Jans, U., Reaction of thiometon and disulfoton with reduced sulfur species in simulated natural environment. *J. Agric. Food. Chem.* **2006,** *54*, 7753-7760.
89. Gan, Q.; Singh, R. M.; Wu, T.; Jans, U., Kinetics and mechanism of degradation of dichlorvos in aqueous solutions containing reduced sulfur species. *Environ. Sci. Technol.* **2006,** *40*, 5717-5723.
90. Wu, T.; Jans, U., Nucleophilic substitution reactions of chlorpyrifos-methyl with sulfur species. *Environ. Sci. Technol.* **2006,** *40*, 784-790.
91. Gan, Q.; Jans, U., Nucleophilic reactions of phorate and terbufos with reduced sulfur species under anoxic conditions. *J. Agric. Food. Chem.* **2007,** *55*, 3546-3554.

Chapter 3: Abiotic Transformation of Pesticides in Prairie Pothole Porewaters: Reduction Reactions[1]

1 A version of this chapter has been published as: Zeng, T.; Chin, Y.-P.; Arnold, W. A., Potential for abiotic reduction of pesticides in prairie pothole porewaters. *Environ. Sci. Technol.* **2012,** *46*, 3177-3187.

Prairie pothole lakes (PPLs) are critical hydrological and ecological components of central North America and represent one of the largest inland wetland systems on Earth. These lakes are located within an agricultural region, and many of them are subject to nonpoint source pesticide pollution. Limited attention, however, has been paid to understanding the impact of PPL water chemistry on the fate and persistence of pesticides. In this study, the abiotic reductive transformation of seven dinitroaniline pesticides was investigated in PPL sediment porewaters containing naturally abundant levels of reduced sulfur species (i.e., bisulfide (HS^-) and polysulfides (S_n^{2-})) and dissolved organic matter (DOM). Target dinitroanilines underwent rapid degradation in PPL porewaters and were transformed into corresponding amine products. While the largest fraction of the transformation could be attributed to reduced sulfur species, experimental evidence suggested that other reactive entities in PPL porewaters, such as DOM and mineral phases, might also affect reaction rates of dinitroanilines. Results from this study highlight the importance of reductive transformation as an abiotic natural attenuation pathway for pesticides entering the PPL sedimentary environment.

3.1 Introduction

Nitroaromatic compounds (NACs) constitute a major class of aquatic contaminants due to their extensive use in pesticides, munitions, dyes, and various other industrial chemicals.[1] In this context, NAC transformation has been investigated in a range of natural systems and model systems mimicking the complex natural environment. One predominant pathway governing the transformation of NACs under anoxic conditions is reduction of the aromatic nitro group(s).[2] Earlier studies have suggested that

abiotic reduction of NACs by dissolved, adsorbed, or solid chemical species can be a major removal mechanism as opposed to biotransformation in reducing environments.[3-11] To date, mechanistic investigations into the abiotic reduction of NACs have focused on several classes of biogeochemically important reductants, including reduced iron compounds, reduced sulfur species, and natural organic matter (NOM). Uncertainty remains, however, concerning the extrapolation of results from model systems to predict the actual transformation of NACs in a given natural system.[12,13] Studies in both heterogeneous and homogeneous systems have demonstrated the significance of ferrous iron species (Fe(II)) in the abiotic reduction of NACs, including structural Fe(II) present in Fe(II) or mixed-valent Fe(III)-Fe(II) minerals,[14-20] Fe(II) sorbed on Fe(III) (hydr)oxides or Fe(II)-bearing minerals,[8,15-18,21-26] Fe(II)-organic ligand complexes,[13,27-30] and some combination of these.[31] Additional efforts have been aimed at characterizing the reduction of NACs by reduced sulfur species and NOM.[8,32-36] In principle, reduced sulfur species, such as bisulfide (HS^-) and polysulfides (S_n^{2-}; n = 2-5), possess sufficiently low reduction potentials to directly reduce NACs through a dissociative electron transfer process (Equations (3.1) and (3.2)):[2]

$$HS\text{:}^- + ArNO_2 = ArNO_2^{\bullet -} + HS^{\bullet} \quad (3.1)$$

$$^-\text{:S-(S)}_n\text{-S:}^- + ArNO_2 = ArNO_2^{\bullet -} + \ ^-\text{:S-(S)}_n\text{-S}^{\bullet} \quad (3.2)$$

The transfer of the first electron from HS^- to NACs is generally considered to be a highly endergonic process,[2] and the direct reduction of some monosubstituted NACs by HS^- has been documented as a slow process with respect to their facile transformations sometimes observed in anoxic environments.[32,33] The addition of NOM or its structural

analogs containing redox-labile functionality often can accelerate rates of NAC reduction by orders of magnitude in the hydrogen sulfide system.[32,33,35] The role of NOM has most commonly been ascribed to its ability to serve as an effective electron transfer mediator that shuttles electrons between HS^- (bulk electron donors) and NACs (electron acceptors).[32,33,37] Such NOM constituents often contain quinone or its sulfur derivatives (e.g., mercaptoquinone) that result from addition reactions with hydrogen sulfide.[38-46] In contrast to HS^-, polysulfide ions are kinetically more reactive reductants towards NACs even though they are more oxidized.[47-49] Nonetheless, the direct reduction of NACs by S_n^{2-} has not been fully explored under environmentally relevant conditions.

The prairie pothole region (PPR) of central North America contains numerous glacially formed water bodies commonly known as prairie pothole lakes (PPLs).[50] Despite serving as pivotal hydrological and ecological units in the PPR,[51] PPLs and related wetlands have undergone severe loss over decades due to large-scale agricultural drainage practices.[52-54] Recent trends in corn-based biofuel production further stimulated the expansion of agricultural land use in the PPR.[55-58] Consequently, the remaining PPLs continue to be directly and indirectly impacted by nonpoint source pesticide pollution from agriculture.[59-63] As such, PPLs represent a unique setting for studying the environmental fate of pesticides.[64-67]

Dinitroanilines rank among the most commonly used nitroaromatic pesticides in the U.S. and are regularly applied in the PPR for pre-emergent control of annual grasses and broadleaf weeds.[68,69] For instance, the U.S. average annual use of pendimethalin in 2002 was approximately 12.5 million pounds of active ingredient, followed by trifluralin

(8.5 million pounds) and ethalfluralin (1.9 million pounds).[69] In North Dakota, the total area of agricultural land treated by pendimethalin has reached approximately 0.20 million acres in 2008, followed by ethalfluralin (0.16 million acres) and trifluralin (0.07 million acres).[70] The past and present use of dinitroanilines has led to their frequent detection in groundwater, surface water, and sediment.[71,72] Some dinitroanilines, such as pendimethalin and trifluralin, have been classified as Persistent Bioaccumulative Toxins by the U.S. Environmental Protection Agency.[73] The ubiquity and toxicity of dinitroanilines and their transformation products have sparked considerable interest in the environmental fate and risk of these pesticides.[74-76] Although dinitroanilines are soil-incorporated when applied, they may enter prairie wetlands by several routes, such as vapor drift, atmospheric deposition, and surface runoff, and eventually become part of the sedimentary environment. Thus, a fundamental understanding of the rates and pathways of abiotic and biotic transformations that may affect the persistence of dinitroanilines is essential.

In many freshwater limnological systems, benthic sediment porewaters may develop abundant reductants, such as Fe(II), dissolved organic matter (DOM), and reduced sulfur species.[77-81] Previous studies in well-defined solutions and freshwater sediment porewaters have demonstrated the significance of these aqueous phase chemical reductants in the abiotic reduction of dinitroanilines in addition to surface-mediated processes.[82-85] We have reported in earlier work that sediment porewaters sampled from PPLs in North Dakota contained hydrogen sulfide and polysulfides that reached concentrations as high as 2.3 mM and 79 μM, respectively.[86] Meanwhile, extremely high

DOM levels (on the order of 100 mg/L as carbon) were also measured in these PPL porewaters.[86] Chloroacetanilide pesticides, which react with reduced sulfur species via nucleophilic substitution reactions, have been found to undergo rapid degradation in PPL porewaters.[86] Given the abundances of the reduced sulfur and DOM present in PPL porewaters, it is also likely that HS^- and S_n^{2-} act as direct or bulk reductants to promote the transformation of dinitroanilines. Such natural attenuation processes in PPLs have not been investigated. The main objective of this study, therefore, was to examine the kinetics and products of abiotic reduction of seven dinitroaniline pesticides in PPL sediment porewaters with particular emphasis on the potential contribution of HS^- and S_n^{2-}.

3.2 Experimental Section

3.2.1 Chemicals, Reagents, and Glassware

All dinitroaniline pesticides were purchased from Fluka, including benfluralin (*N*-butyl-*N*-ethyl-2,6-dinitro-4-(trifluoromethyl)aniline; 99.7%), butralin (*N*-(*sec*-butyl)-4-(*tert*-butyl)-2,6-dinitroaniline; 99.8%), ethalfluralin (*N*-ethyl-*N*-(2-methylallyl)-2,6-dinitro-4-(trifluoromethyl)aniline; 99.5%), isopropalin (4-isopropyl-2,6-dinitro-*N*,*N*-dipropylaniline; 98.2%), nitralin (4-(methylsulfonyl)-2,6-dinitro-*N*,*N*-dipropylaniline; 98.0%), pendimethalin (3,4-dimethyl-2,6-dinitro-*N*-(pentan-3-yl)aniline; 98.8%), and trifluralin (2,6-dinitro-*N*,*N*-dipropyl-4-(trifluoromethyl)aniline; 99.5%). Methanol (Chromasolv for HPLC, ≥99.9%), toluene (Chromasolv for HPLC, ≥99.9%), silver nitrate ($AgNO_3$; ≥99.0%), sodium bisulfite (≥58.5% SO_2 basis), sodium sulfate (≥99.0%), sodium thiosulfate pentahydrate (≥99.5%), sodium azide (NaN_3; ≥99.5%), and methyl

iodide (99.5%) were obtained from Sigma-Aldrich. Ferric chloride hexahydrate (≥98.0%) was obtained from Sigma. Sodium sulfide nonahydrate ($Na_2S·9H_2O$; ≥99.99%), *N*,*N*-dimethyl-*p*-phenylenediamine sulfate salt (98%), 5-hydroxy-1,4-naphthoquinone (juglone; 97%), and tris(hydroxymethyl)aminomethane (Tris; 99.90%) were obtained from Aldrich. Terbuthylazine (N^2-(*tert*-butyl)-6-chloro-N^4-ethyl-1,3,5-triazine-2,4-diamine; 98.8%) was obtained from Fluka. Dimethyldisulfide (Me_2S_2; 99%), dimethyltrisulfide (Me_2S_3; 98%), sodium tetrasulfide (Na_2S_4; technical grade, 90+%), and 2-nitro-*m*-xylene (99%) were obtained from Alfa Aesar. *n*-Hexane (UltimAR grade, ≥95% *n*-hexane), ethyl acetate (AR grade, ≥99.5%), sodium chloride (NaCl; 100%), sodium hydroxide (NaOH; >99%), hydrogen peroxide (H_2O_2; 30% solution, 29.0-32.0%), hydrochloric acid (HCl; ≥36.5-38.0%), and nitric acid (≥68.0-70.0%) were obtained from Mallinckrodt. Difco fluid thioglycollate medium (for sterility testing) was obtained from Becton, Dickinson and Company. All chemicals were used as received without further purification. The glassware cleaning and autoclave procedures were the same as described previously.[86]

Unless otherwise stated, all solutions of redox sensitive solutes were prepared with deoxygenated ultrapure water (resistivity 18.2 MΩ·cm, Millipore Corp.). Standard solutions of dinitroaniline pesticides were prepared either in *n*-hexane or ethyl acetate. Dintroaniline stock solutions for spiking aqueous samples were prepared in deoxygenated methanol. Tris control buffer (5 mM; pH 8.80) was prepared by dilution of Tris stock solution (1.0 M) into deoxygenated ultrapure water with sufficient NaCl added to establish an ionic strength of 0.70 equiv/L. Hydrogen sulfide and polysulfide stock

solutions were prepared by dissolving purified $Na_2S \cdot 9H_2O$ crystals and Na_2S_4 crystals, respectively, in the Tris buffer. Hydrogen sulfide buffers were prepared by diluting an appropriate aliquot of its stock solution into the Tris buffer. Polysulfide buffers were prepared by diluting an aliquot of hydrogen sulfide stock solution into the Tris buffer, followed by the addition of an appropriate amount of polysulfide stock solution. All sulfide redox buffers were then adjusted with deoxygenated HCl or NaOH to the desired pH (~8.80) and equilibrated for 2 weeks to mimic the composition and abundance of reduced sulfur species in PPL sediment porewaters prior to use. The final hydrogen sulfide concentrations (in addition to polysulfide species) in the polysulfide buffers were similar to those employed in the hydrogen sulfide buffers. The pH of porewaters and sulfide redox buffers were measured before and after selected pesticide transformation experiments to confirm that pH was stable to within 0.05 units.

3.2.2 Sample Collection and Analysis

Sediment cores were collected in 2010 from two high-sulfate PPLs (i.e., Lake P1 and P8) in the U.S. Geological Survey (USGS) Cottonwood Lake study area in North Dakota.[86] Whole sediment cores were pressurized to extract porewaters for use in pesticide transformation experiments. All manipulations of air-sensitive samples were performed in an anaerobic glove box (95% N_2/5% H_2, Pd catalyst, 23±2 ℃; Coy Laboratory Products Inc.). Sub-samples of sediments were subjected to elemental analysis and powder X-ray diffraction (XRD) characterization (see Appendix B.8 for additional details). Prior to pesticide transformation experiments, part of the sediment porewaters was filter-sterilized through 0.2 μm syringe filters (PTFE Acrodisc CR13,

Pall Corp.). The sterility of filtered porewaters was verified based on the absence of turbidity in inoculated culture tubes (containing fluid thioglycollate medium) after a 5-day incubation period at 30 ℃.[38] Sub-samples of porewaters (both native and filter-sterilized) and sulfide redox buffers were analyzed for the concentrations of reduced sulfur species. The total hydrogen sulfide concentration ($[H_2S]_T$) was determined by the methylene blue method.[87] The total polysulfide concentration ($[H_2S_n]_T$) was determined by a modified methylation method.[88,89] Details pertaining to the applicability and limitations of these methods in a PPL porewater system have been discussed previously.[86] Dissolved organic carbon (DOC) in the porewaters was measured after proper dilution of the samples with deoxygenated ultrapure water.[86] A series of analyses were also performed to characterize the reactivity discrepancy between native and filter-sterilized porewaters (see Appendix B.9 for additional details). Anion and cation concentrations in the porewaters were analyzed using ion chromatography (IC) and inductively coupled plasma-mass spectrometry (ICP-MS), respectively. The average particle size in both types of porewaters was measured by dynamic light scattering (DLS). Attempts were also made to identify materials collected by the filters after porewater filtration. Due to practical constraints of retrieving intact membranes from 0.2 μm syringe filters, sub-samples of porewaters were passed through 0.22 μm membrane filters (Durapore GCWP, Millipore Corp.) by vacuum filtration. Both unused and used membrane filters were then analyzed for major oxides by inductively coupled plasma-optical emission spectrometry (ICP-OES). Another set of unused and used membrane filters were examined by XRD.

3.2.3 Batch Kinetic Studies

Dinitroaniline transformation studies were performed in the glove box following procedures similar to those described previously.[86] Batch kinetic experiments were conducted in duplicate using porewaters (both native and filter-sterilized) from Lake P8 (sampled in April 2010) in 10-mL foil-wrapped, zero-headspace glass syringes. Individual reactions were initiated by the addition of a 50-μL aliquot of the dinitroaniline methanolic stock solution into the syringes to yield an initial concentration of 0.2-0.5 μM. A 0.5-mL aliquot of aqueous sample was withdrawn periodically and extracted with 0.5 mL of *n*-hexane or ethyl acetate (containing 4.3 μM terbuthylazine as an internal standard) on a vortex mixer for 1 min. Extraction efficiencies for dinitroanilines were >95%. The exact volumes of sample and extraction solvent were determined gravimetrically. Most reactions were allowed to progress over approximately 3 half-lives. Slower reactions (e.g., pendimethalin) at best progressed over approximately 1 half-life. Control syringes containing Tris buffer were spiked, sampled, and extracted in a similar fashion to account for the loss of pesticides via other pathways. Complementary batch experiments were also conducted in well-defined sulfide redox buffers to assess direct reactions of dinitroanilines with concentrations of HS^- and S_n^{2-} comparable to those found in the porewaters. All hexane and ethyl acetate extracts were analyzed by gas chromatography-microelectron capture detection (GC-μECD; see next section). A subset of hexane or ethyl acetate extracts were combined and concentrated to allow identification of possible intermediates and reaction products by gas chromatography-tandem mass spectrometry (GC-MS/MS; see the next section).

3.2.4 Dinitroanilines and Product Analysis

Concentrations of dinitroanilines were analyzed by an Agilent 6890 Series gas chromatograph equipped with a ^{63}Ni microelectron capture detector. Samples (in hexane or ethyl acetate) were injected with an Agilent 7693 autosampler into a split/splitless injector. The GC was equipped with a Rtx-1701 fused silica capillary column (14% cyanopropylphenyl/86% dimethyl polysiloxane bonded phase; 30 m × 0.25 mm i.d. × 0.25 μm film thickness; Restek Crop.). Helium at a constant flow rate of 1.5 mL/min was used as carrier gas. Nitrogen at a constant flow rate of 60.0 mL/min was used as makeup gas. The injector and detector temperatures were set at 250 and 290 ℃, respectively. The injection volume was 1.0 μL in splitless mode. For hexane extracts, the oven temperature was programmed as follows: initial temperature 60 ℃ (hold for 0.5 min), initial rate 60 ℃/min to 215 ℃ (hold for 3 min), then 60 ℃/min to 250 ℃ (hold for 4 min). For ethyl acetate extracts, the oven temperature was programmed as follows: initial temperature 70 ℃ (hold for 0.5 min), initial rate 60 ℃/min to 250 ℃ (hold for 10 min).

Transformation products of dinitroanilines were analyzed by a TSQ Quantum GC tandem mass spectrometer coupled with a TRACE GC Ultra gas chromatograph. Samples (in hexane or ethyl acetate) were injected with a TriPlus autosampler into a split/splitless injector. The GC was equipped with a HP-5MS fused silica capillary column ((5%-phenyl)-methylpolysiloxane bonded phase; 30 m × 0.25 mm i.d. × 0.25 μm film thickness; J & W Scientific Inc.). Helium at a constant flow rate of 1.0 mL/min was used as carrier gas. The injector temperature was set at 250 ℃. The injection volume was 1.0 μL in splitless mode. At 2 min, split mode was switched on with the split flow of 50

mL/min. The oven temperature was programmed as follows: initial temperature 40 ℃ (hold for 2 min), initial rate 25 ℃/min to 140 ℃, then 7 ℃/min to 210 ℃, and then 25 ℃/min to 280 ℃ (hold for 5 min). The mass spectrometer was operated in the positive EI mode at 70 eV. Argon at a pressure of 1.0 mTorr was used as collision gas. The transfer line and ion source temperatures were set at 280 and 200 ℃, respectively. A filament multiplier delay of 4 min was set. The emission current was 100 μA, the scan width was set at *m/z* 0.100, and the scan time was 0.050 sec. Peak widths of Q1 and Q3 were all set at 0.70 amu.

For the optimization of the MS parameters, the instrument was first operated in full scan product mode with the *m/z* ratio ranging from 50-500. According to the selected precursor ions (Table B.1), product ion spectra were acquired by collision-induced dissociation with argon. Collision energies were ramped from 10 to 30 eV. The product spectra were evaluated to determine the most abundant product ion. The instrument was then operated in the selected reaction monitoring mode based on the chosen precursor-product ion pairs. For different *m/z* transitions, the collision energy was optimized for maximum sensitivity separately (Table B.1).

3.2.5 Data Analysis

The pseudo-first-order approximation was used to model reactions of dinitroanilines. Data fitting and analysis were performed using *SigmaPlot 10* (Systat Software Inc.).

3.3 Results and Discussion

3.3.1 Transformations of Pesticides in PPL Porewaters and Sulfide Buffers

Characteristics of porewaters and sulfide redox buffers are summarized in Table 3.1. The time courses in Figure 3.1 show that the degradation of dinitroanilines occurred without any lag phase in both PPL porewaters and sulfide redox buffers. No apparent reaction of dinitroanilines was observed in the Tris control buffer.

Table 3.1 Characteristics of Lake P8 porewaters and sulfide redox buffers

Sample	pH	$[H_2S]_T$ (μM)[a]	$[HS^-]_{calc}$ (μM)[b]	$[H_2S_n]_{T, calc}$ (μM)[c]	$\Sigma[S_n^{2-}]_{calc}$ (μM)[d]	DOC (mg/L)[e]
Native porewater	8.78	1999 ± 16	1984 ± 21	43.5 ± 1.5	43.4 ± 2.1	114.0 ± 0.1
Filtered porewater	8.78	1995 ± 24	1980 ± 34	44.3 ± 2.2	44.2 ± 3.1	110.2 ± 0.1
Hydrogen sulfide buffer	8.82	2012 ± 20	1998 ± 28	0	0	0
Polysulfide buffer	8.84	1985 ± 30	1972 ± 42	47.2 ± 1.6	47.2 ± 2.2	0

[a] Total hydrogen sulfide concentration measured by the methylene blue method. Errors represent one standard deviation from triplicate measurements. [b] Bisulfide concentration calculated from $[H_2S]_T$ and pH, assuming that the sample is not saturated with elemental sulfur. Errors were propagated from $[H_2S]_T$. [c] Total polysulfide concentration calculated as the sum of measured $[Me_2S_2]$ and $[Me_2S_3]$ after correcting for methylation and extraction efficiencies.[86] Errors were calculated through propagation of errors associated with $[Me_2S_2]$ and $[Me_2S_3]$. [d] Polysulfide dianion concentration calculated from $[H_2S_n]_{T, calc}$ and pH, assuming that the relative abundance of HS_n^- and S_n^{2-} species are dictated by equilibrium constants from Shea and Helz.[90] Errors were propagated from $[H_2S_n]_{T, calc}$. [e] Errors represent one standard deviation from triplicate measurements.

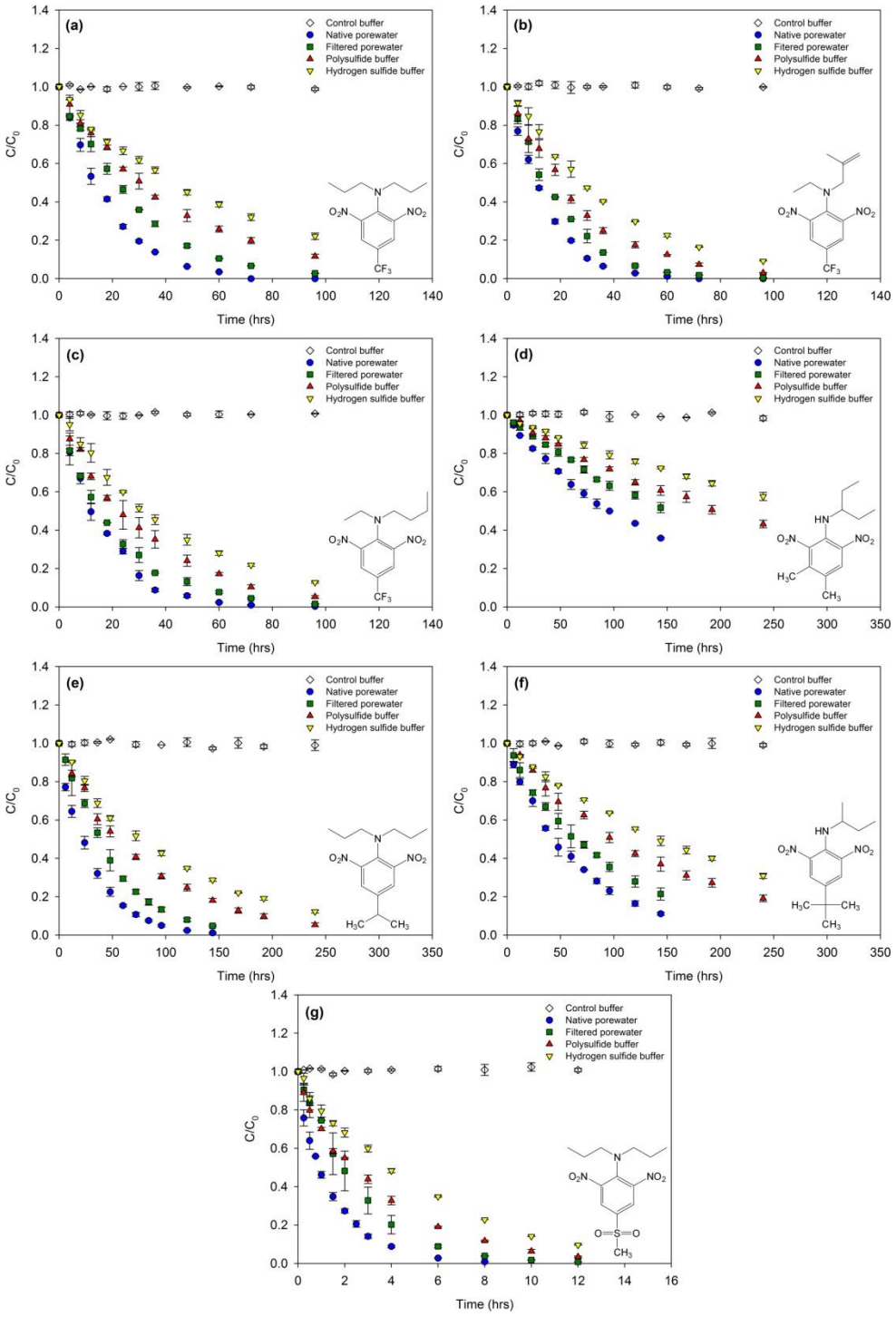

Figure 3.1 Transformations of dinitroanilines in P8 porewaters (Apr 2010) and sulfide redox buffers: (a) trifluralin; (b) ethalfluralin; (c) benfluralin; (d) pendimethalin; (e) isopropalin; (f) butralin; (g) nitralin. Open symbols represent Tris buffer controls. Error bars represent one standard deviation of duplicate samples; where absent, bars fall within symbols. Note differences in time scales.

The reactivity of dinitroanilines differed substantially and decreased in the following order: nitralin > ethalfluralin > benfluralin > trifluralin > isopropalin > butralin > pendimethalin. Depending on the type of substituents on their aromatic rings, electron withdrawing substituents (e.g., $-CF_3$ and $-SO_2CH_3$) accelerate, while electron donating substituents (e.g., $-CH_3$ and $-CHCH_3CH_3$), retard reaction rates. An identical reactivity pattern of dinitroanilines was observed in sulfide redox buffers. Semilogarithmic plots for the transformations of dinitroanilines indicate that all reactions obeyed pseudo-first-order kinetics (see Figure B.1). A summary of rate constants for all batch experiments in the porewaters and sulfide redox buffers is provided in Table 3.2 and Table 3.3, respectively. Pseudo-first-order rate constants (k_{obs}) for dinitroaniline reactions were obtained by linear least-squares fitting. Notably, reactions in native porewaters were faster than those in filter-sterilized porewaters ($k_{obs,\ native}/k_{obs,\ filtered} \approx 1.50$; see Table 3.2), suggesting that the filtration process might have removed certain reactive entities in native porewaters that would otherwise react with dinitroanilines (see further discussion below). In sulfide redox buffers, the reactions of dinitroanilines with HS^- and S_n^{2-} were determined to be first order in $[HS^-]$ and $\Sigma[S_n^{2-}]$, respectively, (see Figure B.2 and Figure B.3), which agrees with previous reports on the reaction order of monosubstituted NACs with HS^- and S_2^{2-}.[47-49] Second-order rate constants for reactions of dinitroanilines with HS^- (k_{HS^-}) were computed by dividing k_{obs} measured in the hydrogen sulfide buffer by $[HS^-]$, while second-order rate constants for reactions of dinitroanilines with S_n^{2-} ($k_{S_n^{2-}}$) were estimated by dividing k_{obs} measured in the polysulfide buffer by $\Sigma[S_n^{2-}]$, after first correcting k_{obs} to account for the contribution from reaction with HS^-.

Table 3.2 Rate constants for reactions of dinitroanilines in PPL porewaters

Dinitroaniline	$k_{obs,\ native}$ (hr^{-1})[a]	$k_{obs,\ filtered}$ (hr^{-1})[b]	$\frac{k_{obs,native}}{k_{obs,\ filtered}}$
Trifluralin	$5.55(\pm0.05)\times10^{-2}$	$3.69(\pm0.05)\times10^{-2}$	1.50
Ethalfluralin	$7.34(\pm0.11)\times10^{-2}$	$5.55(\pm0.07)\times10^{-2}$	1.36
Benfluralin	$6.26(\pm0.21)\times10^{-2}$	$4.35(\pm0.11)\times10^{-2}$	1.44
Pendimethalin	$7.20(\pm0.10)\times10^{-3}$	$4.70(\pm0.40)\times10^{-3}$	1.53
Isopropalin	$2.95(\pm0.05)\times10^{-2}$	$2.08(\pm0.08)\times10^{-2}$	1.50
Butralin	$1.52(\pm0.07)\times10^{-2}$	$1.07(\pm0.08)\times10^{-2}$	1.42
Nitralin	$6.10(\pm0.03)\times10^{-1}$	$4.04(\pm0.14)\times10^{-1}$	1.51

[a] Observed pseudo-first-order rate constant for reactions of dinitroanilines in native P8 porewaters (Apr 2010). Errors represent one standard deviation from duplicate experiments. [b] Observed pseudo-first-order rate constant for reactions of dinitroanilines in filter-sterilized P8 porewaters (Apr 2010). Errors represent one standard deviation from duplicate experiments.

Table 3.3 Rate constants for reactions of dinitroanilines in sulfide redox buffers

Dinitroaniline	$k_{obs,\ H_2S}$ (hr^{-1})[a]	$k_{calc,\ H_2S_n}$ (hr^{-1})[b]	$k_{calc,\ HS^-}$ ($M^{-1}.s^{-1}$)[c]	$k_{calc,\ S_n^{2-}}$ ($M^{-1}.s^{-1}$)[d]	$\frac{k_{calc,\ S_n^{2-}}}{k_{calc,\ HS^-}}$
Trifluralin	$1.60(\pm0.06)\times10^{-2}$	$6.60(\pm1.25)\times10^{-3}$	$2.22(\pm0.07)\times10^{-3}$	$3.88(\pm1.02)\times10^{-2}$	17
Ethalfluralin	$2.49(\pm0.02)\times10^{-2}$	$1.13(\pm0.83)\times10^{-3}$	$3.46(\pm0.03)\times10^{-3}$	$6.66(\pm0.64)\times10^{-2}$	19
Benfluralin	$2.14(\pm0.07)\times10^{-2}$	$9.10(\pm1.75)\times10^{-3}$	$2.97(\pm0.08)\times10^{-3}$	$5.36(\pm1.42)\times10^{-2}$	18
Pendimethalin	$2.30(\pm0.10)\times10^{-3}$	$1.20(\pm0.22)\times10^{-3}$	$3.20(\pm0.13)\times10^{-4}$	$7.06(\pm1.82)\times10^{-3}$	22
Isopropalin	$8.80(\pm0.30)\times10^{-3}$	$3.40(\pm0.67)\times10^{-3}$	$1.22(\pm0.03)\times10^{-3}$	$2.00(\pm0.55)\times10^{-2}$	16
Butralin	$4.90(\pm0.20)\times10^{-3}$	$2.00(\pm0.45)\times10^{-3}$	$6.81(\pm0.26)\times10^{-4}$	$1.18(\pm0.37)\times10^{-2}$	17
Nitralin	$1.91(\pm0.10)\times10^{-1}$	$8.61(\pm0.74)\times10^{-2}$	$2.66(\pm0.04)\times10^{-2}$	$5.07(\pm0.58)\times10^{-1}$	19

[a] Observed pseudo-first-order rate constant for reactions of dinitroanilines in hydrogen sulfide buffer. Errors represent one standard deviation from duplicate experiments. [b]Calculated pseudo-first-order rate constant for reactions of dinitroanilines in polysulfide buffer after subtracting the contribution from hydrogen sulfide. Errors represent one standard deviation from duplicate experiments. [c] Calculated second-order rate constant for reactions of dinitroanilines with HS^- (at 23±2 ℃) calculated as $k_{obs,\ H_2S}$ / $[HS^-]_{calc}$. Errors were calculated through propagation of errors associated with $k_{obs,\ H_2S}$ and $[HS^-]_{calc}$. [d] Calculated second-order rate constant for reactions of dinitroanilines with S_n^{2-} (at 23±2 ℃) calculated as ($k_{obs,\ H_2S+H_2S_n}$ - $k_{obs,\ H_2S}$) / $\Sigma[S_n^{2-}]_{calc}$. Errors were calculated through propagation of errors associated with $k_{obs,\ H_2S}$, $k_{obs,\ H_2S+H_2S_n}$, and $\Sigma[S_n^{2-}]_{calc}$.

For all dinitroanilines, a greater reactivity toward S_n^{2-} than HS^- was found, suggesting that S_n^{2-} species are indeed much more reactive reductants ($k_{S_n^{2-}}/k_{HS^-}$ = 16 to 22; see Table 3.3). Meanwhile, reactions in hydrogen sulfide and polysulfide redox buffers were not markedly slower than those in the porewaters based on the comparison of rate constants. This seems to contrast with the slow direct reduction of monosubstituted NACs by HS^- shown in earlier studies.[32,33,49] A plausible explanation for the significant direct reduction by HS^- and S_n^{2-} is that the two nitro groups on dinitroanilines may exhibit higher electron affinities, making them susceptible to faster reduction. In fact, previous work has shown that the direct reduction of polysubstituted NACs by HS^- can account for up to 35% of their overall reactivities in the H_2S-juglone system.[8] An alternative interpretation is that the transfer of the first electron may not be the actual, or at least is not the only, rate-limiting step in the direct reduction of dinitroanilines. An earlier study has also argued that the mechanism for dinitroaniline reduction in the Fe(II)-goethite system differs from that for monosubstituted NACs.[83] Linear free energy relationships (LFERs) based upon estimated one-electron reduction potential (see Figure B.4) and cross-correlation analysis between the rate constants obtained in the porewaters and sulfide redox buffers (see Figure B.5) were developed to explore such possibility. A detailed interpretation of these analyses is provided in Appendix B.4. The LFERs have slopes of order 4, indicating that processes other than the first electron transfer are rate limiting, violating the underlying assumption of the LFER. The LFERs are still presented given their *potential use* for predicting rate constants (see Table B.3), despite their lack of insight into the rate-limiting step.

It should be pointed out that observed sulfite (SO_3^{2-}) and thiosulfate ($S_2O_3^{2-}$) concentrations in PPL porewaters reached 30 μM and 100 μM, respectively (see Table B.8), which are comparable to the levels reported for marine sediment porewaters.[91,92] In an effort to further assess the possible importance of these species, the transformation of ethalfluralin was investigated in complementary sulfite and thiosulfate control buffers (see Table B.4). It was found that neither SO_3^{2-} nor $S_2O_3^{2-}$ exhibited apparent reactivity towards dinitroanilines both prior to and after juglone was added to serve as an electron transfer mediator (see Figure B.6). According to the standard reduction potentials of relevant sulfur redox couples (e.g., HS^-, S_n^{2-}, SO_3^{2-}, $S_2O_3^{2-}$; see Table B.5), it appears that SO_3^{2-} and $S_2O_3^{2-}$ are thermodynamically capable of reducing dinitroanilines. Previous studies, however, have shown that SO_3^{2-} and $S_2O_3^{2-}$ may only act as nucleophiles and undergo rapid reversible formation of anionic Meisenheimer complexes with NACs including dinitroanilines.[93-96] Such reversible reactions, however, did not seem to compete with the reductive transformation promoted by HS^- and S_n^{2-}.

Analysis of kinetic data allows delineation of the relative importance of dinitroaniline transformation pathways in the porewaters. The observed reaction rate is a joint contribution of all concurrent reaction pathways and can be approximated by summing relevant rates assuming pseudo-first-order kinetics (Equation (3.3)):

$$-\frac{dC}{dt} = k_{obs} \cdot C = \left(k_{HS^-} \cdot [HS^-] + k_{S_n^{2-}} \cdot \Sigma [S_n^{2-}] + k_{other} \right) \cdot C \qquad (3.3)$$

where C is the concentration of target dinitroaniline, k_{HS^-} and $k_{S_n^{2-}}$ are the second-order rate constants for reactions with HS^- and S_n^{2-}, and k_{other} is the rate constant for other processes. The contributions of HS^- and S_n^{2-} to k_{obs} were estimated by multiplying their concentrations in the porewaters (see Table 3.1) and the second-order rate constants determined in the sulfide redox buffers (see Table 3.3). With this assumption, the average percent contributions of HS^- and S_n^{2-} to the overall reactivity of the seven dinitroanilines in native and filter-sterilized porewaters are illustrated in Figure 3.2.

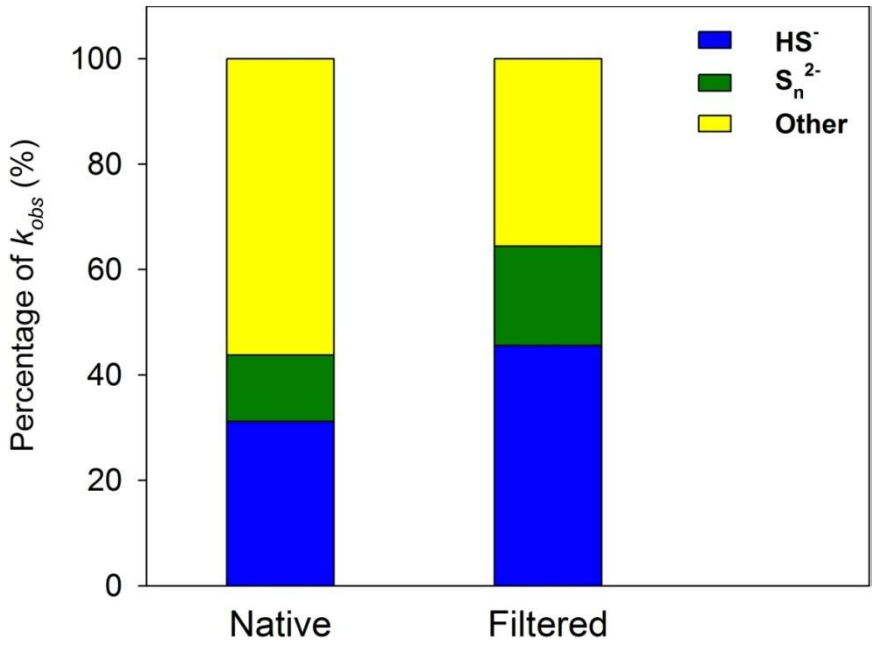

Figure 3.2 Average percent contributions of HS^-, S_n^{2-}, and other processes to dinitroaniline transformation in native and filter-sterilized P8 porewaters (Apr 2010). Stacked bars plotted using calculated values in Table B.6.

In native porewaters, the reaction with HS^- accounts for the largest fraction (~31%) of k_{obs}. Polysulfides are inherently more reactive reductants, but because their concentrations are two orders of magnitude lower than that of the HS^-, the overall influence of S_n^{2-} on k_{obs} is secondary (~13%). Meanwhile, a significant portion (~56%) of

k_{obs} cannot be explained by HS^- and S_n^{2-}, indicating that some porewater constituent(s) other than reduced sulfur species are also responsible for the observed reactions. In filter-sterilized porewaters, the largest fraction (~46%) of k_{obs} can be attributed to HS^-, while a smaller contribution (~19%) to k_{obs} stems from S_n^{2-}. But again, unrecognized reagents or processes are also important contributors to k_{obs} (~35%). Based on these estimations, it is evident that high concentrations of HS^- and S_n^{2-} alone *did not suffice to promote the rapid transformation of dinitroanilines*. The abundance of HS^- and S_n^{2-}, however, is still expected to be a key factor in the abiotic reduction of dinitroanilines in PPL porewaters

To further test the role of reduced sulfur species in direct and DOM-mediated reduction of dinitroanilines, the transformation of ethalfluralin was investigated in silver nitrate-amended and air-sparged (i.e., oxidized) porewaters, respectively (Figure 3.3; see Appendix B.10 for additional details). The purpose of $AgNO_3$ addition was to lower the reduced sulfur concentrations in the porewaters by forming precipitates with HS^- and S_n^{2-} species. Air sparging, on the other hand, was used to remove the reducing capacity of porewaters. As anticipated, the concentrations of reduced sulfur species decreased as increasing amounts of $AgNO_3$ were added into porewaters, while no detectable amounts of reduced sulfur species were found in oxidized porewaters (see Table B.12). The reaction rates of ethalfluralin decreased and correlated well with decreasing total reduced sulfur concentrations (see Figure B.9). No reactivity of ethalfluralin was observed when the reduced sulfur level was lowered down to zero after the addition of excess $AgNO_3$. Similarly, ethalfluralin was unreactive in oxidized porewaters, which could possibly be attributed to the loss of reduced sulfur species and redox-active DOM constituents upon

oxidization. In principle, both the reduced sulfur species and the redox-active DOM could be responsible for the reductive transformation of dinitroanilines in PPL porewaters. Unless the electron accepting capacity (EAC) of DOM present in PPL porewaters is considerably lower than DOM that have been investigated in other studies, these DOM should possess sufficiently high reducing capacity to promote the reduction of dinitroanilines. If one assumes that the EAC and the carbon content of porewater DOM are ~1000 μmol e^-/g and ~45 mmol C/g, respectively (average values reported for a range of terrestrial and aquatic humic and fulvic acids in ref *45*), the predicted reducing capacity of DOM (~110 mg C/L; see Table 3.1) could then explain the transformation of up to half of the amount of dinitroanilines that were initially spiked in PPL porewaters. Thus, removing the reduced sulfur species by precipitation alone should not completely quench the ethalflluralin reactivity because the reducing power of DOM should still persist. It is therefore suspected that the addition of silver ions might simultaneously prevent the interaction of ethalfluralin with porewater DOM by blocking the redox-active sites via complexation and/or chelation.[97] Given that the silver ion is a soft acid and that redox-active mercapto functional groups associated with DOM are soft bases, this explanation appears to be plausible. Overall, the inhibitory influence of $AgNO_3$ addition and oxidation provided strong evidence that reduced sulfur species indeed served critical roles in the transformation of dinitroanilines.

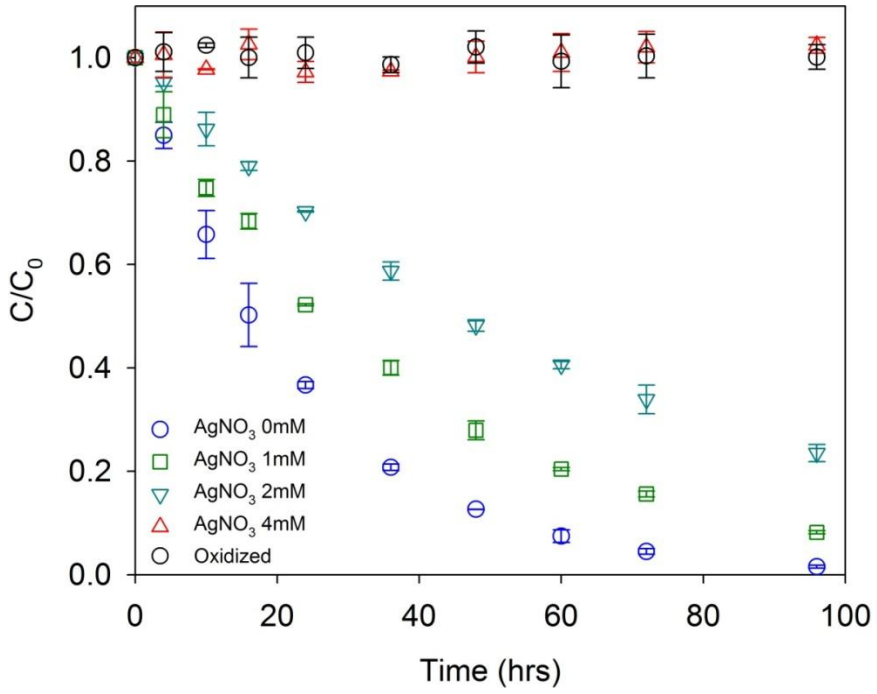

Figure 3.3 Time courses for ethalfluralin transformation in $AgNO_3$-amended and oxidized P8 porewaters (Sep 2010). Error bars represent one standard deviation of duplicate measurements; where absent, bars fall within symbols. "$AgNO_3$ 0mM" to "$AgNO_3$ 4mM" denote reactions in the porewaters that were amended with 0, 1, 2, and 4 mM $AgNO_3$, respectively. "Oxidized" denotes reactions in the air-sparged porewaters. All modified porewaters were filter-sterilized before reactions were initiated. The bisulfide ($[HS^-]$) and polysulfide dianion ($\Sigma[S_n^{2-}]$) concentrations in each modified porewaters are summarized in Table B.13. Note that no hydrogen sulfide or polysulfides was detected in either porewaters amended with 4 mM $AgNO_3$ or porewaters sparged with air.

No attempts were made to quantify the exact contribution of DOM for two reasons. First, the observed rate constants in the porewaters may have resulted from a combination of at least two reactions: slow direct reduction by HS^- or S_n^{2-} and faster DOM-mediated reactions. These two processes are often interconnected and occur simultaneously, rendering it difficult to separate the contribution of DOM from those of HS^- and S_n^{2-}. Second, the redox properties of model NOM or quinone compounds at best bear little similarity to the PPL porewater DOM, so it is difficult to reproduce the actual DOM-mediated processes in the porewaters by using those surrogate compounds.

Ultimately, the interpretation of the role of DOM is limited by our understanding of the nature and abundances of redox-labile functionalities in PPL DOM as well as the dependence of their reactivities on the chemistry of porewaters.

3.3.2 Reactivity Discrepancy between Native and Filtered Porewaters

A series of experiments were performed to further investigate the identity of unknown species that might account for the observed discrepancy in reactivity of native and filter-sterilized porewaters. Several possible reactive entities other than reduced sulfur species were evaluated, including DOM, microorganisms, and filterable mineral phases.

Prior work has demonstrated that reduction rates of dinitroanilines accelerate with increasing juglone concentrations in the H_2S-juglone system.[83] Conversely, elevated DOM levels in the Fe(II)-DOM system were shown to impede the reduction of dinitroanilines,[85] which could in part be explained by the existence of Fe(II) complexing ligands in non-reactive DOM moieties that might decrease the overall reducing capacity of Fe(II) by forming less reactive Fe(II)-DOM complexes.[13,85] In the porewaters, it is expected that the change of DOC level caused by the filtration step, if significant, would affect the reaction rates of dinitroanilines. The difference in the measured DOC between native and filter-sterilized porewaters, however, was only ~4 mg C/L (see Table 3.1). Such slight divergence in the DOC levels was most probably associated with analytical errors and should not account for the pronounced drop of dinitroaniline reaction rates in filter-sterilized porewaters.

Anaerobic biodegradation of dinitroanilines has been well documented, which often involves the reduction of nitro groups followed by dealkylation of propylamines.[98-102] To evaluate the possible contribution of biodegradation, the transformation of ethalfluralin was investigated in sterilized native porewaters. Sodium azide, which has been shown to inhibit microbially-mediated NAC reduction[103] and sulfur transformations,[104] was added into native porewaters as a biological inhibitor. Heat sterilization of porewaters was avoided due to concerns about the unintended shift of original reduced sulfur speciation at high temperatures.[105] It was found that the reaction rates of ethalfluralin in unmodified and NaN_3-treated porewaters were not statistically different from one another (see Figure B.10), indicating that direct biodegradation of dinitroanilines was minimal. This observation further corroborates that the bulk of the dinitroaniline transformation in native porewaters is abiotic in origin. It should be noted that exudates of microorganisms might also function as the electron transfer mediator. The reactivity of these exudates can be two orders of magnitude higher than freshwater DOM isolates, and are on the similar order to that of the model quinone compounds.[33,106] Previous research has demonstrated that the 0.2 μm pore-size filtrate of *Streptomyces sp.* culture could effectively mediate the reduction of nitrobenzenes in the hydrogen sulfide system.[106] Such exudates, if present, might explain a fraction of dinitroaniline reactivity in filter-sterilized porewaters.

Despite the fact that a relatively high iron content was found in PPL sediments (see Table B.7 and Figure B.7), only trace levels of Fe(II) were present in PPL porewaters (~9 μg/L; see Table B.9). The transformation of dinitroanilines promoted by

dissolved Fe(II) or Fe(II)-DOM complexes is therefore considered unimportant in PPL porewaters. In the absence of dissolved Fe(II), Fe(II) associated with minerals (i.e., structural or adsorbed Fe(II)) may represent another major pool of reactive Fe(II) species in the reduction of dinitroanilines. Structural Fe(II) in smectite was previously postulated as a primary reductant in rapid trifluralin transformations in anoxic agricultural soils.[82] In controlled Fe(II)-goethite systems, dinitroanilines have been shown to undergo rapid reduction through a surface-mediated process that typically includes sequential reduction of nitro groups, dealkylation of propylamines, and cyclization between the α carbon of a propylamine and a nitro group.[83,84] Enhanced reaction kinetics of dinitroanilines in native porewaters, therefore, may stem from reaction with filterable mineral phases. To assess such possibility, DLS analysis was first performed to characterize the particle size distribution in native and 0.2 μm filter-sterilized porwaters, followed by ICP-OES and XRD analysis of unused and used 0.22 μm membrane filters to confirm the identity of filtered materials. The use of 0.22 μm membrane filters instead of 0.2 μm syringe filters was justified by experimental data showing no statistical difference in the reaction rates of ethalfluralin in 0.2 μm filtered and 0.22 μm filtered porewaters (see Figure B.11). DLS analysis (see Table B.10) revealed that the average particle size in native porewaters was larger than that in filter-sterilized porewaters, indicating that removal of particles from native porewaters occurred during the filtration. ICP-OES analysis (see Table B.11) and XRD analysis (see Figure B.8) on the identity of filtered materials, however, were inconclusive due to insufficient mass collected plus the background interferences from the filter.

To clarify further the role of filtered materials, the transformation of ethalfluralin was studied in control buffers containing substances sonicated from 0.22 μm membrane filters after vacuum filtration of 10 mL native porewaters (Figure 3.4; see B.13 for additional details).

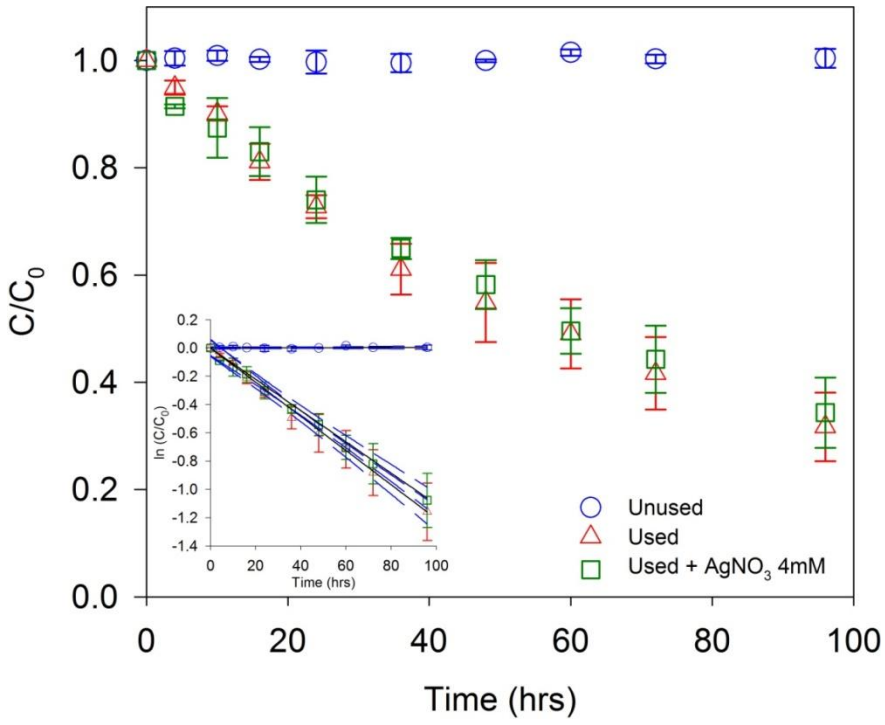

Figure 3.4 Time courses for ethalfluralin transformation in the Tris buffer containing substances sonicated from 0.22 μm membrane filters. Error bars represent one standard deviation of duplicate samples; where absent, bars fall within symbols. Inset depicts the same data plotted in semilogarithmic form. Solid lines represent linear regressions and dashed lines represent 95% confidence intervals. $R^2 > 0.95$. "Unused" and "Used" denote reactions in the Tris buffer sonicated with unused and used membrane filters, respectively. "Used + $AgNO_3$ 4mM" denotes reactions in the Tris buffer sonicated with used membrane filters that were further amended with 4 mM $AgNO_3$.

It was found that materials retained on 0.22 μm membrane filters could promote the reaction of ethalfluralin with the value of k_{obs} (1.23 (±0.22)×10^{-2} hr^{-1}) on the same order of magnitude of that obtained in native porewaters. In this case, reduced sulfur species or DOM did not seem to play a role in that the reaction rate was not significantly

affected by the addition of excess $AgNO_3$; instead, metal sulfide minerals are the most likely source of reactive phases in anoxic environments where excess reduced sulfur exists, such as PPL porewaters.[107,108] In fact, the low concentrations of trace metals in sulfur-rich freshwater sediment has recently been traced to the scavenging of metal ions by sulfide minerals.[109] Depending on their solubility and dissolution rates, a variety of sulfide minerals, such as CoS, FeS_2, MnS, and ZnS have been shown to promote NAC reduction under anoxic conditions.[110-112] An alternative identity hypothesized for filtered materials is black carbon particles given the high organic carbon content in PPL sediments (see Table B.7). Previous research has confirmed that black carbon could serve as a redox mediator to promote NAC reduction in the presence of dithiothreitol or hydrogen sulfide as a bulk reductant.[113-115] Although the observed transformation of ethalfluralin cannot be taken as a quantitative assessment of contribution from the filtered materials, it is a plausible explanation for the unaccounted abiotic processes in native PPL porewaters (yellow bar labeled "other" in Figure 3.2). It also points to the importance of surface-mediated processes to the overall transformation of dinitroanilines in addition to the aqueous phase reduction reactions. The morphology and composition of the substances filtered from native porewaters, therefore, merit further investigation to fully interpret the results obtained herein.

3.3.3 Transformation Products of Dinitroanilines

The primary dinitroaniline transformation products observed in PPL porewaters were diamine (1-NH_2) and/or triamine (2-NH_2) compounds. Neither dealkylation nor cyclization (i.e., benzimidazole) products were detected as reported for the surface-

mediated reduction of dinitroanilines.[83,84] The transformation of dinitroanilines appeared to follow the well-established pathway of sequential reduction of the two nitro groups, each of which involves transfer of six electrons (Figure 3.5). The GC-MS/MS total ion chromatogram and mass spectra of parent pesticides and products are provided in the SI (see Figure B.13-Figure B.26).

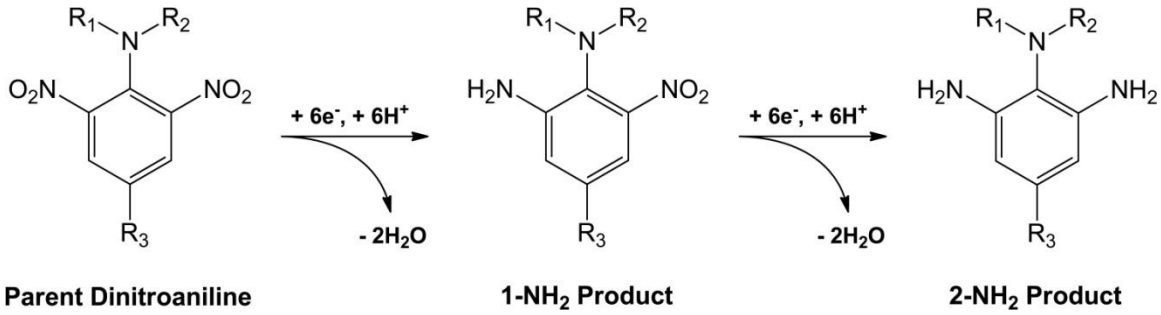

Figure 3.5 Schematic of reductive transformation of dinitroanilines.

Depending on their reaction rates, a distinct trend of product distribution was found for target dinitroanilines. For the faster reacting pesticides (e.g., trifluralin, ethalfluralin, and benfluralin), identified products included both 1-NH_2 and 2-NH_2, implying that the parent compound might initially undergo rapid reduction of the first nitro group to form 1-NH_2, followed by partial reduction of the second nitro group to form 2-NH_2. For the slower reacting pesticides, (e.g., pendimethalin, isopropalin, and butralin), only 1-NH_2 was observed, so it is likely that the second nitro reduction was inhibited or proceeded too slowly to form a detectable amount of 2-NH_2. For the fastest reacting pesticide (i.e., nitralin), only 2-NH_2 was observed, suggesting that 1-NH_2 was an intermediate that was fully reduced to 2-NH_2 within the experimental time scale. Also noteworthy is the fact that the reducible sulfone group on nitralin was not reduced under the experimental conditions. These observations are consistent with previous findings

that the rate of reduction of the first nitro group is generally much faster than the rate of reduction of the remaining nitro groups for polynitroaromatic compounds, which is often attributed to the lower reduction potential of 1-NH_2 relative to the parent compound.[34]

The amine products resulting from dinitroaniline reduction could potentially undergo nucleophilic addition reactions with the carbonyl functionality of DOM and become incorporated in the form of anilinohydroquinone, anilinoquinone, anilide, imine, or heterocyclic nitrogen.[116,117] Thus, an additional role for DOM in PPL porewaters would be to serve as a permanent sink for the amine products of dinitroanilines. The mechanism and the extent to which transformation products may become irreversibly bound to DOM, however, are beyond the scope of the current study.

3.4 Summary

In this study, we demonstrated that dinitroaniline pesticides could be effectively transformed in native and filter-sterilized PPL sediment porewaters to corresponding amine products. The rate and extent of dinitroaniline transformation in PPL porewaters was greater than in sulfide redox buffers containing comparable levels of reduced sulfur species (i.e., HS^- and S_n^{2-}). Specifically, direct reduction by reduced sulfur species and DOM-mediated reduction processes seemed to dominate the abiotic reduction of dinitroanilines. Other porewater constituents, such as filterable mineral particles, might also act as additional redox-active phases. Future studies should also focus on the reactive capacity of the sediments to effect pesticide transformations. These findings, together with a previous report of abiotic transformation of chloroacetanilide pesticides in PPL porewaters,[86] provide compelling evidence that reduced sulfur species can serve as both

reductants and nucleophiles that react with a suite of pesticides. Results from this study may have important implications for understanding how PPLs function to attenuate agrochemicals widely used in the PPR as well as assessment of the environmental significance and fate of their transformation products. Finally, PPLs are highly sensitive to the spatial and temporal variations of temperature and precipitation.[118-120] The effects of transient changes in PPL water chemistry on the abiotic transformation of agrochemicals warrant further study.

3.5 References

1. Ju, K.-S.; Parales, R. E., Nitroaromatic compounds, from synthesis to biodegradation. *Microbiol. Mol. Biol. Rev.* **2010,** *74*, 250-272.
2. Schwarzenbach, R. P.; Gschwend, P. M.; Imboden, D. M., *Environmental Organic Chemistry*. John Wiley & Sons, Inc.: Hoboken, NJ, 2003.
3. Wahid, P. A.; Ramakrishna, C.; Sethunathan, N., Instantaneous degradation of parathion in anaerobic soils. *J. Environ. Qual.* **1980,** *9*, 127-130.
4. Wolfe, N. L.; Kitchens, B. E.; Macalady, D. L.; Grundl, T. J., Physical and chemical factors that influence the anaerobic degradation of methyl parathion in sediment systems. *Environ. Toxicol. Chem.* **1986,** *5*, 1019-1026.
5. Heijman, C. G.; Holliger, C.; Glaus, M. A.; Schwarzenbach, R. P.; Zeyer, J., Abiotic reduction of 4-chloronitrobenzene to 4-chloroaniline in a dissimilatory iron-reducing enrichment culture. *Appl. Environ. Microbiol.* **1993,** *59*, 4350-4353.
6. Heijman, C. G.; Grieder, E.; Holliger, C.; Schwarzenbach, R. P., Reduction of nitroaromatic compounds coupled to microbial iron reduction in laboratory aquifer columns. *Environ. Sci. Technol.* **1995,** *29*, 775-783.
7. Rügge, K.; Hofstetter, T. B.; Haderlein, S. B.; Bjerg, P. L.; Knudsen, S.; Zraunig, C.; Mosbæk, H.; Christensen, T. H., Characterization of predominant reductants in an anaerobic leachate-contaminated aquifer by nitroaromatic probe compounds. *Environ. Sci. Technol.* **1998,** *32*, 23-31.
8. Hofstetter, T. B.; Heijman, C. G.; Haderlein, S. B.; Holliger, C.; Schwarzenbach, R. P., Complete reduction of TNT and other (poly)nitroaromatic compounds under iron-reducing subsurface conditions. *Environ. Sci. Technol.* **1999,** *33*, 1479-1487.
9. Simon, R.; Colón, D.; Tebes-Stevens, C. L.; Weber, E. J., Effect of redox zonation on the reductive transformation of *p*-cyanonitrobenzene in a laboratory sediment column. *Environ. Sci. Technol.* **2000,** *34*, 3617-3622.
10. Hoferkamp, L. A.; Weber, E. J., Nitroaromatic reduction kinetics as a function of dominant terminal electron acceptor processes in natural sediments. *Environ. Sci. Technol.* **2006,** *40*, 2206-2212.

11. Tobler, N. B.; Hofstetter, T. B.; Schwarzenbach, R. P., Assessing iron-mediated oxidation of toluene and reduction of nitroaromatic contaminants in anoxic environments using compound-specific isotope analysis. *Environ. Sci. Technol.* **2007,** *41*, 7773-7780.
12. Tratnyek, P. G.; Weber, E. J.; Schwarzenbach, R. P., Quantitative structure-activity relationships for chemical reductions of organic contaminants. *Environ. Toxicol. Chem.* **2003,** *22*, 1733-1742.
13. Hakala, J. A.; Fimmen, R. L.; Chin, Y.-P.; Agrawal, S. G.; Ward, C. P., Assessment of the geochemical reactivity of Fe-DOM complexes in wetland sediment pore waters using a nitroaromatic probe compound. *Geochim. Cosmochim. Acta* **2009,** *73*, 1382-1393.
14. Yan, L.; Bailey, G. W., Sorption and abiotic redox transformation of nitrobenzene at the smectite-water interface. *J. Colloid Interface Sci.* **2001,** *241*, 142-153.
15. Hofstetter, T. B.; Schwarzenbach, R. P.; Haderlein, S. B., Reactivity of Fe(II) species associated with clay minerals. *Environ. Sci. Technol.* **2003,** *37*, 519-528.
16. Hofstetter, T. B.; Neumann, A.; Schwarzenbach, R. P., Reduction of nitroaromatic compounds by Fe(II) species associated with iron-rich smectites. *Environ. Sci. Technol.* **2005,** *40*, 235-242.
17. Neumann, A.; Hofstetter, T. B.; Lüssi, M.; Cirpka, O. A.; Petit, S.; Schwarzenbach, R. P., Assessing the redox reactivity of structural iron in smectites using nitroaromatic compounds as kinetic probes. *Environ. Sci. Technol.* **2008,** *42*, 8381-8387.
18. Hofstetter, T. B.; Neumann, A.; Arnold, W. A.; Hartenbach, A. E.; Bolotin, J.; Cramer, C. J.; Schwarzenbach, R. P., Substituent effects on nitrogen isotope fractionation during abiotic reduction of nitroaromatic compounds. *Environ. Sci. Technol.* **2008,** *42*, 1997-2003.
19. Gorski, C. A.; Scherer, M. M., Influence of magnetite stoichiometry on Fe^{II} uptake and nitrobenzene reduction. *Environ. Sci. Technol.* **2009,** *43*, 3675-3680.
20. Gorski, C. A.; Nurmi, J. T.; Tratnyek, P. G.; Hofstetter, T. B.; Scherer, M. M., Redox behavior of magnetite: Implications for contaminant reduction. *Environ. Sci. Technol.* **2010,** *44*, 55-60.
21. Klausen, J.; Troeber, S. P.; Haderlein, S. B.; Schwarzenbach, R. P., Reduction of substituted nitrobenzenes by Fe(II) in aqueous mineral suspensions. *Environ. Sci. Technol.* **1995,** *29*, 2396-2404.
22. Schultz, C. A.; Grundl, T. J., pH Dependence on reduction rate of 4-Cl-nitrobenzene by Fe(II)/montmorillonite systems. *Environ. Sci. Technol.* **2000,** *34*, 3641-3648.
23. Elsner, M.; Schwarzenbach, R. P.; Haderlein, S. B., Reactivity of Fe(II)-bearing minerals toward reductive transformation of organic contaminants. *Environ. Sci. Technol.* **2004,** *38*, 799-807.
24. Klupinski, T. P.; Chin, Y.-P.; Traina, S. J., Abiotic degradation of pentachloronitrobenzene by Fe(II): Reactions on goethite and iron oxide nanoparticles. *Environ. Sci. Technol.* **2004,** *38*, 4353-4360.
25. Colón, D.; Weber, E. J.; Anderson, J. L., QSAR study of the reduction of nitroaromatics by Fe(II) species. *Environ. Sci. Technol.* **2006,** *40*, 4976-4982.

26. Larese-Casanova, P.; Cwiertny, D. M.; Scherer, M. M., Nanogoethite formation from oxidation of Fe(II) sorbed on aluminum oxide: Implications for contaminant reduction. *Environ. Sci. Technol.* **2010,** *44*, 3765-3771.
27. Naka, D.; Kim, D.; Strathmann, T. J., Abiotic reduction of nitroaromatic compounds by aqueous iron(II)-catechol complexes. *Environ. Sci. Technol.* **2006,** *40*, 3006-3012.
28. Hakala, J. A.; Chin, Y.-P.; Weber, E. J., Influence of dissolved organic matter and Fe(II) on the abiotic reduction of pentachloronitrobenzene. *Environ. Sci. Technol.* **2007,** *41*, 7337-7342.
29. Naka, D.; Kim, D.; Carbonaro, R. F.; Strathmann, T. J., Abiotic reduction of nitroaromatic contaminants by iron(II) complexes with organothiol ligands. *Environ. Toxicol. Chem.* **2008,** *27*, 1257-1266.
30. Hartenbach, A. E.; Hofstetter, T. B.; Aeschbacher, M.; Sander, M.; Kim, D.; Strathmann, T. J.; Arnold, W. A.; Cramer, C. J.; Schwarzenbach, R. P., Variability of nitrogen isotope fractionation during the reduction of nitroaromatic compounds with dissolved reductants. *Environ. Sci. Technol.* **2008,** *42*, 8352-8359.
31. Colón, D.; Weber, E. J.; Anderson, J. L., Effect of natural organic matter on the reduction of nitroaromatics by Fe(II) species. *Environ. Sci. Technol.* **2008,** *42*, 6538-6543.
32. Schwarzenbach, R. P.; Stierli, R.; Lanz, K.; Zeyer, J., Quinone and iron porphyrin mediated reduction of nitroaromatic compounds in homogeneous aqueous solution. *Environ. Sci. Technol.* **1990,** *24*, 1566-1574.
33. Dunnivant, F. M.; Schwarzenbach, R. P.; Macalady, D. L., Reduction of substituted nitrobenzenes in aqueous solutions containing natural organic matter. *Environ. Sci. Technol.* **1992,** *26*, 2133-2141.
34. Barrows, S. E.; Cramer, C. J.; Truhlar, D. G.; Elovitz, M. S.; Weber, E. J., Factors controlling regioselectivity in the reduction of polynitroaromatics in aqueous solution. *Environ. Sci. Technol.* **1996,** *30*, 3028-3038.
35. Guo, X.; Jans, U., Kinetics and mechanism of the degradation of methyl parathion in aqueous hydrogen sulfide solution: Investigation of natural organic matter effects. *Environ. Sci. Technol.* **2006,** *40*, 900-906.
36. Hartenbach, A.; Hofstetter, T. B.; Berg, M.; Bolotin, J.; Schwarzenbach, R. P., Using nitrogen isotope fractionation to assess abiotic reduction of nitroaromatic compounds. *Environ. Sci. Technol.* **2006,** *40*, 7710-7716.
37. Sposito, G., Electron shuttling by natural organic matter: Twenty years after. In *Aquatic Redox Chemistry*, Tratnyek, P. G.; Grundl, T. J.; Haderlein, S. B., Eds. American Chemical Society: Washington, DC, 2011; Vol. 1071, pp 113-127.
38. Tratnyek, P. G.; Macalady, D. L., Abiotic reduction of nitro aromatic pesticides in anaerobic laboratory systems. *J. Agric. Food. Chem.* **1989,** *37*, 248-254.
39. Perlinger, J. A.; Kalluri, V. M.; Venkatapathy, R.; Angst, W., Addition of hydrogen sulfide to juglone. *Environ. Sci. Technol.* **2002,** *36*, 2663-2669.
40. Nurmi, J. T.; Tratnyek, P. G., Electrochemical properties of natural organic matter (NOM), fractions of NOM, and model biogeochemical electron shuttles. *Environ. Sci. Technol.* **2002,** *36*, 617-624.

41. Cory, R. M.; McKnight, D. M., Fluorescence spectroscopy reveals ubiquitous presence of oxidized and reduced quinones in dissolved organic matter. *Environ. Sci. Technol.* **2005,** *39*, 8142-8149.
42. Heitmann, T.; Blodau, C., Oxidation and incorporation of hydrogen sulfide by dissolved organic matter. *Chem. Geol.* **2006,** *235*, 12-20.
43. Ratasuk, N.; Nanny, M. A., Characterization and quantification of reversible redox sites in humic substances. *Environ. Sci. Technol.* **2007,** *41*, 7844-7850.
44. Macalady, D. L.; Walton-Day, K., New light on a dark subject: On the use of fluorescence data to deduce redox states of natural organic matter (NOM). *Aquat. Sci.* **2009,** *71*, 135-143.
45. Aeschbacher, M.; Sander, M.; Schwarzenbach, R. P., Novel electrochemical approach to assess the redox properties of humic substances. *Environ. Sci. Technol.* **2010,** *44*, 87-93.
46. Aeschbacher, M.; Vergari, D.; Schwarzenbach, R. P.; Sander, M., Electrochemical analysis of proton and electron transfer equilibria of the reducible moieties in humic acids. *Environ. Sci. Technol.* **2011,** *45*, 8385-8394.
47. Hojo, M.; Takagi, Y.; Ogata, Y., Kinetics of the reduction of nitrobenzenes by sodium disulfide. *J. Am. Chem. Soc.* **1960,** *82*, 2459-2462.
48. Cope, O. J.; Brown, R. K., The reduction of nitrobenzene by sodium sulphide in aqueous ethanol. *Can. J. Chem.* **1961,** *39*, 1695-1710.
49. Cope, O. J.; Brown, R. K., The reduction of nitrobenzene by hydrosulphide ion in aqueous media. *Can. J. Chem.* **1962,** *40*, 2317-2328.
50. van der Valk, A. G., The prairie potholes of North America. In *The World's Largest Wetlands*, Fraser, L. H.; Keddy, P. A., Eds. Cambridge University Press: Cambridge, UK, 2005; pp 393-423.
51. Gleason, R. A.; Euliss, N. H.; Tangen, B. A.; Laubhan, M. K.; Browne, B. A., USDA conservation program and practice effects on wetland ecosystem services in the Prairie Pothole Region. *Ecol. Appl.* **2011,** *21*, S65-S81.
52. Dahl, T. E. *Wetland losses in the United States 1780's to 1980's*; U.S. Fish and Wildlife Service: Washington, DC, 1990; pp 1-13.
53. Johnson, R. R.; Oslund, F. T.; Hertel, D. R., The past, present, and future of prairie potholes in the United States. *J. Soil Water Conserv.* **2008,** *63*, 84A-87A.
54. Oslund, F. T.; Johnson, R. R.; Hertel, D. R., Assessing wetland changes in the prairie pothole region of Minnesota from 1980 to 2007. *J. Fish Wildl. Manag.* **2010,** *1*, 131-135.
55. Stubbs, M. *Land conversion in the northern plains*; Resources, Science, and Industry Division, The National Council for Science and the Environment, CRS Report for Congress RL33950: Washington, DC, 2007.
56. Euliss, N. H.; Smith, L. M.; Liu, S.; Feng, M.; Mushet, D. M.; Auch, R. F.; Loveland, T. R., The need for simultaneous evaluation of ecosystem services and land use change. *Environ. Sci. Technol.* **2010,** *44*, 7761-7763.
57. Gascoigne, W. R.; Hoag, D.; Koontz, L.; Tangen, B. A.; Shaffer, T. L.; Gleason, R. A., Valuing ecosystem and economic services across land-use scenarios in the Prairie Pothole Region of the Dakotas, USA. *Ecol. Econ.* **2011,** *70*, 1715-1725.

58. Rashford, B. S.; Walker, J. A.; Bastian, C. T., Economics of grassland conversion to cropland in the prairie pothole region. *Conserv. Biol.* **2011,** *25*, 276-284.
59. Olness, A.; Staricka, J. A.; Daniel, J. A., Oxidation-reduction and groundwater contamination in the Prairie Pothole region of the Northern Great Plains. In *Water for Agriculture and Wildlife and the Environment -- Win-Win Opportunities: Proceedings of the 1996 USCID Wetlands Seminar*, Schaack, J.; Anderson, S. S., Eds. U.S. Committee on Irrigation and Drainage: Denver, CO, 1996; pp 115-131.
60. Goldsborough, L. G.; Crumpton, W. G., Distribution and environmental fate of pesticides in prairie wetlands. *Great Plains Res.* **1998,** *8*, 73-95.
61. Donald, D. B.; Narine, P. G.; Lynne, Q.-A.; Kevin, C., Diffuse geographic distribution of herbicides in northern prairie wetlands. *Environ. Toxicol. Chem.* **2001,** *20*, 273-279.
62. Detenbeck, N. E.; Elonen, C. M.; Taylor, D. L.; Cotter, A. M.; Puglisi, F. A.; Sanville, W. D., Effects of agricultural activities and best management practices on water quality of seasonal prairie pothole wetlands. *Wetlands Ecol. Manage.* **2002,** *10*, 335-354.
63. Degenhardt, D.; Humphries, D.; Cessna, A. J.; Messing, P.; Badiou, P. H.; Raina, R.; Farenhorst, A.; Pennock, D. J., Dissipation of glyphosate and aminomethylphosphonic acid in water and sediment of two Canadian prairie wetlands. *J. Environ. Sci. Health, Part B* **2012,** *47*, 631-639.
64. Huckins, J. N.; Petty, J. D.; England, D. C., Distribution and impact of trifluralin, atrazine, and fonofos residues in microcosms simulating a northern prairie wetland. *Chemosphere* **1986,** *15*, 563-588.
65. Grover, R.; Waite, D. T.; Cessna, A. J.; Nicholaichuk, W.; Irvin, D. G.; Kerr, L. A.; Best, K., Magnitude and persistence of herbicide residues in farm dugouts and ponds in the Canadian prairies. *Environ. Toxicol. Chem.* **1997,** *16*, 638-643.
66. Cessna, A. J.; Donald, D. B.; Bailey, J.; Waiser, M.; Headley, J. V., Persistence of the sulfonylurea herbicides thifensulfuron-methyl, ethametsulfuron-methyl, and metsulfuron-methyl in farm dugouts (ponds). *J. Environ. Qual.* **2006,** *35*, 2395-2401.
67. Degenhardt, D.; Cessna, A. J.; Raina, R.; Farenhorst, A.; Pennock, D. J., Dissipation of six acid herbicides in water and sediment of two Canadian prairie wetlands. *Environ. Toxicol. Chem.* **2011,** *30*, 1982-1989.
68. Helling, C. S., Dinitroaniline herbicides in soils. *J. Environ. Qual.* **1976,** *5*, 1-15.
69. U.S. Geological Survey, Pesticide National Synthesis Project. *2002 Pesticide Use Maps*; http://water.usgs.gov/nawqa/pnsp/usage/maps/compound_listing.php?year=02 (Accessed August, 2011).
70. Zollinger, R.; McMullen, M.; Knodel, J.; Gray, J.; Jantzi, D.; Kimmet, G.; Hagemeister, K.; Schmitt, C. *Pesticide Use and Pest Management Practices in North Dakota, 2008*; North Dakota State University in cooperation with North Dakota Agricultural Statistics Service Extension Publication W-1446: Fargo, ND, 2009.
71. Gilliom, R. J., Pesticides in U.S. streams and groundwater. *Environ. Sci. Technol.* **2007,** *41*, 3408-3414.
72. U.S. Environmental Protection Agency, National Sediment Quality Survey. *Incidence and Severity of Sediment Contamination in Surface Waters of the United States, Second Edition*; EPA 823-R-04-007; U.S. Environmental Protection Agency:

Washington, DC, 2004. http://water.epa.gov/polwaste/sediments/cs/upload/nsqs2ed-complete-2.pdf (Accessed August, 2011).
73. U.S. Environmental Protection Agency, Persistent Bioaccumulative and Toxic (PBT) Chemical Program. *Pesticides and Other Persistent Bioaccumulative Toxic (PBT) Chemicals*; EPA 260-B-01-005; U.S. Environmental Protection Agency: Washington, DC, 2001. http://www.epa.gov/tri/guide_docs/pdf/2001/pest2001.pdf (Accessed August 2011).
74. Rickert, D. E., *Toxicity of Nitroaromatic Compounds*. Hemisphere Publishing Corp.: Washington, DC, 1985.
75. Weber, J. B., Behavior of dinitroaniline herbicides in soils. *Weed Technol.* **1990,** *4*, 394-406.
76. Belden, J. B.; Phillips, T. A.; Henderson, K. L.; Clark, B. W.; Lydy, M. J.; Coats, J. R., Persistence, mobility, and bioavailability of pendimethalin and trifluralin in Soil. In *Environmental Fate and Effects of Pesticides*, American Chemical Society: Washington, DC, 2003; Vol. 853, pp 167-177.
77. Ciglenecki, I.; Kodba, Z.; Cosovic, B., Sulfur species in Rogoznica Lake. *Mar. Chem.* **1996,** *53*, 101-110.
78. Overmann, J.; Beatty, J. T.; Krouse, H. R.; Hall, K. J., The sulfur cycle in the chemocline of a meromictic salt lake. *Limnol. Oceanogr.* **1996,** *41*, 147-156.
79. Miller, P. L.; Vasudevan, D.; Gschwend, P. M.; Roberts, A. L., Transformation of hexachloroethane in a sulfidic natural water. *Environ. Sci. Technol.* **1998,** *32*, 1269-1275.
80. Chin, Y.-P.; Traina, S. J.; Swank, C. R.; Backhus, D., Abundance and properties of dissolved organic matter in pore waters of a freshwater wetland. *Limnol. Oceanogr.* **1998,** *43*, 1287-1296.
81. O'Loughlin, E. J.; Chin, Y.-P., Quantification and characterization of dissolved organic carbon and iron in sedimentary porewater from Green Bay, WI, USA. *Biogeochemistry* **2004,** *71*, 371-386.
82. Tor, J. M.; Xu, C.; Stucki, J. M.; Wander, M. M.; Sims, G. K., Trifluralin degradation under microbiologically induced nitrate and Fe(III) reducing conditions. *Environ. Sci. Technol.* **2000,** *34*, 3148-3152.
83. Wang, S.; Arnold, W. A., Abiotic reduction of dinitroaniline herbicides. *Water Res.* **2003,** *37*, 4191-4201.
84. Klupinski, T. P.; Chin, Y.-P., Abiotic degradation of trifluralin by Fe(II): Kinetics and transformation pathways. *Environ. Sci. Technol.* **2003,** *37*, 1311-1318.
85. Hakala, J. A.; Chin, Y.-P., Abiotic reduction of pendimethalin and trifluralin in controlled and natural systems containing Fe(II) and dissolved organic matter. *J. Agric. Food. Chem.* **2010,** *58*, 12840-12846.
86. Zeng, T.; Ziegelgruber, K. L.; Chin, Y.-P.; Arnold, W. A., Pesticide processing potential in prairie pothole porewaters. *Environ. Sci. Technol.* **2011,** *45*, 6814-6822.
87. Cline, J. D., Spectrophotometric determination of hydrogen sulfide in natural waters. *Limnol. Oceanogr.* **1969,** *14*, 454-458.
88. Heitz, A.; Kagi, R. I.; Alexander, R., Polysulfide sulfur in pipewall biofilms: Its role in the formation of swampy odour in distribution systems. *Water Sci. Technol.* **2000,** *41*, 271-278.

89. Kristiana, I.; Heitz, A.; Joll, C.; Sathasivan, A., Analysis of polysulfides in drinking water distribution systems using headspace solid-phase microextraction and gas chromatography-mass spectrometry. *J. Chromatogr. A* **2010,** *1217*, 5995-6001.
90. Shea, D.; Helz, G. R., The solubility of copper in sulfidic waters - sulfide and polysulfide complexes in equilibrium with covellite. *Geochim. Cosmochim. Acta* **1988,** *52*, 1815-1825.
91. MacCrehan, W.; Shea, D., Temporal relationship of thiols to inorganic sulfur compounds in anoxic Chesapeake Bay sediment porewater. In *Geochemical Transformations of Sedimentary Sulfur*, Vairavamurthy, M. A.; Schoonen, M. A. A.; Eglinton, T. I.; Luther III, G. W.; Manowitz, B., Eds. American Chemical Society: Washington, DC, 1995; Vol. 612, pp 294-310.
92. Zopfi, J.; Ferdelman, T. G.; Fossing, H., Distribution and fate of sulfur intermediates-sulfite, tetrathionate, thiosulfate, and elemental sulfur-in marine sediments. *Geol. Soc. Am. Spec. Pap.* **2004,** *379*, 97-116.
93. Marendic, N.; Norris, A. R., The interaction of sulfite ion with 2,4,6-trinitrobenzaldehyde: Kinetic, equilibrium, and proton magnetic resonance studies. *Can. J. Chem.* **1973,** *51*, 3927-3935.
94. Buncel, E.; Norris, A. R.; Russell, K. E.; Sheridan, P. J., Kinetic and thermodynamic studies of the reactions of sulfite ion with picramide, *N*-methylpicramide, and *N*,*N*-dimethylpicramide in aqueous solution. *Can. J. Chem.* **1974,** *52*, 25-33.
95. Annandale, M. T.; vanLoon, G. W.; Buncel, E., Regioselectivity and stereoelectronic effects in the reactions of the dinitroaniline herbicides trifluralin and benefin with nucleophiles. *Can. J. Chem.* **1998,** *76*, 873-883.
96. Gallardo, I.; Guirado, G., Thermodynamic study of σ^H complexes in nucleophilic aromatic substitution reactions: Relative stabilities of electrochemically generated radicals. *Eur. J. Org. Chem.* **2008**, 2463-2472.
97. Smith, D. S.; Bell, R. A.; Kramer, J. R., Metal speciation in natural waters with emphasis on reduced sulfur groups as strong metal binding sites. *Comp. Biochem. Physiol., Part C: Toxicol. Pharmacol.* **2002,** *133*, 65-74.
98. Willis, G. H.; Wander, R. C.; Southwick, L. M., Degradation of trifluralin in soil suspensions as related to redox potential. *J. Environ. Qual.* **1974,** *3*, 262-265.
99. Kearney, P. C.; Plimmer, J. R.; Wheeler, W. B.; Kontson, A., Persistence and metabolism of dinitroaniline herbicides in soils. *Pestic. Biochem. Physiol.* **1976,** *6*, 229-238.
100. Camper, N. D.; Stralka, K.; Skipper, H. D., Aerobic and anaerobic degradation of profluralin and trifluralin. *J. Environ. Sci. Health Part B-Pestic. Contam. Agric. Wastes* **1980,** *15*, 457-473.
101. Singh, S. B.; Kulshrestha, G., Microbial-degradation of pendimethalin. *J. Environ. Sci. Health Part B-Pestic. Contam. Agric. Wastes* **1991,** *26*, 309-321.
102. Bellinaso, M. D.; Greer, C. W.; Peralba, M. D.; Henriques, J. A. P.; Gaylarde, C. C., Biodegradation of the herbicide trifluralin by bacteria isolated from soil. *FEMS Microbiol. Ecol.* **2003,** *43*, 191-194.

103. Okutman Tas, D.; Pavlostathis, S. G., Microbial reductive transformation of pentachloronitrobenzene under methanogenic conditions. *Environ. Sci. Technol.* **2005,** *39*, 8264-8272.
104. Burton, E. D.; Bush, R. T.; Sullivan, L. A.; Hocking, R. K.; Mitchell, D. R. G.; Johnston, S. G.; Fitzpatrick, R. W.; Raven, M.; McClure, S.; Jang, L. Y., Iron-monosulfide oxidation in natural sediments: Resolving microbially mediated S transformations using XANES, electron microscopy, and selective extractions. *Environ. Sci. Technol.* **2009,** *43*, 3128-3134.
105. Giggenbach, W., Equilibriums involving polysulfide ions in aqueous sulfide solutions up to 240.deg. *Inorg. Chem.* **1974,** *13*, 1724-1730.
106. Glaus, M. A.; Heijman, C. G.; Schwarzenbach, R. P.; Zeyer, J., Reduction of nitroaromatic compounds mediated by *Streptomyces sp.* exudates. *Appl. Environ. Microbiol.* **1992,** *58*, 1945-1951.
107. Luther III, G. W.; Rickard, D., Metal sulfide cluster complexes and their biogeochemical importance in the environment. *J. Nanopart. Res.* **2005,** *7*, 389-407.
108. Rickard, D.; Luther III, G. W., Metal sulfide complexes and clusters. *Rev. Mineral. Geochem.* **2006,** *61*, 421-504.
109. Charriau, A.; Lesven, L.; Gao, Y.; Leermakers, M.; Baeyens, W.; Ouddane, B.; Billon, G., Trace metal behaviour in riverine sediments: Role of organic matter and sulfides. *Appl. Geochem.* **2011,** *26*, 80-90.
110. Yu, Y. S.; Bailey, G. W., Reduction of nitrobenzene by four sulfide minerals: Kinetics, products, and solubility. *J. Environ. Qual.* **1992,** *21*, 86-94.
111. Cheng, J. Y.; Suidan, M. T.; Venosa, A. D., Abiotic reduction of 2,4-dinitrotoluene in the presence of sulfide minerals under anoxic conditions. *Water Sci. Technol.* **1996,** *34*, 25-33.
112. Oh, S.-Y.; Chiu, P. C.; Cha, D. K., Reductive transformation of 2,4,6-trinitrotoluene, hexahydro-1,3,5-trinitro-1,3,5-triazine, and nitroglycerin by pyrite and magnetite. *J. Hazard. Mater.* **2008,** *158*, 652-655.
113. Oh, S.-Y.; Son, J.-G.; Lim, O.-T.; Chiu, P., The role of black carbon as a catalyst for environmental redox transformation. *Environ. Geochem. Health* **2012,** *34*, 105-113.
114. Oh, S.-Y.; Chiu, P. C., Graphite- and soot-mediated reduction of 2,4-dinitrotoluene and hexahydro-1,3,5-trinitro-1,3,5-triazine. *Environ. Sci. Technol.* **2009,** *43*, 6983-6988.
115. Yu, X.; Gong, W.; Liu, X.; Shi, L.; Han, X.; Bao, H., The use of carbon black to catalyze the reduction of nitrobenzenes by sulfides. *J. Hazard. Mater.* **2011,** *198*, 340-346.
116. Weber, E. J.; Spidle, D. L.; Thorn, K. A., Covalent binding of aniline to humic substances. 1. Kinetic studies. *Environ. Sci. Technol.* **1996,** *30*, 2755-2763.
117. Thorn, K. A.; Pettigrew, P. J.; Goldenberg, W. S.; Weber, E. J., Covalent binding of aniline to humic substances. 2. ^{15}N NMR studies of nucleophilic addition reactions. *Environ. Sci. Technol.* **1996,** *30*, 2764-2775.
118. Johnson, W. C.; Millett, B. V.; Gilmanov, T.; Voldseth, R. A.; Guntenspergen, G. R.; Naugle, D. E., Vulnerability of northern prairie wetlands to climate change. *Bioscience* **2005,** *55*, 863-872.

119. Millett, B. V.; Johnson, W. C.; Guntenspergen, G. R., Climate trends of the North American prairie pothole region 1906-2000. *Clim. Change* **2009,** *93*, 243-267.
120. Niemuth, N.; Wangler, B.; Reynolds, R., Spatial and temporal variation in wet area of wetlands in the Prairie Pothole Region of North Dakota and South Dakota. *Wetlands* **2010,** *30*, 1053-1064.

Chapter 4: Abiotic Transformation of Pesticides in Prairie Pothole Surface Water: Photosensitized Reactions

Prairie pothole lakes (PPLs) are glacially-derived, ecologically-important water bodies found in central North America and represent a unique setting in which extensive agriculture occurs within wetland ecosystems. In the Prairie Pothole Region (PPR), elevated pesticide use and increasing hydrologic connectivity have raised concerns about the impact of nonpoint source agricultural pollution on the water quality of PPLs and downstream aquatic systems. Despite containing high dissolved organic matter (DOM) levels, the photoreactivity of PPL water and the photochemical fate of pesticides entering PPLs is largely unknown. In this study, the photodegradation of sixteen pesticides was investigated in PPL waters sampled from North Dakota, USA, under simulated and natural sunlight. Enhanced pesticide removal rates in the irradiated PPL water relative to the control buffer pointed to the importance of indirect photolysis pathways involving photochemically produced reactive intermediates (PPRIs). The steady-state concentrations of carbonate radical, hydroxyl radical, singlet oxygen, and triplet-excited state DOM were measured and second-order rate constants for the pesticide reactions with these PPRIs were calculated. Results from this study underscore the role of DOM as photosensitizer in limiting the persistence of pesticides in prairie wetlands through photochemical reactions.

4.1 Introduction

Prairie pothole lakes (PPLs) are small depressional wetlands scattered across the northern Great Plains of the United States and Canada.[1] They not only provide essential ecological niches for prairie wildlife,[2,3] but also serve as a major component of regional hydrology.[4,5] Throughout the prairie pothole region (PPR), historic and contemporary

conversion of native prairie for agriculture has resulted in a pronounced loss of PPLs.[6-9] Remaining PPLs have become interspersed within a matrix of agricultural landscape and are often artificially connected to rivers and streams through drainage tiles or ditch networks.[10-12] Thus, these lakes trap nonpoint source pollutants such as nutrients and pesticides from adjacent farmland,[13-18] which has raised concerns regarding negative impacts on the water quality of downstream water bodies as well as the overall biodiversity and productivity of the PPR.[11,12,19-22]

Numerous studies have documented that photochemical reactions contribute to the abiotic transformation of a wide array of pesticides via direct and/or indirect pathways.[23-25] Direct photolysis occurs when a contaminant directly absorbs light energy and undergoes chemical reaction.[26] Indirect photolysis occurs when another chemical species (photosensitizer) becomes electronically excited due to light absorption and either reacts directly with the contaminant of interest or produces reactive intermediates which further transform the contaminant.[26] Natural waters contain a variety of photosensitizers, including dissolved organic matter (DOM), nitrate/nitrite, bi/carbonate ions, halide ions, and iron species, which are capable of generating a suite of primary and secondary photochemically produced reactive intermediates (PPRIs).[27-35] Although the steady-state concentrations of PPRIs (e.g., 10^{-18}-10^{-9} M) in natural waters are small, these levels are sufficient to promote the photodegradation of aquatic contaminants.[36,37] In sunlit natural waters, direct photolysis is often a less important pathway for pesticides because of small overlap between their light absorption spectra and that of sunlight.[24] Moreover, the light screening effect of DOM retards direct photolysis.[38] The observed photolysis rates of

pesticides in natural waters, however, may be enhanced via photosensitized processes involving PPRIs.[39-45] Several PPRIs, including carbonate radical ($CO_3^{\bullet-}$),[45-52] hydroxyl radical ($^{\bullet}OH$)[42,44,45,51,53-67], singlet oxygen ($^1O_2$),[68,69] and triplet-excited state DOM ($^3DOM^*$),[66,70,71] react with a wide range of pesticides. Knowing steady-state concentrations of PPRIs, therefore, is critical to accurately predict the fate of pesticides.

The photic zone may comprise a large portion of PPLs due to their shallow depth (<1.5 m).[15] PPL surface water is typically characterized by high DOM concentrations, making them ideal for photosensitized reactions.[72-76] Thus, PPLs may possess high near-surface photoreactivity, which can promote the photodegradation of pesticides. Indeed, it has been suggested that photolysis represents a dissipation route of sulfonylurea herbicides in prairie waters.[77,78] Knowledge gaps, however, exist pertaining to the influence of PPL water constituents, in particular DOM, on the photochemical fate of pesticides commonly applied in the PPR.

The aim of the present work is to elucidate the significance of pesticide photolysis in PPL waters and discern the possible contribution of PPRIs. Sixteen target pesticides (atrazine, cyanazine, acetochlor, alachlor, metolachlor, diuron, isoproturon, metoxuron, mesotrione, bentazon, chlorpyrifos, clopyralid, propiconazole, ethalfluralin, pendimethalin, and trifluralin) were chosen based on their current usage and occurrence in prairie wetlands.[79,80] The photodegradation kinetics were investigated in surface water samples collected from two PPLs in North Dakota under both simulated and natural sunlight. The steady-state concentrations of four PPRIs (i.e., $CO_3^{\bullet-}$, $^{\bullet}OH$, $^1O_2$ and $^3DOM^*$)

were measured. Using quencher experiments, the relative rates of the different photolysis pathways were calculated and second-order rate constants estimated.

4.2 Experimental Section

4.2.1 Chemicals, Reagents, and Glassware

All pesticide standards were purchased from Fluka, including atrazine (6-chloro-N^2-ethyl-N^4-isopropyl-1,3,5-triazine-2,4-diamine; 99.8%), cyanazine (2-((4-chloro-6-(ethylamino)-1,3,5-triazin-2-yl)amino)-2-methylpropanenitrile; 99.7%), acetochlor (2-chloro-*N*-(ethoxymethyl)-*N*-(2-ethyl-6-methylphenyl)acetamide; 97.3%), alachlor (2-chloro-*N*-(2,6-diethylphenyl)-*N*-(methoxymethyl)acetamide; 99.2%), metolachlor (2-chloro-*N*-(2-ethyl-6-methylphenyl)-*N*-(1-methoxypropan-2-yl)acetamide; 97.6%), ethalfluralin (*N*-ethyl-*N*-(2-methylallyl)-2,6-dinitro-4-(trifluoromethyl)aniline; 99.5%), pendimethalin (3,4-dimethyl-2,6-dinitro-*N*-(pentan-3-yl)aniline; 98.8%), trifluralin (2,6-dinitro-*N*,*N*-dipropyl-4-(trifluoromethyl)aniline; 99.5%), diuron (3-(3,4-dichlorophenyl)-1,1-dimethylurea; 99.4%), isoproturon (3-(4-isopropylphenyl)-1,1-dimethylurea; 99.9%), metoxuron (3-(3-chloro-4-methoxyphenyl)-1,1-dimethylurea; 99.4%), mesotrione (2-(4-(methylsulfonyl)-2-nitrobenzoyl)cyclohexane-1,3-dione; 99.9%), bentazon (3-isopropyl-1*H*-benzo[*c*][1,2,6]thiadiazin-4(3*H*)-one 2,2-dioxide; 99.9%), chlorpyrifos (*O*,*O*-diethyl *O*-(3,5,6-trichloropyridin-2-yl) phosphorothioate; 99.9%), clopyralid (2-(4-(methylsulfonyl)-2-nitrobenzoyl)cyclohexane-1,3-dione; 98.7%), and propiconazole (1-((2-(2,4-dichlorophenyl)-4-propyl-1,3-dioxolan-2-yl)methyl)-1*H*-1,2,4-triazole; 98.4%). The physiochemical and light absorption properties of target pesticides are shown in Table C.1, Table C.2 (quantum yield), and Figure C.1(molar absorptivity), respectively.

All natural organic matter (NOM) standards were acquired from the International Humic Substances Society (IHSS), including Suwannee River Fulvic Acid (SRFA; 2S101F), Suwannee River Humic Acid (SRHA; 2S101H), Suwannee River Natural Organic Matter (SRNOM; 1R101N), Elliot Soil Humic Acid (ESHA; 1S102H), and Pony Lake Fulvic Acid (PLFA; 1R109F).

Ammonium phosphate monobasic (≥99.99%), bromocresol green (dye content 95%), methanol (Chromasolv for HPLC, ≥99.9%), isopropyl alcohol (IPA; anhydrous, 99.5%), sodium bicarbonate (99.7-100.3%), sodium acetate trihydrate (≥99.0%), sodium sulfate (≥99.0%) and sodium tetraborate decahydrate (≥99.5%) were obtained from Sigma-Aldrich. *N*,*N*-Dimethylaniline (DMA; purified by redistillation, ≥99.5%), furfuryl alcohol (FFA; ≥98%), and pyridine (PYR; ≥99.0%) were obtained from Aldrich. Terbuthylazine (N^2-(tert-butyl)-6-chloro-N^4-ethyl-1,3,5-triazine-2,4-diamine; 98.8%) was obtained from Fluka. Sorbic acid *(trans,trans*-hexadienoic acid; *t,t*-HDA; 99%) was obtained from Alfa Aesar. *p*-Nitroanisole (PNA; 99+%) and *p*-nitroacetophenone (PNAP; 97%) were obtained from Acros Organics. L-Histidine (HIS; 98.5-101.0%) was obtained from Fisher Scientific. 1,4-Diazabicyclo[2,2,2]octane (DABCO) was obtained from Matheson, Coleman, and Bell. *n*-Hexane (UltimAR grade, ≥95% *n*-hexane), sodium chloride (100%), sodium hydroxide (NaOH; >99%), hydrochloric acid (HCl; ≥36.5-38.0%), and nitric acid (HNO_3; ≥68.0-70.0%) were obtained from Mallinckrodt. Acetonitrile (Baker analyzed HPLC ultra grade, ≥99.9%), *o*-phosphoric acid (85%), and acetic acid (glacial, ≥99.9%) were obtained from J. T. Baker. Terephthalic acid (TPA) and 2-hydroxyterephthalic acid (hTPA) were synthesized and purified by Dr. Sarah E.

Page (University of Minnesota).[81] *p*-Nitroanisole was recrystallized from hexane to remove impurities.[82] All other chemicals were used as received without further purification.

The glassware cleaning procedures were the same as described previously.[76] Unless otherwise stated, all stock solutions were prepared using ultrapure water (resistivity 18.2 MΩ·cm, Millipore Corp.). Pesticide stock solutions for spiking aqueous samples in photolysis experiments were prepared in acetonitrile. Calibration standards of pesticides were prepared either in ultrapure water (for HPLC) or *n*-hexane (for GC-μECD). Borate buffer (10 mM; pH 8.50) was prepared by dissolving sodium tetraborate decahydrate crystals in ultrapure water with appropriate amounts of sodium chloride, sodium sulfate and sodium bicarbonate added to match the composition of the PPL water. SRFA, SRHA, SRNOM, ESHA and PLFA stock solutions were prepared by dissolving organic matter powders in ultrapure water adjusted to pH 10. Each solution was stirred overnight in the dark, filtered through 0.2 μm nylon membrane filters (GNWP, Millipore Corp.), and adjusted back to pH 8.50. SRFA, SRHA, SRNOM, ESHA and PLFA working solutions (i.e., model DOM solutions) were prepared by mixing a predetermined volume of individual stock NOM solution with borate buffer to achieve a final DOC level at ~25 mg C/L, which was meant to match the DOC level measured in P8-Sep-2010 water. PNA (10.0 μM)/PYR (1.0 or 5.0 mM) and PNAP (10.0 μM)/PYR (35.0 or 115.0 mM) actinometer solutions were prepared according to Leifer.[83]

4.2.2 Water Sample Collection and Analysis

Three PPL surface water samples, designated as P8-Sep-2010, P1-Apr-2012, and P8-Apr-2012, were collected from two adjacent prairie potholes (i.e., Lake P1 and P8) in the U.S. Geological Survey (USGS) Cottonwood Lake study area, Jamestown, North Dakota, in September 2010 and April 2012. Water samples were collected in acid-washed glass jars and transported in ice-chilled coolers to the University of Minnesota within 24 h. Whole water samples were then vacuum-filtered through pre-combusted (6 h at 550 ℃) 0.7 μm glass fiber filters (Grade GF/F, Whatman), followed by 0.2 μm nylon membrane filters (GNWP, Millipore Corp.), and stored in the dark at 4 ℃ until use. The pH of water samples was measured by an Orion Ross combination pH electrode. Dissolved oxygen (DO) was measured by a YSI EcoSense DO200 dissolved oxygen/temperature meter. Conductivity and total dissolved solids (TDS) were measured by an Orbeco Model 72 conductance/TDS meter. Total alkalinity (as $CaCO_3$) was determined by titration to the bromocresol green endpoint (pH 4.5). Dissolved organic carbon (DOC) was measured by a Sievers 900 Portable TOC analyzer after water samples were acidified with 2 M HCl and purged with nitrogen. Absorbance spectra of water samples were acquired on a Shimadzu UV-1601 PC spectrophotometer. The collected spectra were used to calculate light screening factors ($S_{\sum\lambda 290\text{-}800nm}$) for each water sample.[42] Anion and cation concentrations were determined using ion chromatography (IC) and inductively coupled plasma-optical emission spectrometry (ICP-OES), respectively.[84]

Indoor and Outdoor Photolysis of Pesticides

Pesticide photolysis in PPL waters was investigated under both simulated (i.e., indoor) and natural (i.e., outdoor) sunlight. For indoor photolysis, all sixteen pesticides were photolyzed in P8-Sep-2010 water using an Atlas Suntest CPS+ solar simulator equipped with a 1500 W xenon arc lamp. The lamp was fitted with a UV-Suprax optical filter (passing wavelengths ranging from 290 to 800 nm), and the light intensity was set at 765 W/m^2. For outdoor photolysis, selected pesticides were photolyzed in P8-Sep-2010, P1-Apr-2012 and P8-Apr-2012 water, respectively. Due to analytical constraints at the field site, outdoor photolysis was performed on the roof of the U of MN Civil Engineering building (44°58'34"N and 93°13'53"W) in Spring 2012. Reaction solutions for photolysis experiments were prepared by addition of a predetermined amount of pesticide stock solution (in acetonitrile) into volumetric flasks, evaporation of all traces of acetonitrile under a gentle nitrogen stream, and reconstitution into either filtered PPL water or borate buffer (10 mM, pH 8.5). The initial pesticide concentrations were 0.4-11 μM, which allowed the direct monitoring of pesticide concentration and minimization of light screening. Selected solutions spiked with either 120 μM *N,N*-dimethylaniline (DMA; a $CO_3^{\bullet-}$ scavenger), 26 mM isopropyl alcohol (IPA; a $^{\bullet}OH$ scavenger), 20 mM L-Histidine (HIS; a $^1O_2$ and $^{\bullet}OH$ scavenger), 10 mM 1,4-diazabicyclo[2,2,2]octane (DABCO; a $^1O_2$ and $^{\bullet}OH$ scavenger), or 10 mM *trans,trans*-hexadienoic acid (HDA; a $^3DOM^*$ scavenger) were concurrently irradiated to evaluate the importance of indirect photolysis processes. For indoor photolysis, tubes containing aerated (i.e., air-purged) and deaerated (i.e., nitrogen-purged) reaction solutions were also irradiated to further probe the role of $^1O_2$ and $^3DOM^*$. Deaerated solutions were prepared and sampled in an

anaerobic glove box (95% N_2/5% H_2, Pd catalyst, Coy Laboratory Products Inc.). Aliquots of 8-mL reaction solutions were placed in quartz test tubes (o.d. = 13 mm, i.d. = 11 mm, V = 10 mL) which were sealed with rubber caps and Teflon tape. The tubes were placed in the solar simulator or on the building roof at an angle of 30 ° from the horizontal. For both indoor and outdoor photolysis, all tubes were irradiated along with foil-wrapped abiotic dark controls and either *p*-nitroanisole/pyridine (PNA/PYR) or *p*-nitroacetophenone/pyridine (PNAP/PYR) actinometer solutions. The actinometers were used to measure light exposure and to allow long-duration time courses to be plotted versus actinometer loss. Determination of quantum yields for direct photolysis was not a goal of this study. Photolysis kinetics were monitored over both a short, 4 h, time period as well as a long, 56 h, time period to capture distinct kinetic time courses. A 0.5-mL aliquot of sub-sample was withdrawn from each tube at selected time points and transferred into amber autosampler vials.

Concentrations of pesticides (except ethalfluralin, pendimethalin and trifluralin) in aqueous samples were directly analyzed by an Agilent 1100 Series high-pressure liquid chromatography equipped with a micro degasser, a quaternary pump and an autosampler coupled to a multi-wavelength UV absorbance detector (MWD) and a fluorescence detector (FLD). Chromatographic separations were performed using a Supelco Discovery RP-Amide C_{16} column (15 cm × 4.6 mm; 5 μm) with an in-line Supelguard Discovery RP-Amide C_{16} cartridge (2 cm × 2.1 mm; 5 μm). PNA and PNAP were analyzed using the same HPLC system. Instrument parameters and retention times for analysis of pesticides, PNA and PNAP are summarized in Table C.3:

Concentrations of ethalfluralin, trifluralin and pendimethalin were analyzed by an Agilent 6890 Series gas chromatograph equipped with an autosampler and a ^{63}Ni microelectron capture detector as described previously.[84] Pesticides in aqueous samples were first extracted into 0.5 mL of *n*-hexane (containing 4.3 μM terbuthylazine as an internal standard), and 1 μL of hexane was injected in splitless mode.

4.2.3 Determination of Steady-State Concentrations of PPRIs

The apparent steady-state concentrations of carbonate radical ($[CO_3^{\bullet-}]_{ss}$), hydroxyl radical ($[^{\bullet}OH]_{ss}$), singlet oxygen ($[^1O_2]_{ss}$) and triplet-excited state DOM ($[^3DOM^*]_{ss}$) were determined under both simulated and natural sunlight. For indoor photolysis, the steady-state concentrations of target PPRIs in P8-Sep-2010 water was measured along with Suwannee River Fulvic Acid (SRFA), Suwannee River Humic Acid (SRHA), Suwannee River Natural Organic Matter (SRNOM), Elliot Soil Humic Acid (ESHA), and Pony Lake Fulvic Acid (PLFA) model solutions (~25 mg C/L) in the solar simulator. For outdoor photolysis, the steady-state concentrations of PPRIs were measured in P8-Sep-2010, P1-Apr-2012 and P8-Apr-2012 water, respectively. Details of these methods are presented below.

Carbonate radical Apparent $[CO_3^{\bullet-}]_{ss}$ was determined by monitoring the decay of DMA as a probe.[85] Triplicate PPL water samples or model DOM solutions were dosed with 2 μM DMA and irradiated. For both indoor and outdoor experiments, photolysis kinetics were monitored over a 4 h time period. A 0.5-mL aliquot of sub-sample was removed from each tube at selected time points and transferred into amber autosampler vials. HPLC parameters for analysis of DMA were 40% ultrapure water and 60%

acetonitrile with an injection volume of 100 µL and a flow rate of 1 mL/min. Fluorescence detection was set at 252 nm for excitation and at 410 nm for emission. The retention time for DMA was 5.4 min. Calibration standards of DMA were prepared either in PPL waters or model DOM solutions to account for the matrix effect. Control experiments in which DMA was irradiated in borate buffer was performed to account for its direct photolysis. Semilogarithmic plots for DMA degradation are shown in Figure C.2. The observed DMA degradation rates in PPL waters and model DOM solutions were corrected by subtraction of the direct photolysis rate of DMA. Apparent $[CO_3^{\bullet-}]_{ss}$ was computed by dividing the corrected DMA degradation rate by its carbonate radical reaction rate constant (i.e., $k_{DMA,\ CO_3^{\bullet-}} = 1.8 \times 10^9\ M^{-1}\ s^{-1}$) using the following equation (Equation (4.1)):[85]

$$\frac{d[DMA]}{dt} = - k_{DMA,\ CO_3^{\bullet-}} \cdot [DMA] \cdot [CO_3^{\bullet-}]_{ss} \quad (4.1)$$

Hydroxyl radical Apparent $[^{\bullet}OH]_{ss}$ was determined by monitoring the formation of 2-hydroxyterephthalic acid (hTPA) using terephthalate as a probe.[81] Triplicate PPL water samples or duplicate model DOM solutions were dosed with 500 µM TPA and irradiated. TPA solutions were prepared in amber volumetric flasks in the dark to minimize exposure to ambient light. For both indoor and outdoor experiments, photolysis kinetics were monitored over a 1 h time period. A 0.5-mL aliquot of sub-sample was removed from each tube at selected time points and transferred into amber autosampler vials preloaded with 10 µL concentrated HCl. HPLC parameters for analysis of hTPA were 70% phosphate buffer (10 mM, pH 3, with 10% ACN) and 30% methanol with an injection volume of 100 µL and a flow rate of 1 mL/min. Fluorescence detection was set

at 250 nm for excitation and at 410 nm for emission. The retention time for hTPA was 5.2 min. Calibration standards of hTPA were prepared either in PPL waters or model DOM solutions to account for the matrix effect. Time courses for hTPA formation are shown in Figure C.3. The formation rate of hTPA was determined in the initial rate kinetics regime. Apparent $[^{\bullet}OH]_{ss}$ was computed by dividing the observed hTPA formation rate (determined in the initial rate kinetics regime) in PPL waters or model DOM solutions by the initial TPA concentration (i.e., $[TPA]_0$ = 500 μM), reaction yield (i.e., 0.35) and its hydroxyl radical reaction rate constant (i.e., $k_{TPA,\ ^{\bullet}OH} = 4.4 \times 10^9\ M^{-1}\ s^{-1}$) using the following equation (Equation (4.2)):[81]

$$\frac{d[hTPA]}{dt} = 0.35 \cdot k_{TPA,\ ^{\bullet}OH} \cdot [TPA] \cdot [^{\bullet}OH]_{ss} \quad (4.2)$$

Singlet oxygen Apparent $[^1O_2]_{ss}$ was determined by monitoring the decay of furfuryl alcohol (FFA) as a probe.[86] Triplicate PPL water samples or model DOM solutions were dosed with 23 μM FFA and irradiated. For both indoor and outdoor experiments, photolysis kinetics were monitored over a 4 h time period. A 0.5-mL aliquot of sub-sample was removed from each tube at selected time points and transferred into amber autosampler vials. HPLC parameters for analysis of FFA were 90% phosphate buffer (10 mM, pH 3, with 10% ACN) and 10% methanol with an injection volume of 35 μL and a flow rate of 1 mL/min. UV detection was set at 219 nm. The retention time for FFA was 4.4 min. Control experiments in which FFA was irradiated in borate buffer were performed to account for its direct photolysis. Semilogarithmic plots for FFA degradation are shown in Figure C.4. The observed FFA degradation rates in PPL waters and model DOM solutions were corrected by subtraction of the direct photolysis rate of FFA.

Apparent $[^1O_2]_{ss}$ was computed by dividing the corrected FFA degradation rate by its singlet oxygen reaction rate constant (i.e., $k_{FFA,\,^1O_2} = 8.3 \times 10^7\ M^{-1}\ s^{-1}$) using the following equation (Equation (4.3)):[86,87]

$$\frac{d[FFA]}{dt} = - k_{FFA,\,^1O_2} \cdot [FFA] \cdot [^1O_2]_{ss} \quad (4.3)$$

Triplet-excited state DOM Apparent $[^3DOM^*]_{ss}$ was determined by monitoring the formation of four isomers using HDA as a probe.[88] Duplicate PPL water samples or model DOM solutions were dosed with *trans,trans*-HDA at five different concentrations ranging from 10 to 1000 μM and irradiated. Three other HDA isomers (i.e., *cis,trans*-HDA, *cis,cis*-HDA and *trans,cis*-HDA) were formed upon irradiation as a result of the interaction of *t,t*-HDA with $^3DOM^*$. A custom-fabricated plastic cover (made of 3M PP2200 transparency film) was used to cut off light below 315 nm to minimize the self-isomerization of *t,t*-HDA (see Figure C.5(a)).[88] For both indoor and outdoor experiments, photolysis kinetics were monitored over a 40 h time period. A 0.5-mL aliquot of sub-sample was withdrawn from each tube at selected time points and transferred into amber autosampler vials preloaded with 50 μL glacial acetic acid. HPLC parameters for baseline resolution of four HDA isomers were 87% acetate buffer (30 mM, pH 4.75) and 13% acetonitrile with an injection volume of 40 μL and a flow rate of 1 mL/min. UV detection was set at 254 nm. Retention times for *c,t*-HDA, *c,c*-HDA, *t,t*-HDA and *t,c*-HDA were 11.3, 12.3, 13.3 and 14.5 min, respectively (see Figure C.5(b)). An external calibration curve was constructed for *t,t*-HDA, while calibration curves for other three HDA isomers were generated based on their relative molar absorption coefficients at 254 nm to *t,t*-HDA.[88] Example time courses for *c,t*-HDA, *c,c*-HDA and *t,c*-HDA isomer formation

along with *t,t*-HDA degradation in P8-Sep-2010 water are shown in Figure C.6. At each *t,t*-HDA dose, the formation rates of *c,t*-HDA, *c,c*-HDA and *t,c*-HDA were experimentally determined in the initial rate kinetics regime, and the reformation rate of the original *t,t*-HDA relative to *c,t*-HDA was calculated to be ~2.18. This value was derived based on a multiple linear regression of data from all *t,t*-HDA photolysis experiments (n = 18) using the following equation (Equation (4.4)):[88]

$$\frac{\mathrm{d}[t,t\text{-HDA}]}{dt} = \frac{R_{t,t\text{-}HDA}}{R_{c,t\text{-}HDA}}\left(\frac{\mathrm{d}[c,t\text{-HDA}]}{dt}\right) - k'_{t,t\text{-}HDA}\cdot[t,t\text{-HDA}] \qquad (4.4)$$

where $k'_{t,t\text{-}HDA}$ is the sum of pseudo-first order rate constant for *t,t*-HDA photodegradation and pseudo-first order rate constant for reaction between *t,t*-HDA and solution scavengers. Solving the above equation yielded $R_{t,t\text{-}HDA}/R_{c,t\text{-}HDA}$ = 2.18 (±0.14), which compares well with the value (i.e., 2.86 (±3.55)) reported previously.[88]

The overall formation rate of four isomers (R_{HDA}) was then calculated as the sum of *c,t*-HDA, *c,c*-HDA and *t,c*-HDA formation rates plus the *t,t*-HDA reformation rate. Minor self-isomerization of *t,t*-HDA was observed during irradiation in the solar simulator even with the presence of custom-made filter, possibly caused by a bleed of wavelengths below 315 nm. Thus, for indoor photolysis, the value of R_{HDA} determined in PPL waters and model DOM solutions were corrected by subtraction of the self-isomerization rate of HDA in borate buffer ($R_{HDA\text{-}SI}$) using the following equation (Equation (4.5)):

$$R_{HDA,\ indoor} = R_{c,t\text{-}HDA} + R_{c,c\text{-}HDA} + R_{t,t\text{-}HDA} + R_{t,c\text{-}HDA} - R_{HDA\text{-}SI} \qquad (4.5)$$

For outdoor photolysis, the self-isomerization of *t,t*-HDA was negligible, and typical loss of original *t,t*-HDA was less than 1% at the end of experiment. The value of R_{HDA} was determined using the following equation (Equation (4.6)):

$$R_{HDA,\ outdoor} = R_{c,t\text{-}HDA} + R_{c,c\text{-}HDA} + R_{t,t\text{-}HDA} + R_{t,c\text{-}HDA} \quad (4.6)$$

At steady state, the relationship between the formation rate of $^3DOM^*$ ($F_{^3DOM^*}$) and R_{HDA} in the presence of scavengers (other than *t,t*-HDA) can be expressed as (Equation (4.7)):[88]

$$R_{HDA} = \frac{F_{^3DOM^*} \cdot k_{t,t\text{-HDA}} \cdot [t,t\text{-HDA}]}{k_{t,t\text{-HDA}} \cdot [t,t\text{-HDA}] + k'_{scavenger}} \quad (4.7)$$

where [*t,t*-HDA] is the initial dose of *t,t*-HDA, $k_{t,t\text{-}HDA}$ is the estimated second-order rate constant (= 4.40 (±4.29) × 10^9 M^{-1} s^{-1}) for reaction between *t,t*-HDA and $^3DOM^*$, and $k'_{scavenger}$ is the pseudo-first order rate constant for reaction between solution scavengers and $^3DOM^*$, assuming that the scavenger concentrations are constant within the experimental time frame.[88] The above equation can be re-arranged as (Equation (4.8)):[88]

$$\frac{[t,t\text{-HDA}]}{R_{HDA}} = \frac{[t,t\text{-HDA}]}{F_{^3DOM^*}} + \frac{k'_{scavenger}}{F_{^3DOM^*} \cdot k_{t,t\text{-HDA}}} \quad (4.8)$$

The intercept determined from the linear regression of [*t,t*-HDA]/R_{HDA} versus [*t,t*-HDA], as shown in Figure C.7, can then be used to compute $[^3DOM^*]_{ss}$ (i.e., the apparent steady-state concentration of triplet-excited state of DOM in the *absence* of HDA) using the following equation (Eqautiu(4.9)):[88]

$$[^3DOM^*]_{ss} = \frac{1}{k_{t,t\text{-HDA}} \cdot \text{Intercept}} \quad (4.9)$$

4.2.4 Data Analysis

Pesticide photolysis was modeled assuming the pseudo-first-order kinetics. The observed photolysis rates for pesticides were corrected by the rates of PNA or PNAP decay so that results from different experiments could be compared to each other. Data fitting and regression analysis were performed using *SigmaPlot 10* (Systat Software Inc.).

4.3 Results and Discussion

4.3.1 Photoreactivity of PPL Surface Water

Characteristics of three PPL water samples are summarized in Table 4.1. All PPL waters were alkaline (pH~8.5) with DOC levels ranging from ~20 to 38 mg C/L and total alkalinity from ~130 to 210 mg/L as $CaCO_3$. Nitrate, nitrite and iron levels were low, suggesting that $^{\bullet}OH$ production from these photosensitizers would be minimal. Halide ions (e.g., Cl^- and Br^-), which generate reactive halogen species by scavenging $^{\bullet}OH$, were also found to be at low levels compared to other natural waters.[89] Overall, DOM appears to be the dominant photosensitizer in the PPL water.

When absorbing sunlight, the chromophoric components of DOM are promoted to short-lived singlet-excited state ($^1DOM^*$), which can either release energy by ejecting solvated electrons (e^-_{aq}),[35,90-92] or undergo intersystem crossing to a more stable, lower-energy $^3DOM^*$. Triplet-excited state DOM can either 1) react directly with contaminants via energy or electron transfer or hydrogen abstraction, 2) generate $^{\bullet}OH$, or 3) transfer energy to ground-state oxygen generating other reactive oxygen species such as $^1O_2$, superoxide radical anion ($O_2^{\bullet-}$), peroxyl radical ($RO_2^{\bullet}$), and hydrogen peroxide (H_2O_2).[28,31-34,37,93-99] Hydroxyl radical can further react with certain inorganic water

constituents and produce secondary transients such as $CO_3^{\bullet-}$.[97] On the other hand, DOM can also scavenge PPRIs[48,100-104] and/or suppress PPRI-mediated reactions, as exemplified by the inhibition of $^3DOM^*$-induced oxidation by phenolic antioxidant moieties.[71,105,106] Given the abundance of DOM, a mixture of PPRIs are presumably present in the PPL water and may participate in an array of photochemical reactions.

Table 4.1 Characteristics of PPL surface water

Parameter[a]	P8-Sep-2010	P1-Apr-2012	P8-Apr-2012
pH	8.46	8.58	8.48
DO (mg/L)	6.63	6.26	6.85
Conductivity (μS/cm)	1.80×10^4	3.00×10^4	1.87×10^4
TDS (mg/L)	1.26×10^4	2.10×10^4	1.31×10^4
DOM (mg C/L)	25.70 ± 0.15	37.91 ± 0.88	20.75 ± 0.13
Total alkalinity (mg/L as $CaCO_3$)	130.2 (±1.1)	197.2 (±1.1)	210.8 (±1.8)
$SUVA_{254nm}$ (L/mg-M)	2.25	1.67	2.26
$S_{\sum\lambda 290\text{-}800nm}$	0.966	0.971	0.972
Anion (mg/L)[b]			
Bromide (Br^-)	0.037 (±0.000)	0.028 (±0.003)	0.061 (±0.001)
Chloride (Cl^-)	14.65 (±0.02)	19.84 (±0.03)	15.70 (±0.02)
Fluoride (F^-)	0.155 (±0.001)	0.112 (±0.001)	0.212 (±0.001)
Nitrate (NO_3^-)	0.016 (±0.000)	0.010 (±0.000)	0.004 (±0.000)
Nitrite (NO_2^-)	< 0.002[d]	< 0.002[d]	< 0.002[d]
Phosphate (PO_4^{3-})	< 0.005[d]	< 0.005[d]	< 0.005[d]
Sulfate (SO_4^{2-})	691.0 (±0.3)	1595.3 (±4.0)	563.3 (±1.0)
Cation (μg/L)[c]			
Al	1.4 (±0.7)	1.4 (±1.2)	0.8 (±0.2)
Ca	35345 (±105)	137500 (±438)	121130 (±234)
Fe	< 1.1[d]	< 1.1[d]	< 1.1[d]
K	9375 (±47)	40460 (±236)	18032 (±239)
Mg	71415 (±666)	317853 (±4576)	123540 (±840)
Mn	1.8 (±1.2)	67.9 (±2.0)	14.0 (±1.1)
Na	52133 (±380)	168707 (±1249)	83655 (±906)

[a] Measured in 0.2 μm filtered PPL waters. Errors represent one standard deviation from triplicate measurements. [b] Concentration measured by IC.[84] [c] Concentration measured by ICP-OES.[84] [d] Concentration below the limit of quantification.

The apparent steady-state concentrations of $CO_3^{\bullet-}$, $^{\bullet}OH$, $^1O_2$ and $^3DOM^*$ were determined in both P8-Sep-2010 water and five model DOM solutions under simulated sunlight. The five DOM isolates (i.e., SRFA, SRHA, SRNOM, ESHA and PLFA) were chosen to represent a spectrum of allochthonous and autochthonous end-members. The pH, DOC and alkalinity of model DOM solutions were adjusted to match the levels found in P8-Sep-2010 water.

Table 4.2 Steady-state concentrations of PPRIs in PPL waters and model DOM solutions

Sample	$[CO_3^{\bullet-}]_{ss}$ (M)[a]	$[^{\bullet}OH]_{ss}$ (M)[a]	$[^1O_2]_{ss}$ (M)[a]	$[^3DOM^*]_{ss}$ (M)[a]
Simulated sunlight				
P8-Sep-2010	$20.41(\pm0.83)\times10^{-15}$	$6.12(\pm0.14)\times10^{-17}$	$7.30(\pm0.22)\times10^{-13}$	$52.49(\pm1.79)\times10^{-16}$
SRFA	$13.32(\pm0.51)\times10^{-15}$	$9.68(\pm0.30)\times10^{-17}$	$4.68(\pm0.10)\times10^{-13}$	$11.43(\pm0.35)\times10^{-16}$
SRHA	$14.77(\pm0.92)\times10^{-15}$	$25.57(\pm0.48)\times10^{-17}$	$4.17(\pm0.13)\times10^{-13}$	$8.23(\pm0.75)\times10^{-16}$
SRNOM	$19.44(\pm1.34)\times10^{-15}$	$17.76(\pm0.24)\times10^{-17}$	$3.68(\pm0.15)\times10^{-13}$	$10.57(\pm0.14)\times10^{-16}$
ESHA	$24.21(\pm0.21)\times10^{-15}$	$28.62(\pm0.38)\times10^{-17}$	$7.71(\pm0.16)\times10^{-13}$	$18.63(\pm0.69)\times10^{-16}$
PLFA	$28.56(\pm0.70)\times10^{-15}$	$21.94(\pm0.72)\times10^{-17}$	$3.34(\pm0.11)\times10^{-13}$	$39.87(\pm1.54)\times10^{-16}$
Natural sunlight				
P8-Sep-2010	$7.22(\pm0.43)\times10^{-15}$	$2.29(\pm0.13)\times10^{-17}$	$2.61(\pm0.26)\times10^{-13}$	$11.71(\pm0.34)\times10^{-16}$
P1-Apr-2012	$18.96(\pm0.24)\times10^{-15}$	$3.06(\pm0.12)\times10^{-17}$	$3.55(\pm0.31)\times10^{-13}$	$14.00(\pm0.22)\times10^{-16}$
P8-Apr-2012	$9.40(\pm0.44)\times10^{-15}$	$2.61(\pm0.14)\times10^{-17}$	$2.22(\pm0.14)\times10^{-13}$	$11.59(\pm0.13)\times10^{-16}$

[a] Steady-state concentration measured in PPL waters and model DOM solutions. Errors represent one standard deviation from duplicate or triplicate measurements. Measured values represent concentrations in the bulk aqueous phase without correction for the microheterogeneity of DOM micelles.[107,108] Concentrations measured in model DOM solutions are comparable to literature data (see Table C.4).

As compiled in Table 4.2, $[CO_3^{\bullet-}]_{ss}$ in P8-Sep-2010 water falls within the median range of concentrations measured in model DOM solutions (PLFA>ESHA>P8-Sep-2010≈SRNOM>SRHA>SRFA). $[^{\bullet}OH]_{ss}$ in P8-Sep-2010 water is the lowest (ESHA>SRHA>PLFA>SRNOM>PLFA>P8-Sep-2010), whereas $[^1O_2]_{ss}$ ranks the second highest among all samples (ESHA>P8-Sep-2010>SRFA≈SRHA>SRNOM≈PLFA). Notably, $[^3DOM^*]_{ss}$ in P8-Sep-2010 water is significantly higher than those measured in

model DOM solutions (P8-Sep-2010>PLFA>ESHA>SRFA≈SRNOM>SRHA). Such distinct patterns of PPRI concentrations reflect differences in the overall photoreactivity between pure DOM isolates and whole PPL water, which likely results from a combination of the variability in composition of DOM from diverse sources and the presence of other water constituents. Earlier studies have demonstrated that the photosensitization efficiency of DOM is a complex function of its chemical and optical properties. For instance, the photoproduction of $^{\bullet}OH$ strongly depends on the relative abundance of carboxylic and phenolic moieties present in the DOM,[63] while the photoreactivity of $^{3}DOM^{*}$ has been found to vary with the content of ketone moieties.[109-114]

Previous studies have documented temporal and spatial changes in the PPL water chemistry in terms of composition and reactivity of DOM.[73,74,115] To probe the differences in photoreactivity of PPL waters, the apparent steady-state concentrations of $CO_3^{\bullet-}$, $^{\bullet}OH$, $^{1}O_2$ and $^{3}DOM^{*}$ were measured in P8-Sep-2010, P1-Apr-2012, and P8-Apr-2012 water under natural sunlight. As shown in Table 4.2, the concentrations of PPRIs measured in P1-Apr-2012 water are consistently higher than those measured in P8-Apr-2012 water, which might be attributed to the elevated DOM level found in P1-Apr-2012 water. The concentrations of PPRIs measured in P8 water sampled on two occasions are similar, with $[CO_3^{\bullet-}]_{ss}$ and $[^{\bullet}OH]_{ss}$ slightly higher in P8-Apr-2012 water. Although the DOM level was lower in P8-Apr-2012 water, the levels of various metal ions were significantly higher than those measured in P8-Sep-2010, suggesting that inhibitory effects on PPRI formation caused by the radical scavenging and/or the fluorescence

quenching abilities of DOM-complexed metal ions were minimal.[116] PPRI concentrations measured in P8-Sep-2010 water under simulated sunlight were approximately three times higher than those measured under natural sunlight.

4.3.2 Pesticide Photodegradation under Simulated Sunlight

For indoor photolysis, all sixteen target pesticides were photolyzed in either borate buffer or P8-Sep-2010 water, with or without additives. As shown in Figure 4.1, pesticide photolysis generally proceeded faster in native P8-Sep-2010 water than in borate buffer, suggesting that indirect photolysis had a large impact. Minimal loss of pesticides was observed in the dark control, indicating that other non-photolytic processes (e.g., biodegradation, hydrolysis, sorption or volatilization) were insignificant relative to photolysis. The only exceptions were dinitroaniline herbicides (i.e., ethalfluralin, pendimethalin, and trifluralin), which mainly underwent direct photolysis and lost up to 20% in the dark control. Logarithmic plots for pesticide photolysis versus actinometer loss indicate that reactions followed pseudo-first-order kinetics (see Figure C.8). The observed indoor photolysis rates of pesticides are summarized in Table C.5.

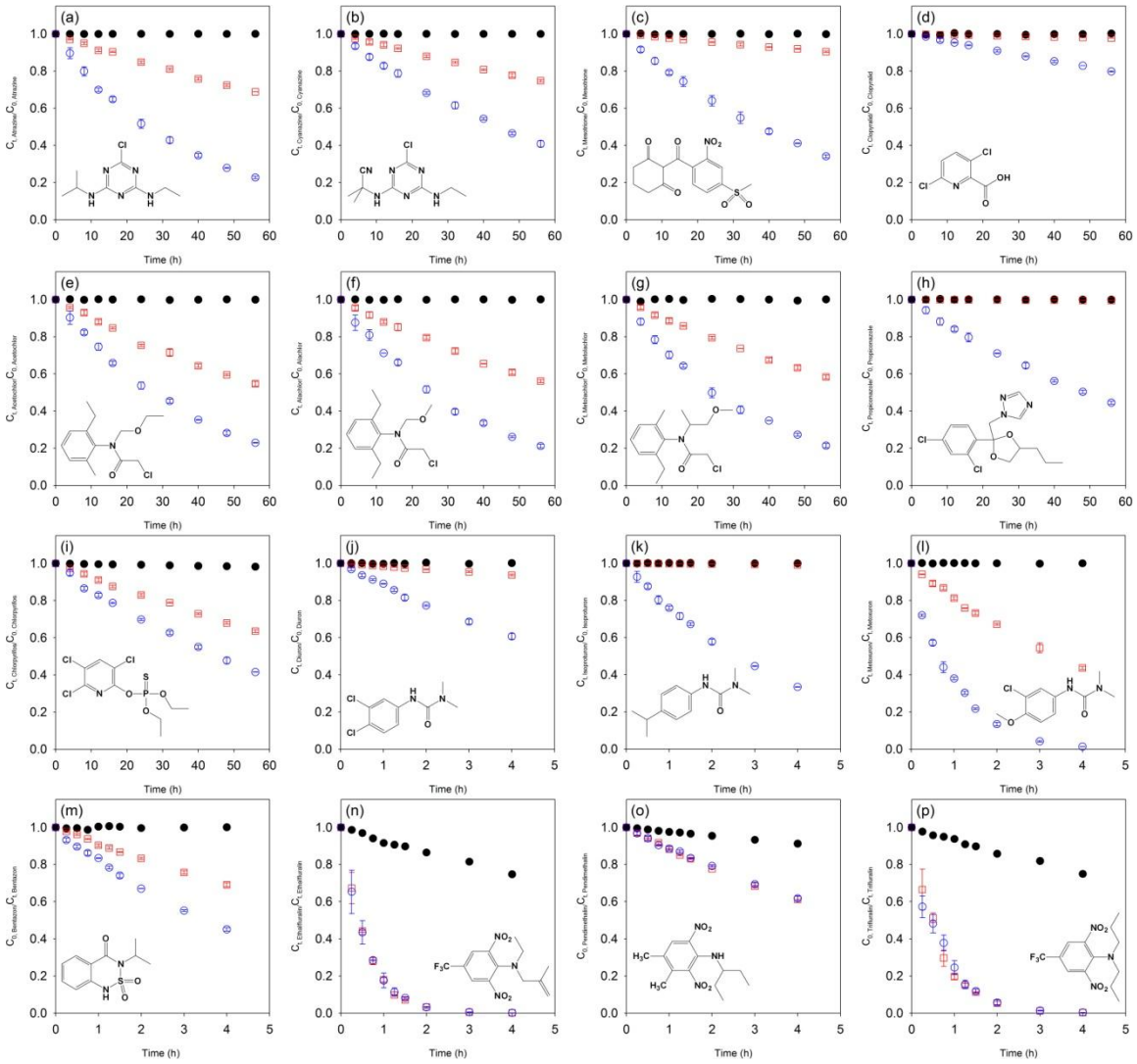

Figure 4.1 Photodegradation of pesticides in P8-Sep-2010 water (○) and borate buffer (□) under simulated sunlight: (a) atrazine; (b) cyanazine; (c) mesotrione; (d) clopyralid; (e) acetochlor; (f) alachlor; (g) metolachlor; (h) propiconazole; (i) chlorpyrifos; (j) diuron; (k) isoproturon; (l) metoxuron; (m) bentazon; (n) ethalfluralin; (o) pendimethalin; (p) trifluralin. Filled symbol (●) represents the dark control. Error bars represent one standard deviation of duplicate samples; where absent, bars fall within symbols. Note differences in time scales.

A series of quencher experiments were conducted using P8-Sep-2010 water to determine the contributions of $CO_3^{\bullet-}$, $^{\bullet}OH$, $^1O_2$ and $^3DOM^*$ to the overall pesticide photolysis. To better illustrate the variation in reactivity of each pesticide, individual photolysis rate constants in P8-Sep-2010 water containing various PPRI quenchers were

normalized to the photolysis rate constant of that pesticide in native P8-Sep-2010 water to obtain relative rates.

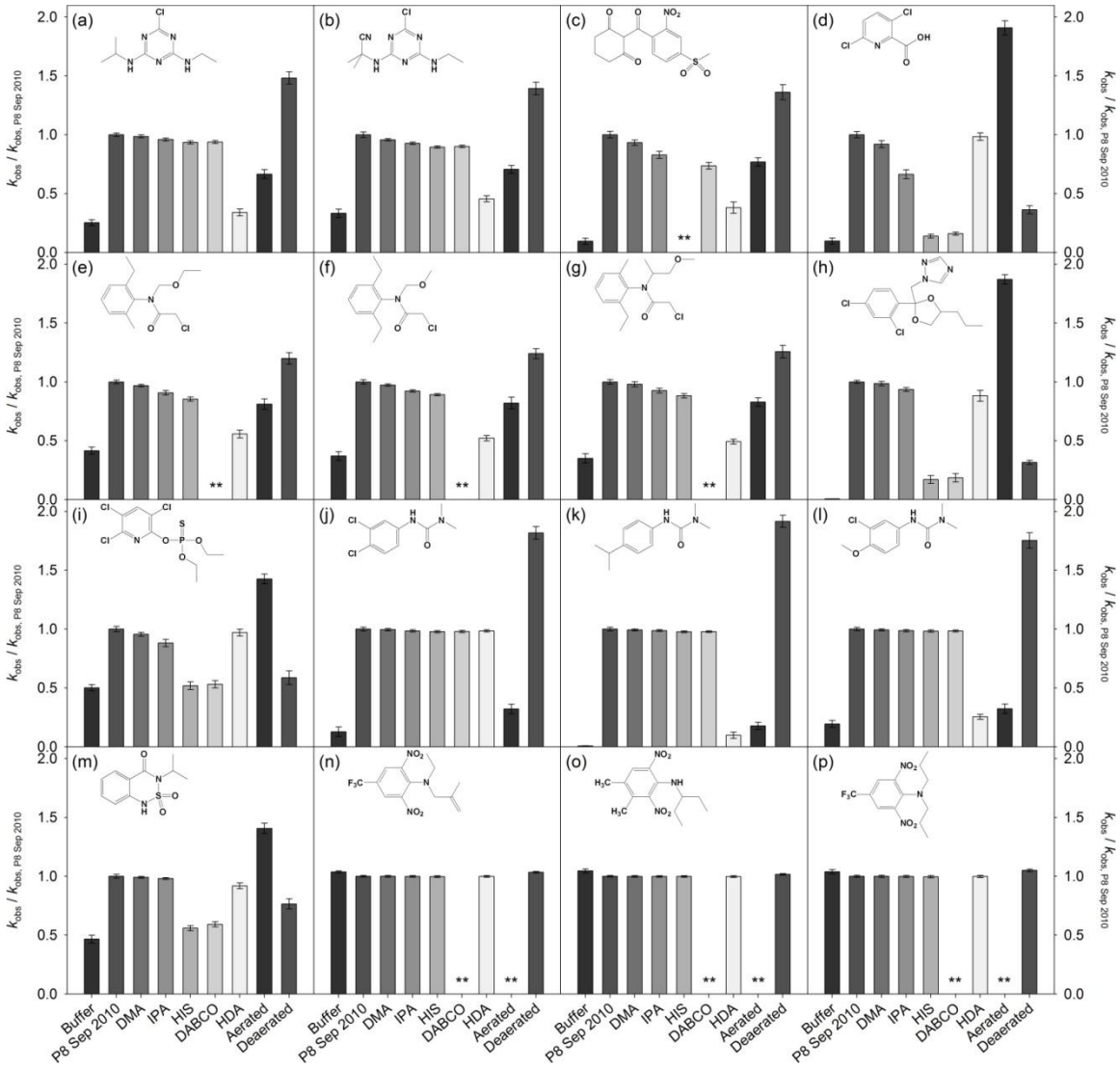

Figure 4.2 Relative rates of pesticide photodegradation in borate buffer and native and modified P8-Sep-2010 water under simulated sunlight: (a) atrazine; (b) cyanazine; (c) mesotrione; (d) clopyralid; (e) acetochlor; (f) alachlor; (g) metolachlor; (h) propiconazole; (i) chlorpyrifos; (j) diuron; (k) isoproturon; (l) metoxuron; (m) bentazon; (n) ethalfluralin; (o) pendimethalin; (p) trifluralin. Error bars represent one standard deviation of duplicate samples. Double asterisk marks designate data not available.

As shown in Figure 4.2, the addition of quenchers did not exert a measurable effect on the photolysis rates of dinitroanilines. In other cases, the addition of DABCO or

HIS (a $^1O_2$ and $^{\bullet}OH$ quencher) and HDA (a $^3DOM^*$ quencher) significantly suppressed the photolysis rates of pesticides. In contrast, the addition of DMA (a $CO_3^{\bullet-}$ quencher) and IPA (a $^{\bullet}OH$ quencher) inhibited the photolysis to a much lesser extent. The role of $^1O_2$ and $^3DOM^*$ was further confirmed by pesticide photolysis in aerated and deaerated P8-Sep-2010 water. Deoxygenation usually led to an enhancement in $^3DOM^*$-mediated reactions but an inhibition in $^1O_2$-mediated reactions, while aeration resulted in an opposite effect. Overall, $^1O_2$ and $^3DOM^*$ seemed to dominate the indirect photolysis of pesticides in P8-Sep-2010 water. It should also be pointed out that the addition of a single quencher did not completely halt pesticide photolysis, suggesting the existence of multiple and possibly interconnected reaction pathways.

4.3.3 Role of PPRIs

Under constant irradiance, the observed pesticide photolysis rate (k_{obs}) is a summation of relevant direct and indirect photolysis pathways assuming pseudo-first-order kinetics and steady-state concentrations of PPRIs (Equation (4.10)):

$$-\frac{dC}{dt} = k_{obs} \cdot C \tag{4.10}$$

$$= \left(k_{Direct} + k_{CO_3^{\bullet-}} \cdot [CO_3^{\bullet-}]_{ss} + k_{^{\bullet}OH} \cdot [^{\bullet}OH]_{ss} + k_{^1O_2} \cdot [^1O_2]_{ss} + k_{^3DOM^*} \cdot [^3DOM^*]_{ss} + k_{Other} \right) \cdot C$$

where C is the concentration of pesticide, k_{Direct} is the rate constant of direct photolysis, $k_{CO_3^{\bullet-}}$, $k_{^{\bullet}OH}$, $k_{^1O_2}$ and $k_{^3DOM^*}$ are the second-order rate constants for reactions with $CO_3^{\bullet-}$, $^{\bullet}OH$, $^1O_2$ and $^3DOM^*$, respectively, and k_{Other} is sum of rate constants for other concurrent processes. A summary of the available second-order rate constants for reactions of pesticides with PPRIs of interest is tabulated in Table C.7. Although the

reactions of many pesticides with $^{\bullet}OH$ are well documented, fewer or no reaction rate constants have been reported for $CO_3^{\bullet-}$, $^1O_2$ and $^3DOM^*$, making it difficult to calculate the contribution of these three PPRIs. In lieu of direct calculation, a decrease in k_{obs} resulting from the quenching of a specific PPRI was assumed to be equivalent to the contribution of that PPRI to the overall photolysis, knowing that quenchers often have a strong, preferential reactivity for a single PPRI. Quenchers, however, may not be completely selective and can simultaneously scavenge multiple PPRIs when used in excessive doses. Based on literature data (see Table C.8), DMA was assumed to quench $CO_3^{\bullet-}$ only, IPA was assumed to quench radicals (e.g., $^{\bullet}OH$ and $CO_3^{\bullet-}$), DABCO and HIS were assumed to quench both $^1O_2$ and radicals, and HDA was assumed to quench $^3DOM^*$ only. For an *upper bound* estimate, the following equations (Equations (4.11), (4.12), (4.13), and (4.14)) were derived to calculate the individual contribution of PPRIs:

$$k_{CO_3^{\bullet-}} \cdot [CO_3^{\bullet-}]_{ss} \approx k_{obs} - k_{obs,\,DMA} \tag{4.11}$$

$$k_{^{\bullet}OH} \cdot [^{\bullet}OH]_{ss} \approx (k_{obs} - k_{obs,\,IPA}) - (k_{obs} - k_{obs,\,DMA}) \tag{4.12}$$

$$k_{^1O_2} \cdot [^1O_2]_{ss} \approx (k_{obs} - k_{obs,\,HIS/DABCO}) - (k_{obs} - k_{obs,\,IPA}) \tag{4.13}$$

$$k_{^3DOM^*} \cdot [^3DOM^*]_{ss} \approx k_{obs} - k_{obs,\,HDA} \tag{4.14}$$

where $k_{obs,\,DMA}$, $k_{obs,\,IPA}$, $k_{obs,\,HIS/DABCO}$, and $k_{obs,\,HDA}$ are the observed photolysis rates in the PPL water amended with DMA, IPA, HIS or DABCO, and HDA, respectively. The validity of such approximation was checked against the predicted contribution of PPRIs computed from available second-order rate constants and measured steady-state concentrations of PPRIs. Despite the simplifications and assumptions, the calculated and predicted contributions of $CO_3^{\bullet-}$, $^{\bullet}OH$ and $^1O_2$ were usually within ±15% agreement (see

Table C.6), suggesting that the extent of quenching is a reasonable proxy for estimating the contribution of PPRIs. Accordingly, the percent contributions of direct photolysis and photosensitized reactions to the overall photolysis of the sixteen pesticides were calculated for native P8-Sep-2010 water under simulated sunlight.

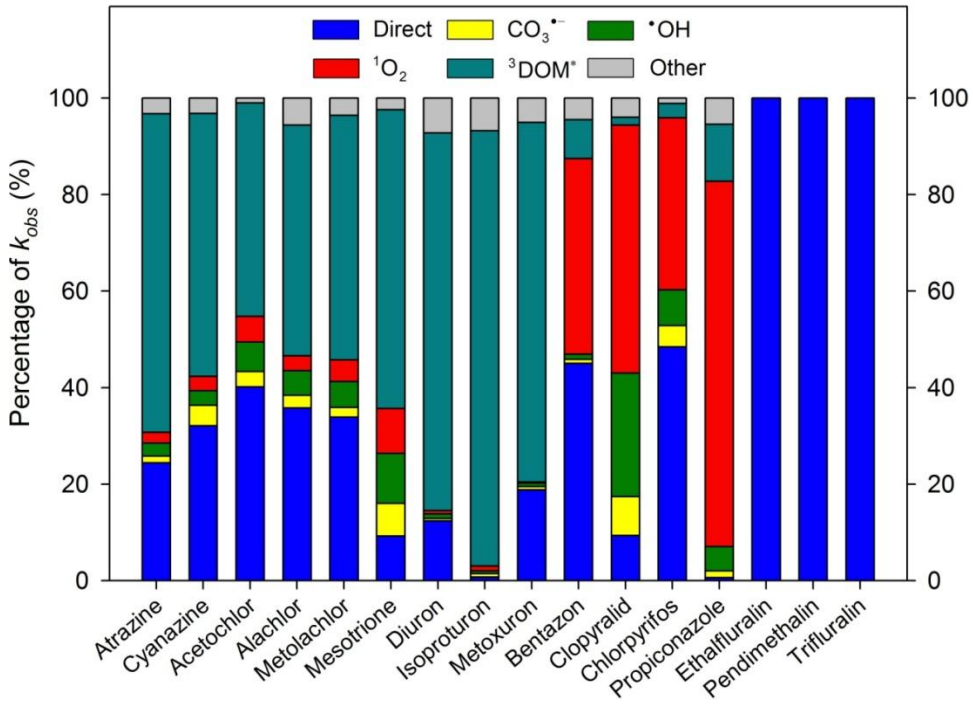

Figure 4.3 Percent contributions of direct photolysis, $CO_3^{\bullet-}$, $^{\bullet}OH$, $^1O_2$, $^3DOM^*$, and other processes to the photodegradation of pesticides in P8-Sep-2010 water under simulated sunlight. Stacked bars plotted based on values calculated from Table C.6. See text and Appendix C.10 for additional details.

As shown by Figure 4.3, for pesticides that were inefficiently degraded by direct photolysis, indirect photolysis induced by $CO_3^{\bullet-}$, $^{\bullet}OH$, $^1O_2$ or $^3DOM^*$ was the main dissipation process, with $^1O_2$ or $^3DOM^*$ often dominating. Unidentified processes constitute a small fraction (<10%) of the observed loss of pesticides. Pesticides from different categories appeared to exhibit contrasting photochemical behavior in the PPL water, as further detailed below.

Atrazine and cyanazine The photodegradation of *s*-triazines proceeds via dechlorination, *N*-dealkylation or *N*-alkyl oxidation.[117-119] Depending on the source and abundance of DOM, atrazine photolysis rates can either be enhanced or retarded.[54,118,120-122] Several studies have shown that indirect photolysis of atrazine occurs mainly through reaction with $^{\bullet}OH$, especially in the presence of nitrate.[55,63,65,118] In carbonate-rich waters, the scavenging of $^{\bullet}OH$ by bi/carbonate ions tends to slow down the overall atrazine photodegradation owing to the lower reactivity of formed $CO_3^{\bullet-}$.[47,50] Unlike $^{\bullet}OH$-mediated processes, $^3DOM^*$ surrogates have been found to accelerate atrazine photolysis via hydrogen abstraction.[71,117,119] Conversely, oxidation by $^1O_2$ is often considered unimportant in *s*-triazine photolysis due to the quenching effect of *N*-ethyl side chain.[117,123] In P8-Sep-2010 water, direct photolysis of atrazine and cyanazine explained 24-32% of k_{obs}, while the largest fraction (55-66%) of k_{obs} stemmed from interaction with $^3DOM^*$. The overall contribution of $CO_3^{\bullet-}$, $^{\bullet}OH$ and $^1O_2$ were much less, summing to only 6-10% of k_{obs}.

Acetochlor, Alachlor and Metolachlor The photodegradation of chloroacetanilides in natural waters has been found to proceed through several routes, including dechlorination, hydroxylation, dehydrochlorination with subsequent cyclization, and *N*-dealkylation.[40,60,124,125] The presence of nitrate can significantly enhance chloroacetanilide photolysis through $^{\bullet}OH$ production, while DOM often inhibits photolysis by acting as a light attenuator and scavenger of $^{\bullet}OH$.[44,56,60,65,124,126,127] A case study of alachlor photolysis in wetland waters has also suggested a negligible role of $^3DOM^*$ but a possible involvement of $^1O_2$.[44] In P8-Sep-2010 water, both direct photolysis

and $^{3}DOM^{*}$-mediated reactions were important contributors to the photodegradation of acetochlor, alachlor and metolachlor, accounting for 34-40% and 44-51% of k_{obs}, respectively. The influence of $CO_3^{\bullet-}$, $^{\bullet}OH$, and $^{1}O_2$ on k_{obs} was relatively small (~2-6%).

Mesotrione Direct photolysis of mesotrione is a relatively slow process that proceeds via hydroxylation, but the presence of nitrate and DOM has been found to increase its photodegradation rate up to a factor of ten, pointing to the significance of $^{\bullet}OH$, $^{1}O_2$ and $^{3}DOM^{*}$.[62,68,128,129] In P8-Sep-2010 water, direct photolysis of mesotrione was only responsible for 9% of k_{obs}., while a significant portion (~62%) of k_{obs} could be explained by reaction with $^{3}DOM^{*}$, followed by $^{\bullet}OH$ (~10%), $^{1}O_2$ (~9%) and $CO_3^{\bullet-}$ (~7%), respectively.

Diuron, Isoproturon and Metoxuron Direct photolysis of phenylurea herbicides mainly involves hydroxylation, *N*-dealkylation or *N*-alkyl oxidation but is generally slow.[130] Both laboratory and field measurements have confirmed that indirect photolysis of phenylurea herbicides in natural waters mainly originates from reactions with $^{3}DOM^{*}$ via electron transfer and/or hydrogen abstraction.[41,70] Recent modeling studies have also predicted that $CO_3^{\bullet-}$ and $^{\bullet}OH$ might serve as additional sinks of diuron, with the latter being more important due to its higher reactivity.[50,65,131] In P8-Sep-2010 water, direct photolysis of diuron, isoproturon and metoxuron was responsible for 1-19% of k_{obs}. The largest fraction (75-90%) of k_{obs} originated from reaction with $^{3}DOM^{*}$, while reactions with $CO_3^{\bullet-}$, $^{\bullet}OH$ and $^{1}O_2$ were minor (~1-2%).

Bentazon Direct photolysis involving hydroxylation or oxidation often dominates the aquatic photochemistry of bentazon.[40,125,132] The presence of DOM, however, has

been shown to enhance its overall photodegradation.[40,66,132] Indirect photolysis of bentazon has previously been suspected to involve photosensitized hydroxylation,[40,132] but a recent study showed that $^{\bullet}OH$-mediated process might only account for less than 3% of bentazon photolysis in estuarine waters.[66] In P8-Sep-2010 water, the largest fraction (~45%) of k_{obs} was attributable to direct photolysis of bentazon, while the contribution of $^{1}O_2$ was at a comparable level, explaining ~41% of k_{obs}. The contribution of $^{3}DOM^{*}$ was limited (~8%), and the role of $CO_3^{\bullet-}$ and $^{\bullet}OH$ was almost negligible (~1%).

Clopyralid Limited quantitative data are available regarding the aquatic photochemistry of clopyralid. In P8-Sep-2010 water, direct photolysis of clopyralid only accounted for ~9% of k_{obs}, corresponding to its slow photolysis in pure water.[133] Conversely, a significant portion (~52%) of k_{obs} was assignable to reaction with $^{1}O_2$, followed by $^{\bullet}OH$ (~26%) and $CO_3^{\bullet-}$ (~8%), respectively. The contribution of $^{3}DOM^{*}$ (~2%) was minimal.

Chlorpyrifos Direct photolysis involving dearylation or oxidative desulfuration represents major reaction routes in the photodegradation of chlorpyrifos,[134,135] while an inconsistent trend of chlorpyrifos loss has been observed increasing DOM.[57,136,137] Earlier work has demonstrated that oxidation induced by $^{\bullet}OH$ may play a key role in chlorpyrifos photolysis.[57,116] A recent study has also illustrated that $CO_3^{\bullet-}$ can potentially contribute to chlorpyrifos dissipation in carbonate-rich waters.[51] In P8-Sep-2010 water, direct photolysis of chlorpyrifos constituted the largest portion (~48%) of k_{obs}, followed by $^{1}O_2$

(~36%), $^{\bullet}OH$ (~7%) and $CO_3^{\bullet-}$ (~4%), respectively. In contrast, the contribution of $^3DOM^*$ was minor (~3%).

Propiconazole Direct photolysis of propiconazole proceeds rather slowly in pure water,[45,138,139] but its photodegradation is often increased in the presence of DOM or in natural waters with oxidation being the major pathway.[138] Elevated nitrate levels has been found to accelerate the photodegradation of propiconazole via reaction with $^{\bullet}OH$, while bi/carbonate retards its photolysis by $^{\bullet}OH$ scavenging.[45] In P8-Sep-2010 water, direct photolysis of propiconazole was negligible (<1%), which is in line with previous findings, while $^1O_2$ contributed up to ~76% of k_{obs}. A smaller fraction of k_{obs} could be explained by $^3DOM^*$ (~12%), but $^{\bullet}OH$ (~5%) and $CO_3^{\bullet-}$ (~2%) were not involved to any significant extent.

Ethafluralin, Pendimethalin, and Trifluralin The photodegradation of trifluralin in natural waters is known to occur primarily through direct photolysis involving oxidative *N*-dealkylation, nitro reduction or cyclization.[59,140,141] Increasing DOM levels often slows down the photodegradation of trifluralin relative to its direct photolysis due to the light screening effect.[59,140] The involvement of photosensitized reactions; however, cannot be completely ruled out. For instance, reaction with $^{\bullet}OH$ has been postulated as a major sink for trifluralin in waters containing high nitrate.[59] Meanwhile, increasing DO levels in waters has also been shown to enhance trifluralin photolysis, which might be interpreted by the participation of $^1O_2$ via reaction with amine intermediates formed upon *N*-dealkylation.[141] In P8-Sep-2010 water, direct photolysis of trifluralin essentially explained 100% of k_{obs} and the role of PPRIs was negligible. Similar patterns were

observed for ethalfuralin and pendimethalin, confirming that indirect photolysis is negligible for dinitroanilines in this system.

4.3.4 Pesticide Photodegradation under Natural Sunlight

To check the transferability of results obtained from indoor photolysis, complementary outdoor experiments were conducted using selected pesticides in P8-Sep-2010, P1-Apr-2012, and P8-Apr-2012 water, respectively. Logarithmic plots for pesticide photolysis versus actinometer loss suggest that outdoor photolysis also followed pseudo-first-order kinetics (see Figure C.9, Figure C.11 and Figure C.14). The observed outdoor photolysis rates of pesticides in three PPL waters are summarized in Table C.9, Table C.11 and Table C.13, respectively. The rates exhibited the same trend as observed in indoor photolysis. The photodegradation of pesticides in P8-Sep-2010 water under natural sunlight proceeded ~60% slower than that under simulated sunlight (see Figure 4.4). Under natural sunlight, the photolysis rates of pesticides in P8-Sep-2010 and P8-Apr-2012 waters were similar, both of which were ~20% slower than those measured in P1-Apr-2012 water which contained higher steady-state concentrations of PPRIs.

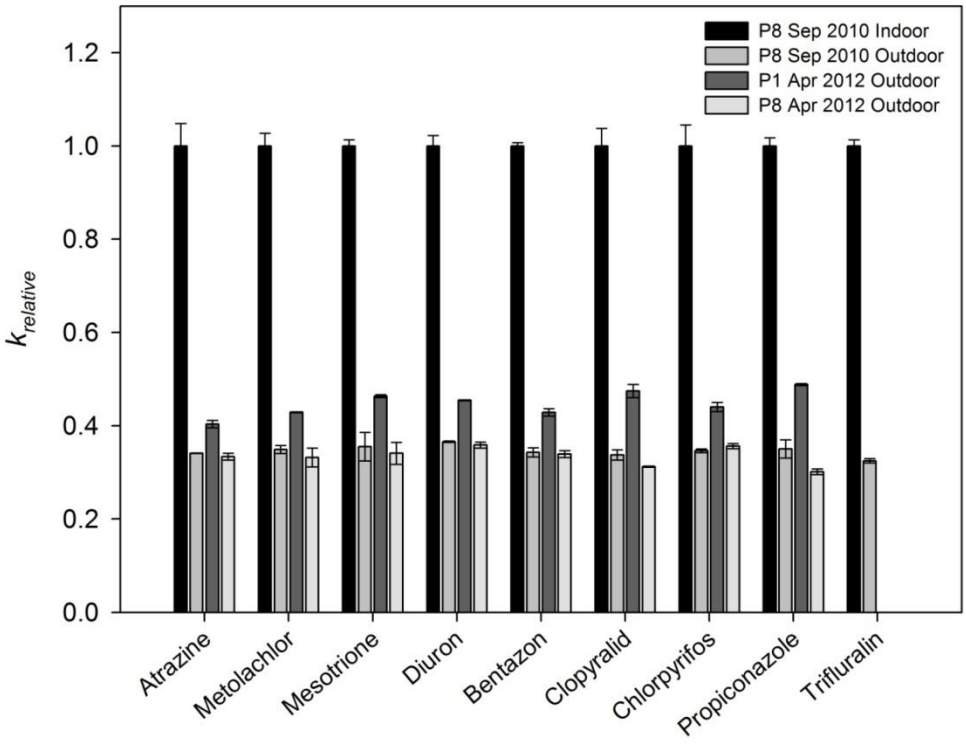

Figure 4.4 Comparison of pesticide photodegradation in PPL waters under simulated and natural sunlight. Observed indoor and outdoor photolysis rates in P8-Sep-2010, P1-Apr-2012, and P8-Apr-2012 waters were normalized to the observed indoor photolysis rates in P8-Sep-2010 water to yield "$k_{relative}$". Error bars represent one standard deviation propagated through observed rate constants.

Quencher experiments were conducted in each PPL water to further evaluate the contribution of PPRIs (see Figure C.10, Figure C.12 and Figure C.14), and the observed outdoor photolysis rate was parsed out as described previously. As shown by Figure 4.5, the relative contributions of direct and indirect reaction pathways to pesticide photolysis under natural sunlight are analogous to those found under simulated sunlight. The second-order rate constants for reactions of pesticides with PPRIs were calculated based on the quenching effect on k_{obs} and measured steady-state concentrations of PPRIs and are tabulated in Table 4.3. Second-order rate constants were not estimated for ethalfluralin, pendiemthalin, and trifluralin because of the dominance of direct photolysis.

In most cases, the rate constants for reactions of pesticides with $CO_3^{\bullet-}$, $^{\bullet}OH$ and $^1O_2$ compare favorably with reported literature values (Table C.7). The rate constants for reactions of pesticides with $^3DOM^*$ spanned from 10^6 to 10^{10} M^{-1} s^{-1}, which concur with rate constants for quenching of triplet-state aromatic ketones by substituted phenols.[109,142] The estimated rate constant was $7.8(\pm1.6)\times10^9$ M^{-1} s^{-1} for diuron, which is of the same order of magnitude as its quenching rate constant with triplet-state benzophenone (i.e., $2.0\ (\pm0.4)\times10^9$ M^{-1} s^{-1}).[70] Due to a lack of knowledge about the structure of DOM derived in PPLs, these second-order rate constants cannot be generalized for DOM in other natural waters, but they may still have practical utility for estimating DOM photochemical reaction rates in addition to data obtained from model aromatic ketones.

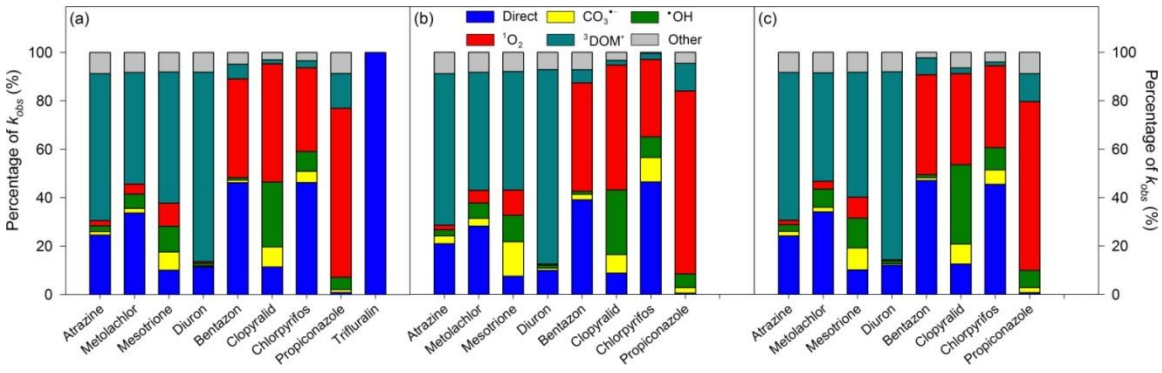

Figure 4.5 Percent contributions of direct photolysis, $CO_3^{\bullet-}$, $^{\bullet}OH$, $^1O_2$, $^3DOM^*$, and other processes to the photodegradation of pesticides in PPL waters under natural sunlight: (a) P8-Sep-2010 water; (b) P1-Apr-2012 water; (c) P8-Apr-2012 water. Stacked bars plotted based on values calculated from Table C.10, Table C.12 and Table C.14, respectively. See text and Appendix C.13, C.14,and C.15 for additional details.

Table 4.3 Estimated second-order rate constants for reactions of target pesticides with PPRIs

Pesticide	$k_{CO_{3,\,est}^{\bullet-}}$ (M^{-1} s^{-1})[a]	$k_{CO_3^{\bullet-}}$ (M^{-1} s^{-1})[b]	$k_{^{\bullet}OH,\,est}$ (M^{-1} s^{-1})[c]	$k_{^{\bullet}OH}$ (M^{-1} s^{-1})[d]
Atrazine	$5.0(\pm1.5)\times10^{6\#}$	$4.4(\pm1.2)\times10^{6}$	$2.7(\pm0.3)\times10^{9\#}$	$2.5(\pm0.4)\times10^{9}$
Cyanazine	$8.8(\pm1.0)\times10^{6*}$	N.A.[h]	$2.1(\pm0.1)\times10^{9*}$	1.9×10^{9}
Acetochlor	$1.1(\pm0.5)\times10^{6*}$	N.A.[h]	$7.3(\pm0.4)\times10^{9*}$	$6.9(\pm1.8)\times10^{9}$
Alachlor	$9.6(\pm1.1)\times10^{6*}$	N.A.[h]	$6.3(\pm0.3)\times10^{9*}$	$6.0(\pm1.4)\times10^{9}$
Metolachlor	$6.2(\pm2.0)\times10^{6\#}$	N.A.[h]	$6.9(\pm0.3)\times10^{9\#}$	$7.0(\pm1.6)\times10^{9}$
Mesotrione	$1.8(\pm0.6)\times10^{7\#}$	N.A.[h]	$8.7(\pm0.3)\times10^{9\#}$	$8.6(\pm0.4)\times10^{9}$
Diuron	$8.1(\pm1.7)\times10^{6\#}$	$7.2(\pm3.1)\times10^{6}$	$6.0(\pm0.2)\times10^{9\#}$	$7.8(\pm1.7)\times10^{9}$
Isoproturon	$2.8(\pm0.3)\times10^{7*}$	$2.7(\pm0.6)\times10^{7}$	$6.4(\pm0.1)\times10^{9*}$	$6.7(\pm1.4)\times10^{9}$
Metoxuron	$9.4(\pm0.9)\times10^{7*}$	$9.6(\pm4.4)\times10^{7}$	$3.4(\pm0.1)\times10^{10*}$	N.A.[h]
Bentazon	$2.5(\pm1.7)\times10^{7\#}$	N.A.[h]	$9.1(\pm0.5)\times10^{9\#}$	$5.7(\pm2.6)\times10^{9}$
Clopyralid	$3.4(\pm1.0)\times10^{6\#}$	N.A.[h]	$4.4(\pm0.2)\times10^{9\#}$	$4.4(\pm0.2)\times10^{9}$
Chlorpyrifos	$9.2(\pm2.6)\times10^{6\#}$	$8.8(\pm0.4)\times10^{6}$	$5.1(\pm0.1)\times10^{9\#}$	$4.7(\pm0.4)\times10^{9}$
Propiconazole	$2.5(\pm1.0)\times10^{6\#}$	N.A.[h]	$3.3(\pm0.2)\times10^{9\#}$	N.A.[h]
Pesticide	$k_{^1O_{2,\,est}}$ (M^{-1} s^{-1})[e]	$k_{^1O_2}$ (M^{-1} s^{-1})[f]	$k_{^3DOM^*,\,est}$ (M^{-1} s^{-1})[g]	$k_{^3DOM^*}$ (M^{-1} s^{-1})
Atrazine	$2.0(\pm0.3)\times10^{5\#}$	N.A.[h]	$1.2(\pm0.2)\times10^{9\#}$	N.A.[h]
Cyanazine	$1.7(\pm0.2)\times10^{5*}$	N.A.[h]	$4.5(\pm0.1)\times10^{8*}$	N.A.[h]
Acetochlor	$5.3(\pm0.1)\times10^{5*}$	N.A.[h]	$6.1(\pm0.3)\times10^{8*}$	N.A.[h]
Alachlor	$3.3(\pm0.1)\times10^{5*}$	N.A.[h]	$6.9(\pm0.7)\times10^{8*}$	N.A.[h]
Metolachlor	$4.4(\pm0.6)\times10^{5\#}$	N.A.[h]	$9.8(\pm1.7)\times10^{8\#}$	N.A.[h]
Mesotrione	$6.9(\pm0.4)\times10^{5\#}$	$6.7(\pm0.3)\times10^{5}$	$7.8(\pm1.1)\times10^{8\#}$	N.A.[h]
Diuron	$2.9(\pm0.6)\times10^{5\#}$	N.A.[h]	$7.8(\pm1.6)\times10^{9\#}$	N.A.[h]
Isoproturon	$1.0(\pm0.1)\times10^{6*}$	N.A.[h]	$1.3(\pm0.3)\times10^{10*}$	N.A.[h]
Metoxuron	$9.6(\pm3.1)\times10^{5*}$	N.A.[h]	$4.2(\pm0.1)\times10^{10*}$	N.A.[h]
Bentazon	$3.1(\pm0.3)\times10^{7\#}$	N.A.[h]	$9.7(\pm2.0)\times10^{8\#}$	N.A.[h]
Clopyralid	$7.0(\pm0.9)\times10^{5\#}$	N.A.[h]	$5.7(\pm3.8)\times10^{6\#}$	N.A.[h]
Chlorpyrifos	$1.9(\pm0.2)\times10^{6\#}$	N.A.[h]	$2.7(\pm1.3)\times10^{7\#}$	N.A.[h]
Propiconazole	$3.9(\pm0.3)\times10^{6\#}$	N.A.[h]	$1.3(\pm0.4)\times10^{8\#}$	N.A.[h]

[a] Calculated as the average of $k_{calc,\,CO_3^{\bullet-}}$ / $[CO_3^{\bullet-}]_{ss}$ from indoor photolysis ($^{\#}$) or from both indoor and outdoor photolysis (*), where $k_{calc,\,CO_3^{\bullet-}}$ is from Table C.6, Table C.10, Table C.12, and Table C.14 and $[CO_3^{\bullet-}]_{ss}$ is from Table 4.1. [b] Average literature value from Table C.7. [c] Calculated as the average of $k_{calc,\,^{\bullet}OH}$ / $[^{\bullet}OH]_{ss}$ from indoor photolysis ($^{\#}$) or from both indoor and outdoor photolysis (*), where $k_{calc,\,^{\bullet}OH}$ is from Table C.6, Table C.10, Table C.12, and Table C.14 and $[^{\bullet}OH]_{ss}$ is from Table 4.1. [d] Average literature value from Table S8. [e] Calculated as the average of $k_{calc,\,^1O_2}$ / $[^1O_2]_{ss}$ from indoor photolysis ($^{\#}$) or from both indoor and outdoor photolysis (*), where $k_{calc,\,^1O_2}$ is from Table C.6, Table C.10, Table C.12, and Table C.14 and $[^1O_2]_{ss}$ is from Table 4.1. [f] Average literature value from Table S7. [g] Calculated as the average of $k_{calc,\,^3DOM^*}$ / $[^3DOM^*]_{ss}$ from indoor photolysis ($^{\#}$) or from both indoor and outdoor photolysis (*), where $k_{calc,\,^3DOM^*}$ is from Table C.6, Table C.10, Table C.12, and Table C.14 and $[^3DOM^*]_{ss}$ is from Table 4.1. [h] N.A. = not available.

4.4 Summary

The current study combines photolysis kinetics and reactive intermediate concentrations to elucidate the photochemical fate of pesticides in PPLs. For most pesticides surveyed, indirect photolysis in the PPL water outweighed direct photolysis under both simulated and natural sunlight. Although a quantitative link of PPRI concentrations to specific water chemistry parameters is difficult to establish, the photoreactivity of PPL water originated from DOM production of PPRIs upon irradiation. Quencher experiments further revealed that $^{1}O_2$ and $^{3}DOM^{*}$ had large effects on pesticide photolysis. For each category of pesticides, the relative contribution of individual PPRIs to the overall photodegradation followed a similar pattern in the three PPL water samples. Results from this study contribute to a systematic evaluation of the potential for photochemical attenuation of pesticides in near-surface PPL water. More detailed knowledge on the chemical properties and toxicity of the photoproducts, however, is necessary to reveal the exact mechanism of the pesticide decomposition and associated ecological risks. Given the interconnectedness of water resources in the PPR, a better understanding of pesticide photolysis in PPLs may shed light on future water and land use management strategies. For instance, optimizing photolysis efficiency by adjustment of water residence time in *drained* PPLs would potentially reduce downstream environmental exposure to pesticides. Similarly, the photochemical processing in *undrained* PPLs may protect groundwater resources and provide an incentive to prevent further drainage of these critical landscape elements. On a broad scale, the spatiotemporal variation of the PPL hydrochemistry (e.g., DOM quantity and quality) driven by

changing land use and climate[73,74,115,143] and its effect on the photochemical fate of pesticides also merit further investigation.

4.5 References

1. van der Valk, A. G., The prairie potholes of North America. In *The World's Largest Wetlands*, Fraser, L. H.; Keddy, P. A., Eds. Cambridge University Press: Cambridge, UK, 2005; pp 393-423.
2. Kantrud, H. A.; Krapu, G. L.; Swanson, G. A. *Prairie basin wetlands of the Dakotas: A community profile*; U.S. Fish and Wildlife Service, Biological Report 85: Washington, DC, 1989; pp 1-111.
3. Ostlie, W. R.; Schneider, R. E.; Aldrich, J. M.; Faust, T. M.; McKim, R. L. B.; Chaplin., S. J. *The status of biodiversity in the Great Plains*; The Nature Conservancy; Arlington, VA, 1997.
4. LaBaugh, J. W.; Winter, T. C.; Rosenberry, D. O., Hydrological functions of prairie wetlands. *Great Plains Res.* **1998,** *8*, 17-37.
5. van der Kamp, G.; Hayashi, M., The groundwater recharge functions of prairie wetlands. *Great Plains Res.* **1998,** *8*, 39-56.
6. Samson, F. B.; Knopf, F. L.; Ostlie, W. R., Great Plains ecosystems: Past, present, and future. *Wildl. Soc. Bull.* **2004,** *32*, 6-15.
7. Stubbs, M. *Land conversion in the northern plains*; Resources, Science, and Industry Division, The National Council for Science and the Environment, CRS Report for Congress RL33950: Washington, DC, 2007.
8. Watmough, M. D.; Schmoll, M. J. *Environment Canada's prairie & northern region habitat monitoring program phase II: Recent habitat trends in the prairie habitat joint venture*; Canadian Wildlife Service, Environment Canada, Report Series Number 493; Ottawa, Canada, 2007.
9. Oslund, F. T.; Johnson, R. R.; Hertel, D. R., Assessing wetland changes in the prairie pothole region of Minnesota from 1980 to 2007. *J. Fish Wildl. Manag.* **2010,** *1*, 131-135.
10. Lenhart, C. F.; Verry, E. S.; Brooks, K. N.; Magner, J. A., Adjustment of prairie pothole streams to land-use, drainage and cliamte changes and consequences for turbidity impairment. *River Res. Appl.* **2011**, DOI: 10.1002/rra.1549.
11. Anteau, M., Do interactions of land use and climate affect productivity of waterbirds and prairie-pothole wetlands? *Wetlands* **2012,** *32*, 1-9.
12. Brunet, N. N.; Westbrook, C. J., Wetland drainage in the Canadian prairies: Nutrient, salt and bacteria characteristics. *Agric. Ecosyst. Environ.* **2012,** *146*, 1-12.
13. Neely, R. K.; Baker, J. L., Nitrogen and phosphorous dynamics and the fate of agricultural runoff. In *Northern Prairie Wetlands*, Van der Valk, A. G., Ed. Iowa State University Press: Ames, IA, 1989; pp 92-131.
14. Olness, A.; Staricka, J. A.; Daniel, J. A., Oxidation-reduction and groundwater contamination in the Prairie Pothole region of the Northern Great Plains. In *Water for Agriculture and Wildlife and the Environment -- Win-Win Opportunities: Proceedings of*

the 1996 USCID Wetlands Seminar, Schaack, J.; Anderson, S. S., Eds. U.S. Committee on Irrigation and Drainage: Denver, CO, 1996; pp 115-131.
15. Goldsborough, L. G.; Crumpton, W. G., Distribution and environmental fate of pesticides in prairie wetlands. *Great Plains Res.* **1998,** *8*, 73-95.
16. Crumpton, W. G.; Goldsborough, L. G., Nitrogen transformation and fate in prairie wetlands. *Great Plains Res.* **1998,** *8*, 57-72.
17. Detenbeck, N. E.; Elonen, C. M.; Taylor, D. L.; Cotter, A. M.; Puglisi, F. A.; Sanville, W. D., Effects of agricultural activities and best management practices on water quality of seasonal prairie pothole wetlands. *Wetlands Ecol. Manage.* **2002,** *10*, 335-354.
18. Ontkean, G. R.; Chanasyk, D. S.; Riemersma, S.; Bennett, D. R.; Brunen, J. M., Enhanced prairie wetland effects on surface water quality in Crowfoot Creek, Alberta. *Water Qual. Res. J. Can.* **2003,** *38*, 335-359.
19. Donald, D. B.; Syrgiannis, J.; Hunter, F.; Weiss, G., Agricultural pesticides threaten the ecological integrity of northern prairie wetlands. *Sci. Total Environ.* **1999,** *231*, 173-181.
20. Whigham, D. F.; Jordan, T. E., Isolated wetlands and water quality. *Wetlands* **2003,** *23*, 541-549.
21. Cessna, A. J.; Sheedy, C.; Farenhorst, A.; McQueen, D. A. R., Indicator of the Risk of Water Contamination by Pesticides. In *Environmental Sustainability of Canadian Agriculture: Agri-Environmental Indicator Report Series - Report No. 3*, Eilers, W.; MacKay, R.; Graham, L.; Lefebvre, A., Eds. Agriculture and Agri-Food Canada: Ottawa, Canada, 2010.
22. Sura, S.; Waiser, M.; Tumber, V.; Lawrence, J. R.; Cessna, A. J.; Glozier, N., Effects of glyphosate and two herbicide mixtures on microbial communities in prairie wetland ecosystems: A mesocosm approach. *J. Environ. Qual.* **2012,** *41*, 732-743.
23. Zabik, M. J.; Leavitt, R. A.; Su, G. C. C., Photochemistry of bioactive compounds: A review of pesticide photochemistry. *Annu. Rev. Entomol.* **1976,** *21*, 61-79.
24. Burrows, H. D.; Canle L, M.; Santaballa, J. A.; Steenken, S., Reaction pathways and mechanisms of photodegradation of pesticides. *J. Photochem. Photobiol. B: Biol.* **2002,** *67*, 71-108.
25. Katagi, T., Photodegradation of pesticides on plant and soil surfaces. In *Reviews of Environmental Contamination and Toxicology, Vol 182*, Springer: New York, 2004; Vol. 182, pp 1-189.
26. Schwarzenbach, R. P.; Gschwend, P. M.; Imboden, D. M., *Environmental Organic Chemistry*. John Wiley & Sons, Inc.: Hoboken, NJ, 2003.
27. Zafiriou, O. C., Sources and Reactions of OH and Daughter Radicals in Seawater. *J. Geophys. Res.* **1974,** *79*, 4491-4497.
28. Zepp, R. G.; Wolfe, N. L.; Baughman, G. L.; Hollis, R. C., Singlet oxygen in natural waters. *Nature* **1977,** *267*, 421-423.
29. Zafiriou, O. C.; True, M. B., Nitrate photolysis in seawater by sunlight. *Mar. Chem.* **1979,** *8*, 33-42.
30. Zafiriou, O. C.; True, M. B., Nitrite photolysis in seawater by sunlight. *Mar. Chem.* **1979,** *8*, 9-32.

31. Mill, T.; Hendry, D. G.; Richardson, H., Free-radical oxidants in natural waters. *Science* **1980,** *207*, 886-887.
32. Baxter, R. M.; Carey, J. H., Evidence for photochemical generation of superoxide ion in humic waters. *Nature* **1983,** *306*, 575-576.
33. Cooper, W. J.; Zika, R. G., Photochemical formation of hydrogen peroxide in surface and ground waters exposed to sunlight. *Science* **1983,** *220*, 711-712.
34. Zepp, R. G.; Schlotzhauer, P. F.; Sink, R. M., Photosensitized transformations involving electronic energy transfer in natural waters: role of humic substances. *Environ. Sci. Technol.* **1985,** *19*, 74-81.
35. Zepp, R. G.; Braun, A. M.; Hoigne, J.; Leenheer, J. A., Photoproduction of hydrated electrons from natural organic solutes in aquatic environments. *Environ. Sci. Technol.* **1987,** *21*, 485-490.
36. Zafiriou, O. C.; Joussot-Dubien, J.; Zepp, R. G.; Zika, R. G., Photochemistry of natural waters. *Environ. Sci. Technol.* **1984,** *18*, 358A-371A.
37. Mill, T., Predicting photoreaction rates in surface waters. *Chemosphere* **1999,** *38*, 1379-1390.
38. Zepp, R. G.; Cline, D. M., Rates of direct photolysis in aquatic environment. *Environ. Sci. Technol.* **1977,** *11*, 359-366.
39. Zepp, R. G.; Wolfe, N. L.; Gordon, J. A.; Fincher, R. C., Light-induced transformations of methoxychlor in aquatic systems. *J. Agric. Food. Chem.* **1976,** *24*, 727-733.
40. Chiron, S.; Barceló, D.; Abian, J.; Ferrer, M.; Sanchez-Baeza, F.; Messeguer, A., Comparative photodegradation rates of alachlor and bentazone in natural water and determination of breakdown products. *Environ. Toxicol. Chem.* **1995,** *14*, 1287-1298.
41. Gerecke, A. C.; Canonica, S.; Muller, S. R.; Scharer, M.; Schwarzenbach, R. P., Quantification of dissolved natural organic matter (DOM) mediated phototransformation of phenylurea herbicides in lakes. *Environ. Sci. Technol.* **2001,** *35*, 3915-3923.
42. Miller, P. L.; Chin, Y.-P., Photoinduced degradation of carbaryl in a wetland surface water. *J. Agric. Food. Chem.* **2002,** *50*, 6758-6765.
43. Schulz, R.; Hahn, C.; Bennett, E. R.; Dabrowski, J. M.; Thiere, G.; Peall, S. K. C., Fate and effects of azinphos-methyl in a flow-through wetland in South Africa. *Environ. Sci. Technol.* **2003,** *37*, 2139-2144.
44. Miller, P. L.; Chin, Y.-P., Indirect photolysis promoted by natural and engineered wetland water constituents: Processes leading to alachlor degradation. *Environ. Sci. Technol.* **2005,** *39*, 4454-4462.
45. Wallace, D. F.; Hand, L. H.; Oliver, R. G., The role of indirect photolysis in limiting the persistence of crop protection products in surface waters. *Environ. Toxicol. Chem.* **2010,** *29*, 575-581.
46. Huang, J.; Mabury, S. A., The role of carbonate radical in limiting the persistence of sulfur-containing chemicals in sunlit natural waters. *Chemosphere* **2000,** *41*, 1775-1782.
47. Lam, M. W.; Tantuco, K.; Mabury, S. A., PhotoFate: A new approach in accounting for the contribution of indirect photolysis of pesticides and pharmaceuticals in surface waters. *Environ. Sci. Technol.* **2003,** *37*, 899-907.

48. Canonica, S.; Kohn, T.; Mac, M.; Real, F. J.; Wirz, J.; von Gunten, U., Photosensitizer method to determine rate constants for the reaction of carbonate radical with organic compounds. *Environ. Sci. Technol.* **2005,** *39*, 9182-9188.
49. Mazellier, P.; Busset, C.; Delmont, A.; De Laat, J., A comparison of fenuron degradation by hydroxyl and carbonate radicals in aqueous solution. *Water Res.* **2007,** *41*, 4585-4594.
50. Vione, D.; Maurino, V.; Minero, C.; Carlotti, M. E.; Chiron, S.; Barbati, S., Modelling the occurrence and reactivity of the carbonate radical in surface freshwater. *C. R. Chim.* **2009,** *12*, 865-871.
51. Wu, C.; Linden, K. G., Phototransformation of selected organophosphorus pesticides: Roles of hydroxyl and carbonate radicals. *Water Res.* **2010,** *44*, 3585-3594.
52. Dell'Arciprete, M. L.; Soler, J. M.; Santos-Juanes, L.; Arques, A.; Mártire, D. O.; Furlong, J. P.; Gonzalez, M. C., Reactivity of neonicotinoid insecticides with carbonate radicals. *Water Res.* **2012**.
53. Haag, W. R.; Yao, C. C. D., Rate constants for reaction of hydroxyl radicals with several drinking water contaminants. *Environ. Sci. Technol.* **1992,** *26*, 1005-1013.
54. Minero, C.; Pramauro, E.; Pelizzetti, E.; Dolci, M.; Marchesini, A., Photosensitized transformations of atrazine under simulated sunlight in aqueous humic acid solution. *Chemosphere* **1992,** *24*, 1597-1606.
55. Mabury, S. A.; Crosby, D. G., Pesticide reactivity toward hydroxyl and its relationship to field persistence. *J. Agric. Food. Chem.* **1996,** *44*, 1920-1924.
56. Fulkerson-Brekken, J.; Brezonik, P. L., Indirect photolysis of acetochlor: Rate constant of a nitrate-mediated hydroxyl radical reaction. *Chemosphere* **1998,** *36*, 2699-2704.
57. Kamiya, M.; Kameyama, K., Photochemical effects of humic substances on the degradation of organophosphorus pesticides. *Chemosphere* **1998,** *36*, 2337-2344.
58. Armbrust, K. L., Pesticide hydroxyl radical rate constants: Measurements and estimates of their importance in aquatic environments. *Environ. Toxicol. Chem.* **2000,** *19*, 2175-2180.
59. Dimou, A. D.; Sakkas, V. A.; Albanis, T. A., Trifluralin photolysis in natural waters and under the presence of isolated organic matter and nitrate ions: Kinetics and photoproduct analysis. *J. Photochem. Photobiol. A: Chem.* **2004,** *163*, 473-480.
60. Dimou, A. D.; Sakkas, V. A.; Albanis, T. A., Metolachlor photodegradation study in aqueous media under natural and simulated solar irradiation. *J. Agric. Food. Chem.* **2005,** *53*, 694-701.
61. Shemer, H.; Sharpless, C. M.; Elovitz, M. S.; Linden, K. G., Relative rate constants of contaminant candidate list pesticides with hydroxyl radicals. *Environ. Sci. Technol.* **2006,** *40*, 4460-4466.
62. Richard, C.; ter Halle, A.; Brahmia, O.; Malouki, M.; Halladja, S., Auto-remediation of surface waters by solar-light: Photolysis of 1-naphthol, and two herbicides in pure and synthetic waters. *Catal. Today* **2007,** *124*, 82-87.
63. Garbin, J. R.; Milori, D. M. B. P.; Simões, M. L.; da Silva, W. T. L.; Neto, L. M., Influence of humic substances on the photolysis of aqueous pesticide residues. *Chemosphere* **2007,** *66*, 1692-1698.

64. Dell'Arciprete, M. L.; Santos-Juanes, L.; Sanz, A. A.; Vicente, R.; Amat, A. M.; Furlong, J. P.; Martire, D. O.; Gonzalez, M. C., Reactivity of hydroxyl radicals with neonicotinoid insecticides: Mechanism and changes in toxicity. *Photochem. Photobiol. Sci.* **2009,** *8*, 1016-1023.
65. Vione, D.; Das, R.; Rubertelli, F.; Maurino, V.; Minero, C.; Barbati, S.; Chiron, S., Modelling the occurrence and reactivity of hydroxyl radicals in surface waters: Implications for the fate of selected pesticides. *Int. J. Environ. Anal. Chem.* **2010,** *90*, 260-275.
66. Al Housari, F.; Höhener, P.; Chiron, S., Factors responsible for rapid dissipation of acidic herbicides in the coastal lagoons of the Camargue (Rhône River Delta, France). *Sci. Total Environ.* **2011,** *409*, 582-587.
67. Ukpebor, J.; Halsall, C., Effects of dissolved water constituents on the photodegradation of fenitrothion and diazinon. *Water, Air, Soil Pollut.* **2012,** *223*, 655-666.
68. ter Halle, A.; Richard, C., Simulated solar light irradiation of mesotrione in natural waters. *Environ. Sci. Technol.* **2006,** *40*, 3842-3847.
69. Dell'Arciprete, M. L.; Santos-Juanes, L.; Arques, A.; Vercher, R. F.; Amat, A. M.; Furlong, J. P.; Mártire, D. O.; Gonzalez, M. C., Reactivity of neonicotinoid pesticides with singlet oxygen. *Catal. Today* **2010,** *151*, 137-142.
70. Canonica, S.; Hellrung, B.; Muller, P.; Wirz, J., Aqueous oxidation of phenylurea herbicides by triplet aromatic ketones. *Environ. Sci. Technol.* **2006,** *40*, 6636-6641.
71. Canonica, S.; Laubscher, H. U., Inhibitory effect of dissolved organic matter on triplet-induced oxidation of aquatic contaminants. *Photochem. Photobiol. Sci.* **2008,** *7*, 547-551.
72. Arts, M. T.; Robarts, R. D.; Kasai, F.; Waiser, M. J.; Tumber, V. P.; Plante, A. J.; Rai, H.; Lange, H. J. d., The attenuation of ultraviolet radiation in high dissolved organic carbon waters of wetlands and lakes on the northern Great Plains. *Limnol. Oceanogr.* **2000,** *45*, 292-299.
73. Waiser, M. J.; Robarts, R. D., Changes in composition and reactivity of allochthonous DOM in a prairie saline lake. *Limnol. Oceanogr.* **2000,** *45*, 763-774.
74. Waiser, M. J., Relationship between hydrological characteristics and dissolved organic carbon concentration and mass in northern prairie wetlands using a conservative tracer approach. *J. Geophys. Res.* **2006,** *111*, G02024.
75. Holloway, J. M.; Goldhaber, M. B.; Mills, C. T., Carbon and nitrogen biogeochemistry of a Prairie Pothole wetland, Stutsman County, North Dakota, USA. *Appl. Geochem.* **2011,** *26*, S44-S47.
76. Zeng, T.; Ziegelgruber, K. L.; Chin, Y.-P.; Arnold, W. A., Pesticide processing potential in prairie pothole porewaters. *Environ. Sci. Technol.* **2011,** *45*, 6814-6822.
77. Cessna, A. J.; Donald, D. B.; Bailey, J.; Waiser, M.; Headley, J. V., Persistence of the sulfonylurea herbicides thifensulfuron-methyl, ethametsulfuron-methyl, and metsulfuron-methyl in farm dugouts (ponds). *J. Environ. Qual.* **2006,** *35*, 2395-2401.
78. Headley, J. V.; Du, J.-L.; Peru, K. M.; McMartin, D. W., Mass spectrometry of the photolysis of sulfonylurea herbicides in prairie waters. *Mass Spectrom. Rev.* **2010,** *29*, 593-605.

79. Zollinger, R.; McMullen, M.; Knodel, J.; Gray, J.; Jantzi, D.; Kimmet, G.; Hagemeister, K.; Schmitt, C. *Pesticide Use and Pest Management Practices in North Dakota, 2008*; North Dakota State University in cooperation with North Dakota Agricultural Statistics Service, Extension Publication W-1446; Fargo, ND, 2009.
80. Johnson, J., Monitoring surface waters for pesticides in North Dakota. In *2012 North Dakota Water Quality Monitoring Conference* Bismarck, ND, 2012.
81. Page, S. E.; Arnold, W. A.; McNeill, K., Terephthalate as a probe for photochemically generated hydroxyl radical. *J. Environ. Monit.* **2010,** *12*, 1658-1665.
82. Ryan, C. C.; Tan, D. T.; Arnold, W. A., Direct and indirect photolysis of sulfamethoxazole and trimethoprim in wastewater treatment plant effluent. *Water Res.* **2011,** *45*, 1280-1286.
83. Leifer, A., *The Kinetics of Environmental Aquatic Photochemistry: Theory and Practice*. American Chemical Society: Washington, DC, 1988.
84. Zeng, T.; Chin, Y.-P.; Arnold, W. A., Potential for abiotic reduction of pesticides in prairie pothole porewaters. *Environ. Sci. Technol.* **2012,** *46*, 3177-3187.
85. Huang, J.; Mabury, S. A., Steady-state concentrations of carbonate radicals in field waters. *Environ. Toxicol. Chem.* **2000,** *19*, 2181-2188.
86. Haag, W. R.; Hoigné, J.; Gassman, E.; Braun, A., Singlet oxygen in surface waters - Part I: Furfuryl alcohol as a trapping agent. *Chemosphere* **1984,** *13*, 631-640.
87. Latch, D. E.; Packer, J. L.; Arnold, W. A.; McNeill, K., Photochemical conversion of triclosan to 2,8-dichlorodibenzo-p-dioxin in aqueous solution. *J. Photochem. Photobiol. A: Chem.* **2003,** *158*, 63-66.
88. Grebel, J. E.; Pignatello, J. J.; Mitch, W. A., Sorbic acid as a quantitative probe for the formation, scavenging and steady-state concentrations of the triplet-excited state of organic compounds. *Water Res.* **2011,** *45*, 6535-6544.
89. Magazinovic, R. S.; Nicholson, B. C.; Mulcahy, D. E.; Davey, D. E., Bromide levels in natural waters: its relationship to levels of both chloride and total dissolved solids and the implications for water treatment. *Chemosphere* **2004,** *57*, 329-335.
90. Fischer, A. M.; Kliger, D. S.; Winterle, J. S.; Mill, T., Direct observation of phototransients in natural waters. *Chemosphere* **1985,** *14*, 1299-1306.
91. Thomas-Smith, T. E.; Blough, N. V., Photoproduction of hydrated electron from constituents of natural waters. *Environ. Sci. Technol.* **2001,** *35*, 2721-2726.
92. Wang, W.; Zafiriou, O. C.; Chan, I.-Y.; Zepp, R. G.; Blough, N. V., Production of hydrated electrons from photoionization of dissolved organic matter in natural waters. *Environ. Sci. Technol.* **2007,** *41*, 1601-1607.
93. Zepp, R. G.; Baughman, G. L.; Schlotzhauer, P. F., Comparison of photochemical behavior of various humic substances in water: II. Photosensitized oxygenations. *Chemosphere* **1981,** *10*, 119-126.
94. Draper, W. M.; Crosby, D. G., The photochemical generation of hydrogen peroxide in natural waters. *Arch. Environ. Contam. Toxicol.* **1983,** *12*, 121-126.
95. Haag, W. R.; Hoigné, J., Photo-sensitized oxidation in natural water via $^{\bullet}OH$ radicals. *Chemosphere* **1985,** *14*, 1659-1671.

96. Haag, W. R.; Hoigné, J., Singlet oxygen in surface waters. 3. Photochemical formation and steady-state concentrations in various types of waters. *Environ. Sci. Technol.* **1986,** *20*, 341-348.
97. Cooper, W. J.; Zika, R. G.; Petasne, R. G.; Fischer, A. M., Sunlight-induced photochemistry of humic substances in natural waters: Major reactive species. In *Aquatic Humic Substances*, Suffet, I. H.; MacCarthy, P., Eds. American Chemical Society: Washington DC, 1989; Vol. 219, pp 333-362.
98. Hoigné, J.; Faust, B. C.; Haag, W. R.; Scully, F. E.; Zepp, R. G., Aquatic humic substances as sources and sinks of photochemically produced transient reactants. In *Aquatic Humic Substances*, Suffet, I. H.; MacCarthy, P., Eds. American Chemical Society: Washington DC, 1989; Vol. 219, pp 363-381.
99. Mopper, K.; Zhou, X., Hydroxyl radical photoproduction in the sea and its potential impact on marine processes. *Science* **1990,** *250*, 661-664.
100. Larson, R. A.; Zepp, R. G., Reactivity of the carbonate radical with aniline derivatives. *Environ. Toxicol. Chem.* **1988,** *7*, 265-274.
101. Brezonik, P. L.; Fulkerson-Brekken, J., Nitrate-induced photolysis in natural waters: Controls on concentrations of hydroxyl radical photo-intermediates by natural scavenging agents. *Environ. Sci. Technol.* **1998,** *32*, 3004-3010.
102. Westerhoff, P.; Mezyk, S. P.; Cooper, W. J.; Minakata, D., Electron pulse radiolysis determination of hydroxyl radical rate constants with Suwannee River fulvic acid and other dissolved organic matter isolates. *Environ. Sci. Technol.* **2007,** *41*, 4640-4646.
103. McKay, G.; Dong, M. M.; Kleinman, J. L.; Mezyk, S. P.; Rosario-Ortiz, F. L., Temperature dependence of the reaction between the hydroxyl radical and organic matter. *Environ. Sci. Technol.* **2011,** *45*, 6932-6937.
104. Katsoyiannis, I. A.; Canonica, S.; von Gunten, U., Efficiency and energy requirements for the transformation of organic micropollutants by ozone, O_3/H_2O_2 and UV/H_2O_2. *Water Res.* **2011,** *45*, 3811-3822.
105. Wenk, J.; von Gunten, U.; Canonica, S., Effect of dissolved organic matter on the transformation of contaminants induced by excited triplet states and the hydroxyl radical. *Environ. Sci. Technol.* **2011,** *45*, 1334-1340.
106. Wenk, J.; Canonica, S., Phenolic antioxidants inhibit the triplet-induced transformation of anilines and sulfonamide antibiotics in aqueous solution. *Environ. Sci. Technol.* **2012,** *46*, 5455-5462.
107. Latch, D. E.; McNeill, K., Microheterogeneity of singlet oxygen distributions in irradiated humic acid solutions. *Science* **2006,** *311*, 1743-1747.
108. Grandbois, M.; Latch, D. E.; McNeill, K., Microheterogeneous concentrations of singlet oxygen in natural organic matter isolate solutions. *Environ. Sci. Technol.* **2008,** *42*, 9184-9190.
109. Canonica, S.; Hellrung, B.; Wirz, J., Oxidation of phenols by triplet aromatic ketones in aqueous solution. *J. Phys. Chem. A* **2000,** *104*, 1226-1232.
110. Richard, C.; Trubetskaya, O.; Trubetskoj, O.; Reznikova, O.; Afanas'eva, G.; Aguer, J. P.; Guyot, G., Key role of the low molecular size fraction of soil humic acids for fluorescence and photoinductive activity. *Environ. Sci. Technol.* **2004,** *38*, 2052-2057.

111. Halladja, S.; ter Halle, A.; Aguer, J.-P.; Boulkamh, A.; Richard, C., Inhibition of humic substances mediated photooxygenation of furfuryl alcohol by 2,4,6-trimethylphenol. Evidence for reactivity of the phenol with humic triplet excited states. *Environ. Sci. Technol.* **2007,** *41*, 6066-6073.
112. Cawley, K. M.; Hakala, J. A.; Chin, Y.-P., Evaluating the triplet state photoreactivity of dissolved organic matter isolated by chromatography and ultrafiltration using an alkylphenol probe molecule. *Limnol. Oceanogr.: Methods* **2009,** *7*, 391-398.
113. Cavani, L.; Halladja, S.; ter Halle, A.; Guyot, G.; Corrado, G.; Ciavatta, C.; Boulkamh, A.; Richard, C., Relationship between photosensitizing and emission properties of peat humic acid fractions obtained by tangential ultrafiltration. *Environ. Sci. Technol.* **2009,** *43*, 4348-4354.
114. Guerard, J.; Miller, P.; Trouts, T.; Chin, Y.-P., The role of fulvic acid composition in the photosensitized degradation of aquatic contaminants. *Aquat. Sci.* **2009,** *71*, 160-169.
115. Waiser, M.; Robarts, R., Photodegradation of DOC in a shallow prairie wetland: Evidence from seasonal changes in DOC optical properties and chemical characteristics. *Biogeochemistry* **2004,** *69*, 263-284.
116. Kamiya, M.; Kameyama, K., Effects of selected metal ions on photodegradation of organophosphorus pesticides sensitized by humic acids. *Chemosphere* **2001,** *45*, 231-235.
117. Rejto, M.; Saltzman, S.; Acher, A. J.; Muszkat, L., Identification of sensitized photooxidation products of *s*-triazine herbicides in water. *J. Agric. Food. Chem.* **1983,** *31*, 138-142.
118. Torrents, A.; Anderson, B. G.; Bilboulian, S.; Johnson, W. E.; Hapeman, C. J., Atrazine photolysis: Mechanistic investigations of direct and nitrate-mediated hydroxy radical processes and the influence of dissolved organic carbon from the Chesapeake Bay. *Environ. Sci. Technol.* **1997,** *31*, 1476-1482.
119. Hartenbach, A. E.; Hofstetter, T. B.; Tentscher, P. R.; Canonica, S.; Berg, M.; Schwarzenbach, R. P., Carbon, hydrogen, and nitrogen isotope fractionation during light-induced transformations of atrazine. *Environ. Sci. Technol.* **2008,** *42*, 7751-7756.
120. Konstantinou, I. K.; Zarkadis, A. K.; Albanis, T. A., Photodegradation of selected herbicides in various natural waters and soils under environmental conditions. *J. Environ. Qual.* **2001,** *30*, 121-130.
121. Navarro, S.; Vela, N.; Jose, G. M.; Navarro, G., Persistence of four s-triazine herbicides in river, sea and groundwater samples exposed to sunlight and darkness under laboratory conditions. *Sci. Total Environ.* **2004,** *329*, 87-97.
122. Prosen, H.; Zupančič-Kralj, L., Evaluation of photolysis and hydrolysis of atrazine and its first degradation products in the presence of humic acids. *Environ. Pollut.* **2005,** *133*, 517-529.
123. Rebelo, S.; Melo, A.; Coimbra, R.; Azenha, M.; Pereira, M.; Burrows, H.; Sarakha, M., Photodegradation of atrazine and ametryn with visible light using water soluble porphyrins as sensitizers. *Environ. Chem. Lett.* **2007,** *5*, 29-33.
124. Kochany, J.; Maguire, R. J., Sunlight photodegradation of metolachlor in water. *J. Agric. Food. Chem.* **1994,** *42*, 406-412.

125. Vialaton, D.; Bagli, D.; Richard, C.; Skejo-Andresen, H.; Paya-Perez, A. B.; Larsen, B., Photochemical transformation of priority organic chemicals and pesticides in water. *Fresenius Environ. Bull.* **2001,** *10*, 554-560.
126. Wilson, R. I.; Mabury, S. A., Photodegradation of metolachlor: Isolation, identification, and quantification of monochloroacetic acid. *J. Agric. Food. Chem.* **2000,** *48*, 944-950.
127. Hua, R.; Yue, Y.; Fan, D., The photodegradation of acetochlor in water. *Chin. J. Pestic. Sci.* **2000,** *2*, 71-74.
128. Chaabane, H.; Vulliet, E.; Joux, F.; Lantoine, F.; Conan, P.; Cooper, J.-F.; Coste, C.-M., Photodegradation of sulcotrione in various aquatic environments and toxicity of its photoproducts for some marine micro-organisms. *Water Res.* **2007,** *41*, 1781-1789.
129. Coelho, C.; Cavani, L.; Halle, A. t.; Guyot, G.; Ciavatta, C.; Richard, C., Rates of production of hydroxyl radicals and singlet oxygen from irradiated compost. *Chemosphere* **2011,** *85*, 630-636.
130. Amine-Khodja, A.; Boulkamh, A.; Boule, P., Photochemical behaviour of phenylurea herbicides. *Photochem. Photobiol. Sci.* **2004,** *3*, 145-156.
131. Al Housari, F.; Vione, D.; Chiron, S.; Barbati, S., Reactive photoinduced species in estuarine waters. Characterization of hydroxyl radical, singlet oxygen and dissolved organic matter triplet state in natural oxidation processes. *Photochem. Photobiol. Sci.* **2010,** *9*, 78-86.
132. Peschka, M.; Petrovic, M.; Knepper, T.; Barceló, D., Determination of two phototransformation products of bentazone using quadrupole time-of-flight mass spectrometry. *Anal. Bioanal. Chem.* **2007,** *388*, 1227-1234.
133. Eyheraguibel, B.; ter Halle, A.; Richard, C., Photodegradation of bentazon, clopyralid, and triclopyr on model leaves: Importance of a systematic evaluation of pesticide photostability on crops. *J. Agric. Food. Chem.* **2009,** *57*, 1960-1966.
134. Barceló, D.; Durand, G.; De Bertrand, N., Photodegradation of the organophosphorus pesticides chlorpyrifos, fenamiphos and vamidothion in water. *Toxicol. Environ. Chem.* **1993,** *38*, 183-199.
135. Bavcon Kralj, M.; Franko, M.; Trebše, P., Photodegradation of organophosphorus insecticides - Investigations of products and their toxicity using gas chromatography-mass spectrometry and AChE-thermal lens spectrometric bioassay. *Chemosphere* **2007,** *67*, 99-107.
136. Dilling, W. L.; Lickly, L. C.; Lickly, T. D.; Murphy, P. G.; McKellar, R. L., Organic photochemistry. 19. Quantum yields for *O,O*-diethyl *O*-(3,5,6-trichloro-2-pyridinyl) phosphorothioate (chlorpyrifos) and 3,5,6-trichloro-2-pyridinol in dilute aqueous solutions and their environmental phototransformation rates. *Environ. Sci. Technol.* **1984,** *18*, 540-543.
137. Wu, X.; Hua, R.; Tang, F.; Li, X.; Cao, H.; Yue, Y., Photochemical degradation of chlorpyrifos in water. *Chin. J. Appl. Ecol.* **2006,** *17*, 1301-1304.
138. Vialaton, D.; Pilichowski, J.-F.; Baglio, D.; Paya-Perez, A.; Larsen, B.; Richard, C., Phototransformation of propiconazole in aqueous media. *J. Agric. Food. Chem.* **2001,** *49*, 5377-5382.

139. Vialaton, D.; Richard, C., Phototransformation of aromatic pollutants in solar light: Photolysis versus photosensitized reactions under natural water conditions. *Aquat. Sci.* **2002,** *64*, 207-215.
140. Dimou, A. D.; Sakkas, V. A.; Albanis, T. A., Photodegradation of trifluralin in natural waters and soils: Degradation kinetics and influence of organic matter. *Int. J. Environ. Anal. Chem.* **2004,** *84*, 173-182.
141. Tagle, M. G. S.; Salum, M. L.; Bujan, E. I.; Arguello, G. A., Time evolution and competing pathways in photodegradation of trifluralin and three of its major degradation products. *Photochem. Photobiol. Sci.* **2005,** *4*, 869-875.
142. Canonica, S.; Jans, U.; Stemmler, K.; Hoigné, J., Transformation kinetics of phenols in water: Photosensitization by dissolved natural organic material and aromatic ketones. *Environ. Sci. Technol.* **1995,** *29*, 1822-1831.
143. Dalzell, B. J.; King, J. Y.; Mulla, D. J.; Finlay, J. C.; Sands, G. R., Influence of subsurface drainage on quantity and quality of dissolved organic matter export from agricultural landscapes. *J. Geophys. Res.* **2011,** *116*, G02023.

Chapter 5: Sulfur Speciation in Prairie Pothole Sediments

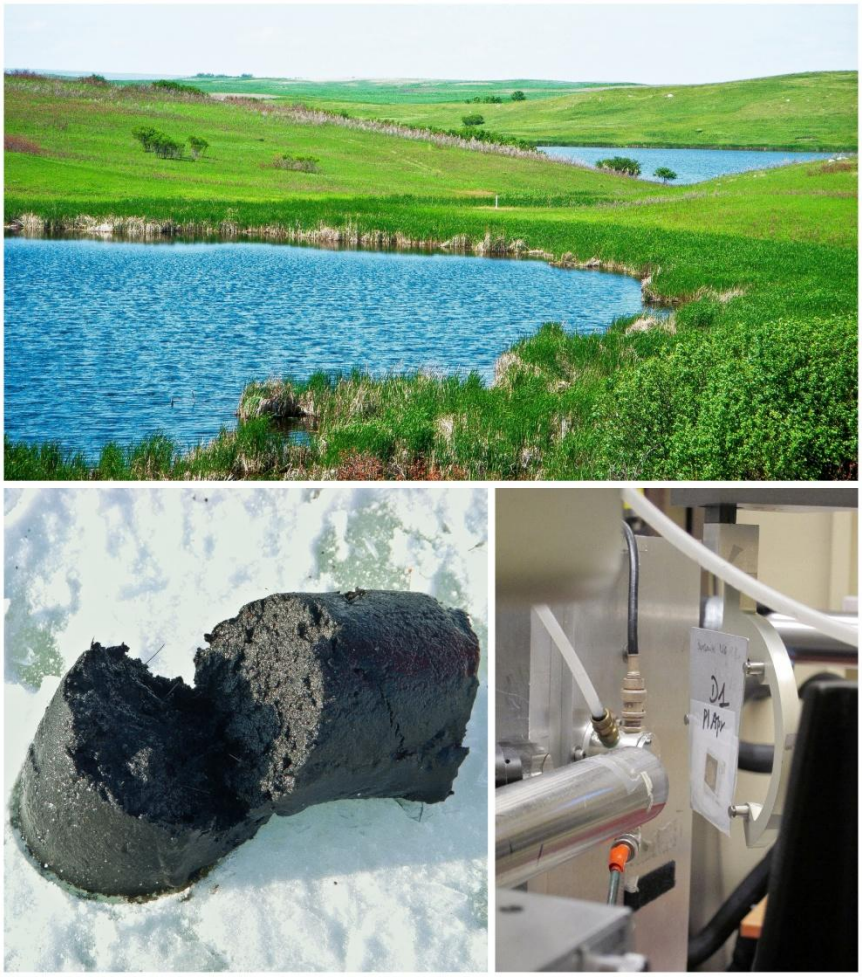

Prairie pothole lakes (PPLs) are biogeochemically diverse wetland ecosystems commonly found in the glaciated prairie of North America and represent a unique landscape because many of them have evolved high levels of sulfate in the water column. The sulfur (S) speciation in the PPL sedimentary environment, however, remains largely unexplored but is important because it may exert a major influence over a variety of environmental processes such as mercury methylation, acidity release, pesticide attenuation, and greenhouse gas emissions. In this study, a microscale sulfur chemical mapping method using sulfur *K*-edge X-ray absorption near-edge structure (XANES) spectroscopy was developed for the first time to quantify the sulfur species in sediments collected from PPLs in North Dakota, USA. Sulfur species in these sediments were best represented by organic (di)sulfide, sulfonate, ester/inorganic sulfate, as well as pyrite. On a seasonal timescale, the fractional abundance of total reduced sulfur was highest in fall, fluctuated over winter and spring, and declined to the lowest levels in summer. Results from this study reflect the seasonal changes in sedimentary sulfur speciation in PPLs and may have implications for evaluation of contaminant fate in prairie wetlands.

5.1 Introduction

The prairie pothole region (PPR), which extends from northwestern Iowa in the United Sates into central Alberta in Canada, features numerous small, shallow water basins typically referred to as prairie pothole lakes (PPLs).[1] These potholes and related aquatic ecosystems comprise one of the largest grassland ecoregions on Earth and play a critical role in maintaining the biodiversity and productivity of the PPR.[1] Since their formation during the late Pleistocene glaciation, PPLs have experienced long-term

hydrogeochemical evolution.[2,3] In particular, high levels of sulfate are frequently measured in the PPL surface water,[2,4-6] which is ascribed to recharge by groundwater saturated with gypsum that results from the oxidation of pyrite in underlying glacial till.[7,8] Despite the lack of direct evidence,[9] microbially-mediated sulfate reduction has been proposed as a key process affecting the water chemistry of PPLs.[9-11] Long-term field research has also confirmed that sediments in PPLs develop anoxic environments that support microbial communities involved in sulfate reduction.[12] Thus, PPL sediments may serve as a primary reservoir of sulfur (S), and the S speciation is likely to be temporally variable owing to the dynamic nature of PPLs.[12]

A holistic picture of S cycling in PPLs is essential to evaluating the ecosystem functions of these water bodies for several reasons. First, recent studies focusing on mercury (Hg(II)) occurrence in the PPR have found elevated concentrations of methylmercury (MeHg) in water sampled from diverse prairie wetlands as well as invertebrates that inhabit these systems.[13-15] In wetland soils and sediments, reduced organic S represents a major pool of high-affinity bonds with both Hg(II) and MeHg.[16-24] A mechanistic characterization of S speciation dynamics in PPL sediments, therefore, is of central importance for predicting the methylation rate and mercury mobility in prairie wetlands. Second, PPL water levels fluctuate widely in response to seasonal and annual wetting and drying cycles,[25] which has been recognized as the sensitivity of prairie ecosystems to climate variability.[26] Low water and occasional drying of the wetland bottom may expose previously anoxic soils and sediments to oxygen,[10] thereby causing the dissolution of pyrite and other sulfide minerals upon re-oxidation.[9,27,28] Assessing

likely consequences of such processes, mainly leaching of acidity and/or heavy metals, requires knowledge of the S speciation in PPLs. Third, the landscape of the PPR has been severely altered by extensive historical and ongoing drainage of PPLs associated with the expansion of agricultural activity.[29] Remaining and restored PPLs often trap non-point source pollutants, especially pesticides and fertilizers, from adjacent farmland.[30-33] Experimental evidence has shown that redox-active phases present in PPL sediments, most likely sulfide minerals, might promote the abiotic degradation of pesticides.[34] Hence, an improved understanding of the identity and abundance of reactive S species in PPL sediments would provide additional insight concerning their natural attenuation potential. Fourth, recent research has demonstrated that prairie wetlands are landscape-scale hotspots for methane (CH_4) emissions.[35-37] The release of CH_4 from prairie wetlands has been shown to closely correlate with the potential of sulfate reduction, and the removal of sulfate through reduction in wetland sediments may trigger the onset of significant CH_4 production.[36,37] Thus, elucidating the S speciation in PPL sediments is not only crucial for the accounting of the effect of S cycling on CH_4 flux across the pothole landscape, but also the development of more regionally specific assessments on the net greenhouse gas budget.

The dynamic cycling of oxidized and reduced S forms in sedimentary environments is mainly governed by the relative rates of biogenic S deposition, sulfate reduction, and diagenetic S interconversion.[38,39] Upon sulfate reduction in sediments, the formed hydrogen sulfide can either undergo re-oxidation, add to organic matter to form organic S, or react with reactive iron to precipitate iron sulfides.[40] Re-oxidation of sulfide

can occur at oxic-anoxic interfaces via abiotic and biotic pathways, including chemical oxidation by oxygen, nitrate, or iron and manganese oxides and aerobic or anaerobic oxidation by phototrophic or chemotrophic bacteria.[41] These processes typically regenerate sulfate but also produce a range of intermediate oxidation products, such as elemental sulfur, polysulfides, sulfite, and thiosulfate.[42-46] Most of these reduced inorganic S species, particularly polysulfides, are strong nucleophiles and can undergo intra- and intermolecular addition reactions with functionalized organic matter (e.g., α,β-unsaturated carbonyl groups) to form low molecular weight organic S compounds and high molecular weight macromolecules.[47-51] For shallow water bodies, photochemical sulfurization of functionalized organic matter may also occur in anoxic photic zones.[52] Alternatively, hydrogen sulfide and polysulfides can directly precipitate dissolved iron(II)[53] or reduce iron(III) (oxyhydr)oxides[54,55] to form metastable iron monosulfides such as greigite (Fe_3S_4) and mackinawite (FeS), which are eventually converted to more thermodynamically stable pyrite (FeS_2).[56] The reactions of reduced S species with organic matter and iron are competing geochemical pathways, and the latter is believed to be a kinetically favored process.[57,58] Studies of organic S formation within marine sediments have often found that the enrichment of S in organic matter is inversely correlated to the availability of reactive iron.[59-62] Reactive iron concentrations, however, do not consistently control organic S formation in lacustrine and estuarine sediments, and iron sulfides and organic S can form concurrently in high levels.[63-66] Although quantifying the relative rates of biochemical and geochemical processes is beyond the

scope of this study, the S speciation in PPL sediments may be intimately controlled by the interactions between the C, S and Fe cycles.

The oxidation state (i.e., ranging from -2 in sulfide to +6 in sulfate), speciation, and distribution of S are critical determinants of the S biogeochemistry. Existing knowledge of S in geochemical materials heavily relies on the application of preferential extraction methods, which provide a useful but operationally defined view of solid-phase S rather than direct speciation data.[67-71] Furthermore, some extraction-based methods are inherently limited by not targeting the intended phases.[72] More recently, synchrotron-based X-ray absorption near-edge structure (XANES) spectroscopy has proven to be a noninvasive and selective technique for determining the distribution and speciation of S and many other elements.[73] For S, the 1s → 3p transition (*K*-edge) of a photoelectron upon X-ray absorption occurs as an intense, well-resolved absorption peak (i.e., white-line) in the XANES spectrum.[74] The intensity and energy position of white-line peaks depend on the electronic structure, oxidation state, and local molecular coordination of S atom, which have allowed for a qualitative and quantitative S speciation in heterogeneous environmental matrices,[74-77] including soils and sediments as well as their organic matter extracts.[28,61,78-101] In addition to its high spectral and spatial resolution, XANES has the capacity for S speciation in whole redox-sensitive samples with minimal pretreatment and chemical alterations.[102] Previous research utilizing S XANES has examined the speciation of various inorganic and organic S in anoxic marine sediments and wetland soils, including iron sulfides (e.g., greigite, mackinawite, and pyrite),[28,78,80,85,93,100,101,103] elemental sulfur,[78,100,101] organic mono-, di-, and polysulfides,[28,78,80-82,85,89,93,101,103]

thiophene,[81,103] sulfoxide,[28,80,81,89,93,103] sulfite,[89,93] sulfone,[81,89,93] sulfonate,[28,61,78,80-82,85,93,101] and sulfate. [28,78,80-82,85,89,93,100,101,103] Despite the utility of S *K*-edge XANES spectroscopy, there has been only one study that applied this technique to describe the solid-phase S speciation in prairie wetland soils collected from Saskatchewan, Canada.[28] This earlier study, however, did not distinguish the relative abundances of different reduced S species.

Previous environmental applications of XANES analyses have mainly focused on: 1) determining the bulk average speciation of an element or, 2) examining speciation at a point location within a sample using a microprobe instrument (i.e. point spectra). Neither approach can adequately capture the elemental speciation present within a complex sample.[104,105] One key objective of this study was to quantify the S species in PPL sediments by developing a S chemical mapping protocol that integrated multi-energy X-ray fluorescence (XRF) mapping with point XANES spectra to ground truth the chemical map. For each sample, XRF maps were collected at multiple energies spanning the S *K*-edge. The individual XRF maps were aligned to create a S chemical map having a seven point absorption spectrum at each pixel within the area of interest. The composite S chemical maps were then fit with reference XANES spectra of identified S species to extract quantitative information on S speciation in samples. A similar approach has recently been applied to quantify the speciation of iron in complex geochemical samples such as water-rock reaction media, suspended marine particulates, and hydrothermal plume particles.[104-107]

5.2 Experimental Section

5.2.1 Site Description and Sample Collection

Benthic sediments were sampled throughout 2010 from two adjacent PPLs in the U.S. Geological Survey (USGS) Cottonwood Lake study area (CLSA), Jamestown, North Dakota, USA (see Figure 5.1).[108] The CLSA, which is situated on the eastern edge of a large glacial drift complex known as the Missouri Coteau, consists of a complex of sixteen temporary, seasonal, and semipermanent wetlands within a 91.8 ha hummocky prairie grassland.[109-111] The semi-arid climate of the CLSA is characterized by long, cold, dry winters and short, mild, wet summers, with a mean annual temperature of 4 ℃ and a mean annual precipitation of 440 mm.[112] Two semipermanent wetlands, P1 and P8,[109] were chosen for this study because they are representative of the biological, chemical, and hydrological conditions in the CLSA.[113] Both P1 and P8 receive their water from direct precipitation, groundwater recharge as well as runoff from surrounding uplands, whereas the greatest loss of water is through evapotranspiration.[112,114] P1 differs hydrologically from P8 in that it has a more dynamic water regime and a lower annual turnover of water due to the lack of an intermittent surface outlet.[10] As a result of the morphometry (area = 3.0 – 4.6 ha, mean depth < 2 m) and continuous wind-induced turbulence, the surface waters of P1 and P8 remains aerobic throughout the year,[115] but the bottom water and sediment may develop persistent anoxia.[116]

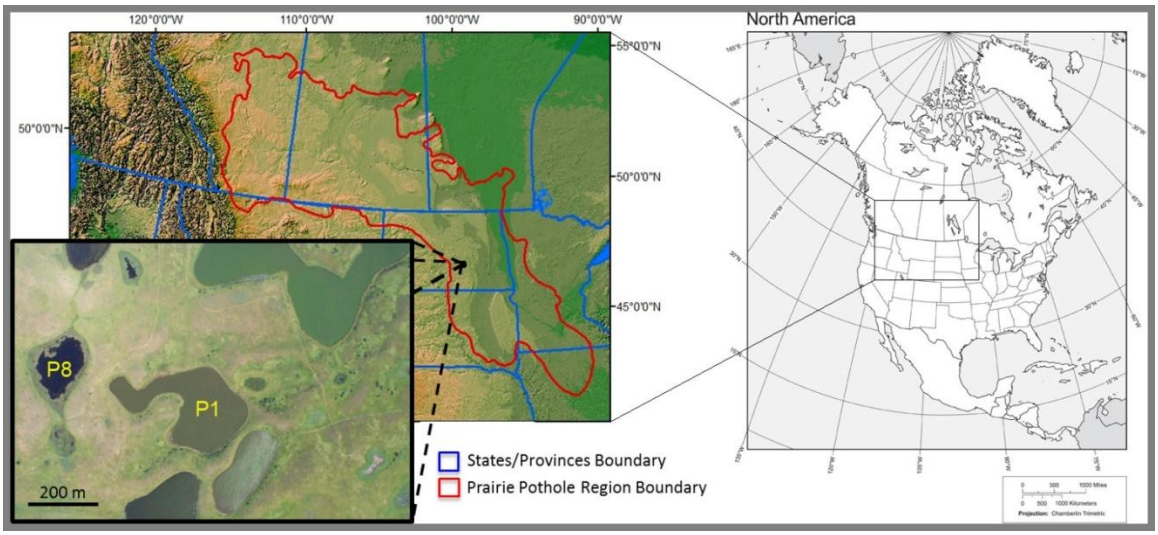

Figure 5.1 Location and photograph of Lake P1 and P8 within the Cottonwood Lake study area, North Dakota, USA. North America map courtesy of Douglas Minnis, Arizona Geographic Alliance and Arizona State University. Inset PPR and CLSA images courtesy of Dr. David N. Mushet, USGS Northern Prairie Wildlife Research Center.[108]

Sediment and surface water samples were collected from P1 and P8 during January, April, June, and September 2010 (hereafter referred as P1Jan/Apr/Jun/Sep and P8Apr/Sep). Sediments were sampled from the center of the lakes using a push corer and transported in sealed core liners to the University of Minnesota within 24 h for processing.[6] For profile porewater collection, sediment samples were pressurized in a Jahnke-type core squeezer and porewaters at different depths were extracted directly into argon-purged glass syringes.[117] For bulk porewater collection, sediment samples were rapidly sliced into Nalgene centrifuge bottles under a stream of nitrogen and centrifuged in a Beckman JA-10 rotor (3 times at 5000 rpm for 30 min).[6] Syringes and centrifuge bottles were then immediately transferred into a glove box (95% N_2/5% H_2, Pd catalyst, Coy Laboratory Products Inc.), and porewaters were stored in serum vials with zero headspace. After porewater collection, bulk sediments were packed into acid-washed glass jars with minimal headspace and kept frozen until use.

5.2.2 Sediment Sample Preparation

Sediment sample preparation for S XANES spectroscopy was performed in the anaerobic glove box to avoid exposure to oxygen. A few grams of dry bulk sediment sample were ground and homogenized using an Agate mortar and pestle. The mortar and pestle were thoroughly rinsed with acetone and ultrapure water between samples to avoid cross contamination. To minimize any potential oxidation of redox-active species during XANES analysis, a thin layer of sediment was spread onto a 4.0 μm thick low-sulfur XRF film (Premier Lab Supply, Inc.) and sealed between two 3.6 μm thick low-sulfur Mylar X-ray films (Premier Lab Supply, Inc.). No visible color change was apparent for an oxygen indicator solution prepared using the same protocol after a 24-hr period of exposure to air, suggesting that such preservation approach was sufficient to maintain the sample redox integrity. The sample film stack was mounted on an aluminum sample holder, which was subsequently sealed within 0.15 mm thick Mylar bags along with an AnaeroPack oxygen scrubber (Mitsubishi Gas Chemical Company, Inc.). The Mylar packages were transported within nitrogen-filled Mylar bags and stored under argon until XANES analysis.

5.2.3 XRF Mapping and XANES Spectra Acquisition

Acquisition of XRF maps and XANES spectra was performed at the microprobe beamline 10.3.2 of the Advanced Light Source, Lawrence Berkeley National Laboratory (Berkeley, California, USA),[118] during November 2011 and May 2012.

During the 2011 analyses, samples P1Sep and P8Sep were analyzed to obtain baseline information on the major S speciation in PPL sediments. XRF maps were

acquired by scanning a 2000 μm × 1000 μm region of interest on samples at two incident X-ray beam energies of 2472.8 eV and 2482.5 eV using a Si(1 1 1) double crystal monochromator with a beam spot size of 15 μm (horizontal) × 6 μm (vertical).[118] These two energies were chosen to represent the white-line peaks of common reduced and oxidized S species, respectively. The absolute energy of the monochromator was periodically calibrated against the white-line peak of gypsum (2482.74 eV). The sample holder was mounted at a 45 ºangle to the incident beam, and the signal was recorded at an angle of 90 º using a 7-element germanium detector in fluorescence mode.[118] Samples were run with helium in the I-zero (I_0) chamber to minimize the beam attenuation by air.[118] Counts in 15 spectral regions of interest were recorded for each map, including S (2120-2350 eV). The distance of the detector relative to the sample was finely adjusted for optimal S counts. The fluorescence signal was collected for each pixel of the map with a scan step of 8 μm × 8 μm, a dwell time of 120 ms, and a monochromator settling time of 500 ms between horizontal scan lines. For each sample, both XRF maps were deadtime corrected, resized, registered, and stacked to create a single dual-energy composite S map using custom beamline software.[118] The composite S maps were subsequently used to identify S-rich points of interest (POIs, bright and diffused spots with S counts > 2000) for XANES scans. For each POI, at least two XANES scans were acquired in the energy range between 2420 and 2625 eV, with a 0.2 eV step size in the XANES region (2465-2486 eV) and coarser step sizes (1 and 2 eV) in the pre-edge and post-edge regions.

During the 2012 analyses, multi-energy XRF maps for samples P1Jan, P1Apr, P1Jun and P1Sep were acquired by sequentially scanning a 1000 μm × 1000 μm region of interest at seven incident beam energies across the S *K*-edge (2466, 2472.6, 2473.6, 2478.5, 2481.2, 2482.5, and 2520 eV). The lowest (2466 eV) and highest (2520 eV) energies were used to determine the background and total counts in the S channel. This approach generates an energy dependent absorption profile at each pixel within the region of interest and will be referred to as "chemical mapping". The five intermediate energies were selected using an error estimator program to best distinguish spectral features of different S species based on the XANES spectra acquired from P1Sep and P8Sep samples (see below for details). The resulting multi-energy S chemical maps for each sample were used to guide the selection of S-rich POIs on which to acquire XANES spectra as described above. For comparison purposes, S chemical maps for samples P8Apr and P8Sep were also acquired for a 600 μm × 600 μm region of interest.

For the acquisition of S reference XANES spectra, a thin layer of finely-ground S compound was spread onto a conductive graphite tape and the signal was recorded in total electron yield (TEY) mode to minimize over-absorption effects.[119] Reference XANES spectra were collected for a suite of S compounds (i.e., 1-amino-2-naphthol-4-sulfonic acid (ANSA), L-cysteine, DL-homocysteic acid, L-methionine, DL-methionine sulfoxide, sodium dodecyl sulfate (SDS), sulfanilamide, and 2-thiophenecarboxylic acid). These spectra were compiled with other donated spectra (i.e., L-cystine, elemental sulfur, greigite, mackinawite, pyrite, sodium sulfite, and sodium thiosulfate[24,96]) to generate a reference database that was used for fitting XANES spectra and composite maps. The

selected reference S compounds exhibited distinct spectral features (e.g., position and intensity of white-line peaks) relative to one another and represent the S species frequently encountered in sedimentary environments (see Table D.1).

5.2.4 XRF Map and XANES Spectra Analysis

All experimental S XANES spectra were deadtime corrected and energy calibrated, followed by the pre-edge background subtraction (2420-2466 eV) and step-edge height normalization to unity (2520-2625 eV). Normalized spectra were first submitted to a principal component analysis (PCA) using SixPACK[120] following previously published protocols.[121] The number of spectral components present in sample XANES spectra was evaluated with the local minimum *IND* value and the quality of reconstruction of the S reference spectra by target transformation with the *SPOIL* value,[119,122,123] which provides a statistical basis for defining the most appropriate subset of S references for spectral fitting.[124] Reference compounds with smaller *SPOIL* values were ranked as the high priority predictors for subsequent least-squares linear combination fittings (LCF). The fitting of XANES spectra was performed with various linear combinations of the spectra of appropriate reference compounds over the energy range of 2460 to 2560 eV using custom beamline software,[125] with the sum of the total S species not constrained to unity (mean sum = 0.935) and minor energy shifts permitted (±0.3 eV). The quality of the LCF fits was quantified with normalized sum of squared residuals (*NSS*), and the addition of a component was justified when *NSS* decreased by at least 10%. The results of the best fit were taken to indicate the S oxidation state and functional moiety rather than actual specific S-containing compounds. Previous XANES

studies on lacustrine sediments and wetland soils have reported that the quantification error associated with LCF is approximately ±5-10%.[28,85]

For quantitative chemical mapping analyses, multi-energy S chemical maps were fitted using S reference spectra along with a background spectrum from a sample blank. The fitting procedure essentially took a 7-point XANES spectrum at each pixel in the map and fit that spectrum with a linear combination of the 7-point XANES spectra of the reference compounds.[126] The quality of the fits was evaluated with the whole-map mean squared error (*MSE*). The total count of each S species was calculated by summing the counts from all pixels in corresponding chemical map channel and normalized by the mapping area. The area-normalized counts of each S species were further corrected by subtracting the background counts from sediment-free areas of the prepared sample (i.e., XRF tape and Mylar film). The background-subtracted counts were then converted to the relative proportion of each S species in the map.

For quantitative XRF mapping analyses, multi-energy composite S chemical maps were fitted using S reference spectra along with a background spectrum. Fittings the chemical maps has the advantage to extract more representative spatial and chemical information of the investigated element by capturing the microspatial heterogeneity of a sample. The fitting procedure essentially took a 7-point XANES spectrum at each pixel in the map and fit that spectrum with a linear combination of the 7-point XANES spectra of the reference compounds.[119] The quality of the fits was evaluated with the whole-map mean squared error (*MSE*). The total count of each S species was calculated by summing the counts from all pixels in corresponding chemical map channel and normalized by the

mapping area. The area-normalized counts of each S species were further corrected by subtracting the background counts. The background-subtracted counts were then converted to the relative proportion of each S species in the map.

5.3 Results and Discussion

5.3.1 Chemistry of PPL Surface Water and Sediment Porewaters

The bulk chemistry of surface water and sediment porewaters from P1 and P8 has been previously characterized and selected results are presented in Table 5.1. In general, PPL surface water contained high sulfate (5-30 mM) with a slightly alkaline pH (~8.0). Sulfide and dissolved iron (Fe) were non-detectable. PPL sediment porewaters had a similar pH range and contained high hydrogen sulfide levels (0.9-2.4 mM) but low sulfate (0.4-1.0 mM). Elevated concentrations of polysulfides, sulfite, and thiosulfate have also been measured in the porewaters.[34] The DOC concentrations in porewaters (6-10 mM) were typically 2-3 times higher than those measured in the surface water (1.8-3.2 mM), while the dissolved iron was low (<1 μM).

A selection of depth profiles (pH, $[SO_4^{2-}]$, $\Sigma[S^{2-}]$, and DOC) are presented in Figure 5.2 for P1Sep and P8Sep sediment porewaters. The porewater pH was near-neutral (7.0-8.0) for all depths. The surficial porewater sulfate concentrations (7-23 mM) fell in the same range with surface water, but decreased rapidly with increasing depth and stayed consistently low below ~10 cm (< 1.0 mM). The porewater sulfide profiles were an inverse of sulfate, increasing before reaching a plateau as sulfate was depleted to minimum. Similarly, the porewater DOC increased with a median of 9.5 mM. The disappearance of porewater sulfate with an increase of hydrogen sulfide indicates that

sulfate reduction was likely to be a dominant process in the near-surface PPL sediments. Below 10 cm in depth, however, the depletion of sulfate coupled with the saturation of sulfide signifies that such process became inhibited, and methanogenesis might take over as the terminal process of organic matter mineralization.[128,129] Given the high S/C weight ratio (~0.04) and Fe content (~1.1 wt%; see Table 5.1) in PPL sediments, both organic S and iron sulfide species were expected to constitute the bulk of the total S, and their relative susceptibility towards oxidation may affect the S speciation.

Table 5.1 Characteristics of PPL surface water, sediment porewaters, and sediments

Bulk surface water					
Sample	pH	$[SO_4^{2-}]$ (mM)	$\Sigma[S^{2-}]$ (mM)	Fe (μM)	DOC (mM)
P1Jan	8.14[a]	30.33 ± 0.76[a]	< 0.01	N.A.	3.25 ± 0.04[a]
P1Apr	8.38[a]	19.04 ± 0.01[a]	< 0.01	< 0.020[c]	2.99 ± 0.07[a]
P1Jun	8.35[a]	19.26 ± 0.31[a]	< 0.01	N.A.	2.51 ± 0.01[a]
P8Apr	7.87[a]	5.17 ± 0.02[a]	< 0.01	< 0.020[c]	1.84 ± 0.02[a]
P8Sep	8.05[a]	6.95 ± 0.07[a]	< 0.01	< 0.020[c]	2.39 ± 0.01[a]
Bulk sediment porewaters					
Sample	pH	$[SO_4^{2-}]$ (mM)	$\Sigma[S^{2-}]$ (mM)	Fe (μM)	DOC (mM)
P1Jan	8.58	N.A.	0.58 ± 0.16	N.A.	24.38 ± 0.04
P1Apr	8.62[a]	1.02 ± 0.01[b]	2.37 ± 0.03[a]	0.618 ± 0.046[c]	6.01 ± 0.03[a]
P1Jun	7.84[a]	N.A.	0.89 ± 0.08[a]	N.A.	8.81 ± 0.02[a]
P1Sep	7.36[a]	N.A.	1.95 ± 0.05[a]	N.A.	9.06 ± 0.02[a]
P8Apr	8.53[a]	0.37 ± 0.03[b]	2.06 ± 0.05[a]	0.162 ± 0.001[b]	10.37 ± 0.03[a]
P8Sep	7.45[a]	N.A.	1.60 ± 0.06[a]	N.A.	10.09 ± 0.04[a]
Bulk sediments					
Sample	Total S(g/kg)	Total C(g/kg)	Organic C(g/kg)	Fe (g/kg)	S/Organic C ratio
P1Apr	5.21 ± 0.07[b]	135.2 ± 0.3[b]	121.8 ± 0.3[b]	11.98 ± 0.76[b]	0.043
P8Apr	5.74 ± 0.07[b]	163.4 ± 0.0[b]	150.5 ± 0.1[b]	10.80 ± 0.83[b]	0.038

[a] Data taken from Zeng et al. (2011).[6] [b] Data taken from Zeng et al. (2012).[34] [c] Data taken from Zeng and Arnold (2012).[127]

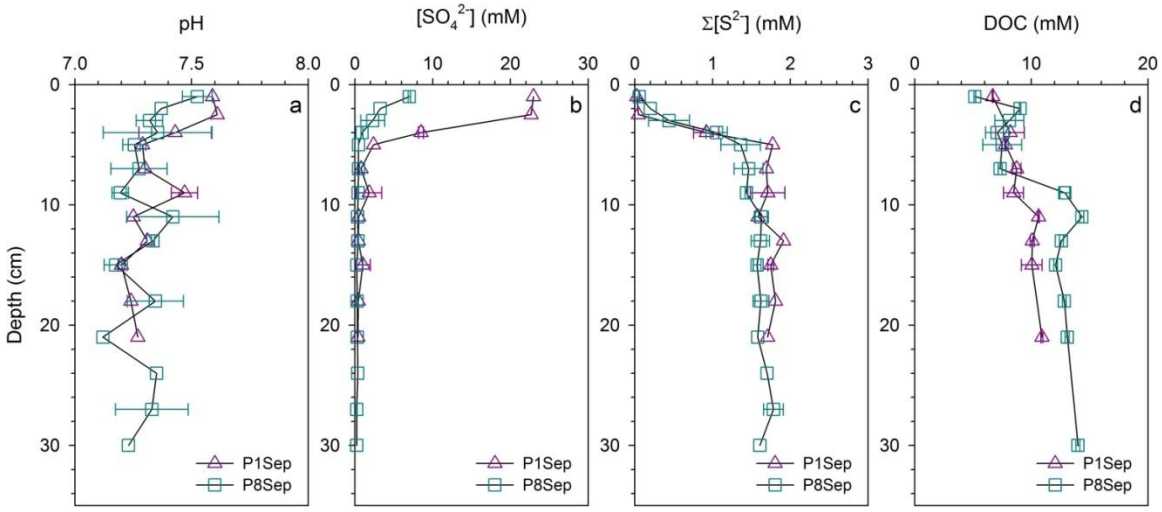

Figure 5.2 Porewater profiles of pH, $[SO_4^{2-}]$, $\Sigma[S^{2-}]$, and DOC for P1Sep and P8Sep sediment samples. The water-sediment interface is dictated by "0 cm". Error bars represent one standard deviation of duplicate samples; where absent, only one sample was analyzed. DOC profile data were averaged from values reported by Ziegelgruber et al. (2012)[117]

5.3.2 Energy Optimization for Chemical Mapping

Figure 5.3 presents the dual-energy composite S maps and XANES spectra of P1Sep and P8Sep sediment samples.

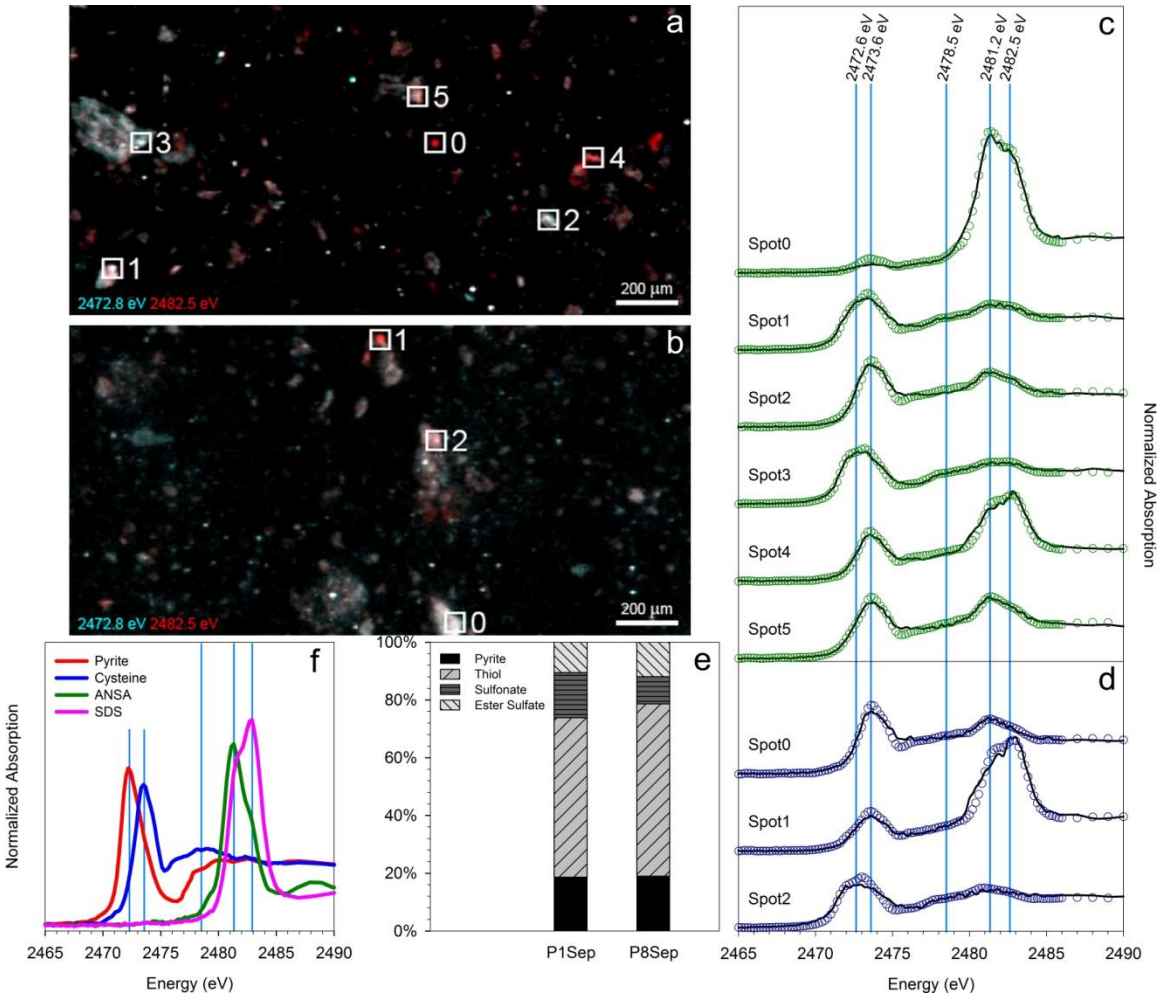

Figure 5.3 Identification of major S species in P1Sep and P8Sep sediment samples: (a) and (b) bicolor composite S maps (energies at 2472.8 and 2482.5 eV) of P1Sep and P8Sep, respectively; (c) and (d) XANES spectra and LCF fittings of POIs on P1Sep and P8Sep, respectively; (e) Fractional contribution of S species averaged from the LCF fittings of XANES spectra of P1Sep and P8Sep, respectively, with the sum of all S species normalized to unity (see Table D.3); (f) Overplot of XANES spectra of four S reference compounds. Blue lines correspond to five intermediate mapping energies at which S chemical maps were scanned.

The maps (Figure 5.3a and Figure 5.3b) reveal a significant heterogeneity of S distribution. Within a distance of several hundred microns, the S aggregates can vary between dominant reduced or oxidized S species and coexistence of both. XANES spectra typically contain two distinct absorption bands, mainly corresponding to the

reduced S and the highly oxidized S (Figure 5.3c and Figure 5.3d). It was expected that the first band near 2470-2475 eV region would consist of both organic (e.g., thiol) and inorganic (e.g., pyrite) reduced S species, while the second band near 2480-2485 eV region would arise from highly oxidized S species (e.g., sulfonate or sulfate). Other intermediate S species (e.g., sulfanilamide) might also exist in the samples as minor components that were not clearly resolved from the major features in these spectra. Such variation of S species was supported by results from PCA and target transformation analyses (Table D.2).

To obtain further information about the different S species involved, XANES spectra were fit using a suite of S reference spectra (Figure 5.4). In this context it should be pointed out that the S reference compounds used in LCF only serve as proxies for different S functional groups, and the quantitative analysis of an XANES spectrum aims to estimate the fractional contribution of these functional groups rather than individual compounds in a sample. Thus, a satisfactory fit does not necessarily imply that chosen reference compounds actually exist in the sample, whereas a poor fit may be indicative of the presence of additional S species that are not well represented by the reference compounds used. Inclusion of a wider range of reference compounds may improve the goodness of the fittings. Knowledge of the chemistry of the sediments along with PCA-target transformation analysis makes this database-dependent approach more robust.

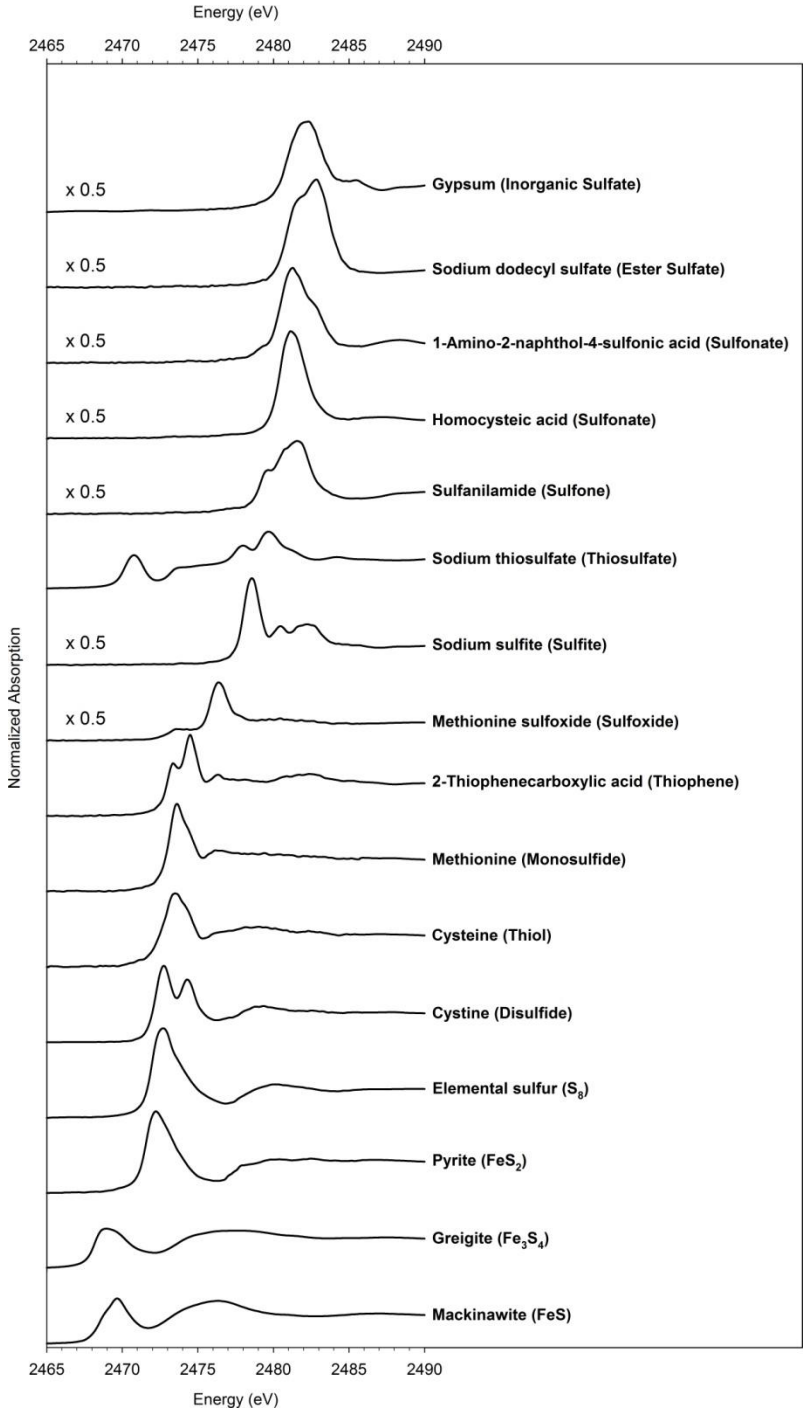

Figure 5.4 Normalized XANES spectra of S reference compounds. "× 2" denotes that the white-line peak intensity of original XANES spectra was scaled down by a factor of 2. XANES spectra of greigite, mackinawite, and sodium thiosulfate courtesy of Dr. Edward D. Burton (Southern Cross GeoScience, Southern Cross University, Australia). XANES spectra of L-cystine, elemental sulfur, pyrite, and sodium sulfite courtesy of Dr. Kathryn L. Nagy (Department of Earth and Environmental Sciences, University of Illinois at Chicago).

According to the LCF analyses of XANES spectra (Figure 5.3e), P1Sep sample contained significant thiol (55%) and a lesser proportion of pyrite (19%). The oxidized S was much less abundant than the reduced S and characterized by sulfonate (16%) and ester sulfate (10%). The dominant S species in P8Sep sample were the same as those found in P1Sep (within the estimated error) and consisted of thiol (60%), pyrite (19%), sulfonate (9%), and ester sulfate (12%). The types of S species identified herein were largely consistent with those from an earlier study focusing on Canadian prairie wetland soils, which found that pyrite and organic monosulfide comprised the main portion of the reduced S, while sulfonate and inorganic sulfate constituted the oxidized S.[28] Consequently, the white-lines of four reference compounds (2472.6 eV for pyrite, 2473.6 eV for cysteine, 2481.2 eV for ANSA, and 2482.5 eV for SDS) were chosen for use in the subsequent multi-energy S chemical mapping (Figure 5.3f).

5.3.3 Seasonal Dynamics of Sulfur Speciation

To track the seasonal dynamics of S speciation in PPL sediments, XRF maps were collected at seven incident energies for both sets of sediment samples, with XANES scans acquired on four P1 samples to ground truth chemical map fit results. Figure 5.5 presents the multi-energy S chemical maps and XANES spectra of P1Jan, P1Apr, P1Jun, and P1Sep samples. The PCA and target transformation analyses of XANES spectra revealed the possible contribution from additional S species such as organic disulfide and inorganic sulfate (Table D.4). Results on S speciation from the fittings of chemical maps and XANES spectra are summarized in Table 5.2.

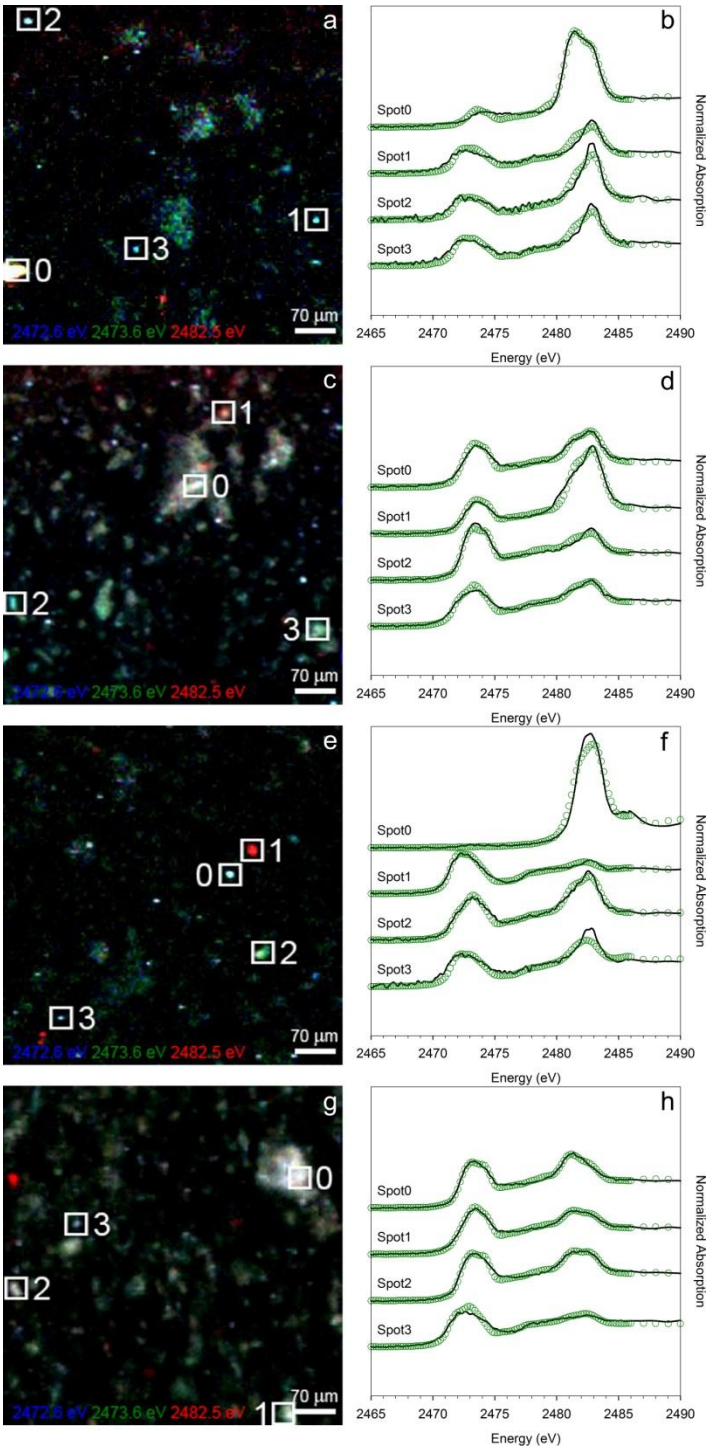

Figure 5.5 Multi-energy S chemical maps and XANES spectra of P1 sediment samples: (a), (c), (e), and (g) Tricolor multi-energy S chemical maps (energies at 2472.6 eV, 2473.6 eV, and 2482.5 eV) of P1Jan, P1Apr, P1Jun, and P1Sep, respectively; (b), (d), (f), and (h) XANES spectra and LCF fittings of P1Jan, P1Apr, P1Jun, and P1Sep.

Table 5.2 Fractional contribution of S species in PPL sediments

Sample	Reduced S			Oxidized S	
	Inorganic	Organic			
	Pyrite (%)	Disulfide (%)	Monosulfide (%)[c]	Sulfonate (%)	Sulfate (%)[d]
Chemical map fit[a]					
P1Jan	43	-	23	-	34
P1Apr	24	12	43	-	21
P1Jun	30	-	15	-	55
P1Sep	12	28	47	6	7
P8Apr	14	36	33	0	17
P8Sep	15	36	33	9	8
XANES spectra fit[b]					
P1Jan	34	-	26	-	40
P1Apr	8	17	52	-	23
P1Jun	32	-	26	-	42
P1Sep	15	15	55	9	6

[a] Fractional contribution of S species calculated from the fitting of multi-energy S chemical maps in Figure 5.5 with the sum of all S species normalized to unity. Raw fitting data presented in Table D.5. [b] Fractional contribution of S species averaged from the LCF fittings of XANES spectra with the sum of all S species normalized to unity. Raw fitting data presented in Table D.6. [c] Sum of thiol (R-SH) and organic monosulfide (R-S-R'). [d] Sum of ester sulfate ($R\text{-}O\text{-}SO_3^-$) and inorganic sulfate (SO_4^{2-}).

According to the chemical map fitting, the reduced S in P1Jan and P1Jun samples was mainly pyrite (30-43%), accompanied by a smaller portion of thiol (15-23%). Conversely, a large portion of reduced S in P1Apr and P1Sep samples could be attributed to thiol (43-47%) with additional fractions ascribed to organic disulfide (12-28%) and pyrite (12-24%), respectively. The oxidized S in P1Jan, P1Apr, and P1Jun samples primarily originated from ester and inorganic sulfate (21-55%), while the composition differed distinctly in P1Sep sample with fairly equal amounts of sulfonate (6%) and ester sulfate (7%). The decreases in abundance of reduced S were balanced by comparable and

concurrent increases in the oxidized S, suggesting that these sediment samples underwent appreciable changes in S speciation. The relative abundances of S species in each sample estimated from the average of LCF fittings of XANES spectra usually agreed within ±15% as those determined by the chemical mapping. As noted above, the discrepancy between XANES spectra and map fittings may be caused by the spatial heterogeneity of S distribution, which should be minimized with more XANES spectra averaged from additional POIs. For comparison purposes, the chemical map fitting results for P8Apr and P8Sep samples are also included in Table 5.2 (see Figure D.1 for chemical maps). These fittings showed similar S speciation in P8 samples as observed in P1 samples, with a considerable amount of reduced S (~83%). The contribution of thiol (33%) and organic disulfide (36%) to the reduced S in the both P8 samples was at a comparable level, followed by pyrite (~14-15%). The presence of ester sulfate (17%) accounted for the oxidized S in P8Apr sample, while both sulfonate (9%) and ester sulfate (8%) played a role in P8Sep sample.

The major forms of reduced organic S in PPL sediments were thiol (R-S-H) and organic disulfide (R-S-S-R'). Studies of marine and estuarine sediments as well as prairie wetland soils have shown that organic sulfides (e.g., thiol, mono-, di-, and polysulfides) can contribute up to 70% of the total S.[28,78,80,85,93,101] In sedimentary environments, thiol can form via the addition of hydrogen sulfide or polysulfides onto functionalized organic matter[48] and further undergo intermolecular reactions to form organic monosulfide (R-S-R').[80] Thiol and organic monosulfide may also originate from decaying organic matter due to their ubiquity in living organisms (e.g., amino acids cysteine and

methionine).[130,131] On the other hand, organic disulfide can be formed through the intermolecular cross-linking of two thiol groups upon oxidation.[132] The strength and rigidity of disulfide cross-linking has been proposed to enhance the stability of organic matter in anoxic depositional environments.[133,134] It should be noted that the S *K*-edge XANES does not allow discrimination between thiol and organic monosulfide because they exhibit fairly similar white-line position and intensity (see cysteine and methionine XANES spectra in Figure 5.4).[93] The inclusion of both species in the fitting caused one to increase and the other to decrease simultaneously. Thus, the fitting results derived from cysteine should be interpreted as the joint contribution from thiol and organic monosulfide.

Pyrite (FeS_2) was another main pool of the reduced S in PPL sediments, suggesting that reactive iron served as another important sink for reduced S. The presence of pyrite in Canadian prairie wetland soils has also been reported, but its relative abundance to reduced organic S species was unclear.[28] Earlier studies have demonstrated that iron-thiolate complexes formed by Fe and thiol (Fe-S-R) can produce spurious features of Fe sulfides in XANES spectra.[94,135] Thus, the fitting results for pyrite must be interpreted with caution in the absence of detailed mineralogical characterization, because the pyrite signal may be complicated by such complexes.

Sulfate was the major oxidized form of S found in PPL sediments. Previous studies have confirmed ester sulfate as a major form of oxidized S in marine and estuarine sediments. [61,78,93,101] In contrast, inorganic sulfate seemed to predominate in prairie wetland soils (39-43%).[28] In sedimentary environments, sulfate may be present in

multiple forms, including ester sulfate, inorganic sulfate, and carbonate-hosted sulfate, and each of these can be differentiated by subtle spectral differences in their XANES spectra.[136] For instance, ester sulfate exhibits a splitting in the white-line peak induced by the asymmetry of S coordination environment, while carbonate-hosted and inorganic sulfate have a more symmetric white-line peak but contains additional features in the post-edge region.[85,137] Although SDS typically yielded better fits than gypsum for most PPL sediment samples, the inclusion of both species in P1Jun sample improved the fitting quality markedly, indicating the co-existence of ester and inorganic sulfate.

Sulfonate was found as a minor component of oxidized S in P1Sep and P8Sep samples. The widespread occurrence of sulfonate in marine and estuarine sediments has been reported.[61,78,80,101] Sulfonate has various biochemically-important structural analogues in living organisms (e.g., the amino acid taurine) and may be directly introduced into sediments from decaying organic matter.[61,101] Alternatively, sulfonate may form upon the oxidation of thiol or organic disulfides or the reaction of sulfite or thiosulfate with organic matter.[58,78] Sulfonate has also been found previously to constitute a major portion of the total S in prairie wetland soils (17-31%).[103] Unlike organic sulfides which are often associated with highly labile organic matter, sulfonate tends to associate with less labile phases of organic matter and therefore is more resistant to mineralization or transformation.[90]

As illustrated in Figure 5.6, the total reduced S (i.e., sum of organic sulfides and pyrite) exhibited the highest fractional abundance in fall (P1Sep), followed by comparable levels in winter (P1Jan) and spring (P1Apr), and dropped to the lowest in

summer (P1Jun). An opposite seasonal dependence was observed for the total oxidized S, with the highest fractional abundance in summer. These data point to seasonal redox cycling of S.

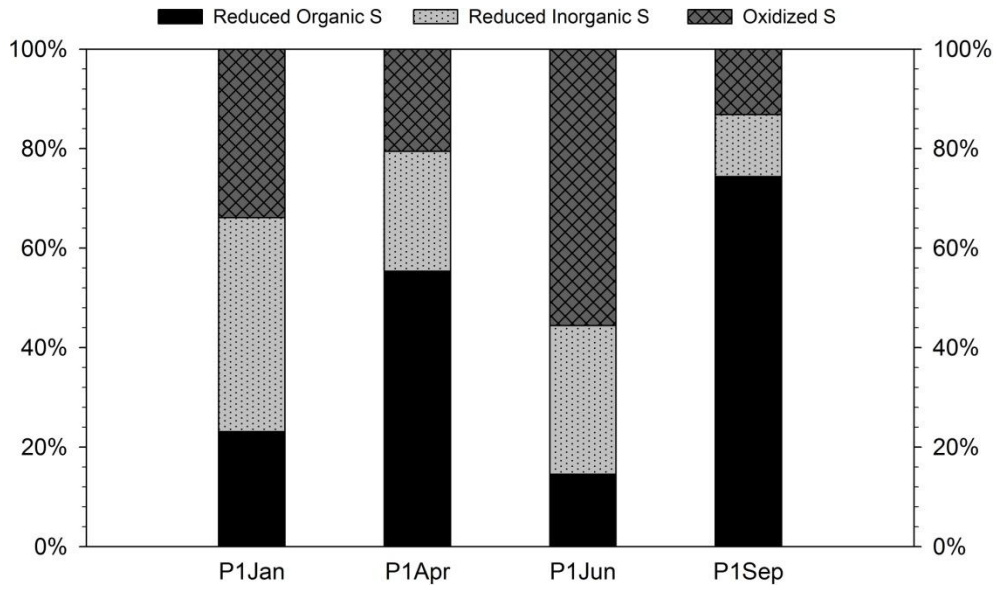

Figure 5.6 Fractional contribution of reduced organic S, reduced inorganic S, and oxidized S in P1 and P8 sediment samples. Stacked bars plotted based on data in Table 5.2.

Earlier investigations have shown that seasonal variation in the sulfate reduction rate (SRR) appears to correlate with temperature and the availability of labile organic matter in salt marsh and marine sediments.[138-144] The acceleration in the SRR, however, is often out of phase with the accumulation of reduced S.[143,145-147] The SRR commonly peaks in summer, while the accumulation of reduced S only becomes apparent until later in fall.[143,145,147] During the summer, substantial amounts of dissolved oxygen may penetrate into surficial sediments due to extensive evapotranspiration or water uptake coupled with increasing productivity.[148,149] Thus, the observed seasonal delay is often attributed to the re-oxidation of sulfide in summer.[141,142,150,151] Given the comparability of sulfate concentrations in P1 surface water and seawater (~28 mM),[39] the influence of

seasonality on S speciation in P1 sediments might follow those of marine environments. By inference, a likely scenario for P1 is that the accumulation of reduced S species in sediments started when sediments became sufficiently anoxic in late summer, and reached their maximum contents in fall. Part of the reduced S was oxidized after lake turnover in winter, but the regenerated sulfate in turn somewhat offset a prolonged decrease in the SRR because of lower temperature. In spring, the SRR was stimulated by increasing temperature and sedimentation of organic matter from the spring bloom, followed by an enrichment of the reduced S. As temperature further increased in early summer, sediments gradually shifted into a more oxidized state and counteracted the enhanced sulfide production caused by an increasing SRR, leading to a low abundance of reduced S. It is noticeable that low pyrite contents appeared to occur with high organic sulfides, indicating the dynamic formation and degradation of organic sulfides in conjunction with pyrite turnover.[150,152-155]

5.4 Summary

The current study demonstrates the utility of S chemical mapping for identifying and quantifying S species in PPL sediments. The method is not limited to microscale S speciation in sediments but also can be extended to detect and quantify the geochemical transformations of S in other complex environmental samples. A major finding of this study was the enrichment of reduced organic sulfides and pyrite in PPL sediments. Meanwhile, sulfonate and sulfate (both ester-linked and inorganic) were the major oxidized S species. The origins of sedimentary organic S species, however, is unclear (i.e., biogenic versus diagenetic), and more detailed knowledge on structural or isotopic

composition of these species is an area requiring further research. Another interesting finding was the appreciable seasonal fluctuation in the oxidized and reduced S. While additional information on biogeochemical processes (e,g, sulfate reduction rate) is necessary to reach a conclusive explanation for such dynamics, the S speciation in PPL sediments might be a sensitive indicator of seasonal changes in environmental variables (e.g., temperature, mixing, and productivity). More importantly, the seasonality of S speciation could have profound effects on the environmental fate of contaminants such as Hg(II) and pesticides in prairie wetlands. For instance, in fall, the potential for reductive transformations of pesticides may decrease as the abundance of pyrite declines, leading to a higher risk of pesticide leaching into groundwater when the pothole serves as a groundwater recharge site. Meanwhile, the extent of Hg(II) complexation by reduced organic S may be enhanced as increasing abundances of organic mono- and disulfides, thereby exacerbating the facilitated uptake of Hg(II) by prairie wildlife. In the future, the characterization of S speciation throughout an entire sediment core section may prove useful to elucidate variable redox conditions and depositional regimes occurring on longer time scales. Such information would be a step forward towards understanding of the nature, formation and transformations of the sedimentary S system of PPLs and interpretation of the S flux and storage in these wetland systems.

5.5 References

1. van der Valk, A. G., The prairie potholes of North America. In *The World's Largest Wetlands*, Fraser, L. H.; Keddy, P. A., Eds. Cambridge University Press: Cambridge, UK, 2005; pp 393-423.
2. LaBaugh, J. W., Chemical characteristics of water in northern prairie wetlands. In *Northern Prairie Wetlands*, Van der Valk, A. G., Ed. Iowa State University Press: Ames, IA, 1989; pp 56-90.

3. Last, W. M.; Ginn, F. M., Saline systems of the Great Plains of western Canada: An overview of the limnogeology and paleolimnology. *Saline Syst.* **2005,** *1*, 1-38.
4. Last, W., Chemical composition of saline and subsaline lakes of the northern Great Plains, western Canada. *Int. J. Salt Lake Res.* **1992,** *1*, 47-76.
5. Waiser, M. J.; Robarts, R. D., Microbial nutrient limitation in prairie saline lakes with high sulfate concentration. *Limnol. Oceanogr*. **1995,** *40*, 566-574.
6. Zeng, T.; Ziegelgruber, K. L.; Chin, Y.-P.; Arnold, W. A., Pesticide processing potential in prairie pothole porewaters. *Environ. Sci. Technol.* **2011,** *45*, 6814-6822.
7. Van Stempvoort, D. R.; Hendry, M. J.; Schoenau, J. J.; Krouse, H. R., Sources and dynamics of sulfur in weathered till, Western Glaciated Plains of North America. *Chem. Geol.* **1994,** *111*, 35-56.
8. Goldhaber, M. B.; Mills, C. T.; Stricker, C. A.; Morrison, J. M., The role of critical zone processes in the evolution of the Prairie Pothole Region wetlands. *Appl. Geochem.* **2011,** *26, Supplement*, S32-S35.
9. Heagle, D.; Hayashi, M.; van der Kamp, G., Use of solute mass balance to quantify geochemical processes in a prairie recharge wetland. *Wetlands* **2007,** *27*, 806-818.
10. LaBaugh, J. W.; Winter, T. C.; Swanson, G. A.; Rosenberry, D. O.; Nelson, R. D.; Euliss, N. H., Changes in atmospheric circulation patterns affect midcontinent wetlands sensitive to climate. *Limnol. Oceanogr.* **1996,** *41*, 864-870.
11. Mills, C. T.; Goldhaber, M. B.; Stricker, C. A.; Holloway, J. M.; Morrison, J. M.; Ellefsen, K. J.; Rosenberry, D. O.; Thurston, R. S., Using stable isotopes to understand hydrochemical processes in and around a Prairie Pothole wetland in the Northern Great Plains, USA. *Appl. Geochem.* **2011,** *26, Supplement*, S97-S100.
12. Biondini, M. E.; Arndt, J. L. *The biogeochemistry of carbon, nitrogen and sulfur transformations in seasonal and semipermanent wetlands*; North Dakota Water Research Institute Technical Report No. ND90-05; Fargo, ND, 1993.
13. Sando, S. K. K., D.P.; Johnson, K. M.; Lundgren, R. F.; Emerson, D. G. *Mercury and methylmercury in water and bottom sediments of wetlands at Lostwood National Wildlife Refuge, North Dakota, 2003-04*; U.S. Geological Survey, Scientific Investigations Report 2007-5219; Reston, VA, 2007; pp 1-74.
14. Hall, B. D.; Baron, L. A.; Somers, C. M., Mercury concentrations in surface water and harvested waterfowl from the prairie pothole region of Saskatchewan. *Environ. Sci. Technol.* **2009,** *43*, 8759-8766.
15. Bates, L. M.; Hall, B. D., Concentrations of methylmercury in invertebrates from wetlands of the Prairie Pothole Region of North America. *Environ. Pollut.* **2012,** *160*, 153-160.
16. Xia, K.; Skyllberg, U. L.; Bleam, W. F.; Bloom, P. R.; Nater, E. A.; Helmke, P. A., X-ray absorption spectroscopic evidence for the complexation of Hg(II) by reduced sulfur in soil humic substances. *Environ. Sci. Technol.* **1999,** *33*, 257-261.
17. Hesterberg, D.; Chou, J. W.; Hutchison, K. J.; Sayers, D. E., Bonding of Hg(II) to reduced organic sulfur in humic acid as affected by S/Hg ratio. *Environ. Sci. Technol.* **2001,** *35*, 2741-2745.

18. Skyllberg, U.; Xia, K.; Bloom, P. R.; Nater, E. A.; Bleam, W. F., Binding of mercury(II) to reduced sulfur in soil organic matter along upland-peat soil transects. *J. Environ. Qual.* **2000,** *29*, 855-865.
19. Wolfenden, S.; Charnock, J. M.; Hilton, J.; Livens, F. R.; Vaughan, D. J., Sulfide species as a sink for mercury in lake sediments. *Environ. Sci. Technol.* **2005,** *39*, 6644-6648.
20. Yoon, S.-J.; Diener, L. M.; Bloom, P. R.; Nater, E. A.; Bleam, W. F., X-ray absorption studies of CH_3Hg^+-binding sites in humic substances. *Geochim. Cosmochim. Acta* **2005,** *69*, 1111-1121.
21. Skyllberg, U.; Bloom, P. R.; Qian, J.; Lin, C.-M.; Bleam, W. F., Complexation of mercury(II) in soil organic matter: EXAFS evidence for linear two-coordination with reduced sulfur groups. *Environ. Sci. Technol.* **2006,** *40*, 4174-4180.
22. Skyllberg, U., Competition among thiols and inorganic sulfides and polysulfides for Hg and MeHg in wetland soils and sediments under suboxic conditions: Illumination of controversies and implications for MeHg net production. *J. Geophys. Res.* **2008,** *113*, G00C03.
23. Skyllberg, U.; Drott, A., Competition between disordered iron sulfide and natural organic matter associated thiols for mercury(II) - An EXAFS study. *Environ. Sci. Technol.* **2010,** *44*, 1254-1259.
24. Nagy, K. L.; Manceau, A.; Gasper, J. D.; Ryan, J. N.; Aiken, G. R., Metallothionein-like multinuclear clusters of mercury(II) and sulfur in peat. *Environ. Sci. Technol.* **2011,** *45*, 7298-7306.
25. LaBaugh, J. W.; Winter, T. C.; Rosenberry, D. O., Hydrological functions of prairie wetlands. *Great Plains Res.* **1998,** *8*, 17-37.
26. Johnson, W. C.; Millett, B. V.; Gilmanov, T.; Voldseth, R. A.; Guntenspergen, G. R.; Naugle, D. E., Vulnerability of northern prairie wetlands to climate change. *Bioscience* **2005,** *55*, 863-872.
27. Adamus, P. R. *Condition, values, and loss of natural functions of prairie wetlands of the north-central United States*; EPA 600-R-92-249; U.S. Environmental Protection Agency: Washington, DC, 1998. http://water.epa.gov/type/wetlands/assessment/appendixb.cfm (Accessed July, 2012).
28. Jokic, A.; Cutler, J. N.; Ponomarenko, E.; van der Kamp, G.; Anderson, D. W., Organic carbon and sulphur compounds in wetland soils: Insights on structure and transformation processes using *K*-edge XANES and NMR spectroscopy. *Geochim. Cosmochim. Acta* **2003,** *67*, 2585-2597.
29. Johnson, R. R.; Oslund, F. T.; Hertel, D. R., The past, present, and future of prairie potholes in the United States. *J. Soil Water Conserv.* **2008,** *63*, 84A-87A.
30. Neely, R. K.; Baker, J. L., Nitrogen and phosphorous dynamics and the fate of agricultural runoff. In *Northern Prairie Wetlands*, Van der Valk, A. G., Ed. Iowa State University Press: Ames, IA, 1989; pp 92-131.
31. Olness, A.; Staricka, J. A.; Daniel, J. A., Oxidation-reduction and groundwater contamination in the Prairie Pothole region of the Northern Great Plains. In *Water for Agriculture and Wildlife and the Environment -- Win-Win Opportunities: Proceedings of*

the 1996 USCID Wetlands Seminar, Schaack, J.; Anderson, S. S., Eds. U.S. Committee on Irrigation and Drainage: Denver, CO, 1996; pp 115-131.
32. Goldsborough, L. G.; Crumpton, W. G., Distribution and environmental fate of pesticides in prairie wetlands. *Great Plains Res.* **1998,** *8*, 73-95.
33. Detenbeck, N. E.; Elonen, C. M.; Taylor, D. L.; Cotter, A. M.; Puglisi, F. A.; Sanville, W. D., Effects of agricultural activities and best management practices on water quality of seasonal prairie pothole wetlands. *Wetlands Ecol. Manage.* **2002,** *10*, 335-354.
34. Zeng, T.; Chin, Y.-P.; Arnold, W. A., Potential for abiotic reduction of pesticides in prairie pothole porewaters. *Environ. Sci. Technol.* **2012,** *46*, 3177-3187.
35. Gleason, R. A.; Tangen, B. A.; Browne, B. A.; Euliss Jr, N. H., Greenhouse gas flux from cropland and restored wetlands in the Prairie Pothole Region. *Soil Biol. Biochem.* **2009,** *41*, 2501-2507.
36. Pennock, D.; Yates, T.; Bedard-Haughn, A.; Phipps, K.; Farrell, R.; McDougal, R., Landscape controls on N_2O and CH_4 emissions from freshwater mineral soil wetlands of the Canadian Prairie Pothole region. *Geoderma* **2010,** *155*, 308-319.
37. Badiou, P.; McDougal, R.; Pennock, D.; Clark, B., Greenhouse gas emissions and carbon sequestration potential in restored wetlands of the Canadian prairie pothole region. *Wetlands Ecol. Manage.* **2011,** *19*, 237-256.
38. Urban, N. R., Retention of sulfur in lake sediments. In *Environmental Chemistry of Lakes and Reservoirs*, Baker, L. A., Ed. American Chemical Society: Washington, DC, 1994; Vol. 237, pp 323-369.
39. Holmer, M.; Storkholm, P., Sulphate reduction and sulphur cycling in lake sediments: a review. *Freshwat. Biol.* **2001,** *46*, 431-451.
40. Vairavamurthy, M. A.; Orr, W. L.; Manowitz, B., Geochemical transformations of sedimentary sulfur: An introduction. In *Geochemical Transformations of Sedimentary Sulfur*, Vairavamurthy, M. A.; Schoonen, M. A. A.; Eglinton, T. I.; Luther III, G. W.; Manowitz, B., Eds. American Chemical Society: Washington, DC, 1995; Vol. 612, pp 1-14.
41. Elsgaard, L.; Jørgensen, B. B., Anoxie transformations of radiolabeled hydrogen sulfide in marine and freshwater sediments. *Geochim. Cosmochim. Acta* **1992,** *56*, 2425-2435.
42. Rickard, D. T., Kinetics and mechanism of pyrite formation at low temperatures. *Am. J. Sci.* **1975,** *275*, 636-652.
43. Pyzik, A. J.; Sommer, S. E., Sedimentary iron monosulfides: Kinetics and mechanism of formation. *Geochim. Cosmochim. Acta* **1981,** *45*, 687-698.
44. Aller, R. C.; Rude, P. D., Complete oxidation of solid phase sulfides by manganese and bacteria in anoxic marine sediments. *Geochim. Cosmochim. Acta* **1988,** *52*, 751-765.
45. Jørgensen, B. B., The sulfur cycle of freshwater sediments: Role of thiosulfate. *Limnol. Oceanogr.* **1990,** *35*, 1329-1342.
46. King, G. M., Effects of added manganic and ferric oxides on sulfate reduction and sulfide oxidation in intertidal sediments. *FEMS Microbiol. Lett.* **1990,** *73*, 131-138.
47. Guerin, W. F.; Braman, R. S., Patterns of organic and inorganic sulfur transformations in sediments. *Org. Geochem.* **1985,** *8*, 259-268.

48. Vairavamurthy, A.; Mopper, K., Geochemical formation of organosulphur compounds (thiols) by addition of H_2S to sedimentary organic matter. *Nature* **1987,** *329*, 623-625.
49. Francois, R., A study of sulphur enrichment in the humic fraction of marine sediments during early diagenesis. *Geochim. Cosmochim. Acta* **1987,** *51*, 17-27.
50. Kohnen, M. E. L.; Sinninghe Damsté, J. S.; ten Haven, H. L.; de Leeuw, J. W., Early incorporation of polysulphides in sedimentary organic matter. *Nature* **1989,** *341*, 640-641.
51. Aizenshtat, Z.; Krein, E. B.; Vairavamurthy, M. A.; Goldstein, T. P., Role of sulfur in the transformations of sedimentary organic matter: A mechanistic overview. In *Geochemical Transformations of Sedimentary Sulfur*, Vairavamurthy, M. A.; Schoonen, M. A. A.; Eglinton, T. I.; Luther III, G. W.; Manowitz, B., Eds. American Chemical Society: Washington, DC, 1995; Vol. 612, pp 16-37.
52. Adam, P.; Philippe, E.; Albrecht, P., Photochemical sulfurization of sedimentary organic matter: A widespread process occurring at early diagenesis in natural environments? *Geochim. Cosmochim. Acta* **1998,** *62*, 265-271.
53. Berner, R. A., Sedimentary pyrite formation: An update. *Geochim. Cosmochim. Acta* **1984,** *48*, 605-615.
54. Canfield, D. E., Reactive iron in marine sediments. *Geochim. Cosmochim. Acta* **1989,** *53*, 619-632.
55. Canfield, D. E.; Raiswell, R.; Bottrell, S. H., The reactivity of sedimentary iron minerals toward sulfide. *Am. J. Sci.* **1992,** *292*, 659-683.
56. Rickard, D.; Luther III, G. W., Chemistry of iron sulfides. *Chem. Rev.* **2007,** *107*, 514-562.
57. Gransch, J. A.; Posthuma, J., On the origin of sulphur in crudes. In *Advances in Organic Geochemistry*, Tissot, B.; Bienner, F., Eds. Editions Technip: Paris, France, 1973; pp 727-739.
58. Luther III, G. W.; Church, T. M., An overview of the environmental chemistry of sulphur in wetland systems. In *Sulphur Cycling on the Continents: Wetlands, Terrestrial Ecosystems, and Associated Water Bodies*, Howarth, R. W.; Stewart, J. W. B.; Ivanov, M. V., Eds. SCOPE, John Wiley & Sons, Inc.: Somerset, NJ, 1992; pp 125-142.
59. Ferdelman, T. G.; Church, T. M.; Luther III, G. W., Sulfur enrichment of humic substances in a Delaware salt marsh sediment core. *Geochim. Cosmochim. Acta* **1991,** *55*, 979-988.
60. Mossmann, J.-R.; Aplin, A. C.; Curtis, C. D.; Coleman, M. L., Geochemistry of inorganic and organic sulphur in organic-rich sediments from the Peru Margin. *Geochim. Cosmochim. Acta* **1991,** *55*, 3581-3595.
61. Vairavamurthy, M. A.; Zhou, W.; Eglinton, T.; Manowitz, B., Sulfonates: A novel class of organic sulfur compounds in marine sediments. *Geochim. Cosmochim. Acta* **1994,** *58*, 4681-4687.
62. Suits, N. S.; Arthur, M. A., Sulfur diagenesis and partitioning in Holocene Peru shelf and upper slope sediments. *Chem. Geol.* **2000,** *163*, 219-234.

63. Bates, A. L.; Spiker, E. C.; Hatcher, P. G.; Stout, S. A.; Weintraub, V. C., Sulfur geochemistry of organic-rich sediments from Mud Lake, Florida, U.S.A. *Chem. Geol.* **1995,** *121*, 245-262.
64. Brüchert, V.; Pratt, L. M., Contemporaneous early diagenetic formation of organic and inorganic sulfur in estuarine sediments from St. Andrew Bay, Florida, USA. *Geochim. Cosmochim. Acta* **1996,** *60*, 2325-2332.
65. Urban, N. R.; Ernst, K.; Bernasconi, S., Addition of sulfur to organic matter during early diagenesis of lake sediments. *Geochim. Cosmochim. Acta* **1999,** *63*, 837-853.
66. Filley, T. R.; Freeman, K. H.; Wilkin, R. T.; Hatcher, P. G., Biogeochemical controls on reaction of sedimentary organic matter and aqueous sulfides in holocene sediments of Mud Lake, Florida. *Geochim. Cosmochim. Acta* **2002,** *66*, 937-954.
67. Freney, J., Some observations on the nature of organic sulphur compounds in soil. *Aust. J. Agric. Res.* **1961,** *12*, 424-432.
68. Pruden, G.; Bloomfield, C., The determination of iron(II) sulphide in soil in the presence of iron(III) oxide. *Analyst* **1968,** *93*, 532-534.
69. Freney, J. R.; Melville, G. E.; Williams, C. H., The determination of carbon bonded sulfur in soil. *Soil Sci.* **1970,** *109*, 310-318.
70. Dick, W. A.; Tabatabai, M. A., Ion chromatographic determination of sulfate and nitrate in soils. *Soil Sci. Soc. Am. J.* **1979,** *43*, 899-904.
71. Canfield, D. E.; Raiswell, R.; Westrich, J. T.; Reaves, C. M.; Berner, R. A., The use of chromium reduction in the analysis of reduced inorganic sulfur in sediments and shales. *Chem. Geol.* **1986,** *54*, 149-155.
72. Rickard, D.; Morse, J. W., Acid volatile sulfide (AVS). *Mar. Chem.* **2005,** *97*, 141-197.
73. Lombi, E.; Hettiarachchi, G. M.; Scheckel, K. G., Advanced in situ spectroscopic techniques and their applications in Environmental Biogeochemistry: Introduction to the special section. *J. Environ. Qual.* **2011,** *40*, 659-666.
74. Fleet, M. E., XANES spectroscopy of sulfur in earth materials. *The Canadian Mineralogist* **2005,** *43*, 1811-1838.
75. Jalilehvand, F., Sulfur: Not a "silent" element any more. *Chem. Soc. Rev.* **2006,** *35*, 1256-1268.
76. Thieme, J.; McNult, I.; Vogt, S.; Paterson; David, X-ray spectromicroscopy - A tool for Environmental Sciences. *Environ. Sci. Technol.* **2007,** *41*, 6885-6889.
77. Lombi, E.; Susini, J., Synchrotron-based techniques for plant and soil science: Opportunities, challenges and future perspectives. *Plant Soil* **2009,** *320*, 1-35.
78. Vairavamurthy, M. A.; Wang, S.; Khandelwal, B.; Manowitz, B.; Ferdelman, T.; Fossing, H., Sulfur transformations in early diagenetic sediments from the Bay of Conception, off Chile. In *Geochemical Transformations of Sedimentary Sulfur*, Vairavamurthy, M. A.; Schoonen, M. A. A.; Eglinton, T. I.; Luther III, G. W.; Manowitz, B., Eds. American Chemical Society: Washington, DC, 1995; Vol. 612, pp 38-58.
79. Morra, M. J.; Fendorf, S. E.; Brown, P. D., Speciation of sulfur in humic and fulvic acids using X-ray absorption near-edge structure (XANES) spectroscopy. *Geochim. Cosmochim. Acta* **1997,** *61*, 683-688.

80. Vairavamurthy, M. A.; Maletic, D.; Wang, S.; Manowitz, B.; Eglinton, T.; Lyons, T., Characterization of sulfur-containing functional groups in sedimentary humic substances by X-ray absorption near-edge structure spectroscopy. *Energy Fuels* **1997,** *11*, 546-553.
81. Xia, K.; Weesner, F.; Bleam, W. F.; Helmke, P. A.; Bloom, P. R.; Skyllberg, U. L., XANES studies of oxidation states of sulfur in aquatic and soil humic substances. *Soil Sci. Soc. Am. J.* **1998,** *62*, 1240-1246.
82. Hutchison, K. J.; Hesterberg, D.; Chou, J. W., Stability of reduced organic sulfur in humic acid as affected by aeration and pH. *Soil Sci. Soc. Am. J.* **2001,** *65*, 704-709.
83. Prietzel, J.; Thieme, J.; Neuhäusler, U.; Susini, J.; Kögel-Knabner, I., Speciation of sulphur in soils and soil particles by X-ray spectromicroscopy. *Eur. J. Soil Sci.* **2003,** *54*, 423-433.
84. Solomon, D.; Lehmann, J.; Martínez, C. E., Sulfur *K*-edge XANES spectroscopy as a tool for understanding sulfur dynamics in soil organic matter. *Soil Sci. Soc. Am. J.* **2003,** *67*, 1721-1731.
85. Bostick, B. C.; Theissen, K. M.; Dunbar, R. B.; Vairavamurthy, M. A., Record of redox status in laminated sediments from Lake Titicaca: A sulfur *K*-edge X-ray absorption near edge structure (XANES) study. *Chem. Geol.* **2005,** *219*, 163-174.
86. Solomon, D.; Lehmann, J.; Lobe, I.; Martinez, C. E.; Tveitnes, S.; Du Preez, C. C.; Amelung, W., Sulphur speciation and biogeochemical cycling in long-term arable cropping of subtropical soils: evidence from wet-chemical reduction and S *K*-edge XANES spectroscopy. *Eur. J. Soil Sci.* **2005,** *56*, 621-634.
87. Zhao, F. J.; Lehmann, J.; Solomon, D.; Fox, M. A.; McGrath, S. P., Sulphur speciation and turnover in soils: Evidence from sulphur *K*-edge XANES spectroscopy and isotope dilution studies. *Soil Biol. Biochem.* **2006,** *38*, 1000-1007.
88. Einsiedl, F.; Schäfer, T.; Northrup, P., Combined sulfur *K*-edge XANES spectroscopy and stable isotope analyses of fulvic acids and groundwater sulfate identify sulfur cycling in a karstic catchment area. *Chem. Geol.* **2007,** *238*, 268-276.
89. Prietzel, J.; Thieme, J.; Salomé, M.; Knicker, H., Sulfur *K*-edge XANES spectroscopy reveals differences in sulfur speciation of bulk soils, humic acid, fulvic acid, and particle size separates. *Soil Biol. Biochem.* **2007,** *39*, 877-890.
90. Schroth, A. W.; Bostick, B. C.; Graham, M.; Kaste, J. M.; Mitchell, M. J.; Friedland, A. J., Sulfur species behavior in soil organic matter during decomposition. *J. Geophys. Res.* **2007,** *112*, G04011.
91. Einsiedl, F.; Mayer, B.; Schäfer, T., Evidence for incorporation of H_2S in groundwater fulvic acids from stable isotope ratios and sulfur *K*-edge X-ray absorption near edge structure spectroscopy. *Environ. Sci. Technol.* **2008,** *42*, 2439-2444.
92. Prietzel, J.; Thieme, J.; Herre, A.; Salomé, M.; Eichert, D., Differentiation between adsorbed and precipitated sulphate in soils and at micro-sites of soil aggregates by sulphur *K*-edge XANES. *Eur. J. Soil Sci.* **2008,** *59*, 730-743.
93. Prietzel, J.; Thieme, J.; Tyufekchieva, N.; Paterson, D.; McNulty, I.; Kögel-Knabner, I., Sulfur speciation in well-aerated and wetland soils in a forested catchment assessed by sulfur *K*-edge X-ray absorption near-edge spectroscopy (XANES). *J. Plant Nutr. Soil Sci.* **2009,** *172*, 393-403.

94. Prietzel, J.; Tyufekchieva, N.; Eusterhues, K.; Kögel-Knabner, I.; Thieme, J.; Paterson, D.; McNulty, I.; de Jonge, M.; Eichert, D.; Salomé, M., Anoxic versus oxic sample pretreatment: Effects on the speciation of sulfur and iron in well-aerated and wetland soils as assessed by X-ray absorption near-edge spectroscopy (XANES). *Geoderma* **2009,** *153*, 318-330.
95. Solomon, D.; Lehmann, J.; Kinyangi, J.; Pell, A.; Theis, J.; Riha, S.; Ngoze, S.; Amelung, W.; Preez, C.; Machado, S.; Ellert, B.; Janzen, H., Anthropogenic and climate influences on biogeochemical dynamics and molecular-level speciation of soil sulfur. *Ecol. Appl.* **2009,** *19*, 989-1002.
96. Burton, E. D.; Bush, R. T.; Sullivan, L. A.; Hocking, R. K.; Mitchell, D. R. G.; Johnston, S. G.; Fitzpatrick, R. W.; Raven, M.; McClure, S.; Jang, L. Y., Iron-monosulfide oxidation in natural sediments: Resolving microbially mediated S transformations using XANES, electron microscopy, and selective extractions. *Environ. Sci. Technol.* **2009,** *43*, 3128-3134.
97. Prietzel, J.; Botzaki, A.; Tyufekchieva, N.; Brettholle, M.; Thieme, J. r.; Klysubun, W., Sulfur speciation in soil by S *K*-edge XANES spectroscopy: Comparison of spectral deconvolution and linear combination fitting. *Environ. Sci. Technol.* **2011,** *45*, 2878-2886.
98. Solomon, D.; Lehmann, J.; de Zarruk, K. K.; Dathe, J.; Kinyangi, J.; Liang, B.; Machado, S., Speciation and long- and short-term molecular-level dynamics of soil organic sulfur studied by X-ray absorption near-edge structure spectroscopy. *J. Environ. Qual.* **2011,** *40*, 704-718.
99. Prietzel, J.; Kögel-Knabner, I.; Thieme, J.; Paterson, D.; McNulty, I., Microheterogeneity of element distribution and sulfur speciation in an organic surface horizon of a forested Histosol as revealed by synchrotron-based X-ray spectromicroscopy. *Org. Geochem.* **2011,** *42*, 1308-1314.
100. Burton, E. D.; Bush, R. T.; Johnston, S. G.; Sullivan, L. A.; Keene, A. F., Sulfur biogeochemical cycling and novel Fe–S mineralization pathways in a tidally re-flooded wetland. *Geochim. Cosmochim. Acta* **2011,** *75*, 3434-3451.
101. Morgan, B.; Burton, E. D.; Rate, A. W., Iron monosulfide enrichment and the presence of organosulfur in eutrophic estuarine sediments. *Chem. Geol.* **2012,** *296–297*, 119-130.
102. Vairavamurthy, M. A.; Manowitz, B.; Zhou, W.; Jeon, Y., Determination of hydrogen sulfide oxidation products by Sulfur *K*-edge X-ray absorption near-edge structure spectroscopy. In *Environmental Geochemistry of Sulfide Oxidation*, Alpers, C. N.; Blowes, D. W., Eds. American Chemical Society: Washington DC, 1994; Vol. 550, pp 412-430.
103. Eglinton, T. I.; Irvine, J. E.; Vairavamurthy, A.; Zhou, W.; Manowitz, B., Formation and diagenesis of macromolecular organic sulfur in Peru margin sediments. *Org. Geochem.* **1994,** *22*, 781-799.
104. Mayhew, L. E.; Webb, S. M.; Templeton, A. S., Microscale imaging and identification of Fe speciation and distribution during fluid–mineral reactions under highly reducing conditions. *Environ. Sci. Technol.* **2011,** *45*, 4468-4474.

105. Lam, P. J.; Ohnemus, D. C.; Marcus, M. A., The speciation of marine particulate iron adjacent to active and passive continental margins. *Geochim. Cosmochim. Acta* **2012,** *80*, 108-124.
106. Toner, B. M.; Marcus, M. A.; Edwards, K. J.; Rouxel, O.; German, C. R., Measuring the form of iron in hydrothermal plume particles. *Oceanography* **2012,** *25*, 209-212.
107. Toner, B. M.; Berquó, T. S.; Michel, F. M.; Sorensen, J. V.; Templeton, A. S.; Edwards, K. J., Mineralogy of iron microbial mats from Loihi Seamount. *Front. Microbiol. Chem.* **2012,** *3*, 1-18.
108. Mushet, D. M.; Euliss, N. H. *The Cottonwood Lake study area, a long-term wetland ecosystem monitoring site*; U.S. Geological Survey Fact Sheet 2012-3040: Reston, VA 2012; pp 1-2.
109. Stewart, R. E.; Kantrud, H. A. *Classification of natural ponds and lakes in the glaciated prairie region*; Bureau of Sport Fisheries and Wildlife, U.S. Fish and Wildlife Service, Resource Publication 92; Washington, DC, 1971; pp 1-57.
110. Winter, T. C.; Carr, M. R. *Hydrologic setting of wetlands in the Cottonwood Lake area, Stutsman County, North Dakota*; U.S. Geological Survey Water Resources Investigations Report 80-99; Denver, CO, 1980; pp 1-42.
111. Euliss, N. H.; Mushet, D. M., A multi-year comparison of IPCI scores for prairie pothole wetlands: Implications of temporal and spatial variation. *Wetlands* **2011,** *31*, 713-723.
112. Winter, T. C.; Rosenberry, D. O., The interaction of ground water with prairie pothole wetlands in the Cottonwood Lake area, east-central North Dakota, 1979-1990. *Wetlands* **1995,** *15*, 193-211.
113. Swanson, G. A.; Winter, T. C.; Adomaitis, V. A.; Labaugh, J. W. *Chemical characteristics of prairie lakes in south-central North Dakota USA - Their potential for influencing use by fish and wildlife*; U.S. Fish and Wildlife Service, Technical Report 18; Washington, DC, 1988; pp 1-44.
114. Winter, T. C.; Rosenberry, D. O., Hydrology of prairie pothole wetlands during drought and deluge: A 17-year study of the cottonwood lake wetland complex in North Dakota in the perspective of longer term measured and proxy hydrological records. *Clim. Change* **1998,** *40*, 189-209.
115. Labaugh, J. W., Spatial and temporal variability in specific conductance and chemical characteristics of wetland water and in water column biota in the wetlands in the Cottonwood Lake area. In *Hydrological, chemical, and biological characteristics of a prairie pothole wetland complex under highly variable climate conditions - the Cottonwood Lake area, east-central North Dakota, U.S. Geological Survey Professional Paper 1675*, Winter, T. C., Ed. U.S. Geological Survey: Denver, CO, 2003; pp 35-53.
116. Rose, C.; Crumpton, W., Effects of emergent macrophytes on dissolved oxygen dynamics in a prairie pothole wetland. *Wetlands* **1996,** *16*, 495-502.
117. Ziegelgruber, K. L.; Zeng, T.; Chin, Y.-P.; Arnold, W. A., Sources and composition of pore water dissolved organic matter in prairie pothole lakes of North Dakota, USA. *Submitted* **2012**.

118. Marcus, M. A.; MacDowell, A. A.; Celestre, R.; Manceau, A.; Miller, T.; Padmore, H. A.; Sublett, R. E., Beamline 10.3.2 at ALS: A hard X-ray microprobe for environmental and materials sciences. *J. Synchrotron Radiat.* **2004,** *11*, 239-247.
119. Marcus, M. A., X-ray photon-in/photon-out methods for chemical imaging. *TrAC, Trends Anal. Chem.* **2010,** *29*, 508-517.
120. Manceau, A.; Marcus, M. A.; Tamura, N., Quantitative speciation of heavy metals in soils and sediments by synchrotron X-ray techniques. In *Applications of synchrotron radiation in low-temperature geochemistry and environmental science*, Fenter, P. A.; Rivers, M. L.; Sturchio, N. C.; Sutton, S. R., Eds. Mineralogical Society of America: Washington, DC, 2002; Vol. 49, pp 341-428.
121. Webb, S. M., SIXpack: A graphical user interface for XAS analysis using IFEFFIT. *Phys. Scr.* **2005,** *2005*, 1011-1014.
122. Toner, B.; Manceau, A.; Webb, S. M.; Sposito, G., Zinc sorption to biogenic hexagonal-birnessite particles within a hydrated bacterial biofilm. *Geochim. Cosmochim. Acta* **2006,** *70*, 27-43.
123. Malinowski, E. R., Determination of the number of factors and the experimental error in a data matrix. *Anal. Chem.* **1977,** *49*, 612-617.
124. Malinowski, E. R., Theory of error for target factor analysis with applications to mass spectrometry and nuclear magnetic resonance spectrometry. *Anal. Chim. Acta* **1978,** *103*, 339-354.
125. Beauchemin, S.; Hesterberg, D.; Beauchemin, M., Principal component analysis approach for modeling sulfur *K*-XANES spectra of humic acids. *Soil Sci. Soc. Am. J.* **2002,** *66*, 83-91.
126. Marcus, M. A.; Westphal, A. J.; Fakra, S. C., Classification of Fe-bearing species from K-edge XANES data using two-parameter correlation plots. *J. Synchrotron Radiat.* **2008,** *15*, 463-468.
127. Zeng, T.; Arnold, W. A., Pesticide photolysis in prairie potholes: Probing photosensitized processes. *Submitted* **2012**.
128. Lovley, D. R.; Klug, M. J., Model for the distribution of sulfate reduction and methanogenesis in freshwater sediments. *Geochim. Cosmochim. Acta* **1986,** *50*, 11-18.
129. Sinke, A. J. C.; Cornelese, A. A.; Cappenberg, T. E.; Zehnder, A. J. B., Seasonal variation in sulfate reduction and methanogenesis in peaty sediments of eutrophic Lake Loosdrecht, the Netherlands. *Biogeochemistry* **1992,** *16*, 43-61.
130. Kiene, R. P.; Visscher, P. T., Production and fate of methylated sulfur compounds from methionine and dimethylsulfoniopropionate in anoxic salt marsh sediments. *Appl. Environ. Microbiol.* **1987,** *53*, 2426-2434.
131. Kiene, R. P.; Malloy, K. D.; Taylor, B. F., Sulfur-containing amino acids as precursors of thiols in anoxic coastal sediments. *Appl. Environ. Microbiol.* **1990,** *56*, 156-161.
132. Risberg, E. D.; Jalilehvand, F.; Leung, B. O.; Pettersson, L. G. M.; Sandstrom, M., Theoretical and experimental sulfur K-edge X-ray absorption spectroscopic study of cysteine, cystine, homocysteine, penicillamine, methionine and methionine sulfoxide. *Dalton Transactions* **2009**, 3542-3558.

133. Schouten, S.; Eglinton Timothy, I.; Sinninghe Damsté Jaap, S.; de Leeuw Jan, W., Influence of sulphur cross-linking on the molecular-size distribution of sulphur-rich macromolecules in bitumen. In *Geochemical Transformations of Sedimentary Sulfur*, Vairavamurthy, M. A.; Schoonen, M. A. A.; Eglinton, T. I.; Luther III, G. W.; Manowitz, B., Eds. American Chemical Society: Washington, DC, 1995; Vol. 612, pp 80-92.
134. van Dongen, B. E.; Schouten, S.; Baas, M.; Geenevasen, J. A. J.; Sinninghe Damsté, J. S., An experimental study of the low-temperature sulfurization of carbohydrates. *Org. Geochem.* **2003,** *34*, 1129-1144.
135. Dey, A.; Glaser, T.; Moura, J. J. G.; Holm, R. H.; Hedman, B.; Hodgson, K. O.; Solomon, E. I., Ligand K-edge X-ray absorption spectroscopy and DFT calculations on $[Fe_3S_4]^{0,+}$ clusters: Delocalization, redox, and effect of the protein environment. *J. Am. Chem. Soc.* **2004,** *126*, 16868-16878.
136. Pingitore Jr, N. E.; Meitzner, G.; Love, K. M., Identification of sulfate in natural carbonates by X-ray absorption spectroscopy. *Geochim. Cosmochim. Acta* **1995,** *59*, 2477-2483.
137. Myneni, S. C. B., X-ray and vibrational spectroscopy of sulfate in earth materials. *Reviews in Mineralogy and Geochemistry* **2000,** *40*, 113-172.
138. Abdollahi, H.; Nedwell, D. B., Seasonal temperature as a factor influencing bacterial sulfate reduction in a saltmarsh sediment. *Microb. Ecol.* **1979,** *5*, 73-79.
139. Howarth, R. W.; Teal, J. M., Sulfate reduction in a New England salt marsh. *Limnol. Oceanogr.* **1979,** *24*, 999-1013.
140. Troelsen, H.; Jørgensen, B. B., Seasonal dynamics of elemental sulfur in two coastal sediments. *Estuar. Coast. Shelf Sci.* **1982,** *15*, 255-266.
141. Westrich, J. T.; Berner, R. A., The effect of temperature on rates of sulfate reduction in marine sediments. *Geomicrobiol. J.* **1988,** *6*, 99-117.
142. Moeslundi, L.; Thamdrup, B.; Jørgensen, B. B., Sulfur and iron cycling in a coastal sediment: Radiotracer studies and seasonal dynamics. *Biogeochemistry* **1994,** *27*, 129-152.
143. Panutrakul, S.; Monteny, F.; Baeyens, W., Seasonal variations in sediment sulfur cycling in the Ballastplaat mudflat, Belgium. *Estuaries Coasts* **2001,** *24*, 257-265.
144. Al-Raei, A. M.; Bosselmann, K.; Bottcher, M. E.; Hespenheide, B.; Tauber, F., Seasonal dynamics of microbial sulfate reduction in temperate intertidal surface sediments: controls by temperature and organic matter. *Ocean Dynam* **2009,** *59*, 351-370.
145. Jørgensen, B. B., The sulfur cycle of a coastal marine sediment (Limfjorden, Denmark). *Limnol. Oceanogr.* **1977,** *22*, 814-832.
146. Sørensen, J.; Jeørgensen, B. B., Early diagenesis in sediments from Danish coastal waters: Microbial activity and Mn-Fe-S geochemistry. *Geochim. Cosmochim. Acta* **1987,** *51*, 1583-1590.
147. King, G. M., Patterns of sulfate reduction and the sulfur cycle in a South Carolina salt marsh. *Limnol. Oceanogr.* **1988,** *33*, 376-390.
148. Dacey, J. W. H.; Howes, B. L., Water uptake by roots controls water table movement and sediment oxidation in short *Spartina* marsh. *Science* **1984,** *224*, 487-489.
149. Morris, J. T.; Whiting, G. J., Gas advection in sediments of a South Carolina salt marsh. *Marine Ecology-Progress Series* **1985,** *27*, 187-194.

150. Luther III, G. W.; Church, T. M., Seasonal cycling of sulfur and iron in porewaters of a Delaware salt marsh. *Mar. Chem.* **1988,** *23*, 295-309.
151. Thamdrup, B.; Finster, K.; Fossing, H.; Hansen, J. W.; Jørgensen, B. B., Thiosulfate and sulfite distributions in porewater of marine sediments related to manganese, iron, and sulfur geochemistry. *Geochim. Cosmochim. Acta* **1994,** *58*, 67-73.
152. Boulegue, J.; Lord III, C. J.; Church, T. M., Sulfur speciation and associated trace metals (Fe, Cu) in the pore waters of Great Marsh, Delaware. *Geochim. Cosmochim. Acta* **1982,** *46*, 453-464.
153. Howarth, R. W.; Merkel, S., Pyrite formation and the measurement of sulfate reduction in salt marsh sediments. *Limnol. Oceanogr.* **1984,** *29*, 598-608.
154. Rudd, J. W. M.; Kelly, C. A.; Furutani, A., The role of sulfate reduction in long term accumulation of organic and inorganic sulfur in lake sediments. *Limnol. Oceanogr.* **1986,** *31*, 1281-1291.
155. Kling, G. W.; Giblin, A. E.; Fry, B.; Peterson, B. J., The role of seasonal turnover in lake alkalinity dynamics. *Limnol. Oceanogr.* **1991,** *36*, 106-122.

Chapter 6: Conclusions and Future Research

6.1 Conclusions

This dissertation demonstrated that several abiotic transformation mechanisms effectively promote the natural attenuation of pesticides in PPLs.

The first mechanism was nucleophilic substitution reactions with HS^- and S_n^{2-} in sediment porewaters. Chloroacetanilide pesticides readily undergo degradation in both native and filter-sterilized porewaters with half-lives on the order of hours. Both HS^- and S_n^{2-} contributed to pesticide transformations. Even though S_n^{2-} is a stronger nucleophile, the greater abundance of HS^- dominated the overall chloroacetanilide reactivity. The contribution of HS^- to the overall reaction decreased with increasing porewater pH, while the contribution of S_n^{2-} increased markedly with increasing pH. The identification of transformation products revealed the presence of mercaptoacetanilides upon chlorine displacement by HS^- and S_n^{2-}, with major products being monosulfur- and disulfur-substituted derivatives.

The second mechanism was reduction reactions with HS^- and S_n^{2-} in sediment porewaters. Dinitroanilines with different electron withdrawing/donating substituents degraded at varying rates with half-lives ranging from hours to days. Polysulfide species proved to be much more reactive reductants than HS^-. Direct reduction by HS^- and S_n^{2-} as well as DOM-mediated reduction seemed to dominate pesticide transformation. Reactions in native porewaters proceeded significantly faster than those in filter-sterilized porewaters, suggesting the possible involvement of other unknown reactive constituents. The identification of transformation products revealed the presence of diamine and/or triamine products corresponding to nitro-reduction.

Photodegradation promoted by DOM occurred in PPL surface water. A variety of pesticides underwent photolysis under both simulated and natural sunlight with half-lives on the order of hours to days. Using selective probe compounds revealed that elevated DOM levels led to increased concentrations of PPRIs such as $CO_3^{\bullet-}$, $^{\bullet}OH$, $^1O_2$ and $^3DOM^*$, indicating higher photoreactivity. While pesticides from different classes exhibited diverse photochemical behavior, most pesticides, with the exception of dinitroanilines, mainly underwent indirect photolysis. Quencher experiments further verified that photosensitized processes mediated by $^1O_2$ and/or $^3DOM^*$ were predominant pathways. By measuring steady-state PPRI concentrations and quenching agents, it was possible to estimate the second-order rate constants for reaction of the pesticides with the PPRIs.

In addition, the S speciation in PPL sediments was examined by S *K*-edge XANES spectroscopy. The multi-energy chemical mapping revealed microspatial heterogeneity of S distribution and speciation. Using linear combination fittings of S chemical maps and XANES spectra, it has been found that the reduced S primarily consisted of organic (di)sulfides and the mineral pyrite, while the oxidized S contained sulfate (both ester-linked and inorganic) and sulfonate to a lesser extent. A closer examination of the fractional contributions of reduced and oxidized S revealed a seasonal fluctuation of S speciation, implying the sensitivity of S biogeochemistry to certain environmental variables (e.g., temperature and productivity).

6.2 Future Research

Overall, this work contributes to our understanding of abiotic natural attenuation processes of pesticides as well as the S cycling in the PPLs. A number of questions raised during the course of this work, however, merit further exploration.

As discussed in Chapter 2 and 3, other dissolved or solid-phase porewater constituents, such as metal sulfides (e.g., pyrite), organic thiol (e.g., glutathione), and DOM, are likely responsible for the enhanced reactivity of pesticides that could not be accounted for by HS^- and S_n^{2-} mediated reactions. The identity and contribution of such chemical species could be further explored through experiments under well-defined laboratory conditions using model compounds. In fact, the possible role of pyrite and organic thiol seems to be supported by the S XANES data, although the abundances of these species in porewaters are unknown. Moreover, the reducing capacity of porewater DOM warrants further research to better differentiate its role as direct reductant and/or electron transfer mediator.

Additional investigations into polysulfide analysis should also be considered. The relative abundance of individual polysulfide species in sediment porewaters remains unknown, as the analytical method used in this work only allows an assessment of total polysulfides. *In situ* analytical techniques to accurately quantify individual polysulfides would enable the identification of the most important species present in sediment porewaters in light of their theoretical reactivity.

As discussed in Chapter 4, the source of DOM may affect the production of reactive intermediates. This suggests a need to further investigate the photoreactivity of

PPLs within different agricultural settings. Future work into the identification, (eco)toxicological evaluations and fate assessment of pesticide photoproducts also deserves consideration.

Field or microcosm studies on sulfate reduction rate may prove useful to better interpret the observed intra-annual variability in S speciation observed in the sediments. Future work might also explore the S speciation throughout an entire sediment core section, which may provide a high resolution depositional record that can be used to examine changes in productivity and redox conditions on longer time scales.

References

Chapter 1 References

1. Tilman, D.; Fargione, J.; Wolff, B.; D'Antonio, C.; Dobson, A.; Howarth, R.; Schindler, D.; Schlesinger, W. H.; Simberloff, D.; Swackhamer, D., Forecasting agriculturally driven global environmental change. *Science* **2001,** *292*, 281-284.
2. Schwarzenbach, R. P.; Egli, T.; Hofstetter, T. B.; von Gunten, U.; Wehrli, B., Global water pollution and human health. *Annu. Rev. Environ. Resour.* **2010,** *35*, 109-136.
3. Gilliom, R. J.; Barbash, J. E.; Crawford, C. G.; Hamilton, P. A.; Martin, J. D.; Nakagaki, N.; Nowell, L. H.; Scott, J. C.; Stackelberg, P. E.; Thelin, G. P.; Wolock, D. M. *The quality of our Nation's waters - Pesticides in the Nation's stream and ground water, 1992-2001*; National Water-Quality Assessment Program, U.S. Geological Survey Circular 1291; Reston, VA, 2006; pp 1-172.
4. Li, Y.; Zhang, J. B., Agricultural diffuse pollution from fertilisers and pesticides in China. *Water Sci. Technol.* **1999,** *39*, 25-32.
5. Huber, A.; Bach, M.; Frede, H. G., Pollution of surface waters with pesticides in Germany: modeling non-point source inputs. *Agric., Ecosyst. Environ.* **2000,** *80*, 191-204.
6. Kishimba, M. A.; Henry, L.; Mwevura, H.; Mmochi, A. J.; Mihale, M.; Hellar, H., The status of pesticide pollution in Tanzania. *Talanta* **2004,** *64*, 48-53.
7. Konstantinou, I. K.; Hela, D. G.; Albanis, T. A., The status of pesticide pollution in surface waters (rivers and lakes) of Greece. Part I. Review on occurrence and levels. *Environ. Pollut.* **2006,** *141*, 555-570.
8. Sarkar, S. K.; Bhattacharya, B. D.; Bhattacharya, A.; Chatterjee, M.; Alam, A.; Satpathy, K. K.; Jonathan, M. P., Occurrence, distribution and possible sources of organochlorine pesticide residues in tropical coastal environment of India: An overview. *Environ. Int.* **2008,** *34*, 1062-1071.
9. Menezes, C. T.; Heller, L., A method for prioritization of areas for pesticides surveillance on surface waters: A study in Minas Gerais, Brazil. *Water Sci. Technol.* **2008,** *57*, 1693-1698.
10. Williamson, S.; Ball, A.; Pretty, J., Trends in pesticide use and drivers for safer pest management in four African countries. *Crop Protect.* **2008,** *27*, 1327-1334.
11. Atapattu, S. S.; Kodituwakku, D. C., Agriculture in South Asia and its implications on downstream health and sustainability: A review. *Agric. Water Manage.* **2009,** *96*, 361-373.
12. Capel, P. D.; Larson, S. J., Effect of scale on the behavior of atrazine in surface waters. *Environ. Sci. Technol.* **2001,** *35*, 648-657.
13. Capel, P. D.; Larson, S. J.; Winterstein, T. A., The behaviour of 39 pesticides in surface waters as a function of scale. *Hydrol. Processes* **2001,** *15*, 1251-1269.
14. Capel, P. D.; McCarthy, K. A.; Barbash, J. E., National, holistic, watershed-scale approach to understand the sources, transport, and fate of agricultural chemicals. *J. Environ. Qual.* **2008,** *37*, 983-993.
15. Katagi, T., Behavior of pesticides in water-sediment systems. In *Reviews of Environmental Contamination and Toxicology*, Ware, G. W.; Albert, L. A.; Voogt, P.;

Gerba, C. P.; Hutzinger, O.; Knaak, J. B.; Mayer, F. L.; Morgan, D. P.; Park, D. L.; Tjeerdema, R. S.; Whitacre, D. M.; Yang, R. S. H.; Gunther, F. A., Eds. Springer-Verlag New York, LLC.: Secaucus, NJ 2006; Vol. 187, pp 133-251.
16. Barbash, J. E., The geochemistry of pesticides. In *Treatise on Geochemistry - Environmental Geochemistry*, Holland, H. D.; Turekian, K. K., Eds. Elsevier Ltd.: Oxford, UK, 2007; Vol. 9, pp 1-43.
17. Zedler, J. B.; Kercher, S., Wetland resources: Status, trends, ecosystem services, and restorability. *Annu. Rev. Environ. Resour.* **2005,** *30*, 39-74.
18. Winter, T. C., Hydrologic studies of wetlands in the Northern Prairie. In *Northern Prairie Wetlands*, Van der Valk, A. G., Ed. Iowa State University Press: Ames, IA, 1989; pp 16-54.
19. van der Valk, A. G., The prairie potholes of North America. In *The World's Largest Wetlands*, Fraser, L. H.; Keddy, P. A., Eds. Cambridge University Press: Cambridge, UK, 2005; pp 393-423.
20. Mitsch, W.; Hernandez, M., Landscape and climate change threats to wetlands of North and Central America. *Aquat. Sci.* **2012**, 1-17.
21. Tiner, R. W., Geographically isolated wetlands of the United States. *Wetlands* **2003,** *23*, 494-516.
22. LaBaugh, J. W.; Winter, T. C.; Rosenberry, D. O., Hydrological functions of prairie wetlands. *Great Plains Res.* **1998,** *8*, 17-37.
23. Stewart, R. E.; Kantrud, H. A. *Classification of natural ponds and lakes in the glaciated prairie region*; Bureau of Sport Fisheries and Wildlife, U.S. Fish and Wildlife Service, Resource Publication 92; Washington, DC, 1971; pp 1-57.
24. Euliss, N. H.; LaBaugh, J. W.; Fredrickson, L. H.; Mushet, D. M.; Laubhan, M. K.; Swanson, G. A.; Winter, T. C.; Rosenberry, D. O.; Nelson, R. D., The wetland continuum: A conceptual framework for interpreting biological studies. *Wetlands* **2004,** *24*, 448-458.
25. Kantrud, H. A.; Krapu, G. L.; Swanson, G. A. *Prairie basin wetlands of the Dakotas: A community profile*; U.S. Fish and Wildlife Service, Biological Report 85: Washington, DC, 1989; pp 1-111.
26. Batt, B. D. J.; Anderson, M. G.; Anderson, C. D.; Caswell, F. D., The use of prairie potholes by North American ducks. In *Northern Prairie Wetlands*, Van der Valk, A. G., Ed. Iowa State University Press: Ames, IA, 1989; pp 204-227.
27. Smith, G. W. *A critical review of the aerial and ground surveys of breeding waterfowl in North America*; U.S. Fish and Wildlife Service, National Biological Service, Biological Science Report 5; Washington, DC, 1995; pp 1-252.
28. Tiner, R. W., *Wetlands of the United States: Current status and recent trends*. National Wetlands Inventory, U.S. Fish and Wildlife Service: Washington, DC, 1984.
29. Adamus, P. R. *Condition, values, and loss of natural functions of prairie wetlands of the north-central United States*; EPA 600-R-92-249; U.S. Environmental Protection Agency: Washington, DC, 1998. http://water.epa.gov/type/wetlands/assessment/appendixb.cfm (Accessed July, 2012).
30. Euliss, J. N. H.; Gleason, R. A.; Olness, A.; McDougal, R. L.; Murkin, H. R.; Robarts, R. D.; Bourbonniere, R. A.; Warner, B. G., North American prairie wetlands are

important nonforested land-based carbon storage sites. *Sci. Total Environ.* **2006,** *361*, 179-188.
31. Gleason, R. A.; Laubhan, M. K.; Euliss, N. H. *Ecosystem services derived from wetland conservation practices in the United States prairie pothole region with an emphasis on the U.S. Department of Agriculture Conservation Reserve and Wetlands Reserve Programs*; U. S. Geological Survey Professional Paper 1745: Reston, VA, 2008; pp 1-58.
32. Johnson, R. R.; Oslund, F. T.; Hertel, D. R., The past, present, and future of prairie potholes in the United States. *J. Soil Water Conserv.* **2008,** *63*, 84A-87A.
33. LaBaugh, J. W., Chemical characterisitcs of water in Northern Prairie Wetlands. *Northern Prairie Wetlands* **1988**, 56-90.
34. Anteau, M., Do interactions of land use and climate affect productivity of waterbirds and prairie-pothole wetlands? *Wetlands* **2012,** *32*, 1-9.
35. Dahl, T. E. *Wetland losses in the United States 1780's to 1980's*; U.S. Fish and Wildlife Service: Washington, DC, 1990; pp 1-13.
36. Oslund, F. T.; Johnson, R. R.; Hertel, D. R., Assessing wetland changes in the prairie pothole region of Minnesota from 1980 to 2007. *J. Fish Wildl. Manag.* **2010,** *1*, 131-135.
37. Dahl, T. E.; Watmough, M. D., Current approaches to wetland status and trends monitoring in prairie Canada and the continental United States of America. *Can. J. Remote Sens.* **2007,** *33*, S17-S27.
38. Samson, F.; Knopf, F., Prairie conservation in North America. *Bioscience* **1994,** *44*, 418-421.
39. Galatowitsch, S. M.; van der Valk, A. G., Natural revegetation during restoration of wetlands in the southern prairie-pothole region of North America. In *Restoration of Temperate Wetlands*, Wheeler, B. D.; Shaw, S. S.; Fojt, W. J.; Robertson, R. A., Eds. John Wiley & Sons, Inc.: Chichester, UK, 1995; pp 129-142.
40. Dahl, T. E. *Status and trends of wetlands in the conterminous United States, 1998-2004*; U.S. Fish and Wildlife Service; U.S. Fish and Wildlife Service: Washington, DC, 2006; pp 1-112.
41. Watmough, M. D.; Schmoll, M. J. *Environment Canada's prairie and northern region habitat monitoring program phase II: Recent habitat trends in the Prairie Habitat Joint Venture*; Environment Canada, Canadian Wildlife Service, Technical Report Series No. 493; Environment Canada, Canadian Wildlife Service, Technical Report Series No. 493: Edmonton, Canada, 2007; pp 1-135.
42. Goldsborough, L. G.; Crumpton, W. G., Distribution and environmental fate of pesticides in prairie wetlands. *Great Plains Res.* **1998,** *8*, 73-95.
43. Neely, R. K.; Baker, J. L., Nitrogen and phosphorous dynamics and the fate of agricultural runoff. In *Northern Prairie Wetlands*, Van der Valk, A. G., Ed. Iowa State University Press: Ames, IA, 1989; pp 92-131.
44. Olness, A.; Staricka, J. A.; Daniel, J. A., Oxidation-reduction and groundwater contamination in the Prairie Pothole region of the Northern Great Plains. In *Water for Agriculture and Wildlife and the Environment -- Win-Win Opportunities: Proceedings of*

the 1996 USCID Wetlands Seminar, Schaack, J.; Anderson, S. S., Eds. U.S. Committee on Irrigation and Drainage: Denver, CO, 1996; pp 115-131.
45. Detenbeck, N. E.; Elonen, C. M.; Taylor, D. L.; Cotter, A. M.; Puglisi, F. A.; Sanville, W. D., Effects of agricultural activities and best management practices on water quality of seasonal prairie pothole wetlands. *Wetlands Ecol. Manage.* **2002,** *10*, 335-354.
46. Goolsby, D. A.; Battaglin, W. A.; Lawrence, G. B.; Artz, R. S.; Aulenbach, B. T.; Hooper, R. P.; Keeny, D. R.; Stensland, G. J. *Flux and sources of nutrients in the Mississippi-Atchafalaya River basin*; Costal Ocean Program, National Oceanic and Atmospheric Administration, Decision Analysis Series No. 17; Silver Spring, MD, 1999; pp 1-151.
47. Wolf, T. M.; Cessna, A. J., Protecting aquatic and riparian areas from pesticide drift. In *International Conference on Pesticide Application for Drift Management*, Washington State University Press: Pullman, WA 2004; pp 59-71.
48. Larney, F. J.; Cessna, A. J.; Bullock, M. S., Herbicide transport on wind-eroded sediment. *J. Environ. Qual.* **1999,** *28*, 1412-1421.
49. Waite, D. T.; Sommerstad, H.; Grover, R.; Kerr, L.; Westcott, N. D., Pesticides in ground water, surface water and spring runoff in a small saskatchewan watershed. *Environ. Toxicol. Chem.* **1992,** *11*, 741-748.
50. Cessna, A. J.; Elliott, J. A.; Best, K. B.; Grover, R.; Nicholaichuk, W., Transport of nutrients and postemergence-applied herbicides in runoff from corrugation irrigation of wheat. In *Herbicide Metabolites in Surface Water and Groundwater*, American Chemical Society: Washington, DC, 1996; Vol. 630, pp 151-164.
51. Yao, Y.; Tuduri, L.; Harner, T.; Blanchard, P.; Waite, D.; Poissant, L.; Murphy, C.; Belzer, W.; Aulagnier, F.; Li, Y.-F.; Sverko, E., Spatial and temporal distribution of pesticide air concentrations in Canadian agricultural regions. *Atmos. Environ.* **2006,** *40*, 4339-4351.
52. Donald, D. B.; Narine, P. G.; Lynne, Q.-A.; Kevin, C., Diffuse geographic distribution of herbicides in northern prairie wetlands. *Environ. Toxicol. Chem.* **2001,** *20*, 273-279.
53. Donald, D. B.; Cessna, A. J.; Sverko, E.; Glozier, N. E., Pesticides in surface drinking-water supplies of the northern Great Plains. *Environ. Health Perspect.* **2007,** *115*, 1183-1191.
54. Degenhardt, D.; Cessna, A. J.; Raina, R.; Farenhorst, A.; Pennock, D. J., Dissipation of six acid herbicides in water and sediment of two Canadian prairie wetlands. *Environ. Toxicol. Chem.* **2011,** *30*, 1982-1989.
55. Johnson, J.; Gray, J. *Surface Water Pesticide Monitoring and Assessment Project, 2010*; Pesticide Water Quality Program, North Dakota Department of Agriculture; Bismarck, ND, 2011.
56. Grue, C. E.; Tome, M. W.; Swanson, G. A.; Borthwick, S. M.; DeWeese, L. R., Agricultural chemicals and the quality of prairie-pothole wetlands for adult and juvenile waterfowl - What are the concerns? In *Proceedings of the National Symposium on Protection of Wetlands from Agricultural Impacts*, Stuber, P. J., Ed. U.S. Fish and Wildlife Service Biological Report 88(16): Washington, DC, 1988; pp 55-64.

57. Donald, D. B.; Syrgiannis, J.; Hunter, F.; Weiss, G., Agricultural pesticides threaten the ecological integrity of northern prairie wetlands. *Sci. Total Environ.* **1999,** *231*, 173-181.
58. Sura, S.; Waiser, M.; Tumber, V.; Lawrence, J. R.; Cessna, A. J.; Glozier, N., Effects of glyphosate and two herbicide mixtures on microbial communities in prairie wetland ecosystems: A mesocosm approach. *J. Environ. Qual.* **2012,** *41*, 732-743.
59. Sievert, S. M.; Kiene, R. P.; Schulz-Vogt, H. N., The sulfur cycle. *Oceanography* **2007,** *20*, 117-123.
60. Vairavamurthy, M. A.; Orr, W. L.; Manowitz, B., Geochemical transformations of sedimentary sulfur: An introduction. In *Geochemical Transformations of Sedimentary Sulfur*, Vairavamurthy, M. A.; Schoonen, M. A. A.; Eglinton, T. I.; Luther III, G. W.; Manowitz, B., Eds. American Chemical Society: Washington, DC, 1995; Vol. 612, pp 1-14.
61. Chen, K. Y.; Morris, J. C., Kinetics of oxidation of aqueous sulfide by oxygen. *Environ. Sci. Technol.* **1972,** *6*, 529-537.
62. Hoffmann, M. R., Kinetics and mechanism of oxidation of hydrogen sulfide by hydrogen peroxide in acidic solution. *Environ. Sci. Technol.* **1977,** *11*, 61-66.
63. Luther III, G. W.; Church, T. M., An overview of the environmental chemistry of sulphur in wetland systems. In *Sulphur Cycling on the Continents: Wetlands, Terrestrial Ecosystems, and Associated Water Bodies*, Howarth, R. W.; Stewart, J. W. B.; Ivanov, M. V., Eds. SCOPE, John Wiley & Sons, Inc.: Somerset, NJ, 1992; pp 125-142.
64. Vairavamurthy, M. A.; Manowitz, B.; Zhou, W.; Jeon, Y., Determination of hydrogen sulfide oxidation products by Sulfur *K*-edge X-ray absorption near-edge structure spectroscopy. In *Environmental Geochemistry of Sulfide Oxidation*, Alpers, C. N.; Blowes, D. W., Eds. American Chemical Society: Washington DC, 1994; Vol. 550, pp 412-430.
65. Giggenbach, W., Optical spectra and equilibrium distribution of polysulfide ions in aqueous solution at 20.deg. *Inorg. Chem.* **1972,** *11*, 1201-1207.
66. Shea, D.; Helz, G. R., The solubility of copper in sulfidic waters - sulfide and polysulfide complexes in equilibrium with covellite. *Geochim. Cosmochim. Acta* **1988,** *52*, 1815-1825.
67. Kamyshny, A.; Goifman, A.; Gun, J.; Rizkov, D.; Lev, O., Equilibrium distribution of polysulfide ions in aqueous solutions at 25 degrees C: A new approach for the study of polysulfides equilibria. *Environ. Sci. Technol.* **2004,** *38*, 6633-6644.
68. Gun, J.; Goifman, A.; Shkrob, I.; Kamyshny, A.; Ginzburg, B.; Hadas, O.; Dor, I.; Modestov, A. D.; Lev, O., Formation of polysulfides in an oxygen rich freshwater lake and their role in the production of volatile sulfur compounds in aquatic systems. *Environ. Sci. Technol.* **2000,** *34*, 4741-4746.
69. MacCrehan, W.; Shea, D., Temporal relationship of thiols to inorganic sulfur compounds in anoxic Chesapeake Bay sediment porewater. In *Geochemical Transformations of Sedimentary Sulfur*, Vairavamurthy, M. A.; Schoonen, M. A. A.; Eglinton, T. I.; Luther III, G. W.; Manowitz, B., Eds. American Chemical Society: Washington, DC, 1995; Vol. 612, pp 294-310.

70. Overmann, J.; Beatty, J. T.; Krouse, H. R.; Hall, K. J., The sulfur cycle in the chemocline of a meromictic salt lake. *Limnol. Oceanogr.* **1996,** *41*, 147-156.
71. Ciglenecki, I.; Kodba, Z.; Cosovic, B., Sulfur species in Rogoznica Lake. *Mar. Chem.* **1996,** *53*, 101-110.
72. Bura-Nakic, E.; Helz, G. R.; Ciglenecki, I.; Cosovic, B., Reduced sulfur species in a stratified seawater lake (Rogoznica Lake, Croatia); seasonal variations and argument for organic carriers of reactive sulfur. *Geochim. Cosmochim. Acta* **2009,** *73*, 3738-3751.
73. Boulegue, J.; Lord III, C. J.; Church, T. M., Sulfur speciation and associated trace metals (Fe, Cu) in the pore waters of Great Marsh, Delaware. *Geochim. Cosmochim. Acta* **1982,** *46*, 453-464.
74. Luther, G. W., III; Meyerson, A. L.; Rogers, K.; Hall, F., Tidal and seasonal variations of sulfate ion in a New Jersey marsh system. *Estuaries* **1982,** *5*, 189-196.
75. Morgan, B.; Burton, E. D.; Rate, A. W., Iron monosulfide enrichment and the presence of organosulfur in eutrophic estuarine sediments. *Chem. Geol.* **2012,** *296–297*, 119-130.
76. Stamper, D. M.; Traina, S. J.; Tuovinen, O. H., Anaerobic transformation of alachlor, propachlor, and metolachlor with sulfide. *J. Environ. Qual.* **1997,** *26*, 488-494.
77. Lippa, K. A.; Roberts, A. L., Nucleophilic aromatic substitution reactions of chloroazines with bisulfide (HS^-) and polysulfides (S_n^{2-}). *Environ. Sci. Technol.* **2002,** *36*, 2008-2018.
78. Wang, S.; Arnold, W. A., Abiotic reduction of dinitroaniline herbicides. *Water Res.* **2003,** *37*, 4191-4201.
79. Jans, U.; Miah, M. H., Reaction of chlorpyrifos-methyl in aqueous hydrogen sulfide/bisulfide solutions. *J. Agric. Food. Chem.* **2003,** *51*, 1956-1960.
80. Lippa, K. A.; Demel, S.; Lau, I. H.; Roberts, A. L., Kinetics and mechanism of the nucleophilic displacement reactions of chloroacetanilide herbicides: Investigation of α-substituent effects. *J. Agric. Food. Chem.* **2004,** *52*, 3010-3021.
81. Yang, W.; Gan, J. J.; Bondarenko, S.; Liu, W., Nucleophilic radical substitution reaction of triazine herbicides with polysulfides. *J. Agric. Food. Chem.* **2004,** *52*, 7051-7055.
82. Lippa, K. A.; Roberts, A. L., Correlation analyses for bimolecular nucleophilic substitution reactions of chloroacetanilide herbicides and their structural analogs with environmentally relevant nucleophiles. *Environ. Toxicol. Chem.* **2005,** *24*, 2401-2409.
83. Bondarenko, S.; Zheng, W.; Yates, S. R.; Gan, J., Dehalogenation of halogenated fumigants by polysulfide salts. *J. Agric. Food. Chem.* **2006,** *54*, 5503-5508.
84. Gan, J. Y., Enhanced degradation of chloroacetanilide herbicides by polysulfide salts. In *Proceedings of the 2006 USDA-CSREES National Water Quality Conference*, USDA-NIFA National Integrated Water Quality Program: Washington, DC, 2006.
85. Gan, Q.; Jans, U., Reaction of thiometon and disulfoton with reduced sulfur species in simulated natural environment. *J. Agric. Food. Chem.* **2006,** *54*, 7753-7760.
86. Gan, Q.; Singh, R. M.; Jans, U., Degradation of naled and dichlorvos promoted by reduced sulfur species in well-defined anoxic aqueous solutions. *Environ. Sci. Technol.* **2006,** *40*, 778-783.

87. Gan, Q.; Singh, R. M.; Wu, T.; Jans, U., Kinetics and mechanism of degradation of dichlorvos in aqueous solutions containing reduced sulfur species. *Environ. Sci. Technol.* **2006,** *40*, 5717-5723.
88. Guo, X.; Jans, U., Kinetics and mechanism of the degradation of methyl parathion in aqueous hydrogen sulfide solution: Investigation of natural organic matter effects. *Environ. Sci. Technol.* **2006,** *40*, 900-906.
89. Wu, T.; Gan, Q.; Jans, U., Nucleophilic substitution of phosphorothionate ester pesticides with bisulfide (HS^-) and polysulfides (S_n^{2-}). *Environ. Sci. Technol.* **2006,** *40*, 5428-5434.
90. Wu, T.; Jans, U., Nucleophilic substitution reactions of chlorpyrifos-methyl with sulfur species. *Environ. Sci. Technol.* **2006,** *40*, 784-790.
91. Zheng, W.; Yates, S. R.; Papiernik, S. K.; Guo, M.; Gan, J., Dechlorination of chloropicrin and 1,3-dichloropropene by hydrogen sulfide species: Redox and nucleophilic substitution reactions. *J. Agric. Food. Chem.* **2006,** *54*, 2280-2287.
92. Gan, Q.; Jans, U., Nucleophilic reactions of phorate and terbufos with reduced sulfur species under anoxic conditions. *J. Agric. Food. Chem.* **2007,** *55*, 3546-3554.
93. Miller, P. L.; Vasudevan, D.; Gschwend, P. M.; Roberts, A. L., Transformation of hexachloroethane in a sulfidic natural water. *Environ. Sci. Technol.* **1998,** *32*, 1269-1275.
94. Lippa, K. A. Reactions of chloro-*s*-triazine and chloroacetanilide agrochemicals with reduced sulfur nucleophiles. Ph.D. Dissertation, The Johns Hopkins University, Baltimore, MD, 2002.
95. Loch, A. R.; Lippa, K. A.; Carlson, D. L.; Chin, Y.-P.; Traina, S. J.; Roberts, A. L., Nucleophilic aliphatic substitution reactions of propachlor, alachlor, and metolachlor with bisulfide (HS^-) and polysulfides (S_n^{2-}). *Environ. Sci. Technol.* **2002,** *36*, 4065-4073.
96. Huckins, J. N.; Petty, J. D.; England, D. C., Distribution and impact of trifluralin, atrazine, and fonofos residues in microcosms simulating a northern prairie wetland. *Chemosphere* **1986,** *15*, 563-588.
97. Cessna, A. J.; Donald, D. B.; Bailey, J.; Waiser, M.; Headley, J. V., Persistence of the sulfonylurea herbicides thifensulfuron-methyl, ethametsulfuron-methyl, and metsulfuron-methyl in farm dugouts (ponds). *J. Environ. Qual.* **2006,** *35*, 2395-2401.
98. Degenhardt, D.; Humphries, D.; Cessna, A. J.; Messing, P.; Badiou, P. H.; Raina, R.; Farenhorst, A.; Pennock, D. J., Dissipation of glyphosate and aminomethylphosphonic acid in water and sediment of two Canadian prairie wetlands. *J. Environ. Sci. Health, Part B* **2012,** *47*, 631-639.
99. Anslyn, E. V.; Dougherty, D. A., *Modern Physical Organic Chemistry*. University Science Books: Sausalito, CA, 2006.
100. Schwarzenbach, R. P.; Gschwend, P. M.; Imboden, D. M., *Environmental Organic Chemistry*. John Wiley & Sons, Inc.: Hoboken, NJ, 2003.
101. Leifer, A., *The Kinetics of Environmental Aquatic Photochemistry: Theory and Practice*. American Chemical Society: Washington, DC, 1988.
102. Larson, R. A.; Weber, E. J., *Reaction Mechanisms in Environmental Organic Chemistry*. CRC Press, Inc.: Boca Raton, FL, 1994.
103. Zepp, R. G.; Cline, D. M., Rates of direct photolysis in aquatic environment. *Environ. Sci. Technol.* **1977,** *11*, 359-366.

104. Arnold, W. A.; McNeill, K.; Petrovic, M.; Barcel, D., Transformation of pharmaceuticals in the environment: Photolysis and other abiotic processes. In *Comprehensive Analytical Chemistry*, Elsevier: 2007; Vol. Volume 50, pp 361-385.
105. Vione, D.; Maurino, V.; Minero, C.; Pelizzetti, E., Reactions induced in natural waters by irradiation of nitrate and nitrite ions. In *The Handbook of Environmental Chemistry Vol. 2-M (Environmental Photochemistry Part II)*, Boule, P.; Bahnemann, D. W.; Robertson, P. K. J., Eds. Springer: Berlin, Germany, 2005; pp 221-253.
106. Chiron, S.; Barcel ó, D.; Abian, J.; Ferrer, M.; Sanchez-Baeza, F.; Messeguer, A., Comparative photodegradation rates of alachlor and bentazone in natural water and determination of breakdown products. *Environ. Toxicol. Chem.* **1995,** *14*, 1287-1298.
107. Dimou, A. D.; Sakkas, V. A.; Albanis, T. A., Trifluralin photolysis in natural waters and under the presence of isolated organic matter and nitrate ions: Kinetics and photoproduct analysis. *J. Photochem. Photobiol. A: Chem.* **2004,** *163*, 473-480.
108. Fasnacht, M. P.; Blough, N. V., Aqueous photodegradation of polycyclic aromatic hydrocarbons. *Environ. Sci. Technol.* **2002,** *36*, 4364-4369.
109. Fasnacht, M. P.; Blough, N. V., Mechanisms of the aqueous photodegradation of polycyclic aromatic hydrocarbons. *Environ. Sci. Technol.* **2003,** *37*, 5767-5772.
110. Fasnacht, M. P.; Blough, N. V., Kinetic analysis of the photodegradation of polycyclic aromatic hydrocarbons in aqueous solution. *Aquat. Sci.* **2003,** *65*, 352-358.
111. Jacobs, L. E.; Weavers, L. K.; Chin, Y. P., Direct and indirect photolysis of polycyclic aromatic hydrocarbons in nitrate-rich surface waters. *Environ. Toxicol. Chem.* **2008,** *27*, 1643-1648.
112. Plumlee, M. H.; Reinhard, M., Photochemical attenuation of *N*-nitrosodimethylamine (NDMA) and other nitrosamines in surface water. *Environ. Sci. Technol.* **2007,** *41*, 6170-6176.
113. Kelly, M. M.; Arnold, W. A., Direct and indirect photolysis of the phytoestrogens genistein and daidzein. *Environ. Sci. Technol.* **2012,** *46*, 5396-5403.
114. Felcyn, J. R.; Davis, J. C. C.; Tran, L. H.; Berude, J. C.; Latch, D. E., Aquatic photochemistry of isoflavone phytoestrogens: Degradation kinetics and pathways. *Environ. Sci. Technol.* **2012,** *46*, 6698-6704.
115. West, C. E.; Rowland, S. J., Aqueous phototransformation of diazepam and related human metabolites under simulated sunlight. *Environ. Sci. Technol.* **2012,** *46*, 4749-4756.
116. Boreen, A. L.; Arnold, W. A.; McNeill, K., Photochemical fate of sulfa drugs in the aquatic environment: Sulfa drugs containing five-membered heterocyclic groups. *Environ. Sci. Technol.* **2004,** *38*, 3933-3940.
117. Edhlund, B. L.; Arnold, W. A.; McNeill, K., Aquatic photochemistry of nitrofuran antibiotics. *Environ. Sci. Technol.* **2006,** *40*, 5422-5427.
118. Ge, L.; Chen, J.; Wei, X.; Zhang, S.; Qiao, X.; Cai, X.; Xie, Q., Aquatic photochemistry of fluoroquinolone antibiotics: Kinetics, pathways, and multivariate effects of main water constituents. *Environ. Sci. Technol.* **2010,** *44*, 2400-2405.
119. Ryan, C. C.; Tan, D. T.; Arnold, W. A., Direct and indirect photolysis of sulfamethoxazole and trimethoprim in wastewater treatment plant effluent. *Water Res.* **2011,** *45*, 1280-1286.

120. Gonçalves, C.; Pérez, S.; Osorio, V.; Petrovic, M.; Alpendurada, M. F.; Barceló, D., Photofate of oseltamivir (Tamiflu) and oseltamivir carboxylate under natural and simulated solar irradiation: Kinetics, identification of the transformation products, and environmental occurrence. *Environ. Sci. Technol.* **2011,** *45*, 4307-4314.
121. Latch, D. E.; Stender, B. L.; Packer, J. L.; Arnold, W. A.; McNeill, K., Photochemical fate of pharmaceuticals in the environment: Cimetidine and ranitidine. *Environ. Sci. Technol.* **2003,** *37*, 3342-3350.
122. Packer, J. L.; Werner, J. J.; Latch, D. E.; McNeill, K.; Arnold, W. A., Photochemical fate of pharmaceuticals in the environment: Naproxen, diclofenac, clofibric acid, and ibuprofen. *Aquatic Sciences - Research Across Boundaries* **2003,** *65*, 342-351.
123. Werner, J. J.; McNeill, K.; Arnold, W. A., Environmental photodegradation of mefenamic acid. *Chemosphere* **2005,** *58*, 1339-1346.
124. Lin, A. Y. C.; Reinhard, M., Photodegradation of common environmental pharmaceuticals and estrogens in river water. *Environ. Toxicol. Chem.* **2005,** *24*, 1303-1309.
125. Liu, Q.-T.; Williams, H. E., Kinetics and degradation products for direct photolysis of β-blockers in water. *Environ. Sci. Technol.* **2007,** *41*, 803-810.
126. Tixier, C.; Singer, H. P.; Canonica, S.; Müller, S. R., Phototransformation of triclosan in surface waters: A relevant elimination process for this widely used biocide - Laboratory studies, field measurements, and modeling. *Environ. Sci. Technol.* **2002,** *36*, 3482-3489.
127. Latch, D. E.; Packer, J. L.; Arnold, W. A.; McNeill, K., Photochemical conversion of triclosan to 2,8-dichlorodibenzo-p-dioxin in aqueous solution. *J. Photochem. Photobiol. A: Chem.* **2003,** *158*, 63-66.
128. Buth, J. M.; Grandbois, M.; Vikesland, P. J.; McNeill, K.; Arnold, W. A., Aquatic photochemistry of chlorinated triclosan derivatives: Potential source of polychlorodibenzo-P-dioxins. *Environ. Toxicol. Chem.* **2009,** *28*, 2555-2563.
129. Zhang, S.; Chen, J.; Qiao, X.; Ge, L.; Cai, X.; Na, G., Quantum chemical investigation and experimental verification on the aquatic photochemistry of the sunscreen 2-phenylbenzimidazole-5-sulfonic acid. *Environ. Sci. Technol.* **2010,** *44*, 7484-7490.
130. MacManus-Spencer, L. A.; Tse, M. L.; Klein, J. L.; Kracunas, A. E., Aqueous photolysis of the organic ultraviolet filter chemical octyl methoxycinnamate. *Environ. Sci. Technol.* **2011,** *45*, 3931-3937.
131. Hoigné, J.; Faust, B. C.; Haag, W. R.; Scully, F. E.; Zepp, R. G., Aquatic humic substances as sources and sinks of photochemically produced transient reactants. In *Aquatic Humic Substances*, Suffet, I. H.; MacCarthy, P., Eds. American Chemical Society: Washington DC, 1989; Vol. 219, pp 363-381.
132. Cooper, W. J.; Zika, R. G.; Petasne, R. G.; Fischer, A. M., Sunlight-induced photochemistry of humic substances in natural waters: Major reactive species. In *Aquatic Humic Substances*, Suffet, I. H.; MacCarthy, P., Eds. American Chemical Society: Washington DC, 1989; Vol. 219, pp 333-362.

133. Zepp, R. G.; Wolfe, N. L.; Baughman, G. L.; Hollis, R. C., Singlet oxygen in natural waters. *Nature* **1977,** *267*, 421-423.
134. Mill, T.; Hendry, D. G.; Richardson, H., Free-radical oxidants in natural waters. *Science* **1980,** *207*, 886-887.
135. Zepp, R. G.; Baughman, G. L.; Schlotzhauer, P. F., Comparison of photochemical behavior of various humic substances in water: II. Photosensitized oxygenations. *Chemosphere* **1981,** *10*, 119-126.
136. Cooper, W. J.; Zika, R. G., Photochemical formation of hydrogen peroxide in surface and ground waters exposed to sunlight. *Science* **1983,** *220*, 711-712.
137. Draper, W. M.; Crosby, D. G., The photochemical generation of hydrogen peroxide in natural waters. *Arch. Environ. Contam. Toxicol.* **1983,** *12*, 121-126.
138. Baxter, R. M.; Carey, J. H., Evidence for photochemical generation of superoxide ion in humic waters. *Nature* **1983,** *306*, 575-576.
139. Zepp, R. G.; Schlotzhauer, P. F.; Sink, R. M., Photosensitized transformations involving electronic energy transfer in natural waters: role of humic substances. *Environ. Sci. Technol.* **1985,** *19*, 74-81.
140. Haag, W. R.; Hoigné, J., Photo-sensitized oxidation in natural water via $^{\bullet}OH$ radicals. *Chemosphere* **1985,** *14*, 1659-1671.
141. Haag, W. R.; Hoigné, J., Singlet oxygen in surface waters. 3. Photochemical formation and steady-state concentrations in various types of waters. *Environ. Sci. Technol.* **1986,** *20*, 341-348.
142. Mopper, K.; Zhou, X., Hydroxyl radical photoproduction in the sea and its potential impact on marine processes. *Science* **1990,** *250*, 661-664.
143. Mill, T., Predicting photoreaction rates in surface waters. *Chemosphere* **1999,** *38*, 1379-1390.
144. Fischer, A. M.; Kliger, D. S.; Winterle, J. S.; Mill, T., Direct observation of phototransients in natural waters. *Chemosphere* **1985,** *14*, 1299-1306.
145. Zepp, R. G.; Braun, A. M.; Hoigne, J.; Leenheer, J. A., Photoproduction of hydrated electrons from natural organic solutes in aquatic environments. *Environ. Sci. Technol.* **1987,** *21*, 485-490.
146. Thomas-Smith, T. E.; Blough, N. V., Photoproduction of hydrated electron from constituents of natural waters. *Environ. Sci. Technol.* **2001,** *35*, 2721-2726.
147. Wang, W.; Zafiriou, O. C.; Chan, I.-Y.; Zepp, R. G.; Blough, N. V., Production of hydrated electrons from photoionization of dissolved organic matter in natural waters. *Environ. Sci. Technol.* **2007,** *41*, 1601-1607.
148. Lam, M. W.; Tantuco, K.; Mabury, S. A., PhotoFate: A new approach in accounting for the contribution of indirect photolysis of pesticides and pharmaceuticals in surface waters. *Environ. Sci. Technol.* **2003,** *37*, 899-907.
149. Kochany, J.; Maguire, R. J., Sunlight photodegradation of metolachlor in water. *J. Agric. Food. Chem.* **1994,** *42*, 406-412.
150. Torrents, A.; Anderson, B. G.; Bilboulian, S.; Johnson, W. E.; Hapeman, C. J., Atrazine photolysis: Mechanistic investigations of direct and nitrate-mediated hydroxy radical processes and the influence of dissolved organic carbon from the Chesapeake Bay. *Environ. Sci. Technol.* **1997,** *31*, 1476-1482.

151. Miller, P. L.; Chin, Y.-P., Photoinduced degradation of carbaryl in a wetland surface water. *J. Agric. Food. Chem.* **2002,** *50*, 6758-6765.
152. Schulz, R.; Hahn, C.; Bennett, E. R.; Dabrowski, J. M.; Thiere, G.; Peall, S. K. C., Fate and effects of azinphos-methyl in a flow-through wetland in South Africa. *Environ. Sci. Technol.* **2003,** *37*, 2139-2144.
153. Miller, P. L.; Chin, Y.-P., Indirect photolysis promoted by natural and engineered wetland water constituents: Processes leading to alachlor degradation. *Environ. Sci. Technol.* **2005,** *39*, 4454-4462.
154. Hedges, J. I.; Oades, J. M., Comparative organic geochemistries of soils and marine sediments. *Org. Geochem.* **1997,** *27*, 319-361.
155. Goldhaber, M. B., Sulfur-rich sediments. In *Treatise on Geochemistry - Sediments, Diagenesis, and Sedimentary Rocks*, Mackenzie, F. T., Ed. Elsevier Ltd.: Oxford, UK, 2003; Vol. 7, pp 257-288.
156. Urban, N. R., Retention of sulfur in lake sediments. In *Environmental Chemistry of Lakes and Reservoirs*, Baker, L. A., Ed. American Chemical Society: Washington, DC, 1994; Vol. 237, pp 323-369.
157. Freney, J., Some observations on the nature of organic sulphur compounds in soil. *Aust. J. Agric. Res.* **1961,** *12*, 424-432.
158. Pruden, G.; Bloomfield, C., The determination of iron(II) sulphide in soil in the presence of iron(III) oxide. *Analyst* **1968,** *93*, 532-534.
159. Freney, J. R.; Melville, G. E.; Williams, C. H., The determination of carbon bonded sulfur in soil. *Soil Sci.* **1970,** *109*, 310-318.
160. Dick, W. A.; Tabatabai, M. A., Ion chromatographic determination of sulfate and nitrate in soils. *Soil Sci. Soc. Am. J.* **1979,** *43*, 899-904.
161. Canfield, D. E.; Raiswell, R.; Westrich, J. T.; Reaves, C. M.; Berner, R. A., The use of chromium reduction in the analysis of reduced inorganic sulfur in sediments and shales. *Chem. Geol.* **1986,** *54*, 149-155.
162. Berner, R. A., Iron sulfides formed from aqueous solution at low temperatures and atmospheric pressure. *J. Geol. (Chicago, IL, U. S.)* **1964,** *72*, 293-306.
163. Rickard, D.; Morse, J. W., Acid volatile sulfide (AVS). *Mar. Chem.* **2005,** *97*, 141-197.
164. Prietzel, J.; Thieme, J.; Neuhäusler, U.; Susini, J.; Kögel-Knabner, I., Speciation of sulphur in soils and soil particles by X-ray spectromicroscopy. *Eur. J. Soil Sci.* **2003,** *54*, 423-433.
165. Vairavamurthy, M. A.; Zhou, W.; Eglinton, T.; Manowitz, B., Sulfonates: A novel class of organic sulfur compounds in marine sediments. *Geochim. Cosmochim. Acta* **1994,** *58*, 4681-4687.
166. Vairavamurthy, M. A.; Wang, S.; Khandelwal, B.; Manowitz, B.; Ferdelman, T.; Fossing, H., Sulfur transformations in early diagenetic sediments from the Bay of Conception, off Chile. In *Geochemical Transformations of Sedimentary Sulfur*, Vairavamurthy, M. A.; Schoonen, M. A. A.; Eglinton, T. I.; Luther III, G. W.; Manowitz, B., Eds. American Chemical Society: Washington, DC, 1995; Vol. 612, pp 38-58.

167. Bostick, B. C.; Theissen, K. M.; Dunbar, R. B.; Vairavamurthy, M. A., Record of redox status in laminated sediments from Lake Titicaca: A sulfur *K*-edge X-ray absorption near edge structure (XANES) study. *Chem. Geol.* **2005,** *219*, 163-174.
168. Burton, E. D.; Bush, R. T.; Sullivan, L. A.; Hocking, R. K.; Mitchell, D. R. G.; Johnston, S. G.; Fitzpatrick, R. W.; Raven, M.; McClure, S.; Jang, L. Y., Iron-monosulfide oxidation in natural sediments: Resolving microbially mediated S transformations using XANES, electron microscopy, and selective extractions. *Environ. Sci. Technol.* **2009,** *43*, 3128-3134.
169. Burton, E. D.; Bush, R. T.; Johnston, S. G.; Sullivan, L. A.; Keene, A. F., Sulfur biogeochemical cycling and novel Fe–S mineralization pathways in a tidally re-flooded wetland. *Geochim. Cosmochim. Acta* **2011,** *75*, 3434-3451.
170. Jokic, A.; Cutler, J. N.; Ponomarenko, E.; van der Kamp, G.; Anderson, D. W., Organic carbon and sulphur compounds in wetland soils: Insights on structure and transformation processes using *K*-edge XANES and NMR spectroscopy. *Geochim. Cosmochim. Acta* **2003,** *67*, 2585-2597.
171. Solomon, D.; Lehmann, J.; Lobe, I.; Martinez, C. E.; Tveitnes, S.; Du Preez, C. C.; Amelung, W., Sulphur speciation and biogeochemical cycling in long-term arable cropping of subtropical soils: evidence from wet-chemical reduction and S *K*-edge XANES spectroscopy. *Eur. J. Soil Sci.* **2005,** *56*, 621-634.
172. Prietzel, J.; Thieme, J.; Tyufekchieva, N.; Paterson, D.; McNulty, I.; Kögel-Knabner, I., Sulfur speciation in well-aerated and wetland soils in a forested catchment assessed by sulfur *K*-edge X-ray absorption near-edge spectroscopy (XANES). *J. Plant Nutr. Soil Sci.* **2009,** *172*, 393-403.
173. Prietzel, J.; Botzaki, A.; Tyufekchieva, N.; Brettholle, M.; Thieme, J. r.; Klysubun, W., Sulfur speciation in soil by S *K*-edge XANES spectroscopy: Comparison of spectral deconvolution and linear combination fitting. *Environ. Sci. Technol.* **2011,** *45*, 2878-2886.
174. Prietzel, J.; Kögel-Knabner, I.; Thieme, J.; Paterson, D.; McNulty, I., Microheterogeneity of element distribution and sulfur speciation in an organic surface horizon of a forested Histosol as revealed by synchrotron-based X-ray spectromicroscopy. *Org. Geochem.* **2011,** *42*, 1308-1314.
175. Solomon, D.; Lehmann, J.; de Zarruk, K. K.; Dathe, J.; Kinyangi, J.; Liang, B.; Machado, S., Speciation and long- and short-term molecular-level dynamics of soil organic sulfur studied by X-ray absorption near-edge structure spectroscopy. *J. Environ. Qual.* **2011,** *40*, 704-718.
176. Boye, K.; Almkvist, G.; Nilsson, S. I.; Eriksen, J.; Persson, I., Quantification of chemical sulphur species in bulk soil and organic sulphur fractions by S K-edge XANES spectroscopy. *Eur. J. Soil Sci.* **2011,** *62*, 874-881.
177. Pickering, I. J.; Prince, R. C.; Divers, T.; George, G. N., Sulfur K-edge X-ray absorption spectroscopy for determining the chemical speciation of sulfur in biological systems. *FEBS Lett.* **1998,** *441*, 11-14.
178. Rompel, A.; Cinco, R. M.; Latimer, M. J.; McDermott, A. E.; Guiles, R. D.; Quintanilha, A.; Krauss, R. M.; Sauer, K.; Yachandra, V. K.; Klein, M. P., Sulfur K-edge

x-ray absorption spectroscopy: A spectroscopic tool to examine the redox state of S-containing metabolites in vivo. *Proc. Natl. Acad. Sci. U. S. A.* **1998,** *95*, 6122-6127.
179. Breier, J. A.; Toner, B. M.; Fakra, S. C.; Marcus, M. A.; White, S. N.; Thurnherr, A. M.; German, C. R., Sulfur, sulfides, oxides and organic matter aggregated in submarine hydrothermal plumes at 9° 50′ N East Pacific Rise. *Geochim. Cosmochim. Acta* **2012,** *88*, 216-236.
180. Lombi, E.; Hettiarachchi, G. M.; Scheckel, K. G., Advanced in situ spectroscopic techniques and their applications in Environmental Biogeochemistry: Introduction to the special section. *J. Environ. Qual.* **2011,** *40*, 659-666.
181. Lombi, E.; Susini, J., Synchrotron-based techniques for plant and soil science: Opportunities, challenges and future perspectives. *Plant Soil* **2009,** *320*, 1-35.
182. Orthous-Daunay, F. R.; Quirico, E.; Lemelle, L.; Beck, P.; deAndrade, V.; Simionovici, A.; Derenne, S., Speciation of sulfur in the insoluble organic matter from carbonaceous chondrites by XANES spectroscopy. *Earth. Planet. Sci. Lett.* **2010,** *300*, 321-328.
183. Almkvist, G.; Boye, K.; Persson, I., *K*-edge XANES analysis of sulfur compounds: An investigation of the relative intensities using internal calibration. *J. Synchrotron Radiat.* **2010,** *17*, 683-688.
184. Beauchemin, S.; Hesterberg, D.; Beauchemin, M., Principal component analysis approach for modeling sulfur *K*-XANES spectra of humic acids. *Soil Sci. Soc. Am. J.* **2002,** *66*, 83-91.
185. Vairavamurthy, M. A.; Maletic, D.; Wang, S.; Manowitz, B.; Eglinton, T.; Lyons, T., Characterization of sulfur-containing functional groups in sedimentary humic substances by X-ray absorption near-edge structure spectroscopy. *Energy Fuels* **1997,** *11*, 546-553.
186. Mushet, D. M.; Euliss, N. H. *The Cottonwood Lake study area, a long-term wetland ecosystem monitoring site*; U.S. Geological Survey Fact Sheet 2012-3040: Reston, VA 2012; pp 1-2.

Chapter 2 References

1. van der Valk, A. G., The prairie potholes of North America. In *The World's Largest Wetlands*, Fraser, L. H.; Keddy, P. A., Eds. Cambridge University Press: Cambridge, UK, 2005; pp 393-423.
2. Kantrud, H. A.; Krapu, G. L.; Swanson, G. A. *Prairie basin wetlands of the Dakotas: A community profile*; U.S. Fish and Wildlife Service, Biological Report 85: Washington, DC, 1989; pp 1-111.
3. Gleason, R. A.; Euliss, N. H.; Tangen, B. A.; Laubhan, M. K.; Browne, B. A., USDA conservation program and practice effects on wetland ecosystem services in the Prairie Pothole Region. *Ecol. Appl.* **2011,** *21*, S65-S81.
4. Johnson, R. R.; Oslund, F. T.; Hertel, D. R., The past, present, and future of prairie potholes in the United States. *J. Soil Water Conserv.* **2008,** *63*, 84A-87A.
5. U.S. Department of Agriculture, National Agricultural Statistical Services. *2009 State Agriculture Overview - North Dakota*; http://www.nass.usda.gov/Statistics_by_State/Ag_Overview/AgOverview_ND.pdf (Accessed February, 2011).
6. U.S. Department of Agriculture, National Agricultural Statistical Services. *Agricultural Chemical Usage - Field Crops*; http://usda.mannlib.cornell.edu/MannUsda/viewDocumentInfo.do?documentID=1560 (Accessed February, 2011).
7. Grue, C. E.; DeWeese, L. R.; Mineau, P.; Swanson, G. A.; Foster, J. R.; Arnold, P. M.; Huckins, J. N.; Sheehan, P. L.; Marshall, W. K.; Ludden, A. P., Potential impacts of agricultural chemicals on waterfowl and other wildlife inhabiting prairie wetlands: An evaluation of research needs and approaches. In *Transactions North American Wildlife and Natural Resources Conference*, McCabe, R. E., Ed. Wildlife Management Institute: Washington, DC, 1986; Vol. 51, pp 357-383.
8. Goldsborough, L. G.; Crumpton, W. G., Distribution and environmental fate of pesticides in prairie wetlands. *Great Plains Res.* **1998,** *8*, 73-95.
9. Olness, A.; Staricka, J. A.; Daniel, J. A., Oxidation-reduction and groundwater contamination in the Prairie Pothole region of the Northern Great Plains. In *Water for Agriculture and Wildlife and the Environment -- Win-Win Opportunities: Proceedings of the 1996 USCID Wetlands Seminar*, Schaack, J.; Anderson, S. S., Eds. U.S. Committee on Irrigation and Drainage: Denver, CO, 1996; pp 115-131.
10. Detenbeck, N. E.; Elonen, C. M.; Taylor, D. L.; Cotter, A. M.; Puglisi, F. A.; Sanville, W. D., Effects of agricultural activities and best management practices on water quality of seasonal prairie pothole wetlands. *Wetlands Ecol. Manage.* **2002,** *10*, 335-354.
11. Grue, C. E.; Tome, M. W.; Swanson, G. A.; Borthwick, S. M.; DeWeese, L. R., Agricultural chemicals and the quality of prairie-pothole wetlands for adult and juvenile waterfowl - What are the concerns? In *Proceedings of the National Symposium on Protection of Wetlands from Agricultural Impacts*, Stuber, P. J., Ed. U.S. Fish and Wildlife Service Biological Report 88(16): Washington, DC, 1988; pp 55-64.

12. Donald, D. B.; Syrgiannis, J.; Hunter, F.; Weiss, G., Agricultural pesticides threaten the ecological integrity of northern prairie wetlands. *Sci. Total Environ.* **1999,** *231*, 173-181.
13. Wolf, T. M.; Cessna, A. J., Protecting aquatic and riparian areas from pesticide drift. In *International Conference on Pesticide Application for Drift Management*, Washington State University Press: Pullman, WA 2004; pp 59-71.
14. Sura, S.; Waiser, M.; Tumber, V.; Lawrence, J. R.; Cessna, A. J.; Glozier, N., Effects of glyphosate and two herbicide mixtures on microbial communities in prairie wetland ecosystems: A mesocosm approach. *J. Environ. Qual.* **2012,** *41*, 732-743.
15. Huckins, J. N.; Petty, J. D.; England, D. C., Distribution and impact of trifluralin, atrazine, and fonofos residues in microcosms simulating a northern prairie wetland. *Chemosphere* **1986,** *15*, 563-588.
16. Cessna, A. J.; Donald, D. B.; Bailey, J.; Waiser, M.; Headley, J. V., Persistence of the sulfonylurea herbicides thifensulfuron-methyl, ethametsulfuron-methyl, and metsulfuron-methyl in farm dugouts (ponds). *J. Environ. Qual.* **2006,** *35*, 2395-2401.
17. Degenhardt, D.; Cessna, A. J.; Raina, R.; Farenhorst, A.; Pennock, D. J., Dissipation of six acid herbicides in water and sediment of two Canadian prairie wetlands. *Environ. Toxicol. Chem.* **2011,** *30*, 1982-1989.
18. Degenhardt, D.; Humphries, D.; Cessna, A. J.; Messing, P.; Badiou, P. H.; Raina, R.; Farenhorst, A.; Pennock, D. J., Dissipation of glyphosate and aminomethylphosphonic acid in water and sediment of two Canadian prairie wetlands. *J. Environ. Sci. Health, Part B* **2012,** *47*, 631-639.
19. Driver, E. A.; Peden, D. G., The chemistry of surface water in prairie ponds. *Hydrobiologia* **1977,** *53*, 33-48.
20. LaBaugh, J. W., Chemical characteristics of water in northern prairie wetlands. In *Northern Prairie Wetlands*, Van der Valk, A. G., Ed. Iowa State University Press: Ames, IA, 1989; pp 56-90.
21. Hall, B. D.; Baron, L. A.; Somers, C. M., Mercury concentrations in surface water and harvested waterfowl from the prairie pothole region of Saskatchewan. *Environ. Sci. Technol.* **2009,** *43*, 8759-8766.
22. Bates, L. M.; Hall, B. D., Concentrations of methylmercury in invertebrates from wetlands of the Prairie Pothole Region of North America. *Environ. Pollut.* **2012,** *160*, 153-160.
23. Grossman, I. G. Origin of the sodium sulfate deposits of the northern Great Plains of Canada and the United States. U.S. Geological Survey Professional Paper 600-B: Denver, CO, 1968; pp B104-B109.
24. Lemke, R. W. Geology of the Souris River area, North Dakota. U.S. Geological Survey Professional Paper 325: Denver, CO, 1960.
25. Goldhaber, M. B.; Mills, C. T.; Stricker, C. A.; Morrison, J. M., The role of critical zone processes in the evolution of the Prairie Pothole Region wetlands. *Appl. Geochem.* **2011,** *26, Supplement*, S32-S35.
26. Mills, C. T.; Goldhaber, M. B.; Stricker, C. A.; Holloway, J. M.; Morrison, J. M.; Ellefsen, K. J.; Rosenberry, D. O.; Thurston, R. S., Using stable isotopes to understand

hydrochemical processes in and around a Prairie Pothole wetland in the Northern Great Plains, USA. *Appl. Geochem.* **2011,** *26, Supplement*, S97-S100.
27. Sloan, C. E. *Ground-water hydrology of prairie potholes in North Dakota. U.S. Geological Survey Professional Paper 585-C*; Department of the Interior: Denver, CO, 1972.
28. MacCrehan, W.; Shea, D., Temporal relationship of thiols to inorganic sulfur compounds in anoxic Chesapeake Bay sediment porewater. In *Geochemical Transformations of Sedimentary Sulfur*, Vairavamurthy, M. A.; Schoonen, M. A. A.; Eglinton, T. I.; Luther III, G. W.; Manowitz, B., Eds. American Chemical Society: Washington, DC, 1995; Vol. 612, pp 294-310.
29. Boulegue, J.; Lord III, C. J.; Church, T. M., Sulfur speciation and associated trace metals (Fe, Cu) in the pore waters of Great Marsh, Delaware. *Geochim. Cosmochim. Acta* **1982,** *46*, 453-464.
30. Morgan, B.; Burton, E. D.; Rate, A. W., Iron monosulfide enrichment and the presence of organosulfur in eutrophic estuarine sediments. *Chem. Geol.* **2012,** *296–297*, 119-130.
31. Vairavamurthy, M. A.; Orr, W. L.; Manowitz, B., Geochemical transformations of sedimentary sulfur: An introduction. In *Geochemical Transformations of Sedimentary Sulfur*, Vairavamurthy, M. A.; Schoonen, M. A. A.; Eglinton, T. I.; Luther III, G. W.; Manowitz, B., Eds. American Chemical Society: Washington, DC, 1995; Vol. 612, pp 1-14.
32. Barbash, J. E.; Reinhard, M., Reactivity of sulfur nucleophiles toward halogenated organic compounds in natural waters. In *Biogenic Sulfur in the Environment*, Saltzman, E. S.; Cooper, W. J., Eds. American Chemical Society: Washington, DC, 1989; Vol. 393, pp 101-138.
33. Miller, P. L.; Vasudevan, D.; Gschwend, P. M.; Roberts, A. L., Transformation of hexachloroethane in a sulfidic natural water. *Environ. Sci. Technol.* **1998,** *32*, 1269-1275.
34. Haag, W. R.; Mill, T., Some reactions of naturally occurring nucleophiles with haloalkanes in water. *Environ. Toxicol. Chem.* **1988,** *7*, 917-924.
35. Roberts, A. L.; Sanborn, P. N.; Gschwend, P. M., Nucleophilic substitution reactions of dihalomethanes with hydrogen sulfide species. *Environ. Sci. Technol.* **1992,** *26*, 2263-2274.
36. Perlinger, J. A.; Angst, W.; Schwarzenbach, R. P., Kinetics of the reduction of hexachloroethane by juglone in solutions containing hydrogen sulfide. *Environ. Sci. Technol.* **1996,** *30*, 3408-3417.
37. Lippa, K. A.; Roberts, A. L., Nucleophilic aromatic substitution reactions of chloroazines with bisulfide (HS^-) and polysulfides (S_n^{2-}). *Environ. Sci. Technol.* **2002,** *36*, 2008-2018.
38. Loch, A. R.; Lippa, K. A.; Carlson, D. L.; Chin, Y.-P.; Traina, S. J.; Roberts, A. L., Nucleophilic aliphatic substitution reactions of propachlor, alachlor, and metolachlor with bisulfide (HS^-) and polysulfides (S_n^{2-}). *Environ. Sci. Technol.* **2002,** *36*, 4065-4073.
39. Wang, S.; Arnold, W. A., Abiotic reduction of dinitroaniline herbicides. *Water Res.* **2003,** *37*, 4191-4201.

40. Gan, Q.; Singh, R. M.; Jans, U., Degradation of naled and dichlorvos promoted by reduced sulfur species in well-defined anoxic aqueous solutions. *Environ. Sci. Technol.* **2006,** *40*, 778-783.
41. Wu, T.; Gan, Q.; Jans, U., Nucleophilic substitution of phosphorothionate ester pesticides with bisulfide (HS^-) and polysulfides (S_n^{2-}). *Environ. Sci. Technol.* **2006,** *40*, 5428-5434.
42. U.S. Geological Survey, Pesticide National Synthesis Project. *2002 Pesticide Use Maps*; http://water.usgs.gov/nawqa/pnsp/usage/maps/compound_listing.php?year=02 (Accessed August, 2011).
43. Stamper, D. M.; Traina, S. J.; Tuovinen, O. H., Anaerobic transformation of alachlor, propachlor, and metolachlor with sulfide. *J. Environ. Qual.* **1997,** *26*, 488-494.
44. Zaugg, S. D.; Sandstrom, M. W.; Smith, S. G.; Fehlberg, K. M. *Methods of analysis by the U.S. Geological Survey National Water Quality Laboratory - Determination of pesticides in water by C-18 solid-phase extraction and capillary-column gas chromatography/mass spectrometry with selected-ion monitoring*; U.S. Geological Survey Open-File Report 95-181: Denver, CO, 1995.
45. Winter, T. C.; Rosenberry, D. O., Hydrology of prairie pothole wetlands during drought and deluge: A 17-year study of the cottonwood lake wetland complex in North Dakota in the perspective of longer term measured and proxy hydrological records. *Clim. Change* **1998,** *40*, 189-209.
46. Hakala, J. A.; Fimmen, R. L.; Chin, Y.-P.; Agrawal, S. G.; Ward, C. P., Assessment of the geochemical reactivity of Fe-DOM complexes in wetland sediment pore waters using a nitroaromatic probe compound. *Geochim. Cosmochim. Acta* **2009,** *73*, 1382-1393.
47. Cline, J. D., Spectrophotometric determination of hydrogen sulfide in natural waters. *Limnol. Oceanogr.* **1969,** *14*, 454-458.
48. Shea, D.; Helz, G. R., The solubility of copper in sulfidic waters - sulfide and polysulfide complexes in equilibrium with covellite. *Geochim. Cosmochim. Acta* **1988,** *52*, 1815-1825.
49. Russell, L. L. Chemical aspects of ground water recharge with treated wastewater Ph.D. Dissertation, University of California, Berkeley, Berkeley, CA, 1976.
50. Mylon, S. E.; Benoit, G., Subnanomolar detection of acid-labile sulfides by the classical methylene blue method coupled to HPLC. *Environ. Sci. Technol.* **2001,** *35*, 4544-4548.
51. Bowles, K. C.; Ernste, M. J.; Kramer, J. R., Trace sulfide determination in oxic freshwaters. *Anal. Chim. Acta* **2003,** *477*, 113-124.
52. Luther III, G. W.; Giblin, A. E.; Varsolona, R., Polarographic analysis of sulfur species in marine porewaters. *Limnol. Oceanogr.* **1985,** *30*, 727-736.
53. Overmann, J.; Beatty, J. T.; Krouse, H. R.; Hall, K. J., The sulfur cycle in the chemocline of a meromictic salt lake. *Limnol. Oceanogr.* **1996,** *41*, 147-156.
54. Wang, F.; Tessier, A., Zero-valent sulfur and metal speciation in sediment porewaters of freshwater lakes. *Environ. Sci. Technol.* **2009,** *43*, 7252-7257.
55. Jacobs, L. A. Metal geochemistry in anoxic marine basins. Ph.D. Dissertation, University of Washington, Seattle, WA, 1984.

56. Heitz, A.; Kagi, R. I.; Alexander, R., Polysulfide sulfur in pipewall biofilms: Its role in the formation of swampy odour in distribution systems. *Water Sci. Technol.* **2000,** *41*, 271-278.
57. Kristiana, I.; Heitz, A.; Joll, C.; Sathasivan, A., Analysis of polysulfides in drinking water distribution systems using headspace solid-phase microextraction and gas chromatography-mass spectrometry. *J. Chromatogr. A* **2010,** *1217*, 5995-6001.
58. Kishore, K.; Ganesh, K., Polymers containing disulfide, tetrasulfide, diselenide and ditelluride linkages in the main chain. In *Polymer Synthesis/Polymer Engineering*, Springer Berlin / Heidelberg: 1995; Vol. 121, pp 81-121.
59. Steudel, R., The chemistry of organic polysulfanes R-S_n-R (n > 2). *Chem. Rev.* **2002,** *102*, 3905-3945.
60. Kamyshny, A.; Goifman, A.; Gun, J.; Rizkov, D.; Lev, O., Equilibrium distribution of polysulfide ions in aqueous solutions at 25 degrees C: A new approach for the study of polysulfides equilibria. *Environ. Sci. Technol.* **2004,** *38*, 6633-6644.
61. Goifman, A.; Ryzkov, D.; Gun, J.; Kamyshny, A.; Modestov, A. D.; Lev, O., Inorganic polysulfides' quantitation by methyl iodide derivatization: Dimethylpolysulfide formation potential. *Water Sci. Technol.* **2004,** *49*, 179-184.
62. Sobek, S.; Tranvik, L. J.; Prairie, Y. T.; Kortelainen, P.; Cole, J. J., Patterns and regulation of dissolved organic carbon: An analysis of 7,500 widely distributed lakes. *Limnol. Oceanogr.* **2007,** *52*, 1208-1219.
63. Holloway, J. M.; Goldhaber, M. B.; Mills, C. T., Carbon and nitrogen biogeochemistry of a Prairie Pothole wetland, Stutsman County, North Dakota, USA. *Appl. Geochem.* **2011,** *26*, S44-S47.
64. Arts, M. T.; Robarts, R. D.; Kasai, F.; Waiser, M. J.; Tumber, V. P.; Plante, A. J.; Rai, H.; Lange, H. J. d., The attenuation of ultraviolet radiation in high dissolved organic carbon waters of wetlands and lakes on the northern Great Plains. *Limnol. Oceanogr.* **2000,** *45*, 292-299.
65. Kuwabara, J. S.; van Geen, A.; McCorkle, D. C.; Bernhard, J. M., Dissolved sulfide distributions in the water column and sediment pore waters of the Santa Barbara Basin. *Geochim. Cosmochim. Acta* **1999,** *63*, 2199-2209.
66. Ciglenecki, I.; Kodba, Z.; Cosovic, B., Sulfur species in Rogoznica Lake. *Mar. Chem.* **1996,** *53*, 101-110.
67. Fritz, M.; Bachofen, R., Volatile organic sulfur compounds in a meromictic alpine lake. *Acta Hydroch. Hydrob.* **2000,** *28*, 185-192.
68. Luthy, L.; Fritz, M.; Bachofen, R., In situ determination of sulfide turnover rates in a meromictic alpine lake. *Appl. Environ. Microbiol.* **2000,** *66*, 712-717.
69. Lippa, K. A. Reactions of chloro-*s*-triazine and chloroacetanilide agrochemicals with reduced sulfur nucleophiles. Ph.D. Dissertation, The Johns Hopkins University, Baltimore, MD, 2002.
70. Chin, Y.-P.; Traina, S. J.; Swank, C. R.; Backhus, D., Abundance and properties of dissolved organic matter in pore waters of a freshwater wetland. *Limnol. Oceanogr.* **1998,** *43*, 1287-1296.

71. O'Loughlin, E. J.; Chin, Y.-P., Quantification and characterization of dissolved organic carbon and iron in sedimentary porewater from Green Bay, WI, USA. *Biogeochemistry* **2004,** *71*, 371-386.
72. Qin, Y. Abiotic reactions of acetanilide herbicides with bisulfide. M.S. Thesis, Oklahoma State University, Stillwater, OK, 1995.
73. Gan, J. Y., Enhanced degradation of chloroacetanilide herbicides by polysulfide salts. In *Proceedings of the 2006 USDA-CSREES National Water Quality Conference*, USDA-NIFA National Integrated Water Quality Program: Washington, DC, 2006.
74. Carlson, D. L.; Than, K. D.; Roberts, A. L., Acid- and base-catalyzed hydrolysis of chloroacetamide herbicides. *J. Agric. Food. Chem.* **2006,** *54*, 4740-4750.
75. Zopfi, J.; Ferdelman, T. G.; Fossing, H., Distribution and fate of sulfur intermediates-sulfite, tetrathionate, thiosulfate, and elemental sulfur-in marine sediments. *Geol. Soc. Am. Spec. Pap.* **2004,** *379*, 97-116.
76. Perlinger, J. A.; Buschmann, J.; Angst, W.; Schwarzenbach, R. P., Iron porphyrin and mercaptojuglone mediated reduction of polyhalogenated methanes and ethanes in homogeneous aqueous solution. *Environ. Sci. Technol.* **1998,** *32*, 2431-2437.
77. Kappler, A.; Haderlein, S. B., Natural organic matter as reductant for chlorinated aliphatic pollutants. *Environ. Sci. Technol.* **2003,** *37*, 2714-2719.
78. Tratnyek, P. G.; Macalady, D. L., Abiotic reduction of nitro aromatic pesticides in anaerobic laboratory systems. *J. Agric. Food. Chem.* **1989,** *37*, 248-254.
79. Guo, X.; Jans, U., Kinetics and mechanism of the degradation of methyl parathion in aqueous hydrogen sulfide solution: Investigation of natural organic matter effects. *Environ. Sci. Technol.* **2006,** *40*, 900-906.
80. Perlinger, J. A.; Kalluri, V. M.; Venkatapathy, R.; Angst, W., Addition of hydrogen sulfide to juglone. *Environ. Sci. Technol.* **2002,** *36*, 2663-2669.
81. Lindley, H., A study of the kinetics of the reaction between thiol compounds and chloroacetamide. *Biochem. J* **1960,** *74*, 577-584.
82. Li, X. Y.; Jiang, X. K.; Pan, H. Q.; Hu, J. S.; Fu, W. M., Nucleophilic substitutions of perhalofluoroalkanes initiated by halophilic attacks. *Pure Appl. Chem.* **1987,** *59*, 1015-1020.
83. Scarponi, L.; Perucci, P.; Martientti, L., Conjugation of 2-chloroacetanilide herbicides with glutathione: Role of molecular structures and of glutathione S-transferase enzymes. *J. Agric. Food. Chem.* **1991,** *39*, 2010-2013.
84. Field, J. A.; Thurman, E. M., Glutathione conjugation and contaminant transformation. *Environ. Sci. Technol.* **1996,** *30*, 1413-1418.
85. Buschmann, J.; Angst, W.; Schwarzenbach, R. P., Iron porphyrin and cysteine mediated reduction of ten polyhalogenated methanes in homogeneous aqueous solution: Product analyses and mechanistic considerations. *Environ. Sci. Technol.* **1999,** *33*, 1015-1020.
86. Yang, W.; Gan, J. J.; Bondarenko, S.; Liu, W., Nucleophilic radical substitution reaction of triazine herbicides with polysulfides. *J. Agric. Food. Chem.* **2004,** *52*, 7051-7055.
87. Jans, U.; Miah, M. H., Reaction of chlorpyrifos-methyl in aqueous hydrogen sulfide/bisulfide solutions. *J. Agric. Food. Chem.* **2003,** *51*, 1956-1960.

88. Gan, Q.; Jans, U., Reaction of thiometon and disulfoton with reduced sulfur species in simulated natural environment. *J. Agric. Food. Chem.* **2006,** *54*, 7753-7760.
89. Gan, Q.; Singh, R. M.; Wu, T.; Jans, U., Kinetics and mechanism of degradation of dichlorvos in aqueous solutions containing reduced sulfur species. *Environ. Sci. Technol.* **2006,** *40*, 5717-5723.
90. Wu, T.; Jans, U., Nucleophilic substitution reactions of chlorpyrifos-methyl with sulfur species. *Environ. Sci. Technol.* **2006,** *40*, 784-790.
91. Gan, Q.; Jans, U., Nucleophilic reactions of phorate and terbufos with reduced sulfur species under anoxic conditions. *J. Agric. Food. Chem.* **2007,** *55*, 3546-3554.

Chapter 3 References

1. Ju, K.-S.; Parales, R. E., Nitroaromatic compounds, from synthesis to biodegradation. *Microbiol. Mol. Biol. Rev.* **2010,** *74*, 250-272.
2. Schwarzenbach, R. P.; Gschwend, P. M.; Imboden, D. M., *Environmental Organic Chemistry*. John Wiley & Sons, Inc.: Hoboken, NJ, 2003.
3. Wahid, P. A.; Ramakrishna, C.; Sethunathan, N., Instantaneous degradation of parathion in anaerobic soils. *J. Environ. Qual.* **1980,** *9*, 127-130.
4. Wolfe, N. L.; Kitchens, B. E.; Macalady, D. L.; Grundl, T. J., Physical and chemical factors that influence the anaerobic degradation of methyl parathion in sediment systems. *Environ. Toxicol. Chem.* **1986,** *5*, 1019-1026.
5. Heijman, C. G.; Holliger, C.; Glaus, M. A.; Schwarzenbach, R. P.; Zeyer, J., Abiotic reduction of 4-chloronitrobenzene to 4-chloroaniline in a dissimilatory iron-reducing enrichment culture. *Appl. Environ. Microbiol.* **1993,** *59*, 4350-4353.
6. Heijman, C. G.; Grieder, E.; Holliger, C.; Schwarzenbach, R. P., Reduction of nitroaromatic compounds coupled to microbial iron reduction in laboratory aquifer columns. *Environ. Sci. Technol.* **1995,** *29*, 775-783.
7. Rügge, K.; Hofstetter, T. B.; Haderlein, S. B.; Bjerg, P. L.; Knudsen, S.; Zraunig, C.; Mosbæk, H.; Christensen, T. H., Characterization of predominant reductants in an anaerobic leachate-contaminated aquifer by nitroaromatic probe compounds. *Environ. Sci. Technol.* **1998,** *32*, 23-31.
8. Hofstetter, T. B.; Heijman, C. G.; Haderlein, S. B.; Holliger, C.; Schwarzenbach, R. P., Complete reduction of TNT and other (poly)nitroaromatic compounds under iron-reducing subsurface conditions. *Environ. Sci. Technol.* **1999,** *33*, 1479-1487.
9. Simon, R.; Colón, D.; Tebes-Stevens, C. L.; Weber, E. J., Effect of redox zonation on the reductive transformation of *p*-cyanonitrobenzene in a laboratory sediment column. *Environ. Sci. Technol.* **2000,** *34*, 3617-3622.
10. Hoferkamp, L. A.; Weber, E. J., Nitroaromatic reduction kinetics as a function of dominant terminal electron acceptor processes in natural sediments. *Environ. Sci. Technol.* **2006,** *40*, 2206-2212.
11. Tobler, N. B.; Hofstetter, T. B.; Schwarzenbach, R. P., Assessing iron-mediated oxidation of toluene and reduction of nitroaromatic contaminants in anoxic environments using compound-specific isotope analysis. *Environ. Sci. Technol.* **2007,** *41*, 7773-7780.
12. Tratnyek, P. G.; Weber, E. J.; Schwarzenbach, R. P., Quantitative structure-activity relationships for chemical reductions of organic contaminants. *Environ. Toxicol. Chem.* **2003,** *22*, 1733-1742.
13. Hakala, J. A.; Fimmen, R. L.; Chin, Y.-P.; Agrawal, S. G.; Ward, C. P., Assessment of the geochemical reactivity of Fe-DOM complexes in wetland sediment pore waters using a nitroaromatic probe compound. *Geochim. Cosmochim. Acta* **2009,** *73*, 1382-1393.
14. Yan, L.; Bailey, G. W., Sorption and abiotic redox transformation of nitrobenzene at the smectite-water interface. *J. Colloid Interface Sci.* **2001,** *241*, 142-153.
15. Hofstetter, T. B.; Schwarzenbach, R. P.; Haderlein, S. B., Reactivity of Fe(II) species associated with clay minerals. *Environ. Sci. Technol.* **2003,** *37*, 519-528.

16. Hofstetter, T. B.; Neumann, A.; Schwarzenbach, R. P., Reduction of nitroaromatic compounds by Fe(II) species associated with iron-rich smectites. *Environ. Sci. Technol.* **2005,** *40*, 235-242.
17. Neumann, A.; Hofstetter, T. B.; Lüssi, M.; Cirpka, O. A.; Petit, S.; Schwarzenbach, R. P., Assessing the redox reactivity of structural iron in smectites using nitroaromatic compounds as kinetic probes. *Environ. Sci. Technol.* **2008,** *42*, 8381-8387.
18. Hofstetter, T. B.; Neumann, A.; Arnold, W. A.; Hartenbach, A. E.; Bolotin, J.; Cramer, C. J.; Schwarzenbach, R. P., Substituent effects on nitrogen isotope fractionation during abiotic reduction of nitroaromatic compounds. *Environ. Sci. Technol.* **2008,** *42*, 1997-2003.
19. Gorski, C. A.; Scherer, M. M., Influence of magnetite stoichiometry on Fe^{II} uptake and nitrobenzene reduction. *Environ. Sci. Technol.* **2009,** *43*, 3675-3680.
20. Gorski, C. A.; Nurmi, J. T.; Tratnyek, P. G.; Hofstetter, T. B.; Scherer, M. M., Redox behavior of magnetite: Implications for contaminant reduction. *Environ. Sci. Technol.* **2010,** *44*, 55-60.
21. Klausen, J.; Troeber, S. P.; Haderlein, S. B.; Schwarzenbach, R. P., Reduction of substituted nitrobenzenes by Fe(II) in aqueous mineral suspensions. *Environ. Sci. Technol.* **1995,** *29*, 2396-2404.
22. Schultz, C. A.; Grundl, T. J., pH Dependence on reduction rate of 4-Cl-nitrobenzene by Fe(II)/montmorillonite systems. *Environ. Sci. Technol.* **2000,** *34*, 3641-3648.
23. Elsner, M.; Schwarzenbach, R. P.; Haderlein, S. B., Reactivity of Fe(II)-bearing minerals toward reductive transformation of organic contaminants. *Environ. Sci. Technol.* **2004,** *38*, 799-807.
24. Klupinski, T. P.; Chin, Y.-P.; Traina, S. J., Abiotic degradation of pentachloronitrobenzene by Fe(II): Reactions on goethite and iron oxide nanoparticles. *Environ. Sci. Technol.* **2004,** *38*, 4353-4360.
25. Colón, D.; Weber, E. J.; Anderson, J. L., QSAR study of the reduction of nitroaromatics by Fe(II) species. *Environ. Sci. Technol.* **2006,** *40*, 4976-4982.
26. Larese-Casanova, P.; Cwiertny, D. M.; Scherer, M. M., Nanogoethite formation from oxidation of Fe(II) sorbed on aluminum oxide: Implications for contaminant reduction. *Environ. Sci. Technol.* **2010,** *44*, 3765-3771.
27. Naka, D.; Kim, D.; Strathmann, T. J., Abiotic reduction of nitroaromatic compounds by aqueous iron(II)-catechol complexes. *Environ. Sci. Technol.* **2006,** *40*, 3006-3012.
28. Hakala, J. A.; Chin, Y.-P.; Weber, E. J., Influence of dissolved organic matter and Fe(II) on the abiotic reduction of pentachloronitrobenzene. *Environ. Sci. Technol.* **2007,** *41*, 7337-7342.
29. Naka, D.; Kim, D.; Carbonaro, R. F.; Strathmann, T. J., Abiotic reduction of nitroaromatic contaminants by iron(II) complexes with organothiol ligands. *Environ. Toxicol. Chem.* **2008,** *27*, 1257-1266.
30. Hartenbach, A. E.; Hofstetter, T. B.; Aeschbacher, M.; Sander, M.; Kim, D.; Strathmann, T. J.; Arnold, W. A.; Cramer, C. J.; Schwarzenbach, R. P., Variability of

nitrogen isotope fractionation during the reduction of nitroaromatic compounds with dissolved reductants. *Environ. Sci. Technol.* **2008,** *42*, 8352-8359.
31. Colón, D.; Weber, E. J.; Anderson, J. L., Effect of natural organic matter on the reduction of nitroaromatics by Fe(II) species. *Environ. Sci. Technol.* **2008,** *42*, 6538-6543.
32. Schwarzenbach, R. P.; Stierli, R.; Lanz, K.; Zeyer, J., Quinone and iron porphyrin mediated reduction of nitroaromatic compounds in homogeneous aqueous solution. *Environ. Sci. Technol.* **1990,** *24*, 1566-1574.
33. Dunnivant, F. M.; Schwarzenbach, R. P.; Macalady, D. L., Reduction of substituted nitrobenzenes in aqueous solutions containing natural organic matter. *Environ. Sci. Technol.* **1992,** *26*, 2133-2141.
34. Barrows, S. E.; Cramer, C. J.; Truhlar, D. G.; Elovitz, M. S.; Weber, E. J., Factors controlling regioselectivity in the reduction of polynitroaromatics in aqueous solution. *Environ. Sci. Technol.* **1996,** *30*, 3028-3038.
35. Guo, X.; Jans, U., Kinetics and mechanism of the degradation of methyl parathion in aqueous hydrogen sulfide solution: Investigation of natural organic matter effects. *Environ. Sci. Technol.* **2006,** *40*, 900-906.
36. Hartenbach, A.; Hofstetter, T. B.; Berg, M.; Bolotin, J.; Schwarzenbach, R. P., Using nitrogen isotope fractionation to assess abiotic reduction of nitroaromatic compounds. *Environ. Sci. Technol.* **2006,** *40*, 7710-7716.
37. Sposito, G., Electron shuttling by natural organic matter: Twenty years after. In *Aquatic Redox Chemistry*, Tratnyek, P. G.; Grundl, T. J.; Haderlein, S. B., Eds. American Chemical Society: Washington, DC, 2011; Vol. 1071, pp 113-127.
38. Tratnyek, P. G.; Macalady, D. L., Abiotic reduction of nitro aromatic pesticides in anaerobic laboratory systems. *J. Agric. Food. Chem.* **1989,** *37*, 248-254.
39. Perlinger, J. A.; Kalluri, V. M.; Venkatapathy, R.; Angst, W., Addition of hydrogen sulfide to juglone. *Environ. Sci. Technol.* **2002,** *36*, 2663-2669.
40. Nurmi, J. T.; Tratnyek, P. G., Electrochemical properties of natural organic matter (NOM), fractions of NOM, and model biogeochemical electron shuttles. *Environ. Sci. Technol.* **2002,** *36*, 617-624.
41. Cory, R. M.; McKnight, D. M., Fluorescence spectroscopy reveals ubiquitous presence of oxidized and reduced quinones in dissolved organic matter. *Environ. Sci. Technol.* **2005,** *39*, 8142-8149.
42. Heitmann, T.; Blodau, C., Oxidation and incorporation of hydrogen sulfide by dissolved organic matter. *Chem. Geol.* **2006,** *235*, 12-20.
43. Ratasuk, N.; Nanny, M. A., Characterization and quantification of reversible redox sites in humic substances. *Environ. Sci. Technol.* **2007,** *41*, 7844-7850.
44. Macalady, D. L.; Walton-Day, K., New light on a dark subject: On the use of fluorescence data to deduce redox states of natural organic matter (NOM). *Aquat. Sci.* **2009,** *71*, 135-143.
45. Aeschbacher, M.; Sander, M.; Schwarzenbach, R. P., Novel electrochemical approach to assess the redox properties of humic substances. *Environ. Sci. Technol.* **2010,** *44*, 87-93.

46. Aeschbacher, M.; Vergari, D.; Schwarzenbach, R. P.; Sander, M., Electrochemical analysis of proton and electron transfer equilibria of the reducible moieties in humic acids. *Environ. Sci. Technol.* **2011,** *45*, 8385-8394.
47. Hojo, M.; Takagi, Y.; Ogata, Y., Kinetics of the reduction of nitrobenzenes by sodium disulfide. *J. Am. Chem. Soc.* **1960,** *82*, 2459-2462.
48. Cope, O. J.; Brown, R. K., The reduction of nitrobenzene by sodium sulphide in aqueous ethanol. *Can. J. Chem.* **1961,** *39*, 1695-1710.
49. Cope, O. J.; Brown, R. K., The reduction of nitrobenzene by hydrosulphide ion in aqueous media. *Can. J. Chem.* **1962,** *40*, 2317-2328.
50. van der Valk, A. G., The prairie potholes of North America. In *The World's Largest Wetlands*, Fraser, L. H.; Keddy, P. A., Eds. Cambridge University Press: Cambridge, UK, 2005; pp 393-423.
51. Gleason, R. A.; Euliss, N. H.; Tangen, B. A.; Laubhan, M. K.; Browne, B. A., USDA conservation program and practice effects on wetland ecosystem services in the Prairie Pothole Region. *Ecol. Appl.* **2011,** *21*, S65-S81.
52. Dahl, T. E. *Wetland losses in the United States 1780's to 1980's*; U.S. Fish and Wildlife Service: Washington, DC, 1990; pp 1-13.
53. Johnson, R. R.; Oslund, F. T.; Hertel, D. R., The past, present, and future of prairie potholes in the United States. *J. Soil Water Conserv.* **2008,** *63*, 84A-87A.
54. Oslund, F. T.; Johnson, R. R.; Hertel, D. R., Assessing wetland changes in the prairie pothole region of Minnesota from 1980 to 2007. *J. Fish Wildl. Manag.* **2010,** *1*, 131-135.
55. Stubbs, M. *Land conversion in the northern plains*; Resources, Science, and Industry Division, The National Council for Science and the Environment, CRS Report for Congress RL33950: Washington, DC, 2007.
56. Euliss, N. H.; Smith, L. M.; Liu, S.; Feng, M.; Mushet, D. M.; Auch, R. F.; Loveland, T. R., The need for simultaneous evaluation of ecosystem services and land use change. *Environ. Sci. Technol.* **2010,** *44*, 7761-7763.
57. Gascoigne, W. R.; Hoag, D.; Koontz, L.; Tangen, B. A.; Shaffer, T. L.; Gleason, R. A., Valuing ecosystem and economic services across land-use scenarios in the Prairie Pothole Region of the Dakotas, USA. *Ecol. Econ.* **2011,** *70*, 1715-1725.
58. Rashford, B. S.; Walker, J. A.; Bastian, C. T., Economics of grassland conversion to cropland in the prairie pothole region. *Conserv. Biol.* **2011,** *25*, 276-284.
59. Olness, A.; Staricka, J. A.; Daniel, J. A., Oxidation-reduction and groundwater contamination in the Prairie Pothole region of the Northern Great Plains. In *Water for Agriculture and Wildlife and the Environment -- Win-Win Opportunities: Proceedings of the 1996 USCID Wetlands Seminar*, Schaack, J.; Anderson, S. S., Eds. U.S. Committee on Irrigation and Drainage: Denver, CO, 1996; pp 115-131.
60. Goldsborough, L. G.; Crumpton, W. G., Distribution and environmental fate of pesticides in prairie wetlands. *Great Plains Res.* **1998,** *8*, 73-95.
61. Donald, D. B.; Narine, P. G.; Lynne, Q.-A.; Kevin, C., Diffuse geographic distribution of herbicides in northern prairie wetlands. *Environ. Toxicol. Chem.* **2001,** *20*, 273-279.

62. Detenbeck, N. E.; Elonen, C. M.; Taylor, D. L.; Cotter, A. M.; Puglisi, F. A.; Sanville, W. D., Effects of agricultural activities and best management practices on water quality of seasonal prairie pothole wetlands. *Wetlands Ecol. Manage.* **2002,** *10*, 335-354.
63. Degenhardt, D.; Humphries, D.; Cessna, A. J.; Messing, P.; Badiou, P. H.; Raina, R.; Farenhorst, A.; Pennock, D. J., Dissipation of glyphosate and aminomethylphosphonic acid in water and sediment of two Canadian prairie wetlands. *J. Environ. Sci. Health, Part B* **2012,** *47*, 631-639.
64. Huckins, J. N.; Petty, J. D.; England, D. C., Distribution and impact of trifluralin, atrazine, and fonofos residues in microcosms simulating a northern prairie wetland. *Chemosphere* **1986,** *15*, 563-588.
65. Grover, R.; Waite, D. T.; Cessna, A. J.; Nicholaichuk, W.; Irvin, D. G.; Kerr, L. A.; Best, K., Magnitude and persistence of herbicide residues in farm dugouts and ponds in the Canadian prairies. *Environ. Toxicol. Chem.* **1997,** *16*, 638-643.
66. Cessna, A. J.; Donald, D. B.; Bailey, J.; Waiser, M.; Headley, J. V., Persistence of the sulfonylurea herbicides thifensulfuron-methyl, ethametsulfuron-methyl, and metsulfuron-methyl in farm dugouts (ponds). *J. Environ. Qual.* **2006,** *35*, 2395-2401.
67. Degenhardt, D.; Cessna, A. J.; Raina, R.; Farenhorst, A.; Pennock, D. J., Dissipation of six acid herbicides in water and sediment of two Canadian prairie wetlands. *Environ. Toxicol. Chem.* **2011,** *30*, 1982-1989.
68. Helling, C. S., Dinitroaniline herbicides in soils. *J. Environ. Qual.* **1976,** *5*, 1-15.
69. U.S. Geological Survey, Pesticide National Synthesis Project. *2002 Pesticide Use Maps*; http://water.usgs.gov/nawqa/pnsp/usage/maps/compound_listing.php?year=02 (Accessed August, 2011).
70. Zollinger, R.; McMullen, M.; Knodel, J.; Gray, J.; Jantzi, D.; Kimmet, G.; Hagemeister, K.; Schmitt, C. *Pesticide Use and Pest Management Practices in North Dakota, 2008*; North Dakota State University in cooperation with North Dakota Agricultural Statistics Service Extension Publication W-1446: Fargo, ND, 2009.
71. Gilliom, R. J., Pesticides in U.S. streams and groundwater. *Environ. Sci. Technol.* **2007,** *41*, 3408-3414.
72. U.S. Environmental Protection Agency, National Sediment Quality Survey. *Incidence and Severity of Sediment Contamination in Surface Waters of the United States, Second Edition*; EPA 823-R-04-007; U.S. Environmental Protection Agency: Washington, DC, 2004. http://water.epa.gov/polwaste/sediments/cs/upload/nsqs2ed-complete-2.pdf (Accessed August, 2011).
73. U.S. Environmental Protection Agency, Persistent Bioaccumulative and Toxic (PBT) Chemical Program. *Pesticides and Other Persistent Bioaccumulative Toxic (PBT) Chemicals*; EPA 260-B-01-005; U.S. Environmental Protection Agency: Washington, DC, 2001. http://www.epa.gov/tri/guide_docs/pdf/2001/pest2001.pdf (Accessed August 2011).
74. Rickert, D. E., *Toxicity of Nitroaromatic Compounds*. Hemisphere Publishing Corp.: Washington, DC, 1985.
75. Weber, J. B., Behavior of dinitroaniline herbicides in soils. *Weed Technol.* **1990,** *4*, 394-406.

76. Belden, J. B.; Phillips, T. A.; Henderson, K. L.; Clark, B. W.; Lydy, M. J.; Coats, J. R., Persistence, mobility, and bioavailability of pendimethalin and trifluralin in Soil. In *Environmental Fate and Effects of Pesticides*, American Chemical Society: Washington, DC, 2003; Vol. 853, pp 167-177.
77. Ciglenecki, I.; Kodba, Z.; Cosovic, B., Sulfur species in Rogoznica Lake. *Mar. Chem.* **1996,** *53*, 101-110.
78. Overmann, J.; Beatty, J. T.; Krouse, H. R.; Hall, K. J., The sulfur cycle in the chemocline of a meromictic salt lake. *Limnol. Oceanogr.* **1996,** *41*, 147-156.
79. Miller, P. L.; Vasudevan, D.; Gschwend, P. M.; Roberts, A. L., Transformation of hexachloroethane in a sulfidic natural water. *Environ. Sci. Technol.* **1998,** *32*, 1269-1275.
80. Chin, Y.-P.; Traina, S. J.; Swank, C. R.; Backhus, D., Abundance and properties of dissolved organic matter in pore waters of a freshwater wetland. *Limnol. Oceanogr.* **1998,** *43*, 1287-1296.
81. O'Loughlin, E. J.; Chin, Y.-P., Quantification and characterization of dissolved organic carbon and iron in sedimentary porewater from Green Bay, WI, USA. *Biogeochemistry* **2004,** *71*, 371-386.
82. Tor, J. M.; Xu, C.; Stucki, J. M.; Wander, M. M.; Sims, G. K., Trifluralin degradation under microbiologically induced nitrate and Fe(III) reducing conditions. *Environ. Sci. Technol.* **2000,** *34*, 3148-3152.
83. Wang, S.; Arnold, W. A., Abiotic reduction of dinitroaniline herbicides. *Water Res.* **2003,** *37*, 4191-4201.
84. Klupinski, T. P.; Chin, Y.-P., Abiotic degradation of trifluralin by Fe(II): Kinetics and transformation pathways. *Environ. Sci. Technol.* **2003,** *37*, 1311-1318.
85. Hakala, J. A.; Chin, Y.-P., Abiotic reduction of pendimethalin and trifluralin in controlled and natural systems containing Fe(II) and dissolved organic matter. *J. Agric. Food. Chem.* **2010,** *58*, 12840-12846.
86. Zeng, T.; Ziegelgruber, K. L.; Chin, Y.-P.; Arnold, W. A., Pesticide processing potential in prairie pothole porewaters. *Environ. Sci. Technol.* **2011,** *45*, 6814-6822.
87. Cline, J. D., Spectrophotometric determination of hydrogen sulfide in natural waters. *Limnol. Oceanogr.* **1969,** *14*, 454-458.
88. Heitz, A.; Kagi, R. I.; Alexander, R., Polysulfide sulfur in pipewall biofilms: Its role in the formation of swampy odour in distribution systems. *Water Sci. Technol.* **2000,** *41*, 271-278.
89. Kristiana, I.; Heitz, A.; Joll, C.; Sathasivan, A., Analysis of polysulfides in drinking water distribution systems using headspace solid-phase microextraction and gas chromatography-mass spectrometry. *J. Chromatogr. A* **2010,** *1217*, 5995-6001.
90. Shea, D.; Helz, G. R., The solubility of copper in sulfidic waters - sulfide and polysulfide complexes in equilibrium with covellite. *Geochim. Cosmochim. Acta* **1988,** *52*, 1815-1825.
91. MacCrehan, W.; Shea, D., Temporal relationship of thiols to inorganic sulfur compounds in anoxic Chesapeake Bay sediment porewater. In *Geochemical Transformations of Sedimentary Sulfur*, Vairavamurthy, M. A.; Schoonen, M. A. A.; Eglinton, T. I.; Luther III, G. W.; Manowitz, B., Eds. American Chemical Society: Washington, DC, 1995; Vol. 612, pp 294-310.

92. Zopfi, J.; Ferdelman, T. G.; Fossing, H., Distribution and fate of sulfur intermediates-sulfite, tetrathionate, thiosulfate, and elemental sulfur-in marine sediments. *Geol. Soc. Am. Spec. Pap.* **2004,** *379*, 97-116.
93. Marendic, N.; Norris, A. R., The interaction of sulfite ion with 2,4,6-trinitrobenzaldehyde: Kinetic, equilibrium, and proton magnetic resonance studies. *Can. J. Chem.* **1973,** *51*, 3927-3935.
94. Buncel, E.; Norris, A. R.; Russell, K. E.; Sheridan, P. J., Kinetic and thermodynamic studies of the reactions of sulfite ion with picramide, *N*-methylpicramide, and *N,N*-dimethylpicramide in aqueous solution. *Can. J. Chem.* **1974,** *52*, 25-33.
95. Annandale, M. T.; vanLoon, G. W.; Buncel, E., Regioselectivity and stereoelectronic effects in the reactions of the dinitroaniline herbicides trifluralin and benefin with nucleophiles. *Can. J. Chem.* **1998,** *76*, 873-883.
96. Gallardo, I.; Guirado, G., Thermodynamic study of σ^H complexes in nucleophilic aromatic substitution reactions: Relative stabilities of electrochemically generated radicals. *Eur. J. Org. Chem.* **2008**, 2463-2472.
97. Smith, D. S.; Bell, R. A.; Kramer, J. R., Metal speciation in natural waters with emphasis on reduced sulfur groups as strong metal binding sites. *Comp. Biochem. Physiol., Part C: Toxicol. Pharmacol.* **2002,** *133*, 65-74.
98. Willis, G. H.; Wander, R. C.; Southwick, L. M., Degradation of trifluralin in soil suspensions as related to redox potential. *J. Environ. Qual.* **1974,** *3*, 262-265.
99. Kearney, P. C.; Plimmer, J. R.; Wheeler, W. B.; Kontson, A., Persistence and metabolism of dinitroaniline herbicides in soils. *Pestic. Biochem. Physiol.* **1976,** *6*, 229-238.
100. Camper, N. D.; Stralka, K.; Skipper, H. D., Aerobic and anaerobic degradation of profluralin and trifluralin. *J. Environ. Sci. Health Part B-Pestic. Contam. Agric. Wastes* **1980,** *15*, 457-473.
101. Singh, S. B.; Kulshrestha, G., Microbial-degradation of pendimethalin. *J. Environ. Sci. Health Part B-Pestic. Contam. Agric. Wastes* **1991,** *26*, 309-321.
102. Bellinaso, M. D.; Greer, C. W.; Peralba, M. D.; Henriques, J. A. P.; Gaylarde, C. C., Biodegradation of the herbicide trifluralin by bacteria isolated from soil. *FEMS Microbiol. Ecol.* **2003,** *43*, 191-194.
103. Okutman Tas, D.; Pavlostathis, S. G., Microbial reductive transformation of pentachloronitrobenzene under methanogenic conditions. *Environ. Sci. Technol.* **2005,** *39*, 8264-8272.
104. Burton, E. D.; Bush, R. T.; Sullivan, L. A.; Hocking, R. K.; Mitchell, D. R. G.; Johnston, S. G.; Fitzpatrick, R. W.; Raven, M.; McClure, S.; Jang, L. Y., Iron-monosulfide oxidation in natural sediments: Resolving microbially mediated S transformations using XANES, electron microscopy, and selective extractions. *Environ. Sci. Technol.* **2009,** *43*, 3128-3134.
105. Giggenbach, W., Equilibriums involving polysulfide ions in aqueous sulfide solutions up to 240.deg. *Inorg. Chem.* **1974,** *13*, 1724-1730.
106. Glaus, M. A.; Heijman, C. G.; Schwarzenbach, R. P.; Zeyer, J., Reduction of nitroaromatic compounds mediated by *Streptomyces sp.* exudates. *Appl. Environ. Microbiol.* **1992,** *58*, 1945-1951.

107. Luther III, G. W.; Rickard, D., Metal sulfide cluster complexes and their biogeochemical importance in the environment. *J. Nanopart. Res.* **2005,** *7*, 389-407.
108. Rickard, D.; Luther III, G. W., Metal sulfide complexes and clusters. *Rev. Mineral. Geochem.* **2006,** *61*, 421-504.
109. Charriau, A.; Lesven, L.; Gao, Y.; Leermakers, M.; Baeyens, W.; Ouddane, B.; Billon, G., Trace metal behaviour in riverine sediments: Role of organic matter and sulfides. *Appl. Geochem.* **2011,** *26*, 80-90.
110. Yu, Y. S.; Bailey, G. W., Reduction of nitrobenzene by four sulfide minerals: Kinetics, products, and solubility. *J. Environ. Qual.* **1992,** *21*, 86-94.
111. Cheng, J. Y.; Suidan, M. T.; Venosa, A. D., Abiotic reduction of 2,4-dinitrotoluene in the presence of sulfide minerals under anoxic conditions. *Water Sci. Technol.* **1996,** *34*, 25-33.
112. Oh, S.-Y.; Chiu, P. C.; Cha, D. K., Reductive transformation of 2,4,6-trinitrotoluene, hexahydro-1,3,5-trinitro-1,3,5-triazine, and nitroglycerin by pyrite and magnetite. *J. Hazard. Mater.* **2008,** *158*, 652-655.
113. Oh, S.-Y.; Son, J.-G.; Lim, O.-T.; Chiu, P., The role of black carbon as a catalyst for environmental redox transformation. *Environ. Geochem. Health* **2012,** *34*, 105-113.
114. Oh, S.-Y.; Chiu, P. C., Graphite- and soot-mediated reduction of 2,4-dinitrotoluene and hexahydro-1,3,5-trinitro-1,3,5-triazine. *Environ. Sci. Technol.* **2009,** *43*, 6983-6988.
115. Yu, X.; Gong, W.; Liu, X.; Shi, L.; Han, X.; Bao, H., The use of carbon black to catalyze the reduction of nitrobenzenes by sulfides. *J. Hazard. Mater.* **2011,** *198*, 340-346.
116. Weber, E. J.; Spidle, D. L.; Thorn, K. A., Covalent binding of aniline to humic substances. 1. Kinetic studies. *Environ. Sci. Technol.* **1996,** *30*, 2755-2763.
117. Thorn, K. A.; Pettigrew, P. J.; Goldenberg, W. S.; Weber, E. J., Covalent binding of aniline to humic substances. 2. ^{15}N NMR studies of nucleophilic addition reactions. *Environ. Sci. Technol.* **1996,** *30*, 2764-2775.
118. Johnson, W. C.; Millett, B. V.; Gilmanov, T.; Voldseth, R. A.; Guntenspergen, G. R.; Naugle, D. E., Vulnerability of northern prairie wetlands to climate change. *Bioscience* **2005,** *55*, 863-872.
119. Millett, B. V.; Johnson, W. C.; Guntenspergen, G. R., Climate trends of the North American prairie pothole region 1906-2000. *Clim. Change* **2009,** *93*, 243-267.
120. Niemuth, N.; Wangler, B.; Reynolds, R., Spatial and temporal variation in wet area of wetlands in the Prairie Pothole Region of North Dakota and South Dakota. *Wetlands* **2010,** *30*, 1053-1064.

Chapter 4 References

1. van der Valk, A. G., The prairie potholes of North America. In *The World's Largest Wetlands*, Fraser, L. H.; Keddy, P. A., Eds. Cambridge University Press: Cambridge, UK, 2005; pp 393-423.
2. Kantrud, H. A.; Krapu, G. L.; Swanson, G. A. *Prairie basin wetlands of the Dakotas: A community profile*; U.S. Fish and Wildlife Service, Biological Report 85: Washington, DC, 1989; pp 1-111.
3. Ostlie, W. R.; Schneider, R. E.; Aldrich, J. M.; Faust, T. M.; McKim, R. L. B.; Chaplin., S. J. *The status of biodiversity in the Great Plains*; The Nature Conservancy; Arlington, VA, 1997.
4. LaBaugh, J. W.; Winter, T. C.; Rosenberry, D. O., Hydrological functions of prairie wetlands. *Great Plains Res.* **1998,** *8*, 17-37.
5. van der Kamp, G.; Hayashi, M., The groundwater recharge functions of prairie wetlands. *Great Plains Res.* **1998,** *8*, 39-56.
6. Samson, F. B.; Knopf, F. L.; Ostlie, W. R., Great Plains ecosystems: Past, present, and future. *Wildl. Soc. Bull.* **2004,** *32*, 6-15.
7. Stubbs, M. *Land conversion in the northern plains*; Resources, Science, and Industry Division, The National Council for Science and the Environment, CRS Report for Congress RL33950: Washington, DC, 2007.
8. Watmough, M. D.; Schmoll, M. J. *Environment Canada's prairie & northern region habitat monitoring program phase II: Recent habitat trends in the prairie habitat joint venture*; Canadian Wildlife Service, Environment Canada, Report Series Number 493; Ottawa, Canada, 2007.
9. Oslund, F. T.; Johnson, R. R.; Hertel, D. R., Assessing wetland changes in the prairie pothole region of Minnesota from 1980 to 2007. *J. Fish Wildl. Manag.* **2010,** *1*, 131-135.
10. Lenhart, C. F.; Verry, E. S.; Brooks, K. N.; Magner, J. A., Adjustment of prairie pothole streams to land-use, drainage and cliamte changes and consequences for turbidity impairment. *River Res. Appl.* **2011**, DOI: 10.1002/rra.1549.
11. Anteau, M., Do interactions of land use and climate affect productivity of waterbirds and prairie-pothole wetlands? *Wetlands* **2012,** *32*, 1-9.
12. Brunet, N. N.; Westbrook, C. J., Wetland drainage in the Canadian prairies: Nutrient, salt and bacteria characteristics. *Agric. Ecosyst. Environ.* **2012,** *146*, 1-12.
13. Neely, R. K.; Baker, J. L., Nitrogen and phosphorous dynamics and the fate of agricultural runoff. In *Northern Prairie Wetlands*, Van der Valk, A. G., Ed. Iowa State University Press: Ames, IA, 1989; pp 92-131.
14. Olness, A.; Staricka, J. A.; Daniel, J. A., Oxidation-reduction and groundwater contamination in the Prairie Pothole region of the Northern Great Plains. In *Water for Agriculture and Wildlife and the Environment -- Win-Win Opportunities: Proceedings of the 1996 USCID Wetlands Seminar*, Schaack, J.; Anderson, S. S., Eds. U.S. Committee on Irrigation and Drainage: Denver, CO, 1996; pp 115-131.
15. Goldsborough, L. G.; Crumpton, W. G., Distribution and environmental fate of pesticides in prairie wetlands. *Great Plains Res.* **1998,** *8*, 73-95.

16. Crumpton, W. G.; Goldsborough, L. G., Nitrogen transformation and fate in prairie wetlands. *Great Plains Res.* **1998,** *8*, 57-72.
17. Detenbeck, N. E.; Elonen, C. M.; Taylor, D. L.; Cotter, A. M.; Puglisi, F. A.; Sanville, W. D., Effects of agricultural activities and best management practices on water quality of seasonal prairie pothole wetlands. *Wetlands Ecol. Manage.* **2002,** *10*, 335-354.
18. Ontkean, G. R.; Chanasyk, D. S.; Riemersma, S.; Bennett, D. R.; Brunen, J. M., Enhanced prairie wetland effects on surface water quality in Crowfoot Creek, Alberta. *Water Qual. Res. J. Can.* **2003,** *38*, 335-359.
19. Donald, D. B.; Syrgiannis, J.; Hunter, F.; Weiss, G., Agricultural pesticides threaten the ecological integrity of northern prairie wetlands. *Sci. Total Environ.* **1999,** *231*, 173-181.
20. Whigham, D. F.; Jordan, T. E., Isolated wetlands and water quality. *Wetlands* **2003,** *23*, 541-549.
21. Cessna, A. J.; Sheedy, C.; Farenhorst, A.; McQueen, D. A. R., Indicator of the Risk of Water Contamination by Pesticides. In *Environmental Sustainability of Canadian Agriculture: Agri-Environmental Indicator Report Series - Report No. 3*, Eilers, W.; MacKay, R.; Graham, L.; Lefebvre, A., Eds. Agriculture and Agri-Food Canada: Ottawa, Canada, 2010.
22. Sura, S.; Waiser, M.; Tumber, V.; Lawrence, J. R.; Cessna, A. J.; Glozier, N., Effects of glyphosate and two herbicide mixtures on microbial communities in prairie wetland ecosystems: A mesocosm approach. *J. Environ. Qual.* **2012,** *41*, 732-743.
23. Zabik, M. J.; Leavitt, R. A.; Su, G. C. C., Photochemistry of bioactive compounds: A review of pesticide photochemistry. *Annu. Rev. Entomol.* **1976,** *21*, 61-79.
24. Burrows, H. D.; Canle L, M.; Santaballa, J. A.; Steenken, S., Reaction pathways and mechanisms of photodegradation of pesticides. *J. Photochem. Photobiol. B: Biol.* **2002,** *67*, 71-108.
25. Katagi, T., Photodegradation of pesticides on plant and soil surfaces. In *Reviews of Environmental Contamination and Toxicology, Vol 182*, Springer: New York, 2004; Vol. 182, pp 1-189.
26. Schwarzenbach, R. P.; Gschwend, P. M.; Imboden, D. M., *Environmental Organic Chemistry*. John Wiley & Sons, Inc.: Hoboken, NJ, 2003.
27. Zafiriou, O. C., Sources and Reactions of OH and Daughter Radicals in Seawater. *J. Geophys. Res.* **1974,** *79*, 4491-4497.
28. Zepp, R. G.; Wolfe, N. L.; Baughman, G. L.; Hollis, R. C., Singlet oxygen in natural waters. *Nature* **1977,** *267*, 421-423.
29. Zafiriou, O. C.; True, M. B., Nitrate photolysis in seawater by sunlight. *Mar. Chem.* **1979,** *8*, 33-42.
30. Zafiriou, O. C.; True, M. B., Nitrite photolysis in seawater by sunlight. *Mar. Chem.* **1979,** *8*, 9-32.
31. Mill, T.; Hendry, D. G.; Richardson, H., Free-radical oxidants in natural waters. *Science* **1980,** *207*, 886-887.
32. Baxter, R. M.; Carey, J. H., Evidence for photochemical generation of superoxide ion in humic waters. *Nature* **1983,** *306*, 575-576.

33. Cooper, W. J.; Zika, R. G., Photochemical formation of hydrogen peroxide in surface and ground waters exposed to sunlight. *Science* **1983,** *220*, 711-712.
34. Zepp, R. G.; Schlotzhauer, P. F.; Sink, R. M., Photosensitized transformations involving electronic energy transfer in natural waters: role of humic substances. *Environ. Sci. Technol.* **1985,** *19*, 74-81.
35. Zepp, R. G.; Braun, A. M.; Hoigne, J.; Leenheer, J. A., Photoproduction of hydrated electrons from natural organic solutes in aquatic environments. *Environ. Sci. Technol.* **1987,** *21*, 485-490.
36. Zafiriou, O. C.; Joussot-Dubien, J.; Zepp, R. G.; Zika, R. G., Photochemistry of natural waters. *Environ. Sci. Technol.* **1984,** *18*, 358A-371A.
37. Mill, T., Predicting photoreaction rates in surface waters. *Chemosphere* **1999,** *38*, 1379-1390.
38. Zepp, R. G.; Cline, D. M., Rates of direct photolysis in aquatic environment. *Environ. Sci. Technol.* **1977,** *11*, 359-366.
39. Zepp, R. G.; Wolfe, N. L.; Gordon, J. A.; Fincher, R. C., Light-induced transformations of methoxychlor in aquatic systems. *J. Agric. Food. Chem.* **1976,** *24*, 727-733.
40. Chiron, S.; Barceló, D.; Abian, J.; Ferrer, M.; Sanchez-Baeza, F.; Messeguer, A., Comparative photodegradation rates of alachlor and bentazone in natural water and determination of breakdown products. *Environ. Toxicol. Chem.* **1995,** *14*, 1287-1298.
41. Gerecke, A. C.; Canonica, S.; Muller, S. R.; Scharer, M.; Schwarzenbach, R. P., Quantification of dissolved natural organic matter (DOM) mediated phototransformation of phenylurea herbicides in lakes. *Environ. Sci. Technol.* **2001,** *35*, 3915-3923.
42. Miller, P. L.; Chin, Y.-P., Photoinduced degradation of carbaryl in a wetland surface water. *J. Agric. Food. Chem.* **2002,** *50*, 6758-6765.
43. Schulz, R.; Hahn, C.; Bennett, E. R.; Dabrowski, J. M.; Thiere, G.; Peall, S. K. C., Fate and effects of azinphos-methyl in a flow-through wetland in South Africa. *Environ. Sci. Technol.* **2003,** *37*, 2139-2144.
44. Miller, P. L.; Chin, Y.-P., Indirect photolysis promoted by natural and engineered wetland water constituents: Processes leading to alachlor degradation. *Environ. Sci. Technol.* **2005,** *39*, 4454-4462.
45. Wallace, D. F.; Hand, L. H.; Oliver, R. G., The role of indirect photolysis in limiting the persistence of crop protection products in surface waters. *Environ. Toxicol. Chem.* **2010,** *29*, 575-581.
46. Huang, J.; Mabury, S. A., The role of carbonate radical in limiting the persistence of sulfur-containing chemicals in sunlit natural waters. *Chemosphere* **2000,** *41*, 1775-1782.
47. Lam, M. W.; Tantuco, K.; Mabury, S. A., PhotoFate: A new approach in accounting for the contribution of indirect photolysis of pesticides and pharmaceuticals in surface waters. *Environ. Sci. Technol.* **2003,** *37*, 899-907.
48. Canonica, S.; Kohn, T.; Mac, M.; Real, F. J.; Wirz, J.; von Gunten, U., Photosensitizer method to determine rate constants for the reaction of carbonate radical with organic compounds. *Environ. Sci. Technol.* **2005,** *39*, 9182-9188.

49. Mazellier, P.; Busset, C.; Delmont, A.; De Laat, J., A comparison of fenuron degradation by hydroxyl and carbonate radicals in aqueous solution. *Water Res.* **2007,** *41*, 4585-4594.
50. Vione, D.; Maurino, V.; Minero, C.; Carlotti, M. E.; Chiron, S.; Barbati, S., Modelling the occurrence and reactivity of the carbonate radical in surface freshwater. *C. R. Chim.* **2009,** *12*, 865-871.
51. Wu, C.; Linden, K. G., Phototransformation of selected organophosphorus pesticides: Roles of hydroxyl and carbonate radicals. *Water Res.* **2010,** *44*, 3585-3594.
52. Dell'Arciprete, M. L.; Soler, J. M.; Santos-Juanes, L.; Arques, A.; Mártire, D. O.; Furlong, J. P.; Gonzalez, M. C., Reactivity of neonicotinoid insecticides with carbonate radicals. *Water Res.* **2012**.
53. Haag, W. R.; Yao, C. C. D., Rate constants for reaction of hydroxyl radicals with several drinking water contaminants. *Environ. Sci. Technol.* **1992,** *26*, 1005-1013.
54. Minero, C.; Pramauro, E.; Pelizzetti, E.; Dolci, M.; Marchesini, A., Photosensitized transformations of atrazine under simulated sunlight in aqueous humic acid solution. *Chemosphere* **1992,** *24*, 1597-1606.
55. Mabury, S. A.; Crosby, D. G., Pesticide reactivity toward hydroxyl and its relationship to field persistence. *J. Agric. Food. Chem.* **1996,** *44*, 1920-1924.
56. Fulkerson-Brekken, J.; Brezonik, P. L., Indirect photolysis of acetochlor: Rate constant of a nitrate-mediated hydroxyl radical reaction. *Chemosphere* **1998,** *36*, 2699-2704.
57. Kamiya, M.; Kameyama, K., Photochemical effects of humic substances on the degradation of organophosphorus pesticides. *Chemosphere* **1998,** *36*, 2337-2344.
58. Armbrust, K. L., Pesticide hydroxyl radical rate constants: Measurements and estimates of their importance in aquatic environments. *Environ. Toxicol. Chem.* **2000,** *19*, 2175-2180.
59. Dimou, A. D.; Sakkas, V. A.; Albanis, T. A., Trifluralin photolysis in natural waters and under the presence of isolated organic matter and nitrate ions: Kinetics and photoproduct analysis. *J. Photochem. Photobiol. A: Chem.* **2004,** *163*, 473-480.
60. Dimou, A. D.; Sakkas, V. A.; Albanis, T. A., Metolachlor photodegradation study in aqueous media under natural and simulated solar irradiation. *J. Agric. Food. Chem.* **2005,** *53*, 694-701.
61. Shemer, H.; Sharpless, C. M.; Elovitz, M. S.; Linden, K. G., Relative rate constants of contaminant candidate list pesticides with hydroxyl radicals. *Environ. Sci. Technol.* **2006,** *40*, 4460-4466.
62. Richard, C.; ter Halle, A.; Brahmia, O.; Malouki, M.; Halladja, S., Auto-remediation of surface waters by solar-light: Photolysis of 1-naphthol, and two herbicides in pure and synthetic waters. *Catal. Today* **2007,** *124*, 82-87.
63. Garbin, J. R.; Milori, D. M. B. P.; Simões, M. L.; da Silva, W. T. L.; Neto, L. M., Influence of humic substances on the photolysis of aqueous pesticide residues. *Chemosphere* **2007,** *66*, 1692-1698.
64. Dell'Arciprete, M. L.; Santos-Juanes, L.; Sanz, A. A.; Vicente, R.; Amat, A. M.; Furlong, J. P.; Martire, D. O.; Gonzalez, M. C., Reactivity of hydroxyl radicals with

neonicotinoid insecticides: Mechanism and changes in toxicity. *Photochem. Photobiol. Sci.* **2009,** *8*, 1016-1023.
65. Vione, D.; Das, R.; Rubertelli, F.; Maurino, V.; Minero, C.; Barbati, S.; Chiron, S., Modelling the occurrence and reactivity of hydroxyl radicals in surface waters: Implications for the fate of selected pesticides. *Int. J. Environ. Anal. Chem.* **2010,** *90*, 260-275.
66. Al Housari, F.; Höhener, P.; Chiron, S., Factors responsible for rapid dissipation of acidic herbicides in the coastal lagoons of the Camargue (Rhône River Delta, France). *Sci. Total Environ.* **2011,** *409*, 582-587.
67. Ukpebor, J.; Halsall, C., Effects of dissolved water constituents on the photodegradation of fenitrothion and diazinon. *Water, Air, Soil Pollut.* **2012,** *223*, 655-666.
68. ter Halle, A.; Richard, C., Simulated solar light irradiation of mesotrione in natural waters. *Environ. Sci. Technol.* **2006,** *40*, 3842-3847.
69. Dell'Arciprete, M. L.; Santos-Juanes, L.; Arques, A.; Vercher, R. F.; Amat, A. M.; Furlong, J. P.; Mártire, D. O.; Gonzalez, M. C., Reactivity of neonicotinoid pesticides with singlet oxygen. *Catal. Today* **2010,** *151*, 137-142.
70. Canonica, S.; Hellrung, B.; Muller, P.; Wirz, J., Aqueous oxidation of phenylurea herbicides by triplet aromatic ketones. *Environ. Sci. Technol.* **2006,** *40*, 6636-6641.
71. Canonica, S.; Laubscher, H. U., Inhibitory effect of dissolved organic matter on triplet-induced oxidation of aquatic contaminants. *Photochem. Photobiol. Sci.* **2008,** *7*, 547-551.
72. Arts, M. T.; Robarts, R. D.; Kasai, F.; Waiser, M. J.; Tumber, V. P.; Plante, A. J.; Rai, H.; Lange, H. J. d., The attenuation of ultraviolet radiation in high dissolved organic carbon waters of wetlands and lakes on the northern Great Plains. *Limnol. Oceanogr.* **2000,** *45*, 292-299.
73. Waiser, M. J.; Robarts, R. D., Changes in composition and reactivity of allochthonous DOM in a prairie saline lake. *Limnol. Oceanogr.* **2000,** *45*, 763-774.
74. Waiser, M. J., Relationship between hydrological characteristics and dissolved organic carbon concentration and mass in northern prairie wetlands using a conservative tracer approach. *J. Geophys. Res.* **2006,** *111*, G02024.
75. Holloway, J. M.; Goldhaber, M. B.; Mills, C. T., Carbon and nitrogen biogeochemistry of a Prairie Pothole wetland, Stutsman County, North Dakota, USA. *Appl. Geochem.* **2011,** *26*, S44-S47.
76. Zeng, T.; Ziegelgruber, K. L.; Chin, Y.-P.; Arnold, W. A., Pesticide processing potential in prairie pothole porewaters. *Environ. Sci. Technol.* **2011,** *45*, 6814-6822.
77. Cessna, A. J.; Donald, D. B.; Bailey, J.; Waiser, M.; Headley, J. V., Persistence of the sulfonylurea herbicides thifensulfuron-methyl, ethametsulfuron-methyl, and metsulfuron-methyl in farm dugouts (ponds). *J. Environ. Qual.* **2006,** *35*, 2395-2401.
78. Headley, J. V.; Du, J.-L.; Peru, K. M.; McMartin, D. W., Mass spectrometry of the photolysis of sulfonylurea herbicides in prairie waters. *Mass Spectrom. Rev.* **2010,** *29*, 593-605.
79. Zollinger, R.; McMullen, M.; Knodel, J.; Gray, J.; Jantzi, D.; Kimmet, G.; Hagemeister, K.; Schmitt, C. *Pesticide Use and Pest Management Practices in North*

Dakota, 2008; North Dakota State University in cooperation with North Dakota Agricultural Statistics Service, Extension Publication W-1446; Fargo, ND, 2009.
80. Johnson, J., Monitoring surface waters for pesticides in North Dakota. In *2012 North Dakota Water Quality Monitoring Conference* Bismarck, ND, 2012.
81. Page, S. E.; Arnold, W. A.; McNeill, K., Terephthalate as a probe for photochemically generated hydroxyl radical. *J. Environ. Monit.* **2010,** *12*, 1658-1665.
82. Ryan, C. C.; Tan, D. T.; Arnold, W. A., Direct and indirect photolysis of sulfamethoxazole and trimethoprim in wastewater treatment plant effluent. *Water Res.* **2011,** *45*, 1280-1286.
83. Leifer, A., *The Kinetics of Environmental Aquatic Photochemistry: Theory and Practice*. American Chemical Society: Washington, DC, 1988.
84. Zeng, T.; Chin, Y.-P.; Arnold, W. A., Potential for abiotic reduction of pesticides in prairie pothole porewaters. *Environ. Sci. Technol.* **2012,** *46*, 3177-3187.
85. Huang, J.; Mabury, S. A., Steady-state concentrations of carbonate radicals in field waters. *Environ. Toxicol. Chem.* **2000,** *19*, 2181-2188.
86. Haag, W. R.; Hoigné, J.; Gassman, E.; Braun, A., Singlet oxygen in surface waters - Part I: Furfuryl alcohol as a trapping agent. *Chemosphere* **1984,** *13*, 631-640.
87. Latch, D. E.; Packer, J. L.; Arnold, W. A.; McNeill, K., Photochemical conversion of triclosan to 2,8-dichlorodibenzo-p-dioxin in aqueous solution. *J. Photochem. Photobiol. A: Chem.* **2003,** *158*, 63-66.
88. Grebel, J. E.; Pignatello, J. J.; Mitch, W. A., Sorbic acid as a quantitative probe for the formation, scavenging and steady-state concentrations of the triplet-excited state of organic compounds. *Water Res.* **2011,** *45*, 6535-6544.
89. Magazinovic, R. S.; Nicholson, B. C.; Mulcahy, D. E.; Davey, D. E., Bromide levels in natural waters: its relationship to levels of both chloride and total dissolved solids and the implications for water treatment. *Chemosphere* **2004,** *57*, 329-335.
90. Fischer, A. M.; Kliger, D. S.; Winterle, J. S.; Mill, T., Direct observation of phototransients in natural waters. *Chemosphere* **1985,** *14*, 1299-1306.
91. Thomas-Smith, T. E.; Blough, N. V., Photoproduction of hydrated electron from constituents of natural waters. *Environ. Sci. Technol.* **2001,** *35*, 2721-2726.
92. Wang, W.; Zafiriou, O. C.; Chan, I.-Y.; Zepp, R. G.; Blough, N. V., Production of hydrated electrons from photoionization of dissolved organic matter in natural waters. *Environ. Sci. Technol.* **2007,** *41*, 1601-1607.
93. Zepp, R. G.; Baughman, G. L.; Schlotzhauer, P. F., Comparison of photochemical behavior of various humic substances in water: II. Photosensitized oxygenations. *Chemosphere* **1981,** *10*, 119-126.
94. Draper, W. M.; Crosby, D. G., The photochemical generation of hydrogen peroxide in natural waters. *Arch. Environ. Contam. Toxicol.* **1983,** *12*, 121-126.
95. Haag, W. R.; Hoigné, J., Photo-sensitized oxidation in natural water via $^{\bullet}OH$ radicals. *Chemosphere* **1985,** *14*, 1659-1671.
96. Haag, W. R.; Hoigné, J., Singlet oxygen in surface waters. 3. Photochemical formation and steady-state concentrations in various types of waters. *Environ. Sci. Technol.* **1986,** *20*, 341-348.

97. Cooper, W. J.; Zika, R. G.; Petasne, R. G.; Fischer, A. M., Sunlight-induced photochemistry of humic substances in natural waters: Major reactive species. In *Aquatic Humic Substances*, Suffet, I. H.; MacCarthy, P., Eds. American Chemical Society: Washington DC, 1989; Vol. 219, pp 333-362.
98. Hoigné, J.; Faust, B. C.; Haag, W. R.; Scully, F. E.; Zepp, R. G., Aquatic humic substances as sources and sinks of photochemically produced transient reactants. In *Aquatic Humic Substances*, Suffet, I. H.; MacCarthy, P., Eds. American Chemical Society: Washington DC, 1989; Vol. 219, pp 363-381.
99. Mopper, K.; Zhou, X., Hydroxyl radical photoproduction in the sea and its potential impact on marine processes. *Science* **1990,** *250*, 661-664.
100. Larson, R. A.; Zepp, R. G., Reactivity of the carbonate radical with aniline derivatives. *Environ. Toxicol. Chem.* **1988,** *7*, 265-274.
101. Brezonik, P. L.; Fulkerson-Brekken, J., Nitrate-induced photolysis in natural waters: Controls on concentrations of hydroxyl radical photo-intermediates by natural scavenging agents. *Environ. Sci. Technol.* **1998,** *32*, 3004-3010.
102. Westerhoff, P.; Mezyk, S. P.; Cooper, W. J.; Minakata, D., Electron pulse radiolysis determination of hydroxyl radical rate constants with Suwannee River fulvic acid and other dissolved organic matter isolates. *Environ. Sci. Technol.* **2007,** *41*, 4640-4646.
103. McKay, G.; Dong, M. M.; Kleinman, J. L.; Mezyk, S. P.; Rosario-Ortiz, F. L., Temperature dependence of the reaction between the hydroxyl radical and organic matter. *Environ. Sci. Technol.* **2011,** *45*, 6932-6937.
104. Katsoyiannis, I. A.; Canonica, S.; von Gunten, U., Efficiency and energy requirements for the transformation of organic micropollutants by ozone, O_3/H_2O_2 and UV/H_2O_2. *Water Res.* **2011,** *45*, 3811-3822.
105. Wenk, J.; von Gunten, U.; Canonica, S., Effect of dissolved organic matter on the transformation of contaminants induced by excited triplet states and the hydroxyl radical. *Environ. Sci. Technol.* **2011,** *45*, 1334-1340.
106. Wenk, J.; Canonica, S., Phenolic antioxidants inhibit the triplet-induced transformation of anilines and sulfonamide antibiotics in aqueous solution. *Environ. Sci. Technol.* **2012,** *46*, 5455-5462.
107. Latch, D. E.; McNeill, K., Microheterogeneity of singlet oxygen distributions in irradiated humic acid solutions. *Science* **2006,** *311*, 1743-1747.
108. Grandbois, M.; Latch, D. E.; McNeill, K., Microheterogeneous concentrations of singlet oxygen in natural organic matter isolate solutions. *Environ. Sci. Technol.* **2008,** *42*, 9184-9190.
109. Canonica, S.; Hellrung, B.; Wirz, J., Oxidation of phenols by triplet aromatic ketones in aqueous solution. *J. Phys. Chem. A* **2000,** *104*, 1226-1232.
110. Richard, C.; Trubetskaya, O.; Trubetskoj, O.; Reznikova, O.; Afanas'eva, G.; Aguer, J. P.; Guyot, G., Key role of the low molecular size fraction of soil humic acids for fluorescence and photoinductive activity. *Environ. Sci. Technol.* **2004,** *38*, 2052-2057.
111. Halladja, S.; ter Halle, A.; Aguer, J.-P.; Boulkamh, A.; Richard, C., Inhibition of humic substances mediated photooxygenation of furfuryl alcohol by 2,4,6-

trimethylphenol. Evidence for reactivity of the phenol with humic triplet excited states. *Environ. Sci. Technol.* **2007,** *41*, 6066-6073.
112. Cawley, K. M.; Hakala, J. A.; Chin, Y.-P., Evaluating the triplet state photoreactivity of dissolved organic matter isolated by chromatography and ultrafiltration using an alkylphenol probe molecule. *Limnol. Oceanogr.: Methods* **2009,** *7*, 391-398.
113. Cavani, L.; Halladja, S.; ter Halle, A.; Guyot, G.; Corrado, G.; Ciavatta, C.; Boulkamh, A.; Richard, C., Relationship between photosensitizing and emission properties of peat humic acid fractions obtained by tangential ultrafiltration. *Environ. Sci. Technol.* **2009,** *43*, 4348-4354.
114. Guerard, J.; Miller, P.; Trouts, T.; Chin, Y.-P., The role of fulvic acid composition in the photosensitized degradation of aquatic contaminants. *Aquat. Sci.* **2009,** *71*, 160-169.
115. Waiser, M.; Robarts, R., Photodegradation of DOC in a shallow prairie wetland: Evidence from seasonal changes in DOC optical properties and chemical characteristics. *Biogeochemistry* **2004,** *69*, 263-284.
116. Kamiya, M.; Kameyama, K., Effects of selected metal ions on photodegradation of organophosphorus pesticides sensitized by humic acids. *Chemosphere* **2001,** *45*, 231-235.
117. Rejto, M.; Saltzman, S.; Acher, A. J.; Muszkat, L., Identification of sensitized photooxidation products of *s*-triazine herbicides in water. *J. Agric. Food. Chem.* **1983,** *31*, 138-142.
118. Torrents, A.; Anderson, B. G.; Bilboulian, S.; Johnson, W. E.; Hapeman, C. J., Atrazine photolysis: Mechanistic investigations of direct and nitrate-mediated hydroxy radical processes and the influence of dissolved organic carbon from the Chesapeake Bay. *Environ. Sci. Technol.* **1997,** *31*, 1476-1482.
119. Hartenbach, A. E.; Hofstetter, T. B.; Tentscher, P. R.; Canonica, S.; Berg, M.; Schwarzenbach, R. P., Carbon, hydrogen, and nitrogen isotope fractionation during light-induced transformations of atrazine. *Environ. Sci. Technol.* **2008,** *42*, 7751-7756.
120. Konstantinou, I. K.; Zarkadis, A. K.; Albanis, T. A., Photodegradation of selected herbicides in various natural waters and soils under environmental conditions. *J. Environ. Qual.* **2001,** *30*, 121-130.
121. Navarro, S.; Vela, N.; Jose, G. M.; Navarro, G., Persistence of four s-triazine herbicides in river, sea and groundwater samples exposed to sunlight and darkness under laboratory conditions. *Sci. Total Environ.* **2004,** *329*, 87-97.
122. Prosen, H.; Zupančič-Kralj, L., Evaluation of photolysis and hydrolysis of atrazine and its first degradation products in the presence of humic acids. *Environ. Pollut.* **2005,** *133*, 517-529.
123. Rebelo, S.; Melo, A.; Coimbra, R.; Azenha, M.; Pereira, M.; Burrows, H.; Sarakha, M., Photodegradation of atrazine and ametryn with visible light using water soluble porphyrins as sensitizers. *Environ. Chem. Lett.* **2007,** *5*, 29-33.
124. Kochany, J.; Maguire, R. J., Sunlight photodegradation of metolachlor in water. *J. Agric. Food. Chem.* **1994,** *42*, 406-412.

125. Vialaton, D.; Bagli, D.; Richard, C.; Skejo-Andresen, H.; Paya-Perez, A. B.; Larsen, B., Photochemical transformation of priority organic chemicals and pesticides in water. *Fresenius Environ. Bull.* **2001,** *10*, 554-560.
126. Wilson, R. I.; Mabury, S. A., Photodegradation of metolachlor: Isolation, identification, and quantification of monochloroacetic acid. *J. Agric. Food. Chem.* **2000,** *48*, 944-950.
127. Hua, R.; Yue, Y.; Fan, D., The photodegradation of acetochlor in water. *Chin. J. Pestic. Sci.* **2000,** *2*, 71-74.
128. Chaabane, H.; Vulliet, E.; Joux, F.; Lantoine, F.; Conan, P.; Cooper, J.-F.; Coste, C.-M., Photodegradation of sulcotrione in various aquatic environments and toxicity of its photoproducts for some marine micro-organisms. *Water Res.* **2007,** *41*, 1781-1789.
129. Coelho, C.; Cavani, L.; Halle, A. t.; Guyot, G.; Ciavatta, C.; Richard, C., Rates of production of hydroxyl radicals and singlet oxygen from irradiated compost. *Chemosphere* **2011,** *85*, 630-636.
130. Amine-Khodja, A.; Boulkamh, A.; Boule, P., Photochemical behaviour of phenylurea herbicides. *Photochem. Photobiol. Sci.* **2004,** *3*, 145-156.
131. Al Housari, F.; Vione, D.; Chiron, S.; Barbati, S., Reactive photoinduced species in estuarine waters. Characterization of hydroxyl radical, singlet oxygen and dissolved organic matter triplet state in natural oxidation processes. *Photochem. Photobiol. Sci.* **2010,** *9*, 78-86.
132. Peschka, M.; Petrovic, M.; Knepper, T.; Barceló, D., Determination of two phototransformation products of bentazone using quadrupole time-of-flight mass spectrometry. *Anal. Bioanal. Chem.* **2007,** *388*, 1227-1234.
133. Eyheraguibel, B.; ter Halle, A.; Richard, C., Photodegradation of bentazon, clopyralid, and triclopyr on model leaves: Importance of a systematic evaluation of pesticide photostability on crops. *J. Agric. Food. Chem.* **2009,** *57*, 1960-1966.
134. Barceló, D.; Durand, G.; De Bertrand, N., Photodegradation of the organophosphorus pesticides chlorpyrifos, fenamiphos and vamidothion in water. *Toxicol. Environ. Chem.* **1993,** *38*, 183-199.
135. Bavcon Kralj, M.; Franko, M.; Trebše, P., Photodegradation of organophosphorus insecticides - Investigations of products and their toxicity using gas chromatography-mass spectrometry and AChE-thermal lens spectrometric bioassay. *Chemosphere* **2007,** *67*, 99-107.
136. Dilling, W. L.; Lickly, L. C.; Lickly, T. D.; Murphy, P. G.; McKellar, R. L., Organic photochemistry. 19. Quantum yields for *O,O*-diethyl *O*-(3,5,6-trichloro-2-pyridinyl) phosphorothioate (chlorpyrifos) and 3,5,6-trichloro-2-pyridinol in dilute aqueous solutions and their environmental phototransformation rates. *Environ. Sci. Technol.* **1984,** *18*, 540-543.
137. Wu, X.; Hua, R.; Tang, F.; Li, X.; Cao, H.; Yue, Y., Photochemical degradation of chlorpyrifos in water. *Chin. J. Appl. Ecol.* **2006,** *17*, 1301-1304.
138. Vialaton, D.; Pilichowski, J.-F.; Baglio, D.; Paya-Perez, A.; Larsen, B.; Richard, C., Phototransformation of propiconazole in aqueous media. *J. Agric. Food. Chem.* **2001,** *49*, 5377-5382.

139. Vialaton, D.; Richard, C., Phototransformation of aromatic pollutants in solar light: Photolysis versus photosensitized reactions under natural water conditions. *Aquat. Sci.* **2002,** *64*, 207-215.
140. Dimou, A. D.; Sakkas, V. A.; Albanis, T. A., Photodegradation of trifluralin in natural waters and soils: Degradation kinetics and influence of organic matter. *Int. J. Environ. Anal. Chem.* **2004,** *84*, 173-182.
141. Tagle, M. G. S.; Salum, M. L.; Bujan, E. I.; Arguello, G. A., Time evolution and competing pathways in photodegradation of trifluralin and three of its major degradation products. *Photochem. Photobiol. Sci.* **2005,** *4*, 869-875.
142. Canonica, S.; Jans, U.; Stemmler, K.; Hoigné, J., Transformation kinetics of phenols in water: Photosensitization by dissolved natural organic material and aromatic ketones. *Environ. Sci. Technol.* **1995,** *29*, 1822-1831.
143. Dalzell, B. J.; King, J. Y.; Mulla, D. J.; Finlay, J. C.; Sands, G. R., Influence of subsurface drainage on quantity and quality of dissolved organic matter export from agricultural landscapes. *J. Geophys. Res.* **2011,** *116*, G02023.

Chapter 5 References

1. van der Valk, A. G., The prairie potholes of North America. In *The World's Largest Wetlands*, Fraser, L. H.; Keddy, P. A., Eds. Cambridge University Press: Cambridge, UK, 2005; pp 393-423.
2. LaBaugh, J. W., Chemical characteristics of water in northern prairie wetlands. In *Northern Prairie Wetlands*, Van der Valk, A. G., Ed. Iowa State University Press: Ames, IA, 1989; pp 56-90.
3. Last, W. M.; Ginn, F. M., Saline systems of the Great Plains of western Canada: An overview of the limnogeology and paleolimnology. *Saline Syst.* **2005,** *1*, 1-38.
4. Last, W., Chemical composition of saline and subsaline lakes of the northern Great Plains, western Canada. *Int. J. Salt Lake Res.* **1992,** *1*, 47-76.
5. Waiser, M. J.; Robarts, R. D., Microbial nutrient limitation in prairie saline lakes with high sulfate concentration. *Limnol. Oceanogr.* **1995,** *40*, 566-574.
6. Zeng, T.; Ziegelgruber, K. L.; Chin, Y.-P.; Arnold, W. A., Pesticide processing potential in prairie pothole porewaters. *Environ. Sci. Technol.* **2011,** *45*, 6814-6822.
7. Van Stempvoort, D. R.; Hendry, M. J.; Schoenau, J. J.; Krouse, H. R., Sources and dynamics of sulfur in weathered till, Western Glaciated Plains of North America. *Chem. Geol.* **1994,** *111*, 35-56.
8. Goldhaber, M. B.; Mills, C. T.; Stricker, C. A.; Morrison, J. M., The role of critical zone processes in the evolution of the Prairie Pothole Region wetlands. *Appl. Geochem.* **2011,** *26, Supplement*, S32-S35.
9. Heagle, D.; Hayashi, M.; van der Kamp, G., Use of solute mass balance to quantify geochemical processes in a prairie recharge wetland. *Wetlands* **2007,** *27*, 806-818.
10. LaBaugh, J. W.; Winter, T. C.; Swanson, G. A.; Rosenberry, D. O.; Nelson, R. D.; Euliss, N. H., Changes in atmospheric circulation patterns affect midcontinent wetlands sensitive to climate. *Limnol. Oceanogr.* **1996,** *41*, 864-870.
11. Mills, C. T.; Goldhaber, M. B.; Stricker, C. A.; Holloway, J. M.; Morrison, J. M.; Ellefsen, K. J.; Rosenberry, D. O.; Thurston, R. S., Using stable isotopes to understand hydrochemical processes in and around a Prairie Pothole wetland in the Northern Great Plains, USA. *Appl. Geochem.* **2011,** *26, Supplement*, S97-S100.
12. Biondini, M. E.; Arndt, J. L. *The biogeochemistry of carbon, nitrogen and sulfur transformations in seasonal and semipermanent wetlands*; North Dakota Water Research Institute Technical Report No. ND90-05; Fargo, ND, 1993.
13. Sando, S. K. K., D.P.; Johnson, K. M.; Lundgren, R. F.; Emerson, D. G. *Mercury and methylmercury in water and bottom sediments of wetlands at Lostwood National Wildlife Refuge, North Dakota, 2003-04*; U.S. Geological Survey, Scientific Investigations Report 2007-5219; Reston, VA, 2007; pp 1-74.
14. Hall, B. D.; Baron, L. A.; Somers, C. M., Mercury concentrations in surface water and harvested waterfowl from the prairie pothole region of Saskatchewan. *Environ. Sci. Technol.* **2009,** *43*, 8759-8766.

15. Bates, L. M.; Hall, B. D., Concentrations of methylmercury in invertebrates from wetlands of the Prairie Pothole Region of North America. *Environ. Pollut.* **2012,** *160*, 153-160.
16. Xia, K.; Skyllberg, U. L.; Bleam, W. F.; Bloom, P. R.; Nater, E. A.; Helmke, P. A., X-ray absorption spectroscopic evidence for the complexation of Hg(II) by reduced sulfur in soil humic substances. *Environ. Sci. Technol.* **1999,** *33*, 257-261.
17. Hesterberg, D.; Chou, J. W.; Hutchison, K. J.; Sayers, D. E., Bonding of Hg(II) to reduced organic sulfur in humic acid as affected by S/Hg ratio. *Environ. Sci. Technol.* **2001,** *35*, 2741-2745.
18. Skyllberg, U.; Xia, K.; Bloom, P. R.; Nater, E. A.; Bleam, W. F., Binding of mercury(II) to reduced sulfur in soil organic matter along upland-peat soil transects. *J. Environ. Qual.* **2000,** *29*, 855-865.
19. Wolfenden, S.; Charnock, J. M.; Hilton, J.; Livens, F. R.; Vaughan, D. J., Sulfide species as a sink for mercury in lake sediments. *Environ. Sci. Technol.* **2005,** *39*, 6644-6648.
20. Yoon, S.-J.; Diener, L. M.; Bloom, P. R.; Nater, E. A.; Bleam, W. F., X-ray absorption studies of CH_3Hg^+-binding sites in humic substances. *Geochim. Cosmochim. Acta* **2005,** *69*, 1111-1121.
21. Skyllberg, U.; Bloom, P. R.; Qian, J.; Lin, C.-M.; Bleam, W. F., Complexation of mercury(II) in soil organic matter: EXAFS evidence for linear two-coordination with reduced sulfur groups. *Environ. Sci. Technol.* **2006,** *40*, 4174-4180.
22. Skyllberg, U., Competition among thiols and inorganic sulfides and polysulfides for Hg and MeHg in wetland soils and sediments under suboxic conditions: Illumination of controversies and implications for MeHg net production. *J. Geophys. Res.* **2008,** *113*, G00C03.
23. Skyllberg, U.; Drott, A., Competition between disordered iron sulfide and natural organic matter associated thiols for mercury(II) - An EXAFS study. *Environ. Sci. Technol.* **2010,** *44*, 1254-1259.
24. Nagy, K. L.; Manceau, A.; Gasper, J. D.; Ryan, J. N.; Aiken, G. R., Metallothionein-like multinuclear clusters of mercury(II) and sulfur in peat. *Environ. Sci. Technol.* **2011,** *45*, 7298-7306.
25. LaBaugh, J. W.; Winter, T. C.; Rosenberry, D. O., Hydrological functions of prairie wetlands. *Great Plains Res.* **1998,** *8*, 17-37.
26. Johnson, W. C.; Millett, B. V.; Gilmanov, T.; Voldseth, R. A.; Guntenspergen, G. R.; Naugle, D. E., Vulnerability of northern prairie wetlands to climate change. *Bioscience* **2005,** *55*, 863-872.
27. Adamus, P. R. *Condition, values, and loss of natural functions of prairie wetlands of the north-central United States*; EPA 600-R-92-249; U.S. Environmental Protection Agency: Washington, DC, 1998. http://water.epa.gov/type/wetlands/assessment/appendixb.cfm (Accessed July, 2012).
28. Jokic, A.; Cutler, J. N.; Ponomarenko, E.; van der Kamp, G.; Anderson, D. W., Organic carbon and sulphur compounds in wetland soils: Insights on structure and transformation processes using *K*-edge XANES and NMR spectroscopy. *Geochim. Cosmochim. Acta* **2003,** *67*, 2585-2597.

29. Johnson, R. R.; Oslund, F. T.; Hertel, D. R., The past, present, and future of prairie potholes in the United States. *J. Soil Water Conserv.* **2008,** *63*, 84A-87A.
30. Neely, R. K.; Baker, J. L., Nitrogen and phosphorous dynamics and the fate of agricultural runoff. In *Northern Prairie Wetlands*, Van der Valk, A. G., Ed. Iowa State University Press: Ames, IA, 1989; pp 92-131.
31. Olness, A.; Staricka, J. A.; Daniel, J. A., Oxidation-reduction and groundwater contamination in the Prairie Pothole region of the Northern Great Plains. In *Water for Agriculture and Wildlife and the Environment -- Win-Win Opportunities: Proceedings of the 1996 USCID Wetlands Seminar*, Schaack, J.; Anderson, S. S., Eds. U.S. Committee on Irrigation and Drainage: Denver, CO, 1996; pp 115-131.
32. Goldsborough, L. G.; Crumpton, W. G., Distribution and environmental fate of pesticides in prairie wetlands. *Great Plains Res.* **1998,** *8*, 73-95.
33. Detenbeck, N. E.; Elonen, C. M.; Taylor, D. L.; Cotter, A. M.; Puglisi, F. A.; Sanville, W. D., Effects of agricultural activities and best management practices on water quality of seasonal prairie pothole wetlands. *Wetlands Ecol. Manage.* **2002,** *10*, 335-354.
34. Zeng, T.; Chin, Y.-P.; Arnold, W. A., Potential for abiotic reduction of pesticides in prairie pothole porewaters. *Environ. Sci. Technol.* **2012,** *46*, 3177-3187.
35. Gleason, R. A.; Tangen, B. A.; Browne, B. A.; Euliss Jr, N. H., Greenhouse gas flux from cropland and restored wetlands in the Prairie Pothole Region. *Soil Biol. Biochem.* **2009,** *41*, 2501-2507.
36. Pennock, D.; Yates, T.; Bedard-Haughn, A.; Phipps, K.; Farrell, R.; McDougal, R., Landscape controls on N_2O and CH_4 emissions from freshwater mineral soil wetlands of the Canadian Prairie Pothole region. *Geoderma* **2010,** *155*, 308-319.
37. Badiou, P.; McDougal, R.; Pennock, D.; Clark, B., Greenhouse gas emissions and carbon sequestration potential in restored wetlands of the Canadian prairie pothole region. *Wetlands Ecol. Manage.* **2011,** *19*, 237-256.
38. Urban, N. R., Retention of sulfur in lake sediments. In *Environmental Chemistry of Lakes and Reservoirs*, Baker, L. A., Ed. American Chemical Society: Washington, DC, 1994; Vol. 237, pp 323-369.
39. Holmer, M.; Storkholm, P., Sulphate reduction and sulphur cycling in lake sediments: a review. *Freshwat. Biol.* **2001,** *46*, 431-451.
40. Vairavamurthy, M. A.; Orr, W. L.; Manowitz, B., Geochemical transformations of sedimentary sulfur: An introduction. In *Geochemical Transformations of Sedimentary Sulfur*, Vairavamurthy, M. A.; Schoonen, M. A. A.; Eglinton, T. I.; Luther III, G. W.; Manowitz, B., Eds. American Chemical Society: Washington, DC, 1995; Vol. 612, pp 1-14.
41. Elsgaard, L.; Jørgensen, B. B., Anoxie transformations of radiolabeled hydrogen sulfide in marine and freshwater sediments. *Geochim. Cosmochim. Acta* **1992,** *56*, 2425-2435.
42. Rickard, D. T., Kinetics and mechanism of pyrite formation at low temperatures. *Am. J. Sci.* **1975,** *275*, 636-652.
43. Pyzik, A. J.; Sommer, S. E., Sedimentary iron monosulfides: Kinetics and mechanism of formation. *Geochim. Cosmochim. Acta* **1981,** *45*, 687-698.

44. Aller, R. C.; Rude, P. D., Complete oxidation of solid phase sulfides by manganese and bacteria in anoxic marine sediments. *Geochim. Cosmochim. Acta* **1988,** *52*, 751-765.
45. Jørgensen, B. B., The sulfur cycle of freshwater sediments: Role of thiosulfate. *Limnol. Oceanogr.* **1990,** *35*, 1329-1342.
46. King, G. M., Effects of added manganic and ferric oxides on sulfate reduction and sulfide oxidation in intertidal sediments. *FEMS Microbiol. Lett.* **1990,** *73*, 131-138.
47. Guerin, W. F.; Braman, R. S., Patterns of organic and inorganic sulfur transformations in sediments. *Org. Geochem.* **1985,** *8*, 259-268.
48. Vairavamurthy, A.; Mopper, K., Geochemical formation of organosulphur compounds (thiols) by addition of H_2S to sedimentary organic matter. *Nature* **1987,** *329*, 623-625.
49. Francois, R., A study of sulphur enrichment in the humic fraction of marine sediments during early diagenesis. *Geochim. Cosmochim. Acta* **1987,** *51*, 17-27.
50. Kohnen, M. E. L.; Sinninghe Damsté, J. S.; ten Haven, H. L.; de Leeuw, J. W., Early incorporation of polysulphides in sedimentary organic matter. *Nature* **1989,** *341*, 640-641.
51. Aizenshtat, Z.; Krein, E. B.; Vairavamurthy, M. A.; Goldstein, T. P., Role of sulfur in the transformations of sedimentary organic matter: A mechanistic overview. In *Geochemical Transformations of Sedimentary Sulfur*, Vairavamurthy, M. A.; Schoonen, M. A. A.; Eglinton, T. I.; Luther III, G. W.; Manowitz, B., Eds. American Chemical Society: Washington, DC, 1995; Vol. 612, pp 16-37.
52. Adam, P.; Philippe, E.; Albrecht, P., Photochemical sulfurization of sedimentary organic matter: A widespread process occurring at early diagenesis in natural environments? *Geochim. Cosmochim. Acta* **1998,** *62*, 265-271.
53. Berner, R. A., Sedimentary pyrite formation: An update. *Geochim. Cosmochim. Acta* **1984,** *48*, 605-615.
54. Canfield, D. E., Reactive iron in marine sediments. *Geochim. Cosmochim. Acta* **1989,** *53*, 619-632.
55. Canfield, D. E.; Raiswell, R.; Bottrell, S. H., The reactivity of sedimentary iron minerals toward sulfide. *Am. J. Sci.* **1992,** *292*, 659-683.
56. Rickard, D.; Luther III, G. W., Chemistry of iron sulfides. *Chem. Rev.* **2007,** *107*, 514-562.
57. Gransch, J. A.; Posthuma, J., On the origin of sulphur in crudes. In *Advances in Organic Geochemistry*, Tissot, B.; Bienner, F., Eds. Editions Technip: Paris, France, 1973; pp 727-739.
58. Luther III, G. W.; Church, T. M., An overview of the environmental chemistry of sulphur in wetland systems. In *Sulphur Cycling on the Continents: Wetlands, Terrestrial Ecosystems, and Associated Water Bodies*, Howarth, R. W.; Stewart, J. W. B.; Ivanov, M. V., Eds. SCOPE, John Wiley & Sons, Inc.: Somerset, NJ, 1992; pp 125-142.
59. Ferdelman, T. G.; Church, T. M.; Luther III, G. W., Sulfur enrichment of humic substances in a Delaware salt marsh sediment core. *Geochim. Cosmochim. Acta* **1991,** *55*, 979-988.

60. Mossmann, J.-R.; Aplin, A. C.; Curtis, C. D.; Coleman, M. L., Geochemistry of inorganic and organic sulphur in organic-rich sediments from the Peru Margin. *Geochim. Cosmochim. Acta* **1991,** *55*, 3581-3595.
61. Vairavamurthy, M. A.; Zhou, W.; Eglinton, T.; Manowitz, B., Sulfonates: A novel class of organic sulfur compounds in marine sediments. *Geochim. Cosmochim. Acta* **1994,** *58*, 4681-4687.
62. Suits, N. S.; Arthur, M. A., Sulfur diagenesis and partitioning in Holocene Peru shelf and upper slope sediments. *Chem. Geol.* **2000,** *163*, 219-234.
63. Bates, A. L.; Spiker, E. C.; Hatcher, P. G.; Stout, S. A.; Weintraub, V. C., Sulfur geochemistry of organic-rich sediments from Mud Lake, Florida, U.S.A. *Chem. Geol.* **1995,** *121*, 245-262.
64. Brüchert, V.; Pratt, L. M., Contemporaneous early diagenetic formation of organic and inorganic sulfur in estuarine sediments from St. Andrew Bay, Florida, USA. *Geochim. Cosmochim. Acta* **1996,** *60*, 2325-2332.
65. Urban, N. R.; Ernst, K.; Bernasconi, S., Addition of sulfur to organic matter during early diagenesis of lake sediments. *Geochim. Cosmochim. Acta* **1999,** *63*, 837-853.
66. Filley, T. R.; Freeman, K. H.; Wilkin, R. T.; Hatcher, P. G., Biogeochemical controls on reaction of sedimentary organic matter and aqueous sulfides in holocene sediments of Mud Lake, Florida. *Geochim. Cosmochim. Acta* **2002,** *66*, 937-954.
67. Freney, J., Some observations on the nature of organic sulphur compounds in soil. *Aust. J. Agric. Res.* **1961,** *12*, 424-432.
68. Pruden, G.; Bloomfield, C., The determination of iron(II) sulphide in soil in the presence of iron(III) oxide. *Analyst* **1968,** *93*, 532-534.
69. Freney, J. R.; Melville, G. E.; Williams, C. H., The determination of carbon bonded sulfur in soil. *Soil Sci.* **1970,** *109*, 310-318.
70. Dick, W. A.; Tabatabai, M. A., Ion chromatographic determination of sulfate and nitrate in soils. *Soil Sci. Soc. Am. J.* **1979,** *43*, 899-904.
71. Canfield, D. E.; Raiswell, R.; Westrich, J. T.; Reaves, C. M.; Berner, R. A., The use of chromium reduction in the analysis of reduced inorganic sulfur in sediments and shales. *Chem. Geol.* **1986,** *54*, 149-155.
72. Rickard, D.; Morse, J. W., Acid volatile sulfide (AVS). *Mar. Chem.* **2005,** *97*, 141-197.
73. Lombi, E.; Hettiarachchi, G. M.; Scheckel, K. G., Advanced in situ spectroscopic techniques and their applications in Environmental Biogeochemistry: Introduction to the special section. *J. Environ. Qual.* **2011,** *40*, 659-666.
74. Fleet, M. E., XANES spectroscopy of sulfur in earth materials. *The Canadian Mineralogist* **2005,** *43*, 1811-1838.
75. Jalilehvand, F., Sulfur: Not a "silent" element any more. *Chem. Soc. Rev.* **2006,** *35*, 1256-1268.
76. Thieme, J.; McNult, I.; Vogt, S.; Paterson; David, X-ray spectromicroscopy - A tool for Environmental Sciences. *Environ. Sci. Technol.* **2007,** *41*, 6885-6889.
77. Lombi, E.; Susini, J., Synchrotron-based techniques for plant and soil science: Opportunities, challenges and future perspectives. *Plant Soil* **2009,** *320*, 1-35.

78. Vairavamurthy, M. A.; Wang, S.; Khandelwal, B.; Manowitz, B.; Ferdelman, T.; Fossing, H., Sulfur transformations in early diagenetic sediments from the Bay of Conception, off Chile. In *Geochemical Transformations of Sedimentary Sulfur*, Vairavamurthy, M. A.; Schoonen, M. A. A.; Eglinton, T. I.; Luther III, G. W.; Manowitz, B., Eds. American Chemical Society: Washington, DC, 1995; Vol. 612, pp 38-58.
79. Morra, M. J.; Fendorf, S. E.; Brown, P. D., Speciation of sulfur in humic and fulvic acids using X-ray absorption near-edge structure (XANES) spectroscopy. *Geochim. Cosmochim. Acta* **1997,** *61*, 683-688.
80. Vairavamurthy, M. A.; Maletic, D.; Wang, S.; Manowitz, B.; Eglinton, T.; Lyons, T., Characterization of sulfur-containing functional groups in sedimentary humic substances by X-ray absorption near-edge structure spectroscopy. *Energy Fuels* **1997,** *11*, 546-553.
81. Xia, K.; Weesner, F.; Bleam, W. F.; Helmke, P. A.; Bloom, P. R.; Skyllberg, U. L., XANES studies of oxidation states of sulfur in aquatic and soil humic substances. *Soil Sci. Soc. Am. J.* **1998,** *62*, 1240-1246.
82. Hutchison, K. J.; Hesterberg, D.; Chou, J. W., Stability of reduced organic sulfur in humic acid as affected by aeration and pH. *Soil Sci. Soc. Am. J.* **2001,** *65*, 704-709.
83. Prietzel, J.; Thieme, J.; Neuhäusler, U.; Susini, J.; Kögel-Knabner, I., Speciation of sulphur in soils and soil particles by X-ray spectromicroscopy. *Eur. J. Soil Sci.* **2003,** *54*, 423-433.
84. Solomon, D.; Lehmann, J.; Martínez, C. E., Sulfur *K*-edge XANES spectroscopy as a tool for understanding sulfur dynamics in soil organic matter. *Soil Sci. Soc. Am. J.* **2003,** *67*, 1721-1731.
85. Bostick, B. C.; Theissen, K. M.; Dunbar, R. B.; Vairavamurthy, M. A., Record of redox status in laminated sediments from Lake Titicaca: A sulfur *K*-edge X-ray absorption near edge structure (XANES) study. *Chem. Geol.* **2005,** *219*, 163-174.
86. Solomon, D.; Lehmann, J.; Lobe, I.; Martinez, C. E.; Tveitnes, S.; Du Preez, C. C.; Amelung, W., Sulphur speciation and biogeochemical cycling in long-term arable cropping of subtropical soils: evidence from wet-chemical reduction and S *K*-edge XANES spectroscopy. *Eur. J. Soil Sci.* **2005,** *56*, 621-634.
87. Zhao, F. J.; Lehmann, J.; Solomon, D.; Fox, M. A.; McGrath, S. P., Sulphur speciation and turnover in soils: Evidence from sulphur *K*-edge XANES spectroscopy and isotope dilution studies. *Soil Biol. Biochem.* **2006,** *38*, 1000-1007.
88. Einsiedl, F.; Schäfer, T.; Northrup, P., Combined sulfur *K*-edge XANES spectroscopy and stable isotope analyses of fulvic acids and groundwater sulfate identify sulfur cycling in a karstic catchment area. *Chem. Geol.* **2007,** *238*, 268-276.
89. Prietzel, J.; Thieme, J.; Salomé, M.; Knicker, H., Sulfur *K*-edge XANES spectroscopy reveals differences in sulfur speciation of bulk soils, humic acid, fulvic acid, and particle size separates. *Soil Biol. Biochem.* **2007,** *39*, 877-890.
90. Schroth, A. W.; Bostick, B. C.; Graham, M.; Kaste, J. M.; Mitchell, M. J.; Friedland, A. J., Sulfur species behavior in soil organic matter during decomposition. *J. Geophys. Res.* **2007,** *112*, G04011.

91. Einsiedl, F.; Mayer, B.; Schäfer, T., Evidence for incorporation of H_2S in groundwater fulvic acids from stable isotope ratios and sulfur *K*-edge X-ray absorption near edge structure spectroscopy. *Environ. Sci. Technol.* **2008,** *42*, 2439-2444.
92. Prietzel, J.; Thieme, J.; Herre, A.; Salomé, M.; Eichert, D., Differentiation between adsorbed and precipitated sulphate in soils and at micro-sites of soil aggregates by sulphur *K*-edge XANES. *Eur. J. Soil Sci.* **2008,** *59*, 730-743.
93. Prietzel, J.; Thieme, J.; Tyufekchieva, N.; Paterson, D.; McNulty, I.; Kögel-Knabner, I., Sulfur speciation in well-aerated and wetland soils in a forested catchment assessed by sulfur *K*-edge X-ray absorption near-edge spectroscopy (XANES). *J. Plant Nutr. Soil Sci.* **2009,** *172*, 393-403.
94. Prietzel, J.; Tyufekchieva, N.; Eusterhues, K.; Kögel-Knabner, I.; Thieme, J.; Paterson, D.; McNulty, I.; de Jonge, M.; Eichert, D.; Salomé, M., Anoxic versus oxic sample pretreatment: Effects on the speciation of sulfur and iron in well-aerated and wetland soils as assessed by X-ray absorption near-edge spectroscopy (XANES). *Geoderma* **2009,** *153*, 318-330.
95. Solomon, D.; Lehmann, J.; Kinyangi, J.; Pell, A.; Theis, J.; Riha, S.; Ngoze, S.; Amelung, W.; Preez, C.; Machado, S.; Ellert, B.; Janzen, H., Anthropogenic and climate influences on biogeochemical dynamics and molecular-level speciation of soil sulfur. *Ecol. Appl.* **2009,** *19*, 989-1002.
96. Burton, E. D.; Bush, R. T.; Sullivan, L. A.; Hocking, R. K.; Mitchell, D. R. G.; Johnston, S. G.; Fitzpatrick, R. W.; Raven, M.; McClure, S.; Jang, L. Y., Iron-monosulfide oxidation in natural sediments: Resolving microbially mediated S transformations using XANES, electron microscopy, and selective extractions. *Environ. Sci. Technol.* **2009,** *43*, 3128-3134.
97. Prietzel, J.; Botzaki, A.; Tyufekchieva, N.; Brettholle, M.; Thieme, J. r.; Klysubun, W., Sulfur speciation in soil by S *K*-edge XANES spectroscopy: Comparison of spectral deconvolution and linear combination fitting. *Environ. Sci. Technol.* **2011,** *45*, 2878-2886.
98. Solomon, D.; Lehmann, J.; de Zarruk, K. K.; Dathe, J.; Kinyangi, J.; Liang, B.; Machado, S., Speciation and long- and short-term molecular-level dynamics of soil organic sulfur studied by X-ray absorption near-edge structure spectroscopy. *J. Environ. Qual.* **2011,** *40*, 704-718.
99. Prietzel, J.; Kögel-Knabner, I.; Thieme, J.; Paterson, D.; McNulty, I., Microheterogeneity of element distribution and sulfur speciation in an organic surface horizon of a forested Histosol as revealed by synchrotron-based X-ray spectromicroscopy. *Org. Geochem.* **2011,** *42*, 1308-1314.
100. Burton, E. D.; Bush, R. T.; Johnston, S. G.; Sullivan, L. A.; Keene, A. F., Sulfur biogeochemical cycling and novel Fe–S mineralization pathways in a tidally re-flooded wetland. *Geochim. Cosmochim. Acta* **2011,** *75*, 3434-3451.
101. Morgan, B.; Burton, E. D.; Rate, A. W., Iron monosulfide enrichment and the presence of organosulfur in eutrophic estuarine sediments. *Chem. Geol.* **2012,** *296–297*, 119-130.
102. Vairavamurthy, M. A.; Manowitz, B.; Zhou, W.; Jeon, Y., Determination of hydrogen sulfide oxidation products by Sulfur *K*-edge X-ray absorption near-edge

structure spectroscopy. In *Environmental Geochemistry of Sulfide Oxidation*, Alpers, C. N.; Blowes, D. W., Eds. American Chemical Society: Washington DC, 1994; Vol. 550, pp 412-430.
103. Eglinton, T. I.; Irvine, J. E.; Vairavamurthy, A.; Zhou, W.; Manowitz, B., Formation and diagenesis of macromolecular organic sulfur in Peru margin sediments. *Org. Geochem.* **1994,** *22*, 781-799.
104. Mayhew, L. E.; Webb, S. M.; Templeton, A. S., Microscale imaging and identification of Fe speciation and distribution during fluid–mineral reactions under highly reducing conditions. *Environ. Sci. Technol.* **2011,** *45*, 4468-4474.
105. Lam, P. J.; Ohnemus, D. C.; Marcus, M. A., The speciation of marine particulate iron adjacent to active and passive continental margins. *Geochim. Cosmochim. Acta* **2012,** *80*, 108-124.
106. Toner, B. M.; Marcus, M. A.; Edwards, K. J.; Rouxel, O.; German, C. R., Measuring the form of iron in hydrothermal plume particles. *Oceanography* **2012,** *25*, 209-212.
107. Toner, B. M.; Berquó, T. S.; Michel, F. M.; Sorensen, J. V.; Templeton, A. S.; Edwards, K. J., Mineralogy of iron microbial mats from Loihi Seamount. *Front. Microbiol. Chem.* **2012,** *3*, 1-18.
108. Mushet, D. M.; Euliss, N. H. *The Cottonwood Lake study area, a long-term wetland ecosystem monitoring site*; U.S. Geological Survey Fact Sheet 2012-3040: Reston, VA 2012; pp 1-2.
109. Stewart, R. E.; Kantrud, H. A. *Classification of natural ponds and lakes in the glaciated prairie region*; Bureau of Sport Fisheries and Wildlife, U.S. Fish and Wildlife Service, Resource Publication 92; Washington, DC, 1971; pp 1-57.
110. Winter, T. C.; Carr, M. R. *Hydrologic setting of wetlands in the Cottonwood Lake area, Stutsman County, North Dakota*; U.S. Geological Survey Water Resources Investigations Report 80-99; Denver, CO, 1980; pp 1-42.
111. Euliss, N. H.; Mushet, D. M., A multi-year comparison of IPCI scores for prairie pothole wetlands: Implications of temporal and spatial variation. *Wetlands* **2011,** *31*, 713-723.
112. Winter, T. C.; Rosenberry, D. O., The interaction of ground water with prairie pothole wetlands in the Cottonwood Lake area, east-central North Dakota, 1979-1990. *Wetlands* **1995,** *15*, 193-211.
113. Swanson, G. A.; Winter, T. C.; Adomaitis, V. A.; Labaugh, J. W. *Chemical characteristics of prairie lakes in south-central North Dakota USA - Their potential for influencing use by fish and wildlife*; U.S. Fish and Wildlife Service, Technical Report 18; Washington, DC, 1988; pp 1-44.
114. Winter, T. C.; Rosenberry, D. O., Hydrology of prairie pothole wetlands during drought and deluge: A 17-year study of the cottonwood lake wetland complex in North Dakota in the perspective of longer term measured and proxy hydrological records. *Clim. Change* **1998,** *40*, 189-209.
115. Labaugh, J. W., Spatial and temporal variability in specific conductance and chemical characteristics of wetland water and in water column biota in the wetlands in the Cottonwood Lake area. In *Hydrological, chemical, and biological characteristics of a*

prairie pothole wetland complex under highly variable climate conditions - the Cottonwood Lake area, east-central North Dakota, U.S. Geological Survey Professional Paper 1675, Winter, T. C., Ed. U.S. Geological Survey: Denver, CO, 2003; pp 35-53.
116. Rose, C.; Crumpton, W., Effects of emergent macrophytes on dissolved oxygen dynamics in a prairie pothole wetland. *Wetlands* **1996,** *16*, 495-502.
117. Ziegelgruber, K. L.; Zeng, T.; Chin, Y.-P.; Arnold, W. A., Sources and composition of pore water dissolved organic matter in prairie pothole lakes of North Dakota, USA. *Submitted* **2012**.
118. Marcus, M. A.; MacDowell, A. A.; Celestre, R.; Manceau, A.; Miller, T.; Padmore, H. A.; Sublett, R. E., Beamline 10.3.2 at ALS: A hard X-ray microprobe for environmental and materials sciences. *J. Synchrotron Radiat.* **2004,** *11*, 239-247.
119. Marcus, M. A., X-ray photon-in/photon-out methods for chemical imaging. *TrAC, Trends Anal. Chem.* **2010,** *29*, 508-517.
120. Manceau, A.; Marcus, M. A.; Tamura, N., Quantitative speciation of heavy metals in soils and sediments by synchrotron X-ray techniques. In *Applications of synchrotron radiation in low-temperature geochemistry and environmental science*, Fenter, P. A.; Rivers, M. L.; Sturchio, N. C.; Sutton, S. R., Eds. Mineralogical Society of America: Washington, DC, 2002; Vol. 49, pp 341-428.
121. Webb, S. M., SIXpack: A graphical user interface for XAS analysis using IFEFFIT. *Phys. Scr.* **2005,** *2005*, 1011-1014.
122. Toner, B.; Manceau, A.; Webb, S. M.; Sposito, G., Zinc sorption to biogenic hexagonal-birnessite particles within a hydrated bacterial biofilm. *Geochim. Cosmochim. Acta* **2006,** *70*, 27-43.
123. Malinowski, E. R., Determination of the number of factors and the experimental error in a data matrix. *Anal. Chem.* **1977,** *49*, 612-617.
124. Malinowski, E. R., Theory of error for target factor analysis with applications to mass spectrometry and nuclear magnetic resonance spectrometry. *Anal. Chim. Acta* **1978,** *103*, 339-354.
125. Beauchemin, S.; Hesterberg, D.; Beauchemin, M., Principal component analysis approach for modeling sulfur *K*-XANES spectra of humic acids. *Soil Sci. Soc. Am. J.* **2002,** *66*, 83-91.
126. Marcus, M. A.; Westphal, A. J.; Fakra, S. C., Classification of Fe-bearing species from K-edge XANES data using two-parameter correlation plots. *J. Synchrotron Radiat.* **2008,** *15*, 463-468.
127. Zeng, T.; Arnold, W. A., Pesticide photolysis in prairie potholes: Probing photosensitized processes. *Submitted* **2012**.
128. Lovley, D. R.; Klug, M. J., Model for the distribution of sulfate reduction and methanogenesis in freshwater sediments. *Geochim. Cosmochim. Acta* **1986,** *50*, 11-18.
129. Sinke, A. J. C.; Cornelese, A. A.; Cappenberg, T. E.; Zehnder, A. J. B., Seasonal variation in sulfate reduction and methanogenesis in peaty sediments of eutrophic Lake Loosdrecht, the Netherlands. *Biogeochemistry* **1992,** *16*, 43-61.
130. Kiene, R. P.; Visscher, P. T., Production and fate of methylated sulfur compounds from methionine and dimethylsulfoniopropionate in anoxic salt marsh sediments. *Appl. Environ. Microbiol.* **1987,** *53*, 2426-2434.

131. Kiene, R. P.; Malloy, K. D.; Taylor, B. F., Sulfur-containing amino acids as precursors of thiols in anoxic coastal sediments. *Appl. Environ. Microbiol.* **1990,** *56*, 156-161.
132. Risberg, E. D.; Jalilehvand, F.; Leung, B. O.; Pettersson, L. G. M.; Sandstrom, M., Theoretical and experimental sulfur K-edge X-ray absorption spectroscopic study of cysteine, cystine, homocysteine, penicillamine, methionine and methionine sulfoxide. *Dalton Transactions* **2009**, 3542-3558.
133. Schouten, S.; Eglinton Timothy, I.; Sinninghe Damsté Jaap, S.; de Leeuw Jan, W., Influence of sulphur cross-linking on the molecular-size distribution of sulphur-rich macromolecules in bitumen. In *Geochemical Transformations of Sedimentary Sulfur*, Vairavamurthy, M. A.; Schoonen, M. A. A.; Eglinton, T. I.; Luther III, G. W.; Manowitz, B., Eds. American Chemical Society: Washington, DC, 1995; Vol. 612, pp 80-92.
134. van Dongen, B. E.; Schouten, S.; Baas, M.; Geenevasen, J. A. J.; Sinninghe Damsté, J. S., An experimental study of the low-temperature sulfurization of carbohydrates. *Org. Geochem.* **2003,** *34*, 1129-1144.
135. Dey, A.; Glaser, T.; Moura, J. J. G.; Holm, R. H.; Hedman, B.; Hodgson, K. O.; Solomon, E. I., Ligand K-edge X-ray absorption spectroscopy and DFT calculations on $[Fe_3S_4]^{0,+}$ clusters: Delocalization, redox, and effect of the protein environment. *J. Am. Chem. Soc.* **2004,** *126*, 16868-16878.
136. Pingitore Jr, N. E.; Meitzner, G.; Love, K. M., Identification of sulfate in natural carbonates by X-ray absorption spectroscopy. *Geochim. Cosmochim. Acta* **1995,** *59*, 2477-2483.
137. Myneni, S. C. B., X-ray and vibrational spectroscopy of sulfate in earth materials. *Reviews in Mineralogy and Geochemistry* **2000,** *40*, 113-172.
138. Abdollahi, H.; Nedwell, D. B., Seasonal temperature as a factor influencing bacterial sulfate reduction in a saltmarsh sediment. *Microb. Ecol.* **1979,** *5*, 73-79.
139. Howarth, R. W.; Teal, J. M., Sulfate reduction in a New England salt marsh. *Limnol. Oceanogr.* **1979,** *24*, 999-1013.
140. Troelsen, H.; Jørgensen, B. B., Seasonal dynamics of elemental sulfur in two coastal sediments. *Estuar. Coast. Shelf Sci.* **1982,** *15*, 255-266.
141. Westrich, J. T.; Berner, R. A., The effect of temperature on rates of sulfate reduction in marine sediments. *Geomicrobiol. J.* **1988,** *6*, 99-117.
142. Moeslundi, L.; Thamdrup, B.; Jørgensen, B. B., Sulfur and iron cycling in a coastal sediment: Radiotracer studies and seasonal dynamics. *Biogeochemistry* **1994,** *27*, 129-152.
143. Panutrakul, S.; Monteny, F.; Baeyens, W., Seasonal variations in sediment sulfur cycling in the Ballastplaat mudflat, Belgium. *Estuaries Coasts* **2001,** *24*, 257-265.
144. Al-Raei, A. M.; Bosselmann, K.; Bottcher, M. E.; Hespenheide, B.; Tauber, F., Seasonal dynamics of microbial sulfate reduction in temperate intertidal surface sediments: controls by temperature and organic matter. *Ocean Dynam* **2009,** *59*, 351-370.
145. Jørgensen, B. B., The sulfur cycle of a coastal marine sediment (Limfjorden, Denmark). *Limnol. Oceanogr.* **1977,** *22*, 814-832.

146. Sørensen, J.; Jørgensen, B. B., Early diagenesis in sediments from Danish coastal waters: Microbial activity and Mn-Fe-S geochemistry. *Geochim. Cosmochim. Acta* **1987,** *51*, 1583-1590.
147. King, G. M., Patterns of sulfate reduction and the sulfur cycle in a South Carolina salt marsh. *Limnol. Oceanogr.* **1988,** *33*, 376-390.
148. Dacey, J. W. H.; Howes, B. L., Water uptake by roots controls water table movement and sediment oxidation in short *Spartina* marsh. *Science* **1984,** *224*, 487-489.
149. Morris, J. T.; Whiting, G. J., Gas advection in sediments of a South Carolina salt marsh. *Marine Ecology-Progress Series* **1985,** *27*, 187-194.
150. Luther III, G. W.; Church, T. M., Seasonal cycling of sulfur and iron in porewaters of a Delaware salt marsh. *Mar. Chem.* **1988,** *23*, 295-309.
151. Thamdrup, B.; Finster, K.; Fossing, H.; Hansen, J. W.; Jørgensen, B. B., Thiosulfate and sulfite distributions in porewater of marine sediments related to manganese, iron, and sulfur geochemistry. *Geochim. Cosmochim. Acta* **1994,** *58*, 67-73.
152. Boulegue, J.; Lord III, C. J.; Church, T. M., Sulfur speciation and associated trace metals (Fe, Cu) in the pore waters of Great Marsh, Delaware. *Geochim. Cosmochim. Acta* **1982,** *46*, 453-464.
153. Howarth, R. W.; Merkel, S., Pyrite formation and the measurement of sulfate reduction in salt marsh sediments. *Limnol. Oceanogr.* **1984,** *29*, 598-608.
154. Rudd, J. W. M.; Kelly, C. A.; Furutani, A., The role of sulfate reduction in long term accumulation of organic and inorganic sulfur in lake sediments. *Limnol. Oceanogr.* **1986,** *31*, 1281-1291.
155. Kling, G. W.; Giblin, A. E.; Fry, B.; Peterson, B. J., The role of seasonal turnover in lake alkalinity dynamics. *Limnol. Oceanogr.* **1991,** *36*, 106-122.

Appendix A: Supporting Information for Chapter 2

A.1 Anion and cation concentrations in PPL porewaters

Sub-samples of native and filter-sterilized P1 porewaters (Apr 2010) were sent to the Analytical Geochemistry Laboratory at the University of Minnesota for IC and ICP-OES analysis.

Concentrations of anions in native and filtered porewaters were analyzed by a Dionex ICS-2000 ion chromatograph equipped with an IonPac AS19 anion-exchange column (150 mm × 4.0 mm i.d.), an ASRS 300 (4 mm) suppressor, an AS40 autosampler, and an integrated dual-piston pump and conductivity detector using the following settings: injection volume: 50 µL; eluent: 2.0 mM sodium hydroxide; flow rate: 1.0 mL/min. Calibration was accomplished by comparing the unknowns to a NIST traceable single or multi-element standard solution. All samples were diluted appropriately such that analyte concentrations were in the linear calibration range of instrument. Results of IC analysis are summarized in Table A.1.

Concentrations of cations in native and filtered porewaters were analyzed by a Thermo Scientific iCAP 6500 dual view inductively coupled plasma-optical emission spectrometer equipped with a Cetac PFA microconcentric nebulizer using the following settings: RF power: 1150 W, cooling gas flow rate: 12 L/min, nebulizer gas flow rate: 0.65 L/min, auxiliary gas flow rate: 0.3 L/min, dwell time: 100 ms, integration: 10 sec/replicate and 5 replicates/sample. For each sample, standard, and blank, triplicate measurements were made to determine a mean and standard deviation for each selected elemental wavelength. Calibration was accomplished by comparing the unknowns to a NIST traceable single or multi-element standard solution. All samples, standards, and

blanks were acid matrix matched to lessen matrix effects. Samples were diluted appropriately before analysis with the addition of a Cs matrix modifier and Y as an internal standard. Results of ICP-OES analysis are summarized in Table A.2.

Table A.1 Anion analysis of PPL porewaters

Analyte	Native (mg/L)[a]	Filtered (mg/L)[b]	Difference (mg/L)[c]
Bromide (Br^-)	0.176 (±0.003)	0.176 (±0.004)	0.000 (±0.005)
Chloride (Cl^-)	33.637 (±0.213)	33.329 (±0.266)	0.308 (±0.341)
Fluoride (F^-)	0.092 (±0.001)	0.066 (±0.001)	0.065 (±0.006)
Formate ($HCOO^-$)	0.020 (±0.000)	0.370 (±0.002)	-0.350 (±0.002)
Acetate (CH_3COO^-)	174.977 (±0.337)	178.093 (±0.137)	-3.117 (±0.364)
Oxalate ($(COO)_2^{2-}$)	0.020 (±0.000)	0.020 (±0.000)	0.000 (±0.000)
Lactate ($CH_3CH(OH)COO^-$)	0.100 (±0.000)	0.100 (±0.000)	0.000 (±0.000)
Nitrate Nitrogen (NO_3^--N)	0.002 (±0.000)	0.002 (±0.000)	0.000 (±0.000)
Nitrite Nitrogen (NO_2^--N)	0.004 (±0.000)	0.004 (±0.000)	0.000 (±0.000)
Phosphate Phosphorous (PO_4^{3-}-P)	0.332 (±0.006)	0.338 (±0.003)	-0.006 (±0.006)
Sulfate (SO_4^{2-})	98.044 (±0.224)	98.210 (±0.327)	-0.167 (±0.396)
Sulfite (SO_3^{2-})	3.164 (±0.051)	3.040 (±0.083)	0.124 (±0.097)
Sulfite (SO_3^{2-}) (µM)	**39.56 (±0.64)**	**38.00 (±1.04)**	**1.55 (±1.22)**
Thiosulfate ($S_2O_3^{2-}$)	9.209 (±0.128)	8.733 (±0.321)	0.476 (±0.345)
Thiosulfate ($S_2O_3^{2-}$) (µM)	**82.22 (±1.62)**	**77.97 (±4.05)**	**4.25 (±4.36)**

[a] Concentration of analyte in native P1 porewaters (Apr 2010). Errors represent one standard deviation from duplicate measurements. [b] Concentration of analyte in filter-sterilized P1 porewaters (Apr 2010). Errors represent one standard deviation from duplicate measurements. [c] Difference in concentrations between native and filter-sterilized porewaters. Calculated as "Native" minus "Filtered". Errors were calculated through propagation of errors associated with "Native" and "Filtered".

Table A.2 Cation analysis of PPL porewaters

Analyte	Native (mg/L)[a]	Filtered (mg/L)[b]	Difference (mg/L)[c]
Al	25.0 (±1.7)	6.9 (±1.9)	18.1 (±2.5)
Ba	11.1 (±0.1)	10.0 (±0.0)	1.1 (±0.1)
Ca	7343.8 (±109.6)	6668.5 (±93.2)	675.3 (±143.9)
Fe	34.5 (±2.6)	38.9 (±2.9)	-4.4 (±3.9)
K	36937.0 (±578.4)	37193.0 (±905.1)	-256.0 (±1074.1)
Li	224.8 (±0.8)	226.6 (±3.1)	-1.7 (±3.2)
Mg	101870.0 (±523.3)	101695.0 (±671.8)	175.0 (±851.5)
Mn	11.0 (±0.1)	2.8 (±0.2)	8.3 (±0.2)
Na	144085.0 (±431.3)	143875.0 (±275.8)	210.0 (±512.0)
P	400.0 (±5243.4)	394.1 (±1.4)	5.9 (±2.0)
Si	5243.4 (±1.8)	4839.7 (±0.1)	403.7 (±1.8)
Sr	133.6 (±0.7)	130.2 (±1.5)	3.4 (±1.6)

[a] Concentration of analyte in native P1 porewaters (Apr 2010). Errors represent one standard deviation from duplicate measurements. [b] Concentration of analyte in filter-sterilized P1 porewaters (Apr 2010). Errors represent one standard deviation from duplicate measurements. [c] Difference in concentrations between native and filter-sterilized porewaters. Calculated as "Native" minus "Filtered". Errors were calculated through propagation of errors associated with "Native" and "Filtered".

A.2 Methylation of sodium tetrasulfide solution

The Na_2S_4 solution was prepared by dissolving purified Na_2S_4 crystals into a deoxygenated sodium borate buffer (0.043 M; pH 9.1). Na_2S_4 crystals were rinsed with deoxygenated toluene to remove excess elemental sulfur. Dissolution of Na_2S_4 in the borate buffer was accompanied by an instantaneous development of turbidity, which could be interpreted as evidence of elemental sulfur precipitation and concurrent disproportionation of S_4^{2-}.[1] The Na_2S_4 solution was then allowed to equilibrate at 23±2 ℃ in the glove box for 1 week prior to methylation.

The GC-MS total ion chromatograms of methylated Na_2S_4 solution and pH-adjusted porewaters are shown in Figure A.1. A comparison of measured dimethylpolysulfide (DMPS) concentrations and predicted polysulfide concentrations is shown in Table A.3. The presence of dimethylated di-, tri-, tetra-, and pentasulfide was evident in the methylated Na_2S_4 solution. Because the standards of Me_2S_4 and Me_2S_5 are not commercially available, the TIC of methylated Na_2S_4 solution provides essential chromatographic information of these two DMPS species and can be used to identify possible DMPS formation in the methylated porewater samples.

Even though Me_2S_4 was predicted to be the predominant DMPS present in the methylated solution, Me_2S_3 appeared to be the most abundant species according to the measured peak area ratios (Table A.3). Quantification of Me_2S_2 and Me_2S_3 using external standards revealed that measured concentrations of these two species were 2-5 orders of magnitude higher than predicted from the equilibrium speciation calculations (Figure A.2). These observations provide direct evidence that partial rearrangement of the DMPS

in the presence of HS^- occurs during the methylation.[1,2] The measured concentration of total DMPS, however, is closely matched by the predicted concentration of total polysulfides ($[H_2S_n]_T$), suggesting that the methylation method can provide reasonable estimates of total polysulfides.

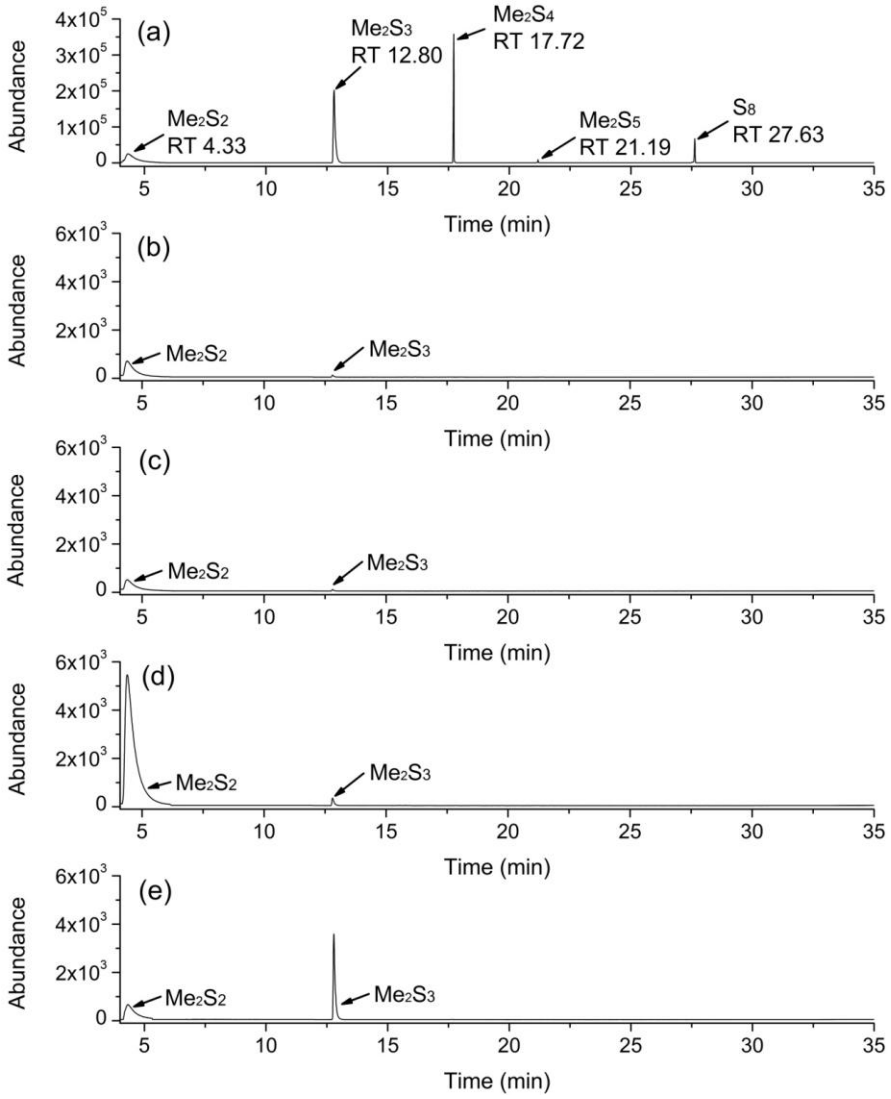

Figure A.1 Total ion chromatograms (TIC) of methylated Na_2S_4 solution and pH-adjusted porewaters: (a) TIC of Na_2S_4 solution; (b) TIC of pH 7.43 porewater; (c) TIC of pH 8.62 porewater; (d) TIC of pH 9.53 porewater; (e) TIC of Me_2S_2 and Me_2S_3 standards. "Me_2S_2", "Me_2S_3", "Me_2S_4", "Me_2S_5", and "S_8" denote dimethyldisulfide, dimethyltrisulfide, dimethyltetrasulfide, dimethylpentasulfide, and elemental sulfur, respectively. "RT" denotes the retention time (min). Note differences in abundance scales.

Table A.3 Measured and predicted polysulfides in a Na_2S_4 solution

DMPS	Measured concentration (mM)[b]	Predicted concentration (mM)[c]	Measured peak area ratio[d]	Predicted concentration ratio[e]
Me_2S_2	1.38 (±0.17)	$4.52\ (\pm 0.12)\times 10^{-5}$	0.874	1.48×10^{-5}
Me_2S_3	2.36 (±0.25)	$2.47\ (\pm 0.01)\times 10^{-2}$	1.775	8.08×10^{-3}
Me_2S_4	~1.33 (±0.10)	3.05 (±0.08)	1.000	1.000
Me_2S_5	$\sim 2.90\ (\pm 0.20)\times 10^{-2}$	2.31 (±0.06)	0.022	0.758
HS^-	N.A.[f]	1.93 (±0.05)	N.A.[f]	N.A.[f]
$(H_2S_n)_T$	5.09 (±0.32)[g]	5.39 (±0.10)[g]	N.A.[f]	N.A.[f]

[a] Solution (pH 9.1 and ionic strength 0.2) containing 7.33(±0.14) mM total divalent sulfide ($[S(-II)]_T$). $[S(-II)]_T$ was measured by iodometric titration.[3] [b] Measured concentration of DMPS obtained upon methylation of Na_2S_4 solution. Concentrations of Me_2S_4 and Me_2S_5 were estimated using the peak area and assuming the same molar response factor as Me_2S_3. Methylation efficiencies for all DMPS are assumed to be 100%. Measured extraction efficiencies for Me_2S_2 and Me_2S_3 are 95.6% and 96.2%, respectively. Extraction efficiencies for Me_2S_4 and Me_2S_5 are assumed to be the same as Me_2S_3. Errors represent one standard deviation from triplicate measurements. [c] Predicted concentration of DMPS using the reduced sulfur prediction model (Figure A.2) and assuming DMPS originate entirely from methylation of polysulfides without any rearrangement. Methylation and extraction efficiencies are both assumed to be 100%. Errors were propagated from $[S(-II)]_T$. [d] Peak area ratio obtained from the GC-MS total ion chromatogram. Values normalized for Me_2S_4. [e] Predicted concentration ratio obtained from the reduced sulfur speciation model (Figure A.2). Values normalized for Me_2S_4. [f] N.A. = not available. [g] Total polysulfide concentration calculated as the sum of measured DMPS concentrations or predicted polysulfide concentrations. Errors were calculated through propagation of errors associated with individual DMPS.

A.3 Equilibrium speciation model of reduced sulfur species

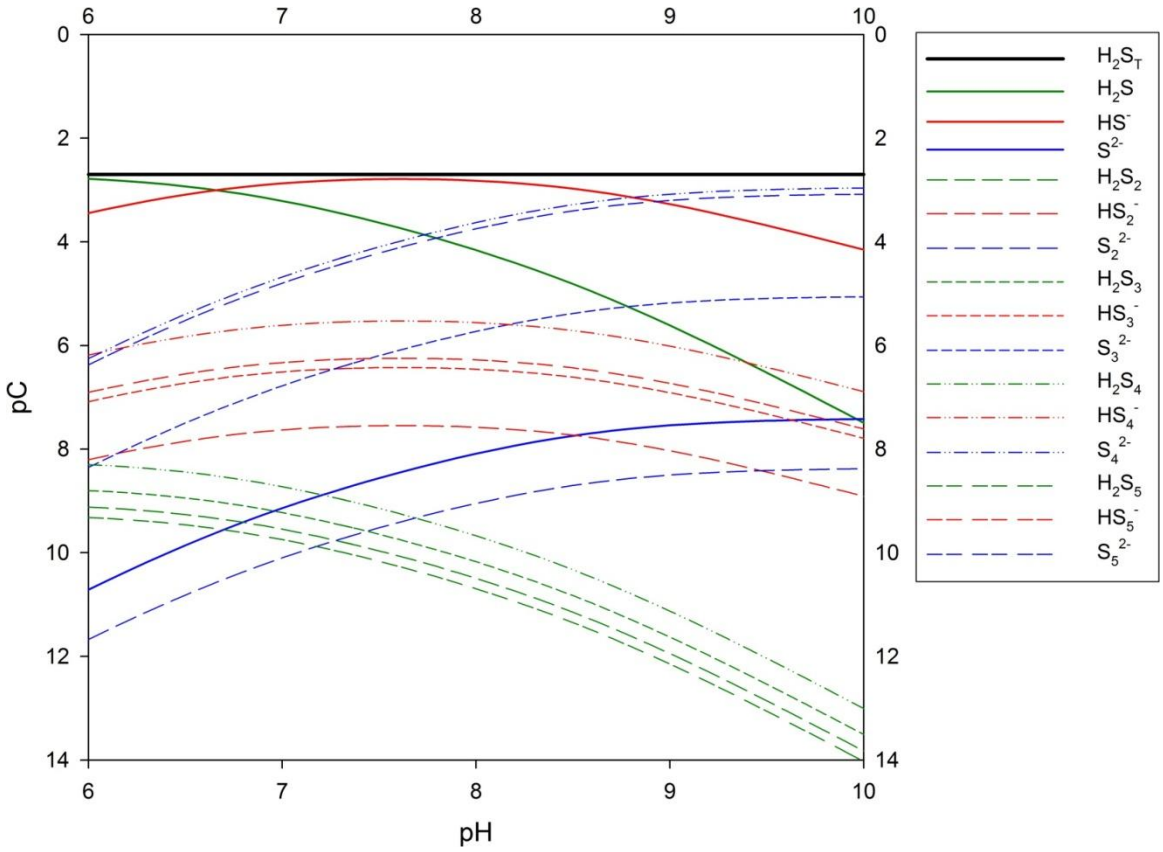

Figure A.2 Predicted reduced sulfur speciation of 2 mM total hydrogen sulfide ($[H_2S]_T$) solution in equilibrium with excess elemental sulfur over pH 6-10. Ionic strength is 0.7. Equilibrium constants from Shea and Helz[4] are used (corrected for appropriate ionic strength).

A.4 Measured, calculated, and predicted reduced sulfur concentrations

Table A.4 Concentrations of HS^- and S_n^{2-} in pH-adjusted porewaters

Filtered[a]							
pH	$[H_2S]_T$ (μM)[c]	$[HS^-]_{calc}$ (μM)[d]	$[Me_2S_2]$ (μM)[e]	$[Me_2S_3]$ (μM)[f]	$[H_2S_n]_{T,\ calc}$ (μM)[g]	$\Sigma[S_n^{2-}]_{calc}$ (μM)[h]	$\Sigma[S_n^{2-}]_{pred}$ (μM)[i]
7.43	2577 (±34)	2203 (±41)	21.6 (±1.2)	0.5 (±0.1)	22.1 (±1.2)	21.4 (±1.2)	154 (±3)
8.62	2372 (±46)	2347 (±64)	74.1 (±3.8)	0.5 (±0.1)	74.6 (±3.8)	74.4 (±3.8)	1297 (±37)
9.53	1705 (±51)	1702 (±72)	282.6 (±14.2)	7.8 (±1.1)	290.4 (±14.2)	290.3 (±14.2)	1801 (±83)
Unfiltered[b]							
pH	$[H_2S]_T$ (μM)[c]	$[HS^-]_{calc}$ (μM)[d]	$[Me_2S_2]$ (μM)[e]	$[Me_2S_3]$ (μM)[f]	$[H_2S_n]_{T,\ calc}$ (μM)[g]	$\Sigma[S_n^{2-}]_{calc}$ (μM)[h]	$\Sigma[S_n^{2-}]_{pred}$ (μM)[i]
7.43	2600 (±70)	2223 (±85)	22.5 (±0.6)	0.8 (±0.0)	23.3 (±0.6)	22.5 (±0.6)	155 (±6)
8.62	2370 (±27)	2345 (±37)	77.8 (±5.9)	1.3 (±0.4)	79.1 (±5.9)	78.9 (±5.9)	1298 (±25)
9.53	1679 (±13)	1676 (±18)	275.7 (±8.1)	8.4 (±1.1)	284.1 (±8.2)	284.0 (±8.2)	1772 (±27)

[a] Filter-sterilized P1 porewaters (Apr 2010). [b] Unfiltered P1 porewaters (Apr 2010). [c] Total hydrogen sulfide concentration measured by the methylene blue method. Errors represent one standard deviation from triplicate measurements. [d] Bisulfide concentration calculated from $[H_2S]_T$ and pH, assuming that the sample is not saturated with elemental sulfur. Errors were propagated from $[H_2S]_T$. [e] Measured dimethyldisulfide concentration after conducting methylation reaction in porewaters. Errors represent one standard deviation from triplicate measurements. [f] Measured dimethyltrisulfide concentration after conducting methylation reaction in porewaters. Errors represent one standard deviation from triplicate measurements. [g] Total polysulfide concentration calculated as the sum of measured $[Me_2S_2]$ and $[Me_2S_3]$ after correcting for methylation and extraction efficiencies. (i.e., $[H_2S_n]_{T,\ calc}$ = ($[Me_2S_2]$ + $[Me_2S_3]$) / (Methylation efficiency × Extraction efficiency)). Methylation efficiencies for Me_2S_2 and Me_2S_3 are assumed to be 100%. Measured extraction efficiencies for Me_2S_2 and Me_2S_3 are 95.6% and 96.2%, respectively. Errors were calculated through propagation of errors associated with $[Me_2S_2]$ and $[Me_2S_3]$. [h] Polysulfide dianion concentration calculated from $[H_2S_n]_{T,\ calc}$ and pH, assuming that the relative abundance of HS_n^- and S_n^{2-} species are dictated by equilibrium constants from Shea and Helz.[1] Errors were propagated from $[H_2S_n]_{T,\ calc}$. [i] Polysulfide dianion concentration predicted from speciation model using an estimated value of total divalent sulfide $[S(-II)]_T$ (calculated as $[H_2S]_T$ + $[H_2S_n]_{T,\ calc}$), assuming that the sample is saturated with elemental sulfur. Errors were calculated through propagation of errors associated with $[H_2S]_T$ and $[H_2S_n]_{T,\ calc}$.

A.5 Transformations of pesticides in unfiltered porewaters

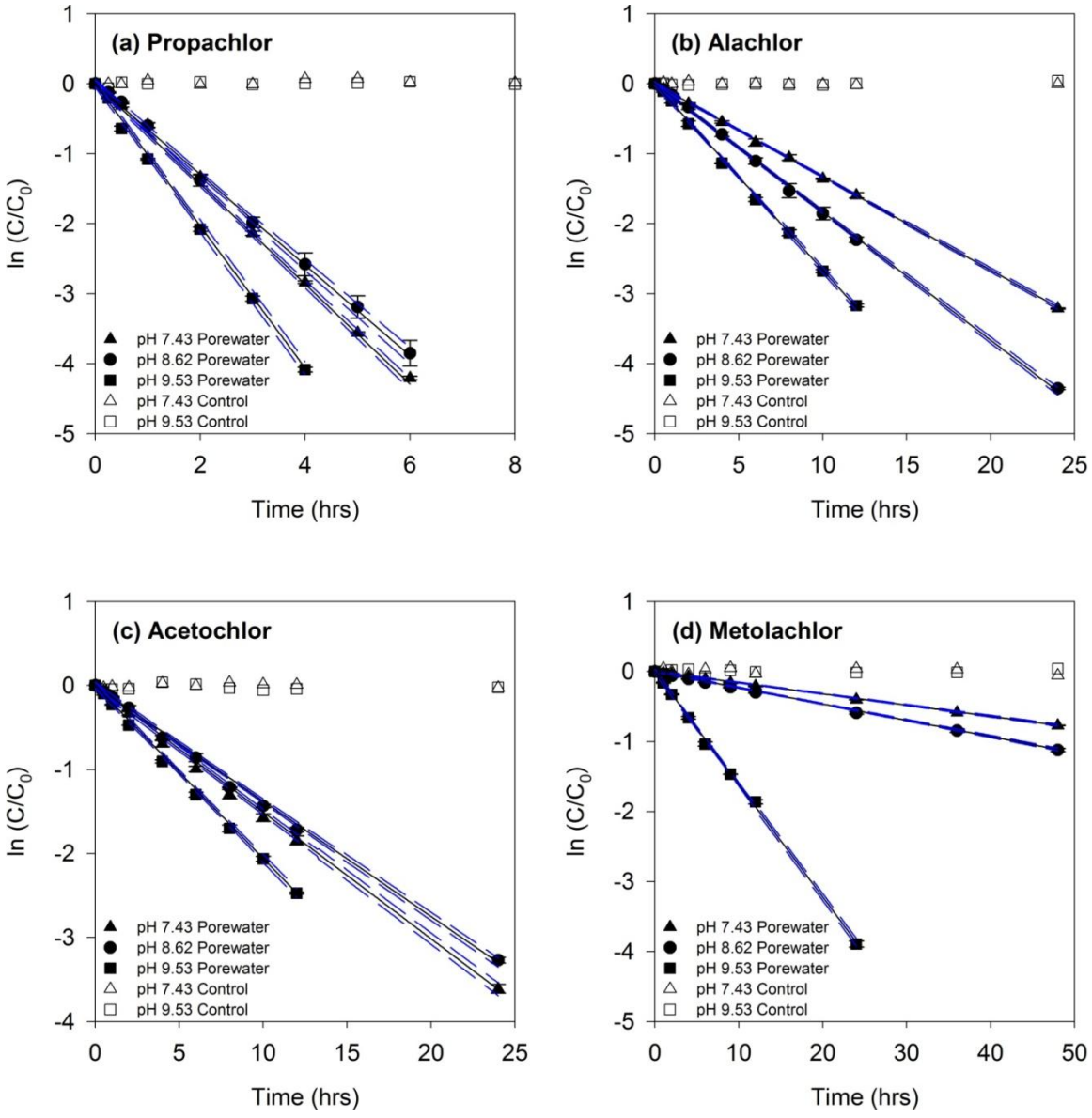

Figure A.3 Comparison of chloroacetanilide reactivity in pH-adjusted, unfiltered P1 porewaters (Apr 2010): (a) propachlor; (b) alachlor; (c) acetochlor; (d) metolachlor. Error bars represent one standard deviation of duplicate (pH 7.43 and 9.53) or triplicate (pH 8.62) samples; where absent, bars fall within symbols. Solid lines represent linear regressions and dashed lines represent 95% confidence intervals. $R^2 > 0.99$ in all cases. $[H_2S]_T$ and $[H_2S_n]_{T,\,calc}$ in unfiltered porewaters are provided in Table A.4.

A.6 Second-order rate constants for pesticide reactions with sulfur species

Table A.5 Second-order rate constants for reactions of chloroacetanilides with HS^-, S_n^{2-}, and other reduced sulfur species

Chloroacetanilide	k_{HS^-} ($M^{-1}.s^{-1}$)	$k_{S_n^{2-}}$ ($M^{-1}.s^{-1}$)	$k_{SO_3^{2-}}$ ($M^{-1}.s^{-1}$)	$k_{S_2O_3^{2-}}$ ($M^{-1}.s^{-1}$)	$k_{S_2O_4^{2-}}$ ($M^{-1}.s^{-1}$)	$k_{S_n^{2-}} / k_{HS^-}$
Propachlor	$5.03 (\pm 0.30) \times 10^{-2}$ [a]	$2.90 (\pm 0.31)$ [a]	$1.04 (\pm 0.07) \times 10^{-4}$ [e]	$3.33 (\pm 0.37) \times 10^{-3}$ [f]	$5.27 (\pm 0.26) \times 10^{-5}$ [g]	58 [h]
Alachlor	$1.50 (\pm 0.19) \times 10^{-2}$ [a]	$1.63 (\pm 0.06) \times 10^{-1}$ [a]	$6.55 (\pm 0.47) \times 10^{-5}$ [d]	$1.68 (\pm 0.08) \times 10^{-3}$ [f]	$3.07 (\pm 0.15) \times 10^{-5}$ [g]	11 [h]
Acetochlor	$1.05 (\pm 0.13) \times 10^{-2}$ [b]	$1.44 (\pm 0.05) \times 10^{-1}$ [c]	$6.57 (\pm 0.68) \times 10^{-5}$ [d]	$1.22 (\pm 0.08) \times 10^{-3}$ [f]	$1.50 (\pm 0.08) \times 10^{-5}$ [g]	14 [h]
Metolachlor	$2.50 (\pm 0.13) \times 10^{-3}$ [a]	$8.05 (\pm 0.30) \times 10^{-2}$ [a]	$1.55 (\pm 0.53) \times 10^{-5}$ [d]	$2.37 (\pm 0.08) \times 10^{-4}$ [f]	$2.89 (\pm 0.14) \times 10^{-6}$ [g]	32 [h]

[a] Reported by Loch et al. (2002)[1]. [b] Extrapolated from the value of second-order rate constant for reaction of alachlor with HS^- reported by Loch et al. (2002)[1] and the relative reactivity of alachlor and acetochlor with HS^- reported by Qin (1995)[2]. [c] Extrapolated from the value of second-order rate constant for reaction of alachlor with S_n^{2-} reported by Loch et al (2002)[1] and the relative reactivity of alachlor and acetochlor with S_n^{2-} reported by Gan (2006)[3]. [d] Calculated from the half-lives for reactions of chloroacetanilides with SO_3^{2-} reported by Bian et al. (2009)[4]. [e] Extrapolated from the value of second-order rate constant for reaction of alachlor with SO_3^{2-} derived from Bian et al. (2009)[4] and the relative reactivity of alachlor and propachlor with HS^- reported by Loch et al. (2002)[1] assuming that the reactivities of HS^- and SO_3^{2-} toward chloroacetanilides were similar.[5] [f] Calculated from the half-lives for reactions of chloroacetanilides with $S_2O_3^{2-}$ reported by Gan et al. (2002)[6]. [g] Calculated from the half-lives for reactions of chloroacetanilides with $S_2O_4^{2-}$ reported by Boparai et al. (2006)[7]. [h] Calculated as $k_{S_n^{2-}} / k_{HS^-}$.

A.7 Contributions of HS^- and S_n^{2-} in unfiltered porewaters

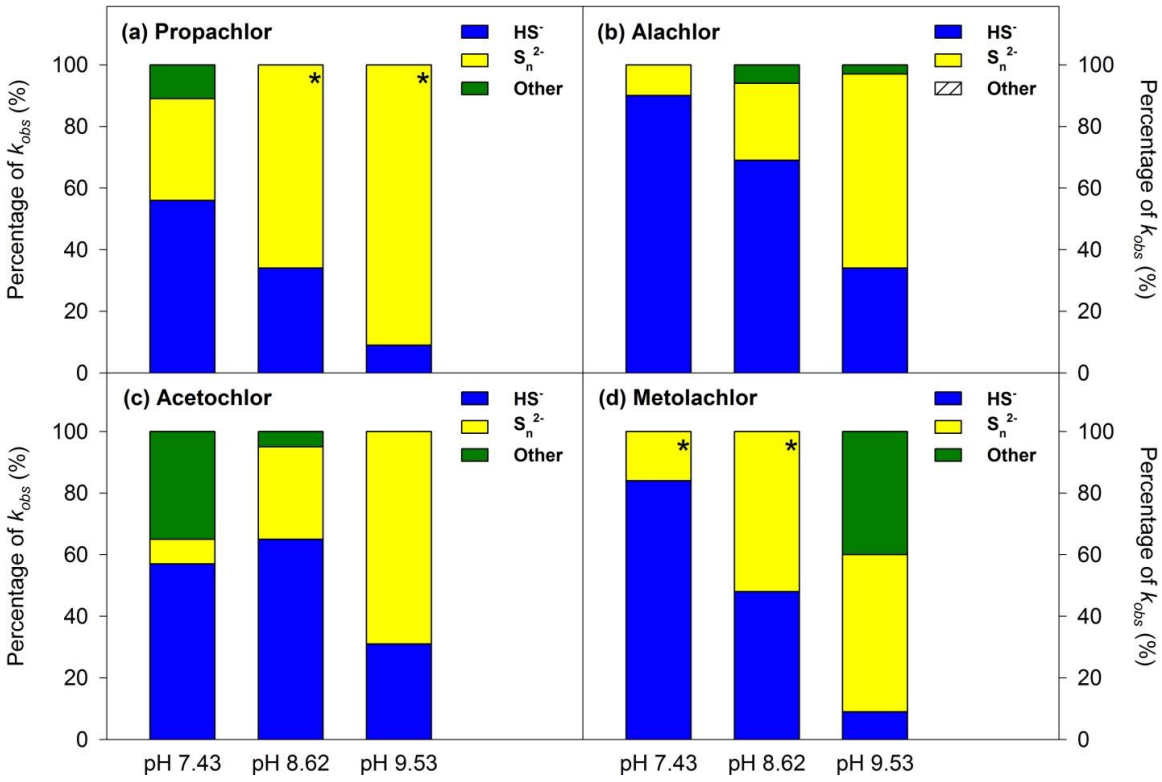

Figure A.4 Percent contributions of HS^-, S_n^{2-}, and other processes to transformations of chloroacetanilides in pH-adjusted, unfiltered P1 porewaters (Apr 2010): (a) propachlor; (b) alachlor; (c) acetochlor; (d) metolachlor. Stacked bars plotted based on values calculated from Table A.4 and Table A.6. Bars with an asterisk mark designate the joint contribution of HS^- and S_n^{2-} up to 100% of k_{obs} even though the predicted contributions of HS^- and S_n^{2-} to k_{obs} are greater than the experimental value of k_{obs} in these cases.

Table A.6 Contributions of HS^-, S_n^{2-}, and other processes to transformations of chloroacetanilides

Propachlor		Filtered[a]			Unfiltered[b]	
pH	k_{HS^-} $[HS^-]$ $(hr^{-1})^c$	$k_{S_n^{2-}}$ $\Sigma[S_n^{2-}]$ $(hr^{-1})^d$	k_{other} $(hr^{-1})^e$	k_{HS^-} $[HS^-]$ $(hr^{-1})^c$	$k_{S_n^{2-}}$ $\Sigma[S_n^{2-}]$ $(hr^{-1})^d$	k_{other} $(hr^{-1})^e$
7.43	0.3989 (±0.0074)	0.2232 (±0.0171)	0.1403 (±0.0246)	0.4025 (±0.0154)	0.2353 (±0.0086)	0.0776 (±0.0239)
8.62	0.4249 (±0.0117)	0.7772 (±0.0560)	-	0.4245 (±0.0068)	0.8241 (±0.0869)	-
9.53	0.3082 (±0.0131)	3.0310 (±0.2096)	-	0.3035 (±0.0033)	2.9652 (±0.1210)	-
Alachlor		Filtered[a]			Unfiltered[b]	
pH	k_{HS^-} $[HS^-]$ $(hr^{-1})^c$	$k_{S_n^{2-}}$ $\Sigma[S_n^{2-}]$ $(hr^{-1})^d$	k_{other} $(hr^{-1})^e$	k_{HS^-} $[HS^-]$ $(hr^{-1})^c$	$k_{S_n^{2-}}$ $\Sigma[S_n^{2-}]$ $(hr^{-1})^d$	k_{other} $(hr^{-1})^e$
7.43	0.1190 (±0.0022)	0.0125 (±0.0010)	0.0147 (±0.0032)	0.1200 (±0.0046)	0.0132 (±0.0005)	0.0000 (±0.0051)
8.62	0.1267 (±0.0035)	0.0437 (±0.0031)	0.0215 (±0.0066)	0.1266 (±0.0020)	0.0463 (±0.0049)	0.0102 (±0.0069)
9.53	0.0919 (±0.0039)	0.1704 (±0.0118)	0.0448 (±0.0157)	0.0914 (±0.0003)	0.1667 (±0.0068)	0.0080 (±0.0065)
Acetochlor		Filtered[a]			Unfiltered[b]	
pH	k_{HS^-} $[HS^-]$ $(hr^{-1})^c$	$k_{S_n^{2-}}$ $\Sigma[S_n^{2-}]$ $(hr^{-1})^d$	k_{other} $(hr^{-1})^e$	k_{HS^-} $[HS^-]$ $(hr^{-1})^c$	$k_{S_n^{2-}}$ $\Sigma[S_n^{2-}]$ $(hr^{-1})^d$	k_{other} $(hr^{-1})^e$
7.43	0.0833 (±0.0018)	0.0111 (±0.0009)	0.0586 (±0.0027)	0.0840 (±0.0014)	0.0117 (±0.0004)	0.0550 (±0.0018)
8.62	0.0887 (±0.0020)	0.0386 (±0.0028)	0.0157 (±0.0048)	0.0886 (±0.0006)	0.0409 (±0.0043)	0.0080 (±0.0038)
9.53	0.0643 (±0.0015)	0.1505 (±0.0104)	0.0021 (±0.0119)	0.0640 (±0.0017)	0.1472 (±0.0060)	0.0000 (±0.0043)
Metolachlor		Filtered[a]			Unfiltered[b]	
pH	k_{HS^-} $[HS^-]$ $(hr^{-1})^c$	$k_{S_n^{2-}}$ $\Sigma[S_n^{2-}]$ $(hr^{-1})^d$	k_{other} $(hr^{-1})^e$	k_{HS^-} $[HS^-]$ $(hr^{-1})^c$	$k_{S_n^{2-}}$ $\Sigma[S_n^{2-}]$ $(hr^{-1})^d$	k_{other} $(hr^{-1})^e$
7.43	0.0198 (±0.0004)	0.0065 (±0.0002)	-	0.0200 (±0.0008)	0.0062 (±0.0005)	-
8.62	0.0211 (±0.0006)	0.0229 (±0.0024)	-	0.0211 (±0.0003)	0.0216 (±0.0016)	-
9.53	0.0153 (±0.0006)	0.0823 (±0.0034)	0.0619 (±0.0065)	0.0152 (±0.0001)	0.0841 (±0.0058)	0.0636 (±0.0033)

[a] Filter-sterilized P1 porewaters (Apr 2010). [b] Unfiltered P1 porewaters (Apr 2010). [c] Calculated as $k_{HS^-} \times [HS^-]_{calc}$, where k_{HS^-} is the second-order rate constant from Table A.5 and $[HS^-]_{calc}$ is the bisulfide concentration from Table A.4. Errors were calculated through propagation of errors associated with rate constants and concentrations. [d] Calculated as $k_{S_n^{2-}} \times \Sigma[S_n^{2-}]_{calc}$, where $k_{S_n^{2-}}$ is the second-order rate constant from Table A.5 and $\Sigma[S_n^{2-}]_{calc}$ is the polysulfide dianion concentration from Table A.4. Errors were calculated through propagation of errors associated with rate constants and concentrations. [e] Calculated as $k_{obs} - k_{HS^-}[HS^-] - k_{S_n^{2-}}\Sigma[S_n^{2-}]$, where k_{obs} is the reaction rate constant from Table 2.3. If the sum of $k_{HS^-}[HS^-] + k_{S_n^{2-}}\Sigma[S_n^{2-}]$ exceeds k_{obs}, k_{other} is designated as "-". Errors were calculated through propagation of errors associated with HS^- and S_n^{2-}.

A.8 Contributions of HS^-, S_n^{2-}, SO_3^{2-}, and $S_2O_3^{2-}$ in native porewaters

Table A.7 Contributions of HS^-, S_n^{2-}, SO_3^{2-}, $S_2O_3^{2-}$, and other processes to transformations of chloroacetanilides (pH 8.62)

Propachlor	k_{HS^-} $[HS^-]$ $(hr^{-1})^a$	$k_{S_n^{2-}}$ $\Sigma[S_n^{2-}]$ $(hr^{-1})^b$	$k_{SO_3^{2-}}$ $[SO_3^{2-}]$ $(hr^{-1})^c$	$k_{S_2O_3^{2-}}$ $[S_2O_3^{2-}]$ $(hr^{-1})^d$	k_{other} $(hr^{-1})^e$
Filtered	0.4249 (±0.0117)	0.7768 (±0.0560)	0.0000 (±0.0000)	0.0010 (±0.0000)	-
Unfiltered	0.4245 (±0.0068)	0.8236 (±0.0869)	0.0000 (±0.0000)	0.0009 (±0.0000)	-
Alachlor	k_{HS^-} $[HS^-]$ $(hr^{-1})^a$	$k_{S_n^{2-}}$ $\Sigma[S_n^{2-}]$ $(hr^{-1})^b$	$k_{SO_3^{2-}}$ $[SO_3^{2-}]$ $(hr^{-1})^c$	$k_{S_2O_3^{2-}}$ $[S_2O_3^{2-}]$ $(hr^{-1})^d$	k_{other} $(hr^{-1})^e$
Filtered	0.1267 (±0.0035)	0.0437 (±0.0031)	0.0000 (±0.0000)	0.0005 (±0.0000)	0.0210 (±0.0066)
Unfiltered	0.1266 (±0.0020)	0.0463 (±0.0049)	0.0000 (±0.0000)	0.0005 (±0.0000)	0.0097 (±0.0069)
Acetochlor	k_{HS^-} $[HS^-]$ $(hr^{-1})^a$	$k_{S_n^{2-}}$ $\Sigma[S_n^{2-}]$ $(hr^{-1})^b$	$k_{SO_3^{2-}}$ $[SO_3^{2-}]$ $(hr^{-1})^c$	$k_{S_2O_3^{2-}}$ $[S_2O_3^{2-}]$ $(hr^{-1})^d$	k_{other} $(hr^{-1})^e$
Filtered	0.0887 (±0.0020)	0.0386 (±0.0028)	0.0000 (±0.0000)	0.0003 (±0.0000)	0.0154 (±0.0048)
Unfiltered	0.0886 (±0.0006)	0.0409 (±0.0043)	0.0000 (±0.0000)	0.0004 (±0.0000)	0.0076 (±0.0038)
Metolachlor	k_{HS^-} $[HS^-]$ $(hr^{-1})^a$	$k_{S_n^{2-}}$ $\Sigma[S_n^{2-}]$ $(hr^{-1})^b$	$k_{SO_3^{2-}}$ $[SO_3^{2-}]$ $(hr^{-1})^c$	$k_{S_2O_3^{2-}}$ $[S_2O_3^{2-}]$ $(hr^{-1})^d$	k_{other} $(hr^{-1})^e$
Filtered	0.0211 (±0.0006)	0.0216 (±0.0016)	0.0000 (±0.0000)	0.0001 (±0.0000)	-
Unfiltered	0.0211 (±0.0003)	0.0229 (±0.0024)	0.0000 (±0.0000)	0.0001 (±0.0000)	-

[a] Calculated as $k_{HS^-} \times [HS^-]_{calc}$, where k_{HS^-} is the second-order rate constant from Table A.5 and $[HS^-]_{calc}$ is the bisulfide concentration from Table A.4. Errors were calculated through propagation of errors associated with rate constants and concentrations. [b] Calculated as $k_{S_n^{2-}} \times \Sigma[S_n^{2-}]_{calc}$, where $k_{S_n^{2-}}$ is the second-order rate constant from Table A.5 and $\Sigma[S_n^{2-}]_{calc}$ is the polysulfide dianion concentration from Table A.4. Errors were calculated through propagation of errors associated with rate constants and concentrations. [c] Calculated as $k_{SO_3^{2-}} \times [SO_3^{2-}]$, where $k_{SO_3^{2-}}$ is the second-order rate constant from Table A.5 and $[SO_3^{2-}]$ is the sulfite concentration from Table A.1. Errors were calculated through propagation of errors associated with rate constants and concentrations. [d] Calculated as $k_{S_2O_3^{2-}} \times [S_2O_3^{2-}]$, where $k_{S_2O_3^{2-}}$ is the second-order rate constant from Table A.5 and $[S_2O_3^{2-}]$ is the thiosulfate concentration from Table A.1. Errors were calculated through propagation of errors associated with rate constants and concentrations. [e]Calculated as $k_{obs} - k_{HS^-}[HS^-] - k_{S_n^{2-}}\Sigma[S_n^{2-}] - k_{SO_3^{2-}}[SO_3^{2-}] - k_{S_2O_3^{2-}}[S_2O_3^{2-}]$, where k_{obs} is the reaction rate constant from Table 2.3. If the sum of $k_{HS^-}[HS^-] + k_{S_n^{2-}}\Sigma[S_n^{2-}] + k_{SO_3^{2-}}[SO_3^{2-}] + k_{S_2O_3^{2-}}[S_2O_3^{2-}]$ exceeds k_{obs}, k_{other} is designated as "-". Errors were calculated through propagation of errors associated with HS^-, S_n^{2-}, SO_3^{2-}, and $S_2O_3^{2-}$.

A.9 Effect of silver nitrate addition on propachlor transformation

The transformation of propachlor was also studied in porewaters from Lake P1 (Sep 2010) amended with varying amounts of silver nitrate ($AgNO_3$). Porewaters amended with $AgNO_3$ were allowed to equilibrate for 1 week and were filter-sterilized through 0.2 μm syringe filters before use. Reactions were initiated by spiking an aliquot of propachlor stock solution into porewaters. The sampling, extraction, and analysis procedures were the same as described in the text. Note that in this set of experiments, P1 porewaters from the Sep 2010 sampling trip were used due to the limited volume of P1 porewaters left from the Apr 2010 sampling trip. The differences and similarities between these two batches of porewaters have been shown in Table 2.2. Briefly, the pH of Sep 2010 porewaters (pH = 7.36) is more neutral compared to Apr 2010 porewaters (pH = 8.62), and the total hydrogen sulfide concentration (~1900 μM) and DOC level (~72 mg/L) are not as high as those measured in Apr 2010 porewaters ($[H_2S]_T$ = ~2400 μM and DOC = ~109 mg/L). The total polysulfide concentrations, however, are very similar between the two different batches of porewaters. The characteristics of $AgNO_3$-amended porewaters and propachlor reaction rates are summarized in Table A.8. The time courses for propachlor degradation and the correlation between reduced sulfur concentration and reaction rate are plotted in Figure A.5. Both HS^- and S_n^{2-} concentrations decreased by a factor of 2-25 as increasing amounts of $AgNO_3$ were added into porewaters. The disappearance of propachlor was slowed in the $AgNO_3$-amended porewaters, and the observed reaction rate was proportional to the total reduced sulfur concentrations (calculated as $[HS^-]+\Sigma[S_n^{2-}]$). Again, the reaction rates calculated from the

second-order rate constants and reduced sulfur concentrations over predicted the observed reaction rates in all cases ($k_{pred}/k_{obs} \approx 1.68$), suggesting that reactions with HS^- and S_n^{2-} were predominant in propachlor transformation.

Table A.8 Reduced sulfur concentrations and propachlor reaction rates in $AgNO_3$-amended porewaters

$AgNO_3$[a]	$[HS^-]_{calc}$ (μM)[b]	$\Sigma[S_n^{2-}]_{calc}$ (μM)[c]	k_{obs} (hr^{-1})[d]	k_{pred} (hr^{-1})[e]	k_{pred} / k_{obs}[f]
0 mM	1675 (±41)	76.6 (±8.6)	0.6562 (±0.0023)	1.1034 (±0.0969)	1.68
0.5 mM	874 (±55)	34.3 (±5.7)	0.3116 (±0.0015)	0.5164 (±0.0690)	1.66
2 mM	419 (±28)	17.1 (±0.7)	0.1507 (±0.0003)	0.2544 (±0.0125)	1.69
3 mM	81 (±11)	3.0 (±0.4)	0.0268 (±0.0001)	0.0459 (±0.0063)	1.71

[a] Amount of silver nitrate added in native P1 porewaters (Sep 2010). [b] Bisulfide concentration calculated from $[H_2S]_T$ and pH, assuming that the sample is not saturated with elemental sulfur. Errors were propagated from $[H_2S]_T$. [c] Polysulfide dianion concentration calculated from measured $[H_2S_n]_{T, calc}$ and pH, assuming that the relative abundance of HS_n^- and S_n^{2-} species are dictated by equilibrium constants from Shea and Helz.[1] Errors were propagated from $[H_2S_n]_{T, calc}$. [d] Rate constant measured in $AgNO_3$-amended, filter-sterilized porewaters. Errors represent one standard deviation from duplicate experiments [e] Rate constant calculated from the sum of $k_{HS^-}[HS^-] + k_{S_n^{2-}}\Sigma[S_n^{2-}]$, where k_{HS^-} and $k_{S_n^{2-}}$ are the second-order rate constants from Table A.5, and $[HS^-]$ and $\Sigma[S_n^{2-}]$ are the bisulfide and polysulfide dianion concentrations listed in the table. Errors were calculated through propagation of errors associated with rate constants and concentrations. [f] Calculated as k_{pred} / k_{obs}.

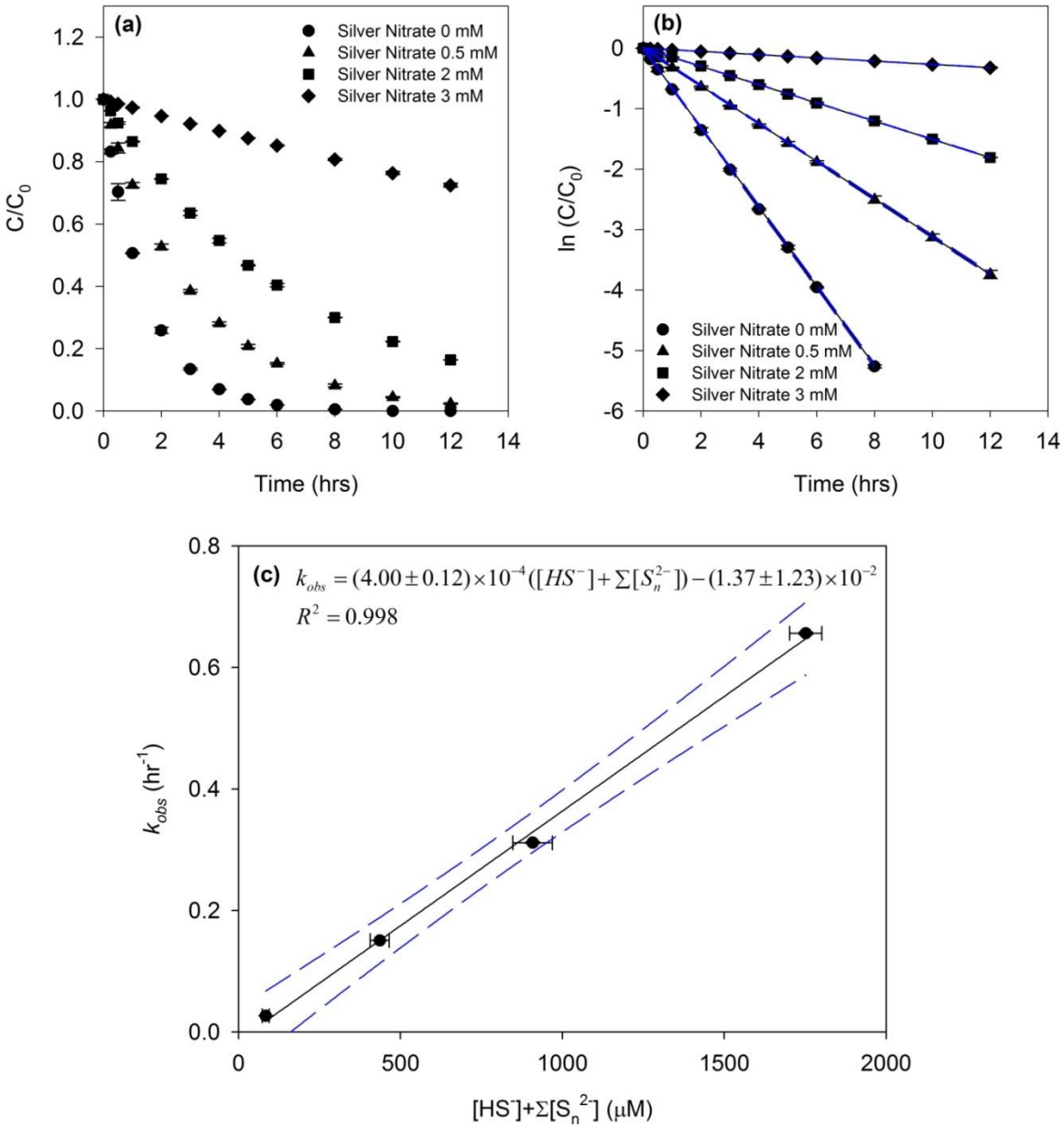

Figure A.5 Transformation of propachlor in $AgNO_3$-amended, filtered-sterilized P1 porewaters (Sep 2010): (a) Time courses for reactions of propachlor in porewaters. Error bars represent one standard deviation of duplicate samples; where absent, bars fall within symbols. (b) Comparison of propachlor reactivity in porewaters Solid lines represent linear regressions and dashed lines represent 95% confidence intervals. R^2 > 0.99 in all cases. (c) Plot of pseudo-first-order rate constant k_{obs} versus $[HS^-] + \Sigma[S_n^{2-}]$ for reactions of propachlor in porewaters. Error bars represent one standard deviation of duplicate samples; where absent, bars fall within symbols. Solid lines represent linear regressions and dashed lines represent 95% confidence intervals.

A.10 Transformation products of alachlor, acetochlor, and metolachlor

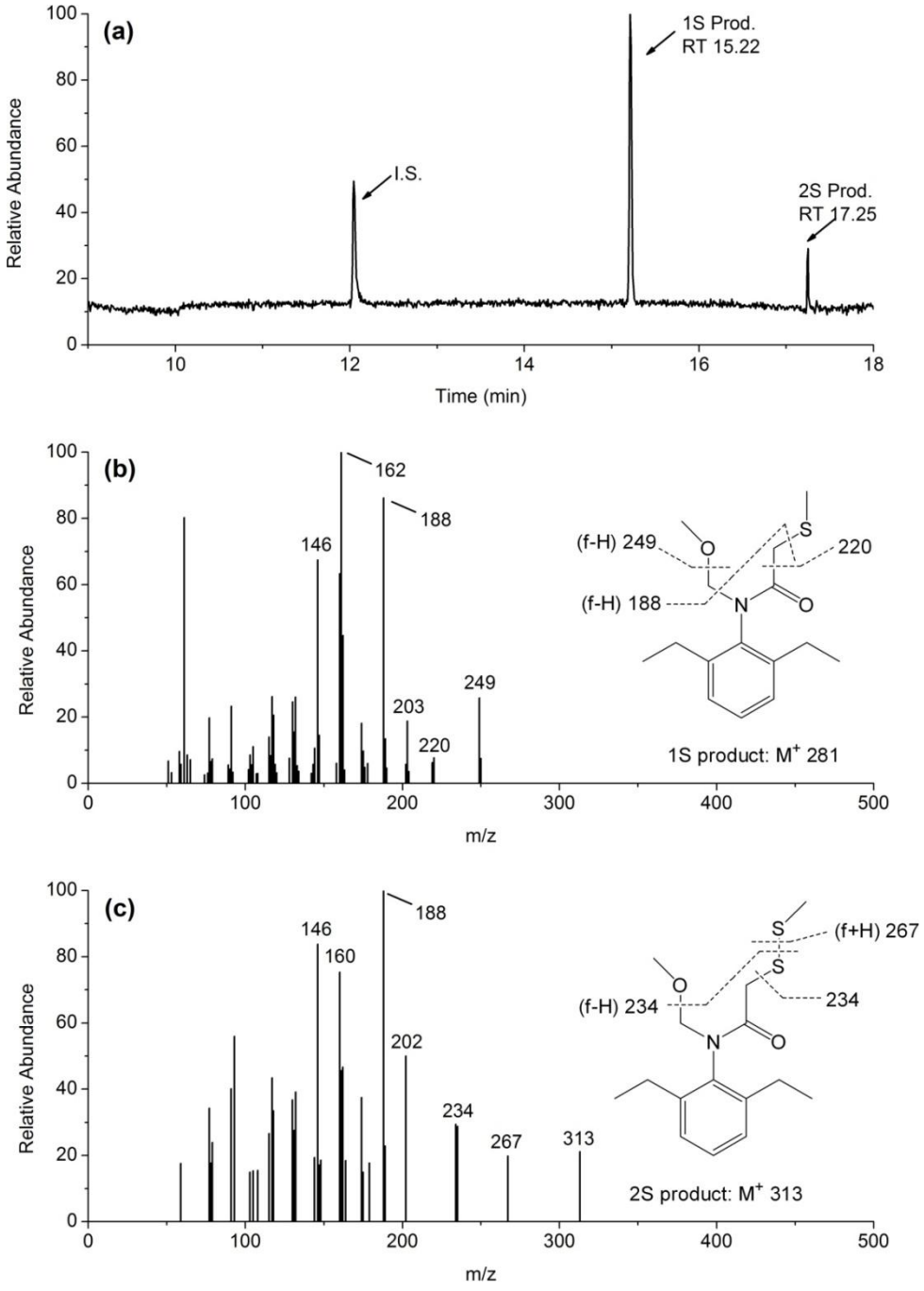

Figure A.6 Total ion chromatogram (TIC) and mass spectra of methylated products obtained in the reaction of alachlor with porewaters: (a) TIC of alachlor products; (b) Mass spectrum of 1S-substituted product; (c) Mass spectrum of 2S-substituted product. "I.S." denotes the internal standard (i.e., terbuthylazine). "RT" denotes the retention time (min). "1S" and "2S" denote the number of sulfur atoms in the products.

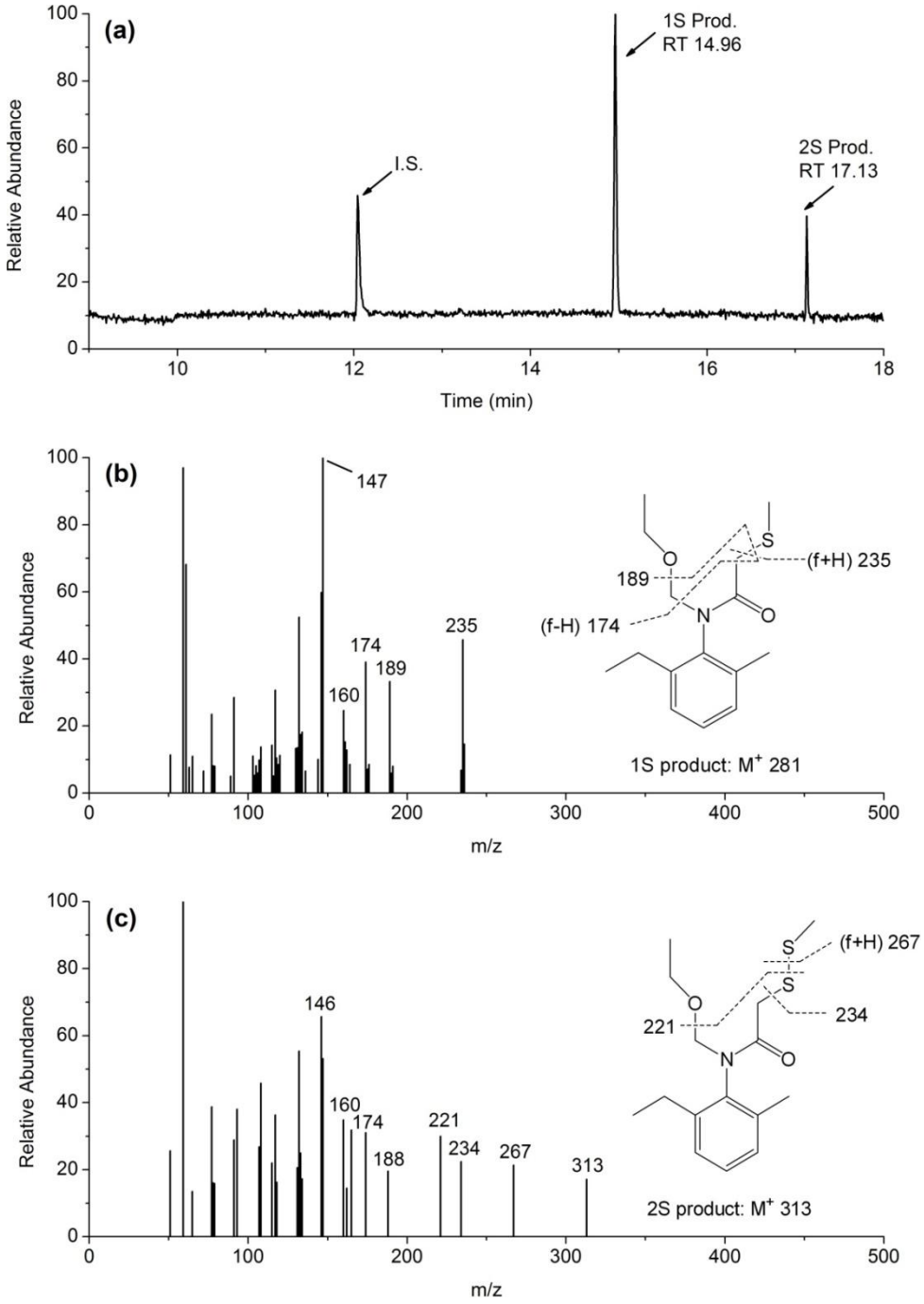

Figure A.7 Total ion chromatogram (TIC) and mass spectra of methylated products obtained in the reaction of acetochlor with porewaters: (a) TIC of acetochlor products; (b) Mass spectrum of 1S-substituted product; (c) Mass spectrum of 2S-substituted product. "I.S." denotes the internal standard (i.e., terbuthylazine). "RT" denotes the retention time (min). "1S" and "2S" denote the number of sulfur atoms in the products.

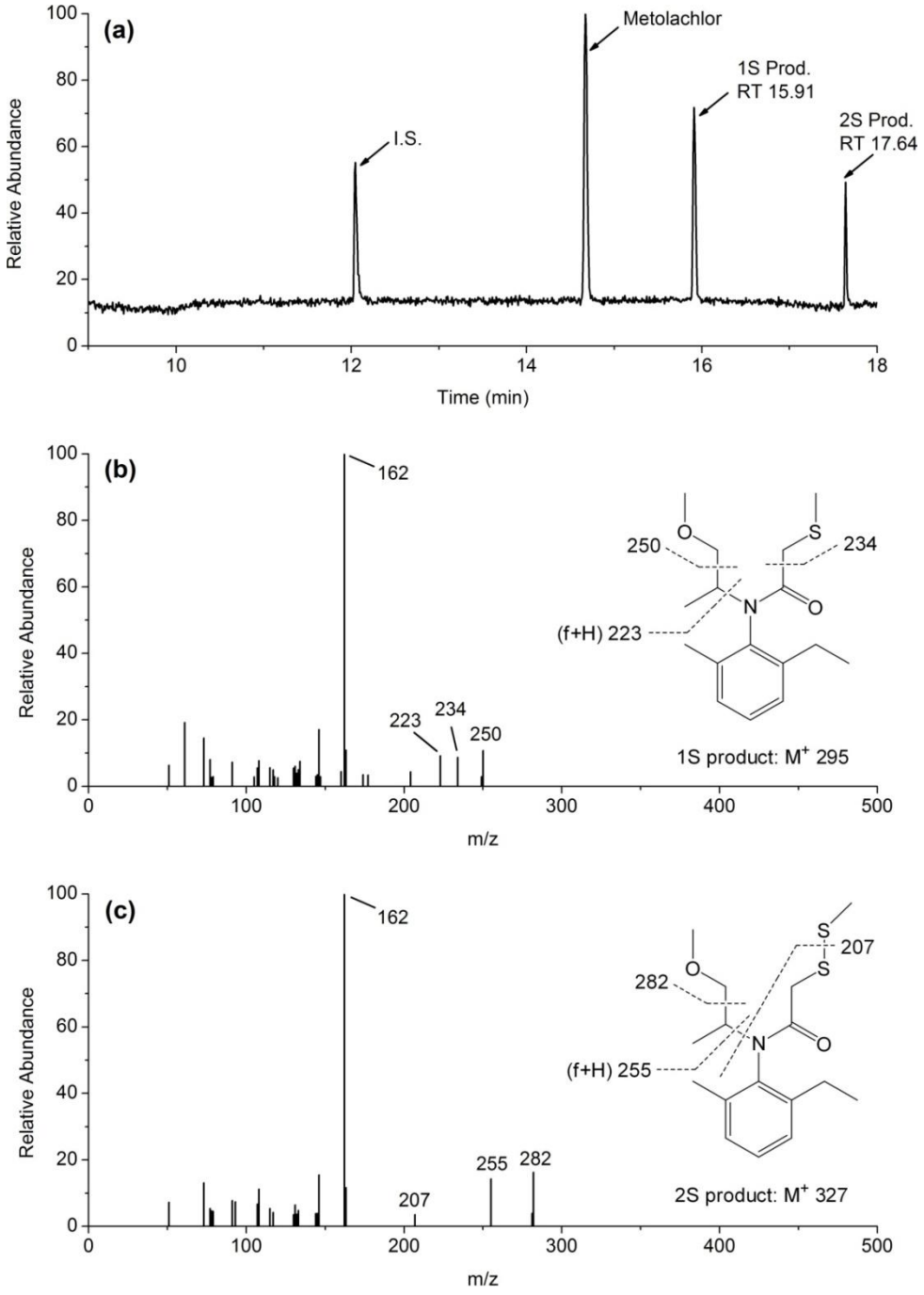

Figure A.8 Total ion chromatogram (TIC) and mass spectra of methylated products obtained in the reaction of metolachlor with porewaters: (a) TIC of metolachlor products; (b) Mass spectrum of 1S-substituted product; (c) Mass spectrum of 2S-substituted product. "I.S." denotes the internal standard (i.e., terbuthylazine). "RT" denotes the retention time (min). "1S" and "2S" denote the number of sulfur atoms in the products.

A.11 References

1. Steudel, R., Inorganic polysulfides S_n^{2-} and radical anions $S_n^{\cdot-}$. In *Elemental Sulfur and Sulfur-Rich Compounds Ii*, Springer-Verlag Berlin: Berlin, 2003; Vol. 231, pp 127-152.
2. Kishore, K.; Ganesh, K., Polymers containing disulfide, tetrasulfide, diselenide and ditelluride linkages in the main chain. In *Polymer Synthesis/Polymer Engineering*, Springer Berlin / Heidelberg: 1995; Vol. 121, pp 81-121.
3. Clesceri, L. S.; Greenberg, A. E.; Eaton, A. D., *Standard Methods for the Examination of Water and Wastewater*. 20th ed.; American Public Health Association (APHA), American Water Works Association (AWWA), Water Environment Federation (WEF): Washington, DC, 1995.
4. Shea, D.; Helz, G. R., The solubility of copper in sulfidic waters - sulfide and polysulfide complexes in equilibrium with covellite. *Geochim. Cosmochim. Acta* **1988,** *52*, 1815-1825.
5. Loch, A. R.; Lippa, K. A.; Carlson, D. L.; Chin, Y.-P.; Traina, S. J.; Roberts, A. L., Nucleophilic aliphatic substitution reactions of propachlor, alachlor, and metolachlor with bisulfide (HS^-) and polysulfides (S_n^{2-}). *Environ. Sci. Technol.* **2002,** *36*, 4065-4073.
6. Qin, Y. Abiotic reactions of acetanilide herbicides with bisulfide. M.S. Thesis, Oklahoma State University, Stillwater, OK, 1995.
7. Gan, J. Y., Enhanced degradation of chloroacetanilide herbicides by polysulfide salts. In *Proceedings of the 2006 USDA-CSREES National Water Quality Conference*, USDA-NIFA National Integrated Water Quality Program: Washington, DC, 2006.
8. Bian, H.; Chen, J.; Cai, X.; Liu, P.; Wang, Y.; Huang, L.; Qiao, X.; Hao, C., Dechlorination of chloroacetanilide herbicides by plant growth regulator sodium bisulfite. *Water Res.* **2009,** *43*, 3566-3574.
9. Barbash, J. E.; Reinhard, M., Reactivity of sulfur nucleophiles toward halogenated organic compounds in natural waters. In *Biogenic Sulfur in the Environment*, Saltzman, E. S.; Cooper, W. J., Eds. American Chemical Society: Washington, DC, 1989; Vol. 393, pp 101-138.
10. Gan, J. Y.; Wang, Q. Q.; Yates, S. R.; Koskinen, W. C.; Jury, W. A., Dechlorination of chloroacetanilide herbicides by thiosulfate salts. *Proc. Natl. Acad. Sci. USA* **2002,** *99*, 5189-5194.
11. Boparai, H. K.; Shea, P. J.; Comfort, S. D.; Snow, D. D., Dechlorinating chloroacetanilide herbicides by dithionite-treated aquifer sediment and surface soil. *Environ. Sci. Technol.* **2006,** *40*, 3043-3049.

Appendix B: Supporting Information for Chapter 3

B.1 Dinitroaniline product identification by gas chromatography

Table B.1 GC-MS/MS conditions for dinitroaniline product identification

Compounds	RT (min)[c]	Precursor ion, *m/z*[d]	Product ion, *m/z*[e]	Precursor-product pair[f]	Collision energy (*eV*)[g]
Trifluralin	12.39	335	264 (*39*), 290 (*100*), 306 (*53*)	335 > 290	15
1-NH_2 Product[a]	13.75	305	234 (*17*), 260 (*36*), 276 (*100*)	305 > 276	14
2-NH_2 Product[b]	13.51	275	204 (*11*), 232 (*2*), 246 (*100*)	275 > 246	15
Ethalfluralin	12.18	333	232 (*29*), 276 (*100*), 316 (*42*)	333 > 276	15
1-NH_2 Product[a]	13.52	303	246 (*100*), 274 (*67*), 287 (*45*)	303 > 246	17
2-NH_2 Product[b]	13.28	273	203 (*48*), 216 (*6*), 230 (*100*)	273 > 230	18
Benfluralin	12.45	335	264 (*76*), 277 (*63*), 292 (*100*)	335 > 292	14
1-NH_2 Product[a]	13.80	305	218 (*39*), 246 (*26*), 262 (*100*)	305 > 262	16
2-NH_2 Product[b]	13.51	275	204 (*6*), 232 (*100*), 246 (*3*)	275 > 232	19
Pendimethalin	17.76	281	162 (*27*), 191 (*18*), 252 (*100*)	281 > 252	17
1-NH_2 Product[a]	16.45	251	208 (*1*), 222 (*28*), 235 (*100*)	251 > 235	17
Isopropalin	17.49	309	264 (*73*), 280 (*100*), 292 (*31*)	309 > 280	15
1-NH_2 Product[a]	17.47	279	208 (*25*), 250 (*100*), 263 (*22*)	279 > 250	17
Butralin	17.23	295	250 (*14*), 266 (*100*), 277 (*20*)	295 > 266	16
1-NH_2 Product[a]	17.34	265	209 (*8*), 220 (*14*), 236 (*100*)	265 > 236	19
Nitralin	21.02	345	274 (*12*), 300 (*5*), 316 (*100*)	345 > 316	13
2-NH_2 Product[b]	22.04	285	214 (*13*), 226 (*26*), 256 (*100*)	285 > 256	16

[a] Diamine reaction product. Proposed structure shown in Figure B.13-Figure B.26. [b] Triamine reaction product. Proposed structure shown in Figure B.13-Figure B.26. [c] Retention time of compounds. [d] Molecular ion of parent and product compounds. [e] Major fragments of precursor ion. Number in parenthesis is the percent relative abundance. [f] Ion pair chosen for the selected reaction monitoring. [g] Collision energy optimized by the energy ramp function.

B.2 Semilogarithmic plots for dinitroaniline transformation

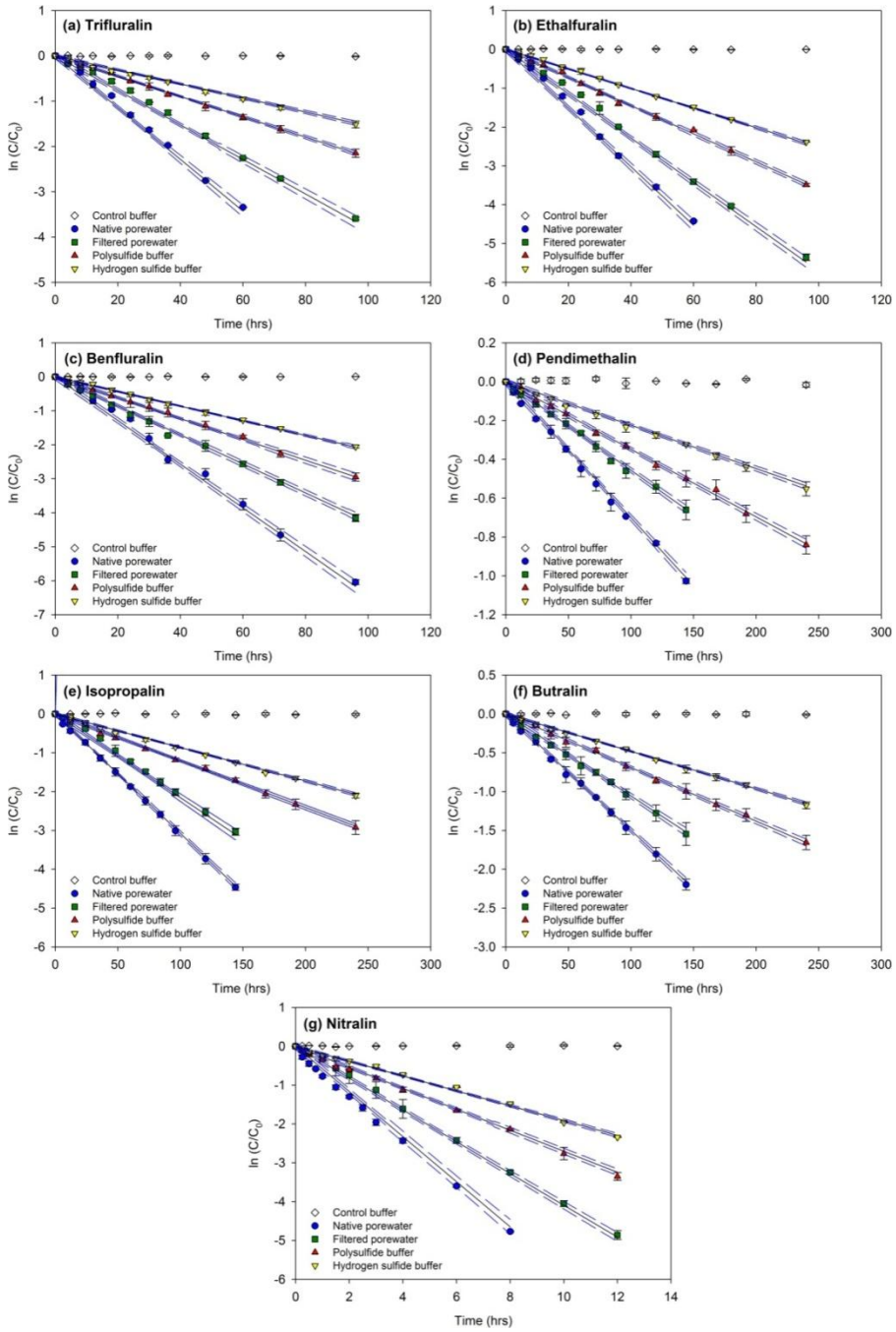

Figure B.1 Semilogarithmic plots for dinitroaniline transformation in P8 porewaters (Apr 2010) and sulfide redox buffers: (a) trifluralin; (b) ethalfluralin; (c) benfluralin; (d) pendimethalin; (e) isopropalin; (f) butralin; (g) nitralin. Open symbols represent Tris buffer controls. Error bars represent one standard deviation of duplicate samples; where absent, bars fall within symbols. Note differences in time scales. Solid lines represent linear regressions and dashed lines represent 95% confidence intervals. $R^2 > 0.99$ in all cases.

B.3 Ethalfluralin reactions with bisulfide and polysulfides

The transformation of ethalfluralin was studied in hydrogen sulfide and polysulfide buffers with varying [HS^-] and $\Sigma[S_n^{2-}]$ (while maintaining pseudo-first-order conditions) at constant pH (~8.80) to verify the reaction order of dinitroanilines with HS^- and S_n^{2-}. The sampling, extraction, and analysis procedures were the same as described in the text. Details pertaining to buffer composition and observed reaction rate constants are summarized in Table B.2.

(1) Ethalfluralin reaction with HS^-

For the reaction of ethalfluralin in hydrogen sulfide buffers, the rate of reaction can be expressed by the following equation:

$$-\frac{d[Ethalfluralin]}{dt} = k_{obs}\cdot[Ethalfluralin]^c = k_{HS^-}\cdot[HS^-]^a\cdot[Ethalfluralin]^c \qquad (B.1)$$

where a and c represent the order of reaction with respect to [HS^-] and [Ethalfluralin], respectively. Assuming c = 1, the above equation can be rewritten as:

$$ln\frac{[Ethalfluralin]}{[Ethalfluralin]_0} = -k_{obs}\cdot t \qquad (B.2)$$

A linear regression of ln [Ethalfluralin]/[Ethalfluralin]$_0$ versus time would yield a slope equal to $-k_{obs}$. The reaction time courses of ethalfluralin in four different hydrogen sulfide buffers are shown in Figure B.2(a). The highly linear semilogarithmic plots in Figure B.2(b) indicate that the reaction is of a first-order dependence on [Ethalfluralin].

The order of reaction with respect to [HS^-] was determined by a linear regression of log k_{obs} versus log [HS^-]:

$$log\ k_{obs} = log\ k_{HS^-} + a\cdot log[HS^-] \qquad (B.3)$$

As shown by Figure B.2(c), the regression yielded a slope *a* equal to 0.993 ± 0.025. Thus, it is reasonable to describe the reaction of ethalfluralin with HS^- as an overall second-order process, first order both in [HS^-] and in [Ethalfluralin]. This agrees with a previous report of first-order dependence on both nitrobenzene and HS^- concentrations in the reduction of nitrobenzene by sodium sulfide.[1]

The value of second-order rate constant for reaction of ethalfluralin with HS^- was then computed by a linear regression of k_{obs} versus [HS^-]:

$$k_{obs} = k_{HS^-} \cdot [HS^-] \tag{B.4}$$

As illustrated in Figure B.2(d), the regression yielded a slope k_{HS^-} equal to 3.48 $\pm(0.06) \times 10^{-3}$ $M^{-1}.s^{-1}$, which is consistent with the value previously measured in the control hydrogen sulfide buffer (k_{HS^-} = 3.46 ($\pm$0.03) $\times 10^{-3}$ $M^{-1}.s^{-1}$; see Table 3.3). The intercept of the regression line is not significantly different from zero, which corresponds to the lack of ethalfluralin reactivity in the Tris control buffer.

(2) Ethalfluralin reaction with S_n^{2-}

For the reaction of ethalfluralin in polysulfide buffers, the rate of reaction can be expressed by the following equation, assuming all polysulfide species have the same rate constants:

$$-\frac{d[Ethalfluralin]}{dt} = k_{obs} \cdot [Ethalfluralin]^c \tag{B.5}$$

$$= (k_{HS^-} \cdot [HS^-]^a + k_{S_n^{2-}} \cdot (\Sigma[S_n^{2-}])^b) \cdot [Ethalfluralin]^c$$

where *a*, *b*, and *c* represent the order of reaction with respect to [HS^-], $\Sigma[S_n^{2-}]$ and [Ethalfluralin], respectively. Assuming c = 1, the above equation can also be simplified as

Equation B.2: A linear regression of ln [Ethalfluralin]/[Ethalfluralin]$_0$ versus time should yield a slope equal to -k_{obs}. The reaction time courses of ethalfluralin in four different polysulfide buffers are shown in Figure S3(a). The highly linear semilogarthmic plots in Figure S3(b) indicate that the reaction is again of a first-order dependence on [Ethalfluralin].

The order of reaction with respect to $\Sigma[S_n^{2-}]$ was estimated by a linear regression of log (k_{obs} - $k_{HS^-}[HS^-]$) versus log $\Sigma[S_n^{2-}]$:

$$log\ (k_{obs} - k_{HS^-} \cdot [HS^-]) = log\ k_{S_n^{2-}} + b \cdot log\ \Sigma[S_n^{2-}] \quad \text{(B.6)}$$

As shown by Figure S3(c), the regression yielded a slope b equal to 0.978 ± 0.037. Thus, it is also reasonable to describe the reaction of ethalfluralin with S_n^{2-} as an overall second-order process, first order both in $\Sigma[S_n^{2-}]$ and in [Ethalfluralin]. This is consistent with previous findings of first-order dependence on both nitrobenzene and S_2^{2-} concentrations in the reduction of nitrobenzene by sodium disulfide.[2,3]

The value of second-order rate constant for reaction of ethalfluralin with S_n^{2-} was then computed by a linear regression of k_{obs} - $k_{HS^-}[HS^-]$ versus $\Sigma[S_n^{2-}]$:

$$k_{obs} - k_{HS^-} \cdot [HS^-] = k_{S_n^{2-}} \cdot \Sigma[S_n^{2-}] \quad \text{(B.7)}$$

As illustrated in Figure S3(d), the regression yielded a slope $k_{S_n^{2-}}$ equal to 6.27 ±(0.10)×10^{-2} $M^{-1}.s^{-1}$, which is not significantly different from the value previously measured in the control polysulfide buffer ($k_{S_n^{2-}}$ = 6.66 (±0.64) ×10^{-2} $M^{-1}.s^{-1}$; see Table 3.3). Again, the intercept of the regression line is not significantly different from zero.

The validity of computing $k_{S_n^{2-}}$ in polysulfide buffers through subtracting k_{HS^-}[HS$^-$] from k_{obs} was tested by comparing the values of k_{HS^-} and $k_{S_n^{2-}}$ obtained from Equations B.4 and B.7, respectively, to those simultaneously derived through a multiple linear regression of the following equation using the measured [HS$^-$], $\Sigma[S_n^{2-}]$, and k_{obs} as the constraints:

$$k_{obs} = k_{HS^-} \cdot [HS^-] + k_{S_n^{2-}} \cdot \Sigma[S_n^{2-}] \quad \text{(B.8)}$$

The resulting regression equation is:

$$k_{obs} = 3.37\ (\pm 0.34) \times 10^{-3} \cdot [HS^-] + 6.62\ (\pm 0.83) \times 10^{-2} \cdot \Sigma[S_n^{2-}] + 8.43\ (\pm 9.25) \times 10^{-8} \quad \text{(B.9)}$$

The value of k_{HS^-}, 3.37 $\pm$(0.34)$\times 10^{-3}$ $M^{-1}.s^{-1}$, is not statistically different from that determined in hydrogen sulfide buffers containing only HS$^-$ (3.46 $\pm$(0.06)$\times 10^{-3}$ $M^{-1}.s^{-1}$; see Table 3.3). Based on the results from ethalfluralin, the reactions of other dinitroanilines in sulfide redox buffers with respect to HS$^-$ and S_n^{2-} are also assumed to be first order in [HS$^-$] and $\Sigma[S_n^{2-}]$, respectively.

Table B.2 Hydrogen sulfide and polysulfide buffer compositions and ethalfluralin reaction rate constants

Hydrogen sulfide buffer	pH	$[H_2S]_T$ (μM)[a]	$[HS^-]_{calc}$ (μM)[b]	$[H_2S_n]_{T,\ calc}$ (μM)[c]	$\Sigma[S_n^{2-}]_{calc}$ (μM)[d]	k_{obs} (s^{-1})[e]	$k_{obs} - k_{HS^-}[HS^-]$ (s^{-1})[f]
A	8.80	509 (±7)	505 (±10)	0	0	1.81 (±0.17) ×10^{-6}	N.A.[g]
B	8.81	1015 (±7)	1007 (±10)	0	0	3.44 (±0.11) ×10^{-6}	N.A.[g]
C	8.81	2020 (±11)	2004 (±16)	0	0	7.00 (±0.33) ×10^{-6}	N.A.[g]
D	8.83	4033 (±19)	4001 (±27)	0	0	1.39 (±0.04) ×10^{-5}	N.A.[g]
Polysulfide buffer	**pH**	$[H_2S]_T$ (μM)[a]	$[HS^-]_{calc}$ (μM)[b]	$[H_2S_n]_{T,\ calc}$ (μM)[c]	$\Sigma[S_n^{2-}]_{calc}$ (μM)[d]	k_{obs} (s^{-1})[e]	$k_{obs} - k_{HS^-}[HS^-]$ (s^{-1})[f]
E	8.82	521 (±8)	517 (±11)	19.8 (±0.7)	19.8 (±1.0)	3.14 (±0.22) ×10^{-6}	1.34 (±0.21) ×10^{-6}
F	8.84	1031 (±11)	1023 (±15)	39.4 (±1.2)	39.3 (±1.7)	6.19 (±0.31) ×10^{-6}	2.64 (±0.26) ×10^{-6}
G	8.84	2047 (±13)	2031 (±18)	81.0 (±5.0)	80.9 (±7.1)	1.22 (±0.05) ×10^{-5}	5.10 (±0.39) ×10^{-6}
H	8.83	4060 (±16)	4027 (±22)	163.5 (±8.3)	163.2 (±11.7)	2.45 (±0.09) ×10^{-5}	1.05 (±0.07) ×10^{-5}

[a] Total hydrogen sulfide concentration measured by the methylene blue method. Errors represent one standard deviation from triplicate measurements. [b] Bisulfide concentration calculated from $[H_2S]_T$ and pH, assuming that the sample is not saturated with elemental sulfur. Errors were propagated from $[H_2S]_T$. [c] Total polysulfide concentration calculated as the sum of measured $[Me_2S_2]$ and $[Me_2S_3]$ after correcting for methylation and extraction efficiencies. Errors were calculated through propagation of errors associated with $[Me_2S_2]$ and $[Me_2S_3]$. [d] Polysulfide dianion concentration calculated from measured $[H_2S_n]_{T,\ calc}$ and pH, assuming that the relative abundance of HS_n^- and S_n^{2-} species are dictated by equilibrium constants from Shea and Helz[4]. Errors were propagated from $[H_2S_n]_{T,\ calc}$. [e] Observed pseudo-first-order rate constants for reactions of ethalfluralin in hydrogen sulfide buffers. Errors represent one standard deviation from duplicate experiments. [f] Calculated pseudo-first-order rate constants for reactions of ethalfluralin in polysulfide buffers after subtracting the contribution from hydrogen sulfide. Errors represent one standard deviation from duplicate experiments. [g] N.A. = not available.

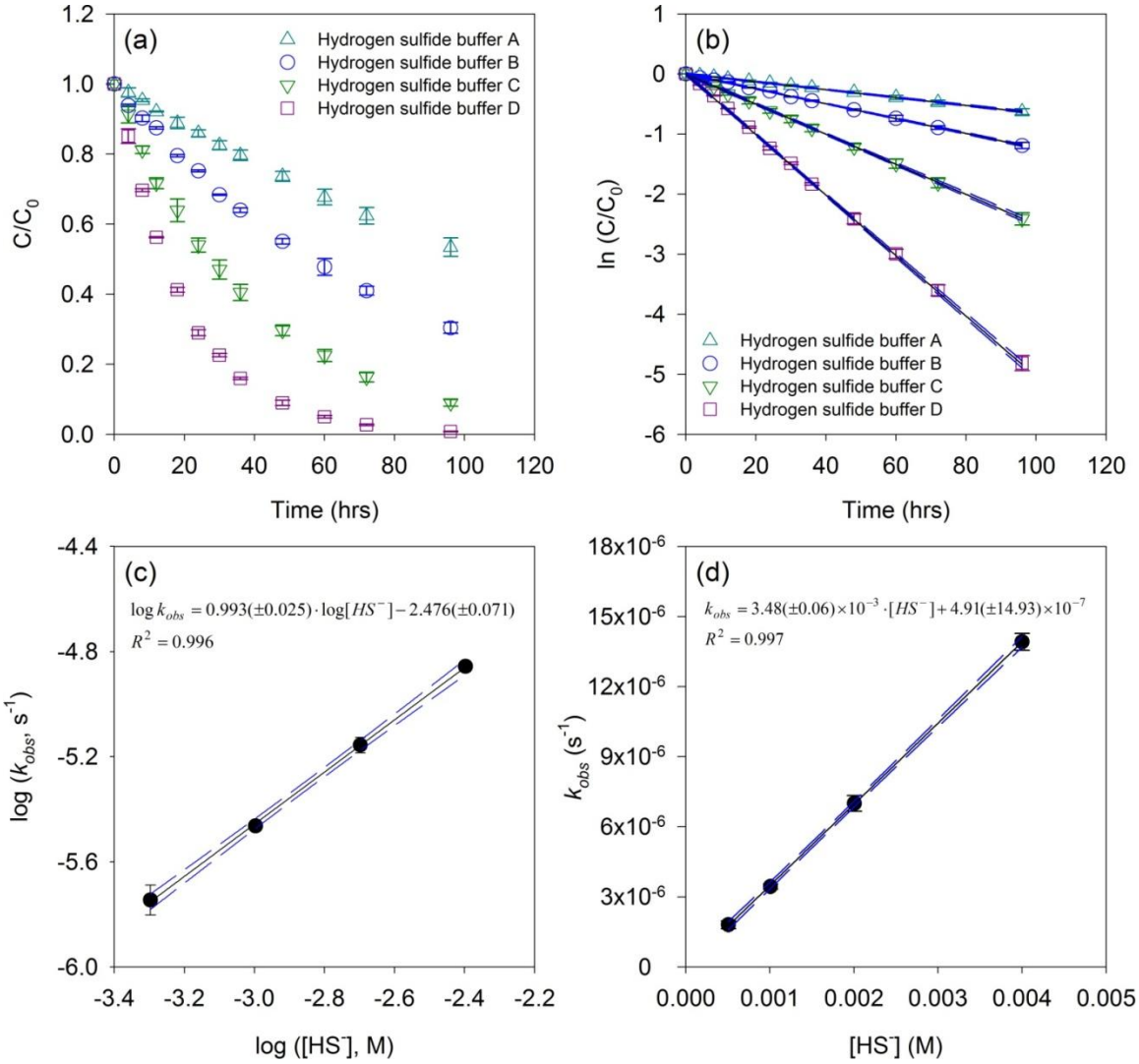

Figure B.2 Transformation of ethalfluralin in hydrogen sulfide buffers (A, B, C, and D; see Table B.2): (a) Time courses for reactions of ethalfluralin in hydrogen sulfide buffers. (b) Semilogarithmic plots for reactions of ethalfluralin in hydrogen sulfide buffers. (c) Plot of log (k_{obs}) versus log [HS^-] for reactions of ethalfluralin with HS^-. (d) Plot of k_{obs} versus [HS^-] for reactions of ethalfluralin with HS^-. Solid lines represent linear regressions and dashed lines represent 95% confidence intervals. $R^2 > 0.99$. Error bars represent one standard deviation of duplicate samples; where absent, bars fall within symbols.

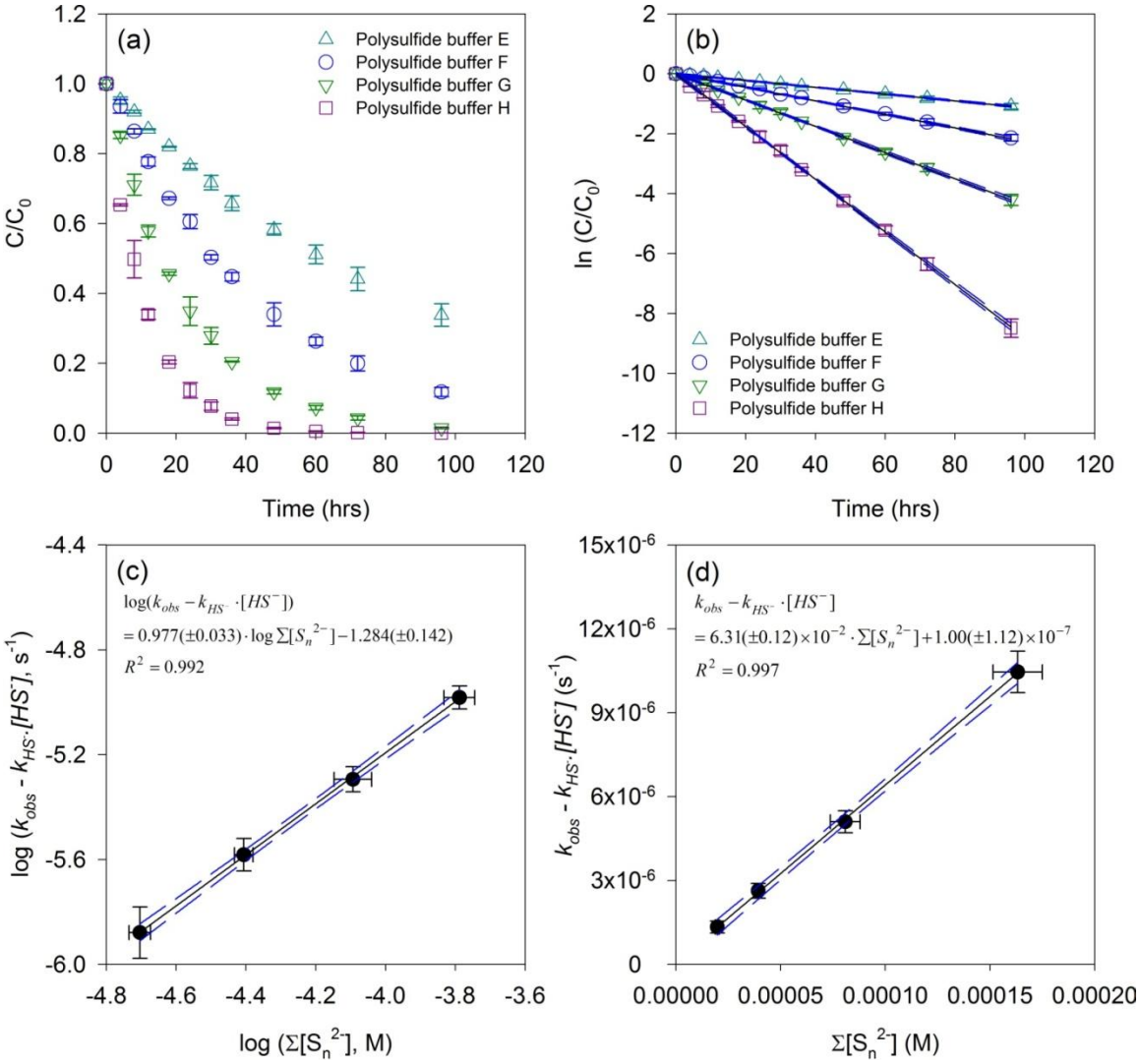

Figure B.3 Transformation of ethalfluralin in polysulfide buffers (E, F, G, and H; see Table B.2): (a) Time courses for reactions of ethalfluralin in polysulfide buffers. (b) Semilogarithmic plots for reactions of ethalfluralin in polysulfide buffers. (c) Plot of log (k_{obs} - k_{HS^-}[HS$^-$]) versus log [HS$^-$] for reactions of ethalfluralin with S_n^{2-}. (d) Plot of k_{obs} - k_{HS^-}[HS$^-$] versus Σ[S_n^{2-}] for reactions of ethalfluralin with S_n^{2-}. Solid lines represent linear regressions and dashed lines represent 95% confidence intervals. $R^2 > 0.99$. Error bars represent one standard deviation of duplicate samples; where absent, bars fall within symbols.

B.4 LFERs and correlation analysis for dinitroaniline transformation

Past research has determined or estimated the one-electron reduction potentials ($E_h^{1'}$) of half reactions for various NACs of environmental relevance. LFERs of the type of Equation B.11 are often developed to evaluate or predict the reactivity of different NACs with their $E_h^{1'}$ values in a given system:[5]

$$ArNO_2 + e^- \leftrightarrow ArNO_2^{\bullet -} \quad E_h^{1'}(ArNO_2) \tag{B.10}$$

$$\log(k) = a\left(\frac{E_h^{1'}}{0.059V}\right) + b \text{ (at 25°C)} \tag{B.11}$$

where slope a and intercept b are constants. Such LFERs *presuppose* that the transfer of the first electron from the reductant to the NACs is the rate-limiting step. Thus, the value of a has long been taken as an indicator of the importance of the first electron transfer in the overall reaction.[5] The actual transfer of first electron from reductants to NACs is considered as the rate-limiting step when $a \approx 1.0$, while other processes become rate limiting when $a \ll 1.0$.[5] Recent studies on nitrogen isotope fractionation during NAC reduction, however, have questioned the validity of the assumption made for such LFERs. Hartenbach and co-workers[6-8] demonstrated that the overall NAC reduction rate might depend on an irreversible reductive cleavage of first N-O bond as well as equilibrium constants of preceding reversible e^- and H^+-transfers to the nitroaryl radical anion. In this case, the slope a in Equation B.11 reflects the relative sensitivity of $E_h^{1'}$ to the collective influence of the NAC substituents on all the preceding elementary reactions.[9,10]

Regardless of the underlying mechanism, a LFER analysis based on Equation B.11 was developed for the target dinitroanilines to assess their relative reactivity in the porewaters. Excellent correlations were found between log k and $E_h^{I'}$ (Figure B.4). Because the $E_h^{I'}$ values of three target dinitroanilines (i.e., ethalfluralin, benfluralin, and butralin) were unavailable in the literature, they were extrapolated using an existing LFER established from other four dinitroanilines with previously estimated $E_h^{I'}$ values. The pseudo-first-order rate constants ($k_{obs,\ native}$ and $k_{obs,\ filtered}$) and second-order rate constants (k_{HS^-} and $k_{S_n^{2-}}$) of nitralin, trifluralin, isopropalin, and pendimethalin obtained in the porewaters and sulfide redox buffers, respectively, were correlated with their $E_h^{I'}$ values reported by Wang and Arnold.[11] Using regression equations derived from Figure B.4, the average $E_h^{I'}$ values of ethalfluralin, benfluralin, and butralin were calculated (Table B.3). The $E_h^{I'}$ values decreased in the order: nitralin > ethalfluralin > benfluralin > trifluralin > isopropalin > butralin > pendimethalin, which can be rationalized by the destabilization and stabilization of nitroaryl radical anions by substituents.[5] Phillips and co-workers[10,12] have recently found that the adiabatic electron affinities and $E_h^{I'}$ values of NACs are linearly correlated with each other. Hence, it would be desirable to use such quantum mechanics method to further verify the $E_h^{I'}$ values of dinitroanilines obtained in this study.

LFERs established for the porewater and sulfide buffer systems also exhibited highly parallel patterns with slopes a equal to 4.35 (±0.02). This value of a is significantly higher than those obtained for reactions of dinitroanilines in the H_2S-juglone (a = 0.94) and Fe(II)-goethite (a = 1.25) systems,[11] as well as those obtained for

reduction of NACs in various model systems (a = 0.94-1.25 for H_2S-juglone;[13,14] a = 0.99 for H_2S-lawsone;[13] a = 0.45-1.00 for H_2S-NOM;[15] a = 0.22-0.43 for Fe(II)-magnetite;[16] a = 0.60 for Fe(II)-goethite;[14] a = 0.67-0.75 for Fe(II)-smectite;[17] a = 0.60-0.93 for Fe(II)-porphyrin;[13] a = 1.11 for Fe(II)-tiron;[18] a = 0.65 for Fe(II)-cysteine;[9] a = 0.91 for Fe(II)-thioglycolate[9]). As reported by Wang and Arnold,[11] with an increase of pH from 6.5 to 7.3, the value of a increased from 0.98 to 2.14 for the reduction of four dinitroanilines in the Fe(II)-goethite system (where a = 1.35pH - 7.63; R^2 = 0.87). If one assumes that such relationship also exists for the porewaters and sulfide buffer systems, the predicted value of a would be close to 4.25 at pH 8.80. As discussed above, the preceding elementary reactions or N-O bond breaking might be the actual (but not necessarily the only) rate-limiting step of the reaction. In fact, this new mechanistic picture may also help explain the relatively fast direct reduction of dintiroanilines by HS^- and S_n^{2-} compared to previously studied mononitroaromtic compounds. That said, the LFERs are potentially useful for the prediction of reduction rate constants for dinitroanilines in sulfide containing systems but cannot provide mechanistic insight into the rate-limiting step.

Finally, Perlinger and co-workers[19] proposed that transformation mechanisms of organic pollutants in an unknown system could be inferred from LFERs by comparing the rate constants obtained in the system of interest to a better-defined one. A slope of unity in a cross-correlation of logarithmic rate constants, therefore, can be interpreted as indication of identical mechanisms with the same rate-limiting step.[19-21] Kohn and co-workers,[22] however, have argued that a slope of unity in correlation analysis is neither necessary nor sufficient evidence of a common mechanism in different systems. This

later argument seems to support the observations in the current study. As shown in Figure B.5, the slopes of the linear regressions in six cross-correlations between porewater and sulfide buffer systems are all very close to unity (i.e., 0.996 ± 0.004) with strong correlation (i.e., R^2 > 0.99). Experimental evidence, however, clearly pointed out that direct reduction reactions with HS^- and S_n^{2-} were not the only operating mechanisms responsible for the transformations of target dinitroanilines in PPL porewaters (see discussion in the text).

Table B.3 $E_h^{l'}$ values of dinitroanilines

Dinitroaniline	$E_h^{l'}$ (mV)
Trifluralin	-414[a]
Ethalfluralin	-411[b]
Benfluralin	-412[b]
Pendimethalin	-425[a]
Isopropalin	-417[a]
Butralin	-421[b]
Nitralin	-399[a]

[a] $E_h^{l'}$ values reported by Wang and Arnold.[11] [b] Average $E_h^{l'}$ values estimated from regression equations obtained in Figure B.4 with 95% confidence intervals at about 0.3 mV.

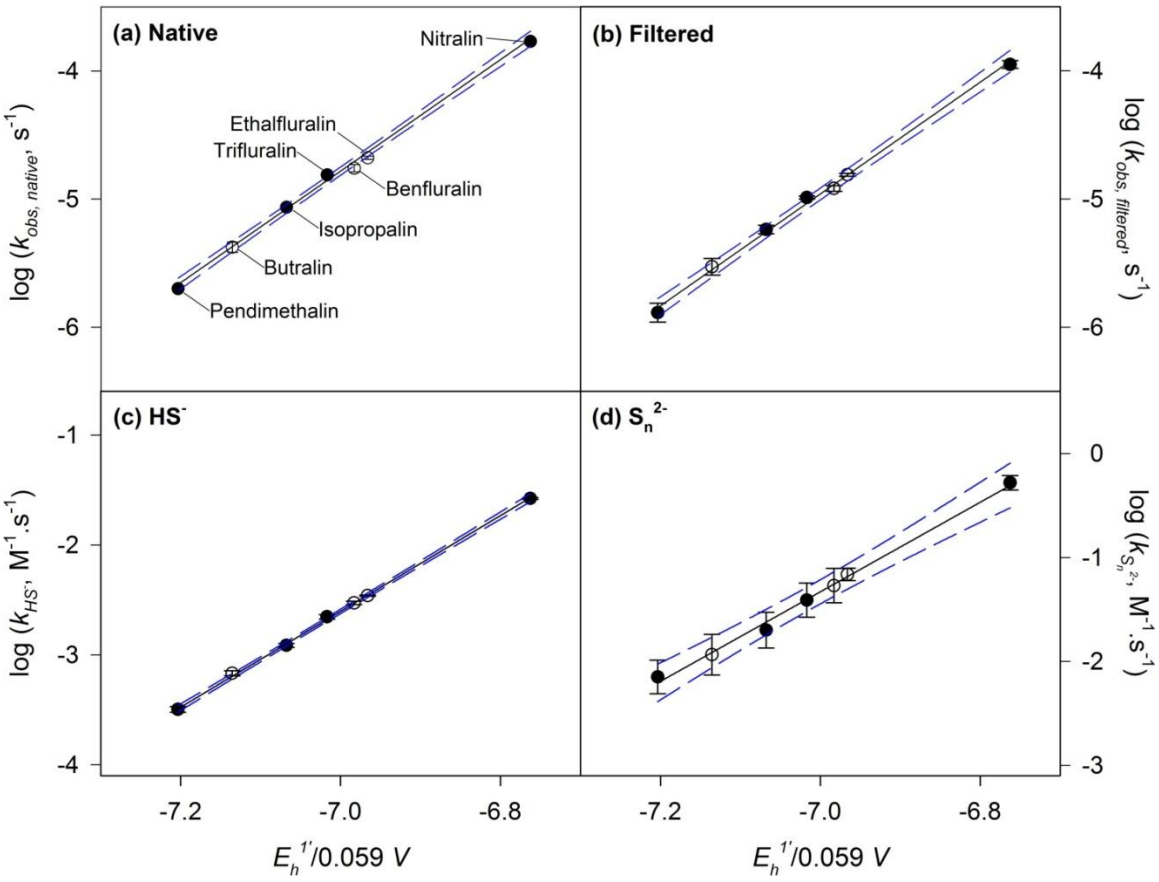

Figure B.4 LFER plots of reaction rate constants of dinitroanilines versus the $E_h^{1'}$ values of the compounds. Filled circles (●) represent reference compounds with known $E_h^{1'}$, whereas open circles (○) represent compounds with unknown $E_h^{1'}$. Solid lines represent linear regressions and dashed lines represent 95% confidence intervals. Error bars represent one standard deviation of duplicate measurements; where absent, bars fall within symbols. Regression equations for the four panels are as follows: (a) $\log(k_{obs,\ native}) = 4.35(\pm0.08)(E_h^{1'}/0.059V) + 25.67(\pm0.57)$, $R^2 = 0.998$; (b) $\log(k_{obs,\ fltered}) = 4.36(\pm0.12)(E_h^{1'}/0.059V) + 25.58(\pm0.82)$, $R^2 = 0.996$; (c) $\log(k_{obs,\ HS^-}) = 4.36(\pm0.05)(E_h^{1'}/0.059V) + 27.91(\pm0.35)$, $R^2 = 0.999$; (d) $\log(k_{obs,\ S_n^{2-}}) = 4.31(\pm0.30)(E_h^{1'}/0.059V) + 28.82(\pm2.08)$, $R^2 = 0.972$.

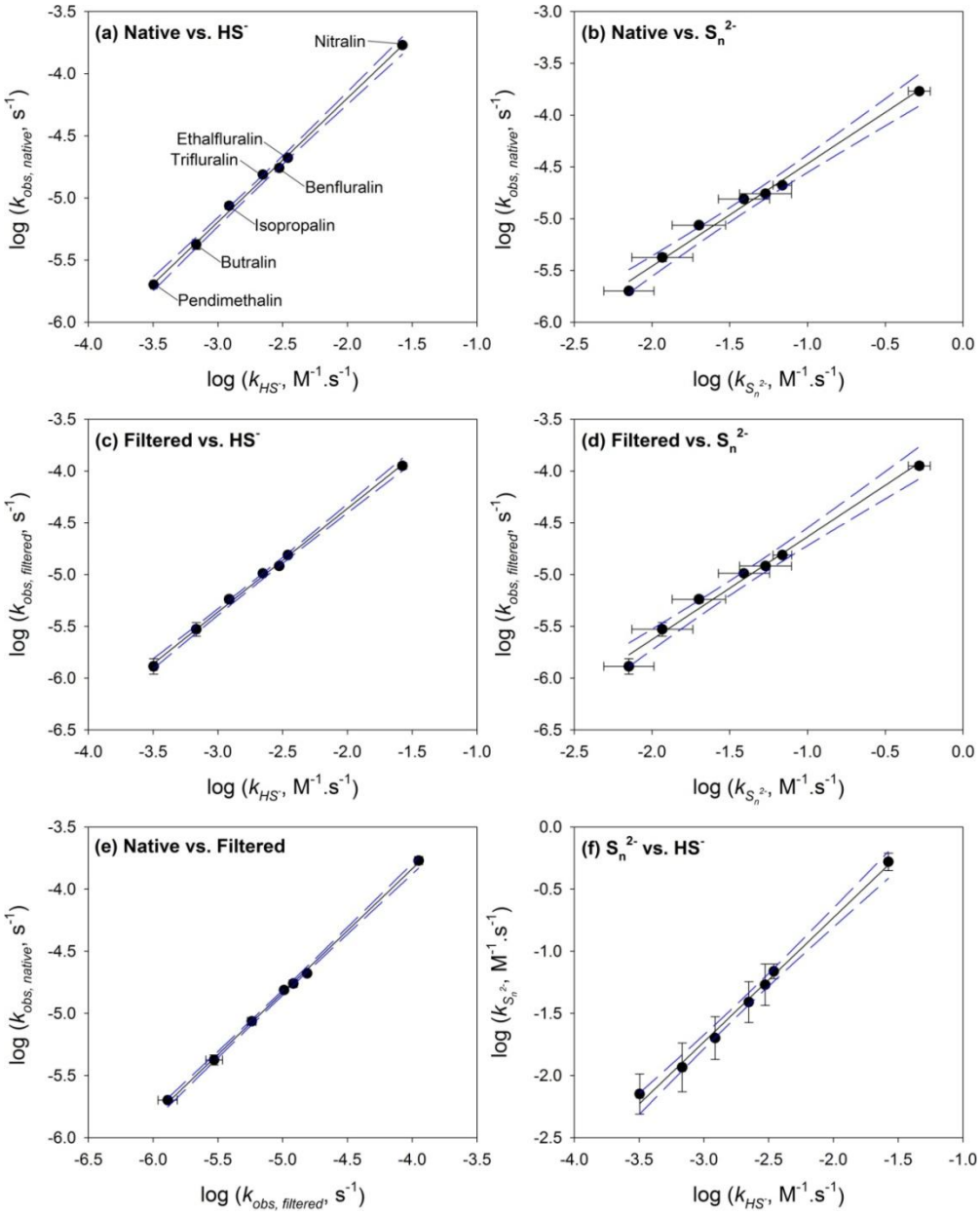

Figure B.5 Cross-correlations of reaction rate constants of dinitroanilines in the porewaters and sulfide redox buffers. Solid lines represent linear regressions and dashed lines represent 95% confidence intervals. Error bars represent one standard deviation of duplicate measurements; where absent, bars fall within symbols. Regression equations for the six panels are as follows: (a) $\log(k_{obs,\ native}) = 0.996(\pm0.022)\log(k_{obs,\ HS^-}) - 2.204(\pm0.060)$, $R^2 = 0.998$; (b) $\log(k_{obs,\ native}) = 0.990(\pm0.047)\log(k_{obs,\ S_n^{2-}}) - 3.480(\pm0.072)$, $R^2 = 0.989$; (c) $\log(k_{obs,\ fltered}) = 1.000(\pm0.019)(k_{obs,\ HS^-}) - 2.362(\pm0.052)$, $R^2 = 0.998$; (d) $\log(k_{obs,\ fltered}) = 0.993(\pm0.045)(k_{obs,\ S_n^{2-}}) - 3.642(\pm0.073)$, $R^2 = 0.989$; (e) $\log(k_{obs,\ native}) = 0.997(\pm0.014)\log(k_{obs,\ fltered}) + 0.150(\pm0.070)$, $R^2 = 0.999$; (f) $\log(k_{obs,\ S_n^{2-}}) = 0.999(\pm0.034)(k_{obs,\ HS^-}) + 1.269(\pm0.092)$, $R^2 = 0.994$.

B.5 Ethalfluralin reactions with sulfite and thiosulfate

The transformation of ethalfluralin was studied in sulfite and thiosulfate control buffers to evaluate direct reactions of dinitroanilines with concentrations of SO_3^{2-} and $S_2O_3^{2-}$ comparable to those found in PPL porewaters. The transformation of ethalfluralin was also investigated in additional control buffers containing juglone as a model NOM electron transfer mediator to assess the potential of SO_3^{2-} and $S_2O_3^{2-}$ to act as bulk reducing agents versus direct reductants. The sampling, extraction, and analysis procedures were the same as described in the text. Details pertaining to buffer composition and observed reaction rate constants are summarized in Table B.4.

The first set of sulfite and thiosulfate buffers were prepared by diluting an appropriate aliquot of their stock solutions into the deoxygenated Tris buffer. The second set of sulfite and thiosulfate buffers were also amended with 100 μM juglone by the addition of an aliquot of juglone methanolic stock solution. All sulfite and thiosulfate buffers were then adjusted with deoxygenated HCl or NaOH to the desired pH (~8.80). The concentrations of sulfite and thiosulfate were determined by IC after an in-sample oxidation by hydrogen peroxide.[23,24] Briefly, a 3-mL aliquot of sulfite or thiosulfate sample or standard solution was treated with 50 μL of H_2O_2 (30% w/w) in the anaerobic glove box and incubated at room temperature for 24 h. At the end of incubation, samples and standards were measured for sulfate concentrations by IC following the method described before.[25]

Table B.4 Sulfite and thiosulfate buffer compositions and ethalfluralin reaction rate constants

Sulfite buffer	pH	$[SO_3^{2-}]$ (μM)[a]	$[S_2O_3^{2-}]$ (μM)[b]	[Juglone] (μM)	k_{obs} (hr^{-1})[c]
A	8.80	31.22 (±0.34)	0	0	0.01 (±0.02) $\times 10^{-2}$
B	8.82	31.20 (±0.25)	0	100	-0.01 (±0.02) $\times 10^{-2}$
Thiosulfate buffer	**pH**	$[SO_3^{2-}]$ (μM)[a]	$[S_2O_3^{2-}]$ (μM)[b]	[Juglone] (μM)	k_{obs} (hr^{-1})[c]
C	8.83	0	98.51 (±2.79)	0	-0.01 (±0.02) $\times 10^{-2}$
D	8.81	0	100.19 (±3.49)	100	-0.03 (±0.02) $\times 10^{-2}$

[a] Sulfite concentration measured by ion chromatography. Errors represent one standard deviation from triplicate measurements. [b] Thiosulfate concentration measured by ion chromatography. Errors represent one standard deviation from triplicate measurements. [c] Observed pseudo-first-order rate constants for reactions of ethalfluralin in sulfite or thiosulfate buffers. Errors represent one standard deviation from duplicate experiments.

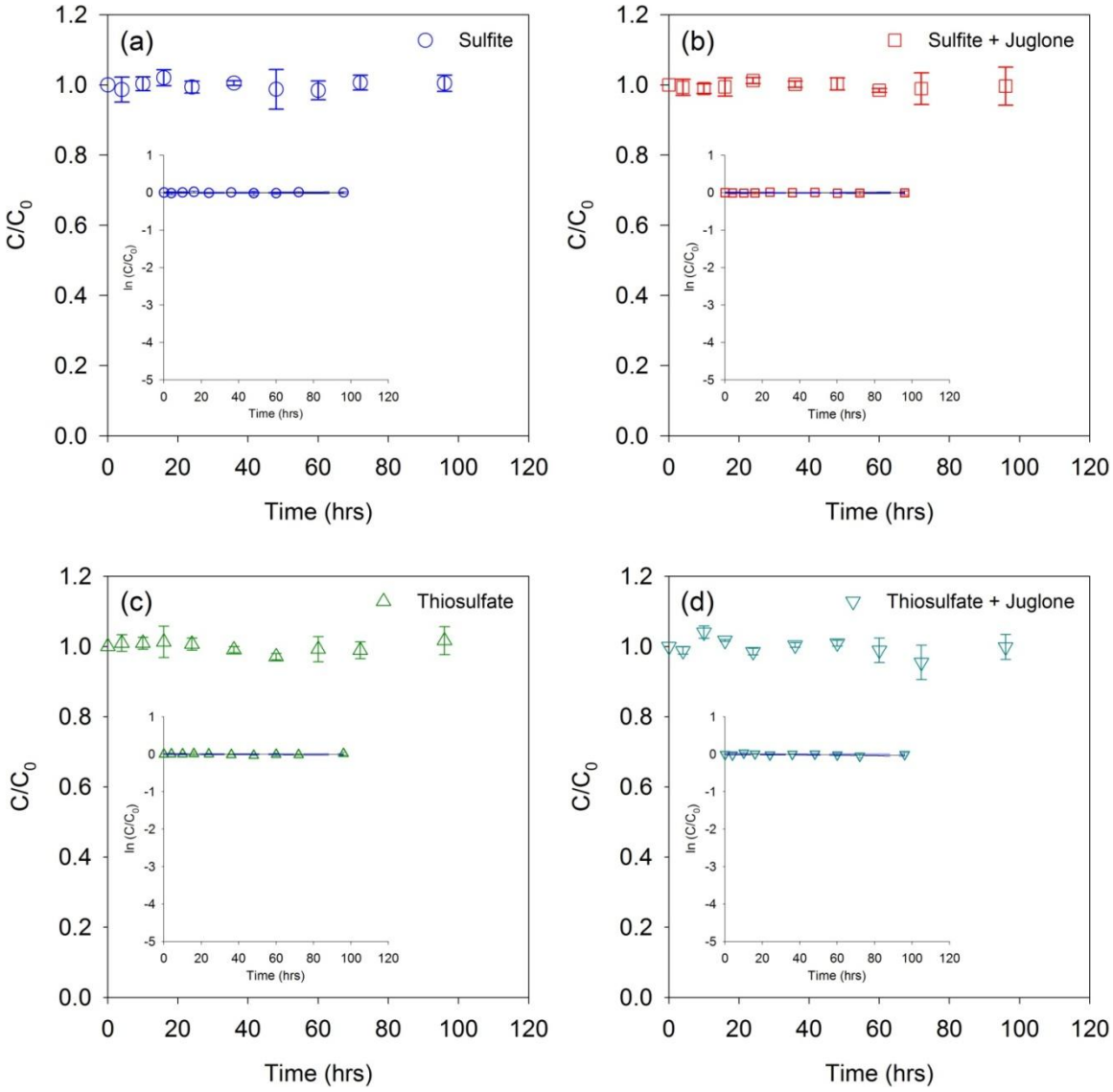

Figure B.6 Transformation of ethalfluralin in sulfite (A and B; see Table B.4) and thiosulfate (C and D; see Table B.4) buffers: (a) Time course for reaction of ethalfluralin in sulfite buffer. (b) Time course for reaction of ethalfluralin in sulfite buffer amended with juglone. (c) Time courses for reaction of ethalfluralin in thiosulfate buffer. (d) Time courses for reaction of ethalfluralin in thiosulfate buffer amended with juglone. Error bars represent one standard deviation of duplicate samples; where absent, bars fall within symbols. Inset depicts the same data plotted in semilogarithmic form. Solid lines represent linear regressions and dashed lines represent 95% confidence intervals.

B.6 Standard reduction potentials of sulfur redox couples

Table B.5 E_h^0 values of sulfur redox couples in aqueous solution

Half reaction[a]	E_h^0 (V)[a]
$S(s) + 2e^- + 2H^+ = H_2S_{(aq)}$	0.144
$S(s) + 2e^- = S^{2-}$	-0.447
$S(s) + 2e^- + H^+ = HS^-$	-0.062
$S(s) + 2e^- + 2H_2O = HS^- + OH^-$	-0.520
$S_2^{2-} + 2e^- = 2S^{2-}$	-0.483
$S_2^{2-} + 2e^- + 2H^+ = 2HS^-$	0.287
$2S_3^{2-} + 2e^- = 3S_2^{2-}$	-0.473
$S_3^{2-} + 4e^- + 3H^+ = 3HS^-$	0.097
$3S_4^{2-} + 2e^- = 4S_3^{2-}$	-0.453
$S_4^{2-} + 6e^- + 4H^+ = 4HS^-$	0.036
$4S_5^{2-} + 2e^- = 5S_4^{2-}$	-0.426
$S_5^{2-} + 8e^- + 5H^+ = 5HS^-$	0.007
$5S(s) + 2e^- = S_5^{2-}$	-0.340
$H_2SO_3 + 4e^- + 4H^+ = S(s) + 3H_2O$	0.500
$SO_3^{2-} + 4e^- + 3H_2O = S(s) + 6OH^-$	-0.659
$SO_4^{2-} + 2e^- + 4H^+ = H_2SO_3 + H_2O$	0.158
$SO_4^{2-} + 2e^- + H_2O = SO_3^{2-} + 2OH^-$	-0.936
$2H_2SO_3 + 4e^- + 2H^+ = S_2O_3^{2-} + 3H_2O$	0.400
$2HSO_3^- + 4e^- + 4H^+ = S_2O_3^{2-} + 3H_2O$	0.453
$2SO_3^{2-} + 4e^- + 6H^+ = S_2O_3^{2-} + 3H_2O$	0.666
$2SO_3^{2-} + 4e^- + 3H_2O = S_2O_3^{2-} + 6OH^-$	-0.576

[a] Half reactions and E_h^0 values taken from Bard et al.[26]

B.7 Contributions of HS^-, S_n^{2-}, and other processes

Table B.6 Contributions of HS^-, S_n^{2-}, and other processes to dinitroaniline transformation

	Native[a]			Filtered[b]		
Dinitroaniline	k_{HS^-} $[HS^-]$ $(hr^{-1})^c$	$k_{S_n^{2-}}$ $\Sigma[S_n^{2-}]$ $(hr^{-1})^d$	k_{other} $(hr^{-1})^e$	k_{HS^-} $[HS^-]$ $(hr^{-1})^c$	$k_{S_n^{2-}}$ $\Sigma[S_n^{2-}]$ $(hr^{-1})^d$	k_{other} $(hr^{-1})^e$
Trifluralin	1.59 (±0.07) $\times 10^{-2}$	0.61 (±0.15) $\times 10^{-2}$	4.37 (±1.58) $\times 10^{-2}$	1.59 (±0.08) $\times 10^{-2}$	0.62 (±0.17) $\times 10^{-2}$	1.49 (±0.18) $\times 10^{-2}$
Ethalfluralin	2.47 (±0.01) $\times 10^{-2}$	1.04 (±0.09) $\times 10^{-2}$	5.75 (±2.36) $\times 10^{-2}$	2.47 (±0.02) $\times 10^{-2}$	1.06 (±0.11) $\times 10^{-2}$	2.02 (±0.04) $\times 10^{-2}$
Benfluralin	2.12 (±0.08) $\times 10^{-2}$	0.84 (±0.21) $\times 10^{-2}$	4.67 (±1.93) $\times 10^{-2}$	2.12 (±0.09) $\times 10^{-2}$	0.85 (±0.24) $\times 10^{-2}$	1.38 (±0.17) $\times 10^{-2}$
Pendimethalin	2.28 (±0.11) $\times 10^{-3}$	1.10 (±0.27) $\times 10^{-3}$	5.36 (±2.43) $\times 10^{-3}$	2.28 (±0.13) $\times 10^{-3}$	1.13 (±0.30) $\times 10^{-3}$	1.29 (±0.13) $\times 10^{-3}$
Isopropalin	8.74 (±0.34) $\times 10^{-3}$	3.13 (±0.82) $\times 10^{-3}$	2.47 (±0.75) $\times 10^{-3}$	8.72 (±0.40) $\times 10^{-3}$	3.19 (±0.90) $\times 10^{-3}$	8.89 (±0.17) $\times 10^{-3}$
Butralin	4.86 (±0.24) $\times 10^{-3}$	1.84 (±0.55) $\times 10^{-3}$	1.16 (±0.41) $\times 10^{-3}$	4.86 (±0.27) $\times 10^{-3}$	1.88 (±0.60) $\times 10^{-3}$	3.97 (±0.27) $\times 10^{-3}$
Nitralin	1.90 (±0.05) $\times 10^{-1}$	0.79 (±0.08) $\times 10^{-1}$	4.72 (±1.89) $\times 10^{-1}$	1.89 (±0.07) $\times 10^{-1}$	0.81 (±0.10) $\times 10^{-1}$	1.33 (±0.09) $\times 10^{-1}$

[a] Native P8 porewaters (Apr 2010). [b] Filter-sterilized P8 porewaters (Apr 2010). [c] Calculated as $k_{HS^-} \times [HS^-]_{calc}$, where k_{HS^-} is the second-order rate constant from Table 3.3 and $[HS^-]_{calc}$ is the bisulfide concentration from Table 3.1. Errors were calculated through propagation of errors associated with rate constants and concentrations. [d] Calculated as $k_{S_n^{2-}} \times \Sigma[S_n^{2-}]_{calc}$, where $k_{S_n^{2-}}$ is the second-order rate constant from Table 3.3 and $\Sigma[S_n^{2-}]_{calc}$ is the polysulfide dianion concentration from Table 3.1. Errors were calculated through propagation of errors associated with rate constants and concentrations. [e] Calculated as $k_{obs} - k_{HS^-}[HS^-] - k_{S_n^{2-}}\Sigma[S_n^{2-}]$, where k_{obs} is the reaction rate constant from Table 3.2. Errors were calculated through propagation of errors associated with rate constants and concentrations.

B.8 Characterization of PPL sediments

(1) Elemental analysis of PPL sediments

Sub-samples of P1 and P8 sediments (Apr 2010) were sent to the Soil Testing Laboratory at the University of Minnesota for elemental analysis. A 0.50 g sample of sediment was mixed with 10 mL of HNO_3 in a polyfluoroacetate vessel and then subject to 10-min microwave heating. Concentrations of trace elements in acid-digested aqueous samples were analyzed by a Perkin-Elmer Optima 3000 inductively coupled plasma-atomic emission spectrometer equipped with a GemTip Cross-Flow II Ryton nebulizer using the following settings: RF power: 1400 W; cooling gas flow rate: 15 L/min; nebulizer gas flow rate: 1.0 L/min; auxiliary gas flow rate: 1.2 L/min; dwell time: 100 ms; sample uptake rate: 0.5 mL/min. For each sample, standard, and blank, five replicate measurements were made to determine a mean and standard deviation for each selected elemental wavelength. Calibration was accomplished by comparing the unknowns to a NIST traceable single or multi-element standard solution. All samples, standards, and blanks were acid matrix matched (in order to lessen matrix effects) and were diluted appropriately such that analyte concentrations were in the linear calibration range of instrument. For *total sulfur* analysis, a 0.30 g sample of sediment was mixed with tungsten oxide powder and combusted at 1350℃ with measurement of evolved sulfur dioxide by infrared absorption on a LECO S144-DR sulfur determinator. For *sulfate sulfur* analysis, sulfate was first extracted by shaking 10 g of sediment in 25 mL of calcium dihydrogen phosphate solution (0.008 M) for 30 min, followed by the addition of 0.15 g of charcoal and shaking for an additional 3 min. The mixture was then filtered. 0.3

g of barium chloride monohydrate was added to 10 mL aliquots of filtrate under constant stirring. The resulting turbidity from the formation of $BaSO_4$ precipitate was measured on a Klett colorimeter at 420 nm. For *total carbon* analysis, a 0.50 g sample of sediment was combusted at 2500 ℉, and carbon dioxide evolution was subsequently measured by infrared absorption using a Skalar Primacs carbon furnace. For *inorganic carbon* analysis, a 0.50 g sample of sediment was added with phosphoric acid in a closed, purged system, and carbon dioxide evolution was measured by infrared absorption. *Organic carbon* was computed as the difference between the total carbon and inorganic carbon. Results of elemental analysis are summarized in Table B.7.

Table B.7 Elemental analysis of PPL sediments

Analyte	P1 (mg/kg)[a]	P8 (mg/kg)[a]
Al	7758.400 (±1542.200)	6668.550 (±1225.911)
B	49.963 (±4.256)	41.108 (±2.618)
Ca	61149.000 (±308.299)	62481.000 (±605.283)
Cd	< 0.880	< 0.880
Cr	14.850 (±1.709)	11.734 (±1.451)
Cu	20.303 (±1.283)	16.900 (±0.588)
Fe	11984.500 (±757.311)	10799.500 (±833.679)
K	3159.300 (±309.571)	2379.700 (±218.920)
Mg	12467.000 (±110.309)	7660.500 (±129.683)
Mn	1249.050 (±7.142)	1040.000 (±0.566)
Na	946.175 (±3.783)	664.910 (±6.859)
Ni	18.831 (±0.238)	16.180 (±0.146)
P	985.625 (±11.703)	1078.550 (±17.183)
Pb	14.211 (±0.185)	14.080 (±0.000)
Zn	64.519 (±0.359)	57.784 (±3.504)
Total sulfur	5210 (±70)	5740 (±70)
Sulfate sulfur[b]	750 (±0)	650 (±0)
Total carbon[b]	135200 (±280)	163400 (±0)
Inorganic carbon[b]	13400 (±140)	12900 (±140)
Organic carbon[b,c]	121800 (±320)	150500 (±140)

[a] Concentration of analyte in acid-digested P1 and P8 sediment (Apr 2010). Results reported on a moist basis. Errors represent one standard deviation from duplicate measurements. [b] Results reported on a dry weight basis. [c] Calculated as "Total carbon" minus "Inorganic carbon". Errors were calculated through propagation of errors associated with "Total carbon" and "Inorganic carbon".

(2) XRD analysis of PPL sediments

Sub-samples of P8 sediments (Apr 2010) were sent to the Department of Chemistry at the University of Minnesota for powder XRD analysis. Native sediment samples (anoxic) were prepared for analysis in the glove box and transferred to air-tight sample holders. Another set of sediment samples (oxidized) were removed from the glove box and flushed with air for 24 h. The XRD analysis of native and oxidized sediments was performed using a PANalytical X'pert PRO MPD X-ray diffractometer equipped with an X'Celerator detector and a cobalt source. Data were collected over the range of 20-105 ° 2θ at a scan rate of 0.0235 °/sec and a revolution time of 4 sec. Diffraction patterns were compared to reference powder diffraction files (PDF) for quartz (SiO_2; PDF# 46-1045), pyrite (FeS_2; PDF# 06-0710), pyrrhotite ($Fe_{1-x}S$; PDF# 22-1120), and magnetite (Fe_3O_4; PDF# 19-0629). Data was plotted as the square root of intensity to better discern smaller peaks from minor phases. No quantitative analysis was pursued. The XRD patterns for native and oxidized sediment samples are shown in Figure B.7. A large portion of the sample was quartz and magnetite. Reduced iron compounds such as pyrite and pyrrhotite were also detected. Oxidized iron compounds such as iron sulfates and iron sulfite hydrate also appeared to be present. Numerous additional small peaks were detected, but they could not be identified by comparison to the PDF database.

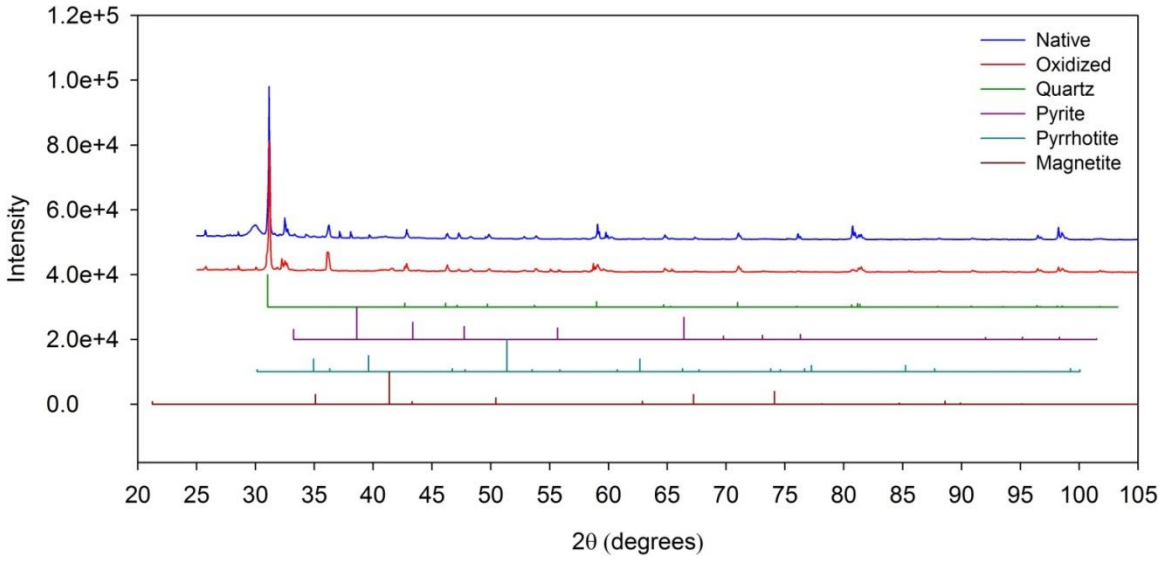

Figure B.7 XRD patterns for native and oxidized P8 sediment (Apr 2010) compared to PDF reference patterns.

B.9 Characterization of native and filter-sterilized PPL porewaters

(1) IC analysis of PPL porewaters

Sub-samples of native and filter-sterilized P8 porewaters (Apr 2010) were sent to the Analytical Geochemistry Laboratory at the University of Minnesota for IC analysis. Concentrations of anions in native and filtered porewaters were analyzed by a Dionex ICS-2000 ion chromatograph equipped with an IonPac AS19 anion-exchange column (150 mm × 4.0 mm i.d.), an ASRS 300 (4 mm) suppressor, an AS40 autosampler, and an integrated dual-piston pump and conductivity detector using the following settings: injection volume: 50 µL; eluent: 2.0 mM sodium hydroxide; flow rate: 1.0 mL/min. Calibration was accomplished by comparing the unknowns to a NIST traceable single or multi-element standard solution. All samples were diluted appropriately such that analyte concentrations were in the linear calibration range of instrument. Results of IC analysis are summarized in Table B.8. The difference between native and filter-sterilized porewaters is used to determine whether anion concentrations were affected by the filtration process using 0.2 µm syringe filters.

Table B.8 IC anion analysis of PPL porewaters

Analyte	Native (mg/L)[a]	Filtered (mg/L)[b]	Difference (mg/L)[c]
Bromide (Br^-)	0.172 (±0.001)	0.168 (±0.002)	0.004 (±0.002)
Chloride (Cl^-)	33.933 (±0.047)	33.573 (±0.062)	0.360 (±0.077)
Fluoride (F^-)	0.092 (±0.001)	0.066 (±0.001)	0.026 (±0.002)
Formate ($HCOO^-$)	< 0.010	< 0.010	N.A.[d]
Acetate (CH_3COO^-)	< 0.010	< 0.010	N.A.[d]
Oxalate ($(COO)_2^{2-}$)	< 0.010	< 0.010	N.A.[d]
Lactate ($CH_3CH(OH)COO^-$)	< 0.010	< 0.010	N.A.[d]
Nitrate Nitrogen (NO_3^--N)	< 0.001	< 0.001	N.A.[d]
Nitrite Nitrogen (NO_2^--N)	0.004 (±0.001)	0.005 (±0.000)	-0.001 (±0.001)
Phosphate Phosphorous (PO_4^{3-}-P)	< 0.005	< 0.005	N.A.[d]
Sulfate (SO_4^{2-})	35.222 (±0.245)	25.338 (±0.320)	9.884 (±0.403)
Sulfite (SO_3^{2-})	2.632 (±0.043)	2.372 (±0.071)	0.260 (±0.083)
Sulfite (SO_3^{2-}) (µM)	**32.90 (±0.76)**	**29.65 (±1.26)**	**3.25 (±1.47)**
Thiosulfate ($S_2O_3^{2-}$)	11.342 (±0.023)	11.171 (±0.003)	0.170 (±0.023)
Thiosulfate ($S_2O_3^{2-}$) (µM)	**101.27 (±0.29)**	**99.74 (±0.04)**	**1.53 (±0.29)**

[a] Concentration of analyte in native P8 porewaters (Apr 2010). Errors represent one standard deviation from duplicate measurements. [b] Concentration of analyte in filter-sterilized P8 porewaters (Apr 2010). Errors represent one standard deviation from duplicate measurements. [c] Difference in concentrations between native and filter-sterilized porewaters. Calculated as "Native (mg/L)" minus "Filtered (mg/L)". Errors were calculated through propagation of errors associated with "Native (mg/L)" and "Filtered (mg/L)". [d] N.A. = not available.

(2) ICP-MS analysis of PPL porewaters

Sub-samples of native and filter-sterilized P8 porewaters (Apr 2010) were sent to the Analytical Geochemistry Laboratory at the University of Minnesota for ICP-MS analysis. Concentrations of trace elements in native and filtered porewaters were analyzed by a Thermo Scientific XSERIES 2 quadrupole inductively coupled plasma-mass spectrometer equipped with an ESI PC3 Peltier cooled spray chamber, a SC-FAST injection loop, and a SC-4 autosampler using the following settings: RF power: 1350 W; cooling gas flow rate: 12 L/min; nebulizer gas flow rate: 0.8 L/min; auxiliary gas flow rate: 1.0 L/min; dwell time: 100 ms; sample uptake rate: 0.5 mL/min; integration: 10 sec/replicate and 5 replicates/sample. Calibration was accomplished by comparing the unknowns to a NIST traceable single or multi-element standard solution. All samples, standards, and blanks were acid matrix matched (in order to lessen matrix effects) and were diluted appropriately such that analyte concentrations were in the linear calibration range of instrument. The internal standard element Y was added to diluted samples to further compensate for drift and for matrix effects. All elements except Li, Be, B, Al, P were analyzed using He/H_2 collision-reaction mode. Results of ICP-MS analysis are summarized in Table B.9. The difference between native and filter-sterilized porewaters is used to determine which elements were filtered out by 0.2 μm syringe filters.

Table B.9 ICP-MS cation analysis of PPL porewaters

Analyte	Native (µg/L)[a]	Filtered (µg/L)[b]	Difference (µg/L)[c]
Li	207.60 (±4.10)	194.70 (±11.60)	12.90 (±12.30)
Be	0.00 (±0.00)	0.00 (±0.00)	0.00 (±0.00)
B	93.53 (±1.29)	85.12 (±4.67)	8.41 (±4.84)
P	577.40 (±17.96)	561.30 (±23.05)	16.10 (±29.22)
Ti	1.35 (±0.09)	0.91 (±0.12)	0.44 (±0.15)
V	0.37 (±0.02)	0.36 (±0.00)	0.01 (±0.02)
Cr	0.31 (±0.00)	0.20 (±0.01)	0.11 (±0.01)
Mn	3.40 (±0.04)	3.10 (±0.01)	0.31 (±0.04)
Fe	**9.08 (±0.08)**	**9.68 (±0.26)**	**-0.59 (±0.27)**
Co	0.28 (±0.00)	0.28 (±0.00)	0.00 (±0.00)
Ni	4.44 (±0.18)	2.89 (±0.09)	1.55 (±0.20)
Cu	0.04 (±0.03)	0.35 (±0.03)	-0.31 (±0.04)
Zn	2.36 (±0.01)	4.50 (±0.11)	-2.14 (±0.11)
As	21.68 (±0.06)	21.59 (±0.52)	0.09 (±0.53)
Se	14.24 (±0.71)	11.85 (±0.94)	2.39 (±1.18)
Sr	283.95 (±0.49)	269.55 (±18.46)	14.40 (±18.46)
Zr	0.73 (±0.04)	0.78 (±0.05)	-0.04 (±0.07)
Nb	0.08 (±0.04)	0.09 (±0.08)	-0.02 (±0.09)
Mo	0.14 (±0.01)	0.23 (±0.02)	-0.09 (±0.03)
Cd	0.01 (±0.01)	0.02 (±0.00)	-0.01 (±0.01)
Sn	0.58 (±0.01)	0.45 (±0.01)	0.13 (±0.01)
Sb	1.22 (±0.04)	1.19 (±0.01)	0.04 (±0.04)
Cs	0.02 (±0.00)	0.02 (±0.00)	0.01 (±0.00)
Ba	14.98 (±0.08)	14.29 (±0.82)	0.69 (±0.82)
W	0.03 (±0.04)	0.07 (±0.05)	-0.03 (±0.06)
Tl	0.00 (±0.01)	0.01 (±0.01)	-0.01 (±0.02)
Pb	0.25 (±0.01)	0.68 (±0.04)	-0.43 (±0.04)
Th	0.03 (±0.03)	0.08 (±0.08)	-0.04 (±0.09)
U	0.19 (±0.01)	0.17 (±0.00)	0.02 (±0.01)

[a] Concentration of analyte in native P8 porewaters (Apr 2010). Errors represent one standard deviation from duplicate measurements. [b] Concentration of analyte in filter-sterilized P8 porewaters (Apr 2010). Errors represent one standard deviation from duplicate measurements. [c] Difference in concentrations between native and filter-sterilized porewaters. Calculated as "Native (µg/L)" minus "Filtered (µg/L)". Errors were calculated through propagation of errors associated with "Native (µg/L)" and "Filtered (µg/L)".

(3) DLS analysis of PPL porewaters

Sub-samples of native and filtered P8 porewaters (Apr 2010) were sent to the Department of Chemistry at the University of Minnesota for DLS analysis. In the glove box, a 10-mL aliquot of porewaters was filtered through 0.2 μm syringe filter, while another 10-mL aliquot of porewaters was filtered through 0.22 μm membrane filters by vacuum filtration. Both native and filtered porewaters were then d into three plastic cuvettes for a total of nine cuvettes for analysis. Each cuvette contained approximately 2.5 mL of native or filtered porewaters. Caps were placed on the cuvettes and sealed with Parafilm to avoid oxidization. All cuvettes were stored in a foil-wrapped beaker before removal from the glove box. The particle size distribution in these porewaters was characterized by a Brookhaven Instruments ZetaPALS particle analyzer (90Plus/BI-MAS, multi angle particle sizing option) with the following specifications: size range: 2 nm to 3 μm; accuracy: ± 1% to 2% with monodisperse samples; repeatability: ± 1% to 2% with dust free samples; laser: 15 mW solid state laser; sample volume: 0.5 to 3 mL. The following parameters were set for porewater analysis: sample run: 1 min/run, 5 runs/sample, and 3 replicates/sample; temperature: 25 ℃; liquid: water; collection angle: 90 °; dust cutoff: 30. Results of DLS analysis are summarized in Table B.10. The intensity-weighted and number-weighted average particle size decreases in the following order: native porewaters > 0.2 μm filtered porewaters > 0.22 μm filtered porewaters, suggesting that filtration of native porewaters indeed removed a fraction of substances with diameters larger than 0.2 μm. The difference in average particle size between 0.2

μm filtered porewaters and 0.22 μm filtered porewaters reveals that the particle size distribution in the porewaters is sensitive to the pore size of filters.

Table B.10 Dynamic light scattering (DLS) analysis of PPL porewaters

Intensity-weighted average size				
Sample ID	Mean (nm)[a]	Standard error (nm)[a]	Combined (nm)[a]	Data included (%)[d]
Native A	812.0	23.1[b]	815.1	97.99
Native B	827.5	34.6[b]	829.8	97.62
Native C	788.9	27.5[b]	789.7	98.19
Average	809.4	49.9[c]	811.5	97.93
0.2 μm Filtered A	458.9	35.9[b]	464.5	98.27
0.2 μm Filtered B	603.1	45.3[b]	620.9	96.13
0.2 μm Filtered C	464.4	28.5[b]	469.4	96.02
Average	508.8	64.4[c]	518.3	96.81
0.22 μm Filtered A	593.0	6.6[b]	593.8	96.65
0.22 μm Filtered B	572.5	11.4[b]	572.1	96.78
0.22 μm Filtered C	570.4	8.3[b]	570.0	96.20
Average	578.6	15.6[c]	578.6	96.54
Number-weighted average size				
Sample ID	Mean (nm)[a]	Median (nm)[a]	Polydispersity	
Native A	178.7	153.5	0.375	
Native B	180.8	155.3	0.376	
Native C	168.5	144.5	0.382	
Average	176.0	151.1	0.378	
0.2 μm Filtered A	108.2	93.5	0.358	
0.2 μm Filtered B	133.1	114.2	0.380	
0.2 μm Filtered C	100.5	86.2	0.381	
Average	113.9	98.0	0.373	
0.22 μm Filtered A	159.7	140.1	0.320	
0.22 μm Filtered B	156.0	137.0	0.317	
0.22 μm Filtered C	159.3	140.3	0.311	
Average	158.4	139.1	0.316	

[a] Measurement of effective diameter. [b] Errors represent one standard deviation from five replicate measurements. [c] Errors were calculated through propagation of errors associated with triplicate measurements. [d] Ideal percentage of "Data included" should be 98% in order to exclude dust particles.

(4) ICP-OES analysis of 0.22 μm membrane filters

Unused (blank) and used 0.22 μm membrane filters were sent to the Analytical Geochemistry Laboratory at the University of Minnesota for ICP-OES analysis. The used membrane filters were prepared by vacuum filtration of 10 mL of P8 porewaters (Apr 2010) in the glove box. Weight percentage of major oxides on unused and used membrane filters were analyzed by a Thermo Scientific iCAP 6500 dual view inductively coupled plasma-optical emission spectrometer equipped with a Cetac PFA microconcentric nebulizer using the following settings: RF power: 1150 W, cooling gas flow rate: 12 L/min, nebulizer gas flow rate: 0.65 L/min, auxiliary gas flow rate: 0.3 L/min, dwell time: 100 ms, integration: 10 sec/replicate and 5 replicates/sample. Powdered samples were diluted 40 fold before analysis with the addition of a Cs matrix modifier and Y as an internal standard. Results of ICP-OES analysis are summarized in Table B.11. The difference between unused and used membrane filters is used to determine which oxides were retained on 0.22 μm membrane filters. The results, however, were inconclusive due to the small amount of materials collected on the filters.

Table B.11 ICP-OES analysis of 0.22 μm membrane filters

Oxide	Unused (wt%)[a]	Used (wt%)[b]	Difference (wt%)[c]
Al_2O_3	0.0049 (±0.0134)	0.0257 (±0.0104)	0.0208 (±0.0170)
BaO	0.0005 (±0.0005)	0.0001 (±0.0002)	-0.0004 (±0.0005)
CaO	0.0318 (±0.0026)	0.1112 (±0.0069)	0.0794 (±0.0073)
Fe_2O_3	0.0905 (±0.0070)	0.1185 (±0.0207)	0.0280 (±0.0218)
K_2O	0.0076 (±0.0257)	0.0352 (±0.0321)	0.0276 (±0.0412)
MgO	0.0124 (±0.0017)	0.0978 (±0.0026)	0.0855 (±0.0031)
MnO	0.0019 (±0.0007)	0.0025 (±0.0004)	0.0006 (±0.0008)
Na_2O	0.0008 (±0.0151)	0.0254 (±0.0097)	0.0246 (±0.0179)
P_2O_5	0.0136 (±0.0056)	0.0237 (±0.0023)	0.0101 (±0.0061)
SiO_2	0.2762 (±0.6926)	0.7479 (±0.6962)	0.4717 (±0.9821)
SrO	0.0008 (±0.0001)	0.0011 (±0.0002)	0.0003 (±0.0002)
TiO_2	0.0369 (±0.0024)	0.0296 (±0.0026)	-0.0073 (±0.0036)
ZrO_2	0.0008 (±0.0001)	0.0011 (±0.0002)	0.0003 (±0.0002)

[a] Elemental percentage of oxide on powdered unused membrane. Errors represent one standard deviation from triplicate measurements. [b] Elemental percentage of oxide on powdered used membrane (vacuum filtration of 10 mL of native P8 porewaters (Apr 2010)). Errors represent one standard deviation from triplicate measurements. [c] Elemental percentage difference between unused and used membranes. Calculated as "Used (wt%)" minus "Unused (wt%)". Errors were calculated through propagation of errors associated with "Used (wt%)" and "Unused (wt%)".

(5) XRD analysis of 0.22 μm membrane filters

Unused (blank) and used 0.22 μm membrane filters were sent to the Department of Chemistry at the University of Minnesota for XRD analysis. The used membrane filters were prepared by vacuum filtration of 10 mL of P8 porewaters (Apr 2010) in the glove box. XRD analysis of unused and used membrane filters was performed using a PANalytical X'pert PRO MPD X-ray diffractometer equipped with an X'Celerator detector and a cobalt source. For both short runs (1 h) and long runs (10.5 h), data were collected over the range of 5-75 °2θ at a scan rate of 0.0193 °/sec and a revolution time of 4 sec. Diffraction patterns were compared to reference powder diffraction files (PDF) for PVDF (PDF# 38-1638, 42-1649, 42-1650, 42-1651). Data was plotted as the square root of intensity to better discern smaller peaks from minor phases. No quantitative analysis was pursued. The XRD patterns for unused and used membranes are shown in Figure B.8. Although the XRD pattern of the used membrane filter reveals the presence of an unknown peak at 35-40 °2θ, the substance is either poorly crystalline or in too small of a quantity to be identified. Thus, it could not be matched to any known materials in the PDF database.

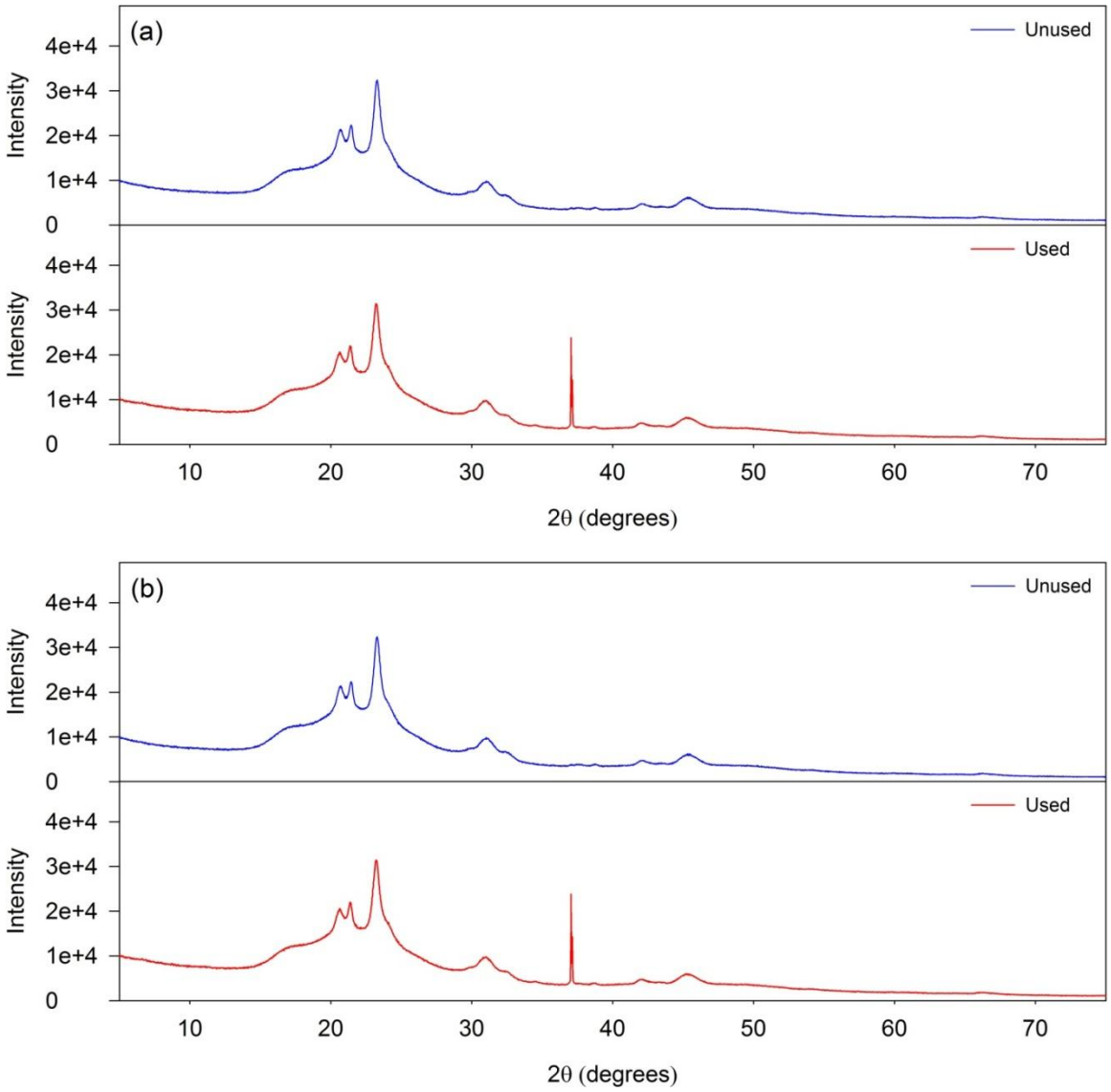

Figure B.8 XRD patterns for unused and used 0.22 μm membrane filters: (a) 1-h short runs; (b) 10.5-h long runs.

B.10 Effect of silver nitrate and oxygen on ethalfluralin transformation

The transformation of ethalfluralin was studied in P8 porewaters (Sep 2010) amended with varying amounts of silver nitrate ($AgNO_3$). Sub-samples of porewaters amended with $AgNO_3$ were allowed to equilibrate for 1 week and filter-sterilized through 0.2 μm syringe filters. The transformation of ethalfluralin was also studied in oxidized P8 porewaters (Sep 2010). Sub-samples of porewaters were sparged with air outside the glove box for 24 h and filter-sterilized through 0.2 μm syringe filters. Reactions were initiated by spiking an aliquot of ethalfluralin stock solution into the above porewaters. The sampling, extraction, and analysis procedures were the same as described in the text. Note that in this set of experiments, P8 porewaters from the Sep 2010 sampling trip were used due to the limited volume of P8 porewaters left from the Apr 2010 sampling trip. The differences and similarities between these two batches of porewaters (native) are summarized in Table B.12. Briefly, the pH of Sep 2010 porewaters (pH = 7.45) is more neutral compared to Apr 2010 porewaters (pH = 8.78), and the total hydrogen sulfide concentration ($[H_2S]_T$ = ~1600 μM) is not as high as that measured in Apr 2010 porewaters ($[H_2S]_T$ = ~2000 μM). The total polysulfide concentrations and DOC levels, however, are very similar between the two different batches of porewaters. The characteristics of $AgNO_3$-amended and oxidized porewaters as well as ethalfluralin reaction rates are summarized in Table B.13. Semilogarithmic plots for ethalfluralin reaction and the correlation between reduced sulfur concentration and reaction rate are shown in Figure B.9. The ratio of predicted rate constant (k_{pred}) to k_{obs} is ~0.6, suggesting that reactions with HS^- and S_n^{2-} indeed played a significant role in the reaction of

ethalfluralin. As shown by Figure B.9(b), the regression of log k_{obs} versus log ($[HS^-]+\Sigma[S_n^{2-}]$) yielded a slope equal to 1.229 ± 0.047. Unlike the reactions of ethalfluralin in hydrogen sulfide and polysulfide buffers, the transformation of ethalfluralin in $AgNO_3$-amended porewaters could not be considered as first order in $[HS^-]$ or $\Sigma[S_n^{2-}]$ even though a strong linear correlation was found between k_{obs} and ($[HS^-]+\Sigma[S_n^{2-}]$). Such deviation might be explained by the involvement of other reactive entities, such as DOM, for reactions in the porewaters.

Table B.12 Characteristics of Lake P8 porewaters from Apr 2010 and Sep 2010 sampling trips

Sample	pH	$[H_2S]_T$ (μM)	$[HS^-]_{calc}$ (μM)	Me_2S_2 (μM)	Me_2S_3 (μM)	$[H_2S_n]_{T,\ calc}$ (μM)	$\Sigma[S_n^{2-}]_{calc}$ (μM)	DOC (mg/L)
P8 Porewater (Apr 2010)	8.78[a]	1999 ± 16[a]	1984 ± 21[a]	42.9 ± 1.5[a]	0.6 ± 0.1[a]	43.5 ± 1.5[a]	43.4 ± 2.1[a]	114.0 ± 0.1[a]
P8 Porewater (Sep 2010)	7.45[b]	1602 ± 64[b]	1357 ± 77[b]	45.0 ± 3.0[b]	1.0 ± 0.1[b]	46.0 ± 3.0[b]	44.2 ± 4.1[b]	121.1 ± 0.5[b]

[a] Values taken from Table 3.1 for comparison purpose. [b] Values reproduced from Zeng et al[1].

Table B.13 Reduced sulfur concentrations and reaction rate constants of ethalfluralin in modified P8 porewaters

$AgNO_3$[a]	$[HS^-]_{calc}$ (μM)[b]	$\Sigma[S_n^{2-}]_{calc}$ (μM)[c]	k_{obs} (hr^{-1})[d]	k_{pred} (hr^{-1})[e]	k_{pred} / k_{obs}[f]
0 mM	1374 (±18)	44.7 (±3.7)	4.34 (±0.18) $\times 10^{-2}$	2.78 (±0.14) $\times 10^{-2}$	0.64
1 mM	944 (±32)	23.0 (±1.5)	2.61 (±0.04) $\times 10^{-2}$	1.73 (±0.08) $\times 10^{-2}$	0.66
2 mM	491 (±12)	11.1 (±1.4)	1.51 (±0.08) $\times 10^{-2}$	0.88 (±0.05) $\times 10^{-2}$	0.58
4 mM	0	0	0.01 (±0.02) $\times 10^{-2}$	0	N.A.[g]
0 mM Oxidized	0	0	0.00 (±0.02) $\times 10^{-2}$	0	N.A.[g]

[a] Amount of silver nitrate added in P8 porewaters (Sep 2010). [b] Bisulfide concentration calculated from $[H_2S]_T$ and pH, assuming that the sample is not saturated with elemental sulfur. Errors were propagated from $[H_2S]_T$. [c] Polysulfide dianion concentration calculated from measured $[H_2S_n]_{T, calc}$ and pH, assuming that the relative abundance of HS_n^- and S_n^{2-} species are dictated by equilibrium constants from Shea and Helz[2]. Errors were propagated from $[H_2S_n]_{T, calc}$. [d] Rate constant measured in $AgNO_3$-amended and oxidized porewaters. Errors represent one standard deviation from duplicate experiments [e] Rate constant calculated from the sum of $k_{HS^-}[HS^-] + k_{S_n^{2-}}\Sigma[S_n^{2-}]$, where k_{HS^-} and $k_{S_n^{2-}}$ are the second-order rate constants from Table 3.3, and $[HS^-]$ and $\Sigma[S_n^{2-}]$ are the bisulfide and polysulfide dianion concentrations listed in the table. Errors were calculated through propagation of errors associated with rate constants and concentrations. [f] Calculated as k_{pred} / k_{obs}. [g] N.A. = not available.

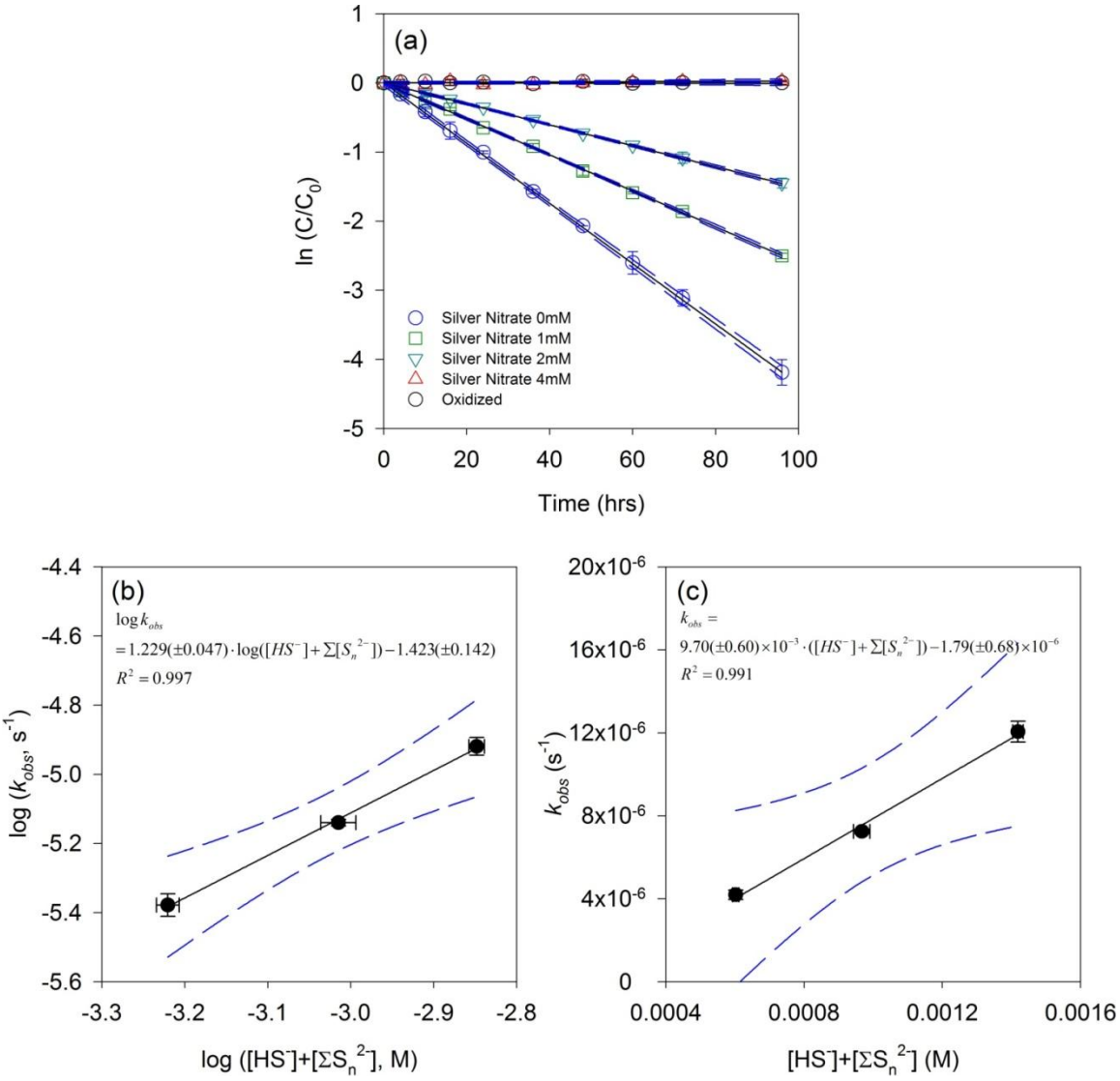

Figure B.9 Transformation of ethalfluralin in $AgNO_3$-amended and oxidized P8 porewaters (Sep 2010): (a) Semilogarithmic plots for reactions of ethalfluralin in P8 porewaters (b) Plot of log (k_{obs}) versus log ($[HS^-] + \Sigma[S_n^{2-}]$) for reactions of ethalfluralin in P8 porewaters. (c) Plot of k_{obs} versus ($[HS^-] + \Sigma[S_n^{2-}]$) for reactions of ethalfluralin in P8 porewaters. Solid lines represent linear regressions and dashed lines represent 95% confidence intervals. $R^2 > 0.99$. Error bars represent one standard deviation of duplicate measurements; where absent, bars fall within symbols.

B.11 Effect of sodium azide on ethalfluralin transformation

The transformation of ethalfluralin was studied in P8 porewaters (Apr 2010) amended with sodium azide (NaN_3). Sub-samples of porewaters treated with 10 mM NaN_3 were allowed to equilibrate for 1 week. Reactions were initiated by spiking an aliquot of ethalfluralin stock solution into the above modified porewaters. The sampling, extraction, and analysis procedures were the same as described in the text.

The time courses for ethalfluralin reaction are shown in Figure B.10. The value of k_{obs} in unmodified native porewaters ($7.39\ (\pm 0.09) \times 10^{-2}$ hr^{-1}) is not statistically different from that in NaN_3-treated porewaters ($7.45\ (\pm 0.10) \times 10^{-2}$ hr^{-1}), which precludes a direct role for biodegradation in the reaction of ethalfluralin.

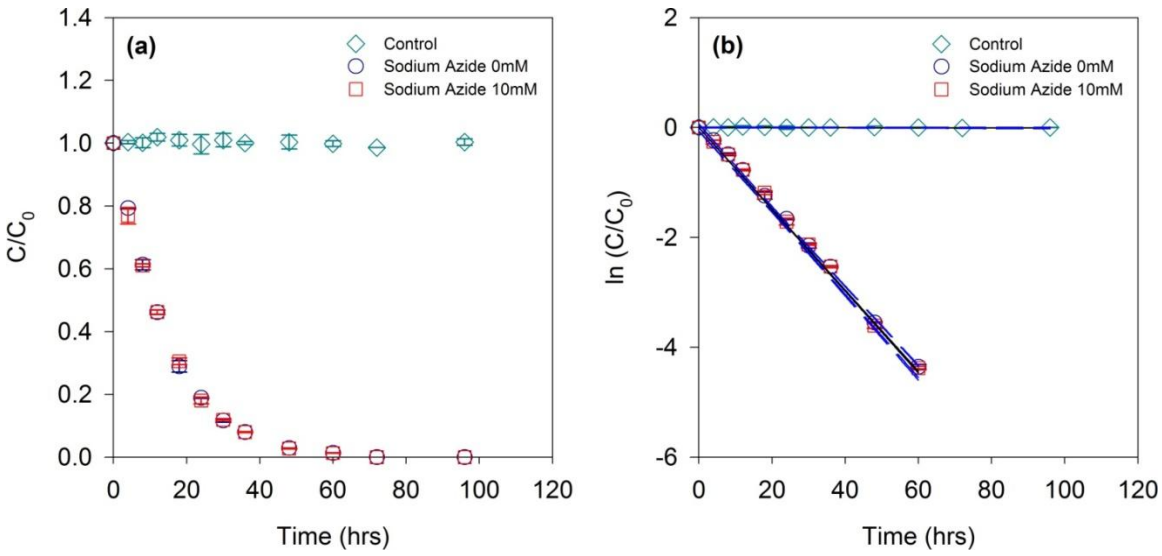

Figure B.10 Transformation of ethalfluralin in NaN_3-treated P8 porewaters (Apr 2010): (a) Time courses for reactions of ethalfluralin in the porewaters and Tris buffer. (b) Semilogarithmic plots for reactions of ethalfluralin in the porewaters and Tris buffer. Solid lines represent linear regressions and dashed lines represent 95% confidence intervals. $R^2 > 0.99$ in both cases. Error bars represent one standard deviation of duplicate samples; where absent, bars fall within symbols.

B.12 Effect of filter pore size on ethalfluralin transformation

The transformation of ethalfluralin was studied in 0.2 μm filtered and 0.22 μm filtered P8 porewaters (Apr 2010). Sub-samples of porewaters were filtered through 0.2 μm syringe filters or 0.22 μm membrane filters. Reactions were initiated by spiking an aliquot of ethalfluralin stock solution into the filtered porewaters. The sampling, extraction, and analysis procedures were the same as described in the text.

The time courses for ethalfluralin reaction are shown in Figure B.11. The value of k_{obs} in 0.2 μm filtered porewaters (5.59 ($\pm$0.10)$\times 10^{-2}$ hr^{-1}) is not statistically different from that in 0.22 μm filtered porewaters (5.62 ($\pm$0.16)$\times 10^{-2}$ hr^{-1}). This suggested that the slight difference in the filter pore size (i.e., 0.02 μm) did not significantly influence the reaction rates of ethalfluralin.

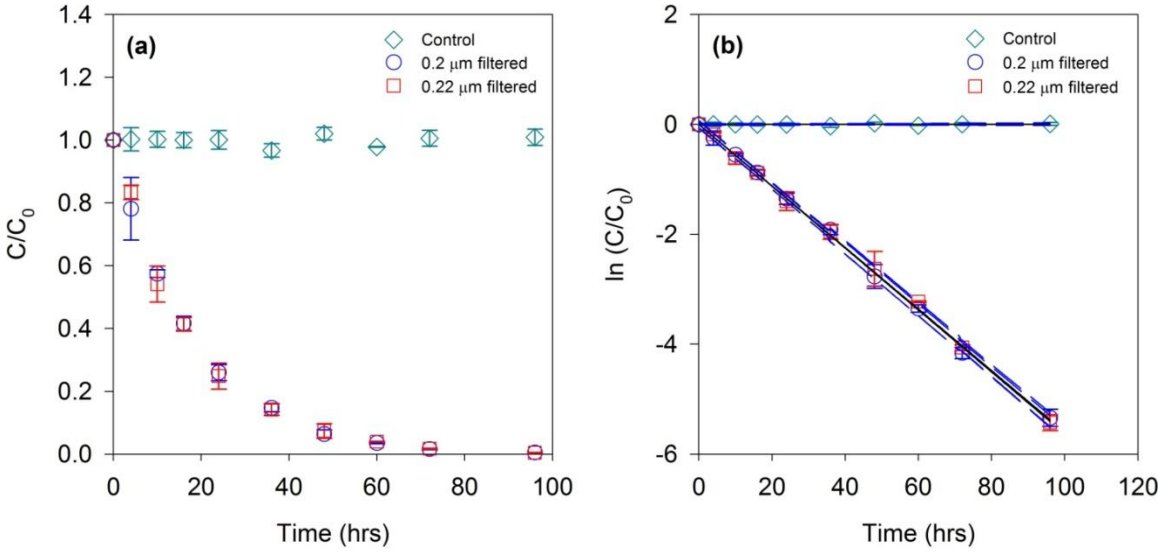

Figure B.11 Transformation of ethalfluralin in 0.2 μm filtered and 0.22 μm filtered P8 porewaters (Apr 2010): (a) Time courses for reactions of ethalfluralin in the porewaters and Tris buffer. (b) Semilogarithmic plots for reactions of ethalfluralin in the porewaters and Tris buffer. Solid lines represent linear regressions and dashed lines represent 95% confidence intervals. R^2 > 0.99 in both cases. Error bars represent one standard deviation of duplicate samples; where absent, bars fall within symbols.

B.13 Effect of filtered materials on ethalfluralin transformation

The transformation of ethalfluralin was studied in the Tris buffer containing 0.22 μm membrane filters. Ten milliliters of P8 porewaters (Apr 2010) was filtered through a 0.22 μm membrane filter by vacuum filtration in the glove box, and the used membrane filters were dried for 24 h. Individual pieces of used membrane filter were then transferred to the glass syringes containing Tris buffer, and the syringes were pre-equilibrated for 1 week. Reactions were initiated by spiking an aliquot of ethalfluralin stock solution into the Tris buffer. The sampling, extraction, and analysis procedures were the same as described in the text. Control syringes containing both Tris buffer and unused membrane filters were spiked, sampled, and extracted in a similar manner.

The transformation of ethalfluralin was also studied in the Tris buffer containing only filtered substances retained on 0.22 μm membrane filters. Ten milliliters of P8 porewaters (Apr 2010) was filtered through a 0.22 μm membrane filter by vacuum filtration in the glove box, and the used membrane filters were dried for 24 h. Individual pieces of used membrane filter were then transferred to foil-wrapped glass vials containing 10 mL of Tris buffer. The vials were sealed and sonicated at 20 ℃ for 6 h in a Branson 2210 ultrasonic cleaner. After sonication, the membrane filters were *removed* and the remaining Tris buffer was transferred into the glass syringes. Another set of Tris buffer was also amended with $AgNO_3$ (4 mM). Reactions were initiated by spiking an aliquot of ethalfluralin stock solution into the Tris buffer. The sampling, extraction, and analysis procedures were the same as described in the text. Control syringes containing

Tris buffer sonicated with unused membrane filters were spiked, sampled, and extracted in a similar manner.

Results of the first experiment are shown in Figure B.12. Although ethalfluralin underwent rapid degradation in the Tris buffer containing unused or used membrane filters (i.e., filters remained in the Tris buffer), the disappearance of ethalfluralin might primarily result from the irreversible sorption to filters. The value of k_{obs} obtained in the Tris buffer containing used filter ($8.11\ (\pm 0.13)\times 10^{-2}$ hr^{-1}) is not statistically different from that in the Tris buffer containing unused filter ($8.23\ (\pm 0.08)\times 10^{-2}$ hr^{-1}), both of which are greater than the value of k_{obs} obtained in native P8 porewaters (see Table 3.2). Results of the second experiment are shown in Figure 3.4 in the text. Slow disappearance of ethalfluralin was observed in the Tris buffer sonicated with used membrane filters (i.e., filters were removed from the Tris buffer). Conversely, ethalfluralin was unreactive in the Tris buffer sonicated with unused membrane filters. In the former case, the value of k_{obs} ($1.23\ (\pm 0.22)\times 10^{-2}$ hr^{-1}) is on the same order of magnitude of k_{obs} obtained in the porewaters and sulfide redox buffers (see Table 3.3). The value of k_{obs} obtained in $AgNO_3$-amended Tris buffer ($1.15\ (\pm 0.19)\times 10^{-2}$ hr^{-1}) is not statistically different from that without $AgNO_3$, suggesting that the contribution of reduced sulfur species was unimportant in these experiments.

As seen from the difference in the particle size distribution between 0.2 μm and 0.22 μm filtered porewaters (see Table B.10), the characteristics and reactivity of substances retained by 0.22 μm membrane filters could be different from those retained by 0.2 μm syringe filters, even though the reactivity of ethalfluralin was similar in the

porewaters filtered by either type of filter (see Figure B.11). Thus, the contribution of filtered materials to the overall k_{obs} in native porewaters might not be fully captured by experiments with 0.22 μm membrane filters.

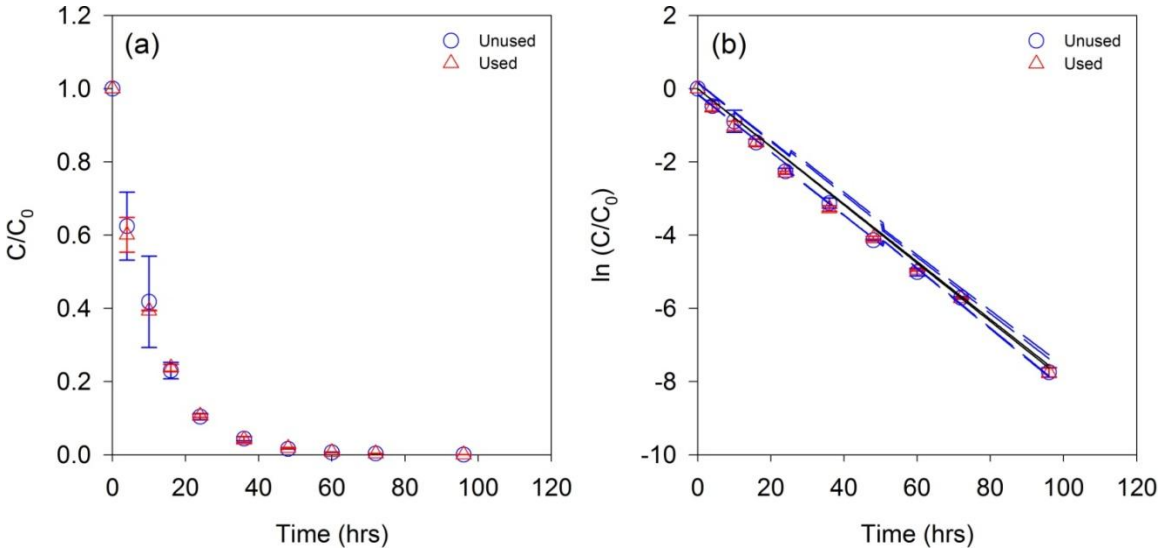

Figure B.12 Transformation of ethalfluralin in the Tris buffer containing 0.22 μm membrane filters: (a) Time courses for reactions of ethalfluralin in the Tris buffer containing unused or used filters. (b) Semilogarithmic plots for reactions of ethalfluralin in the Tris buffer containing unused or used filters. Solid lines represent linear regressions and dashed lines represent 95% confidence intervals. R^2 > 0.98. Error bars represent one standard deviation of duplicate samples; where absent, bars fall within symbols.

B.14 Total ion chromatogram and mass spectra of dinitroaniline products

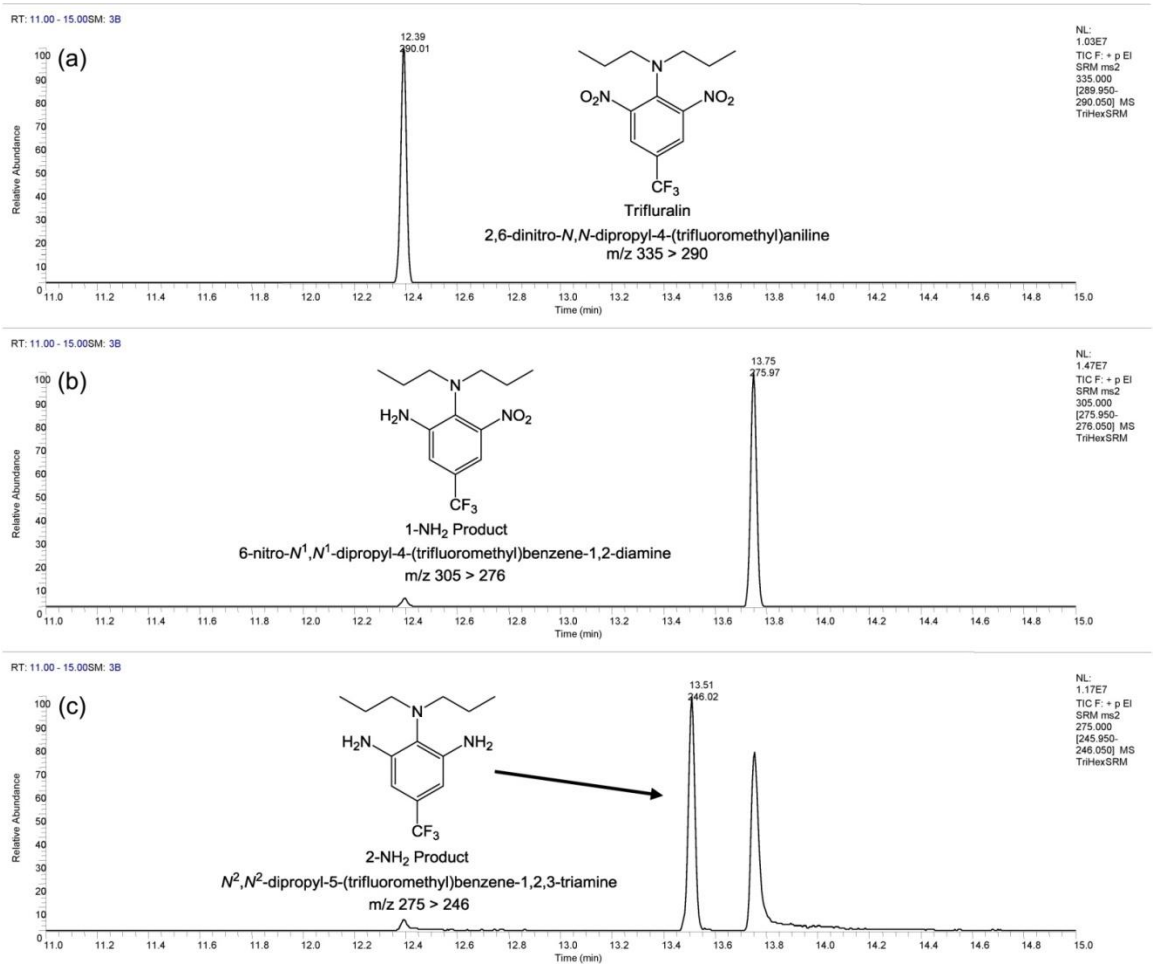

Figure B.13 Total ion chromatogram (TIC) of products obtained in the reaction of trifluralin with porewaters: (a) TIC of parent compound; (b) TIC of 1-NH_2 product; (c) TIC of 2-NH_2 product.

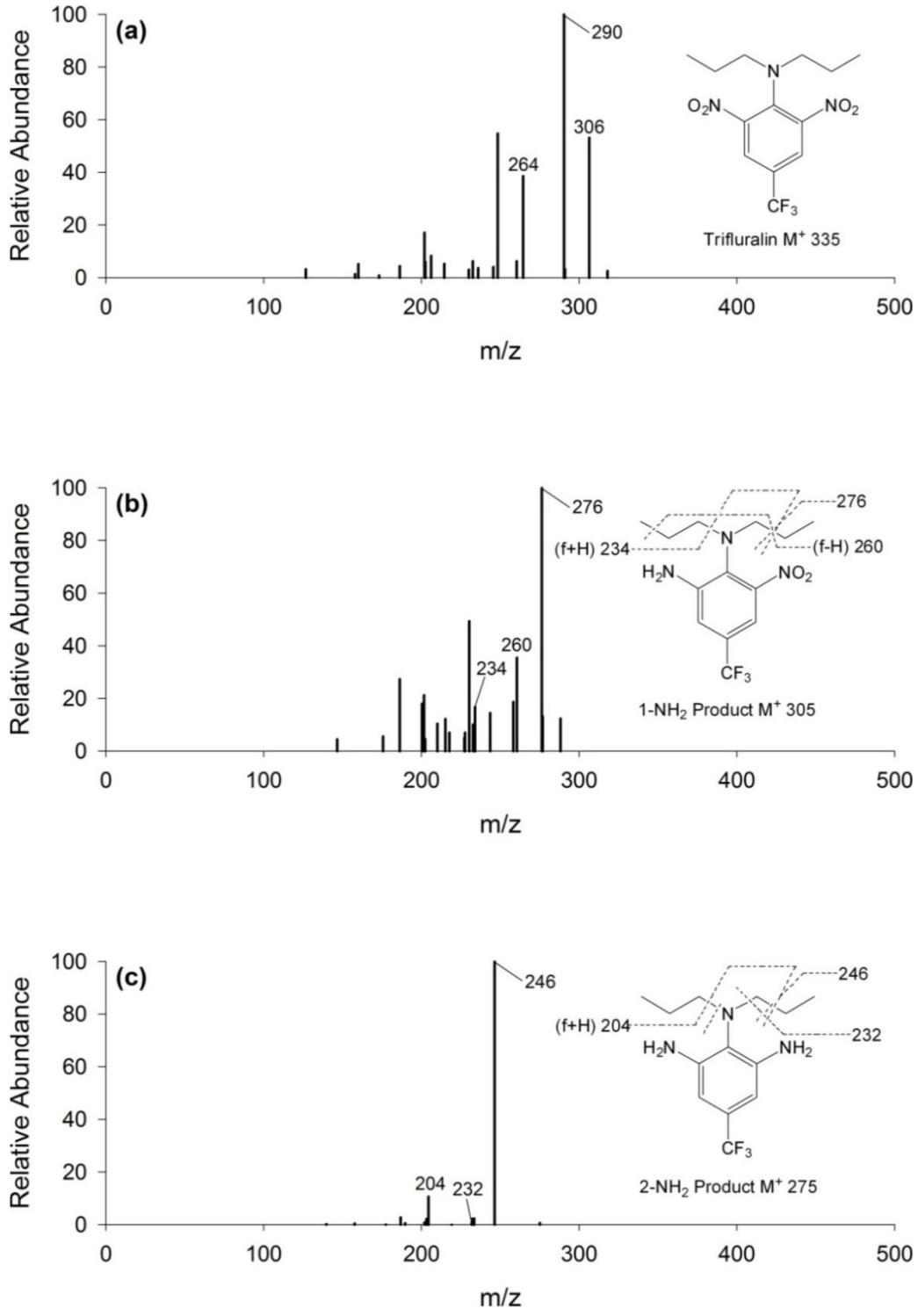

Figure B.14 Mass spectra of products obtained in the reaction of trifluralin with porewaters: (a) Mass spectra of parent compound; (b) Mass spectra of 1-NH_2 product; (c) Mass spectra of 2-NH_2 product.

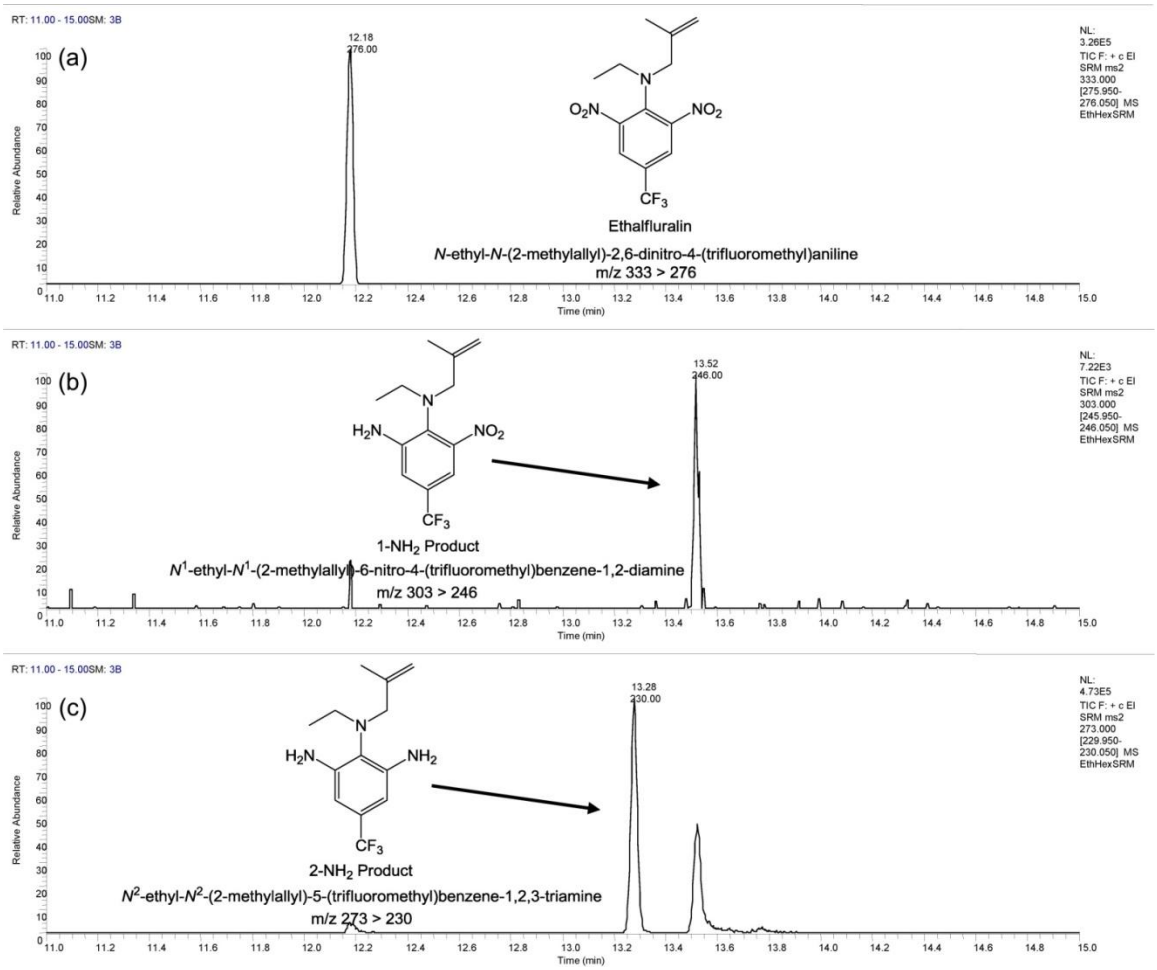

Figure B.15 Total ion chromatogram (TIC) of products obtained in the reaction of ethalfluralin with porewaters: (a) TIC of parent compound; (b) TIC of 1-NH_2 product; (c) TIC of 2-NH_2 product.

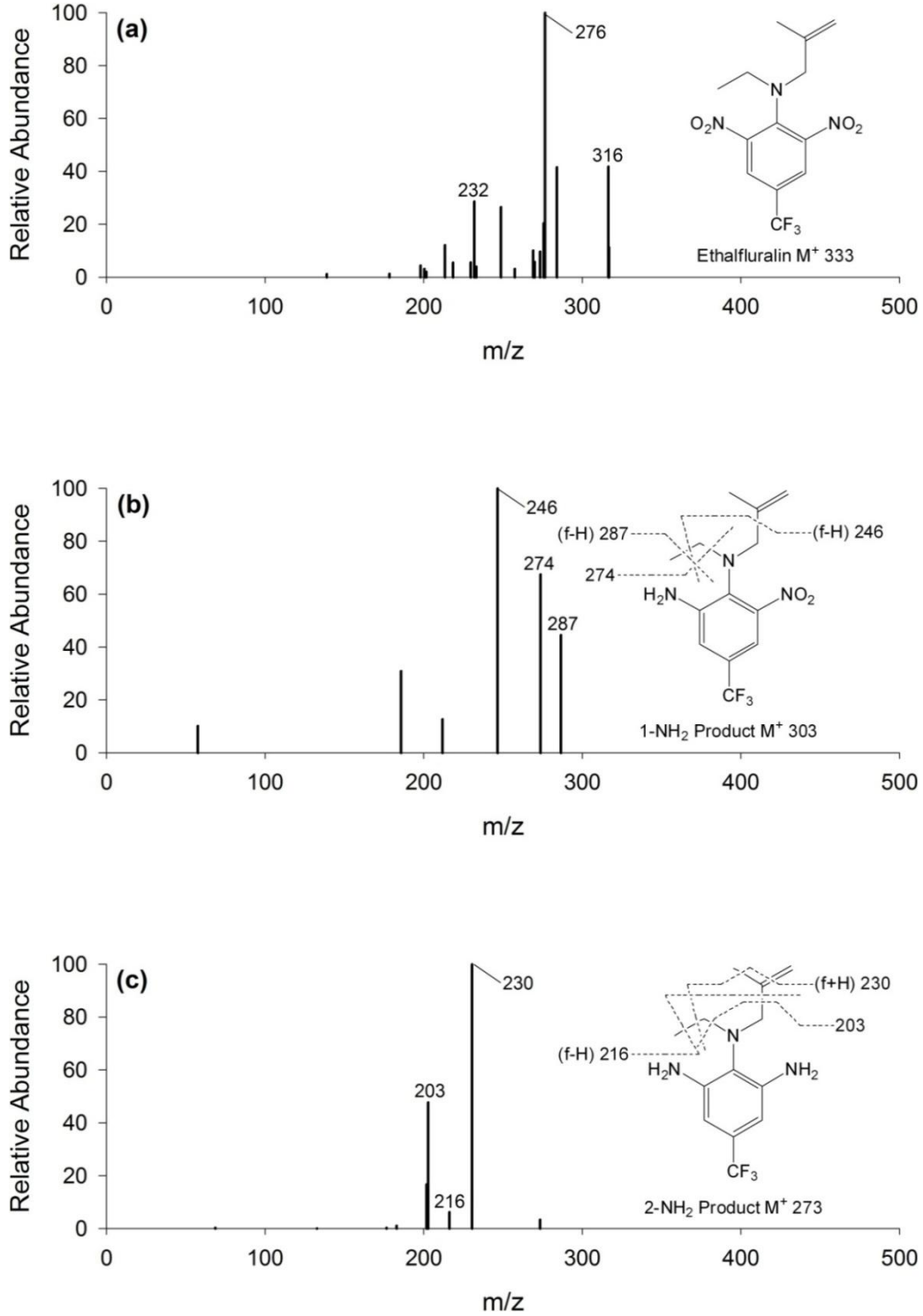

Figure B.16 Mass spectra of products obtained in the reaction of ethalfluralin with porewaters: (a) Mass spectra of parent compound; (b) Mass spectra of 1-NH_2 product; (c) Mass spectra of 2-NH_2 product.

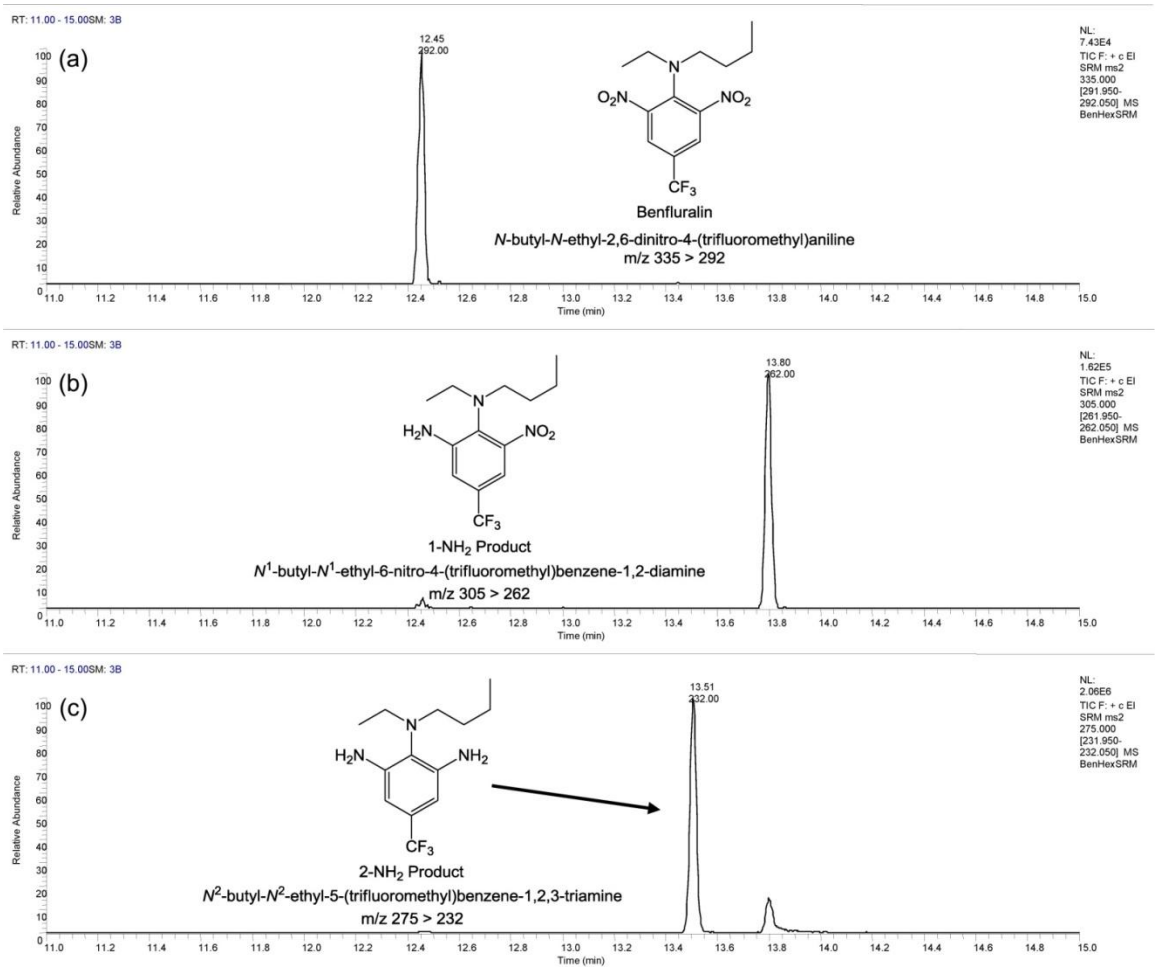

Figure B.17 Total ion chromatogram (TIC) of products obtained in the reaction of benfluralin with porewaters: (a) TIC of parent compound; (b) TIC of 1-NH_2 product; (c) TIC of 2-NH_2 product.

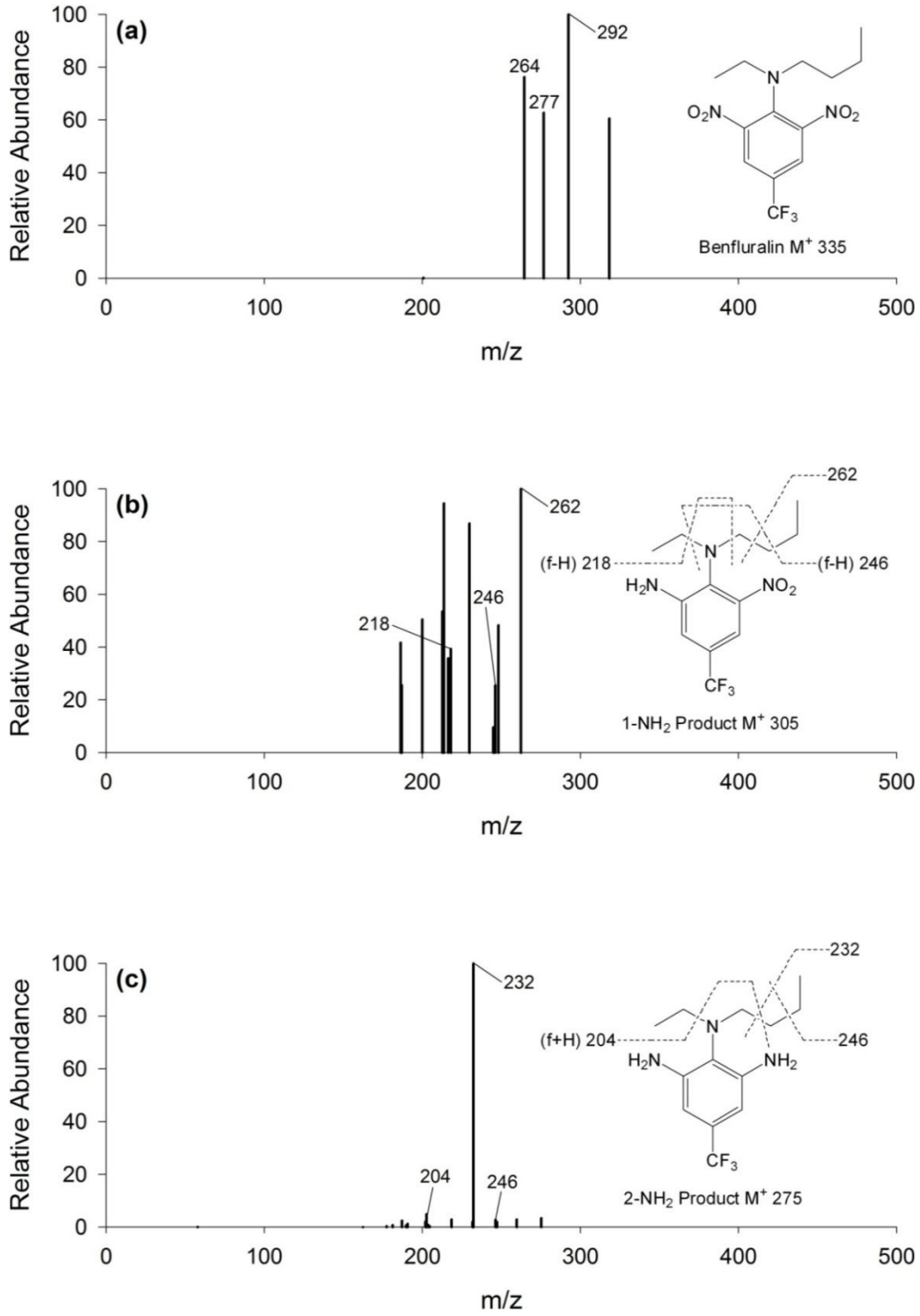

Figure B.18 Mass spectra of products obtained in the reaction of benfluralin with porewaters: (a) Mass spectra of parent compound; (b) Mass spectra of 1-NH_2 product; (c) Mass spectra of 2-NH_2 product.

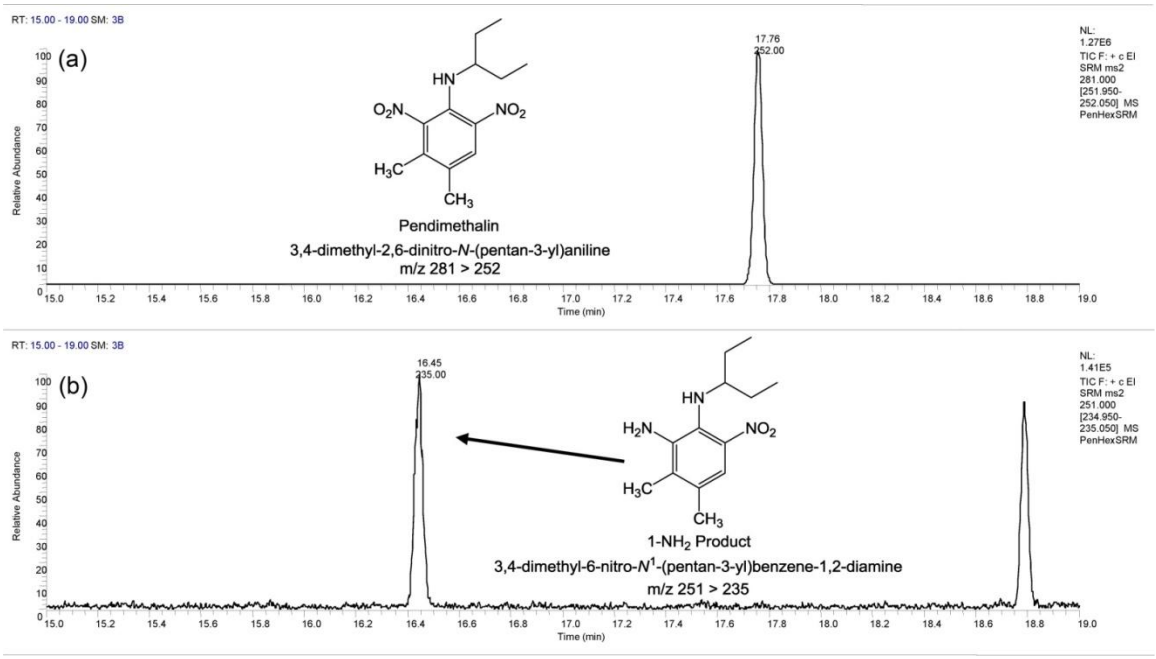

Figure B.19 Total ion chromatogram (TIC) of products obtained in the reaction of pendimethalin with porewaters: (a) TIC of parent compound; (b) TIC of 1-NH_2 product.

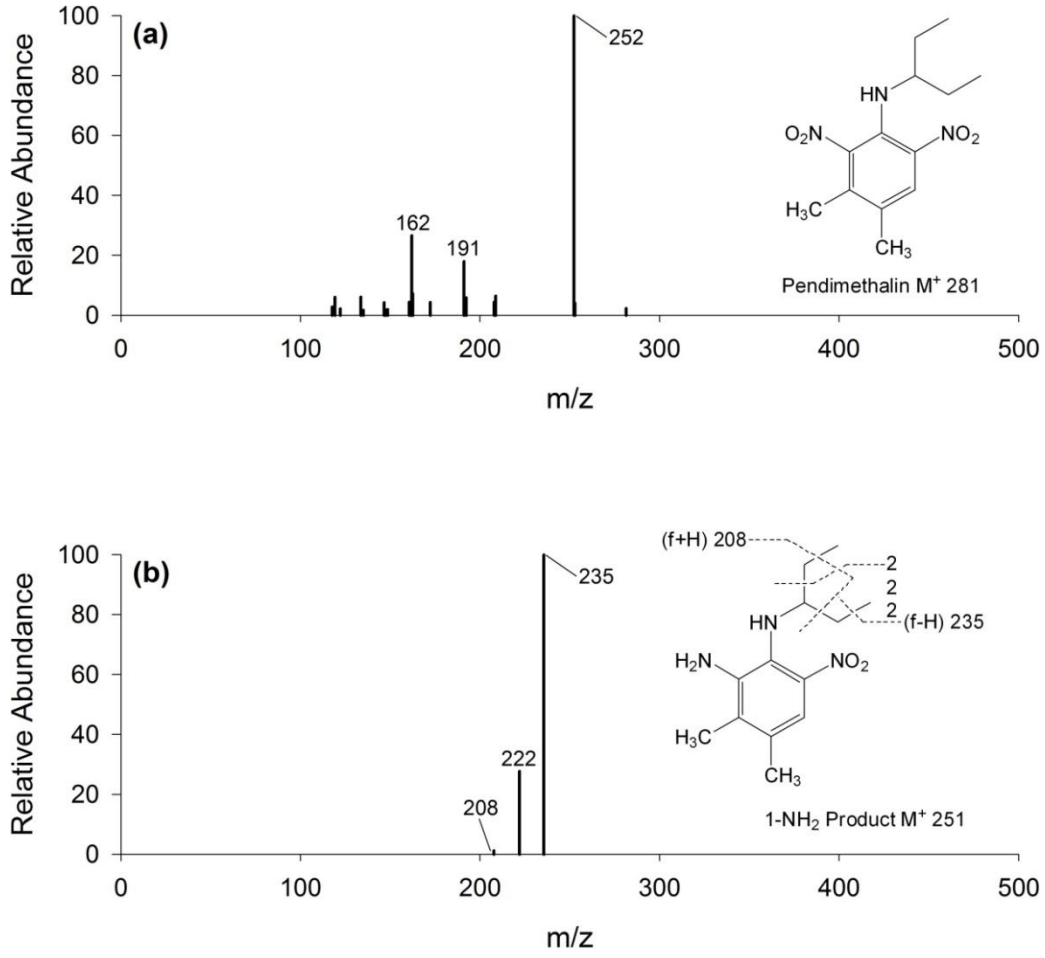

Figure B.20 Mass spectra of products obtained in the reaction of pendimethalin with porewaters: (a) Mass spectra of parent compound; (b) Mass spectra of 1-NH_2 product.

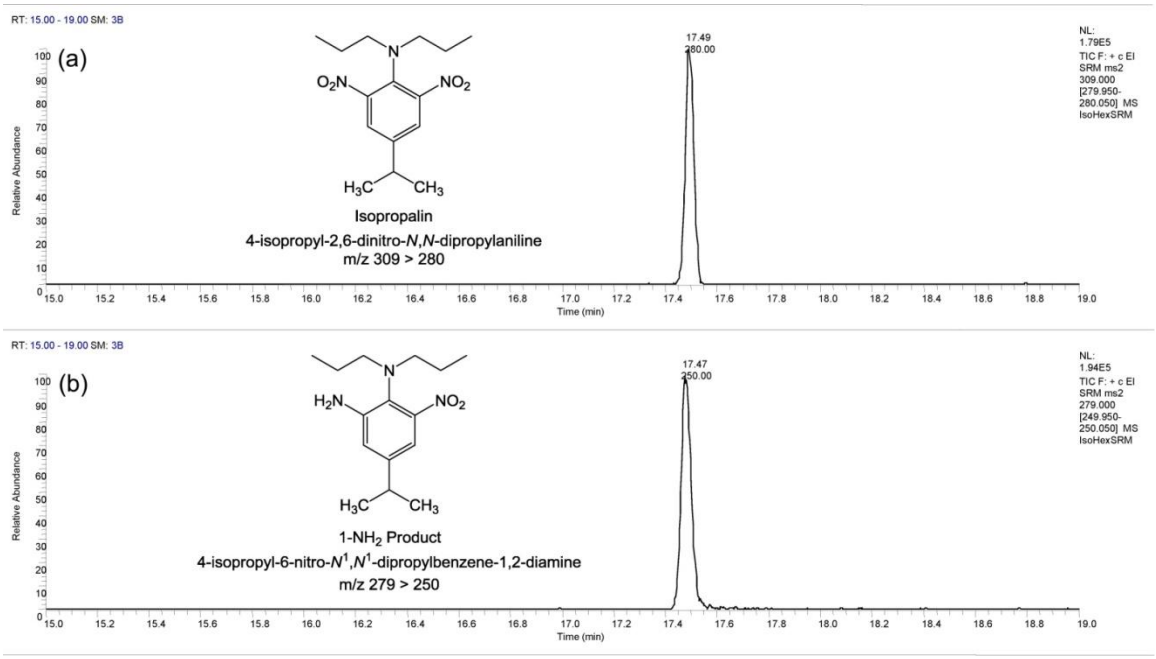

Figure B.21 Total ion chromatogram (TIC) of products obtained in the reaction of isopropalin with porewaters: (a) TIC of parent compound; (b) TIC of 1-NH_2 product.

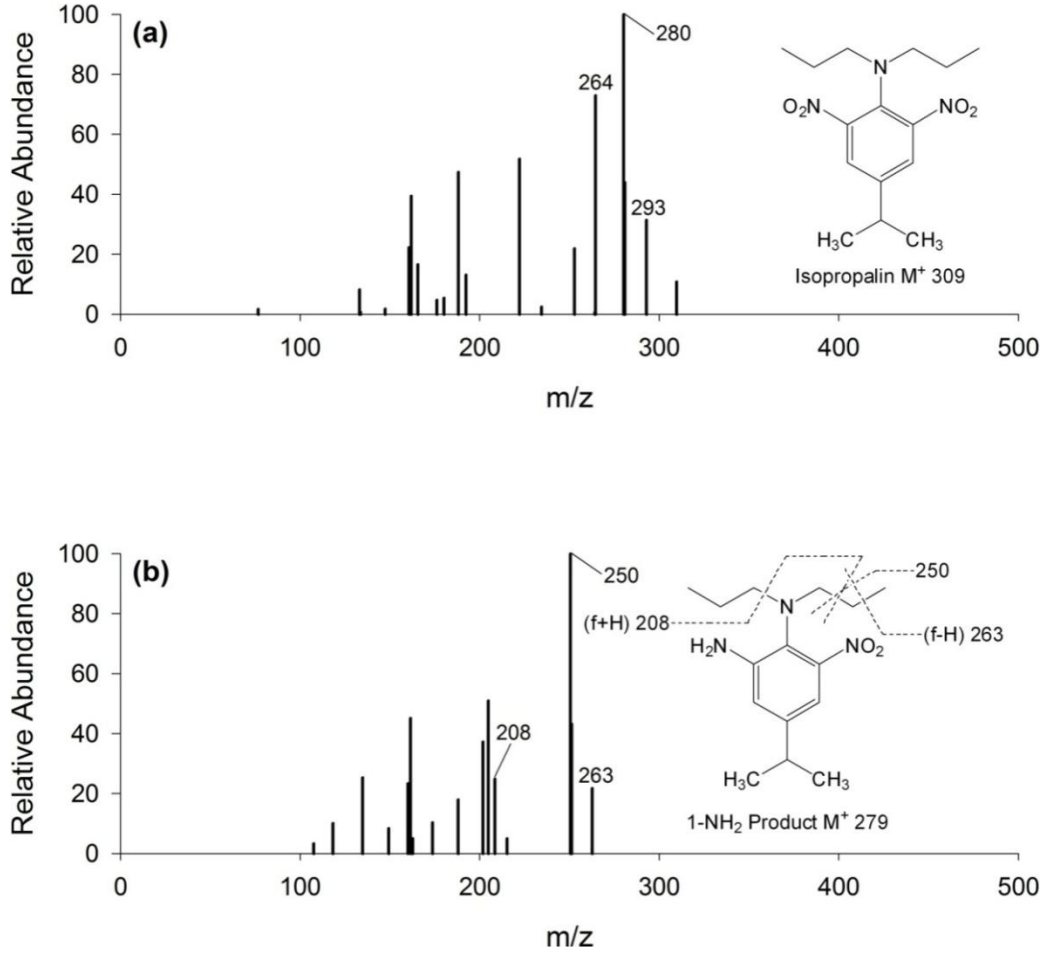

Figure B.22 Mass spectra of products obtained in the reaction of isopropalin with porewaters: (a) Mass spectra of parent compound; (b) Mass spectra of 1-NH_2 product.

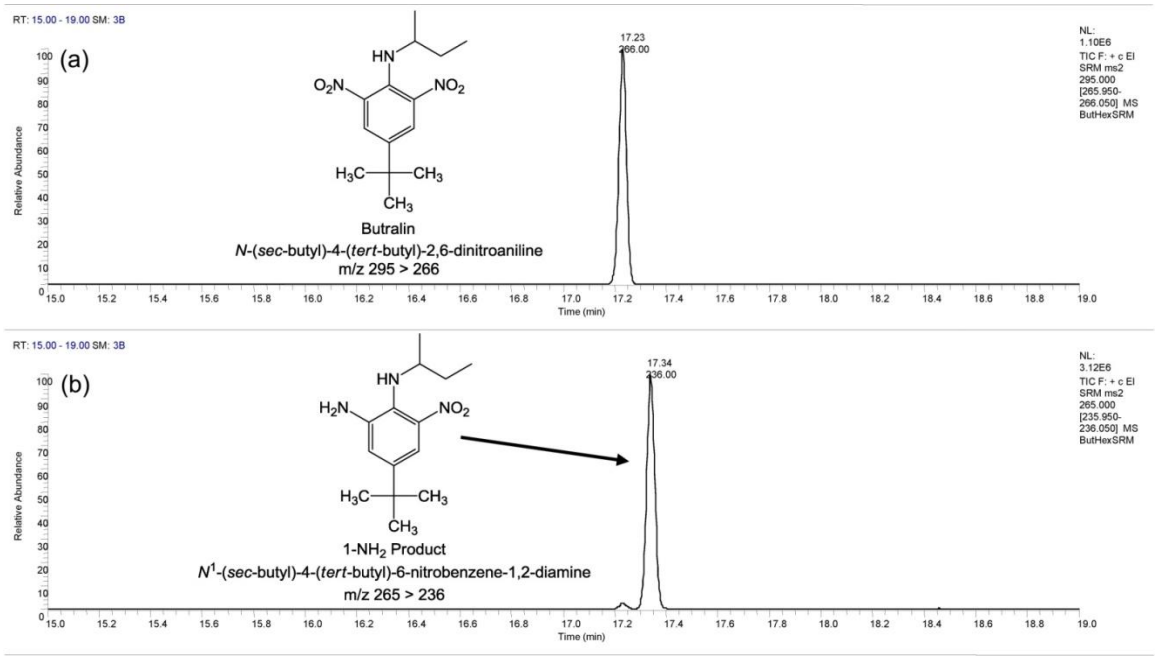

Figure B.23 Total ion chromatogram (TIC) of products obtained in the reaction of butralin with porewaters: (a) TIC of parent compound; (b) TIC of 1-NH_2 product.

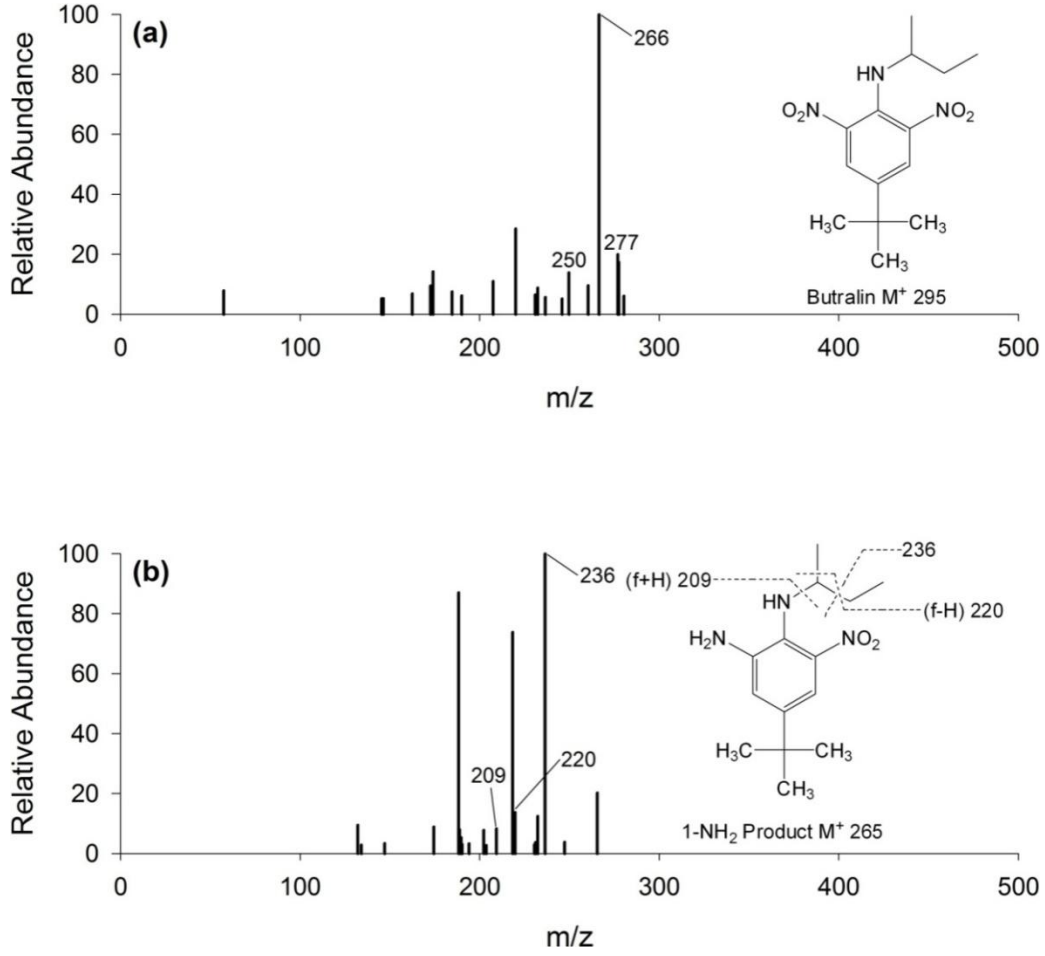

Figure B.24 Mass spectra of products obtained in the reaction of butralin with porewaters: (a) Mass spectra of parent compound; (b) Mass spectra of 1-NH_2 product.

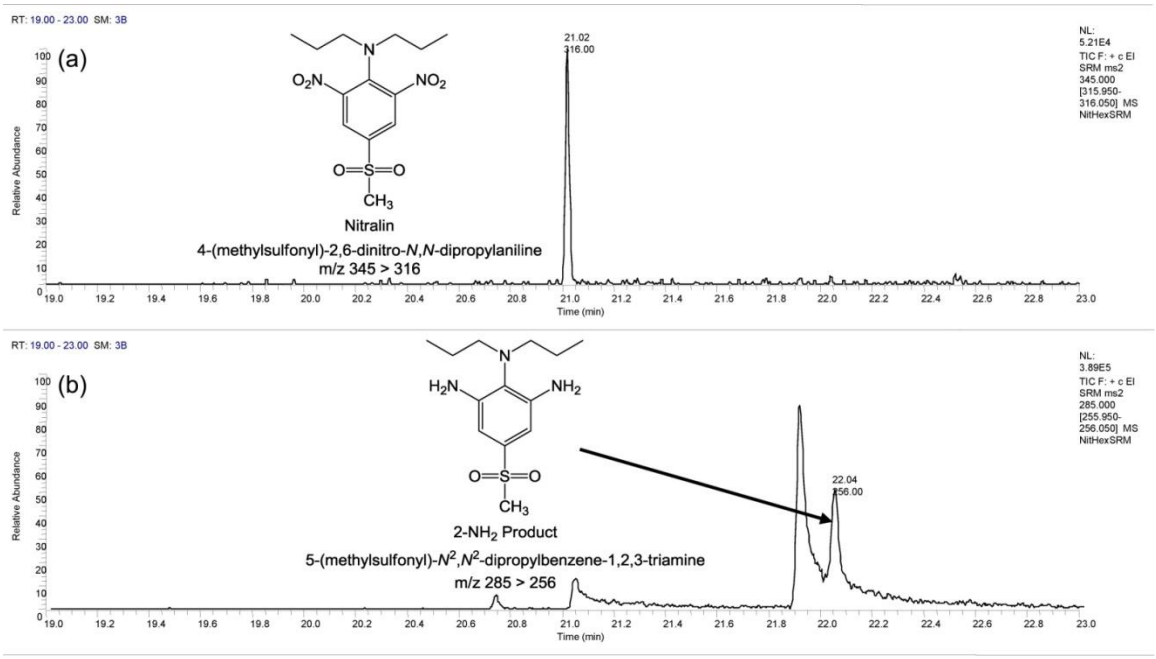

Figure B.25 Total ion chromatogram (TIC) of products obtained in the reaction of nitralin with porewaters: (a) TIC of parent compound; (b) TIC of 1-NH_2 product.

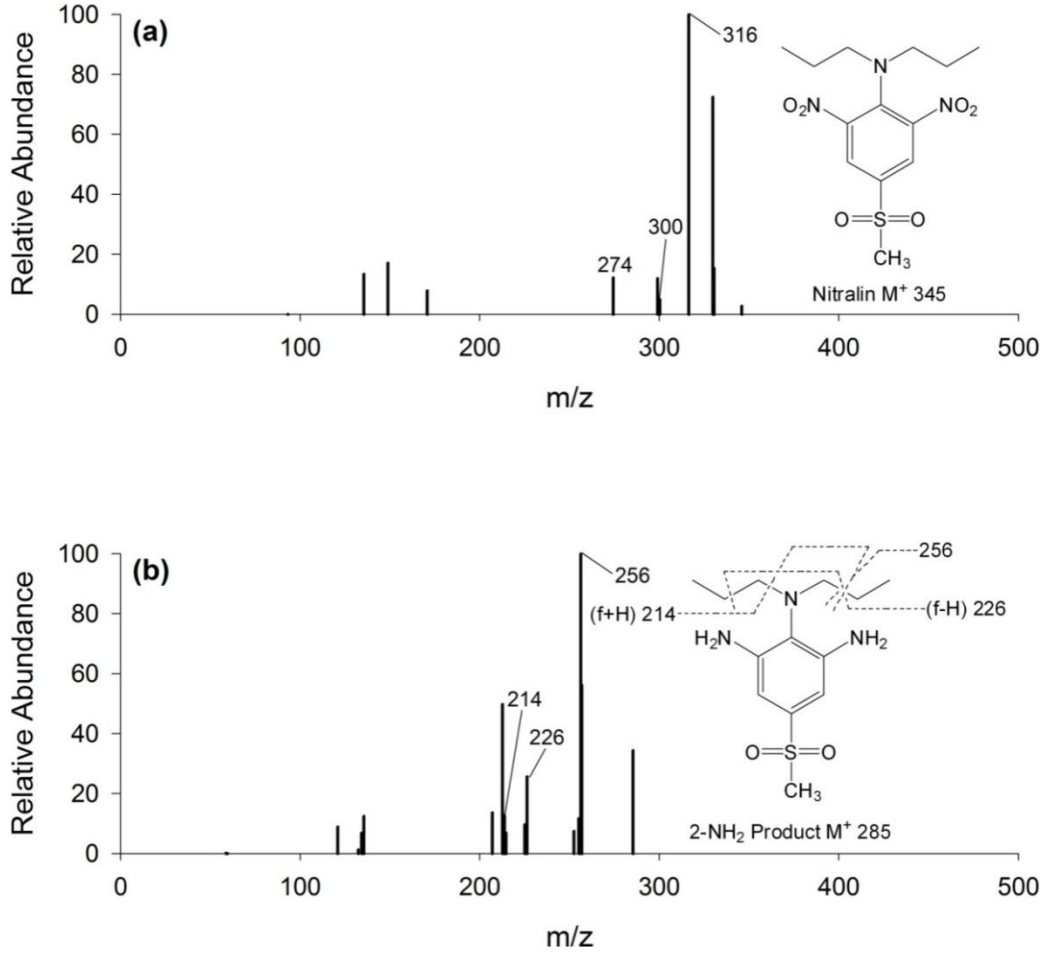

Figure B.26 Mass spectra of products obtained in the reaction of nitralin with porewaters: (a) Mass spectra of parent compound; (b) Mass spectra of 1-NH_2 product.

B.15 References

1. Zeng, T.; Ziegelgruber, K. L.; Chin, Y.-P.; Arnold, W. A., Pesticide processing potential in prairie pothole porewaters. *Environ. Sci. Technol.* **2011,** *45*, 6814-6822.
2. Cope, O. J.; Brown, R. K., The reduction of nitrobenzene by hydrosulphide ion in aqueous media. *Can. J. Chem.* **1962,** *40*, 2317-2328.
3. Hojo, M.; Takagi, Y.; Ogata, Y., Kinetics of the reduction of nitrobenzenes by sodium disulfide. *J. Am. Chem. Soc.* **1960,** *82*, 2459-2462.
4. Cope, O. J.; Brown, R. K., The reduction of nitrobenzene by sodium sulphide in aqueous ethanol. *Can. J. Chem.* **1961,** *39*, 1695-1710.
5. Shea, D.; Helz, G. R., The solubility of copper in sulfidic waters - sulfide and polysulfide complexes in equilibrium with covellite. *Geochim. Cosmochim. Acta* **1988,** *52*, 1815-1825.
6. Schwarzenbach, R. P.; Gschwend, P. M.; Imboden, D. M., *Environmental Organic Chemistry*. John Wiley & Sons, Inc.: Hoboken, NJ, 2003.
7. Hartenbach, A.; Hofstetter, T. B.; Berg, M.; Bolotin, J.; Schwarzenbach, R. P., Using nitrogen isotope fractionation to assess abiotic reduction of nitroaromatic compounds. *Environ. Sci. Technol.* **2006,** *40*, 7710-7716.
8. Hofstetter, T. B.; Neumann, A.; Arnold, W. A.; Hartenbach, A. E.; Bolotin, J.; Cramer, C. J.; Schwarzenbach, R. P., Substituent effects on nitrogen isotope fractionation during abiotic reduction of nitroaromatic compounds. *Environ. Sci. Technol.* **2008,** *42*, 1997-2003.
9. Hartenbach, A. E.; Hofstetter, T. B.; Aeschbacher, M.; Sander, M.; Kim, D.; Strathmann, T. J.; Arnold, W. A.; Cramer, C. J.; Schwarzenbach, R. P., Variability of nitrogen isotope fractionation during the reduction of nitroaromatic compounds with dissolved reductants. *Environ. Sci. Technol.* **2008,** *42*, 8352-8359.
10. Naka, D.; Kim, D.; Carbonaro, R. F.; Strathmann, T. J., Abiotic reduction of nitroaromatic contaminants by iron(II) complexes with organothiol ligands. *Environ. Toxicol. Chem.* **2008,** *27*, 1257-1266.
11. Phillips, K. L.; Chiu, P. C.; Sandler, S. I., Reduction rate constants for nitroaromatic compounds estimated from adiabatic electron affinities. *Environ. Sci. Technol.* **2010,** *44*, 7431-7436.
12. Wang, S.; Arnold, W. A., Abiotic reduction of dinitroaniline herbicides. *Water Res.* **2003,** *37*, 4191-4201.
13. Phillips, K. L.; Sandler, S. I.; Chiu, P. C., A method to calculate the one-electron reduction potentials for nitroaromatic compounds based on gas-phase quantum mechanics. *J. Comput. Chem.* **2011,** *32*, 226-239.
14. Schwarzenbach, R. P.; Stierli, R.; Lanz, K.; Zeyer, J., Quinone and iron porphyrin mediated reduction of nitroaromatic compounds in homogeneous aqueous solution. *Environ. Sci. Technol.* **1990,** *24*, 1566-1574.
15. Hofstetter, T. B.; Heijman, C. G.; Haderlein, S. B.; Holliger, C.; Schwarzenbach, R. P., Complete reduction of TNT and other (poly)nitroaromatic compounds under iron-reducing subsurface conditions. *Environ. Sci. Technol.* **1999,** *33*, 1479-1487.

16. Dunnivant, F. M.; Schwarzenbach, R. P.; Macalady, D. L., Reduction of substituted nitrobenzenes in aqueous solutions containing natural organic matter. *Environ. Sci. Technol.* **1992,** *26*, 2133-2141.
17. Klausen, J.; Troeber, S. P.; Haderlein, S. B.; Schwarzenbach, R. P., Reduction of substituted nitrobenzenes by Fe(II) in aqueous mineral suspensions. *Environ. Sci. Technol.* **1995,** *29*, 2396-2404.
18. Neumann, A.; Hofstetter, T. B.; Lüssi, M.; Cirpka, O. A.; Petit, S.; Schwarzenbach, R. P., Assessing the redox reactivity of structural iron in smectites using nitroaromatic compounds as kinetic probes. *Environ. Sci. Technol.* **2008,** *42*, 8381-8387.
19. Naka, D.; Kim, D.; Strathmann, T. J., Abiotic reduction of nitroaromatic compounds by aqueous iron(II)-catechol complexes. *Environ. Sci. Technol.* **2006,** *40*, 3006-3012.
20. Perlinger, J. A.; Buschmann, J.; Angst, W.; Schwarzenbach, R. P., Iron porphyrin and mercaptojuglone mediated reduction of polyhalogenated methanes and ethanes in homogeneous aqueous solution. *Environ. Sci. Technol.* **1998,** *32*, 2431-2437.
21. Pecher, K.; Haderlein, S. B.; Schwarzenbach, R. P., Reduction of polyhalogenated methanes by surface-bound Fe(II) in aqueous suspensions of iron oxides. *Environ. Sci. Technol.* **2002,** *36*, 1734-1741.
22. Kenneke, J. F.; Weber, E. J., Reductive dehalogenation of halomethanes in iron- and sulfate-reducing sediments. 1. Reactivity pattern analysis. *Environ. Sci. Technol.* **2003,** *37*, 713-720.
23. Kohn, T.; Arnold, W. A.; Roberts, A. L., Reactivity of substituted benzotrichlorides toward granular iron, Cr(II), and an iron(II) porphyrin: A correlation analysis. *Environ. Sci. Technol.* **2006,** *40*, 4253-4260.
24. Koch, M.; Köppen, R.; Siegel, D.; Witt, A.; Nehls, I., Determination of total sulfite in wine by ion chromatography after in-sample oxidation. *J. Agric. Food. Chem.* **2010,** *58*, 9463-9467.
25. Sato, K.; Furuya, S.; Takenaka, N.; Bandow, H.; Maeda, Y.; Furukawa, Y., Oxidative reaction of thiosulfate with hydrogen peroxide by freezing. *Bull. Chem. Soc. Jpn.* **2003,** *76*, 1139-1144.
26. Bard, A. J.; Parsons, R.; Jordan, J., *Standard Potentials in Aqueous Solution*. CRC Press, Inc.: Boca Raton, FL, 1985.

Appendix C: Supporting Information for Chapter 4

C.1 Physiochemical properties, occurrence, and usage of target pesticides

Table C.1 Physiochemical properties, occurrence, and usage of target pesticides

Pesticide	Molecular weight[a]	Water solubility (mg/L)[a]	Log K_{ow}[a]	Henry's law constant (atm-m^3/mol)[a]	pK_a[a]	Occurrence in ND watersheds (Detection frequency)[b]	Usage in ND ($\times 10^3$ acres treated)[c]
Atrazine	215.69	34.7	2.61	2.36×10^{-9}	1.70	9.1%	173.3
Cyanazine	240.70	170	2.22	2.57×10^{-12}	0.87	N.A.[d]	N.A.[d]
Acetochlor	269.77	223	3.03	2.23×10^{-8}	N.A.[d]	N.A.[d]	143.5
Alachlor	269.77	240	3.52	8.32×10^{-9}	N.A.[d]	N.A.[d]	9.3
Metolachlor	283.80	530	3.13	9.00×10^{-9}	N.A.[d]	12.1%	43.6
Mesotrione	339.33	15000	1.49	1.27×10^{-12}	3.12	N.A.[d]	24.4
Diuron	233.10	42	2.68	5.04×10^{-10}	N.A.[d]	3.0%	N.A.[d]
Isoproturon	206.29	65	2.87	1.12×10^{-10}	N.A.[d]	N.A.[d]	N.A.[d]
Metoxuron	228.68	678	1.64	1.48×10^{-8}	N.A.[d]	N.A.[d]	N.A.[d]
Bentazon	240.28	500	2.34	2.18×10^{-9}	2.92	66.7%	856.5
Clopyralid	192.00	7850	1.06	3.03×10^{-9}	2.29	9.1%	3937.2
Chlorpyrifos	350.59	1.12	4.96	2.93×10^{-6}	N.A.[d]	N.A.[d]	1476.9
Propiconazole	342.23	110	3.72	4.12×10^{-9}	1.09	N.A.[d]	1834.7
Ethalfluralin	333.27	0.30	5.11	1.28×10^{-4}	N.A.[d]	N.A.[d]	166.8
Pendimethalin	281.31	0.30	5.18	8.56×10^{-7}	N.A.[d]	3.7%	202.6
Trifluralin	335.29	0.18	5.34	1.03×10^{-4}	N.A.[d]	N.A.[d]	74.0

[a] Data taken from *SRC Interactive PhysProp Database Demo* (http://www.syrres.com/what-we-do/databaseforms.aspx?id=386). [b] Data reported by Johnson (2012)[1]. [c] Data reported by Zollinger et al. (2009)[2]. [d] N.A. = not available.

C.2 Literature data on quantum yield of target pesticides

Table C.2 Quantum yield of target pesticides under environmental relevant conditions

Compound	Quantum yield (mol Einstein^{-1})	Matrix	pH	Light source	Reference
Atrazine	$\Phi_{254nm} = 2.8(\pm0.3)\times10^{-2} - 4.7(\pm0.6)\times10^{-2}$	Ultrapure water	3.0 - 11.0	Low-pressure Hg lamp	Hessler et al. (1993)[1]
	$\Phi_{254nm} = 5.0\times10^{-2}$	Ultrapure water	6.3 - 7.3	Low-pressure Hg lamp	Beltrán et al. (1993)[2]
	$\Phi_{254nm} = 6.1\times10^{-2}$	Ultrapure water	9.0	Xenon lamp	Palm and Zetzsch (1996)[3]
	$\Phi_{254nm} = 3.3\times10^{-2}$	Ultrapure water with 3.3 mg/L	5.6 - 7.8	Medium-pressure Hg lamp	Bolton and Stephan (2002)[4]
	$\Phi_{254nm} = 3.6\times10^{-2}$	Goundwater	N.A.	Low-pressure Hg lamp	McMartin et al. (2003)[5]
	$\Phi_{254nm} = 3.7\times10^{-2}$	Ultrapure water	7.0	High-pressure Hg lamp	Prosen and Zupančič-Kralj (2005)[6]
	$\Phi_{254nm} = 6.0\times10^{-2}$	Ultrapure water	7.0	Low-pressure Hg lamp	Sanches et al. (2010)[7]
Cyanazine	N.A.				
Acetochlor	$\Phi_{313nm} = 6.9\times10^{-2}$	Ultrapure water	6.7	Xenon lamp	Hua et al. (2000)[8]
Alachlor	$\Phi_{254nm} = 1.8\times10^{-1}$	Ultrapure water	7.0	Low-pressure Hg lamp	Beltrán et al. (2000)[9]
	$\Phi_{254nm} = 9.5\times10^{-2}$	Ultrapure water	6.0	Low-pressure Hg lamp	Wong and Chu (2003)[10]
	$\Phi_{254nm} = 5.1\times10^{-2}$	Ultrapure water	6.0	Low-pressure Hg lamp	Wong and Chu (2003)[10]
	$\Phi_{254nm} = 8.0\times10^{-3}$	Ultrapure water	6.0	Low-pressure Hg lamp	Wong and Chu (2003)[10]
	$\Phi_{254nm} = 1.4\times10^{-1}$	Groundwater	7.9 - 8.4	Low-pressure Hg lamp	Song et al. (2008)[11]
	$\Phi_{254nm} = 2.1\times10^{-1}$	Ultrapure water	7.0	Low-pressure Hg lamp	Sanches et al. (2010)[7]
Metolachlor	$\Phi_{313nm} = 2.3\times10^{-5}$	Ultrapure water	4.0	Low-pressure Hg lamp	Kochany and Maguire (1994)[12]
	$\Phi_{313nm} = 2.8\times10^{-5}$	Ultrapure water	6.3	Low-pressure Hg lamp	Kochany and Maguire (1994)[12]
	$\Phi_{313nm} = 3.0\times10^{-5}$	Ultrapure water	7.0	Low-pressure Hg lamp	Kochany and Maguire (1994)[12]
	$\Phi_{313nm} = 3.5\times10^{-5}$	Lake water	8.6	Low-pressure Hg lamp	Kochany and Maguire (1994)[12]

(Continued on next page)

Compound	Quantum yield (mol Einstein^{-1})	Matrix	pH	Light source	Reference
Metolachlor	$\Phi_{313nm} = 2.1\times10^{-5}$	Ultrapure water with 1.6 mg/L $FeCl_3$	6.3	Low-pressure Hg lamp	Kochany and Maguire (1994)[1]
(Continued)	$\Phi_{313nm} = 2.6\times10^{-5}$	Ultrapure water with 0.1 mg/L $MnCl_2$	6.3	Low-pressure Hg lamp	Kochany and Maguire (1994)[1]
	$\Phi_{313nm} = 1.5\times10^{-5}$	Ultrapure water with 5.0 mg/L DOM	6.3	Low-pressure Hg lamp	Kochany and Maguire (1994)[1]
	$\Phi_{Sunlight} = 9.6(\pm1.2)\times10^{-3}$	Ultrapure water	6.3	Sunlight	Kochany and Maguire (1994)[1]
	$\Phi_{Sunlight} = 3.4(\pm0.4)\times10^{-3}$	Ultrapure water with 5.0 mg/L DOM	6.3	Sunlight	Kochany and Maguire (1994)[1]
	$\Phi_{Sunlight} = 6.8(\pm0.8)\times10^{-3}$	Lake water	6.3	Sunlight	Kochany and Maguire (1994)[1]
	$\Phi_{254nm} = 5.6(\pm0.5)\times10^{-1}$	Ultrapure water	2.0 - 9.0	Low-pressure Hg lamp	Benitez et al. (2004)[2]
	$\Phi_{254nm} = 3.0(\pm0.1)\times10^{-1}$	Ultrapure water	6.0 - 8.0	Low-pressure Hg lamp	Wu et al. (2007)[3]
	$\Phi_{254nm} = 4.1(\pm0.6)\times10^{-1}$	Ultrapure water	6.0 - 9.0	Low-pressure Hg lamp	Huntscha et al. (2008)[4]
Mesotrione	$\Phi_{365nm} = 7.0(\pm2.0)\times10^{-1}$	Ultrapure water	6.5	UV lamp	ter Halle and Richard (2006)[5]
Diuron	$\Phi_{254nm} = 2.0\times10^{-2}$	Ultrapure water	7.0	Low-pressure Hg lamp	Jirkovský et al. (1997)[6]
	$\Phi_{296nm} = 1.4\times10^{-2}$	Lake water	7.0 - 9.0	Medium-pressure Hg lamp	Gerecke et al. (2001)[7]
	$\Phi_{254nm} = 1.2(\pm0.1)\times10^{-2}$	Ultrapure water	2.0 - 8.5	Low-pressure Hg lamp	Djebbar et al. (2003)[8]
	$\Phi_{254nm} = 1.1\times10^{-2}$	Ultrapure water	2.0 - 9.0	Low-pressure Hg lamp	Benitez et al. (2006)[9]
	$\Phi_{254nm} = 1.9\times10^{-2}$	Ultrapure water	7.0	Low-pressure Hg lamp	Sanches et al. (2010)[10]
Isoproturon	$\Phi_{254nm} = 4.7\times10^{-3}$	Ultrapure water	7.0	Low-pressure Hg lamp	De St-Laumer et al. (1997)[11]
	$\Phi_{254nm} = 4.0\times10^{-3}$	Ultrapure water	4.0 - 9.0	Xenon lamp	Millet et al. (1998)[12]
	$\Phi_{254nm} = 2.0(\pm0.5)\times10^{-3}$	Ultrapure water	7.0	Low-pressure Hg lamp	Tixier et al. (2000)[13]
	$\Phi_{275nm} = 4.5(\pm0.5)\times10^{-4}$	Ultrapure water	7.0	Xenon lamp	Tixier et al. (2000)[13]
	$\Phi_{275nm} = 4.5\times10^{-3}$	Lake water	7.0 - 9.0	Medium-pressure Hg lamp	Gerecke et al. (2001)[7]

(Continued on next page)

Compound	Quantum yield (mol Einstein^{-1})	Matrix	pH	Light source	Reference
Isoproturon	$\Phi_{290\text{-}800nm} = 2.1\times10^{-6} – 3.3\times10^{-5}$	Ultrapure water	7.0	Xenon lamp	European Commission (2002)[1]
(Continued)	$\Phi_{254nm} = 3.7\times10^{-3}$	Ultrapure water	2.0 - 9.0	Low-pressure Hg lamp	Benitez et al. (2006)[2]
	$\Phi_{254nm} = 2.0\times10^{-3}$	Ultrapure water	7.0	Low-pressure Hg lamp	Sanches et al. (2010)[3]
Metoxuron	$\Phi_{254nm} = 2.0(\pm0.5)\times10^{-3}$	Ultrapure water	7.0	Low-pressure Hg lamp	Boulkamh et al. (2001)[4]
Bentazon	$\Phi_{239\text{-}366nm} = 5.5\times10^{-4} – 1.3\times10^{-3}$	Ultrapure water	7.0 - 9.0	High-pressure Hg lamp	Beltran-Heredia et al. (1996)[5]
	$\Phi_{290\text{-}800nm} = 4.4\times10^{-4}$	Ultrapure water	7.0	Xenon lamp	European Commission (2000)[6]
Clopyralid	N.A.				
Chlorpyrifos	$\Phi_{313nm} = 4.8(\pm0.4)\times10^{-3}$	Ultrapure water	7.0	Medium-pressure Hg lamp	Dilling et al. (1984)[7]
	$\Phi_{254nm} = 4.8(\pm0.4)\times10^{-3}$	Ultrapure water	5.6	Low-pressure Hg lamp	Wan et al. (1994)[8]
	$\Phi_{313nm} = 4.8(\pm0.4)\times10^{-3}$	Ultrapure water	5.6	Medium-pressure Hg lamp	Wan et al. (1994)[8]
	$\Phi_{290\text{-}800nm} = 6.3\times10^{-3}$	Ultrapure water	7.0	Xenon lamp	European Commission (2005)[9]
Propiconazole	$\Phi_{269nm} = 1.1(\pm0.1)\times10^{-1}$	Ultrapure water	7.0	Xenon lamp	Vialaton et al. (2001)[10]
Ethalfluralin	N.A.				
Pendimethalin	N.A.				
Trifluralin	$\Phi_{366nm} = 2.0\times10^{-3}$	Ultrapure water	7.0	Low-pressure Hg lamp	Zepp and Cline (1977)[11]
	$\Phi_{310\text{-}410nm} = 1.4\times10^{-3}$	Ultrapure water	7.0	Low-pressure Hg lamp	Draper (1985)[12]
	$\Phi_{254nm} = 1.2\times10^{-1}$ - 7.2×10^{-1}	Ultrapure water	2.0 - 9.0	Low-pressure Hg lamp	Chelme-Ayala (2010)[13]

C.3 Molar absorption of target pesticides

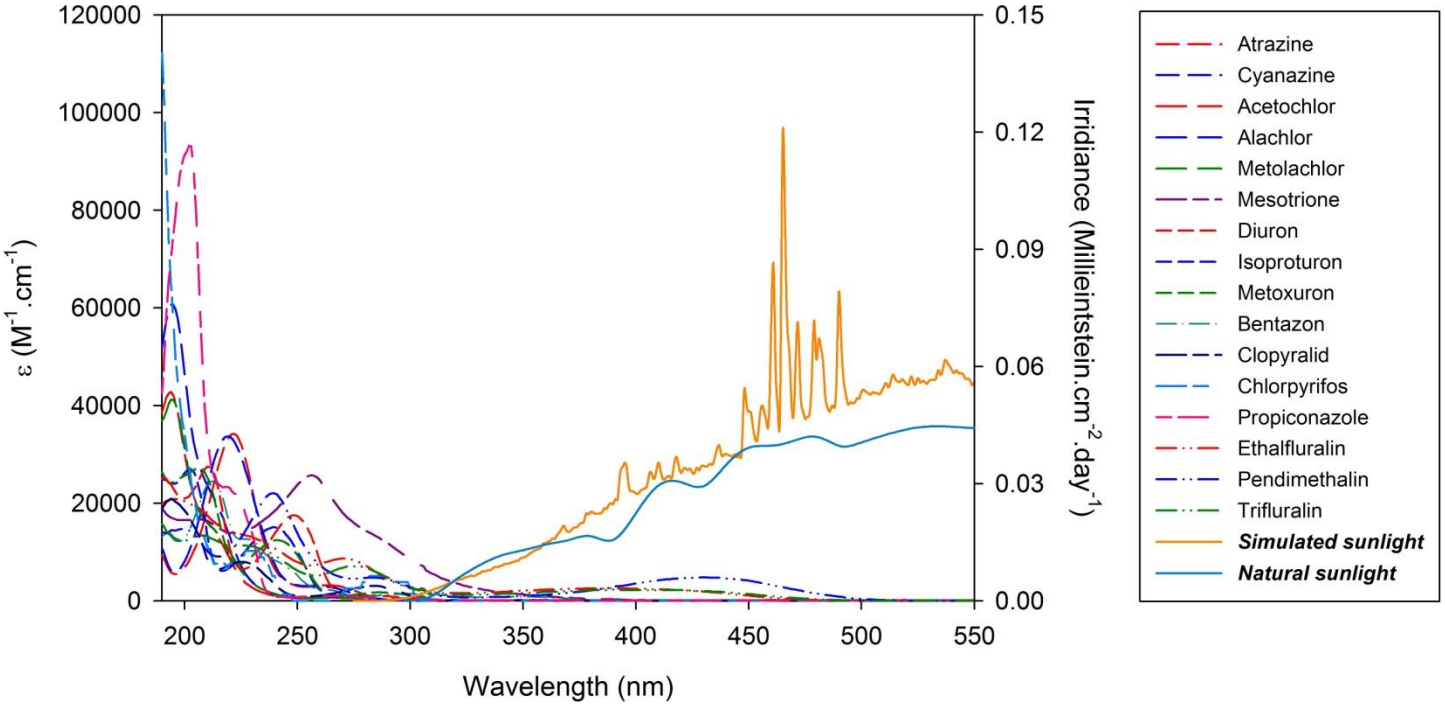

Figure C.1 The molar absorptivity of sixteen target pesticides and spectral irradiance of the simulated sunlight (Filtered xenon arc lamp) and natural sunlight (Spring 2012, Minneapolis, MN, USA).

C.4 HPLC conditions for pesticide analysis

Table C.3 HPLC parameters for pesticide and actinometer analysis

Compound	Mobile phase composition (v:v)	Flow rate (mL/min)	Injection volume (μL)	Detection wavelength (nm)	Retention time (min)
Atrazine	0.1% (v/v) Phosphoric acid (pH 2.85) : ACN (50:50)	1.00	35	220	5.7
Cyanazine	0.1% (v/v) Phosphoric acid (pH 2.85) : ACN (55:45)	1.00	35	220	5.0
Acetochlor	0.1% (v/v) Phosphoric acid (pH 2.85) : ACN (35:65)	1.00	35	220	5.3
Alachlor	0.1% (v/v) Phosphoric acid (pH 2.85) : ACN (35:65)	1.00	35	220	5.3
Metolachlor	0.1% (v/v) Phosphoric acid (pH 2.85) : ACN (35:65)	1.00	35	220	5.2
Mesotrione	0.1% (v/v) Phosphoric acid (pH 2.85) : ACN (55:45)	1.00	35	254	4.8
Diuron	0.1% (v/v) Phosphoric acid (pH 2.85) : ACN (45:55)	1.00	35	254	5.4
Isoproturon	0.1% (v/v) Phosphoric acid (pH 2.85) : ACN (50:50)	1.00	35	254	5.5
Metoxuron	0.1% (v/v) Phosphoric acid (pH 2.85) : ACN (60:40)	1.00	35	254	4.9
Bentazon	0.1% (v/v) Phosphoric acid (pH 2.85) : ACN (45:55)	1.00	35	225	5.5
Clopyralid	0.1% (v/v) Phosphoric acid (pH 2.85) : ACN (70:30)	1.00	35	225	5.6
Chlorpyrifos	0.1% (v/v) Phosphoric acid (pH 2.85) : ACN (45:55)	1.00	35	230	5.6
Propiconazole	0.1% (v/v) Phosphoric acid (pH 2.85) : ACN (35:65)	1.00	35	220	5.3
p-Nitroanisole	Phosphate buffer (10 mM, pH 3, with 10% ACN) : MeOH (30:70)	1.00	35	313	3.6
p-Nitroacetophenone	Phosphate buffer (10 mM, pH 3, with 10% ACN) : MeOH (35:65)	1.00	35	300	3.3

C.5 Measurement of steady-state concentration of carbonate radical

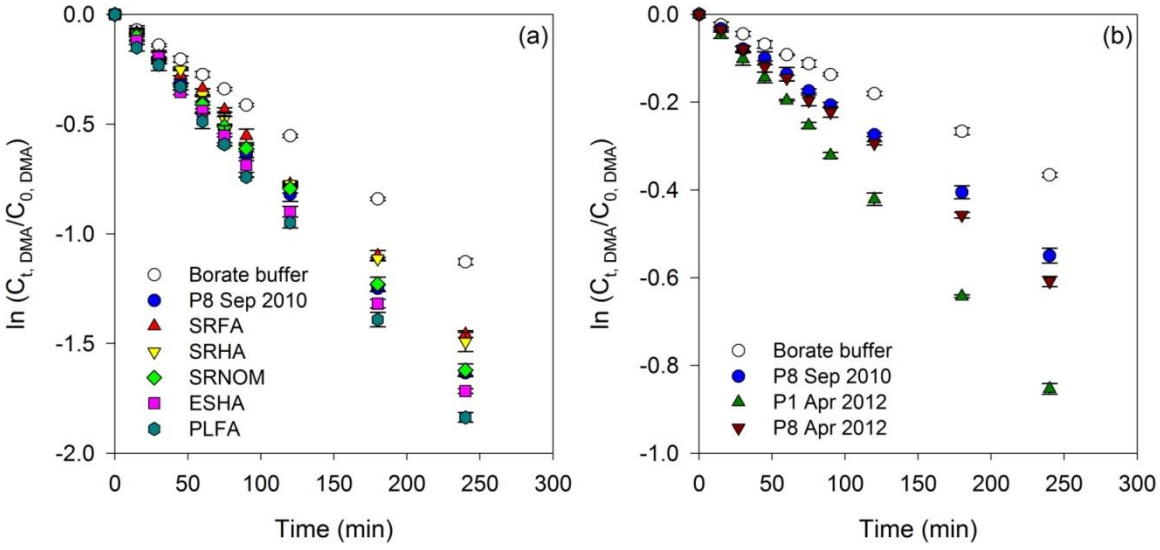

Figure C.2 Semilogarithmic plots for DMA degradation in borate buffer, PPL waters, and model DOM solutions: (a) simulated sunlight; (b) natural sunlight. Error bars represent one standard deviation of duplicate or triplicate samples; where absent, bars fall within symbols.

C.6 Measurement of steady-state concentration of hydroxyl radical

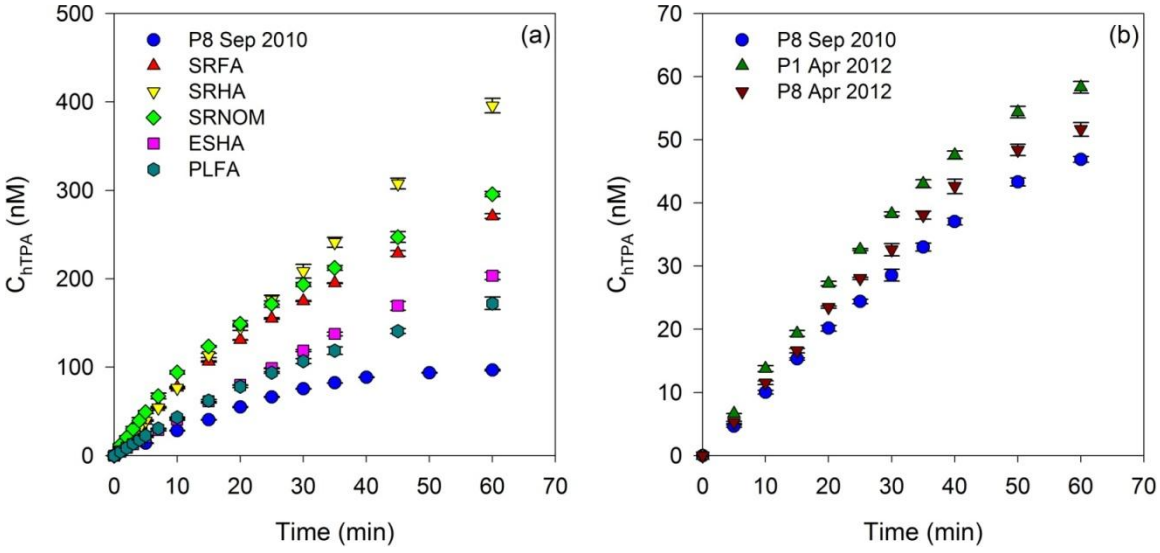

Figure C.3 Time courses for hTPA formation in PPL waters and model DOM solutions: (a) simulated sunlight; (b) natural sunlight. Error bars represent one standard deviation of duplicate or triplicate samples; where absent, bars fall within symbols.

C.7 Measurement of steady-state concentration of singlet oxygen

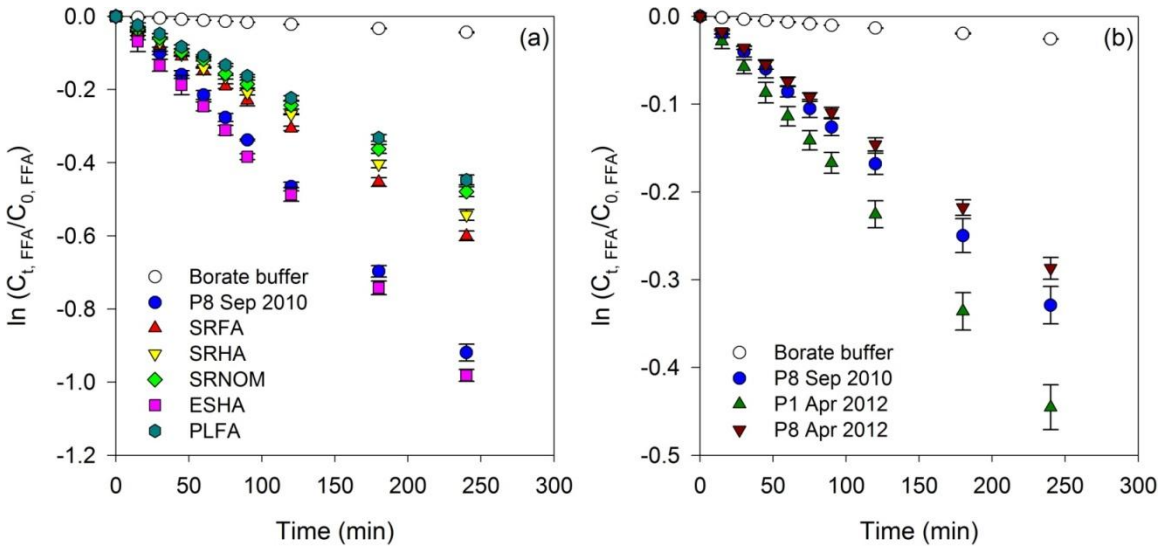

Figure C.4 Semilogarithmic plots for FFA degradation in borate buffer, PPL waters, and model DOM solutions: (a) simulated sunlight; (b) natural sunlight. Error bars represent one standard deviation of duplicate or triplicate samples; where absent, bars fall within symbols.

C.8 Measurement of steady-state concentration of triplet DOM

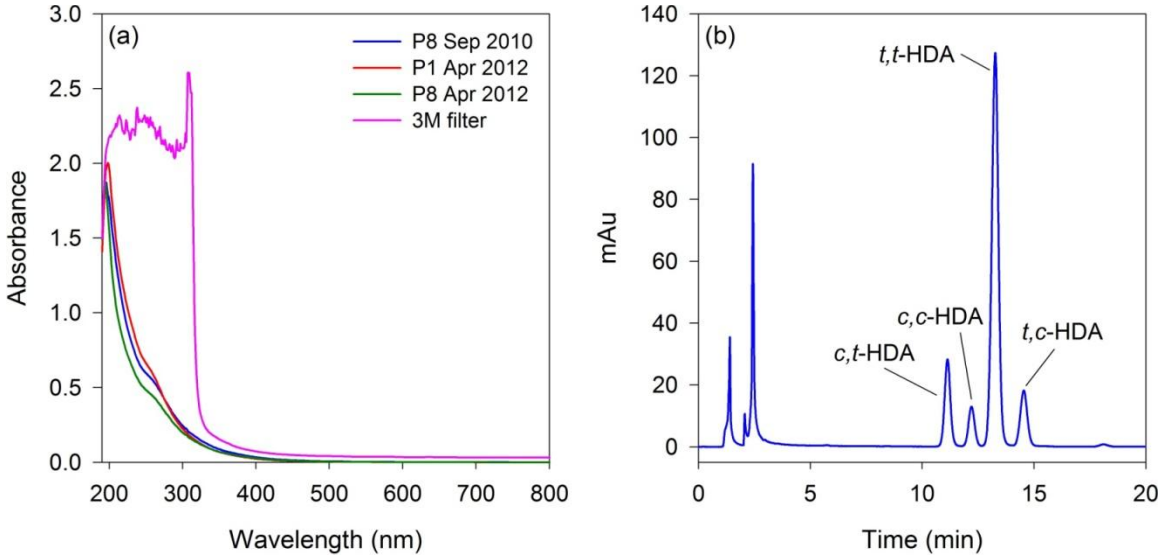

Figure C.5 (a) UV/vis absorbance spectra of PPL waters with 315 nm cutoff filter; (b) HPLC chromatogram of *c*,*t*-HDA, *c*,*c*-HDA, *t*,*t*-HDA and *t*,*c*-HDA.

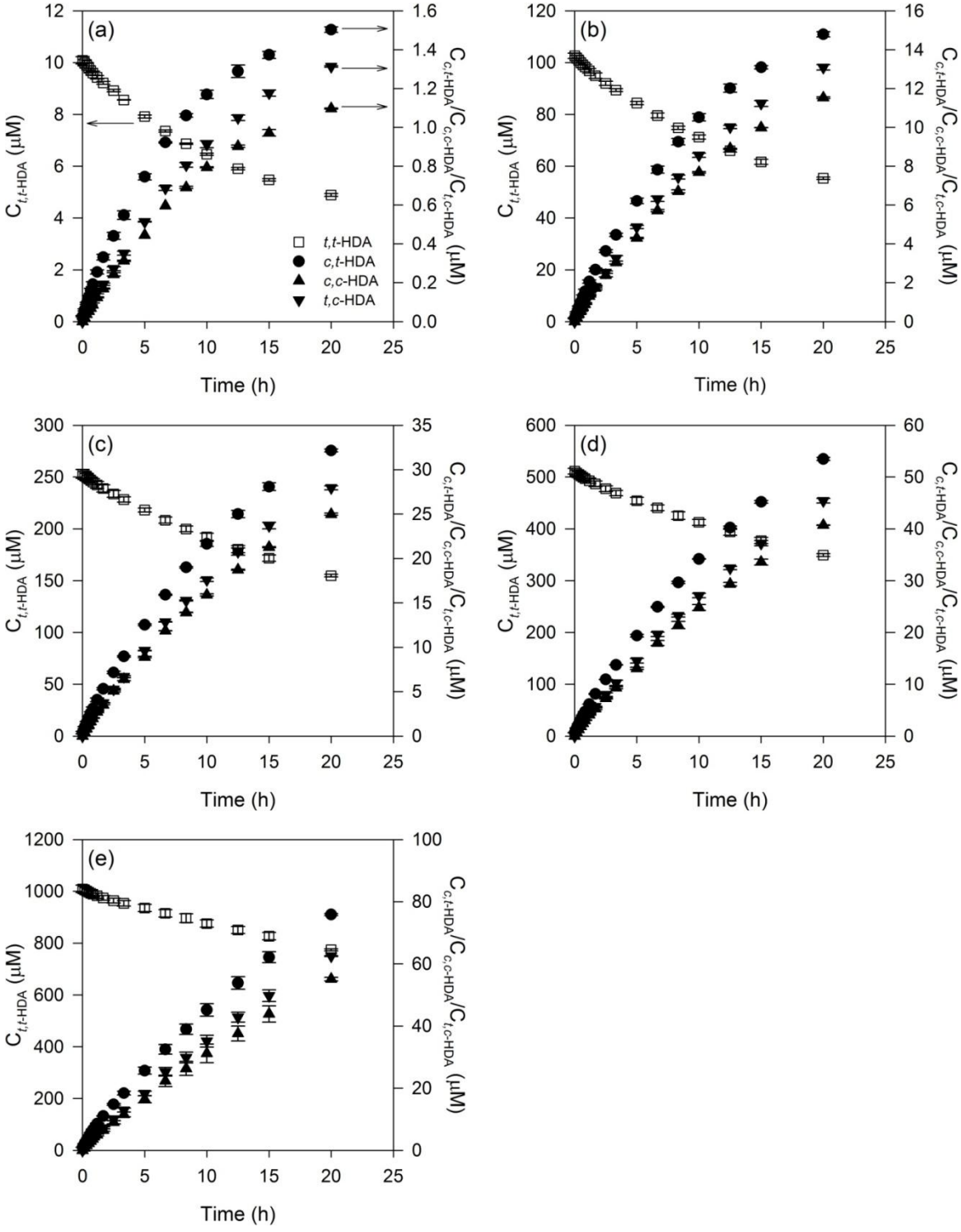

Figure C.6 Time courses for HDA isomer degradation and formation in P8-Sep-2010 water under simulated sunlight: (a) 10 μM *t,t*-HDA; (b) 100 μM *t,t*-HDA; (c) 250 μM *t,t*-HDA; (d) 500 μM *t,t*-HDA; (e) 1000 μM *t,t*-HDA. Error bars represent one standard deviation of duplicate samples; where absent, bars fall within symbols. Note differences in *y*-axis.

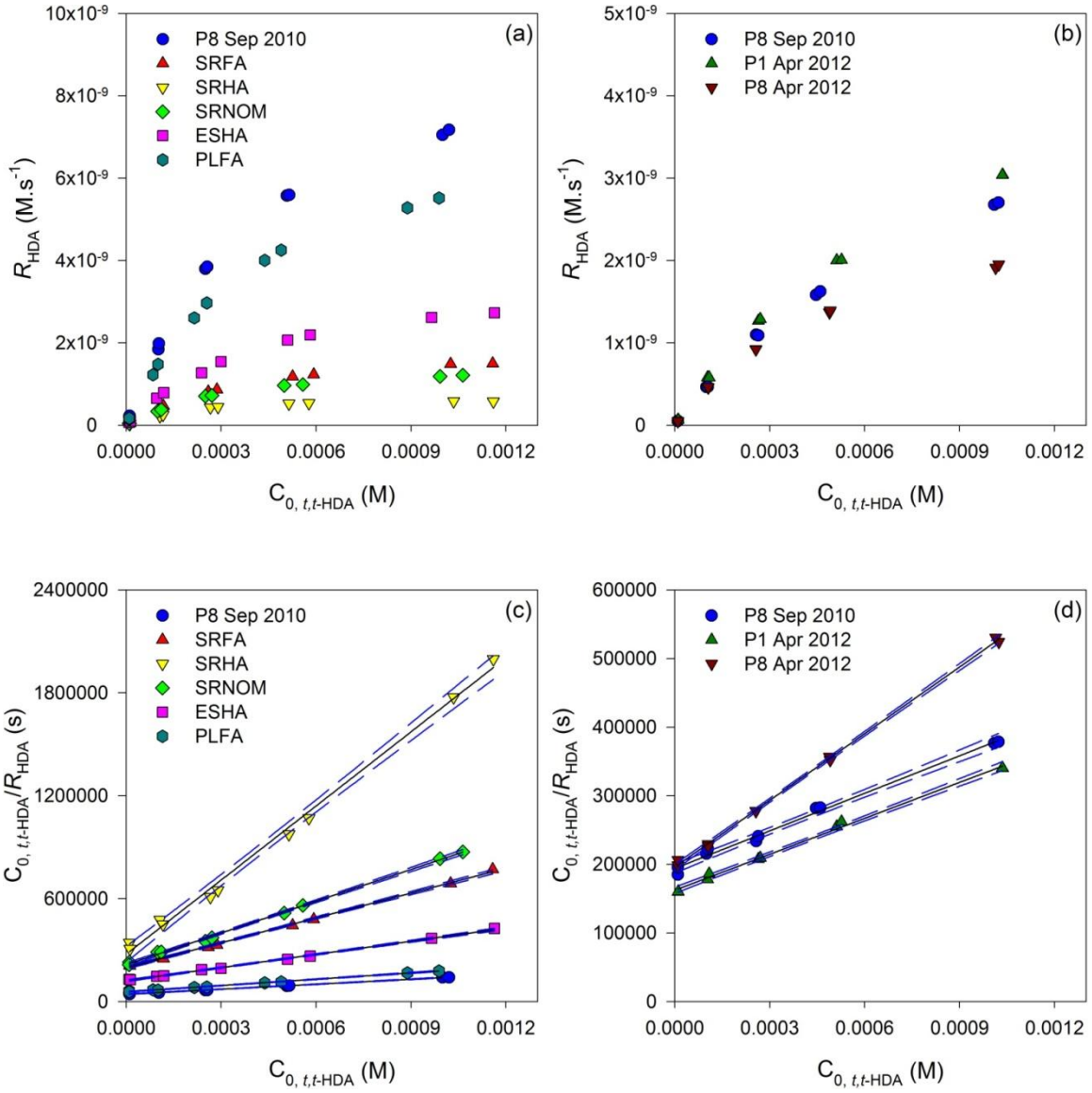

Figure C.7 Graphical data analysis of HDA isomerization in PPL waters and model DOM solutions: (a) Relationship between R_{HDA} and the initial dose of *t*,*t*-HDA ($C_{0,\ t,t\text{-HDA}}$) under simulated sunlight; (b) Relationship between R_{HDA} and $C_{0,\ t,t\text{-HDA}}$ under natural sunlight; (c) Relationship between $C_{0,\ t,t\text{-HDA}}/R_{HDA}$ and $C_{0,\ t,t\text{-HDA}}$ under simulated sunlight; (d) Relationship between $C_{0,\ t,t\text{-HDA}}/R_{HDA}$ and $C_{0,\ t,t\text{-HDA}}$ under natural sunlight. Solid lines represent linear regressions and dashed lines represent 95% confidence intervals. $R^2 > 0.99$ in all cases.

C.9 Literature data on steady-state concentrations of PPRIs

Table C.4 Literature data on steady-state concentrations of PPRIs in IHSS NOM solutions (25 mg C/L)

Sample	DOM solution compositions	Light source (Intensity)	$[^{\bullet}OH]_{ss}$ (M)	Reference
SRFA	pH 7.0, DOC = 25 mg C/L	300 W Xenon lamp	$7.09\ (\pm 0.10)\times 10^{-17}$	Xu et al. (2011)[1]
	pH 7.0, DOC = 0 - 15 mg C/L	175 W Hg-vapor lamp	$3.39\ (\pm 0.10)\times 10^{-16a}$	Page et al. (2011)[2]
SRHA	pH 7.0, DOC = 25 mg C/L	300 W Xenon lamp	$6.50\ (\pm 0.05)\times 10^{-17}$	Xu et al. (2011)[1]
	pH 7.0, DOC = 0 - 15 mg C/L	175 W Hg-vapor lamp	$9.55\ (\pm 0.19)\times 10^{-16a}$	Page et al. (2011)[2]
SRNOM	pH 7.0, DOC = 25 mg C/L	300 W Xenon lamp	$20.12\ (\pm 0.43)\times 10^{-17}$	Xu et al. (2011)[1]
	pH 7.0, DOC = 0 - 15 mg C/L	175 W Hg-vapor lamp	$5.81\ (\pm 0.21)\times 10^{-16a}$	Page et al. (2011)[2]
ESHA	pH 7.0, DOC = 0 - 15 mg C/L	175 W Hg-vapor lamp	$11.51\ (\pm 0.31)\times 10^{-16a}$	Page et al. (2011)[2]
PLFA	pH 7.0, DOC = 0 - 15 mg C/L	175 W Hg-vapor lamp	$7.57\ (\pm 0.40)\times 10^{-16a}$	Page et al. (2011)[2]
Sample	DOM solution compositions	Light source (Intensity)	$[^1O_2]_{ss}$ (M)	Reference
SRFA	pH 7.0, DOC = 25 mg C/L	300 W Xenon lamp	$2.16\ (\pm 0.04)\times 10^{-13}$	Xu et al. (2011)[1]
SRHA	pH 7.0, 10 mM NaCl, DOC = 0 - 25 mg C/L	1000 W Xenon lamp (765 W/m^2)	$1.39\ (\pm 0.07)\times 10^{-13b}$	Kohn et al. (2007)[3]
	pH 7.5, 10 mM NaCl, DOC = 0 - 40 mg C/L	175 W Hg vapor lamp	$2.14\ (\pm 0.11)\times 10^{-13c}$	Grandbois et al. (2008)[4]
	pH 7.0, DOC = 25 mg C/L	300 W Xenon lamp	$1.57\ (\pm 0.05)\times 10^{-13}$	Xu et al. (2011)[1]
SRNOM	pH 6.5, DOC = 30 mg C/L	1000 W Xenon lamp (750 W/m^2)	$6.42\ (\pm 0.32)\times 10^{-13d}$	ter Halle and Richard (2006)[5]
	pH 7.0, DOC = 25 mg C/L	300 W Xenon lamp	$1.58\ (\pm 0.03)\times 10^{-13}$	Xu et al. (2011)[1]
	pH 7.6 – 8.0, DOC = 5 - 40 mg C/L	1000 W Xenon lamp (400 W/m^2)	$3.55\ (\pm 0.18)\times 10^{-13e}$	Romero et al. (2011)[6]
PLFA	pH 7.0, 10 mM NaCl, DOC = 0 - 25 mg C/L	1000 W Xenon lamp (765 W/m^2)	$1.13\ (\pm 0.06)\times 10^{-13b}$	Kohn et al. (2007)[3]
	pH 7.5, 10 mM NaCl, DOC = 0 - 40 mg C/L	175 W Hg vapor lamp	$2.32\ (\pm 0.12)\times 10^{-13c}$	Grandbois et al. (2008)[4]
Sample	DOM solution compositions	Light source (Intensity)	$[^3DOM^*]_{ss}$ (M)	Reference
SRNOM	pH 8.1 (20 mM phosphate buffer), DOC = 0 - 15 mg C/L	15 W Black light fluorescent lamp	$9.37(\pm 0.65)\times 10^{-16f}$	Grebel et al. (2012)[7]

[a] Concentration estimated from Equation 1 with fitting parameters from Figure 1 in Page et al. (2011).[2] [b] Concentration extrapolated from Figure 1 in Kohn et al. (2007).[3] [c] Concentration extrapolated from Figure S1 in Grandbois et al. (2008).[4] [d] Concentration extrapolated for from the value determined at 30 mg C/L in ter Halle and Richard (2006).[5] [e] Concentrations extrapolated from Figure S2 in Romero et al. (2011).[6] [f] Concentration extrapolated from Figure 6c in Grebel et al. (2012).[7] Errors represent 95% confidence intervals.

C.10 Pesticide photolysis in P8-Sep-2010 water under simulated sunlight

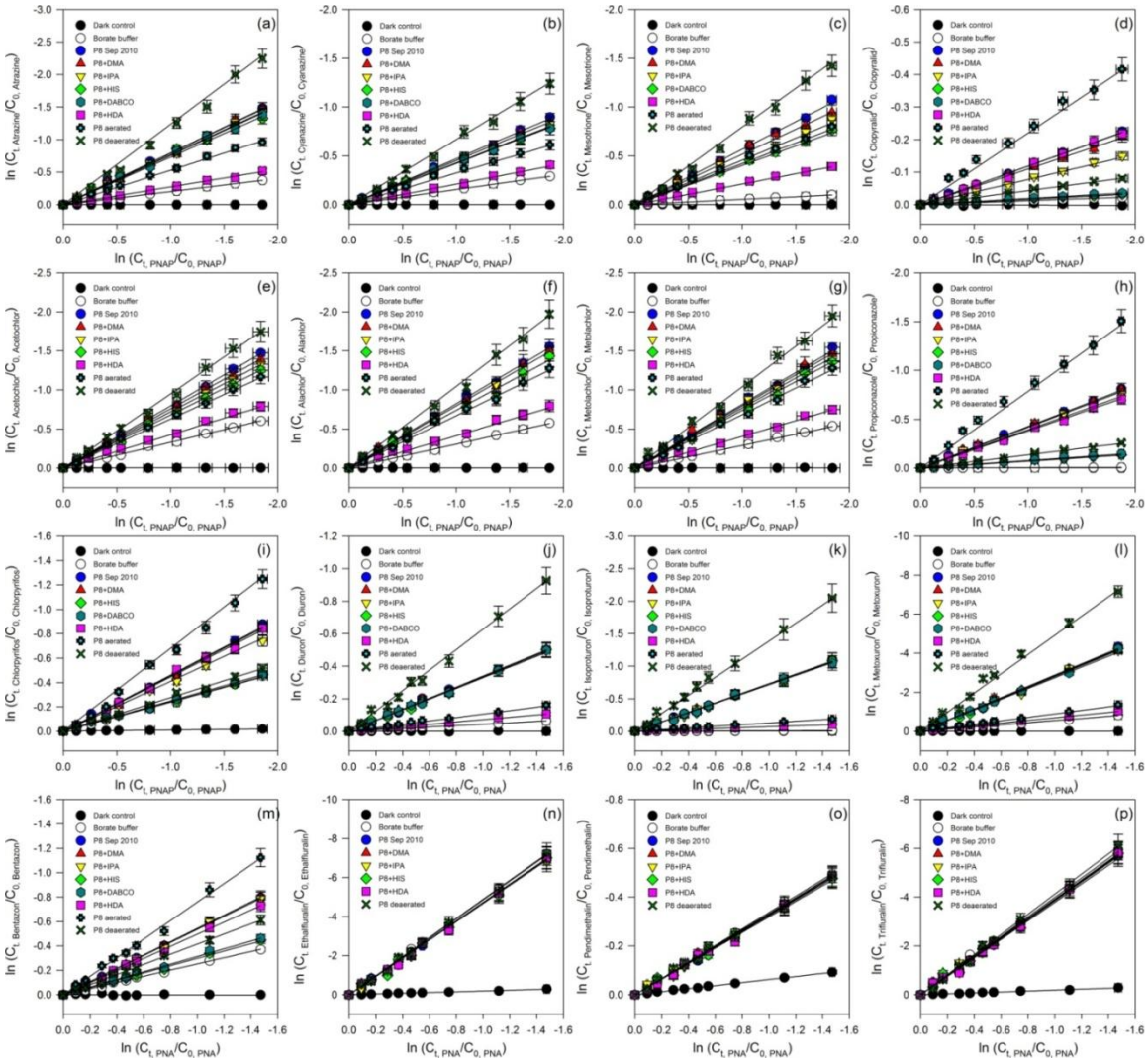

Figure C.8 Logarithmic plots for pesticide photodegradation in borate buffer and native and modified P8-Sep-2010 water under simulated sunlight: (a) atrazine; (b) cyanazine; (c) mesotrione; (d) clopyralid; (e) acetochlor; (f) alachlor; (g) metolachlor; (h) propiconazole; (i) chlorpyrifos; (j) diuron; (k) isoproturon; (l) metoxuron; (m) bentazon; (n) ethalfluralin; (o) pendimethalin; (p) trifluralin. Error bars represent one standard deviation of duplicate samples; where absent, bars fall within symbols. Solid lines represent linear regressions and $R^2 > 0.98$ in all cases. Note differences in *x*-axis.

Table C.5 Pseudo-first-order rate constants of pesticide photodegradation in P8-Sep-2010 water under simulated sunlight

Compound	$k_{obs,\ P8\ Sep}$ (s^{-1})[a]	$k_{obs,\ Buffer}$ (s^{-1})[b]	$k_{obs,\ DMA}$ (s^{-1})[c]	$k_{obs,\ IPA}$ (s^{-1})[d]	$k_{obs,\ HIS}$ (s^{-1})[e]	$k_{obs,\ DABCO}$ (s^{-1})[f]	$k_{obs,\ HDA}$ (s^{-1})[g]	$k_{obs,\ Aerated}$ (s^{-1})[h]	$k_{obs,\ Deaerated}$ (s^{-1})[i]
Atrazine	$7.38(\pm0.15)\times10^{-6}$	$1.86(\pm0.04)\times10^{-6}$	$7.28(\pm0.14)\times10^{-6}$	$7.08(\pm0.13)\times10^{-6}$	$6.91(\pm0.13)\times10^{-6}$	$6.93(\pm0.13)\times10^{-6}$	$2.51(\pm0.06)\times10^{-6}$	$4.91(\pm0.07)\times10^{-6}$	$1.09(\pm0.05)\times10^{-5}$
Cyanazine	$4.34(\pm0.10)\times10^{-6}$	$1.44(\pm0.03)\times10^{-6}$	$4.16(\pm0.04)\times10^{-6}$	$4.02(\pm0.08)\times10^{-6}$	$3.89(\pm0.06)\times10^{-6}$	$3.91(\pm0.08)\times10^{-6}$	$1.97(\pm0.05)\times10^{-6}$	$3.06(\pm0.06)\times10^{-6}$	$6.05(\pm0.06)\times10^{-6}$
Acetochlor	$7.28(\pm0.14)\times10^{-6}$	$3.03(\pm0.06)\times10^{-6}$	$7.05(\pm0.13)\times10^{-6}$	$6.60\ (\pm0.07)\times10^{-6}$	$6.22(\pm0.09)\times10^{-6}$	N.A.[j]	$4.06(\pm0.10)\times10^{-6}$	$5.90(\pm0.06)\times10^{-6}$	$8.73(\pm0.26)\times10^{-6}$
Alachlor	$7.60(\pm0.14)\times10^{-6}$	$2.81(\pm0.06)\times10^{-6}$	$7.39(\pm0.12)\times10^{-6}$	$7.01(\pm0.12)\times10^{-6}$	$6.77(\pm0.12)\times10^{-6}$	N.A.[j]	$3.96(\pm0.09)\times10^{-6}$	$6.23(\pm0.08)\times10^{-6}$	$9.42(\pm0.13)\times10^{-6}$
Metolachlor	$7.66(\pm0.15)\times10^{-6}$	$2.69(\pm0.06)\times10^{-6}$	$7.51(\pm0.11)\times10^{-6}$	$7.09(\pm0.10)\times10^{-6}$	$6.75(\pm0.08)\times10^{-6}$	N.A.[j]	$3.78(\pm0.07)\times10^{-6}$	$6.34(\pm0.08)\times10^{-6}$	$9.63(\pm0.41)\times10^{-6}$
Mesotrione	$5.26(\pm0.10)\times10^{-6}$	$5.01(\pm0.10)\times10^{-7}$	$4.90(\pm0.12)\times10^{-6}$	$4.35(\pm0.10)\times10^{-6}$	N.A.[j]	$3.87(\pm0.10)\times10^{-6}$	$2.00\pm0.09)\times10^{-6}$	$4.04(\pm0.08)\times10^{-6}$	$7.16(\pm0.18)\times10^{-6}$
Diuron	$3.50(\pm0.06)\times10^{-5}$	$4.47(\pm0.09)\times10^{-6}$	$3.48(\pm0.07)\times10^{-5}$	$3.45(\pm0.09)\times10^{-5}$	$3.42(\pm0.07)\times10^{-5}$	$3.43(\pm0.07)\times10^{-5}$	$7.60(\pm0.16)\times10^{-6}$	$1.13(\pm0.05)\times10^{-5}$	$6.36(\pm0.17)\times10^{-5}$
Isoproturon	$7.56(\pm0.12)\times10^{-5}$	$5.64(\pm1.06)\times10^{-7}$	$7.51(\pm0.16)\times10^{-5}$	$7.47(\pm0.16)\times10^{-5}$	$7.39(\pm0.10)\times10^{-5}$	$7.40(\pm0.10)\times10^{-5}$	$7.39(\pm0.13)\times10^{-6}$	$1.34(\pm0.07)\times10^{-5}$	$1.45(\pm0.07)\times10^{-4}$
Metoxuron	$2.93(\pm0.04)\times10^{-4}$	$5.71(\pm0.17)\times10^{-5}$	$2.91(\pm0.06)\times10^{-4}$	$2.89(\pm0.06)\times10^{-4}$	$2.88(\pm0.07)\times10^{-4}$	$2.89(\pm0.06)\times10^{-4}$	$7.46(\pm0.11)\times10^{-5}$	$9.46(\pm0.16)\times10^{-4}$	$5.14(\pm0.09)\times10^{-4}$
Bentazon	$5.53(\pm0.11)\times10^{-5}$	$2.58(\pm0.08)\times10^{-5}$	$5.48(\pm0.11)\times10^{-5}$	$5.43(\pm0.09)\times10^{-5}$	$3.09(\pm0.08)\times10^{-5}$	$3.27(\pm0.07)\times10^{-5}$	$5.08(\pm0.09)\times10^{-5}$	$7.78(\pm0.13)\times10^{-5}$	$4.23(\pm0.07)\times10^{-5}$
Clopyralid	$1.09(\pm0.03)\times10^{-6}$	$1.05(\pm0.06)\times10^{-7}$	$1.00(\pm0.04)\times10^{-6}$	$7.22(\pm0.14)\times10^{-7}$	$1.51(\pm0.06)\times10^{-7}$	$1.73(\pm0.05)\times10^{-7}$	$1.07(\pm0.05)\times10^{-6}$	$2.08(\pm0.06)\times10^{-6}$	$3.94(\pm0.06)\times10^{-7}$
Chlorpyrifos	$4.10(\pm0.13)\times10^{-6}$	$2.05(\pm0.10)\times10^{-6}$	$3.92(\pm0.08)\times10^{-6}$	$3.61(\pm0.07)\times10^{-6}$	$2.13(\pm0.05)\times10^{-6}$	$2.18(\pm0.06)\times10^{-6}$	$3.98(\pm0.08)\times10^{-6}$	$5.85(\pm0.09)\times10^{-6}$	$2.40(\pm0.08)\times10^{-6}$
Propiconazole	$3.96(\pm0.05)\times10^{-6}$	$2.35(\pm0.05)\times10^{-8}$	$3.91(\pm0.07)\times10^{-6}$	$3.71(\pm0.07)\times10^{-6}$	$6.74(\pm0.11)\times10^{-7}$	$7.36(\pm0.14)\times10^{-7}$	$3.49(\pm0.09)\times10^{-6}$	$7.41(\pm0.14)\times10^{-6}$	$1.25(\pm0.06)\times10^{-6}$
Ethalfluralin	$4.60(\pm0.09)\times10^{-4}$	$4.77(\pm0.09)\times10^{-4}$	$4.60(\pm0.09)\times10^{-4}$	$4.59(\pm0.06)\times10^{-4}$	$4.58(\pm0.09)\times10^{-4}$	N.A.[j]	$4.59(\pm0.08)\times10^{-4}$	N.A.[j]	$4.75(\pm0.09)\times10^{-4}$
Pendimethalin	$2.69(\pm0.05)\times10^{-5}$	$2.82(\pm0.05)\times10^{-5}$	$2.69(\pm0.06)\times10^{-5}$	$2.69(\pm0.05)\times10^{-5}$	$2.69(\pm0.06)\times10^{-5}$	N.A.[j]	$2.69(\pm0.06)\times10^{-5}$	N.A.[j]	$2.74(\pm0.06)\times10^{-5}$
Trifluralin	$3.80(\pm0.07)\times10^{-4}$	$3.94(\pm0.07)\times10^{-4}$	$3.79(\pm0.08)\times10^{-4}$	$3.79(\pm0.08)\times10^{-4}$	$3.78(\pm0.09)\times10^{-4}$	N.A.[j]	$3.79(\pm0.06)\times10^{-4}$	N.A.[j]	$3.99(\pm0.09)\times10^{-4}$

[a] Observed pseudo-first-order rate constants for pesticide photolysis in native P8-Sep-2010 water. [b] Observed pseudo-first-order rate constants for pesticide photolysis in borate buffer. [c] Observed pseudo-first-order rate constants for pesticide photolysis in P8-Sep-2010 water with 120 μM DMA. [d] Observed pseudo-first-order rate constants for pesticide photolysis in P8-Sep-2010 water with 26 mM IPA. [e] Observed pseudo-first-order rate constants for pesticide photolysis in P8-Sep-2010 water with 20 mM HIS. [f] Observed pseudo-first-order rate constants for pesticide photolysis in P8-Sep-2010 water with 10 mM DABCO. [g] Observed pseudo-first-order rate constants for pesticide photolysis in P8-Sep-2010 water with 10 mM HDA. [h] Observed pseudo-first-order rate constants for pesticide photolysis in aerated P8-Sep-2010 water. [i] Observed pseudo-first-order rate constants for pesticide photolysis in deaerated P8-Sep-2010 water. [j] N.A. = not available. Errors represent one standard deviation from duplicate experiments.

Table C.6 Contribution of direct and indirect photolysis in P8-Sep-2010 water under simulated sunlight

Compound	$k_{calc,\ Direct}$ (s^{-1})[a]	$k_{calc,\ CO_3^{\bullet-}}$ (s^{-1})[b]	$k_{calc,\ {}^{\bullet}OH}$ (s^{-1})[c]	$k_{calc,\ {}^1O_2}$ (s^{-1})[d]	$k_{calc,\ {}^3DOM^*}$ (s^{-1})[e]	k_{Other} (s^{-1})[f]	$k_{pred,\ CO_3^{\bullet-}}$ (s^{-1})[g]	$k_{pred,\ {}^{\bullet}OH}$ (s^{-1})[h]	$k_{pred,\ {}^1O_2}$ (s^{-1})[i]
Atrazine	$1.80(\pm0.06)\times10^{-6}$	$1.07(\pm0.12)\times10^{-7}$	$1.97(\pm0.37)\times10^{-7}$	$1.65(\pm0.12)\times10^{-7}$	$4.88(\pm0.20)\times10^{-6}$	$2.37(\pm0.62)\times10^{-7}$	$9.50(\pm4.32)\times10^{-8}$	$1.51(\pm0.38)\times10^{-7}$	N.A.[j]
Cyanazine	$1.39(\pm0.03)\times10^{-6}$	$1.86(\pm1.50)\times10^{-7}$	$1.32(\pm0.14)\times10^{-7}$	$1.28(\pm0.12)\times10^{-7}$	$2.37(\pm0.13)\times10^{-6}$	$1.38(\pm0.30)\times10^{-7}$	N.A.[j]	$1.16(\pm0.09)\times10^{-7}$	N.A.[j]
Acetochlor	$2.92(\pm0.21)\times10^{-6}$	$2.32(\pm0.88)\times10^{-7}$	$4.46(\pm0.18)\times10^{-7}$	$3.86(\pm0.16)\times10^{-7}$	$3.22(\pm0.21)\times10^{-6}$	$7.27(\pm2.32)\times10^{-8}$	N.A.[j]	$4.23(\pm0.77)\times10^{-7}$	N.A.[j]
Alachlor	$2.71(\pm0.03)\times10^{-6}$	$2.03(\pm1.62)\times10^{-7}$	$3.84(\pm0.11)\times10^{-7}$	$2.38(\pm0.10)\times10^{-7}$	$3.63(\pm0.15)\times10^{-6}$	$4.22(\pm2.86)\times10^{-7}$	N.A.[j]	$3.68(\pm1.26)\times10^{-7}$	N.A.[j]
Metolachlor	$2.59(\pm0.06)\times10^{-6}$	$1.52(\pm0.17)\times10^{-7}$	$4.14(\pm0.17)\times10^{-7}$	$3.43(\pm0.14)\times10^{-7}$	$3.88(\pm0.12)\times10^{-6}$	$2.72(\pm0.28)\times10^{-7}$	N.A.[j]	$4.14(\pm1.51)\times10^{-7}$	N.A.[j]
Mesotrione	$4.84(\pm0.05)\times10^{-7}$	$3.58(\pm1.71)\times10^{-7}$	$5.45(\pm0.13)\times10^{-7}$	$4.86(\pm0.12)\times10^{-7}$	$3.26(\pm0.10)\times10^{-6}$	$1.25(\pm0.36)\times10^{-7}$	N.A.[j]	$5.20(\pm0.42)\times10^{-7}$	$4.89(\pm0.20)\times10^{-7}$
Diuron	$4.32(\pm0.28)\times10^{-5}$	$1.76(\pm0.20)\times10^{-7}$	$3.50(\pm0.37)\times10^{-7}$	$2.36(\pm0.28)\times10^{-7}$	$2.74(\pm0.05)\times10^{-5}$	$2.52(\pm0.38)\times10^{-6}$	$1.40(\pm0.85)\times10^{-7}$	$4.60(\pm1.70)\times10^{-7}$	N.A.[j]
Isoproturon	$5.44(\pm1.02)\times10^{-7}$	$5.65(\pm0.63)\times10^{-7}$	$3.92(\pm0.32)\times10^{-7}$	$7.63(\pm0.46)\times10^{-7}$	$6.82(\pm0.12)\times10^{-5}$	$5.12(\pm0.26)\times10^{-6}$	$5.53(\pm1.08)\times10^{-7}$	$3.84(\pm1.28)\times10^{-7}$	N.A.[j]
Metoxuron	$5.51(\pm0.17)\times10^{-5}$	$1.98(\pm1.42)\times10^{-6}$	$2.09(\pm0.20)\times10^{-6}$	$7.08(\pm1.83)\times10^{-7}$	$2.19(\pm0.04)\times10^{-4}$	$1.47(\pm0.36)\times10^{-5}$	N.A.[j]	$1.97(\pm0.70)\times10^{-6}$	N.A.[j]
Bentazon	$2.49(\pm0.08)\times10^{-5}$	$4.74(\pm2.08)\times10^{-7}$	$5.84(\pm0.57)\times10^{-7}$	$2.24(\pm0.10)\times10^{-5}$	$4.46(\pm0.21)\times10^{-6}$	$2.48(\pm0.28)\times10^{-6}$	N.A.[j]	$5.14(\pm0.41)\times10^{-7}$	N.A.[j]
Clopyralid	$1.01(\pm0.05)\times10^{-7}$	$8.78(\pm0.74)\times10^{-8}$	$2.79(\pm0.75)\times10^{-7}$	$5.60(\pm0.18)\times10^{-7}$	$1.75(\pm0.56)\times10^{-8}$	$4.32(\pm2.10)\times10^{-8}$	N.A.[j]	$2.69(\pm0.22)\times10^{-7}$	N.A.[j]
Chlorpyrifos	$1.98(\pm0.06)\times10^{-6}$	$1.82(\pm1.06)\times10^{-7}$	$3.03(\pm0.45)\times10^{-7}$	$1.46(\pm0.03)\times10^{-6}$	$1.23(\pm1.07)\times10^{-7}$	$4.52(\pm2.61)\times10^{-8}$	$1.80(\pm0.23)\times10^{-7}$	$2.80(\pm0.65)\times10^{-7}$	N.A.[j]
Propiconazole	$2.27(\pm0.02)\times10^{-8}$	$5.62(\pm2.09)\times10^{-8}$	$1.99(\pm0.35)\times10^{-7}$	$3.00(\pm0.06)\times10^{-6}$	$4.68(\pm0.14)\times10^{-7}$	$2.14(\pm0.65)\times10^{-7}$	N.A.[j]	N.A.[j]	N.A.[j]
Ethalfluralin	$4.60(\pm0.04)\times10^{-4}$	N.A.[j]	N.A.[j]	N.A.[j]	N.A.[j]	N.A.[j]	N.A.[j]	N.A.[j]	N.A.[j]
Pendimethalin	$2.72(\pm0.05)\times10^{-5}$	N.A.[j]	N.A.[j]	N.A.[j]	N.A.[j]	N.A.[j]	N.A.[j]	N.A.[j]	N.A.[j]
Trifluralin	$3.81(\pm0.07)\times10^{-4}$	N.A.[j]	N.A.[j]	N.A.[j]	N.A.[j]	N.A.[j]	N.A.[j]	$4.47(\pm0.22)\times10^{-7}$	N.A.[j]

[a] Calculated as $k_{obs,\ Buffer} \times S_{\sum\lambda 290\text{-}800nm}$, where $k_{obs,\ Buffer}$ is from Table C.5 and $S_{\sum\lambda 290\text{-}800nm}$ is the light screening factor from Table 4.1. [b] Calculated from Eqn (4.11) in the main text. [c] Calculated from Eqn (4.12) in the main text. [d] Calculated from Eqn (4.13) in the main text. [e] Calculated from Eqn (4.14) in the main text. [f] Calculated as $k_{obs,\ P8\ Sep} - k_{calc,\ Direct} - k_{calc,\ CO_3^{\bullet-}} - k_{calc,\ {}^{\bullet}OH} - k_{calc,\ {}^1O_2} - k_{calc,\ {}^3DOM^*}$, where $k_{obs,\ P8\ Sep}$ is from Table C.5. [g] Calculated as $k_{CO_3^{\bullet-}} \times [CO_3^{\bullet-}]_{ss}$, where $k_{CO_3^{\bullet-}}$ is from Table C.7 and $[CO_3^{\bullet-}]_{ss}$ is from Table 4.2. [h] Calculated as $k_{{}^{\bullet}OH} \times [{}^{\bullet}OH]_{ss}$, where $k_{{}^{\bullet}OH}$ is from Table C.7 and $[{}^{\bullet}OH]_{ss}$ is from Table 4.2. [i] Calculated as $k_{{}^1O_2} \times [{}^1O_2]_{ss}$, where $k_{{}^1O_2}$ is from Table C.7 and $[{}^1O_2]_{ss}$ is from Table 4.2. [j] N.A. = not available. Errors were propagated through observed rate constants and PPRI concentrations.

C.11 Second-order reaction rate constants of pesticides with PPRIs

Table C.7 Second-order reaction rate constants of pesticides with carbonate radical, hydroxyl radical, and singlet oxygen

Compound	$k_{CO_3^{\bullet-}}$ (M^{-1} s^{-1})	Reference	$k_{^{\bullet}OH}$ (M^{-1} s^{-1})	Reference	$k_{^1O_2}$ (M^{-1} s^{-1})	Reference
Atrazine	4.0×10^6	Huang and Mabury (2000)[1]	1.7×10^9	Chramosta et al. (1993)[2]	N.A.[b]	
	$3.7(\pm0.2)\times10^6$	Canonica et al. (2005)[3]	$2.1(\pm0.1)\times10^9$	De Laat et al. (1995)[4]		
	6.1×10^6	Larson and Zepp (1988)[5]	2.2×10^9	Azenha et al. (2003)[6]		
			$2.4(\pm0.3)\times10^9$	De Laat et al. (1994)[7]		
			$2.5(\pm0.2)\times10^9$	Balci et al. (2009)[8]		
			$2.6(\pm0.4)\times10^9$	Haag and Yao (1992)[9]		
			$2.7(\pm0.4)\times10^9$	Tace et al. (1992)[10]		
			3.0×10^9	Acero et al. (2000)[11]		
			3.0×10^9	Tauber and von Sonntag (2000)[12]		
Average[a]	**$4.4(\pm1.2)\times10^6$**		**$2.5(\pm0.4)\times10^9$**			
Cyanazine	N.A.		1.9×10^9	De Laat et al. (1995)[4]	N.A.[b]	
Average[a]			**1.9×10^9**			
Acetochlor	N.A.		$6.3(\pm0.5)\times10^9$	Acero et al. (2003)[13]	N.A.[b]	
			$7.5(\pm2.0)\times10^9$	Fulkerson-Brekken and Brezonik (1998)[14]		
Average[a]			**$6.9(\pm1.8)\times10^9$**			
Alachlor	N.A.		5.0×10^9	De Laat et al. (1996)[15]	N.A.[b]	
			7.0×10^9	Haag and Yao (1992)[9]		
Average[a]			**$6.0(\pm1.4)\times10^9$**			
Metolachlor	N.A.		5.1×10^9	De Laat et al. (1996)[15]	N.A.[b]	
			$6.7(\pm0.4)\times10^9$	Acero et al. (2003)[13]		
			$9.1(\pm0.2)\times10^9$	Wu et al. (2007)[16]		
			$6.1(\pm0.6)\times10^9$	Huntscha et al. (2008)[17]		
Average[a]			**$7.0(\pm1.6)\times10^9$**			
Mesotrione	N.A.		8.2×10^9	Murati et al. (2011)[18]	$6.7(\pm0.3)\times10^5$	ter Halle and Richard (2006)[19]
			$8.8(\pm0.2)\times10^9$	Bensalah et al. (2011)[20]		
Average[a]			**$8.6(\pm0.4)\times10^9$**		**$6.7(\pm0.3)\times10^5$**	

(Continued on next page)

Compound	$k_{CO_3^{\bullet-}}$ (M^{-1} s^{-1})	Reference	$k_{^{\bullet}OH}$ (M^{-1} s^{-1})	Reference	$k_{^1O_2}$ (M^{-1} s^{-1})	Reference
Diuron	5.0×10^{6}	Djebbar et al. (2003)[1]	4.6×10^{9}	De Laat et al. (1996)[2]	N.A.[b]	
	$8.3(\pm2.4)\times10^{6}$	Canonica et al. (2005)[3]	$6.6(\pm0.1)\times10^{9}$	Benitez et al. (2007)[4]		
			7.1×10^{9}	Benitez et al. (2007)[5]		
			$7.5(\pm0.2)\times10^{9}$	Shemer et al. (2006)[6]		
			$9.3(\pm0.2)\times10^{9}$	Shemer et al. (2006)[6]		
			$9.9(\pm0.2)\times10^{9}$	Shemer et al. (2006)[6]		
Average[a]	**$7.2(\pm3.1)\times10^{6}$**		**$7.8(\pm1.7)\times10^{9}$**			
Isoproturon	2.5×10^{7}	Canonica et al. (2005)[3]	5.2×10^{9}	De Laat et al. (1996)[2]	N.A.[b]	
	$2.6(\pm0.6)\times10^{7}$	Canonica et al. (2005)[3]	5.7×10^{9}	Benitez et al. (2007)[5]		
	$3.0(\pm0.4)\times10^{7}$	Canonica et al. (2005)[3]	$7.9(\pm0.1)\times10^{9}$	Benitez et al. (2007)[4]		
Average[a]	**$2.7(\pm0.6)\times10^{7}$**		**$6.7(\pm1.4)\times10^{9}$**			
Metoxuron	$8.1(\pm0.6)\times10^{7}$	Canonica et al. (2005)[3]	N.A.[b]		N.A.[b]	
	$11.0(\pm5.0)\times10^{7}$	Canonica et al. (2005)[3]				
Average[a]	**$9.6(\pm4.4)\times10^{7}$**					
Bentazon	N.A.[b]		2.9×10^{9}	Beltran-Heredia et al. (1996)[7]	N.A.[b]	
			$8.4(\pm0.3)\times10^{9}$	Al Housari et al. (2011)[8]		
Average[a]			**$5.7(\pm2.6)\times10^{9}$**			
Clopyralid	N.A.[b]		$4.4(\pm0.2)\times10^{9}$	Özcan et al. (2010)[9]	N.A.[b]	
Average[a]			**$4.4(\pm0.2)\times10^{9}$**			
Chlorpyrifos	$8.8(\pm0.4)\times10^{6}$	Wu and Linden (2010)[10]	4.2×10^{9}	Armbrust (2000)[11]	N.A.[b]	
			$4.9(\pm0.1)\times10^{9}$	Wu and Linden (2010)[10]		
Average[a]	**$8.8(\pm0.4)\times10^{6}$**		**$4.7(\pm0.4)\times10^{9}$**			
Propiconazole	N.A.[b]		N.A.[b]		N.A.[b]	
Ethalfluralin	N.A.[b]		N.A.[b]		N.A.[b]	
Pendimethalin	N.A.[b]		N.A.[b]		N.A.[b]	
Trifluralin	N.A.[b]		$7.1(\pm0.7)\times10^{9}$	Chelme-Ayala (2011)[12]	N.A.[b]	
			$7.5(\pm0.2)\times10^{9}$	Chelme-Ayala (2010)[13]		
Average[a]			**$7.3(\pm0.6)\times10^{9}$**			

[a] Calculated as the average value of reported constants with the standard deviation given in parentheses. [b] N.A. = not available.

C.12 Second-order reaction rate constants of quenchers with PPRIs

Table C.8 Second-order reaction rate constants of quenchers with carbonate radical, hydroxyl radical, and singlet oxygen

Compound	$k_{CO_3^{\bullet-}}$ (M^{-1} s^{-1})	Reference	$k_{^{\bullet}OH}$ (M^{-1} s^{-1})	Reference	$k_{^1O_2}$ (M^{-1} s^{-1})	Reference
DMA	1.8×10^{9}	Chen et al. (1975)[1]	No quenching effect	Huang and Mabury (2000)[2]	No quenching effect	Foote et al. (1970)[3]
	$1.8(\pm0.3)\times10^{9}$	Canonica et al. (2005)[4]			No quenching effect	Huang and Mabury (2000)[2]
IPA	$4.6(\pm0.1)\times10^{4}$	Clifton and Huie (1993)[5]	1.7×10^{9}	Thomas (1965)[6]	No quenching effect	Darmanyan and Foote (1993)[7]
			2.2×10^{9}	Anbar and Neta (1965)[8]		
			1.8×10^{9}	Willson et al. (1971)[9]		
			$1.9(\pm0.1)\times10^{9}$	Wolfenden and Willson (1982)[10]		
			$2.3(\pm0.1)\times10^{9}$	Elliot and Simsons (1984)[11]		
			1.9×10^{9}	Buxton et al. (1988)[12]		
			1.6×10^{9}	Motohashi and Saito (1993)[13]		
			$1.9(\pm0.2)\times10^{9}$	Monod et al. (2005)[14]		
HIS	8.5×10^{6}	Chen and Morton (1975)[15]	5.0×10^{9}	Rao et al. (1975)[16]	1.0×10^{8}	Matheson and Lee (1979)[17]
					$4.0(\pm1.0)\times10^{7}$	Egorov et al. (1997)[18]
					$5.0(\pm0.1)\times10^{7}$	Bisby et al. (1999)[19]
					$8.9(\pm0.5)\times10^{7}$	Boreen et al. (2008)[20]
DABCO	1.7×10^{7}	Elango et al. (1985)[21]	1.2×10^{9}	Anderson and Patel (1978)[22]	1.2×10^{7}	Ogryzlo and Tang (1970)[23]
			6.5×10^{9}	Packer et al. (1980)[24]	1.6×10^{7}	Foote et al. (1970)[3]
HDA	No quenching effect	Grebel et al. (2011)[25]	No quenching effect	Velosa et al. (2007)	$1.0\text{-}2.4\times10^{5}$	Monroe (1981)[26]
					No quenching effect	Velosa et al. (2007)

C.13 Pesticide photolysis in P8-Sep-2010 water under natural sunlight

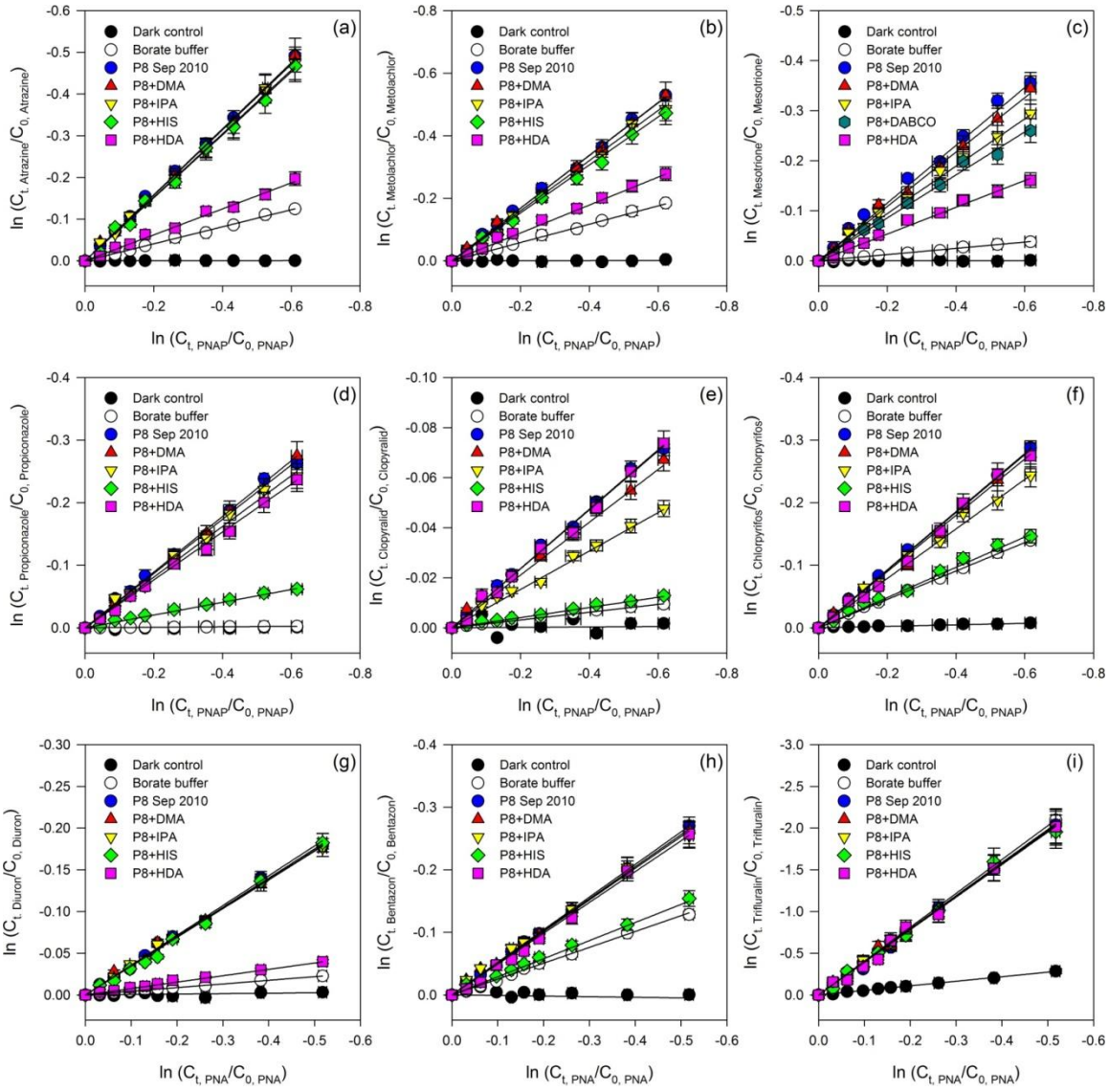

Figure C.9 Logarithmic plots for pesticide photodegradation in borate buffer and native and modified P8-Sep-2010 water under natural sunlight: (a) atrazine; (b) metolachlor; (c) mesotrione; (d) propiconazole; (e) clopyralid; (f) chlorpyrifos; (g) diuron; (h) bentazon; (i) trifluralin. Error bars represent one standard deviation of duplicate samples; where absent, bars fall within symbols. Solid lines represent linear regressions and $R^2 > 0.98$ in all cases. Note differences in *x*-axis.

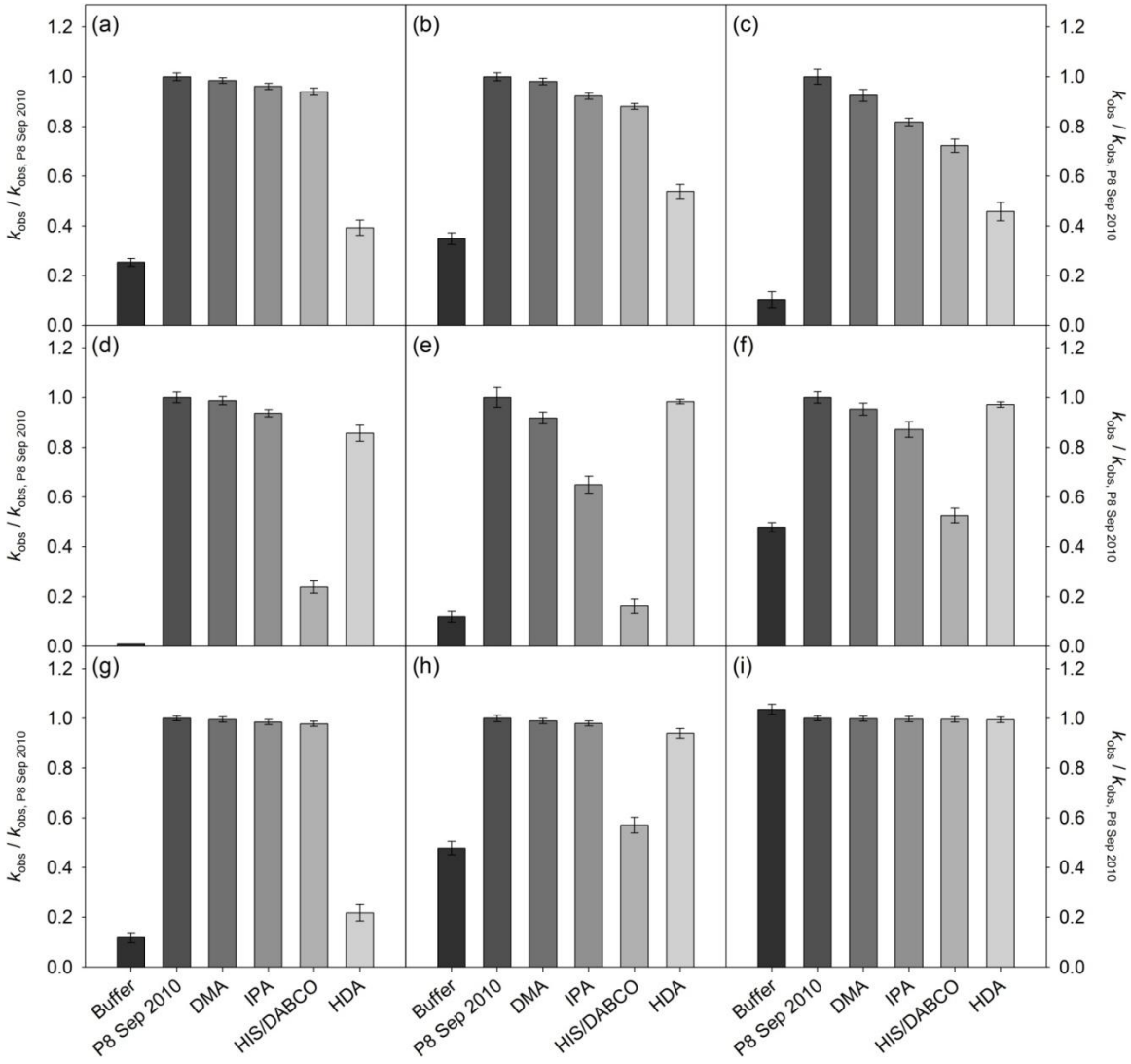

Figure C.10 Relative rates of pesticide photodegradation in borate buffer and native and modified P8-Sep-2010 water under natural sunlight: (a) atrazine; (b) metolachlor; (c) mesotrione; (d) propiconazole; (e) clopyralid; (f) chlorpyrifos; (g) diuron; (h) bentazon; (i) trifluralin. Error bars represent one standard deviation of duplicate samples.

Table C.9 Pseudo-first-order rate constants of pesticide photodegradation in P8-Sep-2010 water under natural sunlight

Compound	$k_{obs,\ P8\ Sep}$ (s^{-1})[a]	$k_{obs,\ Buffer}$ (s^{-1})[b]	$k_{obs,\ DMA}$ (s^{-1})[c]	$k_{obs,\ IPA}$ (s^{-1})[d]	$k_{obs,\ HIS}$ (s^{-1})[e]	$k_{obs,\ DABCO}$ (s^{-1})[f]	$k_{obs,\ HDA}$ (s^{-1})[g]
Atrazine	$2.52(\pm0.09)\times10^{-6}$	$6.40(\pm0.04)\times10^{-7}$	$2.48(\pm0.06)\times10^{-6}$	$2.42(\pm0.08)\times10^{-6}$	$2.37(\pm0.08)\times10^{-6}$	N.A.[h]	$9.90(\pm0.15)\times10^{-7}$
Metolachlor	$2.67(\pm0.10)\times10^{-6}$	$9.34(\pm0.33)\times10^{-7}$	$2.62(\pm0.05)\times10^{-6}$	$2.47(\pm0.07)\times10^{-6}$	$2.36(\pm0.08)\times10^{-6}$	N.A.[h]	$1.44(\pm0.05)\times10^{-6}$
Mesotrione	$1.87(\pm0.08)\times10^{-6}$	$1.95(\pm0.09)\times10^{-7}$	$1.73(\pm0.07)\times10^{-6}$	$1.53(\pm0.06)\times10^{-6}$	N.A.[h]	$1.35(\pm0.05)\times10^{-6}$	$8.57(\pm0.12)\times10^{-7}$
Diuron	$1.28(\pm0.05)\times10^{-5}$	$1.51(\pm0.10)\times10^{-6}$	$1.27(\pm0.05)\times10^{-5}$	$1.26(\pm0.06)\times10^{-5}$	$1.25(\pm0.05)\times10^{-5}$	N.A.[h]	$2.79(\pm0.07)\times10^{-6}$
Bentazon	$1.90(\pm0.07)\times10^{-5}$	$9.07(\pm0.21)\times10^{-6}$	$1.88(\pm0.07)\times10^{-5}$	$1.86(\pm0.05)\times10^{-5}$	$1.08(\pm0.05)\times10^{-5}$	N.A.[h]	$1.78(\pm0.06)\times10^{-5}$
Clopyralid	$3.68(\pm0.10)\times10^{-7}$	$4.35(\pm0.08)\times10^{-8}$	$3.38(\pm0.10)\times10^{-7}$	$2.39(\pm0.09)\times10^{-7}$	$5.94(\pm0.12)\times10^{-8}$	N.A.[h]	$3.62(\pm0.09)\times10^{-7}$
Chlorpyrifos	$1.42(\pm0.06)\times10^{-6}$	$6.80(\pm0.16)\times10^{-7}$	$1.35(\pm0.07)\times10^{-6}$	$1.24(\pm0.06)\times10^{-6}$	$7.46(\pm0.18)\times10^{-7}$	N.A.[h]	$1.38(\pm0.08)\times10^{-6}$
Propiconazole	$1.39(\pm0.07)\times10^{-6}$	$1.16(\pm0.08)\times10^{-8}$	$1.37(\pm0.05)\times10^{-6}$	$1.30(\pm0.05)\times10^{-6}$	$3.31(\pm0.08)\times10^{-7}$	N.A.[h]	$1.19(\pm0.05)\times10^{-6}$
Trifluralin	$1.23(\pm0.05)\times10^{-4}$	$1.28(\pm0.05)\times10^{-4}$	$1.23(\pm0.06)\times10^{-4}$	$1.23(\pm0.06)\times10^{-4}$	$1.23(\pm0.06)\times10^{-4}$	N.A.[h]	$1.23(\pm0.07)\times10^{-4}$

[a] Observed pseudo-first-order rate constants for pesticide photolysis in native P8-Sep-2010 water. [b] Observed pseudo-first-order rate constants for pesticide photolysis in borate buffer. [c] Observed pseudo-first-order rate constants for pesticide photolysis in P8-Sep-2010 water with 120 μM DMA. [d] Observed pseudo-first-order rate constants for pesticide photolysis in P8-Sep-2010 water with 26 mM IPA. [e] Observed pseudo-first-order rate constants for pesticide photolysis in P8-Sep-2010 water with 20 mM HIS. [f] Observed pseudo-first-order rate constants for pesticide photolysis in P8-Sep-2010 water with 10 mM DABCO. [g] Observed pseudo-first-order rate constants for pesticide photolysis in P8-Sep-2010 water with 10 mM HDA. [h] N.A. = not available. Errors represent one standard deviation from duplicate experiments.

Table C.10 Contribution of direct and indirect photolysis in P8-Sep-2010 water under natural sunlight

Compound	$k_{calc,\ Direct}$ (s^{-1})[a]	$k_{calc,\ CO_3^{\bullet-}}$ (s^{-1})[b]	$k_{calc,\ {}^{\bullet}OH}$ (s^{-1})[c]	$k_{calc,\ {}^1O_2}$ (s^{-1})[d]	$k_{calc,\ {}^3DOM^*}$ (s^{-1})[e]	k_{Other} (s^{-1})[f]	$k_{pred,\ CO_3^{\bullet-}}$ (s^{-1})[g]	$k_{pred,\ {}^{\bullet}OH}$ (s^{-1})[h]	$k_{pred,\ {}^1O_2}$ (s^{-1})[i]
Atrazine	$6.18(\pm0.04)\times10^{-7}$	$3.73(\pm0.51)\times10^{-8}$	$5.98(\pm0.93)\times10^{-8}$	$5.41(\pm0.84)\times10^{-8}$	$1.53(\pm0.07)\times10^{-6}$	$2.21(\pm0.07)\times10^{-7}$	$3.38(\pm1.62)\times10^{-8}$	$5.66(\pm1.49)\times10^{-8}$	N.A.[j]
Metolachlor	$9.02(\pm0.61)\times10^{-7}$	$5.00(\pm0.63)\times10^{-8}$	$1.57(\pm0.21)\times10^{-7}$	$1.11(\pm0.15)\times10^{-7}$	$1.23(\pm0.08)\times10^{-6}$	$2.22(\pm0.73)\times10^{-7}$	N.A.[j]	$1.55(\pm0.58)\times10^{-7}$	N.A.[j]
Mesotrione	$1.88(\pm0.08)\times10^{-7}$	$1.40(\pm0.67)\times10^{-7}$	$1.99(\pm0.74)\times10^{-7}$	$1.78(\pm0.66)\times10^{-7}$	$1.01(\pm0.10)\times10^{-6}$	$1.51(\pm0.82)\times10^{-7}$	N.A.[j]	$1.95(\pm0.18)\times10^{-7}$	$1.75(\pm0.25)\times10^{-7}$
Diuron	$1.46(\pm0.10)\times10^{-6}$	$5.83(\pm2.38)\times10^{-8}$	$1.36(\pm0.29)\times10^{-7}$	$9.22(\pm0.20)\times10^{-8}$	$1.00(\pm0.02)\times10^{-5}$	$1.04(\pm0.10)\times10^{-6}$	$5.00(\pm3.13)\times10^{-8}$	$1.72(\pm0.65)\times10^{-7}$	N.A.[j]
Bentazon	$8.76(\pm0.50)\times10^{-6}$	$2.04(\pm0.90)\times10^{-7}$	$1.88(\pm0.40)\times10^{-7}$	$7.75(\pm0.16)\times10^{-6}$	$1.14(\pm0.11)\times10^{-6}$	$9.21(\pm5.33)\times10^{-7}$	N.A.[j]	$1.92(\pm0.17)\times10^{-7}$	N.A.[j]
Clopyralid	$4.20(\pm0.33)\times10^{-8}$	$3.03(\pm0.57)\times10^{-8}$	$9.88(\pm0.37)\times10^{-8}$	$1.79(\pm0.67)\times10^{-7}$	$6.13(\pm4.82)\times10^{-9}$	$1.13(\pm0.84)\times10^{-8}$	N.A.[j]	$1.13(\pm0.84)\times10^{-8}$	N.A.[j]
Chlorpyrifos	$6.56(\pm0.26)\times10^{-7}$	$6.63(\pm0.59)\times10^{-8}$	$1.16(\pm0.43)\times10^{-7}$	$4.91(\pm0.18)\times10^{-7}$	$4.07(\pm0.50)\times10^{-8}$	$4.92(\pm0.39)\times10^{-8}$	$6.38(\pm0.98)\times10^{-8}$	$1.05(\pm0.25)\times10^{-7}$	N.A.[j]
Propiconazole	$1.12(\pm0.01)\times10^{-8}$	$1.79(\pm0.21)\times10^{-8}$	$6.97(\pm0.26)\times10^{-8}$	$9.69(\pm0.36)\times10^{-7}$	$1.99(\pm0.28)\times10^{-7}$	$1.21(\pm0.05)\times10^{-7}$	N.A.[j]	N.A.[j]	N.A.[j]
Trifluralin	$1.23(\pm0.05)\times10^{-4}$	N.A.[j]	N.A.[j]	N.A.[j]	N.A.[j]	N.A.[j]	N.A.[j]	$1.67(\pm0.12)\times10^{-7}$	N.A.[j]

[a] Calculated as $k_{obs,\ Buffer} \times S_{\sum\lambda 290\text{-}800nm}$, where $k_{obs,\ Buffer}$ is from Table C.9 and $S_{\sum\lambda 290\text{-}800nm}$ is the light screening factor from Table 4.1. [b] Calculated from Eqn (4.11) in the main text. [c] Calculated from Eqn (4.12) in the main text. [d] Calculated from Eqn (4.13) in the main text. [e] Calculated from Eqn (4.14) in the main text. [f] Calculated as $k_{obs,\ P8\ Sep} - k_{calc,\ Direct} - k_{calc,\ CO_3^{\bullet-}} - k_{calc,\ {}^{\bullet}OH} - k_{calc,\ {}^1O_2} - k_{calc,\ {}^3DOM^*}$, where $k_{obs,\ P8\ Sep}$ is from Table C.9. [g] Calculated as $k_{CO_3^{\bullet-}} \times [CO_3^{\bullet-}]_{ss}$, where $k_{CO_3^{\bullet-}}$ is from Table C.7 and $[CO_3^{\bullet-}]_{ss}$ is from Table 4.2. [h] Calculated as $k_{{}^{\bullet}OH} \times [{}^{\bullet}OH]_{ss}$, where $k_{{}^{\bullet}OH}$ is from Table C.7and $[{}^{\bullet}OH]_{ss}$ is from Table 4.2. [i] Calculated as $k_{{}^1O_2} \times [{}^1O_2]_{ss}$, where $k_{{}^1O_2}$ is from Table C.7 and $[{}^1O_2]_{ss}$ is from Table 4.2. [j] N.A. = not available. Errors were propagated through observed rate constants and PPRI concentrations.

C.14 Pesticide photolysis in P1-Apr-2012 water under natural sunlight

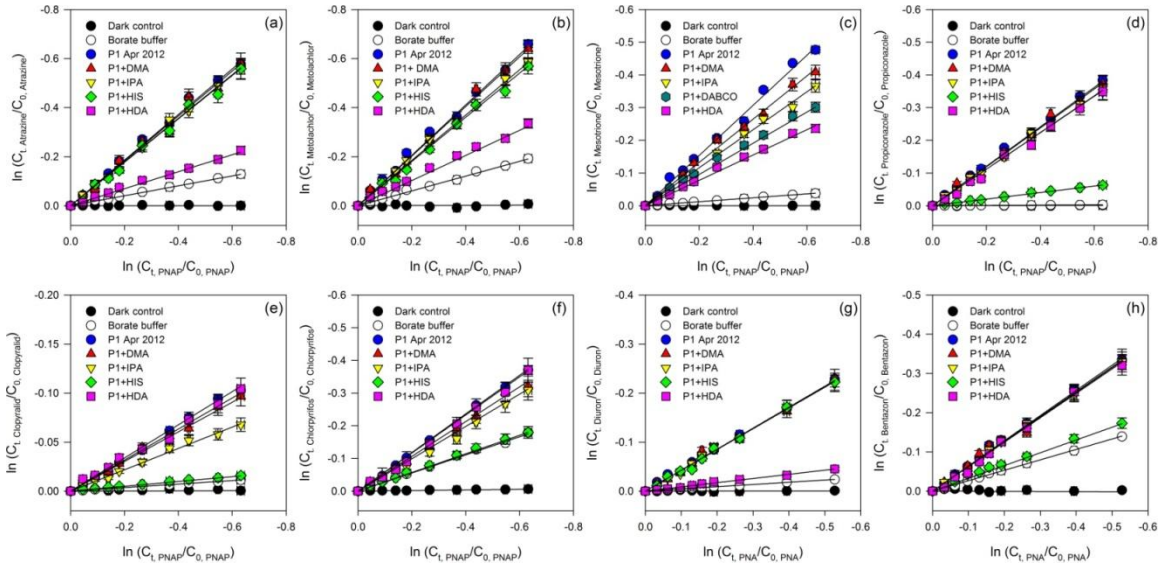

Figure C.11 Logarithmic plots for pesticide photodegradation in borate buffer and native and modified P1-Apr-2012 water under natural sunlight: (a) atrazine; (b) metolachlor; (c) mesotrione; (d) propiconazole; (e) clopyralid; (f) chlorpyrifos; (g) diuron; (h) bentazon. Error bars represent one standard deviation of duplicate samples; where absent, bars fall within symbols. Solid lines represent linear regressions and $R^2 > 0.98$ in all cases. Note differences in *x*-axis.

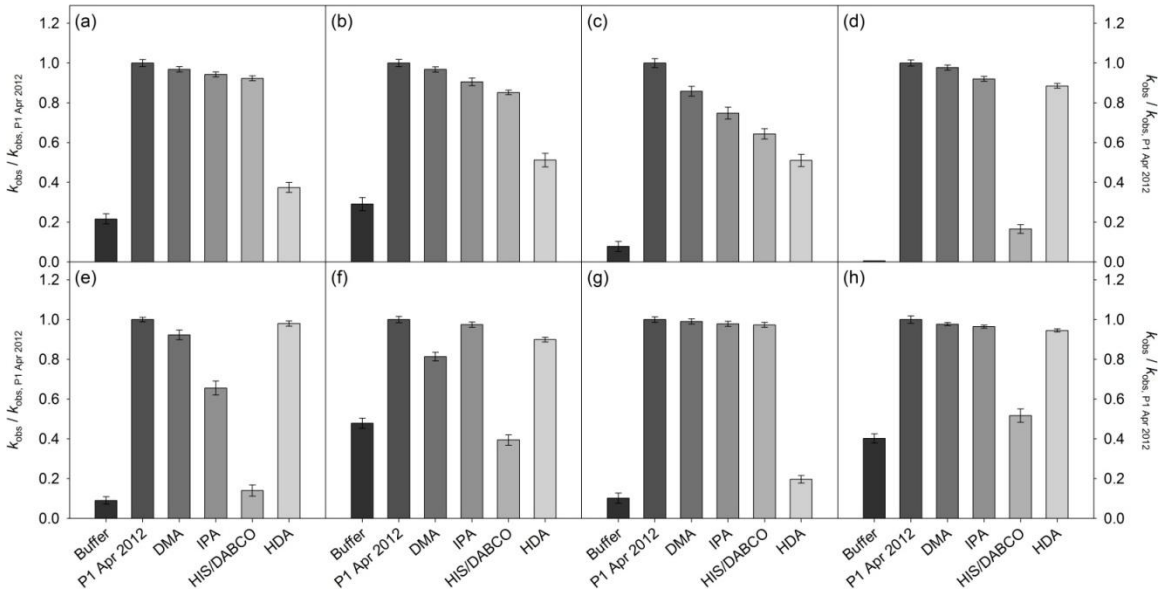

Figure C.12 Relative rates of pesticide photodegradation in borate buffer and native and modified P1-Apr-2012 water under natural sunlight: (a) atrazine; (b) metolachlor; (c) mesotrione; (d) propiconazole; (e) clopyralid; (f) chlorpyrifos; (g) diuron; (h) bentazon. Error bars represent one standard deviation of duplicate samples.

Table C.11 Pseudo-first-order rate constants of pesticide photodegradation in P1-Apr-2012 water under natural sunlight

Compound	$k_{obs,\ P1\ Apr}$ (s^{-1})[a]	$k_{obs,\ Buffer}$ (s^{-1})[b]	$k_{obs,\ DMA}$ (s^{-1})[c]	$k_{obs,\ IPA}$ (s^{-1})[d]	$k_{obs,\ HIS}$ (s^{-1})[e]	$k_{obs,\ DABCO}$ (s^{-1})[f]	$k_{obs,\ HDA}$ (s^{-1})[g]
Atrazine	$2.98(\pm0.06)\times10^{-6}$	$6.44(\pm0.15)\times10^{-7}$	$2.89(\pm0.09)\times10^{-6}$	$2.81(\pm0.08)\times10^{-6}$	$2.75(\pm0.06)\times10^{-6}$	N.A.[h]	$1.12(\pm0.08)\times10^{-6}$
Metolachlor	$3.29(\pm0.06)\times10^{-6}$	$9.56(\pm0.21)\times10^{-7}$	$3.18(\pm0.06)\times10^{-6}$	$2.98(\pm0.07)\times10^{-6}$	$2.80(\pm0.08)\times10^{-6}$	N.A.[h]	$1.68(\pm0.07)\times10^{-6}$
Mesotrione	$2.44(\pm0.07)\times10^{-6}$	$1.89(\pm0.08)\times10^{-7}$	$2.09(\pm0.06)\times10^{-6}$	$1.82(\pm0.05)\times10^{-6}$	N.A.[h]	$1.57(\pm0.02)\times10^{-6}$	$1.24(\pm0.06)\times10^{-6}$
Diuron	$1.59(\pm0.06)\times10^{-5}$	$1.62(\pm0.05)\times10^{-6}$	$1.58(\pm0.08)\times10^{-5}$	$1.56(\pm0.08)\times10^{-5}$	$1.55(\pm0.08)\times10^{-5}$	N.A.[h]	$3.13(\pm0.09)\times10^{-6}$
Bentazon	$2.37(\pm0.07)\times10^{-5}$	$9.54(\pm0.14)\times10^{-6}$	$2.32(\pm0.06)\times10^{-5}$	$2.29(\pm0.06)\times10^{-5}$	$1.23(\pm0.06)\times10^{-5}$	N.A.[h]	$2.24(\pm0.08)\times10^{-5}$
Clopyralid	$5.16(\pm0.06)\times10^{-7}$	$4.67(\pm0.09)\times10^{-8}$	$4.77(\pm0.07)\times10^{-7}$	$3.39(\pm0.05)\times10^{-7}$	$7.24(\pm0.10)\times10^{-8}$	N.A.[h]	$5.06(\pm0.09)\times10^{-7}$
Chlorpyrifos	$1.80(\pm0.06)\times10^{-6}$	$8.64(\pm0.11)\times10^{-7}$	$1.62(\pm0.08)\times10^{-6}$	$1.47(\pm0.07)\times10^{-6}$	$8.92(\pm0.12)\times10^{-7}$	N.A.[h]	$1.76(\pm0.07)\times10^{-6}$
Propiconazole	$1.94(\pm0.05)\times10^{-6}$	$1.05(\pm0.05)\times10^{-8}$	$1.89(\pm0.05)\times10^{-6}$	$1.78(\pm0.08)\times10^{-6}$	$3.20(\pm0.09)\times10^{-7}$	N.A.[h]	$1.71(\pm0.06)\times10^{-6}$

[a] Observed pseudo-first-order rate constants for pesticide photolysis in native P1-Apr-2012 water. [b] Observed pseudo-first-order rate constants for pesticide photolysis in borate buffer. [c] Observed pseudo-first-order rate constants for pesticide photolysis in P1-Apr-2012 water with 120 μM DMA. [d] Observed pseudo-first-order rate constants for pesticide photolysis in P1-Apr-2012 water with 26 mM IPA. [e] Observed pseudo-first-order rate constants for pesticide photolysis in P1-Apr-2012 water with 20 mM HIS. [f] Observed pseudo-first-order rate constants for pesticide photolysis in P1-Apr-2012 water with 10 mM DABCO. [g] Observed pseudo-first-order rate constants for pesticide photolysis in P1-Apr-2012 water with 10 mM HDA. [h] N.A. = not available. Errors represent one standard deviation from duplicate experiments.

Table C.12 Contribution of direct and indirect photolysis in P1-Apr-2012 water under natural sunlight

Compound	$k_{calc,\ Direct}$ (s^{-1})[a]	$k_{calc,\ CO_3^{\bullet-}}$ (s^{-1})[b]	$k_{calc,\ ^{\bullet}OH}$ (s^{-1})[c]	$k_{calc,\ ^1O_2}$ (s^{-1})[d]	$k_{calc,\ ^3DOM^*}$ (s^{-1})[e]	k_{Other} (s^{-1})[f]	$k_{pred,\ CO_3^{\bullet-}}$ (s^{-1})[g]	$k_{pred,\ ^{\bullet}OH}$ (s^{-1})[h]	$k_{pred,\ ^1O_2}$ (s^{-1})[i]
Atrazine	$6.26(\pm0.25)\times10^{-7}$	$9.42(\pm2.07)\times10^{-8}$	$7.57(\pm0.10)\times10^{-8}$	$5.85(\pm0.79)\times10^{-8}$	$1.86(\pm0.04)\times10^{-6}$	$2.62(\pm0.45)\times10^{-7}$	$8.76(\pm3.66)\times10^{-8}$	$7.56(\pm1.92)\times10^{-8}$	N.A.[j]
Metolachlor	$9.28(\pm0.11)\times10^{-7}$	$1.05(\pm0.16)\times10^{-7}$	$2.07(\pm0.28)\times10^{-7}$	$1.73(\pm0.23)\times10^{-7}$	$1.60(\pm0.04)\times10^{-6}$	$2.70(\pm0.14)\times10^{-7}$	N.A.[j]	$2.07(\pm0.76)\times10^{-7}$	N.A.[j]
Mesotrione	$1.84(\pm0.07)\times10^{-7}$	$3.46(\pm0.17)\times10^{-7}$	$2.68(\pm0.36)\times10^{-7}$	$2.55(\pm0.34)\times10^{-7}$	$1.19(\pm0.06)\times10^{-6}$	$1.93(\pm0.38)\times10^{-7}$	N.A.[j]	$2.60(\pm0.21)\times10^{-7}$	$2.38(\pm0.29)\times10^{-7}$
Diuron	$1.58(\pm0.05)\times10^{-6}$	$1.49(\pm0.21)\times10^{-7}$	$1.93(\pm0.31)\times10^{-7}$	$8.25(\pm1.33)\times10^{-8}$	$1.28(\pm0.03)\times10^{-5}$	$1.13(\pm0.09)\times10^{-6}$	$1.27(\pm0.65)\times10^{-7}$	$2.30(\pm0.85)\times10^{-7}$	N.A.[j]
Bentazon	$9.26(\pm0.13)\times10^{-6}$	$5.46(\pm4.04)\times10^{-7}$	$2.89(\pm0.47)\times10^{-7}$	$1.06(\pm0.17)\times10^{-5}$	$1.30(\pm0.41)\times10^{-6}$	$1.70(\pm0.73)\times10^{-6}$	N.A.[j]	$2.57(\pm0.21)\times10^{-7}$	N.A.[j]
Clopyralid	$4.54(\pm0.19)\times10^{-8}$	$3.97(\pm0.35)\times10^{-8}$	$1.38(\pm0.19)\times10^{-7}$	$2.66(\pm0.36)\times10^{-7}$	$1.02(\pm0.39)\times10^{-8}$	$1.68(\pm1.66)\times10^{-8}$	N.A.[j]	$1.35(\pm0.11)\times10^{-7}$	N.A.[j]
Chlorpyrifos	$8.39(\pm0.11)\times10^{-7}$	$1.82(\pm0.66)\times10^{-7}$	$1.53(\pm0.21)\times10^{-7}$	$5.77(\pm0.78)\times10^{-7}$	$4.58(\pm0.48)\times10^{-8}$	$7.83(\pm5.38)\times10^{-9}$	$1.67(\pm0.15)\times10^{-8}$	$1.40(\pm0.33)\times10^{-7}$	N.A.[j]
Propiconazole	$1.02(\pm0.02)\times10^{-8}$	$4.38(\pm0.51)\times10^{-8}$	$1.10(\pm0.15)\times10^{-7}$	$1.46(\pm0.02)\times10^{-6}$	$2.22(\pm0.75)\times10^{-7}$	$8.79(\pm0.46)\times10^{-8}$	N.A.[j]	N.A.[j]	N.A.[j]

[a] Calculated as $k_{obs,\ Buffer} \times S_{\sum\lambda 290\text{-}800nm}$, where $k_{obs,\ Buffer}$ is from Table C.11 and $S_{\sum\lambda 290\text{-}800nm}$ is the light screening factor from Table 4.1. [b] Calculated from Eqn (4.11) in the main text. [c] Calculated from Eqn (4.12) in the main text. [d] Calculated from Eqn (4.13) in the main text. [e] Calculated from Eqn (4.14) in the main text. [f] Calculated as $k_{obs,\ P8\ Sep} - k_{calc,\ Direct} - k_{calc,\ CO_3^{\bullet-}} - k_{calc,\ ^{\bullet}OH} - k_{calc,\ ^1O_2} - k_{calc,\ ^3DOM^*}$, where $k_{obs,\ P8\ Sep}$ is from Table C.11. [g] Calculated as $k_{CO_3^{\bullet-}} \times [CO_3^{\bullet-}]_{ss}$, where $k_{CO_3^{\bullet-}}$ is from Table C.7 and $[CO_3^{\bullet-}]_{ss}$ is from Table 4.2. [h] Calculated as $k_{^{\bullet}OH} \times [^{\bullet}OH]_{ss}$, where $k_{^{\bullet}OH}$ is from Table C.7 and $[^{\bullet}OH]_{ss}$ is from Table 4.2. [i] Calculated as $k_{^1O_2} \times [^1O_2]_{ss}$, where $k_{^1O_2}$ is from Table C.7 and $[^1O_2]_{ss}$ is from Table 4.2. [j] N.A. = not available. Errors were propagated through observed rate constants and PPRI concentrations.

C.15 Pesticide photolysis in P8-Apr-2012 water under natural sunlight

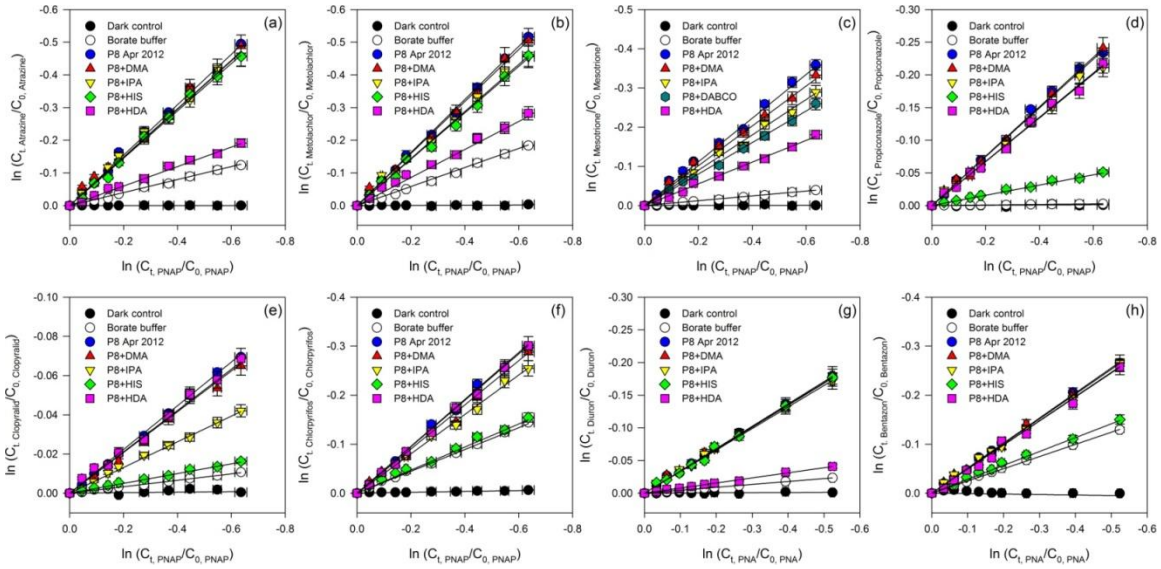

Figure C.13 Logarithmic plots for pesticide photodegradation in borate buffer and native and modified P8-Apr-2012 water under natural sunlight: (a) atrazine; (b) metolachlor; (c) mesotrione; (d) propiconazole; (e) clopyralid; (f) chlorpyrifos; (g) diuron; (h) bentazon. Error bars represent one standard deviation of duplicate samples; where absent, bars fall within symbols. Solid lines represent linear regressions and $R^2 > 0.98$ in all cases. Note differences in *x*-axis.

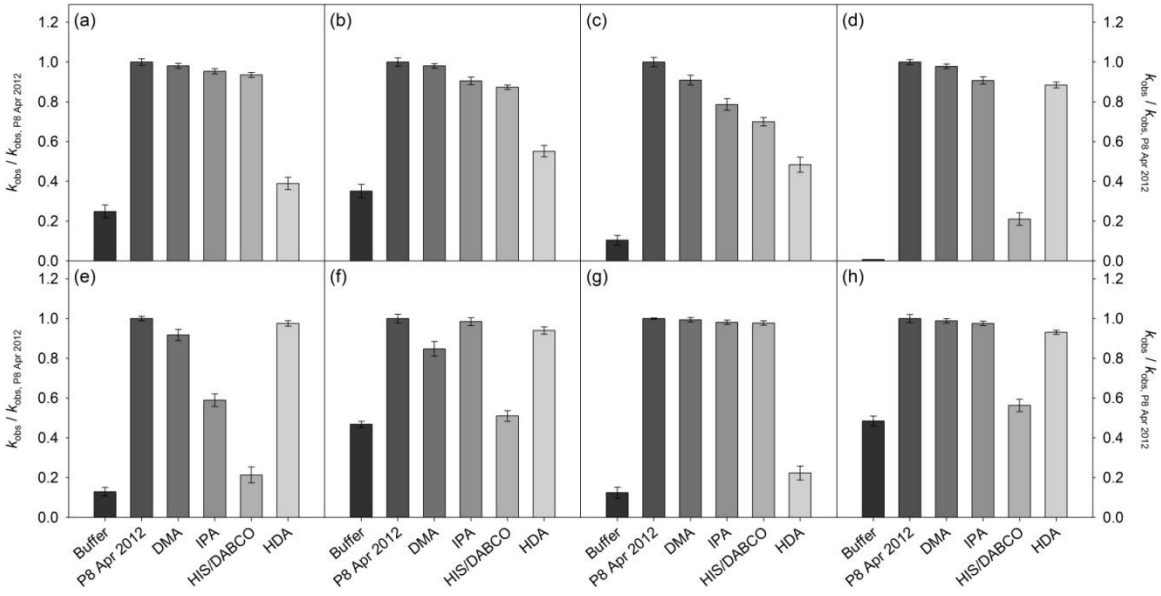

Figure C.14 Relative rates of pesticide photodegradation in borate buffer and native and modified P8-Apr-2012 water under natural sunlight: (a) atrazine; (b) metolachlor; (c) mesotrione; (d) propiconazole; (e) clopyralid; (f) chlorpyrifos; (g) diuron; (h) bentazon. Error bars represent one standard deviation of duplicate samples.

Table C.13 Pseudo-first-order rate constants of pesticide photodegradation in P8-Apr-2012 water under natural sunlight

Compound	$k_{obs,\ P8\ Apr}$ (s^{-1})[a]	$k_{obs,\ Buffer}$ (s^{-1})[b]	$k_{obs,\ DMA}$ (s^{-1})[c]	$k_{obs,\ IPA}$ (s^{-1})[d]	$k_{obs,\ HIS}$ (s^{-1})[e]	$k_{obs,\ DABCO}$ (s^{-1})[f]	$k_{obs,\ HDA}$ (s^{-1})[g]
Atrazine	$2.47(\pm0.08)\times10^{-6}$	$6.14(\pm0.17)\times10^{-7}$	$2.42(\pm0.08)\times10^{-6}$	$2.35(\pm0.09)\times10^{-6}$	$2.31(\pm0.09)\times10^{-6}$	N.A.[h]	$9.61(\pm0.38)\times10^{-7}$
Metolachlor	$2.55(\pm0.06)\times10^{-6}$	$8.93(\pm0.29)\times10^{-7}$	$2.50(\pm0.09)\times10^{-6}$	$2.31(\pm0.09)\times10^{-6}$	$2.22(\pm0.09)\times10^{-6}$	N.A.[h]	$1.41(\pm0.06)\times10^{-6}$
Mesotrione	$1.79(\pm0.07)\times10^{-6}$	$1.87(\pm0.09)\times10^{-7}$	$1.63(\pm0.06)\times10^{-6}$	$1.41(\pm0.06)\times10^{-6}$	N.A.[h]	$1.26(\pm0.05)\times10^{-6}$	$8.68(\pm0.24)\times10^{-7}$
Diuron	$1.25(\pm0.08)\times10^{-5}$	$1.56(\pm0.06)\times10^{-6}$	$1.25(\pm0.07)\times10^{-5}$	$1.23(\pm0.05)\times10^{-5}$	$1.23(\pm0.06)\times10^{-5}$	N.A.[h]	$2.80(\pm0.06)\times10^{-6}$
Bentazon	$1.88(\pm0.08)\times10^{-5}$	$9.10(\pm0.23)\times10^{-6}$	$1.86(\pm0.08)\times10^{-5}$	$1.83(\pm0.06)\times10^{-5}$	$1.06(\pm0.05)\times10^{-5}$	N.A.[h]	$1.75(\pm0.05)\times10^{-5}$
Clopyralid	$3.40(\pm0.08)\times10^{-7}$	$4.40(\pm0.09)\times10^{-8}$	$3.12(\pm0.08)\times10^{-7}$	$2.00(\pm0.08)\times10^{-7}$	$7.26(\pm0.19)\times10^{-8}$	N.A.[h]	$3.32(\pm0.08)\times10^{-7}$
Chlorpyrifos	$1.46(\pm0.06)\times10^{-6}$	$6.84(\pm0.19)\times10^{-7}$	$1.37(\pm0.05)\times10^{-6}$	$1.24(\pm0.05)\times10^{-6}$	$7.46(\pm0.19)\times10^{-7}$	N.A.[h]	$1.44(\pm0.06)\times10^{-6}$
Propiconazole	$1.19(\pm0.05)\times10^{-6}$	$8.93(\pm0.15)\times10^{-9}$	$1.17(\pm0.06)\times10^{-6}$	$1.08(\pm0.06)\times10^{-6}$	$2.51(\pm0.07)\times10^{-7}$	N.A.[h]	$1.06(\pm0.05)\times10^{-6}$

[a] Observed pseudo-first-order rate constants for pesticide photolysis in native P8-Apr-2012 water. [b] Observed pseudo-first-order rate constants for pesticide photolysis in borate buffer. [c] Observed pseudo-first-order rate constants for pesticide photolysis in P8-Apr-2012 water with 120 μM DMA. [d] Observed pseudo-first-order rate constants for pesticide photolysis in P8-Apr-2012 water with 26 mM IPA. [e] Observed pseudo-first-order rate constants for pesticide photolysis in P8-Apr-2012 water with 20 mM HIS. [f] Observed pseudo-first-order rate constants for pesticide photolysis in P8-Apr-2012 water with 10 mM DABCO. [g] Observed pseudo-first-order rate constants for pesticide photolysis in P8-Apr-2012 water with 10 mM HDA. [h] N.A. = not available. Errors represent one standard deviation from duplicate experiments.

Table C.14 Contribution of direct and indirect photolysis in P8-Apr-2012 water under natural sunlight

Compound	$k_{calc,\ Direct}$ (s^{-1})[a]	$k_{calc,\ CO_3^{\bullet-}}$ (s^{-1})[b]	$k_{calc,\ {}^{\bullet}OH}$ (s^{-1})[c]	$k_{calc,\ {}^1O_2}$ (s^{-1})[d]	$k_{calc,\ {}^3DOM^*}$ (s^{-1})[e]	k_{Other} (s^{-1})[f]	$k_{pred,\ CO_3^{\bullet-}}$ (s^{-1})[g]	$k_{pred,\ {}^{\bullet}OH}$ (s^{-1})[h]	$k_{pred,\ {}^1O_2}$ (s^{-1})[i]
Atrazine	$5.96(\pm0.26)\times10^{-7}$	$4.66(\pm2.67)\times10^{-8}$	$6.69(\pm0.26)\times10^{-8}$	$4.62(\pm0.18)\times10^{-8}$	$1.50(\pm0.08)\times10^{-6}$	$2.05(\pm0.27)\times10^{-7}$	$4.38(\pm2.02)\times10^{-8}$	$6.46(\pm1.70)\times10^{-8}$	N.A.[j]
Metolachlor	$8.68(\pm0.28)\times10^{-7}$	$4.86(\pm0.62)\times10^{-8}$	$1.92(\pm0.76)\times10^{-7}$	$8.18(\pm0.32)\times10^{-8}$	$1.14(\pm0.10)\times10^{-6}$	$2.15(\pm0.15)\times10^{-7}$	N.A.[j]	$1.77(\pm0.66)\times10^{-7}$	N.A.[j]
Mesotrione	$1.82(\pm0.08)\times10^{-7}$	$1.63(\pm0.39)\times10^{-7}$	$2.20(\pm0.87)\times10^{-7}$	$1.56(\pm0.61)\times10^{-7}$	$9.26(\pm0.69)\times10^{-7}$	$1.48(\pm0.40)\times10^{-7}$	N.A.[j]	$2.22(\pm0.20)\times10^{-7}$	$1.49(\pm0.13)\times10^{-7}$
Diuron	$1.51(\pm0.11)\times10^{-6}$	$7.73(\pm1.05)\times10^{-8}$	$1.54(\pm0.17)\times10^{-7}$	$5.09(\pm0.57)\times10^{-7}$	$9.75(\pm0.31)\times10^{-6}$	$1.01(\pm0.13)\times10^{-6}$	$6.35(\pm3.51)\times10^{-8}$	$1.97(\pm0.75)\times10^{-7}$	N.A.[j]
Bentazon	$8.84(\pm0.22)\times10^{-6}$	$2.13(\pm1.80)\times10^{-7}$	$2.36(\pm0.26)\times10^{-7}$	$7.75(\pm0.87)\times10^{-6}$	$1.30(\pm0.19)\times10^{-6}$	$4.31(\pm4.21)\times10^{-7}$	N.A.[j]	$2.20(\pm0.20)\times10^{-7}$	N.A.[j]
Clopyralid	$4.27\pm(0.24)\times10^{-8}$	$2.81(\pm0.42)\times10^{-8}$	$1.12(\pm0.44)\times10^{-7}$	$1.28(\pm0.50)\times10^{-7}$	$8.16(\pm5.00)\times10^{-9}$	$2.17(\pm1.83)\times10^{-8}$	N.A.[j]	$1.15(\pm0.10)\times10^{-7}$	N.A.[j]
Chlorpyrifos	$6.65(\pm0.19)\times10^{-7}$	$8.71(\pm0.82)\times10^{-8}$	$1.35(\pm0.53)\times10^{-7}$	$4.94(\pm0.20)\times10^{-7}$	$2.20(\pm0.56)\times10^{-8}$	$5.90(\pm0.69)\times10^{-8}$	$8.29(\pm1.13)\times10^{-8}$	$1.20(\pm0.29)\times10^{-7}$	N.A.[j]
Propiconazole	$8.68(\pm0.02)\times10^{-9}$	$2.54(\pm1.49)\times10^{-8}$	$8.50(\pm0.33)\times10^{-8}$	$8.32(\pm0.33)\times10^{-7}$	$1.37(\pm0.10)\times10^{-7}$	$1.05(\pm0.43)\times10^{-7}$	N.A.[j]	N.A.[j]	N.A.[j]

[a] Calculated as $k_{obs,\ Buffer} \times S_{\sum\lambda 290\text{-}800nm}$, where $k_{obs,\ Buffer}$ is from Table C.13 and $S_{\sum\lambda 290\text{-}800nm}$ is the light screening factor from Table 4.1. [b] Calculated from Eqn (4.11) in the main text. [c] Calculated from Eqn (4.12) in the main text. [d] Calculated from Eqn (4.13) in the main text. [e] Calculated from Eqn (4.14) in the main text. [f] Calculated as $k_{obs,\ P8\ Sep} - k_{calc,\ Direct} - k_{calc,\ CO_3^{\bullet-}} - k_{calc,\ {}^{\bullet}OH} - k_{calc,\ {}^1O_2} - k_{calc,\ {}^3DOM^*}$, where $k_{obs,\ P8\ Sep}$ is from Table C.13. [g] Calculated as $k_{CO_3^{\bullet-}} \times [CO_3^{\bullet-}]_{ss}$, where $k_{CO_3^{\bullet-}}$ is from Table C.7 and $[CO_3^{\bullet-}]_{ss}$ is from Table 4.2. [h] Calculated as $k_{{}^{\bullet}OH} \times [{}^{\bullet}OH]_{ss}$, where $k_{{}^{\bullet}OH}$ is from Table C.7 and $[{}^{\bullet}OH]_{ss}$ is from Table 4.2. [i] Calculated as $k_{{}^1O_2} \times [{}^1O_2]_{ss}$, where $k_{{}^1O_2}$ is from Table C.7 and $[{}^1O_2]_{ss}$ is from Table 4.2. [j] N.A. = not available. Errors were propagated through observed rate constants and PPRI concentrations.

C.16 References

1. Page, S. E.; Arnold, W. A.; McNeill, K., Terephthalate as a probe for photochemically generated hydroxyl radical. *J. Environ. Monit.* **2010,** *12*, 1658-1665.
2. Ryan, C. C.; Tan, D. T.; Arnold, W. A., Direct and indirect photolysis of sulfamethoxazole and trimethoprim in wastewater treatment plant effluent. *Water Res.* **2011,** *45*, 1280-1286.
3. Zeng, T.; Ziegelgruber, K. L.; Chin, Y.-P.; Arnold, W. A., Pesticide processing potential in prairie pothole porewaters. *Environ. Sci. Technol.* **2011,** *45*, 6814-6822.
4. Leifer, A., *The Kinetics of Environmental Aquatic Photochemistry: Theory and Practice*. American Chemical Society: Washington, DC, 1988.
5. Johnson, J., Monitoring surface waters for pesticides in North Dakota. In *2012 North Dakota Water Quality Monitoring Conference* Bismarck, ND, 2012.
6. Zollinger, R.; McMullen, M.; Knodel, J.; Gray, J.; Jantzi, D.; Kimmet, G.; Hagemeister, K.; Schmitt, C. *Pesticide Use and Pest Management Practices in North Dakota, 2008*; North Dakota State University in cooperation with North Dakota Agricultural Statistics Service, Extension Publication W-1446; Fargo, ND, 2009.
7. Hessler, D. P.; Gorenflo, V.; Frimmel, F. H., Degradation of aqueous atrazine and metazachlor solutions by UV and UV/H_2O_2 - Influence of pH and herbicide concentration. *Acta Hydroch. Hydrob.* **1993,** *21*, 209-214.
8. Beltrán, F. J.; Ovejero, G.; Acedo, B., Oxidation of atrazine in water by ultraviolet radiation combined with hydrogen peroxide. *Water Res.* **1993,** *27*, 1013-1021.
9. Palm, W. U.; Zetzsch, C., Investigation of the photochemistry and quantum yields of triazines using polychromatic irradiation and UV-spectroscopy as analytical tool. *Int. J. Environ. Anal. Chem.* **1996,** *65*, 313-329.
10. Bolton, J. R.; Stefan, M. I., Fundamental photochemical approach to the concepts of fluence (UV dose) and electrical energy efficiency in photochemical degradation reactions. *Res. Chem. Intermed.* **2002,** *28*, 857-870.
11. McMartin, D. W.; Headley, J. V.; Wood, B. P.; Gillies, J. A., Photolysis of atrazine and ametryne herbicides in Barbados sugar cane plantation soils and water. *J. Environ. Sci. Health, Part B* **2003,** *38*, 293-303.
12. Prosen, H.; Zupančič-Kralj, L., Evaluation of photolysis and hydrolysis of atrazine and its first degradation products in the presence of humic acids. *Environ. Pollut.* **2005,** *133*, 517-529.
13. Sanches, S.; Barreto Crespo, M. T.; Pereira, V. J., Drinking water treatment of priority pesticides using low pressure UV photolysis and advanced oxidation processes. *Water Res.* **2010,** *44*, 1809-1818.
14. Hua, R.; Yue, Y.; Fan, D., The photodegradation of acetochlor in water. *Chin. J. Pestic. Sci.* **2000,** *2*, 71-74.
15. Beltrán, F. J.; González, M.; Rivas, F. J.; Acedo, B., Determination of kinetic parameters of ozone during oxidations of alachlor in water. *Water Environ. Res* **2000,** *72*, 689-697.
16. Wong, C. C.; Chu, W., The direct photolysis and photocatalytic degradation of alachlor at different TiO_2 and UV sources. *Chemosphere* **2003,** *50*, 981-987.

17. Song, W.; Ravindran, V.; Pirbazari, M., Process optimization using a kinetic model for the ultraviolet radiation-hydrogen peroxide decomposition of natural and synthetic organic compounds in groundwater. *Chem. Eng. Sci.* **2008,** *63*, 3249-3270.
18. Kochany, J.; Maguire, R. J., Sunlight photodegradation of metolachlor in water. *J. Agric. Food. Chem.* **1994,** *42*, 406-412.
19. Benitez, F. J.; Acero, J. L.; Real, F. J.; Maya, C., Modeling of photooxidation of acetamide herbicides in natural waters by UV radiation and the combinations UV/H_2O_2 and UV/O_3. *J. Chem. Technol. Biotechnol.* **2004,** *79*, 987-997.
20. Wu, C.; Shemer, H.; Linden, K. G., Photodegradation of metolachlor applying UV and UV/H_2O_2. *J. Agric. Food. Chem.* **2007,** *55*, 4059-4065.
21. Huntscha, S.; Singer, H.; Canonica, S.; Schwarzenbach, R. P.; Fenner, K., Input dynamics and fate in surface water of the herbicide metolachlor and of its highly mobile transformation product metolachlor ESA. *Environ. Sci. Technol.* **2008,** *42*, 5507-5513.
22. ter Halle, A.; Richard, C., Simulated solar light irradiation of mesotrione in natural waters. *Environ. Sci. Technol.* **2006,** *40*, 3842-3847.
23. Jirkovský, J.; Faure, V.; Boule, P., Photolysis of diuron. *Pestic. Sci.* **1997,** *50*, 42-52.
24. Gerecke, A. C.; Canonica, S.; Muller, S. R.; Scharer, M.; Schwarzenbach, R. P., Quantification of dissolved natural organic matter (DOM) mediated phototransformation of phenylurea herbicides in lakes. *Environ. Sci. Technol.* **2001,** *35*, 3915-3923.
25. Djebbar, K.; Sehili, T.; Mazellier, P.; De Laat, J., Phototransformation of diuron in aqueous solution by UV irradiation in the absence and in the presence of H_2O_2. *Environ. Technol.* **2003,** *24*, 479-489.
26. Benitez, F. J.; Real, F. J.; Acero, J. L.; Garcia, C., Photochemical oxidation processes for the elimination of phenyl-urea herbicides in waters. *J. Hazard. Mater.* **2006,** *138*, 278-287.
27. De St-Laumer, C.; Emmelin, C.; Méallier, P., Photodegradation of isoproturon: Photodegradation of active matter alone and in formulation. *Fresenius Environ. Bull.* **1997,** *6*, 529-535.
28. Millet, M.; Palm, W.-U.; Zetzsch, C., Investigation of the photochemistry of urea herbicides (chlorotoluron and isoproturon) and quantum yields using polychromatic irradiation. *Environ. Toxicol. Chem.* **1998,** *17*, 258-264.
29. Tixier, C.; Meunier, L.; Bonnemoy, F.; Boule, P., Phototransformation of three herbicides: Chlorbufam, isoproturon, and chlorotoluron. Influence of irradiation on toxicity. *Int. J. Photoenergy* **2000,** *2*, 1-8.
30. European Commission, Directorate-General Health & Consumer Protection, Directorate D - Food Safety: Plant health, animal health, and welfare, international questions, Unit E.1 - Plant health. *Review report for the active substance isoproturon*; SANCO/3045/99-Final European Commission: Brussels, Belgium, 2002. http://ec.europa.eu/food/plant/protection/evaluation/existactive/list1-41_en.pdf (Accessed June 2012).
31. Boulkamh, A.; Harakat, D.; Sehili, T.; Boule, P., Phototransformation of metoxuron [3-(3-chloro-4-methoxyphenyl)-1,1-dimethylurea] in aqueous solution. *Pest Manage. Sci.* **2001,** *57*, 1119-1126.

32. Beltran-Heredia, J.; Benitez, F. J.; Gonzalez, T.; Acero, J. L.; Rodriguez, B., Photolytic decomposition of bentazone. *J. Chem. Technol. Biotechnol.* **1996,** *66*, 206-212.
33. European Commission, Directorate-General Health & Consumer Protection, Directorate E - Public, animal and plant health, Unit E.1: Legislation relating to crop products and animal nutrition. *Review report for the active substance bentazone*; 7585/VI/97-Final; European Commission: Brussels, Belgium, 2000. http://ec.europa.eu/food/plant/protection/evaluation/existactive/list1-14_en.pdf (Accessed June 2012).
34. Dilling, W. L.; Lickly, L. C.; Lickly, T. D.; Murphy, P. G.; McKellar, R. L., Organic photochemistry. 19. Quantum yields for *O,O*-diethyl *O*-(3,5,6-trichloro-2-pyridinyl) phosphorothioate (chlorpyrifos) and 3,5,6-trichloro-2-pyridinol in dilute aqueous solutions and their environmental phototransformation rates. *Environ. Sci. Technol.* **1984,** *18*, 540-543.
35. Wan, H. B.; Wong, M. K.; Mok, C. Y., Comparative study on the quantum yields of direct photolysis of organophosphorus pesticides in aqueous solution. *J. Agric. Food. Chem.* **1994,** *42*, 2625-2630.
36. European Commission, Directorate-General Health & Consumer Protection, Directorate D - Food Safety: Production and distribution chain, Unit D.3 - Chemicals, contaminants and pesticides. *Review report for the active substance chlorpyrifos*; SANCO/3059/99 - Rev. 1.5; European Commission: Brussels, Belgium, 2005. http://ec.europa.eu/food/plant/protection/evaluation/existactive/list_chlorpyrifos.pdf (Accessed June 2012).
37. Vialaton, D.; Pilichowski, J.-F.; Baglio, D.; Paya-Perez, A.; Larsen, B.; Richard, C., Phototransformation of propiconazole in aqueous media. *J. Agric. Food. Chem.* **2001,** *49*, 5377-5382.
38. Zepp, R. G.; Cline, D. M., Rates of direct photolysis in aquatic environment. *Environ. Sci. Technol.* **1977,** *11*, 359-366.
39. Draper, W. M., Determination of wavelength-averaged, near UV quantum yields for environmental chemicals. *Chemosphere* **1985,** *14*, 1195-1203.
40. Chelme-Ayala, P.; El-Din, M. G.; Smith, D. W., Degradation of bromoxynil and trifluralin in natural water by direct photolysis and UV plus H_2O_2 advanced oxidation process. *Water Res.* **2010,** *44*, 2221-2228.
41. Zeng, T.; Chin, Y.-P.; Arnold, W. A., Potential for abiotic reduction of pesticides in prairie pothole porewaters. *Environ. Sci. Technol.* **2012,** *46*, 3177-3187.
42. Huang, J.; Mabury, S. A., Steady-state concentrations of carbonate radicals in field waters. *Environ. Toxicol. Chem.* **2000,** *19*, 2181-2188.
43. Haag, W. R.; Hoigné, J.; Gassman, E.; Braun, A., Singlet oxygen in surface waters - Part I: Furfuryl alcohol as a trapping agent. *Chemosphere* **1984,** *13*, 631-640.
44. Latch, D. E.; Packer, J. L.; Arnold, W. A.; McNeill, K., Photochemical conversion of triclosan to 2,8-dichlorodibenzo-p-dioxin in aqueous solution. *J. Photochem. Photobiol. A: Chem.* **2003,** *158*, 63-66.

45. Grebel, J. E.; Pignatello, J. J.; Mitch, W. A., Sorbic acid as a quantitative probe for the formation, scavenging and steady-state concentrations of the triplet-excited state of organic compounds. *Water Res.* **2011,** *45*, 6535-6544.
46. Xu, H.; Cooper, W. J.; Jung, J.; Song, W., Photosensitized degradation of amoxicillin in natural organic matter isolate solutions. *Water Res.* **2011,** *45*, 632-638.
47. Page, S. E.; Arnold, W. A.; McNeill, K., Assessing the contribution of free hydroxyl radical in organic matter-sensitized photohydroxylation reactions. *Environ. Sci. Technol.* **2011,** *45*, 2818-2825.
48. Kohn, T.; Grandbois, M.; McNeill, K.; Nelson, K. L., Association with natural organic matter enhances the sunlight-mediated inactivation of MS2 coliphage by singlet oxygen. *Environ. Sci. Technol.* **2007,** *41*, 4626-4632.
49. Grandbois, M.; Latch, D. E.; McNeill, K., Microheterogeneous concentrations of singlet oxygen in natural organic matter isolate solutions. *Environ. Sci. Technol.* **2008,** *42*, 9184-9190.
50. Romero, O. C.; Straub, A. P.; Kohn, T.; Nguyen, T. H., Role of temperature and Suwannee River natural organic matter on inactivation kinetics of rotavirus and bacteriophage MS2 by solar irradiation. *Environ. Sci. Technol.* **2011,** *45*, 10385-10393.
51. Huang, J.; Mabury, S. A., A new method for measuring carbonate radical reactivity toward pesticides. *Environ. Toxicol. Chem.* **2000,** *19*, 1501-1507.
52. Chramosta, N.; De Laat, J.; Dore, M.; Suty, H.; Pouillot, M., Determination of kinetic constants for reaction of hydroxyl radicals on some s-triazines. *Environ. Technol.* **1993,** *14*, 215-226.
53. Canonica, S.; Kohn, T.; Mac, M.; Real, F. J.; Wirz, J.; von Gunten, U., Photosensitizer method to determine rate constants for the reaction of carbonate radical with organic compounds. *Environ. Sci. Technol.* **2005,** *39*, 9182-9188.
54. De Laat, J.; Doré, M.; Suty, H., Oxidation of *s*-triazines by advances oxidation processes. By-products and kinetic rate constants. *Rev. Sci. Eau.* **1995,** *8*, 23-42.
55. Larson, R. A.; Zepp, R. G., Reactivity of the carbonate radical with aniline derivatives. *Environ. Toxicol. Chem.* **1988,** *7*, 265-274.
56. Azenha, M. E. D. G.; Burrows, H. D.; Canle L, M.; Coimbra, R.; Fernandez, M. I.; Garcia, M. V.; Rodrigues, A. E.; Santaballa, J. A.; Steenken, S., On the kinetics and energetics of one-electron oxidation of 1,3,5-triazines. *Chem. Commun.* **2003**, 112-113.
57. De Laat, J.; Lebarbier, R.; Chramosta, N.; Doré, M., Reactivity of chloro-2, methoxy 2 and methylthio-2 *s*-triazines towards hydroxyl radicals. *J. Euro. Hydrol.* **1994,** *25*, 185-198.
58. Balci, B.; Oturan, N.; Cherrier, R.; Oturan, M. A., Degradation of atrazine in aqueous medium by electrocatalytically generated hydroxyl radicals. A kinetic and mechanistic study. *Water Res.* **2009,** *43*, 1924-1934.
59. Haag, W. R.; Yao, C. C. D., Rate constants for reaction of hydroxyl radicals with several drinking water contaminants. *Environ. Sci. Technol.* **1992,** *26*, 1005-1013.
60. Tace, E.; De Laat, J.; Doré, M., Photodegradation of atrazine by UV-irradation in the absence and in the presence of hydrogen peroxide. *J. Fr. Hydrol.* **1992,** *23*, 233-249.

61. Acero, J. L.; Stemmler, K.; von Gunten, U., Degradation kinetics of atrazine and its degradation products with ozone and OH radicals: A predictive tool for drinking water treatment. *Environ. Sci. Technol.* **2000,** *34*, 591-597.
62. Tauber, A.; von Sonntag, C., Products and kinetics of the OH-radical-induced dealkylation of atrazine. *Acta Hydroch. Hydrob.* **2000,** *28*, 15-23.
63. Acero, J. L.; Benitez, F. J.; Real, F. J.; Maya, C., Oxidation of acetamide herbicides in natural waters by ozone and by the combination of ozone/hydrogen peroxide: Kinetic study and process modeling. *Ind. Eng. Chem. Res.* **2003,** *42*, 5762-5769.
64. Fulkerson-Brekken, J.; Brezonik, P. L., Indirect photolysis of acetochlor: Rate constant of a nitrate-mediated hydroxyl radical reaction. *Chemosphere* **1998,** *36*, 2699-2704.
65. De Laat, J.; Maouala Makata, P.; Doré, M., Rate constants for reactions of ozone and hydroxyl radicals with several phenyl-ureas and acetamides. *Environ. Technol.* **1996,** *17*, 707-716.
66. Murati, M.; Oturan, N.; Aaron, J.-J.; Dirany, A.; Tassin, B.; Zdravkovski, Z.; Oturan, M., Degradation and mineralization of sulcotrione and mesotrione in aqueous medium by the electro-Fenton process: a kinetic study. *Environ. Sci. Pollut. Res.* **2011**, 1-11.
67. Bensalah, N.; Khodary, A.; Abdel-Wahab, A., Kinetic and mechanistic investigations of mesotrione degradation in aqueous medium by Fenton process. *J. Hazard. Mater.* **2011,** *189*, 479-485.
68. Benitez, F. J.; Real, F. J.; Acero, J. L.; Garcia, C., Kinetics of the transformation of phenyl-urea herbicides during ozonation of natural waters: Rate constants and model predictions. *Water Res.* **2007,** *41*, 4073-4084.
69. Benitez, F. J.; Real, F. J.; Acero, J. L.; Garcia, C.; Llanos, E. M., Kinetics of phenylurea herbicides oxidation by Fenton and photo-Fenton processes. *J. Chem. Technol. Biotechnol.* **2007,** *82*, 65-73.
70. Shemer, H.; Sharpless, C. M.; Elovitz, M. S.; Linden, K. G., Relative rate constants of contaminant candidate list pesticides with hydroxyl radicals. *Environ. Sci. Technol.* **2006,** *40*, 4460-4466.
71. Al Housari, F.; Höhener, P.; Chiron, S., Factors responsible for rapid dissipation of acidic herbicides in the coastal lagoons of the Camargue (Rhône River Delta, France). *Sci. Total Environ.* **2011,** *409*, 582-587.
72. Özcan, A.; Oturan, N.; Şahin, Y.; Oturan, M. A., Electro-Fenton treatment of aqueous clopyralid solutions. *Int. J. Environ. Anal. Chem.* **2010,** *90*, 478-486.
73. Wu, C.; Linden, K. G., Phototransformation of selected organophosphorus pesticides: Roles of hydroxyl and carbonate radicals. *Water Res.* **2010,** *44*, 3585-3594.
74. Armbrust, K. L., Pesticide hydroxyl radical rate constants: Measurements and estimates of their importance in aquatic environments. *Environ. Toxicol. Chem.* **2000,** *19*, 2175-2180.
75. Chelme-Ayala, P.; El-Din, M. G.; Smith, D. W.; Adams, C. D., Oxidation kinetics of two pesticides in natural waters by ozonation and ozone combined with hydrogen peroxide. *Water Res.* **2011,** *45*, 2517-2526.

76. Chelme-Ayala, P.; El-Din, M. G.; Smith, D. W., Kinetics and mechanism of the degradation of two pesticides in aqueous solutions by ozonation. *Chemosphere* **2010,** *78*, 557-562.
77. Chen, S.-N.; Hoffman, M. Z.; Parsons, G. H., Reactivity of the carbonate radical toward aromatic compounds in aqueous solution. *J. Phys. Chem.* **1975,** *79*, 1911-1912.
78. Foote, C. S.; Denny, R. W.; Weaver, L.; Chang, Y.; Peters, J., Quenching of singlet oxygen. *Ann. N. Y. Acad. Sci.* **1970,** *171*, 139-148.
79. Clifton, C. L.; Huie, R. E., Rate constants for some hydrogen abstraction reactions of the carbonate radical. *Int. J. Chem. Kinet.* **1993,** *25*, 199-203.
80. Thomas, J. K., Rates of reaction of the hydroxyl radical. *Trans. Faraday Soc.* **1965,** *61*, 702-707.
81. Darmanyan, A. P.; Foote, C. S., Solvent effects on singlet oxygen yield from n,π* and π,π* triplet carbonyl compounds. *J. Phys. Chem.* **1993,** *97*, 5032-5035.
82. Anbar, M.; Neta, P., Tables of bimolecular rate constants of hydrated electrons, hydrogen atoms and hydroxyl radicals with inorganic and organic compounds. *Int. J. Appl. Radiat. Isot.* **1965,** *16*, 227-242.
83. Willson, R. L.; Greenstock, C. L.; Adams, G. E.; Wageman, R.; Dorfman, L. M., The standardization of hydroxyl radical rate data from radiation chemistry. *Int. J. Radiat. Phys. Chem.* **1971,** *3*, 211-220.
84. Wolfenden, B. S.; Willson, R. L., Radical-cations as reference chromogens in kinetic studies of ono-electron transfer reactions: Pulse radiolysis studies of 2,2'-azinobis-(3-ethylbenzthiazoline-6-sulphonate). *J. Chem. Soc., Perkin Trans. 2* **1982**, 805-812.
85. Elliot, A. J.; Simsons, A. S., Rate constants for reactions of hydroxyl radicals as a function of temperature. *Radiat. Phys. Chem.* **1984,** *24*, 229-231.
86. Buxton, G. V.; Greenstock, C. L.; Helman, W. P.; Ross, A. B., Critical review of rate constants for reactions of hydrated electrons and hydroxyl radicals ($^{\bullet}OH/^{\bullet}O^{-}$) in aqueous solution. *J. Phys. Chem. Ref. Data* **1988,** *17*, 513-886.
87. Motohashi, N.; Saito, Y., Competitive measurement of rate constants for hydroxyl radical reactions using radiolytic hydroxylation of benzoate. *Chem. Pharm. Bull.* **1993,** *41*, 1842-1845.
88. Monod, A.; Poulain, L.; Grubert, S.; Voisin, D.; Wortham, H., Kinetics of OH-initiated oxidation of oxygenated organic compounds in the aqueous phase: New rate constants, structure-activity relationships and atmospheric implications. *Atmos. Environ.* **2005,** *39*, 7667-7688.
89. Chen, S.-N.; Morton, Z. H., Effect of pH on the reactivity of the carbonate radical in aqueous solution. *Radiat. Res.* **1975,** *62*, 18-27.
90. Rao, P. S.; Simic, M.; Hayon, E., Pulse radiolysis study of imidazole and histidine in water. *J. Phys. Chem.* **1975,** *79*, 1260-1263.
91. Matheson, I. B. C.; Lee, J., Chemical reaction rates of amino acids with singlet oxygen. *Photochem. Photobiol.* **1979,** *29*, 879-881.
92. Egorov, S. Y.; Kurella, E. G.; Boldyrev, A. A.; Krasnovsky, A. A., Quenching of singlet molecular oxygen by carnosine and related antioxidants. Monitoring 1270-nm phosphorescence in aqueous media. *IUBMB Life* **1997,** *41*, 687-694.

93. Bisby, R. H.; Morgan, C. G.; Hamblett, I.; Gorman, A. A., Quenching of singlet oxygen by Trolox C, ascorbate, and amino acids: Effects of pH and temperature. *J. Phys. Chem. A* **1999,** *103*, 7454-7459.
94. Boreen, A. L.; Edhlund, B. L.; Cotner, J. B.; McNeill, K., Indirect photodegradation of dissolved free amino acids: The contribution of singlet oxygen and the differential reactivity of DOM from various sources. *Environ. Sci. Technol.* **2008,** *42*, 5492-5498.
95. Elango, T. P.; Ramakrishnan, V.; Vancheesan, S.; Kuriacose, J. C., Reactions of the carbonate radical with aliphatic amines. *Tetrahedron* **1985,** *41*, 3837-3843.
96. Anderson, R. F.; Patel, K. B., The effect of 1,4-diazabicyclo[2.2.2]octane on the radiosensitivity of bacteria. *Photochem. Photobiol.* **1978,** *28*, 881-885.
97. Ogryzlo, E. A.; Tang, C. W., Quenching of oxygen($^1\Delta_g$) by amines. *J. Am. Chem. Soc.* **1970,** *92*, 5034-5036.
98. Packer, J. E.; Mahood, J. S.; Mora-Arellano, V. O.; Slater, T. F.; Willson, R. L.; Wolfenden, B. S., Free radicals and singlet oxygen scavengers: Reaction of a peroxy-radical with β-carotene, diphenyl furan and 1,4-diazobicyclo(2,2,2)-octane. *Biochem. Biophys. Res. Commun.* **1981,** *98*, 901-906.
99. Monroe, B. M., Rate constants for the reaction of singlet oxygen with conjugated dienes. *J. Am. Chem. Soc.* **1981,** *103*, 7253-7256.

Appendix D: Supporting Information for Chapter 5

D.1 White-line peak energy and XANES spectra of S reference compounds

Table D.1 Sulfur oxidation state and white-line peak energy of reference compounds

S reference compound	S functional group	Classification	S oxidation state	White-line peak (eV)[a]
Mackinawite (FeS_m)	S^{2-}	Iron monosulfide	-2	2469.8 ± 0.69
Greigite (Fe_3S_{4g})	S^{2-}	Iron monosulfide	-2	2469.8 ± 0.69
Pyrite (FeS_{2p})	S_2^{2-}	Iron disulfide	-1	2471.9 ± 0.40
Sulfur	S_0	Elemental sulfur	0	2472.5 ± 0.20
L-Cystine	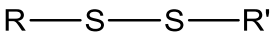	Organic disulfide	+0.2	2472.6 ± 0.39
L-Methionine	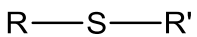	Organic monosulfide	+0.5	2473.4 ± 0.29
L-Cysteine	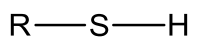	Thiol	+0.5	2473.4 ± 0.08
2-Thiophenecarboxylic acid	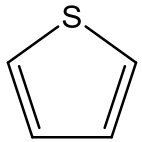	Thiophene	+1	2473.7 ± 0.44
Methionine sulfoxide	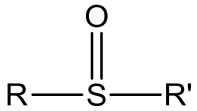	Sulfoxide	+2	2475.8 ± 0.42
Sodium sulfite	SO_3^{2-}	Sulfite	+3.68	2478.6 ± 0.19

S reference compound	S functional group	Classification	S oxidation state	White-line peak (eV)[a]
Sodium thiosulfate	$S_2O_3^{2-}$	Thiosulfate	-1, +5	2472.0 ± 0.33 2480.5 ± 0.65
Sulfanilamide	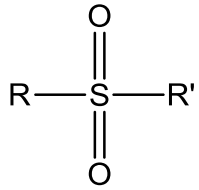	Sulfone	+4	2480.3 ± 0.20
1-Amino-2-naphthol-4-sulfonic acid (ANSA) DL-Homocysteic acid	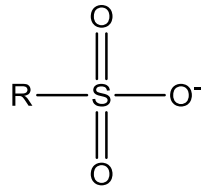	Sulfonate	+5	2481.2 ± 0.16
Sodium dodecyl sulfate (SDS)	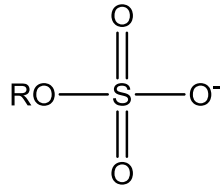	Ester sulfate	+6	2482.6 ± 0.37
Calcium sulfate dihydrate (Gypsum)	SO_4^{2-}	Inorganic sulfate	+6	2482.4 ± 0.41

[a] Average values compiled from literature data reported in Sugiura (1981),[1] Waldo et al. (1991),[2] Vairavamurthy et al. (1993),[3] Vairavamurthy et al. (1994a),[4] Vairavamurthy et al. (1994b),[5] Vairavamurthy et al. (1995),[6] Morra et al. (1997),[7] Vairavamurthy et al. (1997),[8] Rompel et al. (1998),[9] Xia et al. (1998),[10] Prange et al. (1999),[11] Sarret et al. (1999),[12] Prietzel et al. (2003),[13] Bostick et al. (2005),[14] Prietzel et al. (2007),[15] Schroth et al. (2007),[16] Lemelle et al. (2008),[17] Burton et al. (2009),[18] Prietzel et al. (2009),[19] Almkvist et al. (2010),[20] Orthous-Daunay et al. (2010),[21] Prietzel et al. (2011),[22] and references therein.

D.2 PCA and fittings of XANES spectra for P1Sep and P8Sep samples

Table D.2 PCA and target transformation of P1Sep and P8Sep XANES spectra

Component	*IND*[a]	S reference compound	*Chi Sq*	*Rvalue*	*SPOIL*	Quality[c]
Comp1	0.10027	Mackinawite	53.45772	0.05476	15.3222	Unacceptable
Comp2	0.05226	Greigite	55.43212	0.05640	14.8884	Unacceptable
Comp3	0.04777	Pyrite	8.98916	0.00925	2.8183	Good
Comp4[b]	0.03490	Elemental sulfur	20.99603	0.02195	6.7406	Unacceptable
		L-Cystine	10.40519	0.01095	6.9841	Unacceptable
		L-Cysteine	2.49160	0.00245	2.7052	Good
		L-Methionine	5.22578	0.00515	2.8479	Good
		2-Thiophenecarboxylic acid	11.32625	0.01131	4.7710	Poor
		DL-Methionine sulfoxide	110.26920	0.10001	12.5170	Unacceptable
		Sodium sulfite	258.51737	0.17752	26.7369	Unacceptable
		Sulfanilamide	29.48807	0.01933	2.5604	Good
		Sodium thiosulfate	39.16720	0.04031	9.6037	Unacceptable
		DL-Homocysteic acid	30.48381	0.01646	1.8049	Good
		1-Amino-2-naphthol-4-sulfonic acid (ANSA)	12.00095	0.00671	1.5916	Good
		Sodium dodecyl sulfate (SDS)	26.50926	0.01239	2.7394	Good
		Calcium sulfate (Gypsum)	54.57627	0.04257	8.6229	Unacceptable

[a] PCA performed using all XANES spectra acquired on P1Sep and P8Sep samples during November 2011 beamtime. [b] The minimum *IND* value. The number of components used for the target transformation was 4. [c] Values < 1.5 are considered excellent, 1.5-3 good, 3-4.5 fair, 4.5-6 poor, and > 6 unacceptable.

Table D.3 Linear combination fittings of P1Sep and P8Sep XANES spectra

XANES POI[a]	Comp1	Fraction1	Comp2	Fraction2	Comp3	Fraction3	Comp4	Fraction4	*Sum*	*NSS*	*Energy Shift*
P1Sep_spot0	Cystine	0.13752	Cysteine	0.79352	ANSA	0.11618			1.05	3.80×10^{-3}	0.19
P1Sep_spot1	Pyrite	0.09199	Cysteine	0.45269	ANSA	0.10357	SDS	0.36158	1.01	7.39×10^{-3}	0.09
P1Sep_spot2	Pyrite	0.38581	Cysteine	0.39899	ANSA	0.05959			0.84	8.70×10^{-3}	-0.24
P8Sep_spot0	Cysteine	0.12972	Sulfanilamide	0.22064	ANSA	0.25682	SDS	0.30716	0.91	2.30×10^{-3}	-0.03
P8Sep_spot1	Pyrite	0.36031	Cysteine	0.50510	ANSA	0.05948	SDS	0.02516	0.95	2.57×10^{-3}	0.06
P8Sep_spot2	Cystine	0.21824	Cysteine	0.69858	ANSA	0.12341			1.04	2.22×10^{-3}	0.15
P8Sep_spot3	Pyrite	0.47501	Cysteine	0.39504	ANSA	0.03281	SDS	0.02999	0.93	2.27×10^{-3}	-0.03
P8Sep_spot4	Cysteine	0.65397	ANSA	0.06764	SDS	0.24962			0.97	3.85×10^{-3}	0.04
P8Sep_spot5	Pyrite	0.15820	Cysteine	0.70703	ANSA	0.16238			1.03	3.11×10^{-3}	0.20

[a] Linear combination fitting of XANES spectra acquired on P1Sep and P8Sep samples during November 2011 beamtime.

D.3 PCA and fittings of chemical maps and XANES spectra for P1 samples

Table D.4 PCA and target transformation of P1 XANES spectra

Component	*IND*[a]	S reference compound	*Chi Sq*	*Rvalue*	*SPOIL*	Quality[c]
Comp1	0.02525	Mackinawite	50.43828	0.05166	5.8463	Poor
Comp2	0.01739	Greigite	50.50878	0.05139	6.1352	Unacceptable
Comp3	0.01359	Pyrite	7.90102	0.00813	1.9381	Good
Comp4	0.01227	Elemental sulfur	18.10042	0.01892	6.1556	Unacceptable
Comp5	0.01098	L-Cystine	7.47663	0.00787	3.5943	Fair
Comp6[b]	0.01084	L-Cysteine	3.05058	0.00300	1.4527	Excellent
		L-Methionine	9.88791	0.00975	2.0224	Good
		2-Thiophenecarboxylic acid	15.72900	0.01570	2.5613	Good
		DL-Methionine sulfoxide	118.54400	0.10752	7.0625	Unacceptable
		Sodium sulfite	266.04564	0.18268	18.6963	Unacceptable
		Sulfanilamide	48.80931	0.03200	3.3832	Fair
		Sodium thiosulfate	34.90189	0.03592	5.1160	Poor
		DL-Homocysteic acid	17.38154	0.00938	1.04994	Excellent
		1-Amino-2-naphthol-4-sulfonic acid (ANSA)	10.19919	0.00570	0.9333	Excellent
		Sodium dodecyl sulfate (SDS)	13.94573	0.00652	1.3679	Excellent
		Calcium sulfate (Gypsum)	7.89981	0.00616	1.4938	Excellent

[a] PCA performed using all XANES spectra acquired on P1Jan, P1Apr, P1Jun, and P1Sep samples during May 2012 beamtime. [b] The minimum *IND* value. The number of components used for the target transformation was 6. [c] Values < 1.5 are considered excellent, 1.5-3 good, 3-4.5 fair, 4.5-6 poor, and > 6 unacceptable.

Table D.5 Fittings of P1 and P8 chemical maps

Sample[a]	Comp1	Fraction1	Comp2	Fraction2	Comp3	Fraction3	Comp4	Fraction4	Comp5	Fraction5	*Sum*	*MSE*
P1Jan	Pyrite	0.23107	Cysteine	0.43038	Gypsum	0.13290	SDS	0.20565			1.00	4.85×10^{-2}
P1Apr	Pyrite	0.24086	Cystine	0.11966	Cysteine	0.43386	SDS	0.20562			1.00	3.24×10^{-2}
P1Jun	Pyrite	0.29902	Cysteine	0.14524	Gypsum	0.20697	SDS	0.34877			1.00	3.18×10^{-2}
P1Sep	Pyrite	0.12463	Cystine	0.27721	Cysteine	0.46638	ANSA	0.06315	SDS	0.06862	1.00	2.71×10^{-3}
P8Apr	Pyrite	0.14217	Cystine	0.36025	Cysteine	0.33069	SDS	0.16689			1.00	4.34×10^{-2}
P8Sep	Pyrite	0.14600	Cystine	0.35602	Cysteine	0.32830	ANSA	0.08714	SDS	0.08255	1.00	4.32×10^{-3}

[a] Chemical map fitting of P1 and P8 samples during May 2012 beamtime.

Table D.6 Linear combination fittings of P1 and P8 XANES spectra

XANES POI[a]	Comp1	Fraction1	Comp2	Fraction2	Comp3	Fraction3	Comp4	Fraction4	Comp5	Fraction5	*Sum*	*NSS*	*Energy Shift*
P1Jan_spot0	Cysteine	0.27169	Gypsum	0.35143	SDS	0.35244					0.98	9.58×10^{-3}	-0.25
P1Jan_spot1	Pyrite	0.30995	Cysteine	0.18443	SDS	0.16537					0.66[b]	1.51×10^{-2}	0.12
P1Jan_spot2	Pyrite	0.22577	Cysteine	0.12079	SDS	0.20155					0.55[b]	1.51×10^{-2}	0.14
P1Jan_spot3	Pyrite	0.29440	Cysteine	0.16072	SDS	0.15655					0.61[b]	1.46×10^{-2}	0.13
P1Apr_spot0	Cystine	0.20199	Cysteine	0.59832	SDS	0.19311					0.99	3.48×10^{-3}	-0.03
P1Apr_spot1	Cystine	0.14570	Cysteine	0.46311	SDS	0.38258					0.99	5.10×10^{-3}	0.08
P1Apr_spot2	Cystine	0.38212	Cysteine	0.60574	SDS	0.11872					1.11	3.96×10^{-3}	0.04
P1Apr_spot3	Pyrite	0.31416	Cysteine	0.46724	SDS	0.22636					0.91	4.14×10^{-3}	0.02
P1Jun_spot0	Gypsum	0.60344	SDS	0.31360							0.92	1.30×10^{-2}	0.27
P1Jun_spot1	Pyrite	0.51884	Cysteine	0.25948	Gypsum	0.11497					0.89	2.44×10^{-3}	-0.21
P1Jun_spot2	Pyrite	0.28755	Cysteine	0.55282	SDS	0.23223					1.07	3.55×10^{-3}	-0.12
P1Jun_spot3	Pyrite	0.38248	Cysteine	0.20225	Gypsum	0.30137					0.89	2.13×10^{-2}	-0.13
P1Sep_spot0	Cystine	0.15173	Cysteine	0.55147	ANSA	0.17355	SDS	0.02799			1.06	1.73×10^{-3}	-0.02
P1Sep_spot1	Pyrite	0.15012	Cystine	0.13319	Cysteine	0.59305	ANSA	0.09267	SDS	0.04115	1.01	1.63×10^{-3}	0.03
P1Sep_spot2	Cystine	0.33745	Cysteine	0.56350	ANSA	0.08311	SDS	0.09532			1.08	2.26×10^{-3}	-0.09
P1Sep_spot3	Pyrite	0.38513	Cysteine	0.39585	SDS	0.05730					0.84	7.79×10^{-3}	-0.34

[a] Linear combination fitting of XANES spectra acquired on P1Jan, P1Apr, P1Jun, and P1Sep samples during May 2012 beamtime. [b] Poor fitting quality due to weak XANES signal intensity and poorer signal-to-noise ratio than other POIs.

D.4 Chemical maps of P8Apr and P8Sep samples

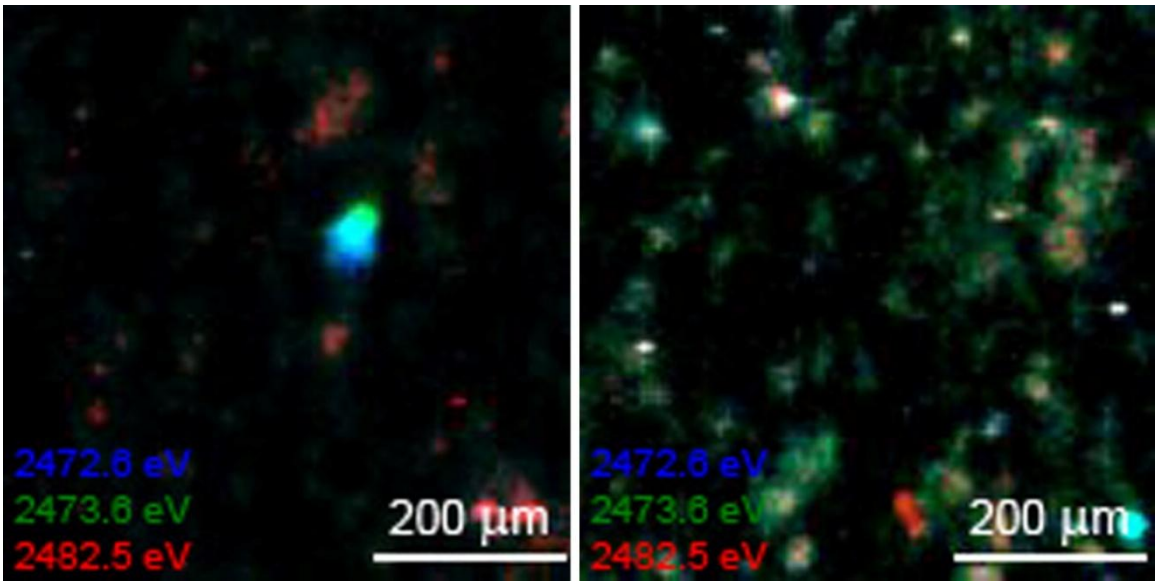

Figure D.1 Tricolor multi-energy S chemical maps (600 µm × 600 µm, energies at 2472.6 eV, 2473.6 eV, and 2482.5 eV) of P8Apr and P8Sep samples.

D.5 References

1. Sugiura, C., Sulfur K x-ray absorption spectra of FeS, FeS_2, and Fe_2S_3. *J. Chem. Phys.* **1981,** *74*, 215-217.
2. Waldo, G. S.; Carlson, R. M. K.; Moldowan, J. M.; Peters, K. E.; Penner-hahn, J. E., Sulfur speciation in heavy petroleums: Information from X-ray absorption near-edge structure. *Geochim. Cosmochim. Acta* **1991,** *55*, 801-814.
3. Vairavamurthy, M. A.; Manowitz, B.; Luther, G. W., III; Jeon, Y., Oxidation state of sulfur in thiosulfate and implications for anaerobic energy metabolism. *Geochim. Cosmochim. Acta* **1993,** *57*, 1619-1623.
4. Vairavamurthy, M. A.; Manowitz, B.; Zhou, W.; Jeon, Y., Determination of hydrogen sulfide oxidation products by Sulfur *K*-edge X-ray absorption near-edge structure spectroscopy. In *Environmental Geochemistry of Sulfide Oxidation*, Alpers, C. N.; Blowes, D. W., Eds. American Chemical Society: Washington DC, 1994; Vol. 550, pp 412-430.
5. Vairavamurthy, M. A.; Zhou, W.; Eglinton, T.; Manowitz, B., Sulfonates: A novel class of organic sulfur compounds in marine sediments. *Geochim. Cosmochim. Acta* **1994,** *58*, 4681-4687.
6. Vairavamurthy, M. A.; Wang, S.; Khandelwal, B.; Manowitz, B.; Ferdelman, T.; Fossing, H., Sulfur transformations in early diagenetic sediments from the Bay of Conception, off Chile. In *Geochemical Transformations of Sedimentary Sulfur*, Vairavamurthy, M. A.; Schoonen, M. A. A.; Eglinton, T. I.; Luther, G. W., III; Manowitz, B., Eds. American Chemical Society: Washington, DC, 1995; Vol. 612, pp 38-58.
7. Morra, M. J.; Fendorf, S. E.; Brown, P. D., Speciation of sulfur in humic and fulvic acids using X-ray absorption near-edge structure (XANES) spectroscopy. *Geochim. Cosmochim. Acta* **1997,** *61*, 683-688.
8. Vairavamurthy, M. A.; Maletic, D.; Wang, S.; Manowitz, B.; Eglinton, T.; Lyons, T., Characterization of sulfur-containing functional groups in sedimentary humic substances by X-ray absorption near-edge structure spectroscopy. *Energy Fuels* **1997,** *11*, 546-553.
9. Rompel, A.; Cinco, R. M.; Latimer, M. J.; McDermott, A. E.; Guiles, R. D.; Quintanilha, A.; Krauss, R. M.; Sauer, K.; Yachandra, V. K.; Klein, M. P., Sulfur K-edge x-ray absorption spectroscopy: A spectroscopic tool to examine the redox state of S-containing metabolites in vivo. *Proc. Natl. Acad. Sci. U. S. A.* **1998,** *95*, 6122-6127.
10. Xia, K.; Weesner, F.; Bleam, W. F.; Helmke, P. A.; Bloom, P. R.; Skyllberg, U. L., XANES studies of oxidation states of sulfur in aquatic and soil humic substances. *Soil Sci. Soc. Am. J.* **1998,** *62*, 1240-1246.
11. Prange, A.; Dahl, C.; Trüper, H. G.; Behnke, M.; Hahn, J.; Modrow, H.; Hormes, J., Investigation of S-H bonds in biologically important compounds by sulfur K-edge X-ray absorption spectroscopy. *Eur. Phys. J. D* **2002,** *20*, 589-596.
12. Sarret, G.; Connan, J.; Kasrai, M.; Bancroft, G. M.; Charrié-Duhaut, A.; Lemoine, S.; Adam, P.; Albrecht, P.; Eybert-Bérard, L., Chemical forms of sulfur in geological and archeological asphaltenes from Middle East, France, and Spain determined by sulfur *K*-

and *L*-edge X-ray absorption near-edge structure spectroscopy. *Geochim. Cosmochim. Acta* **1999,** *63*, 3767-3779.
13. Prietzel, J.; Thieme, J.; Neuhäusler, U.; Susini, J.; Kögel-Knabner, I., Speciation of sulphur in soils and soil particles by X-ray spectromicroscopy. *Eur. J. Soil Sci.* **2003,** *54*, 423-433.
14. Bostick, B. C.; Theissen, K. M.; Dunbar, R. B.; Vairavamurthy, M. A., Record of redox status in laminated sediments from Lake Titicaca: A sulfur *K*-edge X-ray absorption near edge structure (XANES) study. *Chem. Geol.* **2005,** *219*, 163-174.
15. Prietzel, J.; Thieme, J.; Salomé, M.; Knicker, H., Sulfur *K*-edge XANES spectroscopy reveals differences in sulfur speciation of bulk soils, humic acid, fulvic acid, and particle size separates. *Soil Biol. Biochem.* **2007,** *39*, 877-890.
16. Schroth, A. W.; Bostick, B. C.; Graham, M.; Kaste, J. M.; Mitchell, M. J.; Friedland, A. J., Sulfur species behavior in soil organic matter during decomposition. *J. Geophys. Res.* **2007,** *112*, G04011.
17. Lemelle, L.; Labrot, P.; Salomé, M.; Simionovici, A.; Viso, M.; Westall, F., In situ imaging of organic sulfur in 700–800 My-old Neoproterozoic microfossils using X-ray spectromicroscopy at the S *K*-edge. *Org. Geochem.* **2008,** *39*, 188-202.
18. Burton, E. D.; Bush, R. T.; Sullivan, L. A.; Hocking, R. K.; Mitchell, D. R. G.; Johnston, S. G.; Fitzpatrick, R. W.; Raven, M.; McClure, S.; Jang, L. Y., Iron-monosulfide oxidation in natural sediments: Resolving microbially mediated S transformations using XANES, electron microscopy, and selective extractions. *Environ. Sci. Technol.* **2009,** *43*, 3128-3134.
19. Prietzel, J.; Tyufekchieva, N.; Eusterhues, K.; Kögel-Knabner, I.; Thieme, J.; Paterson, D.; McNulty, I.; de Jonge, M.; Eichert, D.; Salomé, M., Anoxic versus oxic sample pretreatment: Effects on the speciation of sulfur and iron in well-aerated and wetland soils as assessed by X-ray absorption near-edge spectroscopy (XANES). *Geoderma* **2009,** *153*, 318-330.
20. Almkvist, G.; Boye, K.; Persson, I., *K*-edge XANES analysis of sulfur compounds: An investigation of the relative intensities using internal calibration. *J. Synchrotron Radiat.* **2010,** *17*, 683-688.
21. Orthous-Daunay, F. R.; Quirico, E.; Lemelle, L.; Beck, P.; deAndrade, V.; Simionovici, A.; Derenne, S., Speciation of sulfur in the insoluble organic matter from carbonaceous chondrites by XANES spectroscopy. *Earth. Planet. Sci. Lett.* **2010,** *300*, 321-328.
22. Prietzel, J.; Kögel-Knabner, I.; Thieme, J.; Paterson, D.; McNulty, I., Microheterogeneity of element distribution and sulfur speciation in an organic surface horizon of a forested Histosol as revealed by synchrotron-based X-ray spectromicroscopy. *Org. Geochem.* **2011,** *42*, 1308-1314.
23. Zeng, T.; Ziegelgruber, K. L.; Chin, Y.-P.; Arnold, W. A., Pesticide processing potential in prairie pothole porewaters. *Environ. Sci. Technol.* **2011,** *45*, 6814-6822.
24. Zeng, T.; Chin, Y.-P.; Arnold, W. A., Potential for abiotic reduction of pesticides in prairie pothole porewaters. *Environ. Sci. Technol.* **2012,** *46*, 3177-3187.
25. Zeng, T.; Arnold, W. A., Pesticide photolysis in prairie potholes: Probing photosensitized processes. *Submitted* **2012**.